frontiers | Research Topics

The role of gut microbiota and probiotics in modulating gut-brain axis of humans and animals

Edited by
Hesong Wang, Xueqin Ni and Yang Bai

Published in
Frontiers in Microbiology

ISSN 1664-8714
ISBN 978-2-8325-2711-5
DOI 10.3389/978-2-8325-2711-5

About Frontiers

Frontiers is more than just an open access publisher of scholarly articles: it is a pioneering approach to the world of academia, radically improving the way scholarly research is managed. The grand vision of Frontiers is a world where all people have an equal opportunity to seek, share and generate knowledge. Frontiers provides immediate and permanent online open access to all its publications, but this alone is not enough to realize our grand goals.

Frontiers journal series

The Frontiers journal series is a multi-tier and interdisciplinary set of open-access, online journals, promising a paradigm shift from the current review, selection and dissemination processes in academic publishing. All Frontiers journals are driven by researchers for researchers; therefore, they constitute a service to the scholarly community. At the same time, the *Frontiers journal series* operates on a revolutionary invention, the tiered publishing system, initially addressing specific communities of scholars, and gradually climbing up to broader public understanding, thus serving the interests of the lay society, too.

Dedication to quality

Each Frontiers article is a landmark of the highest quality, thanks to genuinely collaborative interactions between authors and review editors, who include some of the world's best academicians. Research must be certified by peers before entering a stream of knowledge that may eventually reach the public - and shape society; therefore, Frontiers only applies the most rigorous and unbiased reviews. Frontiers revolutionizes research publishing by freely delivering the most outstanding research, evaluated with no bias from both the academic and social point of view. By applying the most advanced information technologies, Frontiers is catapulting scholarly publishing into a new generation.

What are Frontiers Research Topics?

Frontiers Research Topics are very popular trademarks of the *Frontiers journals series*: they are collections of at least ten articles, all centered on a particular subject. With their unique mix of varied contributions from Original Research to Review Articles, Frontiers Research Topics unify the most influential researchers, the latest key findings and historical advances in a hot research area.

Find out more on how to host your own Frontiers Research Topic or contribute to one as an author by contacting the Frontiers editorial office: frontiersin.org/about/contact

The role of gut microbiota and probiotics in modulating gut-brain axis of humans and animals

Topic editors

Hesong Wang — Southern Medical University, China
Xueqin Ni — Sichuan Agriculture University, China
Yang Bai — Southern Medical University, China

Citation

Wang, H., Ni, X., Bai, Y., eds. (2023). *The role of gut microbiota and probiotics in modulating gut-brain axis of humans and animals*. Lausanne: Frontiers Media SA. doi: 10.3389/978-2-8325-2711-5

Table of contents

frontiers in Microbiology

ORIGINAL RESEARCH
published: 02 November 2021
doi: 10.3389/fmicb.2021.761113

Bifidobacterium infantis Maintains Genome Stability in Ulcerative Colitis *via* Regulating Anaphase-Promoting Complex Subunit 7

Taotao Han[1,2†], Xiaomin Hu[2,3†], Kemin Li[1,2], Di Zhang[1,2], Yan Zhang[4] and Jingnan Li[1,2]*

[1] Department of Gastroenterology, Peking Union Medical College Hospital, Peking Union Medical College, Chinese Academy of Medical Sciences, Beijing, China, [2] Key Laboratory of Gut Microbiota Translational Medicine Research, Chinese Academy of Medical Sciences, Beijing, China, [3] State Key Laboratory of Complex Severe and Rare Diseases, Department of Medical Research Center, Peking Union Medical College Hospital, Chinese Academy of Medical Sciences and Peking Union Medical College, Beijing, China, [4] Institute of Cardiovascular Sciences and Key Laboratory of Molecular Cardiovascular Sciences, School of Basic Medical Sciences, Ministry of Education, Peking University Health Science Center, Beijing, China

OPEN ACCESS

Edited by:
Yang Bai,
Southern Medical University, China

Reviewed by:
Xiuqin Zhang,
Peking University, China
Yongquan Shi,
Fourth Military Medical University, China
Yingxuan Chen,
Shanghai Jiao Tong University, China

***Correspondence:**
Jingnan Li
lijn@pumch.cn

[†] These authors have contributed equally to this work

Specialty section:
This article was submitted to Microbial Symbioses, a section of the journal Frontiers in Microbiology

Received: *19 August 2021*
Accepted: *08 October 2021*
Published: *02 November 2021*

Citation:
Han T, Hu X, Li K, Zhang D, Zhang Y and Li J (2021) Bifidobacterium infantis Maintains Genome Stability in Ulcerative Colitis via Regulating Anaphase-Promoting Complex Subunit 7. Front. Microbiol. 12:761113. doi: 10.3389/fmicb.2021.761113

Probiotics represents a promising intestinal microbiota-targeted therapeutic method for the treatment of ulcerative colitis (UC). Several lines of evidence implicate that *Bifidobacterium infantis* serves as a probiotic strain with proven efficacy in maintaining the remission of UC. However, the exact mechanisms underlying the beneficial effects of *B. infantis* on UC progression have yet to be elucidated. Herein, we provide evidence that *B. infantis* acts as a key predisposing factor for the maintenance of host genome stability. First, we showed that the fecal microbiota transplantation (FMT) of UC-derived feces contributes to more severely DNA damage in dextran sodium sulfate (DSS)-induced mice likely due to mucosa-associated microbiota alterations, as reflected by the rapid appearance of DNA double strand breaks (DSBs), a typical marker of genome instability. Genomic DNA damage analysis of colon tissues derived from healthy controls, patients with UC or dysplasia, and colitis associated cancer (CAC) patients, revealed an enhanced level of DSBs with aggravation in the degree of the intestinal mucosal lesions. To evaluate whether *B. infantis* modulates the host genome stability, we employed the DSS-induced colitis model and a TNFα-induced intestinal epithelial cell model. Following the administration of C57BL/6 mice with *B. infantis via* oral gavage, we found that the development of DSS-induced colitis in mice was significantly alleviated, in contrast to the colitis model group. Notably, *B. infantis* administration decreased DSB levels in both DSS-induced colitis and TNF-treated colonial cell model. Accordingly, our bioinformatic and functional studies demonstrated that *B. infantis* altered signal pathways involved in ubiquitin-mediated proteolysis, transcriptional misregulation in cancer, and the bacterial invasion of epithelial cells. Mechanistically, *B. infantis* upregulated anaphase-promoting complex subunit 7 (APC7), which was significantly suppressed in colitis condition, to activate the DNA repair pathway and alter the genome stability, while downregulation of APC7 abolished the efficiency of *B. infantis* treatment to induce a decrease in the level

of DSBs in TNFα-induced colonial cells. Collectively, our results support that *B. infantis* orchestrates a molecular network involving in APC7 and genome stability, to control UC development at the clinical, biological, and mechanistic levels. Supplying *B. infantis* and targeting its associated pathway will yield valuable insight into the clinical management of UC patients.

Keywords: DSBs, APC7, genome stability, ulcerative colitis, *B. infantis* CGMCC0460.1

INTRODUCTION

Ulcerative colitis (UC), is a chronic inflammatory condition of the colon and is associated with an increased risk for the development of colorectal cancer (CRC). Epidemiological studies demonstrate that more than 20% of worldwide cancers are caused by chronic inflammatory conditions (Grivennikov et al., 2010; Trinchieri, 2012). This increased cancer risk is thought to develop *via* a multistep process involving in cellular genome instability and the progressive accumulation of genetic alterations induced by the chronic inflammation (Loeb and Loeb, 1999). To data, there is no clearly genetic basis explain the alterations in genome stability in patients with UC disease.

Research has demonstrated an increase of higher genomic instability in UC patients, as evidenced by the presence of multiple chromosomal alterations, including DNA double strand breaks (DSBs), DNA replication errors, microsatellite instability (MSI), as well as chromosomal instability, which has been recognized as an early event during the progression of UC-related neoplasia (Willenbucher et al., 1999; Pereira et al., 2016). To further clarify the genetic alterations in UC patients, various of studies depicted the genomic and molecular landscape of inflammatory bowel disease (IBD)-associated CRC, and shown that the main genomic alterations in IBD-CRC, including p53 mutation, p53 loss of heterozygosity (LOH), chromosomic instability, and a high incidence of MSI accompanied by telomere shortening (O'Sullivan et al., 2002), in long standing UC patients with severe inflammation, thus reflecting genomic instability caused by repeated inflammatory stress (Park et al., 1998; Ishitsuka et al., 2001). Notably, continuing chronic inflammation and resultant DNA damage in the setting of UC causes the accumulation of genetic alterations, genomic instability might, therefore, serve as prospective indicators of cancer risk in UC patients. It has been proposed that the anaphase-promoting complex (APC), an E3 ligase enzyme, functions as a tumor suppressor by maintaining genomic stability, whereas the dysregulation of APC/C plays a crucial role in oncogenic processes (Aust et al., 2002; Smolders and Teodoro, 2011). Owing to the heterogeneity of APC subunits expression, the proteins involved in the APC signaling cascade may be altered in UC-related carcinogenesis. As a critical component of APC, the dysregulation of anaphase-promoting complex subunit 7 (APC7) may contribute to the pathogenesis of acute myeloid leukemia (AML) (Rahimi et al., 2015), however, the function roles of APC7 involving in the development of UC remain unclear.

Recent data suggest that microbial factors function as important drivers of inflammation and therefore contribute to carcinogenesis by triggering oxidative stress or changes in genome stability. The high frequency of bacterial cocolonization in colon tissues highlights the importance of understanding the potential effects of gut microbiota in UC development (Guidi et al., 2013). Strong experimental evidence supported the fact that numbers of bacteria that colonized in the intestine could directly affect the genomic integrity of epithelial cells *via* genotoxins. Genotoxin colibactin-producing *pks-Escherichia coli*, was reported to cause cell cycle arrest, DSB, mutations, and promote the development of colitis-associated CRC *in vitro* and *in vivo* (Arthur et al., 2012; Wilson et al., 2019), whereas, *enterotoxigenic Bacteroides fragilis* (ETBF) has been shown to increase the level of interleukin-17 and triggers colon tumorigenesis and DNA damage in the colonic epithelium of Apc Min/+ mice, thus, resulting in faster tumor onset and greater mortality (Wu et al., 2009; Dejea et al., 2018). Thus, it is possible that the intestinal microbiota might affect the ongoing genomic instability of host by direct or indirect ways.

Bifidobacterium infantis is a probiotic strain that naturally resides in the human intestines. A striking reduction in the abundance of *B. infantis* has been observed in the intestinal tissue from UC patients (Frank et al., 2007), thus indicating a potential role of *B. infantis* in human intestines. There is also persuasive evidence from several studies to demonstrate that *B. infantis* acted as a probiotic to protect against inflammatory conditions in several ways, including maintaining the balance of gut flora, modulating the immune system, and by producing metabolites that are involved in the amelioration of intestinal inflammation (Peran et al., 2005, 2007; Javed et al., 2016). Despite the strong link between *B. infantis* and inflammatory disease, multiple complementary approaches have provided indirect information with regards to the proven efficacy of *B. infantis* in inducing and maintaining the remission of UC, then limiting our mechanistic understanding of this direct association.

To address this, we performed a comprehensive analysis of histopathology, molecular damage, and gene expression changes, in DSS induced animal models and TNFα-induced colon epithelial cell culture models, that were treated with *B. infantis* or a vehicle. In these models, we were able to reproduce early responses to acute stimulation, including DSBs and inflammation. Furthermore, we examined whether DNA damage caused by DSS or TNFα resulted in genomic instability. In particular, we investigated the signal pathways involved in *B. infantis* treatment, by applying the transcriptional profiling and analysis of GEO database, which indicated that *B. infantis* might upregulate APC7 expression to maintain genome stability and ameliorate inflammation in the development of UC.

MATERIALS AND METHODS

Cell Line and Small Interfering RNAs

Human intestinal epithelial cell lines (HT29 and HCT116) were purchased from ATCC, and maintained in F12 (Gibco, Carlsbad, CA, United States) and RPMI 1640 (Gibco, Carlsbad, CA, United States), supplemented with 10% fetal bovine serum (FBS, Gibco), respectively. All cells were cultured at 37°C and 5% CO_2. Cells were transiently transfected using Lipofectamine™ 3000 (Thermo Scientific, Worcester, MA, United States). APC7 small interfering RNA (siRNA) and control siRNAs were commercially obtained from Guangzhou RiboBio Co., Ltd. (China). The targeted sequences for si-APC7-1, si-APC7-2, and si-Ctrl were as follows: si-APC7-1: 5′-GGACCAGTATAGTATAGCA-3′; si-APC7-2: 5′-GGAACGCACTGGCTAATCA-3′; si-control: 5′-GGCUCUAGAAAAGCCUAUGCdTdT-3′. The APC7-ovexpressing vectors were purchased from GeneCopoeia, China (#EX-L5377-Lv201).

Animals

A total of 6–8 week-old male C57BL/6 mice were purchased from Beijing Vital River Laboratory Animal Technology Co., Ltd. (China) and housed under a 12-h light and 12-h dark cycle condition. All laboratory animals were cared for and used in accordance with the guidelines of the Animal Care Ethics and Use Committee of Peking Union Medical College Hospital (Beijing, China).

Patients and Specimens

All human tissue samples were obtained from endoscopic biopsies or surgical specimens of patients with UC and colitis associated cancer (CAC), in the Peking Union Medical College Hospital between 2015 and 2021. Written informed consent for the application of specimens was obtained from all the patients. The study was approved by the Ethics Committee of Peking Union Medical College Hospital (Beijing, China).

Administration With *Bifidobacterium infantis* in Dextran Sodium Sulfate-Induced Colitis Model

All mice were initially housed together for adaptive feeding, 1 week later, the mice were randomly divided into control group, colitis model group and *B. infantis* treatment group. The two reference groups (control and colitis model) received sterile saline solution (200 μl/mouse), while the *B. infantis* treatment group received *B. infantis* CGMCC0460.1 powders (7.5×10^9 CFU/ml diluted in 200 μl of sterile saline), purchased from Hangzhou Grand Biologic Pharmaceutical INC. (China). The *B. infantis* treatment group received daily oral administration from day 1 to day 14. Seven days after starting the experiment, 2.5% dextran sodium sulfate (DSS) (Sigma-Aldrich) in drinking water was adequate to induce colitis in the colitis model group and the *B. infantis* treatment group mice for 5 days, and then followed by regulator water for 2 days. Disease activity index (DAI) scores and body weight were recorded throughout the experiments to determine the severity of colitis, as reported previously (Wang et al., 2019). At the end of the experiment, the plasma samples from anesthetized mice was obtained and stored at −80°C. Once the mice were sacrificed, we measured the length of colon and the distal inflamed region of the colon tissues was fixed in 4% buffered paraformaldehyde for histological analysis.

Bifidobacterium infantis Co-cultured With TNFα-Induced Intestinal Epithelial Cells

For *B. infantis* CGMCC0460.1 co-culture, cells at 80% confluency were washed with PBS and incubated in antibiotic-free medium. *B. infantis* CGMCC0460.1 powders were dissolved in antibiotic-free medium, and added to the colon epithelial cells at the indicated concentrations [Multiplicity of Infection (MOI) at 1:100].

Histological and Immunohistochemical Analysis

Hematoxylin and eosin (H&E) staining was performed on the paraffin-embedded sections from formalin-fixed colonic tissues. Histologic analysis was carried out independently by two pathologists, according to previously validated criteria (Ameho et al., 1997). For IHC analysis, colon sections obtained from patients with UC or CAC, and DSS-induced models were stained with the indicated antibodies, including γH2Ax (CST, Danvers, MA, United States, #9718), p-ATM (Abcam, ab36810) and APC7 (Santa Curze, sc-365649).

cDNA Synthesis, Genomic DNA Extraction, and Quantitative Real-Time PCR

Total RNA was isolated from indicated colon tissues or cells using TRIzol reagent (Invitrogen), and then subjected to reverse transcription with M-MLV (Promega) in accordance with the manufacturer's instructions. Quantitative real-time PCR (qRT-PCR) was performed with SYBR Green in an ABI 7500 system (Life Technologies). The primer sequences used for real-time PCR are summarized in **Supplementary Table 1**, GAPDH was chosen as the internal control for the quantitative analysis. Gene expression levels were determined relative to GAPDH. For the detection of *B. infantis* level, we isolated genomic DNA from indicated feces using Genomic DNA extraction Kit (TIANGEN, Beijing), the concentration of extracted DNA was calculated using a Nanodrop LITE (Thermo Scientific). Then, a total of 25 ng of genomic DNA of each sample was used as a template. Quantification of the total *B. infantis* was performed by qRT-PCR assay, 16 s rRNA was performed as an internal control regarding to the bacteria level quantitation.

Western Blotting Assay

For western blotting, colon tissues or cell extracts were collected and quantified by the BCA Protein Assay Kit (Thermo Fisher Scientific). Thirty micrograms of each protein sample was resolved by 12% SDS-PAGE (Thermo Fisher Scientific), transferred to PVDF membranes, and then incubated with the indicated primary antibodies at 4°C overnight. Then, the membranes were washed and incubated with secondary anti-rabbit or mouse IgG (CST) antibodies. Subsequently, the binding

signals were visualized with an ECL Kit (Pierce Biotech, Thermo Fisher Scientific). GAPDH (Proteintech, HRP-60004) or β-actin (CST, 3700) antibodies was used as an endogenous control.

Comet Assay

The comet assay was performed using a Comet assay Kit (Trevigen, 4250-050-K), as described previously (Han et al., 2020). In brief, colon epithelial cells were harvested after the indicated treatment, and then mixed with 0.5% low-melting-point agarose, and immediately pipetted onto Cometslide^{TM}, which were then placed at 4°C in the dark for 10 min. And, the slides were immersed in 4°C lysis solution for 1 h. Then, the slides were placed in fresh Alkaline Unwinding Solution for 1 h at 4°C, and immersed the slides in Alkaline Electrophoresis Solution for 30 min at 21 volts. After electrophoresis, the slides were gently immersed twice in ddH_2O for 5 min, and then in 70% ethanol for 5 min, and dried at 37°C for 30 min. Then, the slides were stained with 20 μg/ml of PI (Sigma-Aldrich, St. Louis, MO, United States) and observed under a fluorescence microscope. The comet tails were quantified using CASP software.

RNA Sequencing

The RNA sequencing was performed by Novogene Co. Ltd. (Beijing, China). Total RNAs were extracted from specimens using TRIzol reagent (Invitrogen, Carlsbad, CA, United States). The concentration of extracted RNA was measured using the Qubit® RNA Assay Kit in a Qubit® 2.0 Fluorometer (Life Technologies, CA, United States). Then, sequencing libraries were generated using the NEBNext® Ultra^{TM} RNA library Prep Kit for Illumina® (NEB, United States). The library preparations were sequenced on an Illumina HiSeq platform. Raw data was firstly processed using in-house perl scripts. The clean data was mapped to the reference genome using STAR (v2.5.1b). The number of reads was counted by HTSeq v 0.6.0 and the Fragments Per Kilobase Million (FPKM) of each gene was calculated to estimate gene expression levels. Gene quantification data were analyzed in R using the DESeq2 package to screen differentially expressed genes. Genes with an adjusted p-value < 0.05 and absolute fold change >0, as determined by DESeq2 were considered as significantly differentially expressed.

Metagenomic Sequencing

Fecal samples were obtained from mice after DSS treatment, then the samples were frozen immediately and underwent DNA extraction using standard protocols. Illumina GAIIX and HiSeq 2000 platform were performed to sequence the samples. Then, clean data was blasted to the host database and were quality filtered using Bowtie 2.2.4 software (Bowtie2.2.4[1]), as described previously (Nielsen et al., 2014).

Fecal Microbial Transplantation in an Antibiotic-Depletion Model

Mice aged 4–5 weeks were treated with antibiotic and anti-fungal water, in order to deplete the gut microbiota. Briefly, mice were treated with an antibiotic cocktail consisting of 0.5 g/L vancomycin (Sigma-Aldrich), 2 g/L streptomycin (Selleck), 0.75 g/L metronidazole (Sigma-Aldrich), and 0.5 g/L fluconazole (Selleck) for 1 week (Kennedy et al., 2018). Then, the feces were dissolved in 10 g/L sterile saline, 20 μl were cultured on the brain heart infusion (BHI) broth (Biobw, Beijing). The plates were placed in a 37°C incubator, after drying, the plates was inverted and cultured for 24 h under anaerobic condition. The number of colonies on each plate was calculated to evaluate the success of the antibiotic-depletion model. Following the depletion of gut microbiota, fresh stools were collected from the healthy control (healthy volunteers were omnivorous and were not taking antibiotics within 8 weeks before stool collection) or a patient with severe UC (an endoscopic Mayo score of ≥2, and do not use antibiotics or probiotics within 6 weeks before stool collection). Specifically, the stools were dissolved in 10 g/L sterile saline and centrifuged at 2000 rpm for 5 min. The supernatants of stools were administered to the antibiotic-treated mice (200 μl/mice) for 5 consecutive days, then DSS treatment 4 weeks later to induce colitis.

Statistical Analysis

Statistical analysis was carried out using SPSS version 26.0 software. Data from at least three independent experiments are presented as the means ± SEM. The student's two-tailed t-test or one way analysis of variance (ANOVA) with Tukey's *post hoc* test were used to determine significant differences among groups. p-Value < 0.05 was considered statistically significant. All graphs in this study were prepared using GraphPad Prism version 8.0 software.

RESULTS

The Development of Ulcerative Colitis Was Associated With Genome Instability, Which Was Partially Mediated by Alteration in the Gut Microbiota

Since previous studies reported that genome instability is an early event during the progression of UC-related neoplasia (Willenbucher et al., 1999), we aimed to test whether the progression of UC was associated with genome instability, by evaluating the expression of S139-phosphorylation of histone H2Ax (γH2Ax), a sensitive marker of DSBs, using immunohistology. As outlined in **Figure 1**, γH2Ax foci were localized to the nucleus of epithelial cells, and an increased intensity of γH2Ax foci were seen in biopsies of the colon from UC patients; only very week expression of γH2Ax foci was observed in normal colon tissues. According to the Montreal classification system, the normal colonic mucosa could progress into moderate UC, severe UC, dysplasia, and eventually developed into colitis-associated cancer (Allen and Sears, 2019). Next, we analyzed the relative numbers of γH2Ax foci in different stages of UC progression. Immunohistological analysis showed that the number of positively stained nuclei was significantly higher in inflamed ($p < 0.05$), dysplastic ($p < 0.001$), and CAC tissues ($p < 0.0001$) than that in normal mucosal tissues, thus

[1]http://bowtie-bio.sourceforge.net/bowtie2/index.shtml

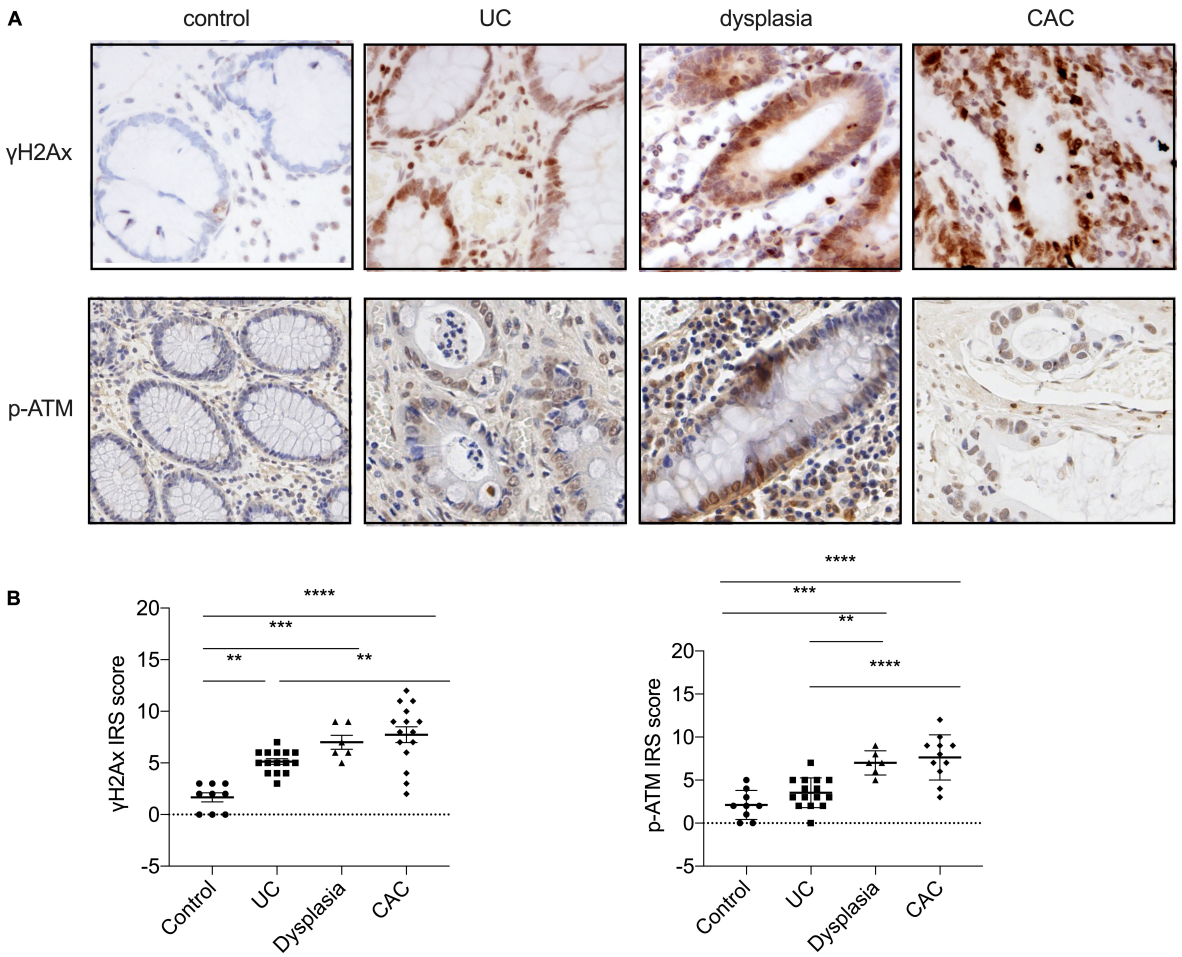

FIGURE 1 | Ulcerative colitis development is associated with genome instability. **(A)** The expression of S139-phosphorylation of histone H2Ax (γH2Ax) and ATM phosphorylation (*p*-ATM) levels were determined by immunohistology assay in healthy controls, patients with UC or dysplasia, and patients with colitis-associated cancer (CAC). (Magnification, ×20.) **(B)** Statistical analysis of γH2Ax and ATM phosphorylation levels determined by immunohistology assay. $^{*}p < 0.05$, $^{**}p < 0.01$, $^{***}p < 0.001$, $^{****}p < 0.0001$.

indicating that γH2Ax expression was sequentially upregulated from normal, UC, dysplasia to CAC. Consistently, the level of ataxia telangiectasia mutated (ATM) phosphorylation was also showed a gradual increase among with aggravation of the degree of the colonic mucosal lesion (**Figure 1**). These results suggested that genome instability, as indicated by γH2Ax and p-ATM, was involved in the progression of UC.

Indeed, the intestinal microbiome has long been suggested to be involved in UC development and genome stability modulation. Hence, to determine whether the microbiome differences between healthy control and severe UC microbiomes are responsible for the regulation of genome stability in colitis, we performed fecal microbiota transplantation (FMT) assay to determine the influence of microbiota derived from UC patients or healthy controls with regards to the pathogenesis of UC. Firstly, the mice were pretreated with antibiotic cocktail for 1 week to target bacteria and fungal blooms, as the colony formation results suggested, the number of colony derived from antibiotic and antifungal treatment mice was significantly decreased than those from the control mice (**Supplementary Figure 1**). Then, the microbiomes derived from UC patients or healthy controls were transplanted into the antibiotics-pretreated mice for 5 days. After 4 weeks of colonization to allow microbiota reconstitution in the intestine, we induced colitis by administering 2.5% DSS to mice. We found that feces derived from UC patients aggravated DSS-induced colitis in mice when compared with those derived from healthy controls (**Figures 2A–E**). Next, immunohistology was performed to investigate the expression levels of γH2Ax. Significant numbers of γH2Ax foci were identified in the nuclei of enterocytes exposed to fecal microbiota derived from UC patients when compared with those from healthy controls, which indicated that gut microbiota is responsible for the genome stability in DSS-induced colitis (**Figure 2F**).

As previous suggested, the gut microbiomes between healthy controls and UC patients were differently abundant in certain bacterial species. Microbiomes derived from healthy control have increased *Akkermansia*, *Bifidobacterium*, *Lactobacillus*, while those derived from severe UC patients have increased with *Bacteroides, Escherichia-Shigella,* and *Enterococcus* (Sood et al.,

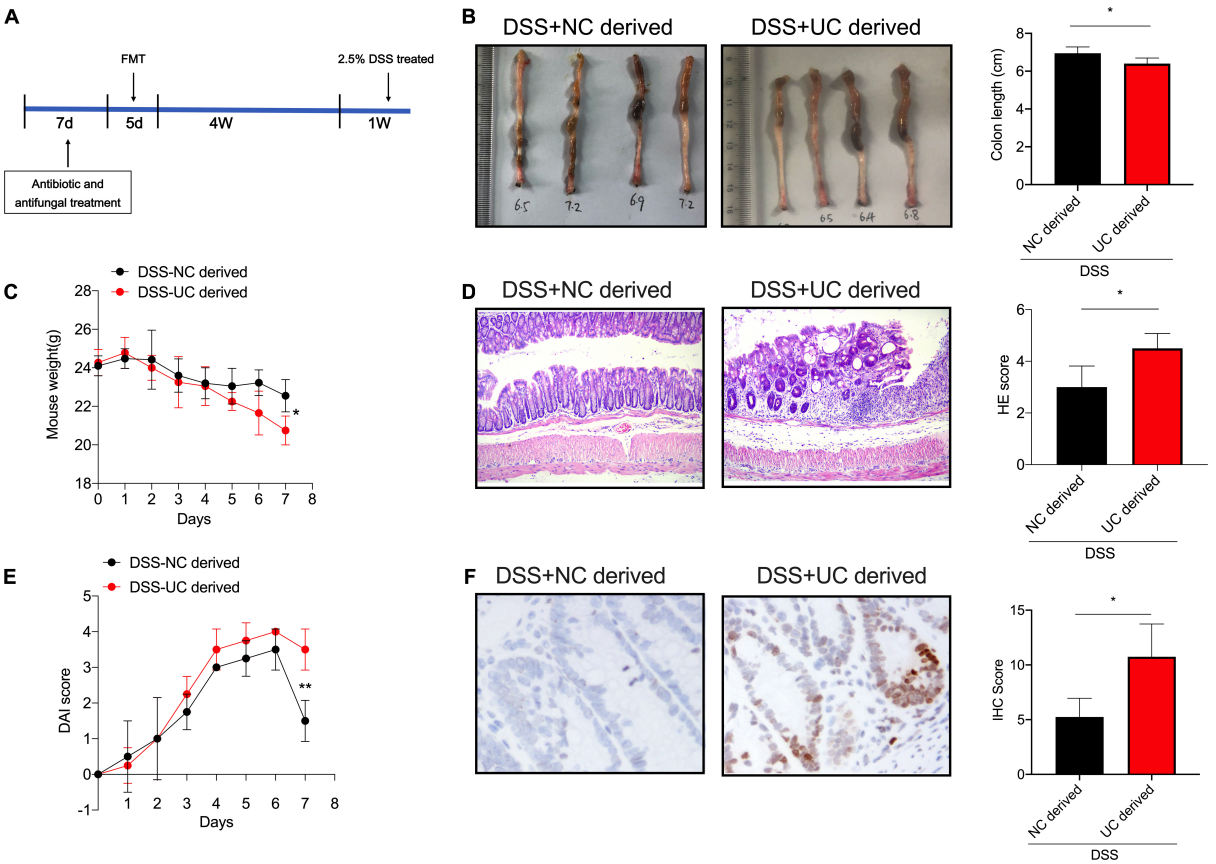

FIGURE 2 | DSS-induced colitis was evaluated among the mice administrated with feces derived from UC patients or healthy controls. **(A)** Schema of FMT model. The colon length **(B)**, body weight **(C)**, the H&E staining of sections **(D)**, and DAI score **(E)**, in colon tissues of mice between the two groups. (Magnification, ×20.) **(F)** The expression levels of γH2Ax were determined by immunohistology in colon tissues of mice administered with feces derived from UC patients and healthy controls. (Magnification, ×20.) $^{*}p < 0.05$, $^{**}p < 0.01$.

2009). In turn, we explored to detect the level of *B. infantis,* belongs to the *Bifidobacterium*, in feces of healthy control and UC patient, and found that *B. infantis* was significantly downregulated in UC patient than those from the healthy control (**Supplementary Figure 2**). Therefore, our data indicated that genome instability was associated with the development of UC and was partially mediated by alteration of intestinal microbiota.

The Administration of *Bifidobacterium infantis* Promoted the Recovery of Dextran Sodium Sulfate-Induced Intestinal Injury and Modulated the Composition of Gut Microbiota in Mice

To investigate the effect of *B. infantis* on intestinal colitis, we administered DSS-treated mice with *B. infantis* by oval gavage. The schema of DSS-induced colitis model was presented as in **Figure 3A**. The mice receiving *B. infantis* presented a milder form of colitis than the mice receiving DSS containing drinking water, as evidenced by the significant lengthening of the colon (**Figure 3B**). Maximum body weight loss of the mice in the colitis model group was observed on day 7. In contrast, the mice that were given an oral dose of *B. infantis* rapidly recovered weight from day 6 to day 7 (**Figure 3C**). The DAI score in DSS-treated mice showed an obvious increase on day 7 compared with the control mice, but was downregulated in mice following *B. infantis* administration (**Figure 3D**). In the colitis model group, the upregulation of DAI score corresponded with increased intestinal permeability, as evidenced by a fluorescein isothiocyanate (FITC) dextran and western blotting assays. However, following exposure to *B. infantis*, the intestinal permeability was decreased and components of the tight junctions, including ZO-1, Claudin-1, and Occludin, were found to be upregulated in the colon by the end of the experiment (**Figures 3E,F**). In addition, H&E stained sections of colonic tissue showed a significantly higher level of inflammatory cell infiltration and total histological score, along with severe disruption of the mucosal epithelium, in DSS-induced mice, but not in *B. infantis*-treated mice (**Figures 3G,H**). These results suggested that the administration of *B. infantis* plays a beneficial role in DSS-induced colitis, and helps to alleviate epithelial damage and promote the remission of inflammation.

In addition, we performed metagenomic sequencing to examine the composition of gut microbiota in DSS-induced mice. Although no difference in species richness was measured between the gut microbiotas of DSS-treated mice and the control group, the Shannon index and gene richness were decreased

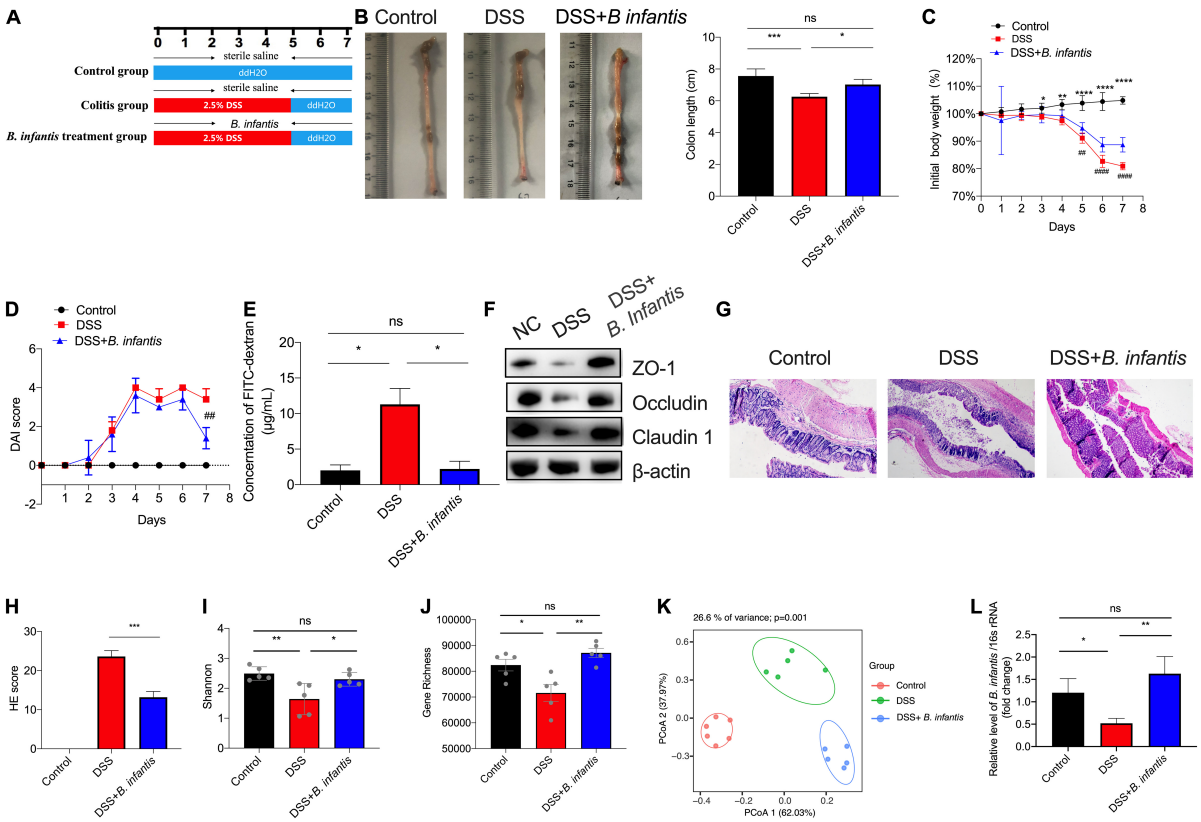

FIGURE 3 | The administration of *B. infantis* relieved colitis in a dextran sodium sulfate (DSS) mouse model of acute colitis. **(A)** Schema of DSS-induced colitis model. Mice in the control group and the colitis model group were pretreated with sterile saline, and the *B. infantis* treatment group was pretreated with *B. infantis* for 7 days. Then, DSS treated mice receiving *B. infantis* by oral gavage as indicated; mice were sacrificed on day 8 and colon length was measured **(B)**. **(C)** Body weight of mice in each group was measured during the experiment period. *Control vs. DSS $p < 0.05$, **Control vs. DSS $p < 0.01$, *****Control vs. DSS $p < 0.0001$, ## Control vs. DSS + *B. infantis* $p < 0.01$. **(D)** DAI score was monitored each day during the experiment period. ## control vs. DSS + *B. infantis* $p < 0.01$. **(E)** The FITC assay was performed to determine intestinal permeability. **(F)** The expression levels of tight junction components, including ZO-1, Claduin-1, and Occludin, were detected by western blot assays. H&E staining of sections **(G)** and the total histological score **(H)**. (Magnification, ×20.) **(I–K)** The Shannon index **(I)**, gene richness **(J)** and Principal Coordinates Analysis (PCoA) plot of Bray–Curtis **(K)** regarding to the gut microbiota in DSS-treated models using metagenomic sequencing. **(L)** The level of *B. infantis* in feces of DSS-induced model detected by qRT-PCR assay. Results represent mean ± SEM; *$p < 0.05$, **$p < 0.01$, ***$p < 0.001$, ****$p < 0.0001$, ns, no significance.

in the DSS-treated group, in contrast to the control group, while following *B. infantis* treatment, the Shannon and gene richness were significantly elevated (**Figures 3I–J**). PCoA of control, colitis model and *B. infantis* treatment mice from samples indicated significant difference among the three groups (**Figure 3K**). Subsequently, we detected the level of *B. infantis* in DSS-induced model, and found that *B. infantis* was decreased after DSS treatment, which was partially restored after treatment with *B. infantis* (**Figure 3L**). Thus, these results indicated that supplementation of *B. infantis* modulated the composition of the gut bacteria, particularly the level of *B. infantis*.

Bifidobacterium infantis Maintained Genome Stability in Dextran Sodium Sulfate-Induced Colitis and TNFα-Treated Intestinal Epithelial Cells

Since gut microbes can elicit their effects on the genome or epigenome *via* direct or indirect mechanisms (Allen and Sears, 2019), we hypothesized that *B. infantis* might exert impact on genome instability triggered by intestinal inflammation. Consistent with this hypothesis, γH2Ax immunohistochemistry and western blot assays revealed significantly enhanced DNA damage in the colon epithelial cells of DSS-induced mice; however, the levels of γH2Ax were obviously decreased after treatment with *B. infantis* (**Figures 4A,B**). Furthermore, we also investigated the phosphorylation of ATM, a core component of the DNA repair system (Marechal and Zou, 2013). Interestingly, the staining of phosphorylated ATM revealed a similar pattern as seen in the colon tissues with regards to γH2Ax staining (**Figures 4,B**). These findings show that *B. infantis* exerts impact on DNA damage in intestinal colitis.

To validate the *in vivo* findings observed in DSS-induced mice, we used an *ex vivo* model of cultured-human intestinal cells that were treated with a proinflammatory cytokine (TNFα). When compared with control cells, the levels of phosphorylated H2Ax were significantly higher in TNFα-treated cells (**Figures 4C**, **6A**). Subsequently, we investigated the direct effects of *B. infantis*

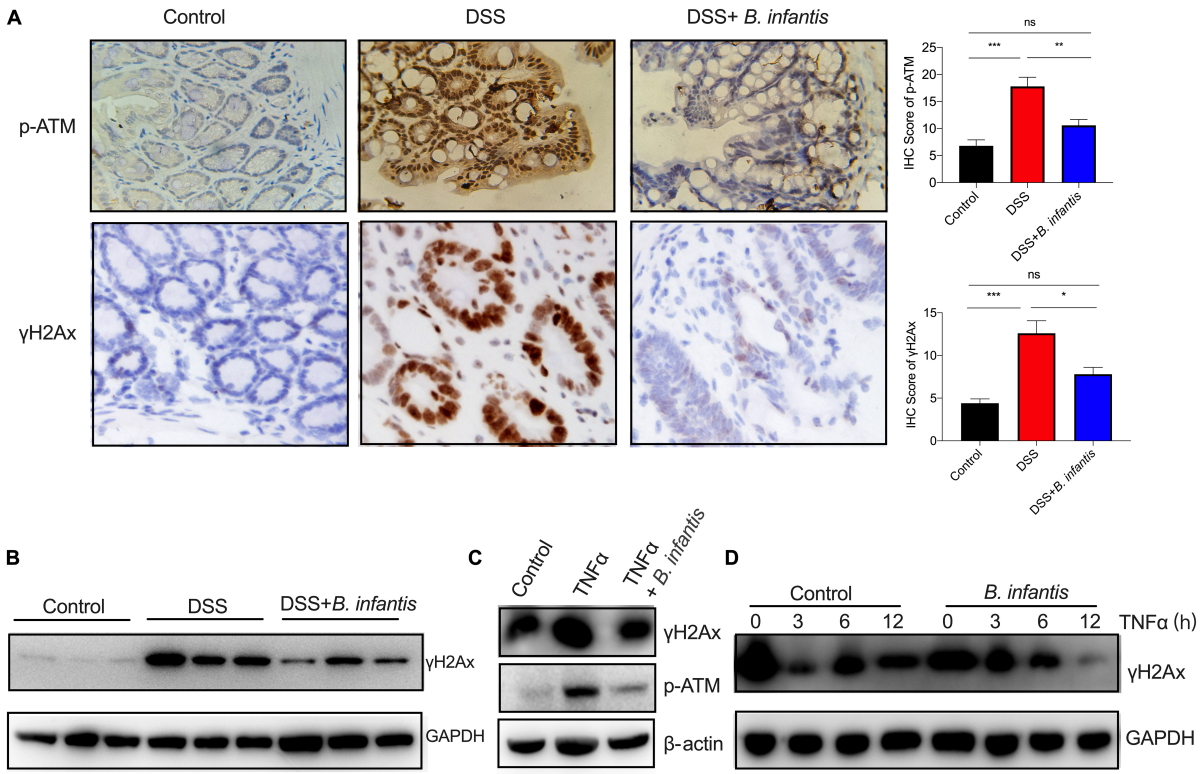

FIGURE 4 | *Bifidobacterium infantis* protected against genome instability in DSS-induced colitis and TNFα-treated intestinal epithelial cells. γH2Ax expression and ATM phosphorylation were determined in DSS-induced mice that had been administered with *B. infantis*, as determined by IHC assays **(A)** and western blotting **(B)**, respectively. (Magnification, ×20.) **(C)** The expression of γH2Ax was examined in TNFα-treated colon epithelial cells that had been co-cultured with *B. infantis*. **(D)** HT29 cells were pretreated with TNFα for 6 h, after which media was replaced with fresh media containing vehicle or *B. infantis* to allow the cells to recover. Western blotting analysis of phosphorylation of γH2Ax was performed. $^{*}p < 0.05$, $^{**}p < 0.01$, $^{***}p < 0.001$, ns, no significance.

on the genomic stability of colon epithelial cells. To do this, we developed a co-culture protocol in which *B. infantis* was added into the *ex vivo* model of colon epithelial cells treated with TNFα. Cells were then immunostained for γH2Ax; we observed a notable increase in the expression levels of γH2Ax in cultures treated with TNFα. In contrast, *B. infantis* treatment reduced the amount of DSBs in intestinal cells after cultured for 6 h (**Figure 4C**). To analyze whether *B. infantis* regulated DSB repairs, we pretreated HT29 cells with TNFα for 6 h, replaced the media with fresh media containing *B. infantis*, and allowed the cells to recover. As shown in **Figure 4D**, the level of DNA damage gradually reduced in colonial cells after TNFα treatment, thus suggesting the efficient repair of DSBs. In contrast, DNA repair was shown to be advanced in colonial cells that were co-cultured with *B. infantis* (**Figure 4D**). These data suggest that the increased basal levels of DSBs in TNFα-induced intestinal cells were attenuated by *B. infantis* treatment.

Identification of Anaphase-Promoting Complex Subunit 7 as a Molecule Related to *Bifidobacterium infantis* Treatment

Next, to determine the protective mechanisms underlying the anti-colitis activity of *B. infantis*, we used RNA sequencing to analyze the transcriptome of colon tissue obtained from control, DSS-induced, and *B. infantis*-treated mice (**Figure 5A**). As the heatmap suggests, there were systematic variations ($p < 0.05$, absolute fold change ≥ 0) in the expression levels of mRNA related to intestinal colitis (**Figure 5A**). Gene set enrichment analysis (GSEA) revealed a significant enrichment in genes related to the ubiquitin-mediated proteolysis pathway (**Figure 5C**). This result was further supported by the transcriptome profiling data from healthy controls, patients with UC in GSE47908 (**Figures 5B,D**). Then, we screened critical molecules that cause or favor the development of UC, as based on a comparison of the overlapping mRNAs involved in the ubiquitin-mediated proteolysis pathway, enriched in the two RNA-sequencing results (**Figure 5E** and **Supplementary Table 2**). Given that the ubiquitin-mediated proteolysis pathway was significantly enriched with regards to the RNA sequencing results, we analyzed the expression of overlapping mRNAs that were enriched in the ubiquitin pathway in public GEO database, and found that APC7 was remarkably downregulated in UC tissues and CAC tissues, compared with normal mucosal tissues in GSE47908 and GSE9452, while there was no significance in APC7 expression between UC tissues and the normal mucosal tissues in GSE47908 (**Figures 5F–G**). Moreover, we determined the expression of APC7 in colon tissues obtained from DSS-induced colitis by western blotting assays. Comparison between

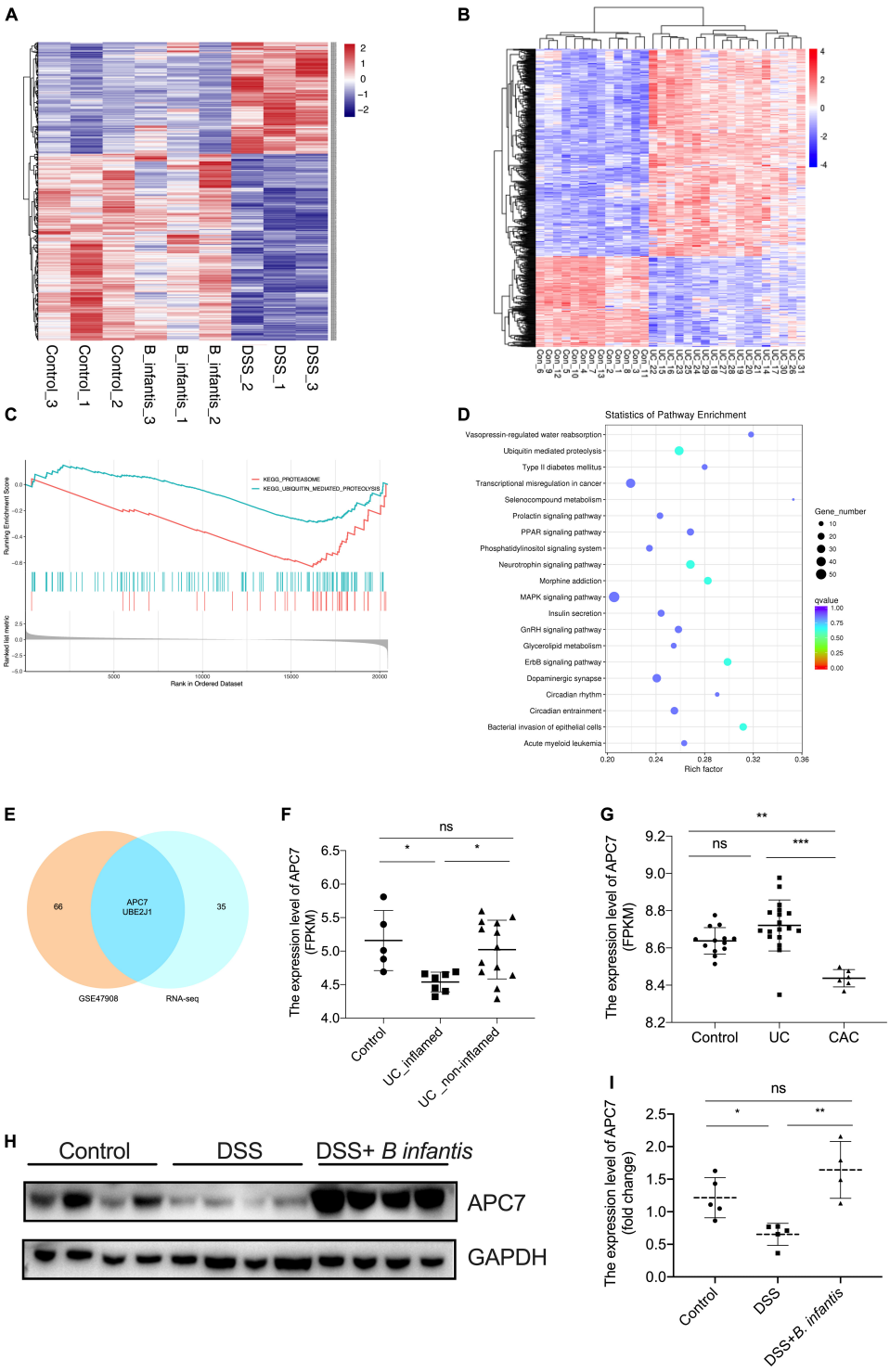

FIGURE 5 | Identification of APC7 as a molecule related to *B. infantis* treatment. **(A)** Heatmap of differentially expressed mRNAs in colon tissues from mice in the control, DSS-treated, and *B. infantis* treatment groups. **(B)** Heatmap of differentially expressed mRNA in colons tissues obtained from healthy controls, patients with UC, from GSE47908. **(C)** GSEA analysis of differentially expressed mRNAs in colon tissues of mice obtained from control, DSS-treated, and *B. infantis* administration groups. **(D)** KEGG analysis of differentially expressed mRNA in colon tissues obtained from healthy controls, patients with UC from GSE47908. **(E)** Venn plot of genes involved in the ubiquitin-mediated proteolysis pathway enriched in RNA-seq results and GSE47908. **(F,G)** The expression level of APC7 were analyzed in colon tissues obtained from healthy controls, patients with UC, and patients with CAC, from GSE47908 and GSE9452. The expression of APC7 was determined using western blotting assays **(H)** and qRT-PCR **(I)** in colon tissues of mice obtained from control, DSS-treated, and *B. infantis* administration groups. $^{*}p < 0.05$, $^{**}p < 0.01$, $^{***}p < 0.001$, ns, no significance.

control and DSS-treated tissues shown a marked decrease of APC7 expression level upon DSS treatment, while enhanced following administration with *B. infantis* (**Figure 5H**). Also, qRT-PCR assay conformed that induction of colitis by DSS led to a significant decrease in the mRNA expression of APC7 in colon tissues when compared to vehicle-treated mice, whereas it upregulated in mice exposed to *B. infantis* in colon tissues; these findings were consistent with the RNA sequencing results (**Figure 5I**). In conclusion, we speculate that APC7 expression can be affected by *B. infantis* and might be required for the progression of UC.

Bifidobacterium infantis Protected Against Genome Stability by Upregulating Anaphase-Promoting Complex Subunit 7 Expression

To test *in vitro* whether *B. infantis* intervention alters APC7 expression, we first assessed whether APC7 can be affected by TNFα challenge in colon epithelial cells. We found that the expression of APC7 was strongly reduced since TNFα treatment for 3 h, whereas γH2Ax level gradually increased with TNFα treatment and reached peak at 6 h, then returned to the baseline (**Figure 6A**). Then, the colon epithelial cells were co-cultured with *B. infantis* without inflammation, and the western blot results revealed that *B. infantis* directly upregulated APC7 expression in colon epithelial cells following cocultured with *B. infantis* for 6 h (**Supplementary Figure 3**).

Previous studies have reported that APC7 plays an important role in the ubiquitin pathway, which was usually related to the maintenance of genome stability (Ghosh and Saha, 2012). Therefore, we investigated whether APC7 played a role in the reduction of DSBs following treatment with *B. infantis*. To characterize the potential effect of APC7 on genome stability in colonial cells, we generated APC7-overexpressing colon epithelial cells using lentivirus-mediated overexpression. As expected, the overexpression of APC7 led to a reduction in the level of γH2Ax in TNFα-induced colonial cells when compared with control cells, as demonstrated by western blotting (**Figure 6B**). Conversely, the depletion of APC7 abolished the capacity of *B. infantis* treatment to reduce the levels of γH2Ax in TNFα-induced colonial cells, as examined by western blotting assay (**Figure 6C**). In addition, a neutral comet assay was employed to compare the level of DNA damage in response to APC7 knockdown (**Figure 6D**). The results also revealed that knockdown of APC7 in colonial cells resulted in longer comet tails than those in the control group upon TNFα treatment, thus indicating that *B. infantis* treatment maintain genome stability partially by upregulating the expression of APC7.

DISCUSSION

As mentioned previously, widespread genomic instability is known to occur in patients with UC who develop colonic neoplasia, this may, therefore, represent as a marker of cancer risk in UC patients (Itzkowitz and Yio, 2004). Thus, there is a clear need to investigate this mechanism further to explain the genomic instability associated with UC in this process. The non-oncogenic or oncogenic activity of the human gut microbiota has recently become the focus of intense research efforts. However, despite extensive studies on the protective effects of *B. infantis*, there is still no evidence to support the exact mechanisms of underlying the effects of *B. infantis* on the alleviation of colitis. In this study, we demonstrated here APC7, screened by RNA sequencing, may be associated with *B. infantis*-mediated maintain of genome stability and thus might aggravate the progression of UC. Specifically, gut microbiota derived from UC patients promoted genome instability and increased the susceptibility of mice with DSS-induced colitis. With regards to the composition of gut microbiota, our previous studies suggested that an obvious decrease of *B. infantis* was identified in UC patients, and that might play important roles in UC development. In turn, our results supported the fact that *B. infantis* effectively promotes DNA repair by upregulating APC7 expression under colitis conditions.

Patients who suffer from UC symptoms have an increased risk of developing CRC that is thought to develop through genomic instability, thus resulting in the accumulation of genetic alterations that drive tumor progression (Ekbom et al., 1990; Loeb and Loeb, 1999; O'Sullivan et al., 2002; Bartkova et al., 2006; Iftekhar et al., 2021). Previous studies investigated the expression of the DSB marker γH2Ax in patients with longstanding UC, CRC and normal colonic mucosal biopsies and indicted that dysplastic UC was associated with high levels of the DNA damage (De Angelis et al., 2018). Also, oxidative DNA lesions were accompanied with the upregulation of DSB response and repair components in IBD and CAC tissues, indicating that DSBs are the core molecular lesion under inflammatory stress (Frick et al., 2018). Thus, we considered that the grade of colitis inflammation might be associated with the level of genome instability. Here, we evaluated the degree of DNA damage in colon tissues obtained from healthy controls, along with tissues obtained from patients with colitis, dysplasia, and CAC, by γH2Ax immunohistochemistry, and found that the level of γH2Ax was sequential upregulated with increasing grades of inflammation and dysplasia, consistent with previous results (Frick et al., 2018). Nevertheless, the mechanisms of the ongoing genomic instabilities involved in the progression of UC remain poorly understood. There was one explanation mentioned that chromosomal instability in UC might be related to telomere shortening (O'Sullivan et al., 2002). Metagenomic and transcriptomic analysis have revealed that the intestinal microbiome involved in UC development, and that various species of gut microbes have been reported to be altered in stool and mucosal samples from patients with UC (Machiels et al., 2017). Various bacterial strains can produce metabolites or toxins that induce host-cell DNA DSBs and activate of the DNA damage signaling pathway. As a result, when examining the impact of the gut microbiota from UC patients on UC development, we reported that feces, obtained from patients with longstanding severe UC symptoms, were transplanted into the mice that has been pretreated with antibiotics, this resulted enhanced DNA damage in the colon tissues, compared with those from the

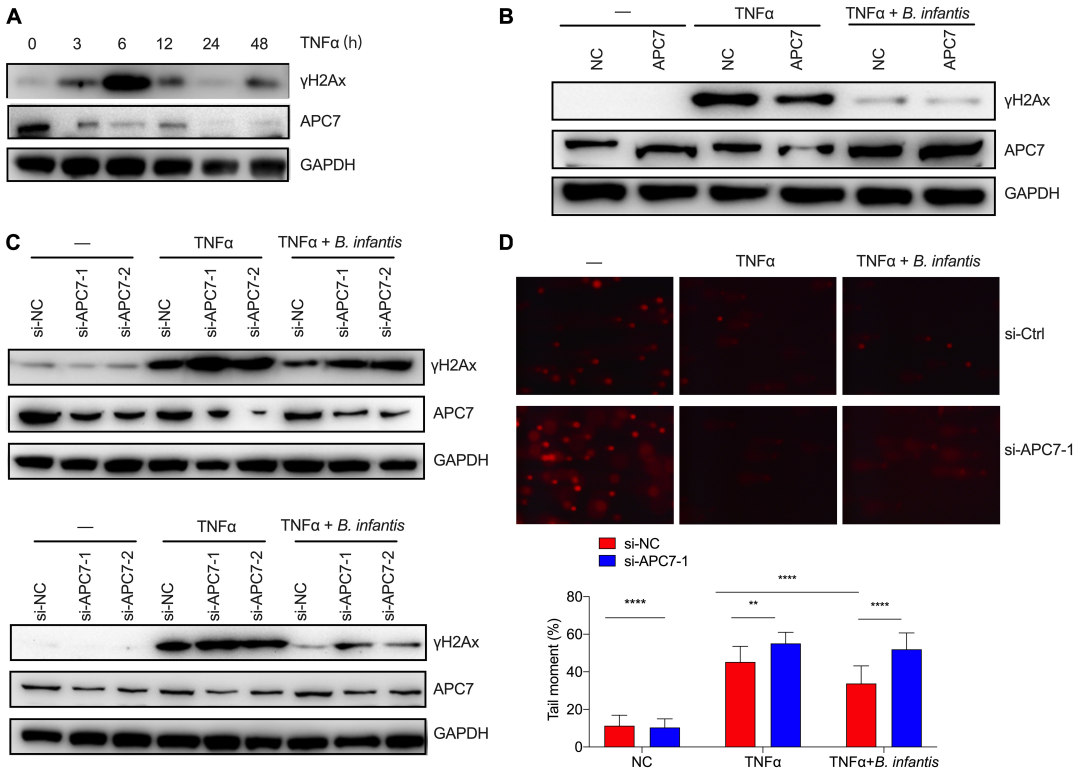

FIGURE 6 | *Bifidobacterium infantis* protected against genome stability partially by upregulating APC7 expression. **(A)** The expression level of APC7 and γH2Ax were determined in TNFα-treated colon cells that had been co-cultured with *B. infantis*. **(B)** γH2Ax levels were investigated by western blotting in APC7-overexpressing HCT116 cells co-cultured with *B. infantis* for 6 h. **(C)** The expression levels of γH2Ax and APC7 were determined in APC7-knockdown colon epithelial cells, including HT29 (top) and HCT116 (bottom), co-cultured with *B. infantis* for 6 h. **(D)** The comet assay was used to determine DNA damage level in APC7-knockdown HT29 cells co-cultured with *B. infantis* for 6 h. (Magnification, ×20.) $^{**}p < 0.01$, $^{****}p < 0.0001$.

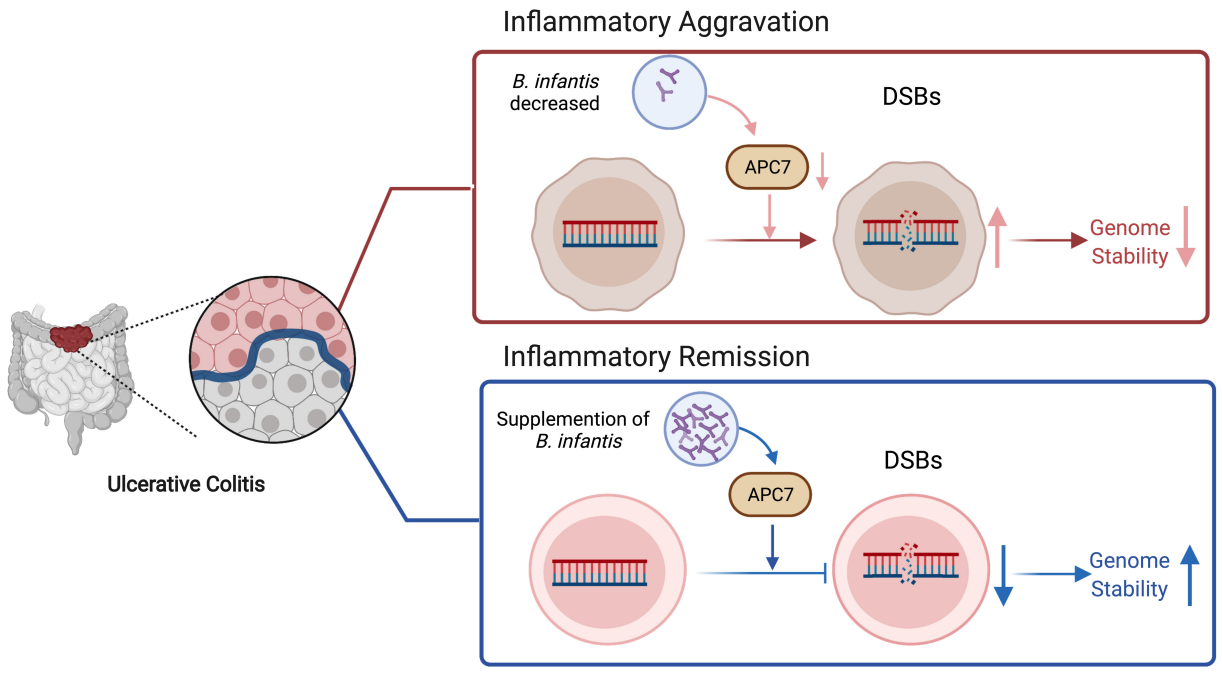

FIGURE 7 | Proposed work model for *B. infantis* to regulate genome stability through upregulating of APC7 expression in colitis, created with BioRender.com.

healthy controls, these results supported that the gut microbiota derived from UC patient is considered as the driving force for genome instability in the development of UC.

Several Gram-negative bacteria, such as *E. coli* and *ETBF*, have been reported to induce DNA damage caused by their secreted toxins that may contribute to the oncogenic process (Guidi et al., 2013; Allen and Sears, 2019). In studies conducted by Dejea et al. (2018), *pks* + *E. coli* were found to work synergistically with ETBF to cause increased DSBs, chromosomal aberrations and cell cycle arrest, *in vitro*. In another study, Yu et al. (2017), showed that, *Fusobacterium nucleatum* promotes chemoresistance *via* the autophagy network to CRC. Together, this evidence points to a direct interaction between specific gut microbes and DNA damage.

Except for the gut microbes mentioned above, there are several beneficial microbes that were remarkedly reduced in the feces of UC patients, including *B. infantis*, *Faecalibacterium*, and *Lactobacillus* (El-Baz et al., 2020; Nishihara et al., 2021). Our previous results also confirmed that the amount of *B. infantis* was reduced upon colitis inflammation (Wang et al., 2019). With the increasing number of reports on the roles of *B. infantis*, there has been significant interest in investigating the specific mechanism of action that is involved. We aimed to explore whether *B. infantis* impact the genome stability. The administration of DSS-induced mice with *B. infantis* could promote an ATM-dependent DNA damage response that was characterized by the formation of γH2Ax foci in the nucleus of colon epithelial cells. Additionally, we also used a TNFα-treated colonial cell model to evaluate the functional roles of *B. infantis in vitro* study. Our results support the importance of *B. infantis* in colitis by modulating DNA damage repair. Accordingly, we dissected the underlying mechanisms by which *B. infantis* treatment maintains genomic stability by applying RNA sequencing and public database analysis. Our results showed that in response to colitis, epithelial APC7 was increased by *B. infantis* administration, this was found to be dysregulated in the colon of UC patients. APC7, one component of the APC with E3 ubiquitin ligase activity, controls mitotic cell cycle progression. The timely activation of APC is thought to be important to maintain accurate chromosome separation, whereas the dysregulation of APC may give rise to abnormal chromosome segregation, then leading to chromosome instability (Sudakin et al., 2001; Greil et al., 2016). Considering that APC is required to maintain genomic stability in primary human cells (Engelbert et al., 2008), we detected whether APC was associated with the effect of *B. infantis*-treatment on maintaining of genomic stability. Our experiments indicated that overexpression of APC7 enhanced DNA genomic stability in TNFα-treated colon epithelial cells, while APC7 knockdown promoted DNA damage upon co-culture with *B. infantis*. However, future research should clarify whether this is also the case *in vivo*, and in patients treated with *B. infantis* strains.

CONCLUSION

In summary, these data suggest that genomic instability is associated with UC development. In this process, co-colonization with *B. infantis* strains enhanced genomic stability by increasing APC7 expression in colon tissues, therefore alleviating colitis inflammation (**Figure 7**). This study implies that the evaluation of probiotic strains, could reduce the risk of colitis related cancer.

DATA AVAILABILITY STATEMENT

The data presented in the study are deposited in the https://bigd.big.ac.cn/gsa/browse/CRA005171; repository, accession number CRA005171.

ETHICS STATEMENT

The studies involving human participants were reviewed and approved by the Ethics Committee of Peking Union Medical College Hospital (Beijing, China). The patients/participants provided their written informed consent to participate in this study. The animal study was reviewed and approved by the Ethics Committee of Peking Union Medical College Hospital, Beijing, China (protocol code: XHDW-2019-031).

AUTHOR CONTRIBUTIONS

TH, XH, and JL were involved in the overall design of the experiments. TH, XH, KL, and DZ participated in the experiments. TH and XH wrote the manuscript. YZ and JL assessed and interpreted the results. All authors have read and approved the published version of the manuscript.

FUNDING

This work was funded by the Natural Science Foundation of China (Grant Nos. 81730016 and 81900483 to JL), the fellowship of China Postdoctoral Science Foundation (Grant No. 2021T140069 to TH).

SUPPLEMENTARY MATERIAL

The Supplementary Material for this article can be found online at: https://www.frontiersin.org/articles/10.3389/fmicb.2021.761113/full#supplementary-material

Supplementary Figure 1 | Evaluation of antibiotic-depletion model. **(A)** Represent plates of colonies derived from the healthy control and the UC patient. **(B)** Evaluation of antibiotic-depletion model by calculating the colony formation units (CFU) in each plate. $^{*}p < 0.05$.

Supplementary Figure 2 | The levels of *B. infantis* in feces derived from the healthy control and UC patient, detected by qRT-PCR assay. $^{**}p < 0.01$.

Supplementary Figure 3 | The expression levels of APC7 in colon epithelial cells co-cultured with *B. infantis* for 6, 12, 24, and 48 h, respectively.

REFERENCES

Allen, J., and Sears, C. L. (2019). Impact of the gut microbiome on the genome and epigenome of colon epithelial cells: contributions to colorectal cancer development. *Genome Med.* 11:11. doi: 10.1186/s13073-019-0621-2

Ameho, C. K., Adjei, A. A., Harrison, E. K., Takeshita, K., Morioka, T., Arakaki, Y., et al. (1997). Prophylactic effect of dietary glutamine supplementation on interleukin 8 and tumour necrosis factor alpha production in trinitrobenzene sulphonic acid induced colitis. *Gut* 41, 487–493. doi: 10.1136/gut.41.4.487

Arthur, J. C., Perez-Chanona, E., Muhlbauer, M., Tomkovich, S., Uronis, J. M., Fan, T. J., et al. (2012). Intestinal inflammation targets cancer-inducing activity of the microbiota. *Science* 338, 120–123. doi: 10.1126/science.1224820

Aust, D. E., Terdiman, J. P., Willenbucher, R. F., Chang, C. G., Molinaro-Clark, A., Baretton, G. B., et al. (2002). The APC/beta-catenin pathway in ulcerative colitis-related colorectal carcinomas: a mutational analysis. *Cancer* 94, 1421–1427. doi: 10.1002/cncr.10334

Bartkova, J., Rezaei, N., Liontos, M., Karakaidos, P., Kletsas, D., Issaeva, N., et al. (2006). Oncogene-induced senescence is part of the tumorigenesis barrier imposed by DNA damage checkpoints. *Nature* 444, 633–637. doi: 10.1038/nature05268

De Angelis, P. M., Schjolberg, A. R., Hughes, J. B., Huitfeldt, H. S., Norheim Andersen, S., and Ostvold, A. C. (2018). Nondysplastic ulcerative colitis has high levels of the homologous recombination repair protein NUCKS1 and low levels of the DNA damage marker gamma-H2AX. *Inflamm. Bowel. Dis.* 24, 593–600. doi: 10.1093/ibd/izx071

Dejea, C. M., Fathi, P., Craig, J. M., Boleij, A., Taddese, R., Geis, A. L., et al. (2018). Patients with familial adenomatous polyposis harbor colonic biofilms containing tumorigenic bacteria. *Science* 359, 592–597. doi: 10.1126/science.aah3648

Ekbom, A., Helmick, C., Zack, M., and Adami, H. O. (1990). Ulcerative colitis and colorectal cancer. A population-based study. *N. Engl. J. Med.* 323, 1228–1233. doi: 10.1056/NEJM199011013231802

El-Baz, A. M., Khodir, A. E., Adel El-Sokkary, M. M., and Shata, A. (2020). The protective effect of *Lactobacillus* versus 5-aminosalicylic acid in ulcerative colitis model by modulation of gut microbiota and Nrf2/Ho-1 pathway. *Life Sci.* 256:117927. doi: 10.1016/j.lfs.2020.117927

Engelbert, D., Schnerch, D., Baumgarten, A., and Wasch, R. (2008). The ubiquitin ligase APC(Cdh1) is required to maintain genome integrity in primary human cells. *Oncogene* 27, 907–917. doi: 10.1038/sj.onc.1210703

Frank, D. N., St Amand, A. L., Feldman, R. A., Boedeker, E. C., Harpaz, N., and Pace, N. R. (2007). Molecular-phylogenetic characterization of microbial community imbalances in human inflammatory bowel diseases. *Proc. Natl. Acad. Sci. U.S.A.* 104, 13780–13785. doi: 10.1073/pnas.0706625104

Frick, A., Khare, V., Paul, G., Lang, M., Ferk, F., Knasmuller, S., et al. (2018). Overt increase of oxidative stress and dna damage in murine and human colitis and colitis-associated neoplasia. *Mol. Cancer Res.* 16, 634–642. doi: 10.1158/1541-7786.MCR-17-0451

Ghosh, S., and Saha, T. (2012). Central role of ubiquitination in genome maintenance: DNA replication and damage repair. *ISRN Mol. Biol.* 2012:146748. doi: 10.5402/2012/146748

Greil, C., Krohs, J., Schnerch, D., Follo, M., Felthaus, J., Engelhardt, M., et al. (2016). The role of APC/C(Cdh1) in replication stress and origin of genomic instability. *Oncogene* 35, 3062–3070. doi: 10.1038/onc.2015.367

Grivennikov, S. I., Greten, F. R., and Karin, M. (2010). Immunity, inflammation, and cancer. *Cell* 140, 883–899. doi: 10.1016/j.cell.2010.01.025

Guidi, R., Guerra, L., Levi, L., Stenerlow, B., Fox, J. G., Josenhans, C., et al. (2013). Chronic exposure to the cytolethal distending toxins of Gram-negative bacteria promotes genomic instability and altered DNA damage response. *Cell Microbiol.* 15, 98–113. doi: 10.1111/cmi.12034

Han, T., Jing, X., Bao, J., Zhao, L., Zhang, A., Miao, R., et al. (2020). H. pylori infection alters repair of DNA double-strand breaks via SNHG17. *J. Clin. Invest.* 130, 3901–3918. doi: 10.1172/JCI125581

Iftekhar, A., Berger, H., Bouznad, N., Heuberger, J., Boccellato, F., Dobrindt, U., et al. (2021). Genomic aberrations after short-term exposure to colibactin-producing E. coli transform primary colon epithelial cells. *Nat. Commun.* 12:1003. doi: 10.1038/s41467-021-21162-y

Ishitsuka, T., Kashiwagi, H., and Konishi, F. (2001). Microsatellite instability in inflamed and neoplastic epithelium in ulcerative colitis. *J. Clin. Pathol.* 54, 526–532. doi: 10.1136/jcp.54.7.526

Itzkowitz, S. H., and Yio, X. (2004). Inflammation and cancer IV. Colorectal cancer in inflammatory bowel disease: the role of inflammation. *Am. J. Physiol. Gastrointest. Liver Physiol.* 287, G7–G17. doi: 10.1152/ajpgi.00079.2004

Javed, N. H., Alsahly, M. B., and Khubchandani, J. (2016). Oral feeding of probiotic bifidobacterium infantis: colonic morphological changes in rat model of TNBS-induced colitis. *Scientifica* 2016:9572596. doi: 10.1155/2016/9572596

Kennedy, E. A., King, K. Y., and Baldridge, M. T. (2018). Mouse microbiota models: comparing germ-free mice and antibiotics treatment as tools for modifying gut bacteria. *Front. Physiol.* 9:1534. doi: 10.3389/fphys.2018.01534

Loeb, K. R., and Loeb, L. A. (1999). Genetic instability and the mutator phenotype. Studies in ulcerative colitis. *Am. J. Pathol.* 154, 1621–1626. doi: 10.1016/S0002-9440(10)65415-6

Machiels, K., Sabino, J., Vandermosten, L., Joossens, M., Arijs, I., de Bruyn, M., et al. (2017). Specific members of the predominant gut microbiota predict pouchitis following colectomy and IPAA in UC. *Gut* 66, 79–88. doi: 10.1136/gutjnl-2015-309398

Marechal, A., and Zou, L. (2013). DNA damage sensing by the ATM and ATR kinases. *Cold Spring Harb. Perspect. Biol.* 5:a012716. doi: 10.1101/cshperspect.a012716

Nielsen, H. B., Almeida, M., Juncker, A. S., Rasmussen, S., Li, J., Sunagawa, S., et al. (2014). Identification and assembly of genomes and genetic elements in complex metagenomic samples without using reference genomes. *Nat. Biotechnol.* 32, 822–828. doi: 10.1038/nbt.2939

Nishihara, Y., Ogino, H., Tanaka, M., Ihara, E., Fukaura, K., Nishioka, K., et al. (2021). Mucosa-associated gut microbiota reflects clinical course of ulcerative colitis. *Sci. Rep.* 11:13743. doi: 10.1038/s41598-021-92870-0

O'Sullivan, J. N., Bronner, M. P., Brentnall, T. A., Finley, J. C., Shen, W. T., Emerson, S., et al. (2002). Chromosomal instability in ulcerative colitis is related to telomere shortening. *Nat. Genet.* 32, 280–284. doi: 10.1038/ng989

Park, W. S., Pham, T., Wang, C., Pack, S., Mueller, E., Mueller, J., et al. (1998). Loss of heterozygosity and microsatellite instability in non-neoplastic mucosa from patients with chronic ulcerative colitis. *Int. J. Mol. Med.* 2, 221–224.

Peran, L., Camuesco, D., Comalada, M., Bailon, E., Henriksson, A., Xaus, J., et al. (2007). A comparative study of the preventative effects exerted by three probiotics, Bifidobacterium lactis, Lactobacillus casei and Lactobacillus acidophilus, in the TNBS model of rat colitis. *J. Appl. Microbiol.* 103, 836–844. doi: 10.1111/j.1365-2672.2007.03302.x

Peran, L., Camuesco, D., Comalada, M., Nieto, A., Concha, A., Diaz-Ropero, M. P., et al. (2005). Preventative effects of a probiotic, Lactobacillus salivarius ssp. salivarius, in the TNBS model of rat colitis. *World J. Gastroenterol.* 11, 5185–5192. doi: 10.3748/wjg.v11.i33.5185

Pereira, C., Coelho, R., Gracio, D., Dias, C., Silva, M., Peixoto, A., et al. (2016). DNA damage and oxidative DNA damage in inflammatory bowel disease. *J. Crohns. Colitis* 10, 1316–1323. doi: 10.1093/ecco-jcc/jjw088

Rahimi, H., Ahmadzadeh, A., Yousef-amoli, S., Kokabee, L., Shokrgozar, M. A., Mahdian, R., et al. (2015). The expression pattern of APC2 and APC7 in various cancer cell lines and AML patients. *Adv. Med. Sci.* 60, 259–263. doi: 10.1016/j.advms.2015.04.007

Smolders, L., and Teodoro, J. G. (2011). Targeting the anaphase promoting complex: common pathways for viral infection and cancer therapy. *Expert. Opin. Ther. Targets* 15, 767–780. doi: 10.1517/14728222.2011.558008

Sood, A., Midha, V., Makharia, G. K., Ahuja, V., Singal, D., Goswami, P., et al. (2009). The probiotic preparation, VSL#3 induces remission in patients with mild-to-moderately active ulcerative colitis. *Clin. Gastroenterol. Hepatol.* 7, 1202–1209, 1209.e1. doi: 10.1016/j.cgh.2009.07.016

Sudakin, V., Chan, G. K., and Yen, T. J. (2001). Checkpoint inhibition of the APC/C in HeLa cells is mediated by a complex of BUBR1, BUB3, CDC20, and MAD2. *J. Cell Biol.* 154, 925–936. doi: 10.1083/jcb.200102093

Trinchieri, G. (2012). Cancer and inflammation: an old intuition with rapidly evolving new concepts. *Annu. Rev. Immunol.* 30, 677–706. doi: 10.1146/annurev-immunol-020711-075008

Wang, Y. N., Meng, X. C., Dong, Y. F., Zhao, X. H., Qian, J. M., Wang, H. Y., et al. (2019). Effects of probiotics and prebiotics on intestinal microbiota in mice with

acute colitis based on 16S rRNA gene sequencing. *Chin. Med. J.* 132, 1833–1842. doi: 10.1097/CM9.0000000000000308

Willenbucher, R. F., Aust, D. E., Chang, C. G., Zelman, S. J., Ferrell, L. D., Moore, D. H. II, et al. (1999). Genomic instability is an early event during the progression pathway of ulcerative-colitis-related neoplasia. *Am. J. Pathol.* 154, 1825–1830. doi: 10.1016/S0002-9440(10)65438-7

Wilson, M. R., Jiang, Y., Villalta, P. W., Stornetta, A., Boudreau, P. D., Carra, A., et al. (2019). The human gut bacterial genotoxin colibactin alkylates DNA. *Science* 363:eaar7785. doi: 10.1126/science.aar7785

Wu, S., Rhee, K. J., Albesiano, E., Rabizadeh, S., Wu, X., Yen, H. R., et al. (2009). A human colonic commensal promotes colon tumorigenesis via activation of T helper type 17 T cell responses. *Nat. Med.* 15, 1016–1022. doi: 10.1038/nm.2015

Yu, T., Guo, F., Yu, Y., Sun, T., Ma, D., Han, J., et al. (2017). *Fusobacterium nucleatum* promotes chemoresistance to colorectal cancer by modulating autophagy. *Cell* 170, 548.e16–563.e16. doi: 10.1016/j.cell.2017.07.008

Conflict of Interest: The authors declare that the research was conducted in the absence of any commercial or financial relationships that could be construed as a potential conflict of interest.

frontiers in Microbiology

MINI REVIEW
published: 23 December 2021
doi: 10.3389/fmicb.2021.817433

Gut Microbiome Regulation of Autophagic Flux and Neurodegenerative Disease Risks

Andrew P. Shoubridge[1,2], Célia Fourrier[3], Jocelyn M. Choo[1,2], Christopher G. Proud[4,5], Timothy J. Sargeant[3†] and Geraint B. Rogers[1,2†]*

[1]*Microbiome and Host Health, Lifelong Health, South Australian Health and Medical Research Institute, Adelaide, SA, Australia,* [2]*Infection and Immunity, Flinders Health and Medical Research Institute, College of Medicine and Public Health, Flinders University, Bedford Park, SA, Australia,* [3]*Lysosomal Health in Ageing, Hopwood Centre for Neurobiology, Lifelong Health, South Australian Health and Medical Research Institute, Adelaide, SA, Australia,* [4]*Nutrition, Diabetes and Gut Health, Lifelong Health, South Australian Health and Medical Research Institute, Adelaide, SA, Australia,* [5]*School of Biological Sciences, University of Adelaide, Adelaide, SA, Australia*

The gut microbiome-brain axis exerts considerable influence on the development and regulation of the central nervous system. Numerous pathways have been identified by which the gut microbiome communicates with the brain, falling largely into the two broad categories of neuronal innervation and immune-mediated mechanisms. We describe an additional route by which intestinal microbiology could mediate modifiable risk for neuropathology and neurodegeneration in particular. Autophagy, a ubiquitous cellular process involved in the prevention of cell damage and maintenance of effective cellular function, acts to clear and recycle cellular debris. In doing so, autophagy prevents the accumulation of toxic proteins and the development of neuroinflammation, both common features of dementia. Levels of autophagy are influenced by a range of extrinsic exposures, including nutrient deprivation, infection, and hypoxia. These relationships between exposures and rates of autophagy are likely to be mediated, as least in part, by the gut microbiome. For example, the suppression of histone acetylation by microbiome-derived short-chain fatty acids appears to be a major contributor to upregulation of autophagic function. We discuss the potential contribution of the microbiome-autophagy axis to neurological health and examine the potential of exploiting this link to predict and prevent neurodegenerative diseases.

Keywords: microbiome, autophagy, pathway, neurodegenerative, dementia, risk exposure

OPEN ACCESS

Edited by:
Hesong Wang,
Southern Medical University, China

Reviewed by:
Cinzia Fabrizi,
Sapienza University of Rome, Italy

****Correspondence:***
Geraint B. Rogers
geraint.rogers@sahmri.com

†These authors share senior authorship

Specialty section:
This article was submitted to Microbial Symbioses, a section of the journal Frontiers in Microbiology

Received: *18 November 2021*
Accepted: *02 December 2021*
Published: *23 December 2021*

Citation:
Shoubridge AP, Fourrier C, Choo JM, Proud CG, Sargeant TJ and Rogers GB (2021) Gut Microbiome Regulation of Autophagic Flux and Neurodegenerative Disease Risks. Front. Microbiol. 12:817433. doi: 10.3389/fmicb.2021.817433

THE GUT MICROBIOME, THE CENTRAL NERVOUS SYSTEM, AND NEURODEGENERATION

Relationships between the gut microbiome and human neurophysiology are increasingly well-recognized (Rogers et al., 2016). A growing body of research now supports the causal contribution of gut microbiome-host interactions to the development of neurodegenerative disorders, including Alzheimer's (Vogt et al., 2017; Kim et al., 2020), Huntington's (Bjorkqvist et al., 2008;

Du et al., 2020; Wasser et al., 2020) and Parkinson's disease (Sampson et al., 2016; Sun et al., 2018), and multiple sclerosis (Jangi et al., 2016).

The influence of the gut microbiome on neurophysiology, central nervous system (CNS) function, and neurodegenerative disease, in particular, can act *via* many different pathways (Rogers et al., 2016; Sharon et al., 2016; Cryan et al., 2019), including the biosynthesis of metabolites, such as short-chain fatty acids (SCFAs; Erny et al., 2015; Correa-Oliveira et al., 2016; Dalile et al., 2019), stimulation of the vagus nerve (Raybould, 2010; Kaelberer et al., 2018; Fulling et al., 2019), tryptophan production (Bellono et al., 2017; Ye et al., 2021) and inflammatory cytokine release (Kim et al., 2013; Erny et al., 2015; Correa-Oliveira et al., 2016; Arentsen et al., 2017; Dalile et al., 2019). Currently, these pathways are broadly defined to act *via* two main routes: immune-mediated mechanisms and direct neuronal innervation. An additional pathway that sits alongside these categories, the process of autophagy, could represent a major mediator of modifiable risk for neurodegeneration.

THE CRITICAL ROLE OF AUTOPHAGY IN NORMAL PHYSIOLOGY

Autophagy is a cellular process that regenerates nutrients from macromolecules in response to nutrient deficiency (Mizushima et al., 2004) and clears damaged material from the cellular environment (Lazarou et al., 2015). Autophagy involves the transport of unwanted material within cellular vesicles (autophagosomes) to the lysosome. Upon fusion, the material is enzymatically degraded (Kaur and Debnath, 2015), a process that is termed "autophagic flux."

The maintenance of cells and tissues within the body relies on efficient autophagy for normal physiology, and dysfunction results in pathological disease (Klionsky et al., 2021). For example, in the heart, autophagy is essential for organelle turnover, with autophagic markers upregulated following ischemia and cardiovascular disease (Nishida et al., 2009). Genetic defects to autophagic function affect bone formation and resorption, with suppressed autophagy in osteocytes mimicking skeletal aging (Onal et al., 2013), potentially contributing to osteoporosis (Yin et al., 2019). In the liver, autophagic markers are downregulated in hepatocytes in mouse models of obesity and insulin resistance (Yang et al., 2010). The importance of autophagic flux is highlighted by the consequences of deleting an essential autophagic gene, *ATG7*, which results in the death of adult mice due to generalized tissue degradation (Karsli-Uzunbas et al., 2014). However, pharmaceutical inhibition of autophagy to treat disease (for example, through exposure to chloroquine or hydroxychloroquine to prevent fusion of the autophagosome with the lysosome) is effective clinically, impairing the growth of established cancers and preventing chronic cellular damage (Bedoya, 1970; Mulcahy Levy and Thorburn, 2020).

The importance of autophagy is no less significant in the CNS. Neurons are postmitotic cells and cannot dilute toxic substances by dividing and therefore rely on autophagy to clear harmful substrates and maintain homeostasis (Son et al., 2012). Autophagy has heightened efficiency in young compared to aged neurons (Boland et al., 2008). This is particularly the case in age-associated neurological diseases, such as Alzheimer's disease, where severe autophagic impairment occurs and results in dystrophic neuronal processes that form around plaques formed in the human brain (Hassiotis et al., 2018; Lie et al., 2021).

Neuronal autophagy is also essential for synaptic plasticity, which is required for learning and memory and is impaired in dementia (Son et al., 2012). Autophagy in microglia, the immunoregulatory cells of the CNS, plays an important role in maintaining the microenvironment around neurons (Plaza-Zabala et al., 2017). Decreasing basal autophagy in microglia through the deletion of autophagy-related genes results in the accumulation of toxic proteins, and as a consequence, reactive microglia (Choi et al., 2020).

REGULATION OF AUTOPHAGIC FLUX

The process of autophagy involves a set of genes that are evolutionarily conserved from yeast to humans. The autophagy-related genes (*ATG*) are predominantly required for the efficient formation of autophagosomes and their fusion with lysosomes to enable the subsequent degradation of material within them (Klionsky et al., 2003; Levine and Kroemer, 2019).

Autophagic flux can be altered by a variety of stressors, including nutrient starvation, oxidative stress, and infection (Hansen et al., 2018). By altering autophagic function, these exposures impact biological aging and the risk of associated disease (Simonsen et al., 2008; Karsli-Uzunbas et al., 2014; Yamamoto et al., 2016; Papadopoulos et al., 2017). Continuing research is increasing the clarity on the precise mechanisms regulating autophagy. For example, activation of the nuclear factor-κB (NF-κB) pathway suppresses autophagy (Lu et al., 2014; Nguyen et al., 2014). Perhaps most significantly, the mechanistic target of rapamycin complex 1 (mTORC1) senses nutrient availability (especially amino acids) and growth factors to support cell growth; mTORC1 also suppresses autophagy and lysosome biogenesis (Ballabio and Bonifacino, 2020; Klionsky et al., 2021).

AUTOPHAGY AND NEUROLOGICAL/ PSYCHIATRIC DISEASE

Interest in the role of autophagy in the context of stress-related and psychiatric conditions, particularly neuronal autophagy, has grown considerably. Altered autophagy gene expression has been reported in individuals with major depressive disorder (MDD; Alcocer-Gomez et al., 2017). Furthermore, antidepressants induce autophagy in the brain and reverse biochemical and behavioral signs of stress-induced MDD (Gulbins et al., 2018). Markers of mTORC1 activity were reduced in cortical post-mortem tissue of MDD individuals (Jernigan et al., 2011) and in individuals with bipolar disorder (Machado-Vieira et al., 2015) compared with healthy individuals. Further,

pharmacological administration of rapamycin, which inhibits mTORC1, exerts antidepressant-like effects (Cleary et al., 2008; Kara et al., 2018).

One of the key proteins in the autophagy pathway, BECN1, was reduced in the post-mortem hippocampus of schizophrenia patients (Merenlender-Wagner et al., 2015), while impairment of autophagy in murine microglia resulted in social behavioral defects and repetitive behaviors, which resemble characteristic features of autism spectrum disorders (Kim et al., 2017). In addition to these extrinsic factors, genetic alterations play a role in altering autophagic function. Indeed, numerous human pathologies arise from mutations in core *ATG* genes, as well as in a wider group of genes that are essential to autolysosomal function. For example, alterations in *ATG16L1* are linked with decreased intestinal bacterial clearance in Crohn's disease (Murthy et al., 2014), while heterozygous loss of progranulin caused by loss-of-function mutations in *GRN* reduced autophagic flux in frontotemporal dementia (Chang et al., 2017) and mutated *Vps15* impairs endosomal-lysosomal trafficking in cortical atrophy and epilepsy [Gstrein et al., 2018; for a detailed review, see (Levine and Kroemer, 2019)].

Preliminary investigations into therapeutic interventions to the autophagic process, such as the proposal of calorie restriction on autophagic induction (Bagherniya et al., 2018), have indicated antidepressant effects in both preclinical models and humans (Zhang et al., 2015). Additionally, physical exercise has been shown to induce autophagy in cardiac and skeletal muscle and adipose tissue in mice (He et al., 2012) and reduce depressive symptoms in humans (Brosse et al., 2002). However, deeper investigation is required into these interventions as they may be acting *via* additional pathways to achieve a clinical outcome (Bagherniya et al., 2018). Furthermore, and crucially, while an increase in markers of autophagy can indicate elevated autophagic cargo transported to the lysosome, it can also suggest that delivery to the lysosome is disrupted, resulting in an accumulation of autophagosomes. This underlines the importance of measuring autophagic flux rather than using a static measurement of autophagy-related markers, such as LC3-II, or other autophagy-related proteins, as a measure of autophagy. A newly adapted method that can directly measure autophagic flux in humans (Bensalem et al., 2021) now provides the opportunity to properly assess these previously reported effects.

THE POTENTIAL INFLUENCE OF THE GUT MICROBIOME ON AUTOPHAGIC FLUX

Autophagy is integral to the maintenance of intestinal homeostasis and host defense against intestinal pathogens (**Figure 1**; Mizushima, 2018). Dysfunctional autophagy has been shown to result in disrupted intestinal epithelial function, defects in anti-microbial peptide secretion by Paneth cells, endoplasmic reticulum stress response, and aberrant immune responses to pathogenic bacteria (Larabi et al., 2020). However, while dysfunctional intestinal autophagic function has been implicated in the development of human disease, such associations are currently restricted to intestinal pathologies, such as inflammatory bowel disease (Nguyen et al., 2013).

In the opposite direction, changes in the characteristics of the intestinal microbiota have been linked to altered regulation of autophagy in host tissues (Larabi et al., 2020). *Escherichia coli* modulate autophagy in host cells by NF-κB, resulting in upregulated levels of select microRNA that lead to downstream inhibition of ATG-specific proteins and ultimate suppression of autophagy (Lu et al., 2014; Nguyen et al., 2014).

The Effect of Gut Microbes on Autophagy in the Immune System

Dysfunctional autophagy in the intestinal tract is also intrinsically linked with the interactions between gut microbes and host immunity (Clarke and Simon, 2019). *Bacteroides fragilis*, a bacterial species abundant throughout the intestinal tract, produces polysaccharide A that is taken up by dendritic cells (DCs; Zheng et al., 2020). DCs utilize major histocompatibility complex (MHC) class II molecules to facilitate the presentation of polysaccharide A and additional lysosomal degradation products to prime naïve helper T cells, which then coordinate host immune responses (Munz, 2016). In addition to regulating the transcription of genes responsible for T-cell stimulation, inflammation, and antiviral immune responses, Toll-like receptors (TLRs) on the apical surface of the gut epithelium also regulate autophagy. Lipopolysaccharide (LPS), a cell wall component of many Gram-negative bacteria (and some Gram-positive ones), is an important inducer of autophagy in macrophages by activating TLR4 (Xu et al., 2007; Shi and Kehrl, 2008). TLR4 activation leads to the recruitment of the adaptor proteins myeloid differentiation primary response 88 (MyD88) and Toll/IL-1 receptor (TIR) domain-containing adaptor inducing interferon β (TRIF), which bind to BECN1 to initiate autophagy by phosphorylation (Shi and Kehrl, 2008). However, the precise impact of LPS on autophagy remains controversial, as it has also recently been reported to inhibit autophagy and autophagosome formation by activating the mTORC1 pathway (Ye et al., 2020).

While the best characterized example, TLR4 is not alone in mediating microbial influence on autophagy. Activation of TLR1, 2, 3, 5, 6, and 7 by pathogen-associated molecular patterns (PAMPs) induce autophagy *in vitro*, particularly *via* PAMP ssRNA and poly(I:C; Delgado et al., 2008; Shi and Kehrl, 2008; Fang et al., 2014). Ligands for TLR2 and TLR6 have been detected in extracellular vesicles released from *Mycobacterium tuberculosis*-infected neutrophils, which corresponded with elevated expression of the autophagy-related marker LC3-II in macrophages (Alvarez-Jimenez et al., 2018; Germic et al., 2019). However, as this is not an accurate measure of autophagic activity, it should be interpreted with caution. Alternatively, CD40-activated macrophages responding to infectious pathogens direct internalized pathogens to the lysosome for removal (Andrade et al., 2006). Furthermore, the bacterial compounds muramyl dipeptide and peptidoglycan also trigger autophagy intracellularly by activating macrophage and DC cytosolic nucleotide-binding oligomerization

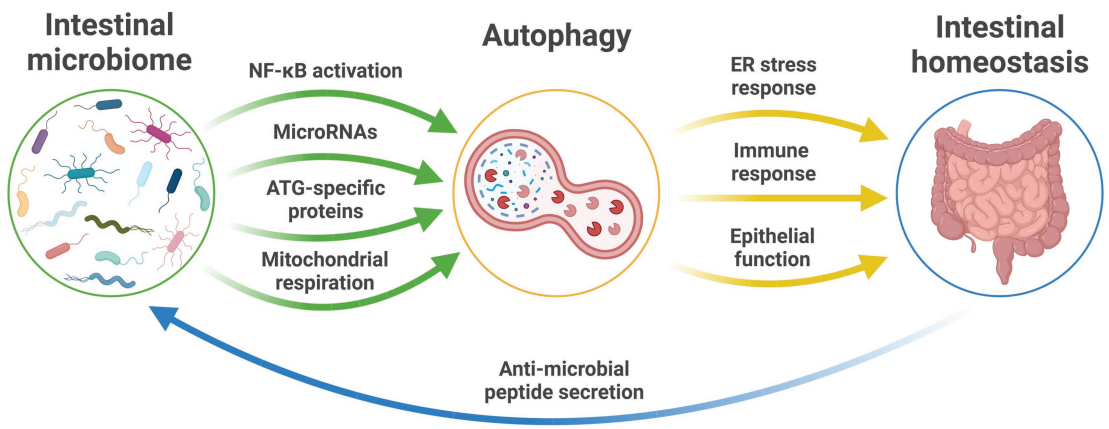

FIGURE 1 | The microbiome and autophagy relationship in intestinal health. The established pathways between the intestinal microbiome and autophagic function that maintain intestinal homeostasis and intestinal health and provide feedback to influence microbiota profiles and function. ATG, autophagy-related genes; ER, endoplasmic reticulum; NF-κB, nuclear factor-κB; RNA, ribonucleic acid.

domain 1 and 2 receptors following the internalization of pathogens (Cooney et al., 2010; Travassos et al., 2010).

The effect of LPS on autophagy was also recorded in an *Atg7*-deficient mouse model, where LPS triggered upregulated expressions of proinflammatory interleukin 1β and tumor necrosis factor-α mRNA in small intestinal epithelium of autophagy-deficient mice, which are integral to NF-κB activation (Fujishima et al., 2011). These changes in host immune regulation are implicated in inflammatory disorders, such as inflammatory bowel disorder (Schreiber et al., 1998). The proinflammatory actions of LPS also occur in a mitochondrial reactive oxygen species-dependent manner that corresponds with reduced autophagic flux (Lee et al., 2016). To prevent elimination by autophagy, Gram-negative bacteria, such as *Salmonella typhimurium* and *Shigella flexneri*, inhibit or alter the autophagic pathway by interfering with ATG proteins, removal of autophagic components and escaping LC3-associated phagocytosis (Huang and Brumell, 2014; Jiao and Sun, 2019).

The Direct Effect of Microbial Metabolites on Autophagy

Autophagy is also regulated by histone acetylation, an epigenetic cellular process involved in the activation and suppression of gene transcription (Bannister and Kouzarides, 2011; Graff et al., 2011). Agents that inhibit histone deacetylases (HDACs) result in upregulation of autophagic activity (Oh et al., 2008). One such agent, butyrate, a SCFA and major product of anaerobic bacterial fermentation in the gut, promotes histone hyperacetylation and increases autophagic flux in human cancer *in vitro* cell lines (Marks et al., 2004; Shao et al., 2004). Acetate, another SCFA produced by commensal gut microbes, also regulates immune responses through inhibition of HDAC9. Furthermore, where butyrate is available to act as an energy source for colonocytes (Donohoe et al., 2011), it rescues deficits in mitochondrial respiration to maintain ATP production and inhibit autophagy within these cells (Donohoe et al., 2011).

The net result of SCFAs produced by bacteria, such as by members of the *Bifidobacterium* genus, is influenced by cross-feeding of intermediary metabolites between diverse microbes. For example, acetate and lactate produced by *Bifidobacterium* species are utilized in cross-feeding interactions by members of the Ruminococcaceae and Lachnospiraceae families (including *Roseburia*, *Anaerostipes*, *Faecalibacterium*, and *Eubacterium* species) to produce butyrate (Parada Venegas et al., 2019). Notably, aging-associated changes in the gut microbiome that predict cognitive decline largely involve the loss of bacterial species involved in these biosynthetic pathways (Jackson et al., 2016).

In addition to SCFAs, intestinal bacterial species, such as bifidobacterial, clostridia, lactobacilli, enterococci, and streptococci, are involved in the metabolism of amino acids, and therefore in the regulation of autophagy (Pugin et al., 2017; Oliphant and Allen-Vercoe, 2019). The catabolism of arginine by intestinal microbes into putrescine, spermidine, and spermine promotes autophagy (Eisenberg et al., 2009) and is essential for the proliferation and longevity of intestinal enterochromaffin cells (Mouille et al., 2003; Oliphant and Allen-Vercoe, 2019). Most importantly, alterations in the genetic transcripts for AZIN2, which influence the deposition of tau (a protein that accumulates in dementia-causing diseases) and production of putrescine, spermidine, and spermine, have recently been uncovered in humans with Alzheimer's disease (Sandusky-Beltran et al., 2021), lending to the development of the idea that polyamines are integral to the accumulation of toxic protein in the development and progression of tauopathies and similar diseases (Sandusky-Beltran et al., 2021). Ultimately, dysregulated intestinal autophagy leads to disrupted intestinal epithelial barrier function by altering the expression of claudin 2, a tight junction protein, in the intestinal mucosa (Nighot et al., 2015; Zhang et al., 2017), causing the systemic circulation of proinflammatory compounds. The shift to a systemic proinflammatory state as a result of intestinal dysbiosis and autophagy dysregulation along the gut microbiome-brain

axis may lead to neuroinflammation and the development of neurodegenerative disease (Capuron and Miller, 2011).

The Impact of Modifiable Risk Factors on Gut Microbiota and Autophagy

Interactions between extrinsic exposures and the microbiome are likely to be important in shaping microbiome-autophagy relationships, an important consideration where modifiable exposures are linked to the risk of neurological disease incidence and progression (Jackson et al., 2016; Rogers et al., 2016). Modifiable risk factors, including smoking, alcohol intake, and physical inactivity, contribute to approximately 40% of worldwide dementia cases (Livingston et al., 2020). Diet, genetic and environmental factors known to influence frailty in aging humans are strongly associated with gut microbiota diversity, particularly with the abundance of *Faecalibacterium prausnitzii* (Jackson et al., 2016). In the context of intestinal diseases, specifically inflammatory bowel disease, risk variants in genes directly involved in intestinal bacterial handling (including *ATG16LI*, *NOD2*, and *FUT2*) correlate with specific decreases in the microbe *Roseburia* spp., which is involved in the metabolism of acetate (Imhann et al., 2018). Furthermore, links between defective autophagy and intestinal dysbiosis have also been connected following exposure to additional infectious pathogens, for example, exposure of *E. coli* to mice with genetically defective autophagy induced chronic intestinal inflammation and microbe dysbiosis compared with control mice (Bretin et al., 2018). Given the independent yet strong correlations between gut microbiome traits, autophagic function, and neurodegenerative disease, it is therefore highly likely that exposure-mediated changes to the gut microbiome contribute to altered autophagic flux and the etiology of neurological disease.

THE CASE FOR MICROBIOME REGULATION OF AUTOPHAGY-MEDIATED NEUROLOGICAL DISEASE RISK

Evidence suggests the gut microbiome acts as a pivotal link between external risk exposures and dysregulation of host immunity and cellular metabolism. In turn, this mechanism is likely to act as a pathway that influences the function and pathology of the CNS and, therefore, the risk of neurological disease (**Figure 2**).

Indeed, significant alterations to autophagic function are implicated in many aspects of biological aging, including age-associated neurodegeneration (Nah et al., 2015). Moreover, levels of autophagy-related proteins, including Atg5, Atg7, and BECN1, decrease with age (Shibata et al., 2006; Lipinski et al., 2010) and preclinical studies have demonstrated that inefficient autophagic function contributes to the development of dementia (Pickford et al., 2008). In humans, variation in genes that regulate autophagy has been linked to numerous neurodegenerative diseases including Alzheimer's, Parkinson's, Huntington's, and Lewy-body disease, frontotemporal dementia, and amyotrophic lateral sclerosis (Tsuang et al., 2012; Nixon, 2013; Fujikake et al., 2018; Gan et al., 2018; Gao et al., 2018). Similarly, microbiome dysbiosis and microbial metabolite production, particularly proinflammatory metabolites, are associated with age and the development of neurodegenerative disease (Rogers et al., 2016; Franceschi et al., 2018).

Neuronal autophagy is involved in the degradation of neurofibrillary tangles of hyperphosphorylated and misfolded tau in Alzheimer's disease brain tissue and is susceptible to changes in inflammatory state (Silva et al., 2020). In particular, deficient autophagosome formation is linked with neuroinflammation and increased intraneuronal tau pathology in preclinical models of Alzheimer's disease (Xu et al., 2021). The microbiome influences the inflammatory state of the brain through the chronic and systemic circulation of proinflammatory cells, cytokines, and metabolites throughout an individual's life, in a process termed "inflammaging" (Franceschi and Campisi, 2014; Frasca and Blomberg, 2016; Franceschi et al., 2018), which may be driving the systemic and neurological autophagic response and, thereby, the development of neurodegenerative disease. During later life, microglia in the brain are primed by these circulating inflammatory markers and become reactive, "pruning" away excessive neuronal tissue across a range of neurodegenerative diseases, including Alzheimer's disease, multiple sclerosis, and motor neuron disease (Liddelow et al., 2017). Remarkably, the amount of soluble amyloid-beta in endosomes and lysosomes greatly increases before the extracellular deposition of amyloid-beta (Yu et al., 2005), leading to abnormalities in the lysosomal pathway that occur earlier than the pathological manifestation of neurofibrillary tangles and senile plaques. Indeed, the importance of declining levels of autophagy to aging-associated neurodegeneration is highlighted by the fact that increasing autophagic flux results in a reversal of aging-related cognitive decline in mice (Glatigny et al., 2019). This connection was demonstrated following the injection of genetic and pharmacological modulators of autophagy directly into the hippocampus of aged mice. Hippocampal neurons (responsible for memory formation and retention) exhibited enhanced autophagic flux and synaptic plasticity following the intervention, which resulted in greater cognitive behavioural performance (Glatigny et al., 2019).

Our understanding of the contribution of microbiome-autophagy-related mechanisms to the development of neurological conditions remains limited. However, an increasing body of circumstantial evidence supports such a relationship. For example, gut bacteria-derived LPS has been shown in a preclinical model to activate the NLRP3 inflammasome and reduce the expression of autophagic markers in the rat hippocampus and induce depression-like symptoms (Jiang et al., 2017). Psychosocial stress has also been correlated with enhanced intestinal autophagy in humans with inflammatory bowel diseases (Wang et al., 2019).

Notably, the impact of external risk exposures on chronic disease is not limited to neurological health. Other age-related diseases, including cardiovascular disease, share common risk profiles that include obesity and chronic inflammation (Ferrucci and Fabbri, 2018). These relationships are influenced by both the gut microbiome and autophagy, suggesting the microbiome-autophagy axis may be regulating not only neurological health but host health more widely.

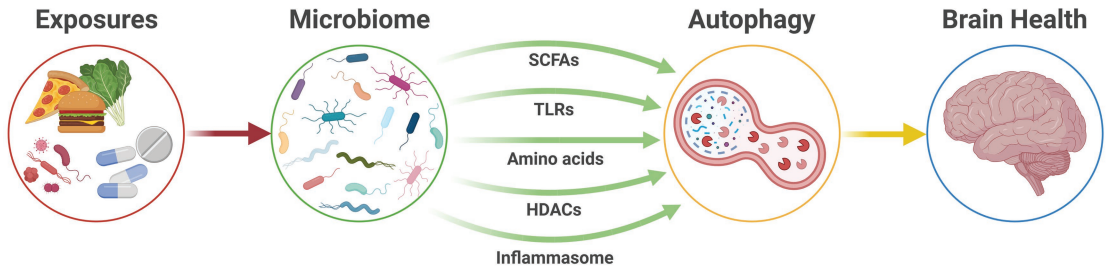

FIGURE 2 | The microbiome-autophagy-brain axis. Active communication pathways between the gut microbiome and autophagic activity that connect modifiable exposures and host health to ultimately affect brain health. HDACs, histone deacetylases; SCFAs, short-chain fatty acids; TLRs, Toll-like receptors.

REDUCING DISEASE RISK BY TARGETING MICROBIOME-AUTOPHAGY INTERACTIONS

Linking modifiable risk exposures to microbiome and autophagic function could prove transformative in providing tractable targets for intervention across the spectrum of neurodegenerative and psychiatric conditions. The ability to readily alter microbiome characteristics, for example, through dietary measures, might enable alteration of autophagic flux. Indeed, foods that promote SCFA biosynthesis through microbial fermentation in the colon, such as those found in the Mediterranean diet, reduce signs of frailty and cognitive impairment in elderly humans by altering the diversity and profile of the intestinal microbiota (Ghosh et al., 2020).

In preclinical models, the potential therapeutic benefit of transplanting healthy microbiota in the form of fecal matter transplants (FMTs), resulting in increased SCFA biosynthesis, has been demonstrated (Jing et al., 2021). Investigations into the impact of FMT on autophagy have also reported increases in autophagy-related protein levels in the intestinal mucosa (Cheng et al., 2018). However, while FMT has proven clinical utility in a number of contexts (Settanni et al., 2021), more readily translated measures, such as synbiotic interventions (Ke et al., 2019; Morshedi et al., 2020), are likely to have greater translational potential for the treatment of neurological disease in the short-term.

CONCLUSION

Despite its considerable biological plausibility, the possibility of a microbiome-autophagy-brain axis has not yet been investigated in detail. We propose that a greater understanding of this pathway could be transformative for individuals at greatest risk of developing age-associated neurodegeneration and offer avenues for therapeutic interventions that may provide significant impact, especially considering the increasing burden of declining neurological health in the community.

AUTHOR CONTRIBUTIONS

TS and GR conceptualized the idea for the manuscript. AS, CF, TS, and GR reviewed the literature and edited the manuscript. AS drafted the manuscript. AS, CF, JC, CP, TS, and GR revised, edited, and approved the final version of the manuscript.

FUNDING

GR is also supported by an NHMRC Senior Research Fellowship (GNT1155179) and a Matthew Flinders Professorial Fellowship.

ACKNOWLEDGMENTS

The authors gratefully acknowledge support from the South Australian Health and Medical Research Institute.

REFERENCES

Alcocer-Gomez, E., Casas-Barquero, N., Nunez-Vasco, J., Navarro-Pando, J. M., and Bullon, P. (2017). Psychological status in depressive patients correlates with metabolic gene expression. *CNS Neurosci. Ther.* 23, 843–845. doi: 10.1111/cns.12755

Alvarez-Jimenez, V. D., Leyva-Paredes, K., Garcia-Martinez, M., Vazquez-Flores, L., Garcia-Paredes, V. G., Campillo-Navarro, M., et al. (2018). Extracellular vesicles released from mycobacterium tuberculosis-infected neutrophils promote macrophage autophagy and decrease intracellular mycobacterial survival. *Front. Immunol.* 9:272. doi: 10.3389/fimmu.2018.00272

Andrade, R. M., Wessendarp, M., Gubbels, M. J., Striepen, B., and Subauste, C. S. (2006). CD40 induces macrophage anti-toxoplasma gondii activity by triggering autophagy-dependent fusion of pathogen-containing vacuoles and lysosomes. *J. Clin. Invest.* 116, 2366–2377. doi: 10.1172/JCI28796

Arentsen, T., Qian, Y., Gkotzis, S., Femenia, T., Wang, T., Udekwu, K., et al. (2017). The bacterial peptidoglycan-sensing molecule Pglyrp2 modulates brain development and behavior. *Mol. Psychiatry* 22, 257–266. doi: 10.1038/mp.2016.182

Bagherniya, M., Butler, A. E., Barreto, G. E., and Sahebkar, A. (2018). The effect of fasting or calorie restriction on autophagy induction: a review of the literature. *Ageing Res. Rev.* 47, 183–197. doi: 10.1016/j.arr.2018.08.004

Ballabio, A., and Bonifacino, J. S. (2020). Lysosomes as dynamic regulators of cell and organismal homeostasis. *Nat. Rev. Mol. Cell Biol.* 21, 101–118. doi: 10.1038/s41580-019-0185-4

Bannister, A. J., and Kouzarides, T. (2011). Regulation of chromatin by histone modifications. *Cell Res.* 21, 381–395. doi: 10.1038/cr.2011.22

Bedoya, V. (1970). Effect of chloroquine on malignant lymphoreticular and pigmented cells in vitro. *Cancer Res.* 30, 1262–1275.

Bellono, N. W., Bayrer, J. R., Leitch, D. B., Castro, J., Zhang, C., O'Donnell, T. A., et al. (2017). Enterochromaffin cells are gut chemosensors that couple to sensory neural pathways. *Cell* 170, 185–98.e16. doi: 10.1016/j.cell.2017.05.034

Bensalem, J., Hattersley, K. J., Hein, L. K., Teong, X. T., Carosi, J. M., Hassiotis, S., et al. (2021). Measurement of autophagic flux in humans: an optimized method for blood samples. *Autophagy* 17, 3238–3255. doi: 10.1080/15548627.2020.1846302

Bjorkqvist, M., Wild, E. J., Thiele, J., Silvestroni, A., Andre, R., Lahiri, N., et al. (2008). A novel pathogenic pathway of immune activation detectable before clinical onset in Huntington's disease. *J. Exp. Med.* 205, 1869–1877. doi: 10.1084/jem.20080178

Boland, B., Kumar, A., Lee, S., Platt, F. M., Wegiel, J., Yu, W. H., et al. (2008). Autophagy induction and autophagosome clearance in neurons: relationship to autophagic pathology in Alzheimer's disease. *J. Neurosci.* 28, 6926–6937. doi: 10.1523/JNEUROSCI.0800-08.2008

Bretin, A., Lucas, C., Larabi, A., Dalmasso, G., Billard, E., Barnich, N., et al. (2018). AIEC infection triggers modification of gut microbiota composition in genetically predisposed mice, contributing to intestinal inflammation. *Sci. Rep.* 8:12301. doi: 10.1038/s41598-018-30055-y

Brosse, A. L., Sheets, E. S., Lett, H. S., and Blumenthal, J. A. (2002). Exercise and the treatment of clinical depression in adults: recent findings and future directions. *Sports Med.* 32, 741–760. doi: 10.2165/00007256-200232120-00001

Capuron, L., and Miller, A. H. (2011). Immune system to brain signaling: neuropsychopharmacological implications. *Pharmacol. Ther.* 130, 226–238. doi: 10.1016/j.pharmthera.2011.01.014

Chang, M. C., Srinivasan, K., Friedman, B. A., Suto, E., Modrusan, Z., Lee, W. P., et al. (2017). Progranulin deficiency causes impairment of autophagy and TDP-43 accumulation. *J. Exp. Med.* 214, 2611–2628. doi: 10.1084/jem.20160999

Cheng, S., Ma, X., Geng, S., Jiang, X., Li, Y., Hu, L., et al. (2018). Fecal microbiota transplantation beneficially regulates intestinal mucosal autophagy and alleviates gut barrier injury. *mSystems* 3, e00137–e00118. doi: 10.1128/mSystems.00137-18

Choi, I., Zhang, Y., Seegobin, S. P., Pruvost, M., Wang, Q., Purtell, K., et al. (2020). Microglia clear neuron-released alpha-synuclein via selective autophagy and prevent neurodegeneration. *Nat. Commun.* 11:1386. doi: 10.1038/s41467-020-15119-w

Clarke, A. J., and Simon, A. K. (2019). Autophagy in the renewal, differentiation and homeostasis of immune cells. *Nat. Rev. Immunol.* 19, 170–183. doi: 10.1038/s41577-018-0095-2

Cleary, C., Linde, J. A., Hiscock, K. M., Hadas, I., Belmaker, R. H., Agam, G., et al. (2008). Antidepressive-like effects of rapamycin in animal models: implications for mTOR inhibition as a new target for treatment of affective disorders. *Brain Res. Bull.* 76, 469–473. doi: 10.1016/j.brainresbull.2008.03.005

Cooney, R., Baker, J., Brain, O., Danis, B., Pichulik, T., Allan, P., et al. (2010). NOD2 stimulation induces autophagy in dendritic cells influencing bacterial handling and antigen presentation. *Nat. Med.* 16, 90–97. doi: 10.1038/nm.2069

Correa-Oliveira, R., Fachi, J. L., Vieira, A., Sato, F. T., and Vinolo, M. A. (2016). Regulation of immune cell function by short-chain fatty acids. *Clin. Transl. Immunol.* 5:e73. doi: 10.1038/cti.2016.17

Cryan, J. F., O'Riordan, K. J., Cowan, C. S. M., Sandhu, K. V., Bastiaanssen, T. F. S., Boehme, M., et al. (2019). The microbiota-gut-brain axis. *Physiol. Rev.* 99, 1877–2013. doi: 10.1152/physrev.00018.2018

Dalile, B., Van Oudenhove, L., Vervliet, B., and Verbeke, K. (2019). He role of short-chain fatty acids in microbiota-gut-brain communication. *Nat. Rev. Gastroenterol. Hepatol.* 16, 461–478. doi: 10.1038/s41575-019-0157-3

Delgado, M. A., Elmaoued, R. A., Davis, A. S., Kyei, G., and Deretic, V. (2008). Toll-like receptors control autophagy. *EMBO J.* 27, 1110–1121. doi: 10.1038/emboj.2008.31

Donohoe, D. R., Garge, N., Zhang, X., Sun, W., O'Connell, T. M., Bunger, M. K., et al. (2011). The microbiome and butyrate regulate energy metabolism and autophagy in the mammalian colon. *Cell Metab.* 13, 517–526. doi: 10.1016/j.cmet.2011.02.018

Du, G., Dong, W., Yang, Q., Yu, X., Ma, J., Gu, W., et al. (2020). Altered gut microbiota related to inflammatory responses in patients with Huntington's disease. *Front. Immunol.* 11:603594. doi: 10.3389/fimmu.2020.603594

Eisenberg, T., Knauer, H., Schauer, A., Buttner, S., Ruckenstuhl, C., Carmona-Gutierrez, D., et al. (2009). Induction of autophagy by spermidine promotes longevity. *Nat. Cell Biol.* 11, 1305–1314. doi: 10.1038/ncb1975

Erny, D., Hrabe de Angelis, A. L., Jaitin, D., Wieghofer, P., Staszewski, O., David, E., et al. (2015). Host microbiota constantly control maturation and function of microglia in the CNS. *Nat. Neurosci.* 18, 965–977. doi: 10.1038/nn.4030

Fang, L., Wu, H. M., Ding, P. S., and Liu, R. Y. (2014). TLR2 mediates phagocytosis and autophagy through JNK signaling pathway in Staphylococcus aureus-stimulated RAW264.7 cells. *Cell. Signal.* 26, 806–814. doi: 10.1016/j.cellsig.2013.12.016

Ferrucci, L., and Fabbri, E. (2018). Inflammageing: chronic inflammation in ageing, cardiovascular disease, and frailty. *Nat. Rev. Cardiol.* 15, 505–522. doi: 10.1038/s41569-018-0064-2

Franceschi, C., and Campisi, J. (2014). Chronic inflammation (inflammaging) and its potential contribution to age-associated diseases. *J. Gerontol. A Biol. Sci. Med. Sci.* 69(Suppl 1), S4–S9. doi: 10.1093/gerona/glu057

Franceschi, C., Garagnani, P., Parini, P., Giuliani, C., and Santoro, A. (2018). Inflammaging: a new immune-metabolic viewpoint for age-related diseases. *Nat. Rev. Endocrinol.* 14, 576–590. doi: 10.1038/s41574-018-0059-4

Frasca, D., and Blomberg, B. B. (2016). Inflammaging decreases adaptive and innate immune responses in mice and humans. *Biogerontology* 17, 7–19. doi: 10.1007/s10522-015-9578-8

Fujikake, N., Shin, M., and Shimizu, S. (2018). Association between autophagy and neurodegenerative diseases. *Front. Neurosci.* 12:255. doi: 10.3389/fnins.2018.00255

Fujishima, Y., Nishiumi, S., Masuda, A., Inoue, J., Nguyen, N. M., Irino, Y., et al. (2011). Autophagy in the intestinal epithelium reduces endotoxin-induced inflammatory responses by inhibiting NF-kappaB activation. *Arch. Biochem. Biophys.* 506, 223–235. doi: 10.1016/j.abb.2010.12.009

Fulling, C., Dinan, T. G., and Cryan, J. F. (2019). Gut microbe to brain signaling: what happens in Vagus. *Neuron* 101, 998–1002. doi: 10.1016/j.neuron.2019.02.008

Gan, L., Cookson, M. R., Petrucelli, L., and La Spada, A. R. (2018). Converging pathways in neurodegeneration, from genetics to mechanisms. *Nat. Neurosci.* 21, 1300–1309. doi: 10.1038/s41593-018-0237-7

Gao, S., Casey, A. E., Sargeant, T. J., and Makinen, V. P. (2018). Genetic variation within endolysosomal system is associated with late-onset Alzheimer's disease. *Brain* 141, 2711–2720. doi: 10.1093/brain/awy197

Germic, N., Frangez, Z., Yousefi, S., and Simon, H. U. (2019). Regulation of the innate immune system by autophagy: monocytes, macrophages, dendritic cells and antigen presentation. *Cell Death Differ.* 26, 715–727. doi: 10.1038/s41418-019-0297-6

Ghosh, T. S., Rampelli, S., Jeffery, I. B., Santoro, A., Neto, M., Capri, M., et al. (2020). Mediterranean diet intervention alters the gut microbiome in older people reducing frailty and improving health status: the NU-AGE 1-year dietary intervention across five European countries. *Gut* 69, 1218–1228. doi: 10.1136/gutjnl-2019-319654

Glatigny, M., Moriceau, S., Rivagorda, M., Ramos-Brossier, M., Nascimbeni, A. C., Lante, F., et al. (2019). Autophagy is required for memory formation and reverses age-related memory decline. *Curr. Biol.* 29, 435–48.e8. doi: 10.1016/j.cub.2018.12.021

Graff, J., Kim, D., Dobbin, M. M., and Tsai, L. H. (2011). Epigenetic regulation of gene expression in physiological and pathological brain processes. *Physiol. Rev.* 91, 603–649. doi: 10.1152/physrev.00012.2010

Gstrein, T., Edwards, A., Pristoupilova, A., Leca, I., Breuss, M., Pilat-Carotta, S., et al. (2018). Mutations in Vps15 perturb neuronal migration in mice and are associated with neurodevelopmental disease in humans. *Nat. Neurosci.* 21, 207–217. doi: 10.1038/s41593-017-0053-5

Gulbins, A., Schumacher, F., Becker, K. A., Wilker, B., Soddemann, M., Boldrin, F., et al. (2018). Antidepressants act by inducing autophagy controlled by sphingomyelin-ceramide. *Mol. Psychiatry* 23, 2324–2346. doi: 10.1038/s41380-018-0090-9

Hansen, M., Rubinsztein, D. C., and Walker, D. W. (2018). Autophagy as a promoter of longevity: insights from model organisms. *Nat. Rev. Mol. Cell Biol.* 19, 579–593. doi: 10.1038/s41580-018-0033-y

Hassiotis, S., Manavis, J., Blumbergs, P. C., Hattersley, K. J., Carosi, J. M., Kamei, M., et al. (2018). Lysosomal LAMP1 immunoreactivity exists in both diffuse and neuritic amyloid plaques in the human hippocampus. *Eur. J. Neurosci.* 47, 1043–1053. doi: 10.1111/ejn.13913

He, C., Bassik, M. C., Moresi, V., Sun, K., Wei, Y., Zou, Z., et al. (2012). Exercise-induced BCL2-regulated autophagy is required for muscle glucose homeostasis. *Nature* 481, 511–515. doi: 10.1038/nature10758

Huang, J., and Brumell, J. H. (2014). Bacteria-autophagy interplay: a battle for survival. *Nat. Rev. Microbiol.* 12, 101–114. doi: 10.1038/nrmicro3160

Imhann, F., Vich Vila, A., Bonder, M. J., Fu, J., Gevers, D., Visschedijk, M. C., et al. (2018). Interplay of host genetics and gut microbiota underlying the

onset and clinical presentation of inflammatory bowel disease. *Gut* 67, 108–119. doi: 10.1136/gutjnl-2016-312135

Jackson, M. A., Jeffery, I. B., Beaumont, M., Bell, J. T., Clark, A. G., Ley, R. E., et al. (2016). Signatures of early frailty in the gut microbiota. *Genome Med.* 8:8. doi: 10.1186/s13073-016-0262-7

Jangi, S., Gandhi, R., Cox, L. M., Li, N., von Glehn, F., Yan, R., et al. (2016). Alterations of the human gut microbiome in multiple sclerosis. *Nat. Commun.* 7:12015. doi: 10.1038/ncomms12015

Jernigan, C. S., Goswami, D. B., Austin, M. C., Iyo, A. H., Chandran, A., Stockmeier, C. A., et al. (2011). The mTOR signaling pathway in the prefrontal cortex is compromised in major depressive disorder. *Prog. Neuro-Psychopharmacol. Biol. Psychiatry* 35, 1774–1779. doi: 10.1016/j.pnpbp.2011.05.010

Jiang, P., Guo, Y., Dang, R., Yang, M., Liao, D., Li, H., et al. (2017). Salvianolic acid B protects against lipopolysaccharide-induced behavioral deficits and neuroinflammatory response: involvement of autophagy and NLRP3 inflammasome. *J. Neuroinflammation* 14:239. doi: 10.1186/s12974-017-1013-4

Jiao, Y., and Sun, J. (2019). Bacterial manipulation of autophagic responses in infection and inflammation. *Front. Immunol.* 10:2821. doi: 10.3389/fimmu.2019.02821

Jing, Y., Yu, Y., Bai, F., Wang, L., Yang, D., Zhang, C., et al. (2021). Effect of fecal microbiota transplantation on neurological restoration in a spinal cord injury mouse model: involvement of brain-gut axis. *Microbiome* 9:59. doi: 10.1186/s40168-021-01007-y

Kaelberer, M. M., Buchanan, K. L., Klein, M. E., Barth, B. B., Montoya, M. M., Shen, X., et al. (2018). A gut-brain neural circuit for nutrient sensory transduction. *Science* 361:eaat5236. doi: 10.1126/science.aat5236

Kara, N. Z., Flaisher-Grinberg, S., Anderson, G. W., Agam, G., and Einat, H. (2018). Mood-stabilizing effects of rapamycin and its analog temsirolimus: relevance to autophagy. *Behav. Pharmacol.* 29, 379–384. doi: 10.1097/FBP.0000000000000334

Karsli-Uzunbas, G., Guo, J. Y., Price, S., Teng, X., Laddha, S. V., Khor, S., et al. (2014). Autophagy is required for glucose homeostasis and lung tumor maintenance. *Cancer Discov.* 4, 914–927. doi: 10.1158/2159-8290.CD-14-0363

Kaur, J., and Debnath, J. (2015). Autophagy at the crossroads of catabolism and anabolism. *Nat. Rev. Mol. Cell Biol.* 16, 461–472. doi: 10.1038/nrm4024

Ke, X., Walker, A., Haange, S. B., Lagkouvardos, I., Liu, Y., Schmitt-Kopplin, P., et al. (2019). Synbiotic-driven improvement of metabolic disturbances is associated with changes in the gut microbiome in diet-induced obese mice. *Mol. Metab.* 22, 96–109. doi: 10.1016/j.molmet.2019.01.012

Kim, H. J., Cho, M. H., Shim, W. H., Kim, J. K., Jeon, E. Y., Kim, D. H., et al. (2017). Deficient autophagy in microglia impairs synaptic pruning and causes social behavioral defects. *Mol. Psychiatry* 22, 1576–1584. doi: 10.1038/mp.2016.103

Kim, M. H., Kang, S. G., Park, J. H., Yanagisawa, M., and Kim, C. H. (2013). Short-chain fatty acids activate GPR41 and GPR43 on intestinal epithelial cells to promote inflammatory responses in mice. *Gastroenterology* 145, 396–406.e1-10. doi: 10.1053/j.gastro.2013.04.056

Kim, M. S., Kim, Y., Choi, H., Kim, W., Park, S., Lee, D., et al. (2020). Transfer of a healthy microbiota reduces amyloid and tau pathology in an Alzheimer's disease animal model. *Gut* 69, 283–294. doi: 10.1136/gutjnl-2018-317431

Klionsky, D. J., Cregg, J. M., Dunn, W. A. Jr., Emr, S. D., Sakai, Y., Sandoval, I. V., et al. (2003). A unified nomenclature for yeast autophagy-related genes. *Dev. Cell* 5, 539–545. doi: 10.1016/S1534-5807(03)00296-X

Klionsky, D. J., Petroni, G., Amaravadi, R. K., Baehrecke, E. H., Ballabio, A., Boya, P., et al. (2021). Autophagy in major human diseases. *EMBO J.* 40:e108863. doi: 10.15252/embj.2021108863

Larabi, A., Barnich, N., and Nguyen, H. T. T. (2020). New insights into the interplay between autophagy, gut microbiota and inflammatory responses in IBD. *Autophagy* 16, 38–51. doi: 10.1080/15548627.2019.1635384

Lazarou, M., Sliter, D. A., Kane, L. A., Sarraf, S. A., Wang, C., Burman, J. L., et al. (2015). The ubiquitin kinase PINK1 recruits autophagy receptors to induce mitophagy. *Nature* 524, 309–314. doi: 10.1038/nature14893

Lee, J. P., Foote, A., Fan, H., Peral de Castro, C., Lang, T., Jones, S. A., et al. (2016). Loss of autophagy enhances MIF/macrophage migration inhibitory factor release by macrophages. *Autophagy* 12, 907–916. doi: 10.1080/15548627.2016.1164358

Levine, B., and Kroemer, G. (2019). Biological functions of autophagy genes: a disease perspective. *Cell* 176, 11–42. doi: 10.1016/j.cell.2018.09.048

Liddelow, S. A., Guttenplan, K. A., Clarke, L. E., Bennett, F. C., Bohlen, C. J., Schirmer, L., et al. (2017). Neurotoxic reactive astrocytes are induced by activated microglia. *Nature* 541, 481–487. doi: 10.1038/nature21029

Lie, P. P. Y., Yang, D. S., Stavrides, P., Goulbourne, C. N., Zheng, P., Mohan, P. S., et al. (2021). Post-Golgi carriers, not lysosomes, confer lysosomal properties to pre-degradative organelles in normal and dystrophic axons. *Cell Rep.* 35:109034. doi: 10.1016/j.celrep.2021.109034

Lipinski, M. M., Zheng, B., Lu, T., Yan, Z., Py, B. F., Ng, A., et al. (2010). Genome-wide analysis reveals mechanisms modulating autophagy in normal brain aging and in Alzheimer's disease. *Proc. Natl. Acad. Sci. U. S. A.* 107, 14164–14169. doi: 10.1073/pnas.1009485107

Livingston, G., Huntley, J., Sommerlad, A., Ames, D., Ballard, C., Banerjee, S., et al. (2020). Dementia prevention, intervention, and care: 2020 report of the lancet commission. *Lancet* 396, 413–446. doi: 10.1016/S0140-6736(20)30367-6

Lu, C., Chen, J., Xu, H. G., Zhou, X., He, Q., Li, Y. L., et al. (2014). MIR106B and MIR93 prevent removal of bacteria from epithelial cells by disrupting ATG16L1-mediated autophagy. *Gastroenterology* 146, 188–199. doi: 10.1053/j.gastro.2013.09.006

Machado-Vieira, R., Zanetti, M. V., Teixeira, A. L., Uno, M., Valiengo, L. L., Soeiro-de-Souza, M. G., et al. (2015). Decreased AKT1/mTOR pathway mRNA expression in short-term bipolar disorder. *Eur. Neuropsychopharmacol.* 25, 468–473. doi: 10.1016/j.euroneuro.2015.02.002

Marks, P. A., Richon, V. M., Miller, T., and Kelly, W. K. (2004). Histone deacetylase inhibitors. *Adv. Cancer Res.* 91, 137–168. doi: 10.1016/S0065-230X(04)91004-4

Merenlender-Wagner, A., Malishkevich, A., Shemer, Z., Udawela, M., Gibbons, A., Scarr, E., et al. (2015). Autophagy has a key role in the pathophysiology of schizophrenia. *Mol. Psychiatry* 20, 126–132. doi: 10.1038/mp.2013.174

Mizushima, N. (2018). A brief history of autophagy from cell biology to physiology and disease. *Nat. Cell Biol.* 20, 521–527. doi: 10.1038/s41556-018-0092-5

Mizushima, N., Yamamoto, A., Matsui, M., Yoshimori, T., and Ohsumi, Y. (2004). In vivo analysis of autophagy in response to nutrient starvation using transgenic mice expressing a fluorescent autophagosome marker. *Mol. Biol. Cell* 15, 1101–1111. doi: 10.1091/mbc.e03-09-0704

Morshedi, M., Saghafi-Asl, M., and Hosseinifard, E. S. (2020). The potential therapeutic effects of the gut microbiome manipulation by synbiotic containing-lactobacillus plantarum on neuropsychological performance of diabetic rats. *J. Transl. Med.* 18, 18. doi: 10.1186/s12967-019-02169-y

Mouille, B., Delpal, S., Mayeur, C., and Blachier, F. (2003). Inhibition of human colon carcinoma cell growth by ammonia: a non-cytotoxic process associated with polyamine synthesis reduction. *Biochim. Biophys. Acta* 1624, 88–97. doi: 10.1016/j.bbagen.2003.09.014

Mulcahy Levy, J. M., and Thorburn, A. (2020). Autophagy in cancer: moving from understanding mechanism to improving therapy responses in patients. *Cell Death Differ.* 27, 843–857. doi: 10.1038/s41418-019-0474-7

Munz, C. (2016). Autophagy Beyond intracellular MHC class II antigen presentation. *Trends Immunol.* 37, 755–763. doi: 10.1016/j.it.2016.08.017

Murthy, A., Li, Y., Peng, I., Reichelt, M., Katakam, A. K., Noubade, R., et al. (2014). A Crohn's disease variant in Atg16l1 enhances its degradation by caspase 3. *Nature* 506, 456–462. doi: 10.1038/nature13044

Nah, J., Yuan, J., and Jung, Y. K. (2015). Autophagy in neurodegenerative diseases: from mechanism to therapeutic approach. *Mol. Cell* 38, 381–389. doi: 10.14348/molcells.2015.0034

Nguyen, H. T., Dalmasso, G., Muller, S., Carriere, J., Seibold, F., and Darfeuille-Michaud, A. (2014). Crohn's disease-associated adherent invasive *Escherichia coli* modulate levels of microRNAs in intestinal epithelial cells to reduce autophagy. *Gastroenterology* 146, 508–519. doi: 10.1053/j.gastro.2013.10.021

Nguyen, H. T., Lapaquette, P., Bringer, M. A., and Darfeuille-Michaud, A. (2013). Autophagy and Crohn's disease. *J. Innate Immun.* 5, 434–443. doi: 10.1159/000345129

Nighot, P. K., Hu, C. A., and Ma, T. Y. (2015). Autophagy enhances intestinal epithelial tight junction barrier function by targeting claudin-2 protein degradation. *J. Biol. Chem.* 290, 7234–7246. doi: 10.1074/jbc.M114.597492

Nishida, K., Kyoi, S., Yamaguchi, O., Sadoshima, J., and Otsu, K. (2009). The role of autophagy in the heart. *Cell Death Differ.* 16, 31–38. doi: 10.1038/cdd.2008.163

Nixon, R. A. (2013). The role of autophagy in neurodegenerative disease. *Nat. Med.* 19, 983–997. doi: 10.1038/nm.3232

Oh, M., Choi, I. K., and Kwon, H. J. (2008). Inhibition of histone deacetylase1 induces autophagy. *Biochem. Biophys. Res. Commun.* 369, 1179–1183. doi: 10.1016/j.bbrc.2008.03.019

Oliphant, K., and Allen-Vercoe, E. (2019). Macronutrient metabolism by the human gut microbiome: major fermentation by-products and their impact on host health. *Microbiome* 7:91. doi: 10.1186/s40168-019-0704-8

Onal, M., Piemontese, M., Xiong, J., Wang, Y., Han, L., Ye, S., et al. (2013). Suppression of autophagy in osteocytes mimics skeletal aging. *J. Biol. Chem.* 288, 17432–17440. doi: 10.1074/jbc.M112.444190

Papadopoulos, C., Kirchner, P., Bug, M., Grum, D., Koerver, L., Schulze, N., et al. (2017). VCP/p97 cooperates with YOD1, UBXD1 and PLAA to drive clearance of ruptured lysosomes by autophagy. *EMBO J.* 36, 135–150. doi: 10.15252/embj.201695148

Parada Venegas, D., De la Fuente, M. K., Landskron, G., Gonzalez, M. J., Quera, R., Dijkstra, G., et al. (2019). Short chain fatty acids (SCFAs)-mediated gut epithelial and immune regulation and its relevance for inflammatory bowel diseases. *Front. Immunol.* 10:277. doi: 10.3389/fimmu.2019.00277

Pickford, F., Masliah, E., Britschgi, M., Lucin, K., Narasimhan, R., Jaeger, P. A., et al. (2008). The autophagy-related protein beclin 1 shows reduced expression in early Alzheimer disease and regulates amyloid beta accumulation in mice. *J. Clin. Invest.* 118, 2190–2199. doi: 10.1172/JCI33585

Plaza-Zabala, A., Sierra-Torre, V., and Sierra, A. (2017). Autophagy and microglia: novel partners in neurodegeneration and aging. *Int. J. Mol. Sci.* 18:598. doi: 10.3390/ijms18030598

Pugin, B., Barcik, W., Westermann, P., Heider, A., Wawrzyniak, M., Hellings, P., et al. (2017). A wide diversity of bacteria from the human gut produces and degrades biogenic amines. *Microb. Ecol. Health Dis.* 28:1353881. doi: 10.1080/16512235.2017.1353881

Raybould, H. E. (2010). Gut chemosensing: interactions between gut endocrine cells and visceral afferents. *Auton. Neurosci.* 153, 41–46. doi: 10.1016/j.autneu.2009.07.007

Rogers, G. B., Keating, D. J., Young, R. L., Wong, M. L., Licinio, J., and Wesselingh, S. (2016). From gut dysbiosis to altered brain function and mental illness: mechanisms and pathways. *Mol. Psychiatry* 1, 738–748. doi: 10.1038/mp.2016.50

Sampson, T. R., Debelius, J. W., Thron, T., Janssen, S., Shastri, G. G., Ilhan, Z. E., et al. (2016). Gut microbiota regulate motor deficits and neuroinflammation in a model of Parkinson's disease. *Cell* 167, 1469–80.e12. doi: 10.1016/j.cell.2016.11.018

Sandusky-Beltran, L. A., Kovalenko, A., Placides, D. S., Ratnasamy, K., Ma, C., Hunt, J. B. Jr., et al. (2021). Aberrant AZIN2 and polyamine metabolism precipitates tau neuropathology. *J. Clin. Invest.* 131:e126299. doi: 10.1172/JCI126299

Schreiber, S., Nikolaus, S., and Hampe, J. (1998). Activation of nuclear factor kappa B inflammatory bowel disease. *Gut* 42, 477–484. doi: 10.1136/gut.42.4.477

Settanni, C. R., Ianiro, G., Bibbo, S., Cammarota, G., and Gasbarrini, A. (2021). Gut microbiota alteration and modulation in psychiatric disorders: current evidence on fecal microbiota transplantation. *Prog. Neuro-Psychopharmacol. Biol. Psychiatry* 109:110258. doi: 10.1016/j.pnpbp.2021.110258

Shao, Y., Gao, Z., Marks, P. A., and Jiang, X. (2004). Apoptotic and autophagic cell death induced by histone deacetylase inhibitors. *Proc. Natl. Acad. Sci. U. S. A.* 101, 18030–18035. doi: 10.1073/pnas.0408345102

Sharon, G., Sampson, T. R., Geschwind, D. H., and Mazmanian, S. K. (2016). The central nervous system and the gut microbiome. *Cell* 167, 915–932. doi: 10.1016/j.cell.2016.10.027

Shi, C. S., and Kehrl, J. H. (2008). MyD88 and Trif target Beclin 1 to trigger autophagy in macrophages. *J. Biol. Chem.* 283, 33175–33182. doi: 10.1074/jbc.M804478200

Shibata, M., Lu, T., Furuya, T., Degterev, A., Mizushima, N., Yoshimori, T., et al. (2006). Regulation of intracellular accumulation of mutant Huntingtin by Beclin 1. *J. Biol. Chem.* 281, 14474–14485. doi: 10.1074/jbc.M600364200

Silva, M. C., Nandi, G. A., Tentarelli, S., Gurrell, I. K., Jamier, T., Lucente, D., et al. (2020). Prolonged tau clearance and stress vulnerability rescue by pharmacological activation of autophagy in tauopathy neurons. *Nat. Commun.* 11:3258. doi: 10.1038/s41467-020-16984-1

Simonsen, A., Cumming, R. C., Brech, A., Isakson, P., Schubert, D. R., and Finley, K. D. (2008). Promoting basal levels of autophagy in the nervous system enhances longevity and oxidant resistance in adult drosophila. *Autophagy* 4, 176–184. doi: 10.4161/auto.5269

Son, J. H., Shim, J. H., Kim, K. H., Ha, J. Y., and Han, J. Y. (2012). Neuronal autophagy and neurodegenerative diseases. *Exp. Mol. Med.* 44, 89–98. doi: 10.3858/emm.2012.44.2.031

Sun, M. F., Zhu, Y. L., Zhou, Z. L., Jia, X. B., Xu, Y. D., Yang, Q., et al. (2018). Neuroprotective effects of fecal microbiota transplantation on MPTP-induced Parkinson's disease mice: gut microbiota, glial reaction and TLR4/TNF-alpha signaling pathway. *Brain Behav. Immun.* 70, 48–60. doi: 10.1016/j.bbi.2018.02.005

Travassos, L. H., Carneiro, L. A., Ramjeet, M., Hussey, S., Kim, Y. G., Magalhaes, J. G., et al. (2010). Nod1 and Nod2 direct autophagy by recruiting ATG16L1 to the plasma membrane at the site of bacterial entry. *Nat. Immunol.* 11, 55–62. doi: 10.1038/ni.1823

Tsuang, D., Leverenz, J. B., Lopez, O. L., Hamilton, R. L., Bennett, D. A., Schneider, J. A., et al. (2012). GBA mutations increase risk for Lewy body disease with and without Alzheimer disease pathology. *Neurology* 79, 1944–1950. doi: 10.1212/WNL.0b013e3182735e9a

Vogt, N. M., Kerby, R. L., Dill-McFarland, K. A., Harding, S. J., Merluzzi, A. P., Johnson, S. C., et al. (2017). Gut microbiome alterations in Alzheimer's disease. *Sci. Rep.* 7:13537. doi: 10.1038/s41598-017-13601-y

Wang, S. L., Shao, B. Z., Zhao, S. B., Chang, X., Wang, P., Miao, C. Y., et al. (2019). Intestinal autophagy links psychosocial stress with gut microbiota to promote inflammatory bowel disease. *Cell Death Dis.* 10:391. doi: 10.1038/s41419-019-1634-x

Wasser, C. I., Mercieca, E. C., Kong, G., Hannan, A. J., McKeown, S. J., Glikmann-Johnston, Y., et al. (2020). Gut dysbiosis in Huntington's disease: associations among gut microbiota, cognitive performance and clinical outcomes. *Brain Commun.* 2:fcaa110. doi: 10.1093/braincomms/fcaa110

Xu, Y., Jagannath, C., Liu, X. D., Sharafkhaneh, A., Kolodziejska, K. E., and Eissa, N. T. (2007). Toll-like receptor 4 is a sensor for autophagy associated with innate immunity. *Immunity* 27, 135–144. doi: 10.1016/j.immuni.2007.05.022

Xu, Y., Propson, N. E., Du, S., Xiong, W., and Zheng, H. (2021). Autophagy deficiency modulates microglial lipid homeostasis and aggravates tau pathology and spreading. *Proc. Natl. Acad. Sci. U. S. A.* 118:e2023418118. doi: 10.1073/pnas.2023418118

Yamamoto, T., Takabatake, Y., Kimura, T., Takahashi, A., Namba, T., Matsuda, J., et al. (2016). Time-dependent dysregulation of autophagy: implications in aging and mitochondrial homeostasis in the kidney proximal tubule. *Autophagy* 12, 801–813. doi: 10.1080/15548627.2016.1159376

Yang, L., Li, P., Fu, S., Calay, E. S., and Hotamisligil, G. S. (2010). Defective hepatic autophagy in obesity promotes ER stress and causes insulin resistance. *Cell Metab.* 11, 467–478. doi: 10.1016/j.cmet.2010.04.005

Ye, L., Bae, M., Cassilly, C. D., Jabba, S. V., Thorpe, D. W., Martin, A. M., et al. (2021). Enteroendocrine cells sense bacterial tryptophan catabolites to activate enteric and vagal neuronal pathways. *Cell Host Microbe* 29, 179–96.e9. doi: 10.1016/j.chom.2020.11.011

Ye, X., Zhu, M., Che, X., Wang, H., Liang, X. J., Wu, C., et al. (2020). Lipopolysaccharide induces neuroinflammation in microglia by activating the MTOR pathway and downregulating Vps34 to inhibit autophagosome formation. *J. Neuroinflammation* 17:18. doi: 10.1186/s12974-019-1644-8

Yin, X., Zhou, C., Li, J., Liu, R., Shi, B., Yuan, Q., et al. (2019). Autophagy in bone homeostasis and the onset of osteoporosis. *Bone Res.* 7:28. doi: 10.1038/s41413-019-0058-7

Yu, W. H., Cuervo, A. M., Kumar, A., Peterhoff, C. M., Schmidt, S. D., Lee, J. H., et al. (2005). Macroautophagy--a novel Beta-amyloid peptide-generating pathway activated in Alzheimer's disease. *J. Cell Biol.* 171, 87–98. doi: 10.1083/jcb.200505082

Zhang, Y., Liu, C., Zhao, Y., Zhang, X., Li, B., and Cui, R. (2015). The effects of calorie restriction in depression and potential mechanisms. *Curr. Neuropharmacol.* 13, 536–542. doi: 10.2174/1570159x13666150326003852

Zhang, C., Yan, J., Xiao, Y., Shen, Y., Wang, J., Ge, W., et al. (2017). Inhibition of autophagic degradation process contributes to claudin-2 expression increase and epithelial tight junction dysfunction in TNF-alpha treated cell monolayers. *Int. J. Mol. Sci.* 18:157. doi: 10.3390/ijms18122754

Zheng, D., Liwinski, T., and Elinav, E. (2020). Interaction between microbiota and immunity in health and disease. *Cell Res.* 30, 492–506. doi: 10.1038/s41422-020-0332-7

Conflict of Interest: The authors declare that the research was conducted in the absence of any commercial or financial relationships that could be construed as a potential conflict of interest.

Publisher's Note: All claims expressed in this article are solely those of the authors and do not necessarily represent those of their affiliated organizations, or those of the publisher, the editors and the reviewers. Any product that may be evaluated in this article, or claim that may be made by its manufacturer, is not guaranteed or endorsed by the publisher.

frontiers in Microbiology

ORIGINAL RESEARCH
published: 11 February 2022
doi: 10.3389/fmicb.2022.819523

Marked Response of Rat Ileal and Colonic Microbiota After the Establishment of Alzheimer's Disease Model With Bilateral Intraventricular Injection of Aβ (1-42)

Qing Xu[1†], Lingmiao Wen[1†], Guihua Wei[1†], Xiaoqin Zhao[1], Yanjun Liu[1], Wei Xiong[1], Tinglan Zhang[1,2], Yuqing Fan[1,2], Chunlan Chen[1], Chunxiao Xiang[1], Chang Chen[2], Yunhui Chen[3], Qiaozhi Yin[3], Tian-e Zhang[3] and Zhiyong Yan[1]**

[1] School of Life Science and Engineering, Southwest Jiaotong University, Chengdu, China, [2] Institute of Chinese Materia Medica, China Academy of Chinese Medical Sciences, Beijing, China, [3] School of Basic Medicine, Chengdu University of Traditional Chinese Medicine, Chengdu, China

OPEN ACCESS

Edited by:
Hesong Wang,
Southern Medical University, China

Reviewed by:
Hu T. Huang,
Syapse Inc., United States
Bahman Sadeghi,
Virginia Tech, United States

***Correspondence:**
Tian-e Zhang
zhte2003@cdutcm.edu.cn
Zhiyong Yan
yzhiy@swjtu.edu.cn

[†] These authors have contributed equally to this work and share first authorship

Specialty section:
This article was submitted to Microbial Symbioses, a section of the journal Frontiers in Microbiology

Received: 21 November 2021
Accepted: 10 January 2022
Published: 11 February 2022

Citation:
Xu Q, Wen L, Wei G, Zhao X, Liu Y, Xiong W, Zhang T, Fan Y, Chen C, Xiang C, Chen C, Chen Y, Yin Q, Zhang T-e and Yan Z (2022) Marked Response of Rat Ileal and Colonic Microbiota After the Establishment of Alzheimer's Disease Model With Bilateral Intraventricular Injection of Aβ (1-42). Front. Microbiol. 13:819523. doi: 10.3389/fmicb.2022.819523

Alzheimer's disease (AD) is a common neurodegenerative disease. More evidence has shown that gut microbiota is closely associated with AD. Also, studies have shown that the distribution of gut microbiota vary in different sections of the intestine. In this study, a rat model of AD was established using a bilateral intraventricular injection of β-amyloid (1-42) [Aβ (1-42)], and the behavior of rats, hippocampal Aβ (1-42) deposition, and the ileal and colonic microbiota in each group were analyzed. We observed that the model rats had obvious memory and cognitive impairment, increased Aβ (1-42) deposition, indicating that the AD model was successfully established. Through 16S rRNA-sequencing analysis, we found that α diversity, β diversity, and dominant microbiota in the ileum and colon of normal rats were significantly different, showing spatial heterogeneity. Additionally, the surgery and injection of Aβ (1-42) caused various degrees of disturbances in the ileal and colonic microbiota of rats. These findings provide new insights for the study of the gut microbiota of AD rats and help advance the development of therapeutic strategies for intervening AD through the gut microbiota.

Keywords: Alzheimer's disease, β-amyloid (1-42), surgery, ileal microbiota, colonic microbiota, 16S rRNA

INTRODUCTION

Alzheimer's disease (AD) is an age-related neurodegenerative disease. Its main characteristics are β-amyloid deposition and neurofibrillary tangles, and its clinical manifestations begin with slight memory decline and can eventually develop into severe self-care and cognitive impairment (Mathys et al., 2019; Kim et al., 2020). According to the Alzheimer's Disease International (2016), the number

Abbreviations: AD, Alzheimer's disease; Aβ, β-amyloid; BDNF, brain derived neurotrophic factor; 5-HT, 5-hydroxytryptamine; SPF, specific pathogen free; MWM, morris water maze; OTU, operational taxonomic unit; ANOVA, one-way analysis of variance; LSD, least significant difference; HE, hematoxylin-eosin; CA, cornu ammonis; DG, dentate gyrus; PCoA, principal co-ordinates analysis; PCR: polymerase chain reaction; SCFAs: short chain fatty acids.

of people with dementia in the world is about 50 million (Alzheimer's Disease International, 2016). The etiology of AD is still unclear. Some studies have suggested that accumulation of Aβ in the brain is the primary influence driving AD pathogenesis (Gitter et al., 2000; Hardy and Selkoe, 2002), and others show that tau protein hyperphosphorylation leads to neurofibrillary tangles, resulting in neurotoxicity (Iqbal et al., 2016; Wesseling et al., 2020). Also, some studies consider AD as a chronic inflammatory disease of the central nervous system (Sierra-Filardi et al., 2011; Krabbe et al., 2013). In addition, the concept of Brain-Gut-Microbiota Axis has been proposed in recent years and suggests that gut microbiota can influence neurodegenerative disorders (Cryan et al., 2019; Kowalski and Mulak, 2019; Sun et al., 2020). In this study, we established an AD model by bilateral intraventricular injection of Aβ (1-42) based on the β-amyloid cascade hypothesis. This method has been widely used (Yang et al., 2018; Xu et al., 2019), and many studies have shown that Aβ (1-42) injection can cause memory impairment and changes Brain Derived Neurotrophic Factor (BDNF) or 5-hydroxytryptamine(2A)[5-HT(2A)] receptor levels in the serum and brain (O'Hare et al., 1999; Christensen et al., 2008).

Gut microbiota is a complex microbial community that is symbiotic in the intestines of humans or animals. Different microbiota in the intestine maintains the micro ecological balance of the intestine and participates in the body's digestion and metabolism, biosynthesis of vitamins, immune regulation, energy conversion, and other functions (Chow et al., 2010). There is increasing evidence that gut microbiota affects gut-brain interaction at different points in time (from early life to neurodegeneration) and at different levels (from the intestinal cavity to the central nervous system) (Dinan and Cryan, 2017; Kowalski and Mulak, 2019). Changes in the gut microbiota can act on various neurodegenerative diseases, including Parkinson's disease, AD, multiple sclerosis, and amyotrophic lateral sclerosis, etc., (Sarkar and Banerjee, 2019). Recently, the new AD drug "GV-971" developed by China (Shanghai Green Valley Pharmaceutical Co., Ltd., Shanghai, China) reshapes the balance of the gut microbiota, inhibits the abnormal increase in specific metabolites of the gut microbiota, reduces the peripheral and central inflammation, and reduces β-amyloid protein deposition and Tau protein hyper phosphorylation, thereby improving patients' cognitive dysfunction. This is also the first new drug for AD targeting the gut-brain axis (Wang et al., 2019).

The mammalian intestine is divided into different intestinal segments, including the jejunum, ileum, cecum, and colon (Li et al., 2020). As a result of various factors, including the pH value, oxygen content, intestinal peristalsis intensity, etc., there are certain differences in the composition, number, and diversity of colony between different individuals or different intestinal segments of the same individual (Eckburg et al., 2005; Donaldson et al., 2016; Tropini et al., 2017; Martinez-Guryn et al., 2019). In the same body, the number of microbiota gradually increases from top to bottom with the direction of the intestine and is more distributed in the ileum and colon, more especially, the colon is the main site of habitation for bacterial residents with an estimated concentration of 10^{12}/ml (Sender et al., 2016). Current studies on gut microbiota mostly use colonic or fecal microbiota as samples (Bhattarai et al., 2021; Jing et al., 2021). Most of the colon or fecal contents contain large intestine microorganisms, but they lack small intestine microorganisms. Therefore, this research focuses on the ileum and colon to explore the composition and changes in the microbiota.

This study established an AD animal model by bilateral intraventricular injection of Aβ (1-42), and the composition of the microbiota in different intestinal segments of normal rats was compared and analyzed. Furthermore, the effects of model-making surgery and injection of Aβ (1-42) on rat ileal and colonic microbiota were analyzed. Present, there are many studies on AD and gut microbiota, but studies on the microbial variation in different sections of the intestine are still rare. This study explores the specific changes in the ileal and colonic microbiota during AD lesions, to promote follow-up research of intervention or treatment of AD using the gut microbiota.

MATERIALS AND METHODS

Animals

A total of 36 specific pathogen free (SPF) adult Sprague–Dawley rats aged 6∼7 weeks, half male and half female, were purchased from Chengdu Dashuo Experimental Animal Co., Ltd., Chengdu, China, and the production license is SCXK (Sichuan) 2015–030. The animals were raised in the Animal Laboratory of the School of Life Sciences and Engineering, Southwest Jiaotong University, and the temperature was maintained at 25°C ± 2°C, alternating light and dark for 12 h, and had access to food and water *ad libitum*. The animal study was reviewed and approved by the Animal Ethics Committee of Southwest Jiaotong University (No. SWJTU-2010-001) and performed in compliance with the Guidelines for Animal Experimentation of the university. After being adaptively reared for 7 days, they were randomly divided into three groups: the normal group, the sham-operated group, and the model group, each with 12 animals, half male, and half female.

Establishment of Alzheimer's Disease Animal Model

The AD model was established by referring to the methods of Granic et al. (2010), Xu et al. (2019). Diluted Aβ (1-42) (J0426A, meilunbio) to 2 μg/μL with sterile saline incubated it in a constant temperature incubator at 37°C for 7 days to make it into an aggregated state and then stored it at 4°C. After placed in an induction chamber and anesthetized with 3% isoflurane, the rats in the model group used surgical scissors to clean their head hair and fixed it on the stereotaxic instrument. The skin of the operation area was first disinfected and then the fontanelle was found. With Bregma as the origin, the two-puncture point was located 3.2 mm after Bregma and 2.0 mm to the left and right of Lambda, and the needle of microinjector was inserted vertically 2.9 mm (AP = −3.2 mm, ML = 2.0 mm, DV = 2.9 mm). In the model group, 2-μL Aβ (1-42) was slowly injected into the bilateral hippocampal CA1 area, and the wound was sutured and disinfected after the needle was withdrawn. The rats in the sham-operated group were

injected with 2-μL sterile saline, and the normal group was not treated in any way.

Morris Water Maze Test

One month after the Aβ (1-42) injection, Morris water maze (MWM) test was conducted (Kelley et al., 2011). The experimental system consists of a pool, a movable platform, an image acquisition and analysis system. The pool was divided into four quadrants, and a platform 2-cm below the water surface was set in the third quadrant. The test was divided into two parts: place navigation test and spatial probe test. Briefly, rats were subjected to acquisition training for 4 consecutive days, then place navigation test on the 5th day. The time(s) spent by each rat to locate the platform (the platform incubation period) was recorded. The rats were placed into the water facing the wall of the pool. If they found the platform within 120 s, they were allowed to stay on the platform for 20 s; if they were not found, they were guided to find the platform and stay for 20 s. On the 6th day of the experiment, the platform was removed for the spatial probe test, and the rats were placed in the swimming pool from the same position. The target quadrant dwell time(s) and crossings(n), and the number of platform crossings(n) within the specified time (120 s) were recorded.

Sampling for Aβ Detection of Hippocampus

After the Morris water maze test, the rats were sacrificed and the hippocampal region of the brain was extracted. The appropriate amount of hippocampal tissue was mixed with nine times the amount of saline and ground into a homogenate. The supernatant was centrifuged at 3,000 rpm for 10 min after which testing was conducted according to the Aβ (1-42) assay kit (6C739NJDT9, Elabscience Biotechnology Co., Ltd., Wuhan, China).

Sampling for Microbiota Detection

While taking the hippocampal tissue, the contents of the ileum and colon were collected and stored in freezer at −80°C. Four samples were taken from each group, and 24 samples were analyzed using 16S rRNA gene amplicon sequencing. According to the manufacturer's instructions, Zymo Research BIOMICS DNA Microprep Kit (Cat# D4301) was used for sample DNA extraction and purification. The 16S rDNA V4 region of the samples was then amplified using Applied Biosystems® PCR System 9700, which primer sequences were as follows: Primer 5′-3′: 515F (5′-GTGYCAGCMGCCGCGGTAA-3′) and 806R (5′- GGACTACHVGGGTWTCTAAT-3′) with an amplification length of 292 bp (Chengdu Ronin Biotechnology Co., Ltd., Chengdu, China). And the products were detected, purified, and quantified. Libraries were built using NEW ENGLAND BioLabs NEBNext Ultra II DNA Library Prep Kit for Illumina (NEB# E7645L), and high-throughput sequencing was conducted using the Hiseq 2500 platform in PE250 mode.

Analysis of Bacterial Microbiota Detection Results

The original sequence of each sample was quality-controlled and filtered using the QIIME (v1.9.0) software package (Caporaso et al., 2010). Based on the Usearch (10.0.240) software, the UPARSE algorithm (Edgar, 2013) was used to conduct operational taxonomic unit(OUT) clustering at a consistency level of 97%, and the sequence with the highest frequency in each OTU was selected as the representative sequence of OTU. The UCLUST classification (Edgar, 2010) is used for annotation analysis, and FastTree (Price et al., 2010) is used to construct phylogenetic tree. The community composition analysis, α diversity, and β diversity analysis were conducted using the R language, which included the Vegan package for Chao1 and Shannon indices analysis, the GuniFrac package to calculate Unifrac distances, the ape package for PCoA analysis, and the ggplot2 package for community composition analysis. Different species analysis was conducted using LEfSe analysis (Segata et al., 2011).

Data Analysis

The experimental data were analyzed using IBM SPSS Statistics 20 and Graphpad Prism 8.0, and the comparison of sample parameters between groups were conducted using the one-way analysis of variance (ANOVA) followed by least significant difference (LSD) tests and Tukey test for multiple comparisons. The data are all expressed as mean ± Standard Error of Mean ($\bar{x}$ + SEM), and $P < 0.05$ indicates that the difference is statistically significant.

RESULTS

Effect of Surgery and Aβ (1-42) Injection on the Rat Behavior

After modeling, a water maze experiment was conducted to evaluate the spatial memory of rats in the normal, sham-operated, and model groups. According to the results (**Table 1**), there were no significant differences between the normal and sham-operated groups in platform incubation period, target quadrant dwell time and crossings, number of platform crossings. While the platform incubation period of the model group rats was significantly longer ($F = 3.986$, $P < 0.05$). The target quadrant dwell time ($F = 7.974$, $P < 0.05$, $P < 0.01$) and crossings ($F = 7.459$, $P < 0.01$) and the number of platform crossings ($F = 8.095$, $P < 0.05$, $P < 0.01$) were significantly shortened. It was observed that the injection of Aβ (1-42) caused damage to the memory and cognitive function of rats, but it was not affected by the surgery.

Effect of Surgery and Aβ (1-42) Injection on the Content of Aβ (1-42) in Hippocampus of Rats

After the water maze experiment, the effects of surgery and Aβ (1-42) injection on the content of Aβ (1-42) in the hippocampus of rats were explored. There was no significant difference in the levels of Aβ (1-42) (pg/ml) in the hippocampus of rats in the normal group and the sham-operated group (**Figure 1**).

TABLE 1 | Effect of surgery and Aβ (1-42) injection on rat behavior.

Group	Platform incubation period(s)	Target quadrant dwell time(s)	Target quadrant crossings(n)	Number of platform crossings(n)
Normal group	11.52 ± 2.53	43.603 ± 2.209	45.830 ± 8.185	8.330 ± 1.639
Sham-operated group	12.95 ± 4.08	39.777 ± 2.096	39.080 ± 7.638	5.580 ± 0.557
Model group	29.20 ± 7.04$^{*\#}$	31.833 ± 2.071$^{**\#}$	12.250 ± 1.256$^{**\#\#}$	2.500 ± 0.399$^{**\#}$

*Mean ± SEM, n = 12. *P < 0.05, **P < 0.01 compared with the normal group.*
$^{\#}$P < 0.05, $^{\#\#}$P < 0.01 compared with the sham-operated group.

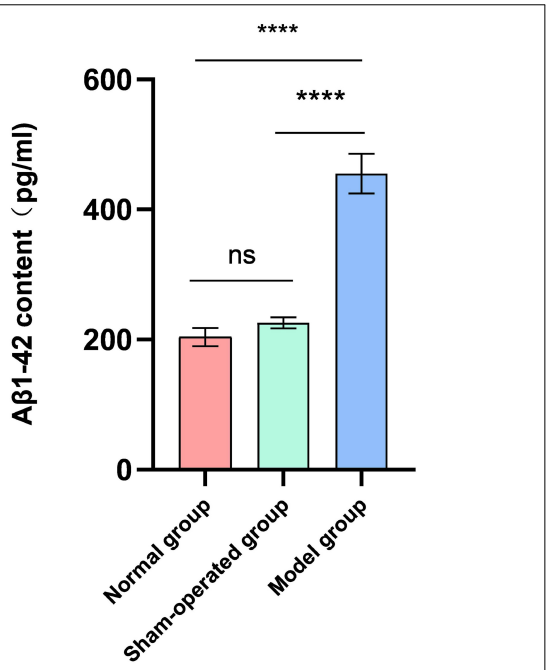

FIGURE 1 | Effect of surgery and Aβ (1-42) injection on the content of Aβ (1-42). *n* = 6. ****$P < 0.0001$.

In contrast, the deposition of Aβ (1-42) in the model group significantly increased ($F = 48.51$, $P < 0.0001$, **Figure 1**).

Effect of Surgery and Aβ (1-42) Injection on the Diversity of the Ileal and Colonic Microbiota of Rats

We read a total of 5,48,256 effective tags from 24 samples, with an average of 22,844 sequence reads per sample for subsequent analysis. As the sequencing depth increases, the species richness of each group of samples increased, and the Rarefaction Curve (**Figure 2A**) and Rank-Abundance (**Figure 2B**) are gradually flattening out. The sequencing depth basically covered all species in the sample, and the species distribution in each sample is also relatively uniform. The Venn diagram displayed 1,336 unique OTUs in the IN, 763 unique OTUs in the IS, 70 unique OTUs in the IM, 17 unique OTUs in the CN, 33 unique OTUs in the CS, and 472 unique OTUs in the CM. In total, 202 OTUs are shared in all groups (**Figure 2C**).

The Chao1 index is commonly used to estimate the total number of species, and the Shannon index is commonly used to assess the number of species and homogeneity of microorganisms. In the normal group and the sham-operated group, the Chao1 index ($F = 44.34$, $P < 0.0001$, **Figure 2D**) and Shannon index ($F = 20.67$, $P < 0.0001$, $P < 0.001$, **Figure 2E**) of the ileal microbiota were significantly higher than those of the colonic microbiota; while in the model group, Chao1 and Shannon index in the ileal and colonic microbiota are not statistically different. In the ileum samples (**Figures 2D,E**), compared with the normal group, the Chao1 index of the sham-operated group was significantly lower ($F = 44.34$, $P < 0.001$). Still, there was no significant difference between the model group and the sham-operated group, and the Shannon index was not significantly different in the three groups. In the colon samples (**Figures 2D,E**), the two indices of the normal group and the sham-operated group were not significantly different, while the Chao1 ($F = 44.34$, $P < 0.001$) and Shannon ($F = 20.67$, $P < 0.01$) indices of the model group were significantly higher than those of the sham-operated group. The Unweighted Unifrac distance matrix was utilized in analyzing the colony structure between each group of samples, the more similar the community composition of the samples, the closer their distance is in the figure. The results showed (**Figure 2F**) that the ileal and colonic microbiota in the normal group, sham-operated group, or model group were significantly separated. In the ileum samples, the structure of the microbiota in the normal group, the sham-operated group, and the model group were clearly separated. In the colon samples, the community distribution of the normal group, the sham-operated group, and the model group were relatively clustered. This indicated that the ileal and colonic microbiota of normal rats were significantly different, and the species number and diversity of the ileal microbiota were significantly higher than that of the colonic microbiota. The surgery has significantly reduced the number of species in the ileal microbiota and changed its structure, but had no significant effect on the colon; the injection of Aβ (1-42) changed the colony structure of the ileum and increased the species number and diversity of the colonic microbiota.

Effect of Surgery and Aβ (1-42) Injection on the Composition of the Bacterial Community in the Ileum and Colon of Rats

To further explore the changes in the ileal and colonic microbiota during the modeling process, the relative composition of the communities of different intestinal segments at the phylum and genus level were analyzed. At the phylum level (**Figure 3**), the

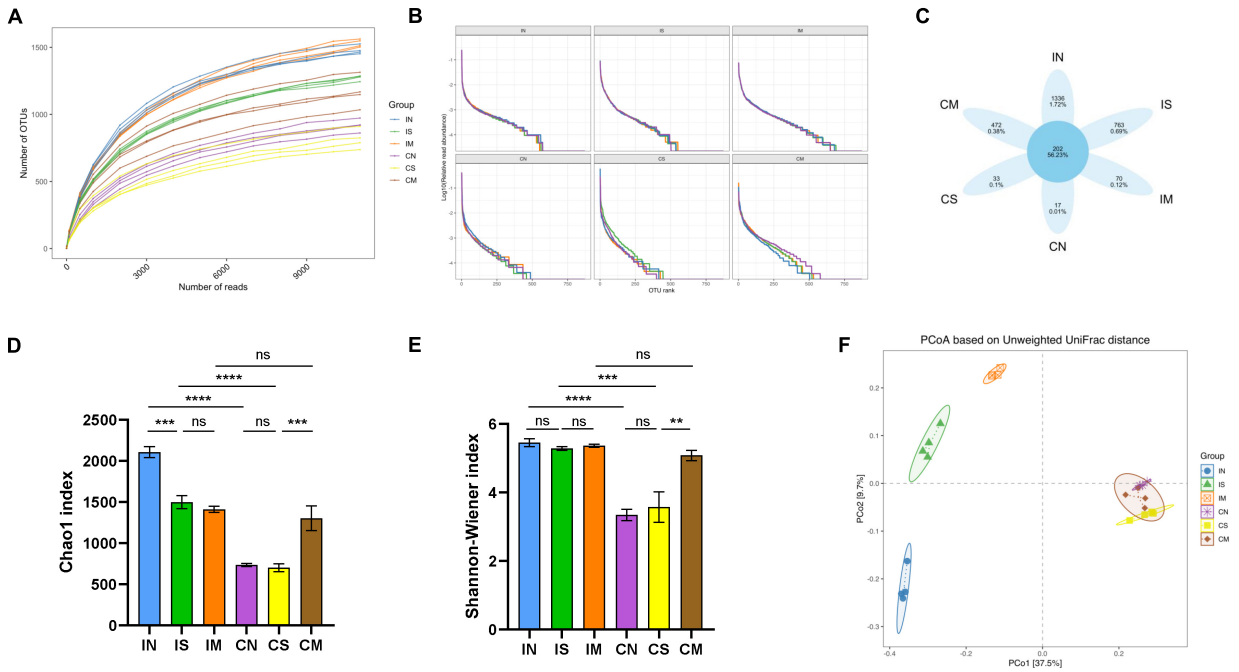

FIGURE 2 | Effect of surgery and Aβ (1-42) injection on the diversity of the ileal and colonic microbiota of rats. **(A)** Rarefaction Curve shows the variation trend of the species richness of each sample with the sequencing depth. **(B)** Rank-Abundance shows the relationship between the abundance of individual species and the type of individual species in each sample. **(C)** Venn diagram shows the OTU unique to each sample and shared by different samples. Chao1 index **(D)** and Shannon–Wiener index **(E)** of α-diversity of 16S rRNA sequencing of each sample in different groups. **(F)** Principal co-ordinates analysis (PCoA) for β-diversity shows the clustering of gut microbial communities in different groups. IN: the ileal microbiota of the normal group; IS: the ileal microbiota of the sham-operated group; IM: the ileal microbiota of the model group; CN: the colonic microbiota of the normal group; CS: the colonic microbiota of the sham-operated group; CM: the colonic microbiota of the model group. $^{**}P < 0.01$; $^{***}P < 0.001$; and $^{****}P < 0.0001$.

most important phyla in rat intestines are Firmicutes (from 26.56 to 83.72%), Bacteroidetes (from 11.08 to 39.84%), Proteobacteria (from 0.45 to 40.82%), and Actinobacteria (from 0.19 to 8.91%). In the normal group, the abundance of Proteobacteria ($F = 29.41$, $P < 0.0001$) and Actinobacteria ($F = 122.3$, $P < 0.0001$) in the ileal microbiota was significantly higher than that of the colonic microbiota, and the abundance of the Firmicutes of the colonic microbiota was significantly higher than that of the ileal microbiota ($F = 35.32$, $P < 0.0001$). In the sham-operated group, the abundance of Bacteroidetes ($F = 23.71$, $P < 0.001$) and Actinobacteria ($F = 122.3$, $P < 0.01$) in the ileal microbiota was higher than that of the colonic microbiota, and the Firmicutes in the colonic microbiota was significantly higher than that of the ileal microbiota ($F = 35.32$, $P < 0.0001$). There was no significant difference in the abundance of each dominant phyla in the ileum and colon. Additionally, in the ileum samples, Bacteroidetes in the sham-operated group were significantly increased compared to the normal group ($F = 23.71$, $P < 0.0001$), Proteobacteria ($F = 29.41$, $P < 0.0001$) and Actinobacteria ($F = 122.3$, $P < 0.0001$) were significantly decreased, and the abundance of Firmicutes in the model group was significantly increased compared to the sham-operated group ($F = 35.32$, $P < 0.05$), Actinobacteria abundance decreased significantly ($F = 122.3$, $P < 0.05$). In the colon sample, Firmicutes in the sham-operated group was significantly lower than that in the normal group ($F = 35.32$, $P < 0.05$), but the dominant phyla of the model group had no significant difference compared with the sham-operated group.

At the genus level (**Figure 4**), the most important bacterial genera in rat intestines are *Lactobacillus* (from 1.68 to 56.62%), *Bacteroides* (from 0.77 to 24.03%), *Escherichia-Shigella* (from 0.06 to 21.91%), *Lachnospiraceae NK4A136 group* (From 1.13 to 10.94%). In the normal group, the abundance of the colonic microbiota of *Lactobacillus* ($F = 16.61$, $P < 0.0001$) and *Lachnospiraceae NK4A136 group* ($F = 14.27$, $P < 0.01$) were significantly higher than that of the ileal microbiota, while the abundance of the ileal microbiota of *Escherichia-Shigella* was significantly higher than that of the colonic microbiota ($F = 9.586$, $P < 0.001$). In the sham-operated group, the abundance of *Lactobacillus* in the colon was significantly higher than that of the ileal microbiota ($F = 16.61$, $P < 0.05$), and the *Bacteroides* of the ileal microbiota were significantly higher than that of the colonic microbiota ($F = 124.1$, $P < 0.0001$). In the model group, there was no significant difference in the abundance of each dominant genus in the ileum and colon. Additionally, in the ileum samples, *Bacteroides* in the sham-operated group were significantly increased compared with the normal group ($F = 124.1$, $P < 0.0001$), while *Escherichia-Shigella* was significantly decreased ($F = 9.586$, $P < 0.01$); the abundance of *Lachnospiraceae NK4A136 group* in the model group was

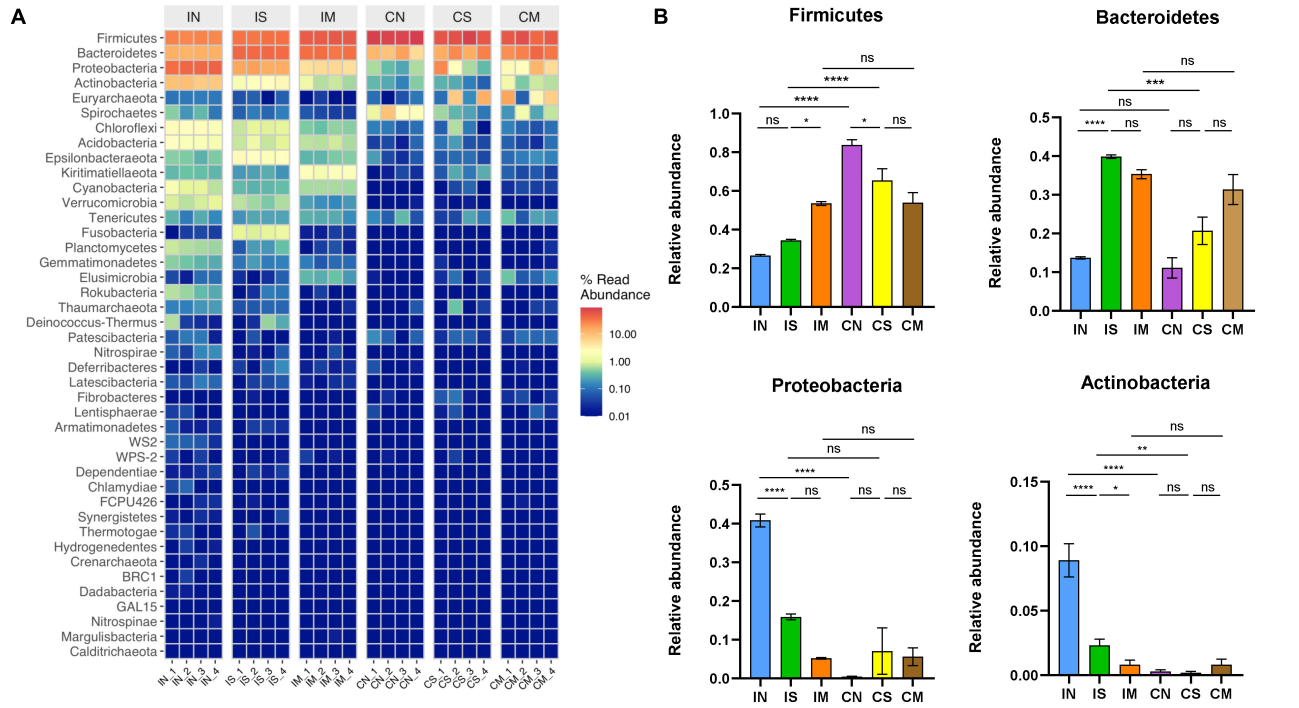

FIGURE 3 | Effect of surgery and Aβ (1-42) injection on the composition of the bacterial community at the phylum level. **(A)** The distribution of the top 50 species with the highest abundance at the phylum level **(B)** the distribution of the top four dominant bacteria phyla with the highest abundance at the phylum level in each group of samples. IN: the ileal microbiota of the normal group; IS: the ileal microbiota of the sham-operated group; IM: the ileal microbiota of the model group; CN: the colonic microbiota of the normal group; CS: the colonic microbiota of the sham-operated group; CM: the colonic microbiota of the model group. Data are reported as the mean ± SEM. $^{*}P < 0.05$; $^{**}P < 0.01$; $^{***}P < 0.001$; and $^{****}P < 0.0001$.

significantly increased compared with the sham-operated group ($F = 14.27$, $P < 0.001$), while the abundance of *Bacteroides* was also significantly decreased ($F = 124.1$, $P < 0.0001$). In the colon sample, the *Lactobacillus* of the sham-operated group was significantly decreased compared with the normal group ($F = 16.61$, $P < 0.05$), and the abundance of *Lachnospiraceae NK4A136 group* in the model group was significantly increased compared with the sham-operated group ($F = 14.27$, $P < 0.01$).

LEfSe analysis enables comparison between multiple groups to find biomarkers with significant differences in abundance between groups. LEfSe analysis was used to further identify the species with significant differences in three groups (**Figure 5**) and to show similar findings. In the normal rats, Proteobacteria, Actinobacteria, *Escherichia-Shigella,* etc., are enriched in the ileum, and Firmicutes, *Lactobacillus*, etc., are enriched in the colon. In the sham-operated rats, Bacteroidetes and *Bacteroides* were enriched in the ileum, but there was no enrichment of high abundance microbiota in the colon. In the model rats, *Lachnospiraceae NK4A136 group* was enriched in the colon.

DISCUSSION

The Morris water maze is currently recognized as a classic experiment for studying spatial learning and memory in rodents. It is the most essential behavioral experiment for evaluating AD animal models (Pereira and Burwell, 2015). The behavioral results of this study showed significant changes in the water maze experiment in the model group rats compared with the normal and sham-operated groups, which indicates that bilateral ventricular injection of Aβ (1-42) impaired memory and cognitive functions in rats and successfully established the rat model of AD. Additionally, the significant increase in the content of Aβ (1-42) in the hippocampus of the model group also confirmed this.

The gut microbiota in the intestine is spatially heterogeneous, and different communities were observed along the length of the intestinal tract (Choi et al., 2014). There are also many previous reports on the segmental distribution of gut microbiota in mice, chickens, and pigs (Looft et al., 2014; Zhao et al., 2015). In this study, we found that the ileal and colonic microbiota were significantly different in terms of diversity and species by analyzing the α-diversity, β-diversity, and community composition of the ileal and colonic microbiota of normal rats. These results indicate that the ileal and colonic microbiota of normal SD rats also showed spatial heterogeneity, and the number of species and diversity of the ileal microbiota were significantly higher than that of the colonic microbiota.

In the process of exploring the difference between ileal and colonic microbiota of AD model rats, we found an interesting phenomenon: several indices of the ileal and colonic microbiota

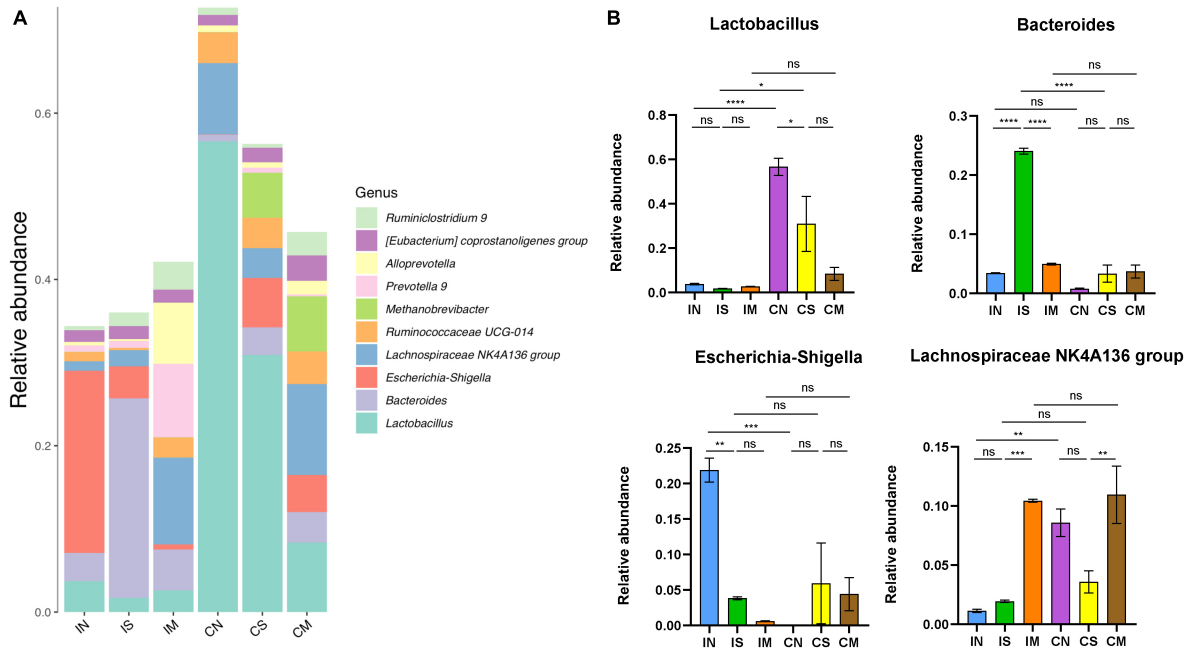

FIGURE 4 | Effect of surgery and Aβ (1-42) injection on the composition of the bacterial community at the genus level. **(A)** The distribution of the top 10 species with the highest abundance at the genus level. **(B)** The abundance distribution of the top four bacterial genera with the highest abundance at the genus level in each group of samples. IN: the ileal microbiota of the normal group; IS: the ileal microbiota of the sham-operated group; IM: the ileal microbiota of the model group; CN: the colonic microbiota of the normal group; CS: the colonic microbiota of the sham-operated group; CM: the colonic microbiota of the model group. Data are reported as the mean ± SEM. $^{*}P < 0.05$; $^{**}P < 0.01$; $^{***}P < 0.001$; and $^{****}P < 0.0001$.

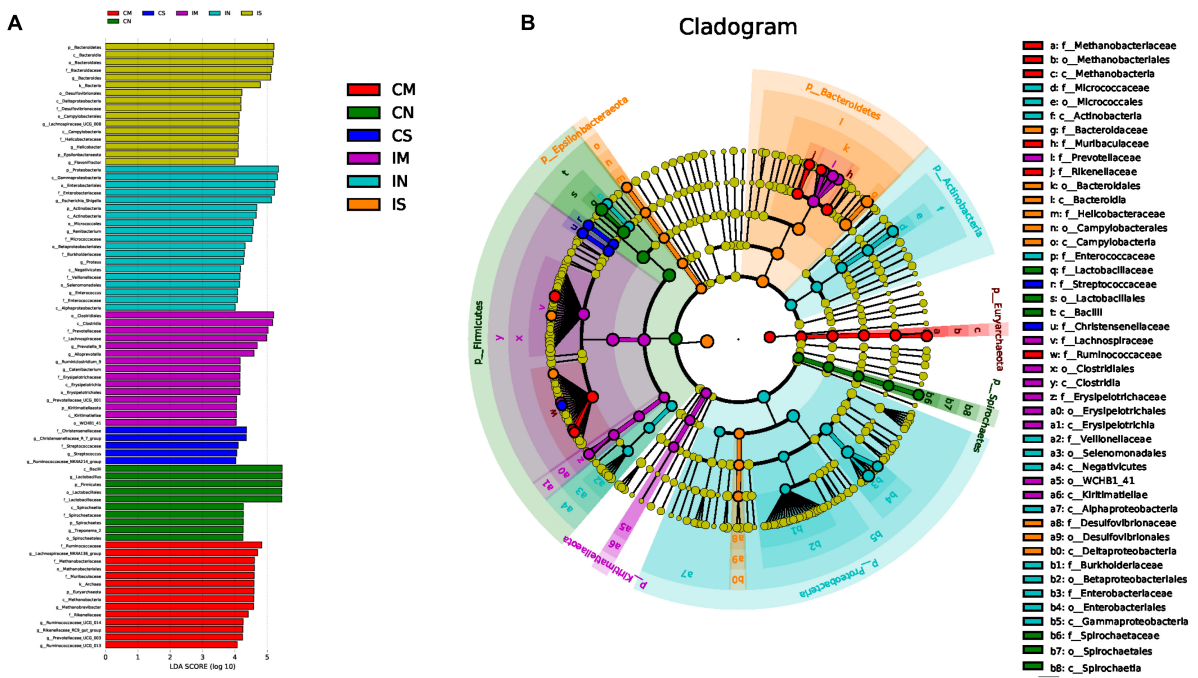

FIGURE 5 | Effect of surgery and Aβ (1-42) injection on the composition of the significantly enriched species. **(A)** LDA score of LEfse (LDA > 4.0), used to show the significantly enriched species in each group and their degree of importance. **(B)** Cladogram of LEfse, used to show the evolutionary laws of species branching that play an important role in each group of samples. IN: the ileal microbiota of the normal group; IS: the ileal microbiota of the sham-operated group; IM: the ileal microbiota of the model group; CN: the colonic microbiota of the normal group; CS: the colonic microbiota of the sham-operated group; CM: the colonic microbiota of the model group.

of normal rats were significantly different, showing spatial heterogeneity, while the ileal microbiota of rats in the sham-operated group, in which only surgery was conducted, showed reduced diversity and altered community structure, making the differences between the ileal and colonic microbiota narrow. And finally there were no significant differences between the ileal and colonic microbiota in Chao1 and Shannon index, the relative abundance of dominant phyla and genera of rats in the model group injected with Aβ (1-42). Therefore, we hypothesized that both the surgery and the injection of Aβ (1-42) caused the alteration of the gut microbiota.

Gut microbiota imbalance often occurs after major surgery or intestinal surgery and in critically ill patients (Earley et al., 2015; Mondot et al., 2015; Hamilton et al., 2020; Wang et al., 2020, 2021). Brain injury alters the composition of the intestinal microbiota, decreasing the intestinal microbial diversity (Wang et al., 2021). This phenomenon was reconfirmed using changes in the microbiota of sham-operated rats in the current study. Additionally, it was shown that traumatic frontal lobe knockout brain injury could lead to extensive changes in intestinal structures and function, affecting intestinal permeability (Feighery et al., 2008; Sundman et al., 2017). Particularly, the surgery in this study significantly increased the relative abundance of Bacteroidetes in sham-operated rats and significantly decreased the relative abundance of Proteobacteria and Actinobacteria, suggesting that it may be related to the effects of surgery on the gut microbiota. Additionally, the surgery also significantly increased the relative abundance of *Bacteroides* and significantly decreased the abundance of *Escherichia-Shigella*.

The departure of gut microbiota from a healthy state was considered a marker of disease onset and progression (Gilbert et al., 2016; Lynch and Pedersen, 2016). In recent years, many people have paid more attention to the study of gut microbiota and AD. Harach et al. (2017) found that the abundance of *Firmicutes*, *Verrucomicrobia, Proteobacteria*, and *Actinomycota* in the gut microbiota of AD model mice of the same age was significantly lower than the wild-type mice, while the abundance of *Bacteroidetes* was significantly higher. The gut microbiota plays an essential role in the regulation of neuroinflammation and neurodegeneration in AD (Goyal et al., 2021).

Senile plaques composed of β-amyloid protein (Aβ) are one of the classic pathological changes of AD. Harach et al. (2017) compared the Aβ content of sterilely-raised amyloid precursor protein transgenic AD model (APP/PS1) mice and conventionally raised APP/PS1 mice. They found that the Aβ content of germ-free mice was reduced compared with conventionally raised mice. Additionally, they also transplanted the microbiota of conventionally raised wild-type mice and APP/PS1 mice into sterilely-raised APP/PS1 mice, and discovered that the colonization of germ-free APP/PS1 mice with microbiota from conventionally raised APP /PS1 mice increased cerebral Aβ pathology, and the amount of Aβ deposition was similar to that of conventionally raised APP/PS1 mice, while colonization with microbiota from wild-type mice was less effective in increasing cerebral Aβ levels. Another study has shown that long-term treatment of APP/PS1 mice with broad-spectrum antibiotics will significantly reduce the diversity of gut microbiota and reduce Aβ plaque deposition in the cerebral cortex and hippocampus of mice (Minter et al., 2016). These findings confirmed that the gut microbiota can affect the production and deposition of Aβ.

In this study, we found that Aβ deposition in the hippocampus of the AD rat model established by bilateral intracerebroventricular injection of Aβ (1-42) was significantly increased. Concurrently, compared with the sham-operated mice, the colony structure of the ileum was significantly changed, the number and diversity of the colonic microbiota was also significantly increased. Therefore, we believe that artificially injecting Aβ into the brain of animals can also cause disorders of the gut microbiota. Particular, injection of Aβ (1-42) significantly increased *Lachnospiraceae NK4A136 group* in the ileum and colon of model rats. *Lachnospiraceae NK4A136 group* represents a kind of bacteria that produces butyrate, which has been found to maintain the integrity of the mouse intestinal barrier and is negatively correlated with intestinal permeability (Hu et al., 2019). As one of the main SCFAs produced by the microbiota, butyrate is essential in maintaining the health of the gastrointestinal tract because it can enhance the integrity of the epithelial barrier and inhibit inflammation (Hamer et al., 2008). Notably, the significant increase in the abundance of *Lachnospiraceae NK4A136 group* also highlights its underlying mechanism in AD lesions.

CONCLUSION

In conclusion, this study used 16S rRNA high-throughput sequencing to compare and analyze the changes in the ileal and colonic microbiota of Alzheimer's disease model rats established using bilateral intraventricular injection of Aβ (1-42), indicating that the microbiota of different intestinal segments of normal rats presents spatial heterogeneity. Both the surgery and injection of Aβ caused various degrees of disturbances in the ileal and colonic microbiota of rats. Particular, more in-depth analysis and discussion of the specific changes of the ileal and colonic microbiota during the modeling process was conducted, which can provide clues for a clearer understanding of the underlying mechanisms of AD lesions. This study allows us to clearly understand the impact of AD lesions on the different gut microbiota and provide more possibilities for intervention in AD from the perspective of gut microbiota. Disturbance of the gut microbiota may be of great significance to the pathogenesis of AD based on the brain-gut axis, and further studies are needed to confirm the connection between surgery, Aβ (1-42) injection, and disturbance of the gut microbiota. Also, whether the effect of Aβ (1-42) induced AD on gut microbiota between males and females is distinct needs to be further investigated.

DATA AVAILABILITY STATEMENT

The datasets generated for this study can be found in the NCBI SRA data with accession number PRJNA762025.

ETHICS STATEMENT

The animal study was reviewed and approved by the Animal Ethics Committee of Southwest Jiaotong University (No. SWJTU-2010-001).

AUTHOR CONTRIBUTIONS

ZY and TZ conceived the project and designed the experiments. QX, LW, GW, XZ, YL, WX, TLZ, YF, CLC, CX, CC, YC, and QY performed the experiments. QX, LW, and GW wrote the manuscript. All authors read and approved the manuscript.

FUNDING

This work was supported by the Fundamental Research Funds for the Central Universities (2682020ZT81), the Special Research Project of Sichuan Provincial Administration of Traditional Chinese Medicine (2020JC0127 and 2021MS099), the Key Project of Research and Development Plan of Science and Technology Department of Sichuan Province (2020JDZH0018), the Sichuan Provincial Famous TCM Doctor Studio Construction Project (202120), and Technological Innovation Research and Development Projects of Chengdu Science and Technology Bureau (2021-YF05-02379-SN).

REFERENCES

Alzheimer's Disease International (2016). *World Alzheimer Report 2016: Improving Healthcare for People with Dementia. Coverage, Quality and Costs now and in the Future*. London: Alzheimer's Disease International.

Bhattarai, Y., Si, J., Pu, M., Ross, O. A., McLean, P. J., Till, L., et al. (2021). Role of gut microbiota in regulating gastrointestinal dysfunction and motor symptoms in a mouse model of Parkinson's disease. *Gut Microbes* 13:1866974. doi: 10.1080/19490976.2020.1866974

Caporaso, J. G., Kuczynski, J., Stombaugh, J., Bittinger, K., Bushman, F. D., Costello, E. K., et al. (2010). QIIME allows analysis of high-throughput community sequencing data. *Nat Methods* 7, 335–336. doi: 10.1038/nmeth.f.303

Choi, J. H., Kim, G. B., and Cha, C. J. (2014). Spatial heterogeneity and stability of bacterial community in the gastrointestinal tracts of broiler chickens. *Poultry Sci.* 93, 1942–1950. doi: 10.3382/ps.2014-03974

Chow, J., Lee, S. M., Shen, Y., Khosravi, A., and Mazmanian, S. K. (2010). Host-bacterial symbiosis in health and disease. *Mucosal Immun.* 107, 243–274. doi: 10.1016/S0065-2776(10)07001-X

Christensen, R., Marcussen, A. B., Wortwein, G., Knudsen, G. M., and Aznar, S. (2008). A beta((1-42)) injection causes memory impairment, lowered cortical and serum BDNF levels, and decreased hippocampal 5-HT2A levels. *Exp. Neurol.* 210, 164–171. doi: 10.1016/j.expneurol.2007.10.009

Cryan, J. F., O'Riordan, K. J., Cowan, C. S. M., Sandhu, K. V., Bastiaanssen, T. F. S., Boehme, M., et al. (2019). The microbiota-gut-brain axis. *Physiol. Rev.* 99, 1877–2013. doi: 10.1152/physrev.00018.2018

Dinan, T. G., and Cryan, J. F. (2017). Gut instincts: microbiota as a key regulator of brain development, ageing and neurodegeneration. *J. Physiol. Lond.* 595, 489–503. doi: 10.1113/Jp273106

Donaldson, G. P., Lee, S. M., and Mazmanian, S. K. (2016). Gut biogeography of the bacterial microbiota. *Nat. Rev. Microbiol.* 14, 20–32. doi: 10.1038/nrmicro3552

Earley, Z. M., Akhtar, S., Green, S. J., Naqib, A., Khan, O., Cannon, A. R., et al. (2015). Burn injury alters the intestinal microbiome and increases gut permeability and bacterial translocation. *PLoS One* 10:e0129996. doi: 10.1371/journal.pone.0129996

Eckburg, P. B., Bik, E. M., Bernstein, C. N., Purdom, E., Dethlefsen, L., Sargent, M., et al. (2005). Diversity of the human intestinal microbial flora. *Science* 308, 1635–1638. doi: 10.1126/science.1110591

Edgar, R. C. (2010). Search and clustering orders of magnitude faster than BLAST. *Bioinformatics* 26, 2460–2461. doi: 10.1093/bioinformatics/btq461

Edgar, R. C. (2013). UPARSE: highly accurate OTU sequences from microbial amplicon reads. *Nat. Methods* 10, 996–998. doi: 10.1038/nmeth.2604

Feighery, L., Smyth, A., Keely, S., Baird, A. W., O'Connor, W. T., Callanan, J. J., et al. (2008). Increased intestinal permeability in rats subjected to traumatic frontal lobe percussion brain injury. *J. Trauma Inj. Infect. Crit. Care* 64, 131–137. doi: 10.1097/TA.0b013e3181568d9f

Gilbert, J. A., Quinn, R. A., Debelius, J., Xu, Z. J. Z., Morton, J., Garg, N., et al. (2016). Microbiome-wide association studies link dynamic microbial consortia to disease. *Nature* 535, 94–103. doi: 10.1038/nature18850

Gitter, B. D., Boggs, L. N., May, P. C., Czilli, D. L., and Carlson, C. D. (2000). Regulation of cytokine secretion and amyloid precursor protein processing by proinflammatory amyloid beta (A beta). *Ann. N. Y. Acad. Sci.* 917, 154–164. doi: 10.1111/j.1749-6632.2000.tb05379.x

Goyal, D., Ali, S. A., and Singh, R. K. (2021). Emerging role of gut microbiota in modulation of neuroinflammation and neurodegeneration with emphasis on Alzheimer's disease. *Prog. Neuro Psychopharmacol. Biol. Psychiatry* 106:110112. doi: 10.1016/j.pnpbp.2020.110112

Granic, I., Masman, M. F., Mulder, C. K., Nijholt, I. M., Naude, P. J. W., Haan, A. D., et al. (2010). LPYFDa neutralizes amyloid-β-induced memory impairment and toxicity. *J. Alzheimers Dis. Jad.* 19, 991–1005. doi: 10.3233/JAD-2010-1297

Hamer, H. M., Jonkers, D., Venema, K., Vanhoutvin, S., Troost, F. J., and Brummer, R. J. (2008). Review article: the role of butyrate on colonic function. *Aliment. Pharmacol. Therap.* 27, 104–119. doi: 10.1111/j.1365-2036.2007.03562.x

Hamilton, A. L., Kamm, M. A., De Cruz, P., Wright, E. K., Feng, H., Wagner, J., et al. (2020). Luminal microbiota related to Crohn's disease recurrence after surgery. *Gut Microbes* 11, 1713–1728. doi: 10.1080/19490976.2020.1778262

Harach, T., Marungruang, N., Duthilleul, N., Cheatham, V., Mc Coy, K. D., Frisoni, G., et al. (2017). Reduction of Abeta amyloid pathology in APPPS1 transgenic mice in the absence of gut microbiota. *Sci. Rep.* 7:41802. doi: 10.1038/srep41802

Hardy, J., and Selkoe, D. J. (2002). The amyloid hypothesis of Alzheimer's disease: progress and problems on the road to therapeutics. *Science* 297, 353–356. doi: 10.1126/science.1072994

Hu, S. W., Wang, J. H., Xu, Y. L., Yang, H. C., Wang, J. F., Xue, C. H., et al. (2019). Anti-inflammation effects of fucosylated chondroitin sulphate from *Acaudina molpadioides* by altering gut microbiota in obese mice. *Food Funct.* 10, 1736–1746. doi: 10.1039/c8fo02364f

Iqbal, K., Liu, F., and Gong, C. X. (2016). Tau and neurodegenerative disease: the story so far. *Nat. Rev. Neurol.* 12, 15–27. doi: 10.1038/nrneurol.2015.225

Jing, Y. L., Yu, Y., Bai, F., Wang, L. M., Yang, D. G., Zhang, C., et al. (2021). Effect of fecal microbiota transplantation on neurological restoration in a spinal cord injury mouse model: involvement of brain-gut axis. *Microbiome* 9, 1–21. doi: 10.1186/s40168-021-01007-y

Kelley, B.-B., Yu, D., and Weihong, S. (2011). Morris water maze test for learning and memory deficits in Alzheimer's disease model mice. *J. Visual. Exp.* 53:2920. doi: 10.3791/2920

Kim, M. S., Kim, Y., Choi, H., Kim, W., Park, S., Lee, D., et al. (2020). Transfer of a healthy microbiota reduces amyloid and tau pathology in an Alzheimer's disease animal model. *Gut* 69, 283–294. doi: 10.1136/gutjnl-2018-317431

Kowalski, K., and Mulak, A. (2019). Brain-gut-microbiota axis in Alzheimer's disease. *J. Neurogastroenterol. Motil.* 25, 48–60. doi: 10.5056/jnm18087

Krabbe, G., Halle, A., Matyash, V., Rinnenthal, J. L., Eom, G. D., Bernhardt, U., et al. (2013). Functional impairment of microglia coincides with beta-amyloid

deposition in mice with Alzheimer-like pathology. *PLoS One* 8:e60921. doi: 10.1371/journal.pone.0060921

Li, N., Zuo, B., Huang, S., Zeng, B., Han, D., Li, T., et al. (2020). Spatial heterogeneity of bacterial colonization across different gut segments following inter-species microbiota transplantation. *Microbiome* 8:161. doi: 10.1186/s40168-020-00917-7

Looft, T., Allen, H. K., Cantarel, B. L., Levine, U. Y., Bayles, D. O., Alt, D. P., et al. (2014). Bacteria, phages and pigs: the effects of in-feed antibiotics on the microbiome at different gut locations. *ISME J.* 8, 1566–1576. doi: 10.1038/ismej.2014.12

Lynch, S. V., and Pedersen, O. (2016). The human intestinal microbiome in health and disease. *N. Engl. J. Med.* 375, 2369–2379. doi: 10.1056/NEJMra1600266

Martinez-Guryn, K., Leone, V., and Chang, E. B. (2019). Regional diversity of the gastrointestinal microbiome. *Cell Host Microbe* 26, 314–324. doi: 10.1016/j.chom.2019.08.011

Mathys, H., Davila-Velderrain, J., Peng, Z., Gao, F., Mohammadi, S., Young, J. Z., et al. (2019). Single-cell transcriptomic analysis of Alzheimer's disease. *Nature* 570, 332–337. doi: 10.1038/s41586-019-1195-2

Minter, M. R., Zhang, C., Leone, V., Daina, L. R., Zhang, X., Oyler-Castrillo, P., et al. (2016). Antibiotic-induced perturbations in gut microbial diversity influences neuro-inflammation and amyloidosis in a murine model of Alzheimer's disease. *Sci. Rep.* 6:30028. doi: 10.1038/srep30028

Mondot, S., Lepage, P., Seksik, P., Allez, M., and Marteau, P. F. J. G. (2015). Structural robustness of the gut mucosal microbiota is associated with Crohn's disease remission after surgery. *Gut* 65, 954–962. doi: 10.1136/gutjnl-2015-309184

O'Hare, E., Weldon, D. T., Mantyh, P. W., Ghilardi, J. R., Finke, M. P., Kuskowski, M. A., et al. (1999). Delayed behavioral effects following intrahippocampal injection of aggregated A beta((1-42). *Brain Res.* 815, 1–10. doi: 10.1016/S0006-8993(98)01002-6

Pereira, I. T., and Burwell, R. D. (2015). Using the spatial learning index to evaluate performance on the water maze. *Behav. Neurosci.* 129, 533–539. doi: 10.1037/bne0000078

Price, M. N., Dehal, P. S., and Arkin, A. P. (2010). FastTree 2–approximately maximum-likelihood trees for large alignments. *PLoS One* 5:e9490. doi: 10.1371/journal.pone.0009490

Sarkar, S. R., and Banerjee, S. (2019). Gut microbiota in neurodegenerative disorders. *J. Neuroimmunol.* 328, 98–104. doi: 10.1016/j.jneuroim.2019.01.004

Segata, N., Izard, J., Waldron, L., Gevers, D., Miropolsky, L., Garrett, W. S., et al. (2011). Metagenomic biomarker discovery and explanation. *Genome Biol.* 12:R60. doi: 10.1186/gb-2011-12-6-r60

Sender, R., Fuchs, S., and Milo, R. (2016). Revised estimates for the number of human and bacteria cells in the body. *PLoS Biol.* 14:e1002533. doi: 10.1371/journal.pbio.1002533

Sierra-Filardi, E., Puig-Kroger, A., Blanco, F. J., Nieto, C., Bragado, R., Palomero, I., et al. (2011). Activin A skews macrophage polarization by promoting a proinflammatory phenotype and inhibiting the acquisition of anti-inflammatory macrophage markers. *Blood* 117, 5092–5101. doi: 10.1182/blood-2010-09-306993

Sun, M., Ma, K., Wen, J., Wang, G. X., Zhang, C. L., Li, Q., et al. (2020). A review of the brain-gut-microbiome axis and the potential role of microbiota in Alzheimer's disease. *J. Alzheimers Dis.* 73, 849–865. doi: 10.3233/Jad-190872

Sundman, M. H., Chen, N. K., Subbian, V., and Chou, Y. H. (2017). The bidirectional gut-brain-microbiota axis as a potential nexus between traumatic brain injury, inflammation, and disease. *Brain Behav. Immun.* 66, 31–44. doi: 10.1016/j.bbi.2017.05.009

Tropini, C., Earle, K. A., Huang, K. C., and Sonnenburg, J. L. (2017). The gut microbiome: connecting spatial organization to function. *Cell Host Microbe* 21, 433–442. doi: 10.1016/j.chom.2017.03.010

Wang, S. H., Zhu, K. X., Hou, X. X., and Hou, L. J. (2021). The association of traumatic brain injury, gut microbiota and the corresponding metabolites in mice. *Brain Res.* 1762:147450. doi: 10.1016/j.brainres.2021.147450

Wang, W. T., Li, Y. B., Wu, Q. J., Pan, X., He, X. H., and Ma, X. X. (2020). High-throughput sequencing study of the effect of transabdominal hysterectomy on intestinal flora in patients with uterine fibroids. *BMC Microbiol.* 20:98. doi: 10.1186/s12866-020-01779-7

Wang, X. Y., Sun, G. Q., Feng, T., Zhang, J., Huang, X., Wang, T., et al. (2019). Sodium oligomannate therapeutically remodels gut microbiota and suppresses gut bacterial amino acids-shaped neuroinflammation to inhibit Alzheimer's disease progression. *Cell Res.* 29, 787–803. doi: 10.1038/s41422-019-0216-x

Wesseling, H., Mair, W., Kumar, M., Schlaffner, C. N., Tang, S. J., Beerepoot, P., et al. (2020). Tau PTM profiles identify patient heterogeneity and stages of Alzheimer's disease. *Cell* 183, 1699–1713. doi: 10.1016/j.cell.2020.10.029

Xu, M. J., Yan, T. X., Fan, K. Y., Wang, M. S., Qi, Y., Xiao, F., et al. (2019). Polysaccharide of *Schisandra chinensis* Fructus ameliorates cognitive decline in a mouse model of Alzheimer's disease. *J. Ethnopharmacol.* 237, 354–365. doi: 10.1016/j.jep.2019.02.046

Yang, B. Y., Tan, J. Y., Liu, Y., Liu, B., Jin, S., Guo, H. W., et al. (2018). A UPLC-TOF/MS-based metabolomics study of rattan stems of *Schisandra chinensis* effects on Alzheimer's disease rats model. *Biomed. Chromatogr.* 32:e4037. doi: 10.1002/bmc.4037

Zhao, W. J., Wang, Y. P., Liu, S. Y., Huang, J. J., Zhai, Z. X., He, C., et al. (2015). The dynamic distribution of porcine microbiota across different ages and gastrointestinal tract segments. *PLoS One* 10:e0117441. doi: 10.1371/journal.pone.0117441

Conflict of Interest: The authors declare that the research was conducted in the absence of any commercial or financial relationships that could be construed as a potential conflict of interest.

Publisher's Note: All claims expressed in this article are solely those of the authors and do not necessarily represent those of their affiliated organizations, or those of the publisher, the editors and the reviewers. Any product that may be evaluated in this article, or claim that may be made by its manufacturer, is not guaranteed or endorsed by the publisher.

frontiers | Frontiers in Microbiology

ORIGINAL RESEARCH
published: 01 April 2022
doi: 10.3389/fmicb.2022.847468

Psychoactive Effects of *Lactobacillus johnsonii* BS15 on Preventing Memory Dysfunction Induced by Acute Ethanol Exposure Through Modulating Intestinal Microenvironment and Improving Alcohol Metabolic Level

Ning Sun[1†], Bin Zhu[2†], Jinge Xin[1,3†], Lianxin Li[1†], Baoxing Gan[1], Xi Cao[1], Jing Fang[4], Kangcheng Pan[1], Bo Jing[1], Yan Zeng[1], Cheng Lv[5], Ling Zhao[5], Dong Zeng[1], Peng Xu[2], Hesong Wang[3]* and Xueqin Ni[1]**

[1] Animal Microecology Institute, College of Veterinary Medicine, Sichuan Agricultural University, Chengdu, China, [2] MOE Key Laboratory for Neuroinformation, Center for Information in Medicine, The School of Life Sciences and Technology, Clinical Hospital of Chengdu Brain Science Institute, University of Electronic Science and Technology of China, Chengdu, China, [3] Guangzhou Beneco Biotechnology Co., Ltd., Guangzhou, China, [4] Key Laboratory of Animal Diseases and Environmental Hazards of Sichuan Province, College of Veterinary Medicine, Sichuan Agricultural University, Chengdu, China, [5] Department of Pharmacy, College of Veterinary Medicine, Sichuan Agricultural University, Chengdu, China

The negative effects of ethanol (EtOH) abuse on the body have been widely reported in recent years. Building on the microbiota-gut-brain axis hypothesis, our study aimed to demonstrate the potential psychobiotic role of *Lactobacillus johnsonii* BS15 in the preventive effects of acute EtOH intake on memory impairment. We also determined whether *L. johnsonii* BS15 intake could effectively improve resistance to acute drinking and alleviate the adverse effects of EtOH. Male mice were fed *L. johnsonii* BS15 orally with (Probiotic group) or without (Control and Alcohol groups) daily dose of 0.2×10^9 CFU/ml per mouse for 28 days. Gavage with *L. johnsonii* BS15 significantly modified the ileal microbial ecosystem (assessed by 16S rRNA gene sequencing) in favor of Firmicutes and *Lactobacillus,* indicating the ability of BS15 to restore the gut microbiota. The acute EtOH exposure model (7 g/kg EtOH per mice) was established by gavage, which was administered to the alcohol and probiotic groups on day 28 of the experiment. The *L. johnsonii* BS15 intake effectively reduced alcohol unconsciousness time, blood alcohol concentration, and serum aspartate aminotransferase (AST) and alanine aminotransferase (ALT) levels. Meanwhile, the improvement of ethanol resistance time and the activities of alcohol dehydrogenase (ADH) and aldehyde dehydrogenase (ALDH) in the liver were shown by BS15 in acute alcohol-induced mice. We found that acute EtOH exposure reduced the exploration ratio (assessed by the novel object recognition test), escape latency, number of errors (assessed by passive avoidance test), and spontaneous exploration (assessed by T-maze test) in mice, which were

OPEN ACCESS

Edited by:
Lifeng Zhu,
Nanjing Normal University, China

Reviewed by:
Mindy Engevik,
Medical University of South Carolina, United States
Tongjie Chai,
Shandong Agricultural University, China
Wen-Tao Yang,
Jilin Agricultural University, China

***Correspondence:**
Peng Xu
xupeng@uestc.edu.cn
Hesong Wang
sunasa1030@foxmail.com
Xueqin Ni
xueqinni@foxmail.com

[†] These authors have contributed equally to this work

Specialty section:
This article was submitted to Microbial Symbioses, a section of the journal Frontiers in Microbiology

Received: *02 January 2022*
Accepted: *28 February 2022*
Published: *01 April 2022*

Citation:
Sun N, Zhu B, Xin J, Li L, Gan B, Cao X, Fang J, Pan K, Jing B, Zeng Y, Lv C, Zhao L, Zeng D, Xu P, Wang H and Ni X (2022) Psychoactive Effects of Lactobacillus johnsonii BS15 on Preventing Memory Dysfunction Induced by Acute Ethanol Exposure Through Modulating Intestinal Microenvironment and Improving Alcohol Metabolic Level. Front. Microbiol. 13:847468. doi: 10.3389/fmicb.2022.847468

obviously improved by *L. johnsonii* BS15. In the hippocampus, *L. johnsonii* BS15 significantly reversed the decrease in antioxidant capacity of superoxide dismutase (SOD), malondialdehyde (MDA), and glutathione (GSH) and mRNA expression of memory-related functional proteins of brain-derived neurotrophic factor (BDNF) and cyclic ampresponse element binding protein (CREB) in the hippocampal tissue after acute EtOH exposure. In conclusion, *L. johnsonii* BS15 intake appears as a promising psychoactive therapy to ameliorate alcohol-mediated memory impairment by increasing EtOH metabolic levels.

Keywords: abuse ethanol, *Lactobacillus johnsonii* BS15, memory impairment, microbiota-gut-brain axis, hippocampus

INTRODUCTION

Alcoholism is an alarming global issue (Neyrinck et al., 2017). Alcohol-related injuries are one of the most common preventable diseases worldwide, with 3.3 million deaths, accounting for 6% of all global deaths (World Health Organization, 2014; Asrani et al., 2019). It is well known that alcohol abuse can damage multiple organs, mainly the liver, intestine, and brain (Bajaj, 2019). Studies have shown that long-term drinking can change the intestinal microbial composition, damage the intestinal mucosal barrier, and destroy intestinal homeostasis (Stärkel and Schnabl, 2016). Additionally, dopamine, glutamate, and γ-changes in aminobutyric acid (GABA) release are associated with excessive alcohol exposure (Alasmari et al., 2018). These neuroadaptations of psychoneuroimmunity promote mood regulation disorders and further trigger inflammation, leading to alcohol use disorder (AUD) and related affective comorbidities (Koob, 2013; Hillemacher et al., 2018). Based on preclinical studies, there is increasing evidence that alcoholism negatively affects brain memory and cognitive function (Scholey et al., 2019). A recent study reported that alcohol addiction could promote rapid acetylation of histones in the brain, thereby affecting the expression of learning and memory genes (Mews et al., 2019). Moreover, long-term intake of high-dose alcohol can induce cognitive impairment, improve the activity of β-amyloid precursor protein (β-APP)-related enzymes, increase the content and deposition of amyloid β-protein (Aβ), and trigger the progression of Alzheimer's disease (AD) (Gong et al., 2021). Unfortunately, the exact mechanism of alcohol-induced memory and cognitive impairment remains unclear, making it difficult to prevent acute or chronic ethanol exposure.

The microbiota, comprising trillions of microbes in the gut, has become a major driver of the gut-brain axis (GBA). Most surprisingly, the microbiota largely shapes the structure and function of the nervous system (Cryan et al., 2019). Perhaps the most specific effect of the microbiota on the host is the regulation of brain physiology and behavior (Hao et al., 2019). Over the past two decades, explosive research has been conducted in the field of microbiota-host interaction. Symbiotic microorganisms have been shown to alter host neurophysiology and pathophysiology, leading to changes in neurological and mental diseases, including depression, anxiety, and social behavior (Sharon et al., 2016; Vuong et al., 2017; Cryan et al., 2019; Fang et al., 2020; Morais et al., 2021). Interestingly, probiotics, composed of different strains of lactic acid bacteria and/or *Bifidobacteria*, have been shown to affect the behavior of mice, including reduced anxiety-related symptoms (Bravo et al., 2011; Messaoudi et al., 2011; Mohammadi et al., 2016) and improved memory (Smith et al., 2014; O'Hagan et al., 2017). The use of probiotic strains can improve the memory of objects and object positions (Smith et al., 2014; Liang et al., 2015; Warburton and Brown, 2015; O'Hagan et al., 2017), rather than object chronological memory (O'Hagan et al., 2017). By analyzing the metabolic characteristics of specific lactic acid bacteria strains in the mouse brain, metabolic clues to enhance memory have been identified. However, metabolic mediators, if any, between the gut and brain remain unknown. To date, it is certain that reduction of the intestinal microbial community can prevent alcohol-induced neuroinflammation, resulting in changes in the expression of inflammatory bodies in the intestine and brain (Lowe et al., 2018). In conclusion, the interaction between alcohol-related brain dysfunction and communication *via* the gut microbiota axis remains unclear. Therefore, more animal experimental evidence is needed to prove the relationship between intestinal flora and the hippocampus under different conditions.

Lactobacillus johnsonii BS15 (CCTCC M2013663) was isolated from self-made yogurt in Hongyuan Prairie, Aba Autonomous Prefecture, China (Xin et al., 2014). The potential probiotic effects of *L. johnsonii* BS15 have been demonstrated in our previous studies (Xin et al., 2014; Sun et al., 2020). A recent study (Wang et al., 2021) reported that BS15 could resist demyelination and neuroinflammation in the brain by reducing impairment and improving fluoride-induced memory dysfunction. Therefore, we studied the effects of acute ethanol (EtOH) exposure and supplementation with *L. johnsonii* BS15 on hippocampal memory and cognitive functions in mice using high-throughput sequencing, behavioral testing, and biochemical analysis. From the perspective of the gut-brain axis, it is unclear whether *L. johnsonii* BS15 reconstructs the community composition and diversity in the intestinal microbiome before alcohol abuse and whether different gut species patterns could effectively prevent liver injury and memory dysfunction in mice after acute EtOH exposure. Therefore, under the same experimental conditions, combining these two aspects in animal experiments could explore the influence of excessive EtOH intake and beneficial treatment on alcohol metabolism and hippocampal memory function.

MATERIALS AND METHODS

Culture and Treatment With BS15

In this study, *L. johnsonii* BS15 was cultured anaerobically in de Man, Rogosa, and Sharpe (MRS) broth (QDRS Biotec, Qingdao, Shandong, China). The plate count method was used to count the bacterial cells. Briefly, the bacterial solution was diluted 10 times with phosphate-buffered saline (PBS) (pH 7.0). Dilution gradients of 10^{-5}, 10^{-6}, and 10^{-7} were chosen, and 10 μl of each gradient was drawn to drop onto the MRS agar medium and repeated thrice. MRS agar medium was then cultured for 36 h at 37°C. An appropriate gradient (easy to count bacteria) was selected for bacterial counting. Next, centrifugation (3,000 rpm, 4℃, 15 min) and washing were done to separate the cells from the cultures and were resuspended in PBS for experimental use. The concentration of the suspension was 1×10^9 CFU BS15/ml (daily consumption dose: 0.2 ml/mice; Xin et al., 2014).

Study Design and Animal Treatment

A total of 146 male Institute of Cancer Research (ICR) mice (22 ± 2 g) were purchased from the Chengdu Dashuo Biological Research Institute (Chengdu, Sichuan, China). All animals were fed normally for 7 days (adaptation period). In this study, the first day after the adaptation period was defined as day 1, as the experiment started. Mice were divided into three groups: control (C), alcohol (A), and probiotics (P). The mice in the P group were fed (gavage) the suspension of *L. johnsonii* BS15 once a day at 8 a.m (day 1–day 28). Groups C and A were treated with an equal PBS volume. All animals were kept in a room where temperature (22 ± 2°C) and a 12-h/12-h light/dark cycle (dark period: 7 p.m.–7 a.m.) could be controlled. The acute EtOH exposure model was induced by a single intragastric administration of 32% (v/v) EtOH at a dose of 7 g/kg on day 28 in the A and P groups (Carson and Pruett, 1996). Group C was treated with the same PBS volume. All animal experiments were performed in accordance with the Guidelines for the Care and Use of Laboratory Animals and approved by the Institutional Animal Care and Use Committee of Sichuan Agricultural University (approval number: SYXKchuan2019–187). All behavioral tasks were conducted between 7 a.m. and 1 p.m. **Figure 1** illustrates the experimental design of this study.

Measurement of Ethanol Resistance Time, Unconsciousness Time, and Blood Ethanol Concentration

On day 28 of the experiment, 6–10 mice from A and P groups were selected for the measurement of ethanol resistance time, unconsciousness time, and blood ethanol concentration after acute EtOH exposure.

Ethanol resistance time was measured as the time interval between acute exposure to EtOH and the loss of righting reflex. Unconsciousness time was measured as the duration of loss of righting reflex. In our study, mice were administered a high dose of EtOH and were determined to have lost the righting reflex when ataxia developed. Meanwhile, the loss of return to normal reflex time was evaluated as the time taken for the animals to return to normal. At 30, 60, 90, and 150 min after acute EtOH exposure, the blood of the orbital venous plexus was taken from a heparinized tube. Subsequently, the blood samples were centrifuged at 1,000 × *g* at 4°C for 15 min (Chen et al., 2014).

Passive Avoidance Test

Habituation and Training Phase

On day 27 of the experiment, 10 mice from each group were put into the central platform to adapt to the testing device, and then, the grid was powered on (36 V, 50 Hz, 1 mA, 2 s) for 3 min to train. When the mouse's foot touches the grid, the animal can obtain an electric shock that keeps it on the central platform. The mice were then put back into the cage, and the testing phase was conducted 24 h later.

During the testing phase, the mice, approximately 8 h after acute EtOH exposure, were placed on the central platform of the testing device again and were required to stay for 3 min. Subsequently, the grid in the device was powered during the testing period. Briefly, the interval when the animal walked off the platform for the first time was denoted as escape latency. In addition, the total number of times the mice left the platform within 3 min was recorded as the time of error. Therefore, shorter escape latency or greater error times in mice indicate memory dysfunction (Chen et al., 2014).

T-Maze

On day 23 of the experiment, eight mice from each group were selected for the T-maze test. We conducted a T-maze test on the animals based on the method outlined by Deacon and Rawlins (2006). This included a feeding point for food provided at the distal end of each goal arm. The proximal end had a regulable door for controlling the open or closed goal arm. Besides, the food made up of 1:1 (v/v) water/full-fat sweetened condensed milk (Nestle, Qingdao, Shandong, China) was provided as a reward, of which 0.07 ml was given per trial by preset pipette.

Habituation and Exploration Phases

During the habituation phase (2 days), animals were softly stroked five times every day (3 min per time) to make the mice adapt to the smell and touch from the experimenters. The mice were then fed with reward food (0.5 ml) each day to reduce their fear of new things. Finally, the exploration phase (3 days) was conducted after the habituation phase, and mice were placed into a testing apparatus in which two goal arms were opened and allowed to move freely for 10 min. Subsequently, the mice were allowed to explore from the start arm to one goal arm (no more than 3 min), where the reward food was given to the food point. Simultaneously, the other goal arm was closed by the door. Each mouse was trained four times every day (equal numbers of left and right goal arms opened).

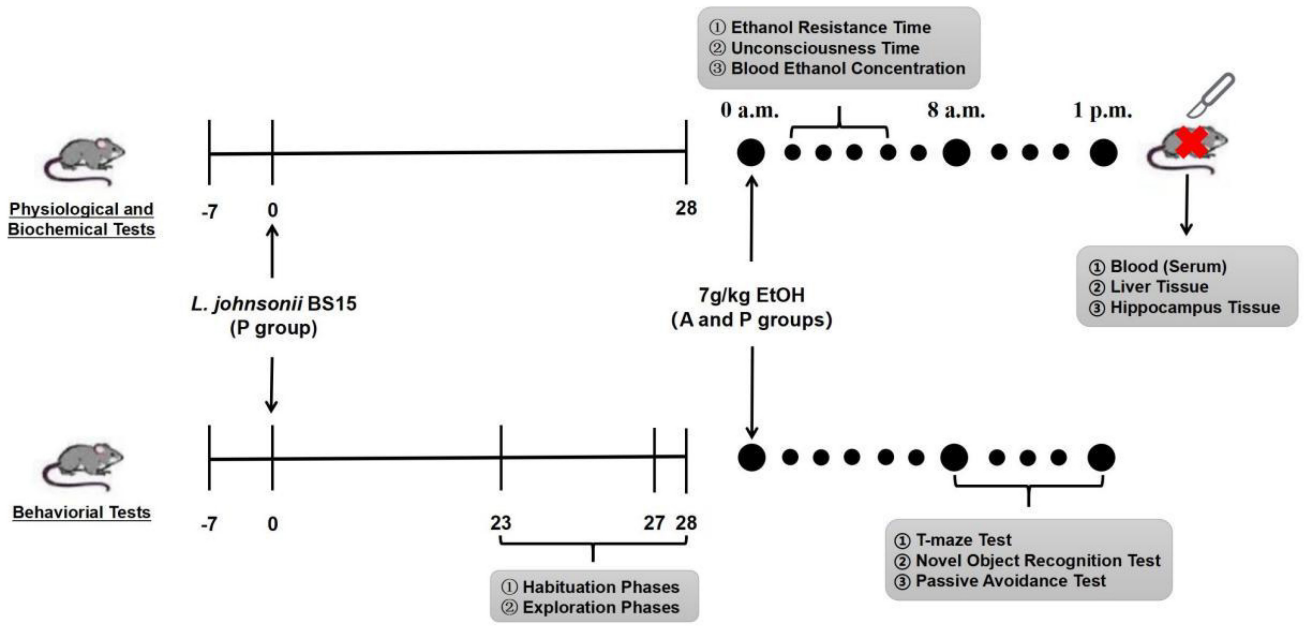

FIGURE 1 | Flow diagram of experimental design. Mice were infected with EtOH (7 g/kg mice) at 28th day after orogastric challenge with either *L. johnsonii* BS15 suspension or PBS solution. Habituation, exploration, and training phase of behavioral tasks were conducted at 23rd day (T-maze test), 27th day (passive avoidance test), and 28th day (novel object recognition test), respectively, then the testing phase of all behavioral tasks was performed about 8 h after acute EtOH exposure at 28th day; 8–10 mice in each group were required to participate in T-maze test, novel object recognition test, and passive avoidance test, respectively. Besides, blood ethanol concentration, ethanol resistance, and unconsciousness time were evaluated by additional 6–10 mice in each group in the presence of acute EtOH exposure. In the end, blood, liver, and hippocampal tissues were collected to measure biochemical tests.

Testing Phase

One goal arm of the apparatus was closed, while the other goal arm remained open (equal times of left and right goal arm) and provided rewarding food at the corresponding point. One mouse, approximately 8 h after acute EtOH exposure, was allowed to explore freely in the apparatus for no more than 3 min and was subsequently removed. After waiting for 0 or 1 min, the mouse was again placed in the maze device. At the same time, the previously closed goal arm was opened, and rewarding food was given at the food point. If different goal arms were entered by the same mice in the two trials, it was recorded as correct. If the same goal arm was entered twice continuously, it was recorded as an error. Every mouse underwent the same process for 10 rounds (Deacon and Rawlins, 2006; Gareau et al., 2011).

Novel Object Recognition Test

The test procedure consisted of three phases: habituation, exploration, and testing (Antunes and Biala, 2012). After 28 days of experimentation, 10 mice from each group were selected for the novel object recognition test (NOR).

Habituation and Exploration Phase

Each mouse was allowed to move freely in the open-field area (l × b × h = 40 × 40 × 45 cm) for 1 h in the absence of objects. The mouse was then removed from the area and placed in its home cage. Each mouse was placed in the area to freely explore two different objects (#A and #B) for 5 min during the familiarization phase. The two objects were placed at opposite positions in the cage.

Testing Phase

The mouse was given an intermediate retention interval of 20 min and then placed in the same area and re-exposed to object (#B) along with a new object (#C, distinguishable from object #A). The exploration ratio [F#C/(F#C + F#B) × 100, where F#C = frequency of exploring object #C, and F#B = frequency of exploring object #B] was calculated to evaluate memory function. The objects used in this study included a gray hard stone (#A), white hard stone (#B), and small blue cap (#C).

Biochemical Analysis

On day 28 of this study, six mice from each treatment group were selected for biochemical measurements approximately 8 h after acute EtOH exposure. The hippocampus, liver, and blood were collected, and the serum was separated. The liver and part of the hippocampus were collected. Serum and tissue supernatants were prepared for subsequent biochemical analysis. The activities of aspartate aminotransferase (AST) and alanine aminotransferase (ALT) in the serum and the activities of superoxide dismutase (SOD), glutathione peroxidase (GSH-Px), GSH, and malondialdehyde (MDA) in the hippocampus were determined using kits purchased from Nanjing Jiancheng Institute of Biological Engineering (Nanjing, China). ADH and ALDH levels in the liver were determined using kits purchased from Abcam (Cambridge, MA, United States). The

detailed procedures followed the manufacturer's instructions, using different reagent kits.

Real-Time Quantitative Polymerase Chain Reaction Analysis of Gene Expression

Residual hippocampal RNA during the above sampling process was extracted using E.Z.N.A.® Total RNA Kit (OMEGA Bio-Tek, Doraville, GA, United States) based on the method outlined by product instructions. The total RNA was detected by the ratio of absorbance at 260 nm and 280 nm and by agarose gel electrophoresis for quantitative and qualitative assessments. Then, the total RNA was transcribed into first-strand complementary DNA (cDNA) using the PrimeScript RT reagent kit with gDNA Eraser (Thermo Scientific, Waltham, MA, United States) according to the method outlined by the manufacturer's instructions. Finally, the cDNA products were stored at -80°C until further study. Real-time quantitative polymerase chain reaction (RT-qPCR) test was conducted using LightCycle 96 Real-Time System (Boehringer Mannheim GmbH, Germany) and SYBR Green Supermix (Bio-Rad, Hercules, CA, United States) to detect the relative expression levels of memory-related functional proteins in the hippocampus tissue. The reaction mixture (10 μl) included cDNA products (1 μl), forward and reverse primers (2 μl), SYBR Green Supermix (5 μl), and sterile deionized water (2 μl). The thermocycling protocol was as follows: 5 min at 95°C, followed by 40 cycles of 10 s denaturation at 95°C, and 30 s annealing/extension at the optimum temperature (**Table 1**). A melting curve analysis was performed to monitor the purity of the PCR product. β-actin was used to normalize the relative mRNA expression levels of target genes, with values presented as $2^{-\Delta\Delta Cq}$. Primer sequences and optimum annealing temperatures are listed in **Table 1** (Niu et al., 2018).

Intestinal Microbial Compositions in the Ileum

Before establishing the acute EtOH exposure model, the ileal contents of six mice were collected from the C and P groups for 16S rRNA gene sequencing.

Microbial DNA was obtained using an E.Z.N.A.TM stool DNA isolation kit (Omega Bio-Tek, Doraville, CA, United States). The final elution volume was 100 μl, and the purity, concentration, integrity, and fragment size were evaluated by electrophoresis on a 1% agarose gel. The 16S V4 region was amplified by PCR using the primer 515F/806R of the 16S rRNA gene. Then, the purified PCR products were formed into a library with Ion Plus Fragment Library Kit 48 rxns (Thermo Fisher Scientific, United States) and sequenced on the IonS5 XL platform (Thermo Fisher Scientific, United States) using single-end sequencing. The primers contained adapter sequences and single-end barcodes, which allowed pooling and direct sequencing of PCR products. Cutadapt (V1.9.1)[1] was applied to the high-quality 16S rRNA gene reads. Subsequently, the 16S rRNA gene read pairs were demultiplexed based on their unique barcodes, and the reads were merged using VSEARCH (Rognes et al., 2016). Sequences were clustered into operational taxonomic units (OTUs) with a similarity cutoff value of 97%. OTU representative sequences were produced using Uparse v7.0.1001. Species annotation analysis was performed on the OTU representative sequences through the SILVA database (SILVA database).[2] These samples were used for downstream analyses of alpha-diversity, beta-diversity, species composition, between-group variance, and correlation analysis in R v4.0.2.

[1]http://cutadapt.readthedocs.io/en/stable/

Statistical Analysis

The 16S rRNA sequencing data were analyzed using the Kruskal-Wallis test, followed by the Wilcoxon rank-sum test to assess significant differences between the different treatments.

Normality was evaluated using the Shapiro-Wilk normality test. If the data were not normally distributed, they were log-transformed for analysis. Data that remained non-normally distributed were analyzed using the Kruskal-Wallis test followed by the Wilcoxon rank-sum test. Normally distributed data were analyzed using one-way ANOVA followed by the least significant difference (LSD) test. Differences were considered statistically significant at $P < 0.05$. Differences were counted using IBM SPSS Statistics 25.0 and R v4.0.2.

RESULTS

The Diversity and Composition of Gut Microbial Community

Through 16s rRNA gene sequencing, we determined whether *L. johnsonii* BS15 supplementation influenced the gut microbiota. As shown in **Figures 2A,B**, the Shannon and Chao1 indices of the ileal microbiome in the P group were significantly lower than those of the control group ($P < 0.01$). Moreover, the high relative abundances of the other genera in the P group were different from those in the control group. Moreover, principal coordinate analysis (PCoA) based on Bray-Curtis showed a clear separation (**Figure 2C**) between the ileal microbiota of the control and P groups. Additionally, the ileal

[2]http://www.arb-silva.de/

TABLE 1 | Primer sequences for RT-qPCR in hippocampus.

Gene	Tm (°C)	Sequence
β-actin	60	Forward: GCTCTTTTCCAGCCTTCCTT Reverse: GATGTCAACGTCACACTT
BDNF	60	Forward: GCGCCCATGAAAGAAGTAAA Reverse: TCGTCAGACCTCTCGAACCT
CREB	60	Forward: CCAGTTGCAAACATCAGTGG Reverse: TTGTGGGCATGAAGCAGTAG
NCAM	60	Forward: GGGAACTCCATCAAGGTGAA Reverse: TTGAGCATGACGTGGACACT
c-Fos	59.5	Forward: CAGAGCGGGAATGGTGAAGA Reverse: CTGTCTCCGCTTGGAGTGTA

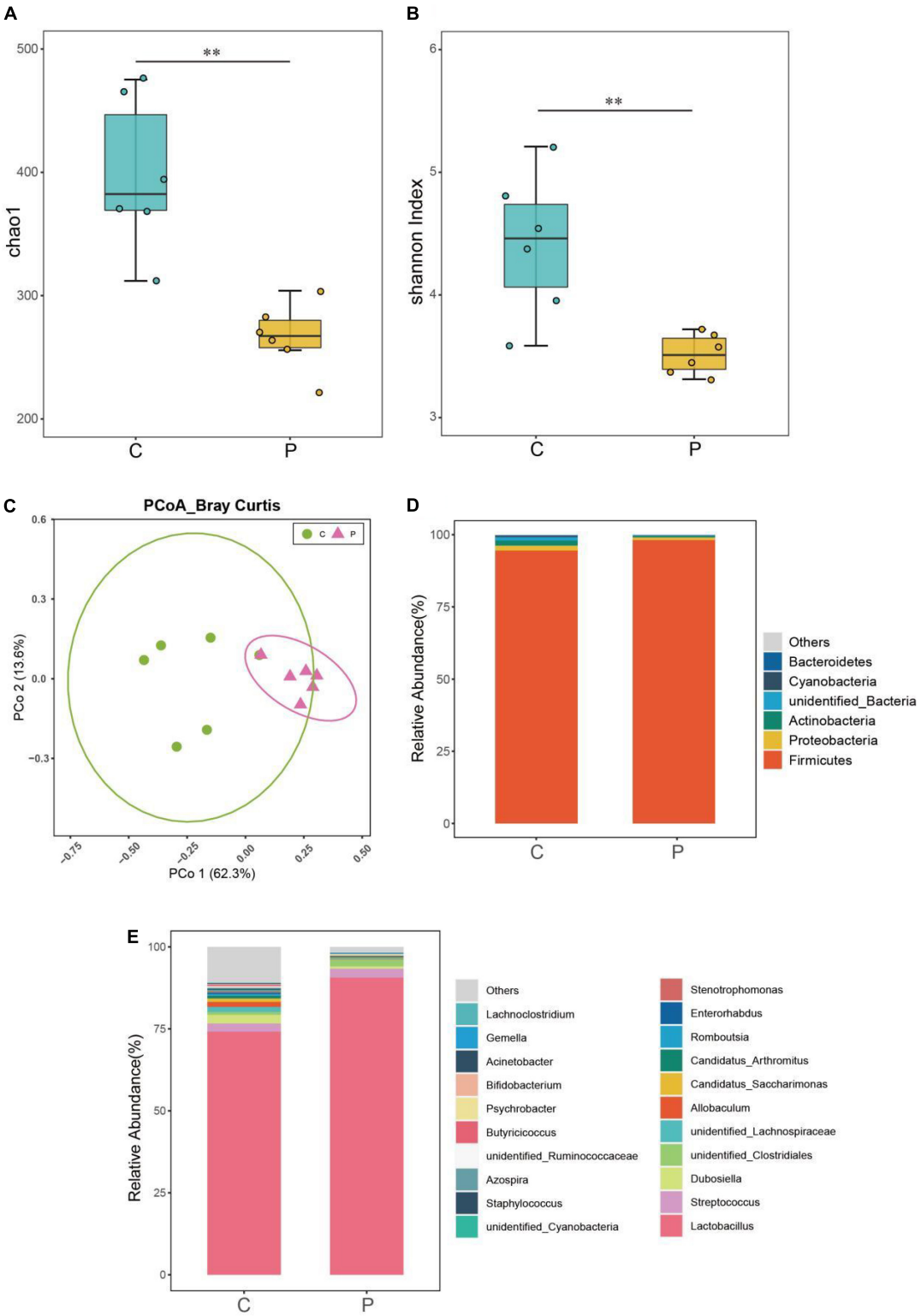

FIGURE 2 | Effects of *L. johnsonii* BS15 on the gut microbial diversity and composition in BS15-pretreated mice. Microbial **(A)** richness (Chao1) and **(B)** evenness (Shannon indexes) in ileal samples of each group. The difference in alpha diversity index was analyzed by Kruskal-Wallis test followed by Wilcoxon rank-sum test. $^{**}P < 0.01$ represents extremely significant differences between groups. **(C)** Principal coordinate analysis (PCoA) of Bray-Curtis distances between groups with or without BS15. The taxa of high relative abundance (>1%) at the **(D)** phylum level and **(E)** genus level of each group.

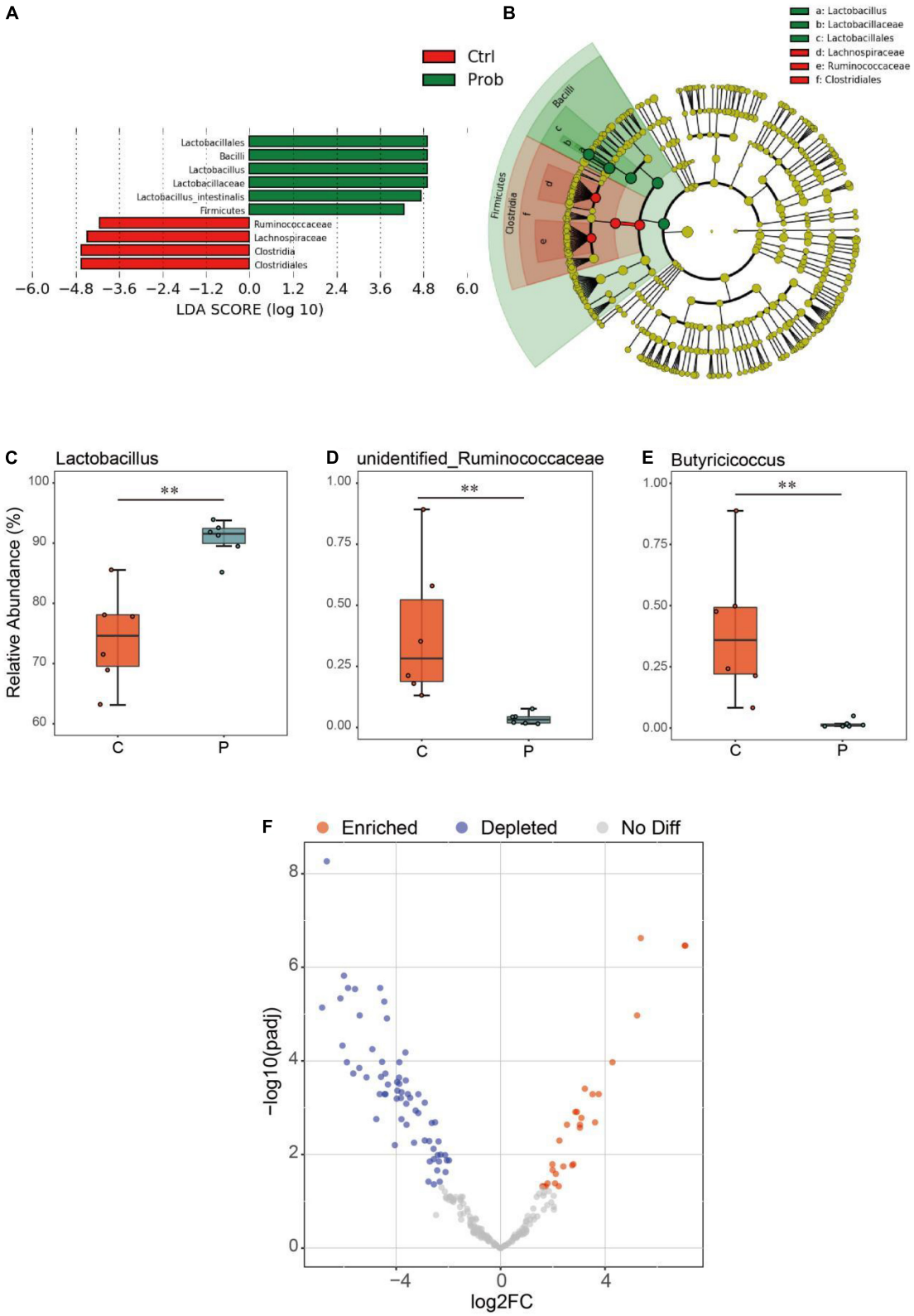

FIGURE 3 | Differential analysis of ileal microbiota in mice. The **(A)** linear discriminant analysis (LDA) score and **(B)** cladogram were generated from LDA effect size (LEfSe). Relative abundance (%) of the **(C)** *Lactobacillus*, **(D)** unidentified Ruminococcaceae, and **(E)** *Butyricicoccus* in each group. $^{**}P < 0.01$ represents extremely significant differences between groups.**(F)** Enrichment and depletion of the significant differentiated OTUs included in the ileal microbiome. Each point represents an individual species.

microbial communities in these two groups were dominated by Firmicutes at the phylum level (**Figure 2D**). The relative abundance of Firmicutes in the P group was significantly higher than that in the control group (**Figure 2E**). Conversely, the relative abundance of Actinobacteria, Bacteroidetes, and Proteobacteria decreased markedly in the P group compared with that in the control group. At the genus level (**Figure 2D**), *Lactobacillus* was the most abundant species in the control and P groups.

As shown in **Figures 3A,B**, compared with the control and P groups, the biomarkers in the control group were Ruminococcaceae, Lachnospiraceae, *Clostridia*, and Clostridiales, and those in the P group were Lactobacillales, Bacilli, *Lactobacillus*, Lactobacillaceae, *Lactobacillus intestinalis*, and Firmicutes. Compared with the C group, the relative abundance of *Lactobacillus* in the P group was significantly increased (**Figure 3C**, $P < 0.01$), and the relative abundance of unidentified Ruminococcaceae and *Butyricicoccus* of P group in the ileum decreased significantly (**Figures 3D,E**, $P < 0.01$). It was possible to quantify the microbial effects of *L. johnsonii* BS15 by analyzing significant differences in OTU abundance relative to the original ileal species (**Figure 3F**). Under the influence of *L. johnsonii* BS15, partial OTUs were enriched or competitively excluded in the ileum. For instance, 24 OTUs were significantly higher in the P group than that in the control group.

Effect of BS15 on Ethanol Resistance and Unconsciousness Time Following Acute Ethanol Exposure in Mice

The tolerance time (**Figure 4A**) and unconsciousness time (**Figure 4B**) were significantly altered by BS15 in the P group. In contrast to the A group, mice pretreated with *L. johnsonii* BS15 showed significantly prolonged body-righting reflex disappearance and shortened unconsciousness time ($P < 0.05$).

Effect of BS15 on Alcohol Metabolism Following Acute Ethanol Exposure in Mice

As shown in **Figures 5A,B**, AST and ALT activities in the serum were significantly elevated in group A compared with those in the control group. *L. johnsonii* BS15 pretreatment markedly decreased AST and ALT activities after acute EtOH exposure ($P < 0.05$). This indicated that pretreatment with *L. johnsonii* BS15 could effectively protect the liver from alcohol-induced injury.

Acute EtOH administration in mice induced a significant increase in ADH activity in the liver ($P < 0.05$), and the elevated ADH activity in BS15 pretreated groups was much higher than that in group A (**Figure 5C**, $P < 0.05$). A similar tendency was observed for ALDH activity between groups A and P (**Figure 5D**, $P < 0.05$).

The blood alcohol concentration reached a peak at 90 min after alcohol intake, and compared with the A group, the blood alcohol concentration was significantly lower at 60 and 90 min after alcohol administration in the *L. johnsonii* BS15 pretreated group (**Figure 5E**, $P < 0.05$).

Behavioral Tests

Figures 6–8 show the results of the behavioral tests for the memory abilities of the mice. Significantly lower exploration ratio (**Figure 6**) and escape latency (**Figure 7A**) were observed ($P < 0.05$) in group A than that in the control group. Correct times for 0 s and 1 min of retention intervals (**Figure 8**) in group A were also significantly lower ($P < 0.05$) than that in the control group. The error numbers (**Figure 7B**) in group A were significantly higher than that in the control group. In contrast, the exploration ratio (**Figure 6**), escape latency (**Figure 7A**), and correct times for 0 s and 1 min retention intervals (**Figure 8**) were significantly higher ($P < 0.05$) in the P group. The error numbers (**Figure 7B**) in group A were significantly lower ($P < 0.05$) than that in group P. Moreover, significant differences ($P < 0.05$) in escape latency and error numbers were observed between the control and P groups (**Figure 7**), whereas the number of correct responses and exploration ratio were not significant (**Figures 6**, **8**, $P > 0.05$).

The mRNA Expression of Memory-Related Functional Proteins in the Hippocampus

Figure 9 illustrates the differences in the mRNA expression levels of memory-related functional proteins in the hippocampus among the three groups. The mRNA expression levels of BDNF and CREB were significantly downregulated (**Figures 9A,B**, $P < 0.05$) in group A compared with those in the control group. However, the mRNA expression levels of NCAM and c-Fos did not change significantly (**Figures 9C,D**, $P > 0.05$) between these two groups. Moreover, *L. johnsonii* BS15 pretreatment significantly increased (**Figures 9A,B**, $P < 0.05$) the mRNA expression levels of BDNF and CREB in response to acute alcohol unconsciousness; their mRNA expression levels in the P group were significantly higher (**Figures 9A,B**, $P < 0.05$) than that in the A group. However, the mRNA expression levels of NCAM and c-Fos remained unchanged (**Figures 9C,D**, $p > 0.05$) between the control and P groups.

Antioxidant Capacity in the Hippocampus

Figure 10 illustrates the antioxidant indices in the hippocampus. As shown in **Figure 10A**, SOD levels were significantly lower ($P < 0.05$) in group A than that in the control group, but no difference ($P > 0.05$) was observed between the control and P groups. **Figure 10B** shows higher ($P < 0.05$) MDA content in group A than that in the other two groups, while the MDA content in the P group was higher ($P < 0.05$) than that in the control group. Meanwhile, the activity of GSH-Px was significantly lower ($P < 0.05$) in group A (**Figure 10C**) than that in the control group, but no significant difference ($P > 0.05$) was observed between groups A and P. Moreover, GSH content was significantly decreased ($P < 0.05$) in group A (**Figure 10D**),

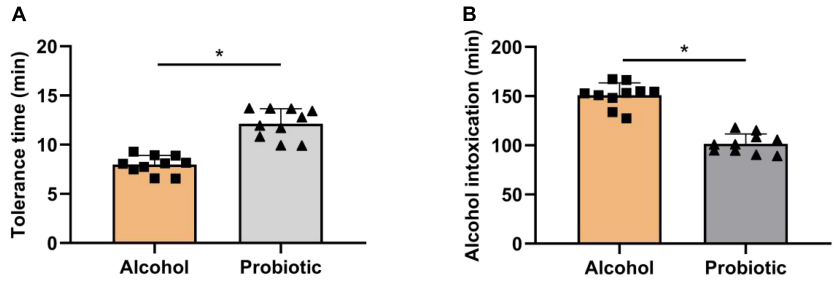

FIGURE 4 | Role of BS15 on resistance and unconsciousness time following acute EtOH exposure in mice. Data are displayed with the mean ± SD (n = 10). **(A)** Ethanol resistance time was measured as the interval between acute EtOH exposure and loss of righting reflex. **(B)** Ethanol unconsciousness time was measured as the duration of loss of righting reflex. Significant change between different treatments in same time point is expressed on the basis of T-test. Significant difference is shown at $^*P < 0.05$.

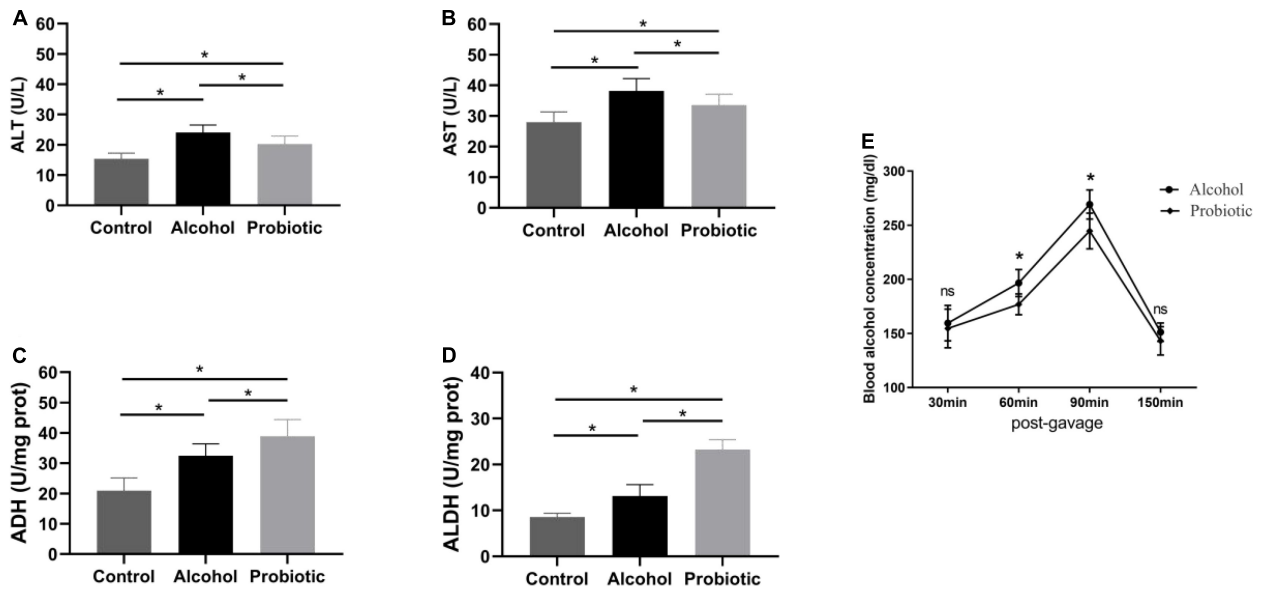

FIGURE 5 | Effect of BS15 on ethanol metabolism following acute EtOH exposure in mice. Data are displayed with the mean ± SD (n = 6). **(A)** ALT and **(B)** AST activities in serum following acute EtOH exposure in mice. **(C)** ADH and **(D)** ALDH activities in liver following acute EtOH exposure in mice. Significant difference between groups is expressed on the basis of one-way ANOVA statistical analysis followed by LSD test. **(E)** Blood ethanol concentration following acute EtOH exposure in mice. Significant change between different treatments in same time point is expressed on the basis of T-test. Significant difference is shown at $^*P < 0.05$. AST, aspartate amino transferase; ALT, alanine amino transferase; ADH, alcohol dehydrogenase; ALDH, aldehyde dehydrogenase.

but showed no differences ($P > 0.05$) compared with that in the control and P groups.

DISCUSSION

In earlier studies on the pathology of organs with regard to excessive drinking, most studies focused on changes in physiological and biochemical parameters of the liver, brain, or gut tissue itself (Bajaj, 2019; Carbia et al., 2021). The motivation of this study was to explore the mechanism of memory dysfunction induced by acute EtOH exposure by observing changes in the intestinal flora. Our study also verified the preventative influence of *L. johnsonii* BS15 on drunkenness. The normal animal memory level relies upon a delicate change in the intestinal flora, organizational barrier, and circulation system (Sun et al., 2020; Xin et al., 2020, 2021a; Wang et al., 2021). Although various factors, such as neuroinflammation, lipid peroxidation, autophagy, and apoptosis, can affect brain health, the gut microbiome plays a significant role as one of the main drivers.

16S rRNA high-throughput sequencing was performed on the ileal microbiome to determine whether the structure of the gut microbiota was altered by *L. johnsonii* BS15 supplementation. According to the results shown in the Shannon index and Chao1 index, the bacteria richness was significantly decreased. The above observation indicates that the administration of *L. johnsonii* BS15 stabilizes the intestinal flora. This conclusion is consistent with the results of previous studies, which suggest that *Lactobacillus* can interfere with the normal colonization of other bacteria, especially pernicious bacteria, owing to its enzymatic,

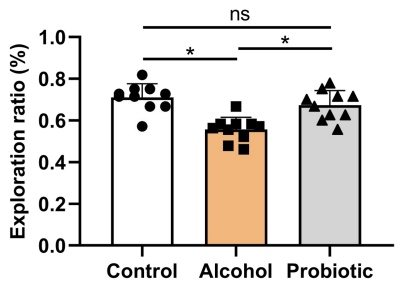

FIGURE 6 | Effects of *L. johnsonii* BS15 on exploration ratio by novel object recognition test. Data are displayed with the mean ± SD (n = 10). Significant difference between groups is expressed on the basis of one-way ANOVA statistical analysis followed by LSD test (*P < 0.05). The "ns" means there is no significant difference between groups.

fibrinolytic, and broad-spectrum antibacterial activities (Eom et al., 2015). Sepp et al. (2018) found that *Lactobacillus* ME-3 contributed to the species richness, diversity, and abundance of *Lactobacillus* in the intestinal tract, which was related to the increase in the diversity of the entire intestinal flora in 71 volunteers. Moreover, as shown in the PCoA of Bray Curtis distances, we observed an apparent inconsistency between the C and P groups, which manifested the compositional differences of the gut microbiota in probiotic-pretreated mice. Therefore, we believe that the reduction of gut microbiota diversity proves the main effect on intestinal microbiota by BS15 supplementation, and the different microbiota structures could be beneficial to the health of the host.

The ileal microenvironment mainly contributes to the normal colonization of microbes from seven predominant taxa, namely, Firmicutes, Bacteroidetes, Actinobacteria, Fusobacteria, Proteobacteria, Verrucomicrobia, and Cyanobacteria. Among them, Firmicutes, which accounted for up to 90% of the relative abundance, was the dominant phylum in all treatments. Normal intestinal microbes of the same strain of animals have shown different compositional patterns in various studies (Cryan et al., 2019). Even genetically identical rodents may have different microbiota owing to environmental factors, including diet, garbage, suppliers, transportation, and facilities (Knight et al., 2018). Based on our previous findings, mouse models reared under certain experimental conditions showed similar microbial composition characteristics in the gut, such as a high relative abundance of Firmicutes and *Lactobacillus* (Xin et al., 2021a,b). Although these results differ from those of other studies, reconciling microbiome data generated using different methods remains an unsolved challenge. The intestinal microbial community in the BS15 supplement was primarily manifested by an increase in the relative abundance of Firmicutes at the phylum level and *Lactobacillus* at the genus level. *Lactobacillus* is an important genus in Firmicutes and is also a well-known

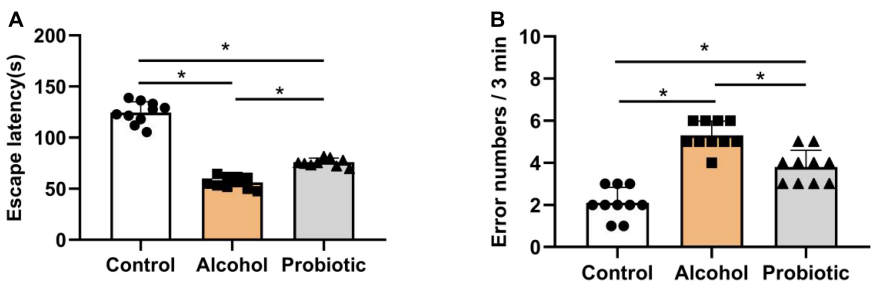

FIGURE 7 | Effects of *L. johnsonii* BS15 on the escape latency and error numbers by passive avoidance test. Data are displayed with the mean ± SD (n = 10). **(A)** Escape latency was the interval when the animal walked off the platform for the first time. **(B)** Error number was the total number of times the mice left the platform within 3 min. Significant difference between groups is expressed on the basis of one-way ANOVA statistical analysis followed by LSD test (*P < 0.05).

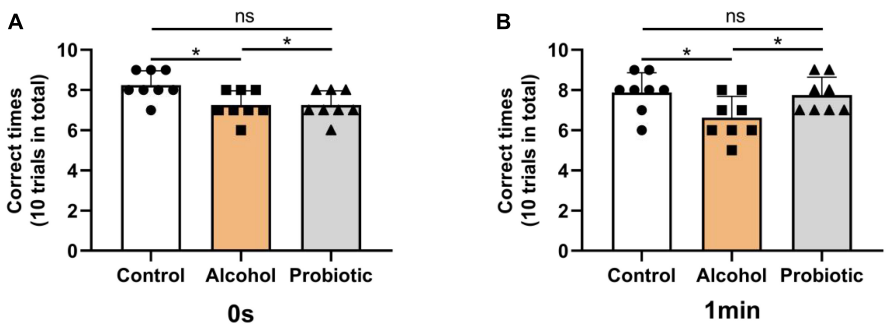

FIGURE 8 | Effects of *L. johnsonii* BS15 on the correct times with both 0 s and 1 min of retention interval by *T*-maze test. Data are displayed with the mean ± SD (n = 8). The correct times with **(A)** 0 s or **(B)** 1 min of retention interval by T-maze test. Significant difference between groups is expressed on the basis of one-way ANOVA statistical analysis followed by LSD test (*P < 0.05). The "ns" means there is no significant difference between groups.

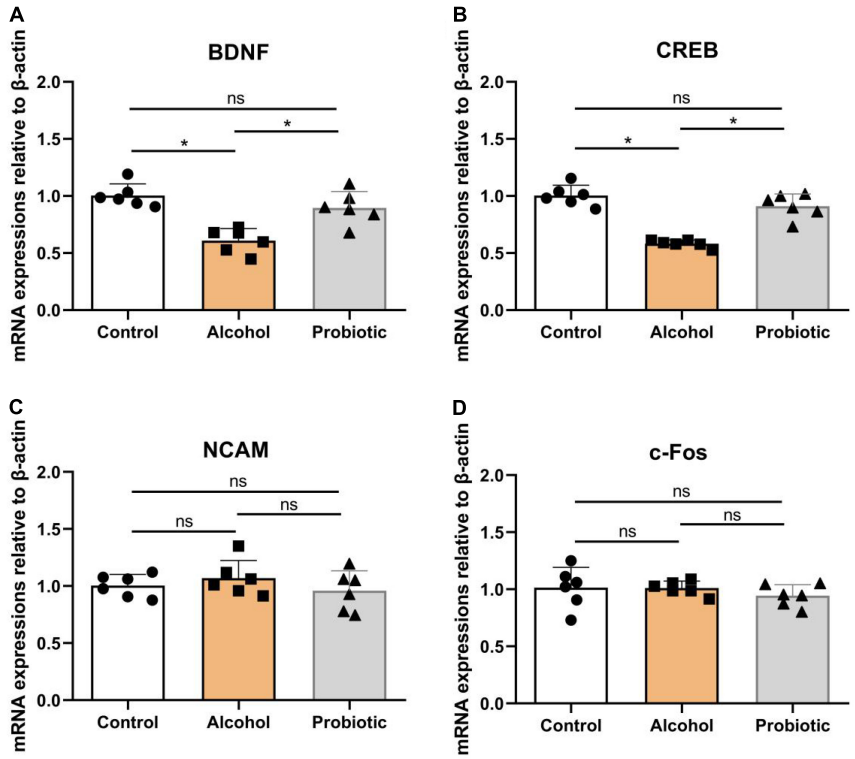

FIGURE 9 | Expression levels of memory-related functional proteins in the hippocampus. **(A–D)** Relative expression of **(A)** BDNF, **(B)** CREB, **(C)** NCAM, and **(D)** c-Fos. Data are displayed with the mean ± SD ($n = 6$). Significant difference between groups is expressed on the basis of one-way ANOVA statistical analysis followed by LSD test (*$P < 0.05$). The "ns" means there is no significant difference between groups. BDNF, brain-derived neurotrophic factor; CREB, cyclic ampresponse element binding protein; NCAM, neural cell adhesion molecule; c-Fos, immediate early gene.

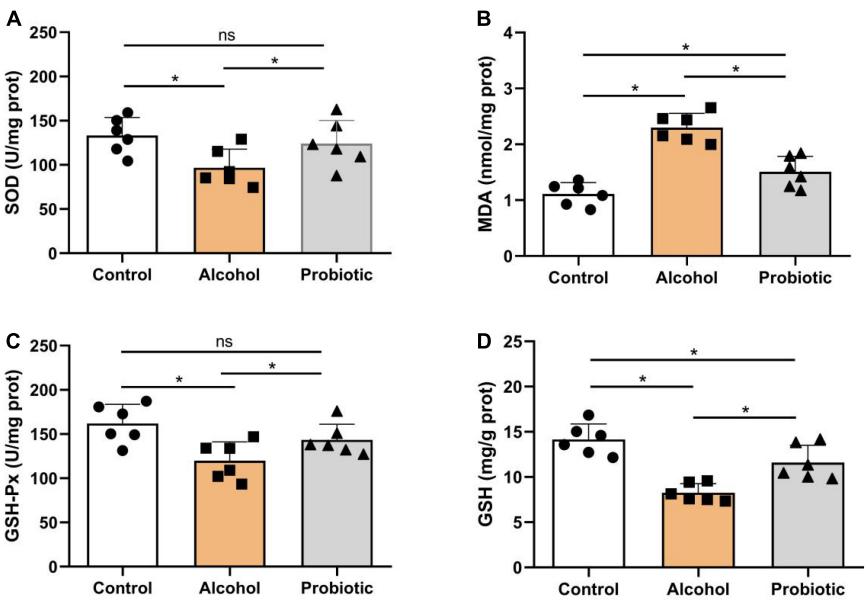

FIGURE 10 | Oxidation and antioxidant levels in the hippocampus. Activities or contents of **(A)** SOD, **(B)** MDA, **(C)** GSH-Px, and **(D)** GSH. Data are displayed with the mean ± SD ($n = 6$). Significant difference between groups is expressed on the basis of one-way ANOVA statistical analysis followed by LSD test (*$P < 0.05$). The "ns" means there is no significant difference between groups. SOD, superoxide dismutase; MDA, malondialdehyde; GSH-Px, glutathione peroxidase; GSH, glutathione.

intestinal probiotic. *Lactobacillus* not only resisted colonization by pathogenic bacteria but also was significantly related to the protein expression level of TNF-α, which supported that it is an anti-inflammatory bacterium (Ait-Belgnaoui et al., 2014; Roychowdhury et al., 2018). Therefore, *Lactobacillus* is actively used for the treatment of various intestinal disorders, including alcoholic liver disease (Lovinger, 1997). A growing body of evidence has revealed a frequent rate of psychological and psychiatric problems among patients suffering from alcohol abuse, and these changes in the central nervous system due to the concept of the gut-brain axis are often accompanied by dysbacteriosis. Yan et al. (2011) reported that alcoholic dysbiosis is characterized by reduced proportions of commensal probiotic bacteria such as *Lactobacillus* species in animal models and humans. In our previous studies, *L. johnsonii* BS15, a potential psychobiotic, was shown to have an impact on higher nervous functions, including behavior, which supports the hypothesis that the gut microbiota may play a beneficial role in alcohol-related diseases (Wang et al., 2020, 2021).

Once consumed, alcohol is absorbed mainly in the gastrointestinal tract by diffusion, enters the liver *via* the portal vein, and is distributed rapidly throughout the body. However, as the primary site for alcohol absorption, mounting evidence shows that the GI tract can be affected by alcohol and its metabolites, which experience symptoms such as intestinal bacterial dysbiosis and disruption of tissue homeostasis (Engen et al., 2015). However, probiotics, the key regulators of the intestinal environment, may become a new target for alcoholism. An early study reported an obvious alteration in the intestinal microbiome in rats chronically fed alcohol, but they could benefit from these changes by supplementing rats with *Lactobacillus* GG (Mutlu et al., 2009). Furthermore, alcohol-mediated tissue injury is commonly accompanied by increased intestinal permeability (Tang et al., 2015). Probiotics, such as *Lactobacillus* (Chen et al., 2016) and *Bifidobacterium* (Ewaschuk et al., 2008), or candidate probiotics, such as *Akkermansia* (Everard et al., 2013), have been shown to enhance intestinal integrity through various mechanisms, such as upregulation of tight junction protein expression, improvement of intestinal villus/crypt histology, and thickening of the mucous layer. In this study, *L. johnsonii* BS15 pretreatment significantly prolonged the resistance time and shortened the unconsciousness time in mice after acute EtOH exposure. These results suggest that amelioration of the gut environment by probiotic supplementation may represent a promising and safe approach to promote alcohol metabolism and increase tolerance to alcoholism.

To gain further insight into the degradation mechanism of probiotics, we detected the related enzymes in mice by biochemical analysis. The body typically processes ingested alcohol through a process called oxidative conversion, which predominantly occurs in the liver. Almost 80–90% of EtOH is metabolized by hepatic metabolic enzymes, which are considered necessary for the metabolism of EtOH, including alcohol dehydrogenase (ADH) and acetaldehyde dehydrogenase (ALDH). In short, ADH converts alcohol into acetaldehyde, and ALDH converts acetaldehyde into acetate. Previous studies have suggested that these enzymes can be expressed by some probiotics (Jing et al., 2018). Similarly, Chen et al. (2015) showed that the absence of the intestinal microbiome in germ-free mice was related to the modulation of the gut and hepatic expression of ethanol-metabolizing enzymes. In this study, we showed that the activities of ADH and ALDH were markedly enhanced after acute EtOH exposure, which is considered an adaptive response to alcohol stimulation. Administration of BS15 further upregulated ADH and ALDH activities in liver tissue after EtOH administration. Based on these facts, we speculated that alcohol metabolism could be accelerated by BS15 pretreatment, which is consistent with the obviously suppressed peaking of the blood alcohol concentration. These results indicate that *L. johnsonii* BS15 mediates EtOH metabolism by increasing the activity of related metabolic enzymes. Ferrere et al. (2017) reported that EtOH-fed mice showed a downregulation of the relative abundance of *Bacteroides*, and fecal microbiota transplantation (FMT) from healthy animals markedly reduced EtOH-induced liver injury. In this study, hepatic injury was determined by detecting aspartate aminotransferase (AST) and alanine aminotransferase (ALT) activities in the blood, which are considered the most sensitive indices for hepatic injury. *L. johnsonii* BS15 pretreatment significantly improved AST and ALT activities after acute EtOH intake. These results demonstrate that supplementation with *L. johnsonii* B15 could improve liver impairment under acute EtOH exposure.

In addition to negatively affecting the liver, alcohol impairs brain function, behavior, and cognition. In this study, three behavioral tasks were used to assess hippocampus-associated memory impairments. The T-maze is an elevated or enclosed equipment in the form of a horizontally placed T, which is used in a variety of ways to evaluate the cognitive and memory capability of an animal (Deacon and Rawlins, 2006). NOR is an efficient and flexible assay for investigating various aspects of learning and memory in animals (Lueptow, 2017). The main advantage of NOR is that it relies on rodents' natural proclivity to explore novelty (Berlyne, 1950). Finally, the passive avoidance test has been widely employed in studies on learning and memory in experimental animals (Jarvik and Essman, 1960). Poor memory ability can be determined by short escape latency and high error numbers (Malekmohamadi et al., 2007; Chen et al., 2014). Notably, the behavioral performance of mice with acute alcohol intake was significantly ameliorated by BS15 pretreatment; thus, the positive effects of *L. johnsonii* BS15 prove it as a potentially beneficial bacterium. The changes in the behavioral tests induced by *L. johnsonii* BS15 pretreatment were consistent with the conclusions of our earlier research (Sun et al., 2020; Xin et al., 2020; Wang et al., 2021).

The hippocampus is an essential brain area for cognitive and memory capabilities and is particularly vulnerable to the damaging effects of acute EtOH exposure (Agartz et al., 1999; Sullivan and Pfefferbaum, 2005; Beresford et al., 2006). Mounting evidence has shown that hippocampal impairment can lead to memory impairment (Guimarães et al., 1993; Molteni et al., 2002). We observed alterations in some pivotal

memory-associated functional proteins and antioxidant capacity in hippocampal tissue to elucidate the mechanism underlying the promising performance of *L. johnsonii* BS15. While the mechanisms of alcohol-induced memory deficits are not completely understood, increased oxidative stress may be a major factor contributing to selective neuronal impairment and cognitive deficits secondary to EtOH abuse (Haorah et al., 2008; Crews and Nixon, 2009). Lipid peroxidation is a critical process in molecular injury during oxidative stress that induces hippocampal-dependent memory impairment. The reactive oxygen species generated by stress are responsible for lipid peroxidation, which is determined by the upregulation of MDA formation (Niki, 2012). CAT, SOD, and GSH-Px are important enzymes that protect against oxidative stress by decreasing the activity of superoxide anions and hydrogen peroxide (Thakare et al., 2017). In our study, acute EtOH exposure downregulated the activities or content of SOD, GSH-Px, and GSH and upregulated MDA formation in the hippocampal tissue, implying an improvement in oxidative stress to a certain extent related to alcohol-induced memory impairment. Furthermore, *L. johnsonii* BS15 pretreatment markedly ameliorated EtOH-induced memory disruption, and this effect may be attributed to accelerated EtOH clearance (McGregor, 2007) and attenuation of oxidative stress by increased antioxidant enzyme activities in the hippocampal tissue.

Further studies are needed to identify the exact mechanism by which key intestinal microbes directly or indirectly mediate EtOH-induced memory function damage. Since it is quite difficult to identify key species based only on 16S rDNA high-throughput sequencing, more technology (such as metagenomics) should be considered in future studies to increase the possibility of eventual identification of these species. Meanwhile, we need a specific application of the above treatment method, requiring further studies with greater grouping design, from multiple bowels, across different time points, and accounting for the alteration of metabolic material in the gut, blood, and injured organs.

CONCLUSION

These findings indicate that *L. johnsonii* BS15 has beneficial effects against excessive alcohol intake-induced impairment of memory functions and activities of oxidative stress-related enzymes. These alterations could be caused by the improved microbial microenvironment in the gut and alcohol metabolic abilities in the serum and liver of mice. This study deepens our understanding of the link between memory function and the intestinal microenvironment under acute EtOH exposure and provides insights for the therapy of future alcoholism.

DATA AVAILABILITY STATEMENT

The datasets presented in this study can be found in online repositories. The names of the repository/repositories and accession number(s) can be found below: https://www.ncbi.nlm.nih.gov/search/all/?term=PRJNA791154.

ETHICS STATEMENT

The animal study was reviewed and approved by the Institutional Animal Care and Use Committee of Sichuan Agricultural University (approval number: SYXKchuan2019–187).

AUTHOR CONTRIBUTIONS

NS, JX, and HW: conceptualization and methodology. NS, BG, and XC: project administration and data curation. NS and LL: writing—original draft. NS and HW: writing—review and editing. XN, HW, DZ, JF, KP, BJ, YZ, CL, LZ, and PX: supervision. All authors contributed to the article and approved the submitted version.

FUNDING

This study was supported by the Guangdong Basic and Applied Basic Research Foundation (Grant No: 2020A1515110693), the Sichuan Science and Technology Program (Grant No: 2021YFH0097), and the Sichuan Youth Software Innovation Project (Grant No: 2021058).

ACKNOWLEDGMENTS

We gratefully acknowledge the help from Peng Xueji, Zhang Shuai, Wang Yiyang, Huang Yujie, and Su Chang for all the hard work during the behavioral tests. Also, they appreciate the support provided by all other undergraduates during the animal feeding and sampling.

REFERENCES

Agartz, I., Momenan, R., Rawlings, R. R., Kerich, M. J., and Hommer, D. W. (1999). Hippocampal volume in patients with alcohol dependence. *Arch. Gen. Psychiatry* 56, 356–363. doi: 10.1001/archpsyc.56.4.356

Ait-Belgnaoui, A., Colom, A., Braniste, V., Ramalho, L., Marrot, A., Cartier, C., et al. (2014). Probiotic gut effect prevents the chronic psychological stress-induced brain activity abnormality in mice. *Neurogastroenterol. Motil.* 26, 510–520. doi: 10.1111/nmo.12295

Alasmari, F., Goodwani, S., McCullumsmith, R. E., and Sari, Y. (2018). Role of glutamatergic system and mesocorticolimbic circuits in alcohol dependence. *Prog. Neurobiol.* 171, 32–49. doi: 10.1016/j.pneurobio.2018.10.001

Antunes, M., and Biala, G. (2012). The novel object recognition memory: neurobiology, test procedure, and its modifications. *Cogn. Process.* 13, 93–110. doi: 10.1007/s10339-011-0430-z

Asrani, S. K., Devarbhavi, H., Eaton, J., and Kamath, P. S. (2019). Burden of liver diseases in the world. *J. Hepatol.* 70, 151–171. doi: 10.1016/j.jhep.2018.09.014

Bajaj, J. S. (2019). Alcohol, liver disease and the gut microbiota. *Nat. Rev. Gastroenterol. Hepatol.* 16, 235–246. doi: 10.1038/s41575-018-0099-1

Beresford, T. P., Arciniegas, D. B., Alfers, J., Clapp, L., Martin, B., Du, Y., et al. (2006). Hippocampus volume loss due to chronic heavy drinking. *Alcohol. Clin. Exp. Res.* 30, 1866–1870. doi: 10.1111/j.1530-0277.2006.00223.x

Berlyne, D. E. (1950). Novelty and curiosity as determinants of exploratory behavior. *Br. J. Psychol.* 41, 68–80. doi: 10.1111/j.2044-8295.1950.tb00262.x

Bravo, J. A., Forsythe, P., Chew, M. V., Escaravage, E., Savignac, H. M., Dinan, T. G., et al. (2011). Ingestion of *Lactobacillus* strain regulates emotional behavior and central GABA receptor expression in a mouse via the vagus nerve. *Proc. Natl. Acad. Sci. U.S.A.* 108, 16050–16055. doi: 10.1073/pnas.1102999108

Carbia, C., Lannoy, S., Maurage, P., López-Caneda, E., O'Riordan, K. J., Dinan, T. G., et al. (2021). A biological framework for emotional dysregulation in alcohol misuse: from gut to brain. *Mol. Psychiatry* 26, 1098–1118. doi: 10.1038/s41380-020-00970-6

Carson, E. J., and Pruett, S. B. (1996). Development and characterization of a binge drinking model in mice for evaluation of the immunological effects of ethanol. *Alcohol. Clin. Exp. Res.* 20, 132–138. doi: 10.1111/j.1530-0277.1996.tb01055.x

Chen, P., Miyamoto, Y., Mazagova, M., Lee, K. C., Eckmann, L., and Schnabl, B. (2015). Microbiota protects mice against acute alcohol-induced liver injury. *Alcohol. Clin. Exp. Res.* 39, 2313–2323. doi: 10.1111/acer.12900

Chen, R. C., Xu, L. M., Du, S. J., Huang, S. S., Wu, H., Dong, J. J., et al. (2016). *Lactobacillus rhamnosus* GG supernatant promotes intestinal barrier function, balances Treg and TH17 cells and ameliorates hepatic injury in a mouse model of chronic-binge alcohol feeding. *Toxicol. Lett.* 241, 103–110. doi: 10.1016/j.toxlet.2015.11.019

Chen, X., Cai, F., Guo, S., Ding, F., He, Y., Wu, J., et al. (2014). Protective effect of Flos puerariae extract following acute alcohol intoxication in mice. *Alcohol. Clin. Exp. Res.* 38, 1839–1846. doi: 10.1111/acer.12437

Crews, F. T., and Nixon, K. (2009). Mechanisms of neurodegeneration and regeneration in alcoholism. *Alcohol. Alcohol.* 44, 115–127. doi: 10.1093/alcalc/agn079

Cryan, J. F., O'Riordan, K. J., Cowan, C. S. M., Sandhu, K. V., Bastiaanssen, T. F. S., Boehme, M., et al. (2019). The microbiota-gut-brain axis. *Physiol. Rev.* 99, 1877–2013. doi: 10.1152/physrev.00018.2018

Deacon, R. M. J., and Rawlins, J. N. P. (2006). T-maze test alternation in the rodent. *Nat. Protoc.* 1:712. doi: 10.1038/nprot.2006.2

Engen, P. A., Green, S. J., Voigt, R. M., Forsyth, C. B., and Keshavarzian, A. (2015). The gastrointestinal microbiome: alcohol effects on the composition of intestinal microbiota. *Alcohol. Res.* 37, 223–236.

Eom, J. S., Song, J., and Choi, H. S. (2015). Protective effects of a novel probiotic strain of *Lactobacillus plantarum* JSA22 from traditional fermented soybean food against infection by *Salmonella enterica Serovar typhimurium*. *J. Microbiol. Biotechnol.* 25, 479–491. doi: 10.4014/jmb.1501.01006

Everard, A., Belzer, C., Geurts, L., Ouwerkerk, J. P., Druart, C., Bindels, L. B., et al. (2013). Cross-talk between *Akkermansia muciniphila* and intestinal epithelium controls diet-induced obesity. *Proc. Natl. Acad. Sci. U.S.A.* 110, 9066–9071. doi: 10.1073/pnas.1219451110

Ewaschuk, J. B., Diaz, H., Meddings, L., Diederichs, B., Dmytrash, A., Backer, J., et al. (2008). Secreted bioactive factors from *Bifidobacterium infantis* enhance epithelial cell barrier function. *Am. J. Physiol. Gastrointest. Liver Physiol.* 295, G1025–G1034. doi: 10.1152/ajpgi.90227.2008

Fang, P., Kazmi, S. A., Jameson, K. G., and Hsiao, E. Y. (2020). The microbiome as a modifier of neurodegenerative disease risk. *Cell Host Microbe* 28, 201–222. doi: 10.1016/j.chom.2020.06.008

Ferrere, G., Wrzosek, L., Cailleux, F., Turpin, W., Puchois, V., Spatz, M., et al. (2017). Fecal microbiota manipulation prevents dysbiosis and alcohol-induced liver injury in mice. *J. Hepatol.* 66, 806–815. doi: 10.1016/j.jhep.2016.11.008

Gareau, M. G., Wine, E., Rodrigues, D. M., Cho, J. H., Whary, M. T., Philpott, D. J., et al. (2011). Bacterial infection causes stress-induced memory dysfunction in mice. *Gut* 60, 307–317. doi: 10.1136/gut.2009.202515

Gong, Y. S., Hou, F. L., Guo, J., Lin, L., and Zhu, F. Y. (2021). Effects of alcohol intake on cognitive function and β-amyloid protein in APP/PS1 transgenic mice. *Food Chem. Toxicol.* 151:112105. doi: 10.1016/j.fct.2021.112105

Guimarães, F. S., Del Bel, E. A., Padovan, C. M., Netto, S. M., and de Almeida, R. T. (1993). Hippocampal 5-HT receptors and consolidation of stressful memories. *Behav. Brain Res.* 58, 133–139. doi: 10.1016/0166-4328(93)90098-b

Hao, Z., Wang, W., Guo, R., and Liu, H. (2019). *Faecalibacterium prausnitzii* (ATCC 27766) has preventive and therapeutic effects on chronic unpredictable mild stress-induced depression-like and anxiety-like behavior in rats. *Psychoneuroendocrinology* 104, 132–142. doi: 10.1016/j.psyneuen.2019.02.025

Haorah, J., Ramirez, S. H., Floreani, N., Gorantla, S., Morsey, B., and Persidsky, Y. (2008). Mechanism of alcohol-induced oxidative stress and neuronal injury. *Free Radic Biol. Med.* 45, 1542–1550. doi: 10.1016/j.freeradbiomed.2008.08.030

Hillemacher, T., Bachmann, O., Kahl, K. G., and Frieling, H. (2018). Alcohol, microbiome, and their effect on psychiatric disorders. *Prog. Neuropsychopharmacol. Biol. Psychiatry* 85, 105–115. doi: 10.1016/j.pnpbp.2018.04.015

Jarvik, M., and Essman, W. (1960). A simple one-trial learning situation for mice. *Psychol. Rep.* 6:290. doi: 10.2466/PR0.6.2.290-290

Jing, L., Yunbin, L., Li, M., Jing, S., Huang, Z., Lu, F., et al. (2018). Alleviating acute alcoholic liver injury in mice with *Bacillus subtilis* co-expressing alcohol dehydrogenase and acetaldehyde dehydrogenase. *J. Funct. Foods* 49, 342–350. doi: 10.1016/j.jff.2018.09.006

Knight, R., Vrbanac, A., Taylor, B. C., Aksenov, A., Callewaert, C., Debelius, J., et al. (2018). Best practices for analysing microbiomes. *Nat. Rev. Microbiol.* 16, 410–422. doi: 10.1038/s41579-018-0029-9

Koob, G. F. (2013). Negative reinforcement in drug addiction: the darkness within. *Curr. Opin. Neurobiol.* 23, 559–563. doi: 10.1016/j.conb.2013.03.011

Liang, S., Wang, T., Hu, X., Luo, J., Li, W., Wu, X., et al. (2015). Administration of *Lactobacillus helveticus* NS8 improves behavioral, cognitive, and biochemical aberrations caused by chronic restraint stress. *Neuroscience* 310, 561–577. doi: 10.1016/j.neuroscience.2015.09.033

Lovinger, D. M. (1997). Serotonin's role in alcohol's effects on the brain. *Alcohol. Health Res. World* 21, 114–120.

Lowe, P. P., Gyongyosi, B., Satishchandran, A., Iracheta-Vellve, A., Cho, Y., Ambade, A., et al. (2018). Reduced gut microbiome protects from alcohol-induced neuroinflammation and alters intestinal and brain inflammasome expression. *J. Neuroinflammation* 15:298. doi: 10.1186/s12974-018-1328-9

Lueptow, L. M. (2017). Novel object recognition test for the investigation of learning and memory in mice. *J. Vis. Exp.* 126:55718. doi: 10.3791/55718

Malekmohamadi, N., Heidari, P., Sahebgharani, M., and Zarrindast, M. R. (2007). Effects of clozapine and sulpiride on morphine state-dependent memory in the step-down passive avoidance test. *Pharmacology* 79, 149–153. doi: 10.1159/000098151

McGregor, N. R. (2007). *Pueraria lobata* (Kudzu root) hangover remedies and acetaldehyde-associated neoplasm risk. *Alcohol* 41, 469–478. doi: 10.1016/j.alcohol.2007.07.009

Messaoudi, M., Violle, N., Bisson, J. F., Desor, D., Javelot, H., and Rougeot, C. (2011). Beneficial psychological effects of a probiotic formulation (*Lactobacillus helveticus* R0052 and *Bifidobacterium longum* R0175) in healthy human volunteers. *Gut Microbes* 2, 256–261. doi: 10.4161/gmic.2.4.16108

Mews, P., Egervari, G., Nativio, R., Sidoli, S., Donahue, G., Lombroso, S. I., et al. (2019). Alcohol metabolism contributes to brain histone acetylation. *Nature* 574, 717–721. doi: 10.1038/s41586-019-1700-7

Mohammadi, A. A., Jazayeri, S., Khosravi-Darani, K., Solati, Z., Mohammadpour, N., Asemi, Z., et al. (2016). The effects of probiotics on mental health and hypothalamic-pituitary-adrenal axis: a randomized, double-blind, placebo-controlled trial in petrochemical workers. *Nutr. Neurosci.* 19, 387–395. doi: 10.1179/1476830515Y.0000000023

Molteni, R., Barnard, R. J., Ying, Z., Roberts, C. K., and Gómez-Pinilla, F. (2002). A high-fat, refined sugar diet reduces hippocampal brain-derived neurotrophic factor, neuronal plasticity, and learning. *Neuroscience* 112, 803–814. doi: 10.1016/s0306-4522(02)00123-9

Morais, L. H., Schreiber, H. L. IV, and Mazmanian, S. K. (2021). The gut microbiota-brain axis in behaviour and brain disorders. *Nat. Rev. Microbiol.* 19, 241–255. doi: 10.1038/s41579-020-00460-0

Mutlu, E., Keshavarzian, A., Engen, P., Forsyth, C. B., Sikaroodi, M., and Gillevet, P. (2009). Intestinal dysbiosis: a possible mechanism of alcohol-induced endotoxemia and alcoholic steatohepatitis in rats. *Alcohol. Clin. Exp. Res.* 33, 1836–1846. doi: 10.1111/j.1530-0277.2009.01022.x

Neyrinck, A. M., Etxeberria, U., Taminiau, B., Daube, G., Van Hul, M., Everard, A., et al. (2017). Rhubarb extract prevents hepatic inflammation induced by acute alcohol intake, an effect related to the modulation of the gut microbiota. *Mol. Nutr. Food Res.* 61:899. doi: 10.1002/mnfr.201500899

Niki, E. (2012). Do antioxidants impair signaling by reactive oxygen species and lipid oxidation products? *FEBS Lett.* 586, 3767–3770. doi: 10.1016/j.febslet.2012.09.025

Niu, R., Chen, H., Manthari, R. K., Sun, Z., Wang, J., Zhang, J., et al. (2018). Effects of fluoride on synapse morphology and myelin damage in mouse hippocampus. *Chemosphere* 194, 628–633. doi: 10.1016/j.chemosphere.2017.12.027

O'Hagan, C., Li, J. V., Marchesi, J. R., Plummer, S., Garaiova, I., and Good, M. A. (2017). Long-term multi-species *Lactobacillus* and *Bifidobacterium* dietary supplement enhances memory and changes regional brain metabolites in middle-aged rats. *Neurobiol. Learn. Mem.* 144, 36–47. doi: 10.1016/j.nlm.2017.05.015

Rognes, T., Flouri, T., Nichols, B., Quince, C., and Mahé, F. (2016). VSEARCH: a versatile open source tool for metagenomics. *PeerJ* 4:e2584. doi: 10.7717/peerj.2584

Roychowdhury, S., Cadnum, J., Glueck, B., Obrenovich, M., Donskey, C., and Cresci, G. A. M. (2018). *Faecalibacterium prausnitzii* and a prebiotic protect intestinal health in a mouse model of antibiotic and *Clostridium difficile* exposure. *JPEN J. Parenter. Enteral. Nutr.* 42, 1156–1167. doi: 10.1002/jpen.1053

Scholey, A., Benson, S., Kaufman, J., Terpstra, C., Ayre, E., Verster, J. C., et al. (2019). Effects of alcohol hangover on cognitive performance: findings from a field/internet mixed methodology study. *J. Clin. Med.* 8:440. doi: 10.3390/jcm8040440

Sepp, E., Smidt, I., Tepetova, J., Rp, T., Hütt, P., Rtsep, M., et al. (2018). The effect of *Lactobacillus fermentum* ME-3 on the intestinal microbiota and urine polyamines content: a double-blind placebo-controlled pilot trial. *J. Funct. Foods* 48, 430–438. doi: 10.1016/j.jff.2018.04.053

Sharon, G., Sampson, T. R., Geschwind, D. H., and Mazmanian, S. K. (2016). The central nervous system and the gut microbiome. *Cell* 167, 915–932. doi: 10.1016/j.cell.2016.10.027

Smith, C. J., Emge, J. R., Berzins, K., Lung, L., Khamishon, R., Shah, P., et al. (2014). Probiotics normalize the gut-brain-microbiota axis in immunodeficient mice. *Am. J. Physiol. Gastrointest. Liver Physiol.* 307, G793–G802. doi: 10.1152/ajpgi.00238.2014

Stärkel, P., and Schnabl, B. (2016). Bidirectional communication between liver and gut during alcoholic liver disease. *Semin. Liver Dis.* 36, 331–339. doi: 10.1055/s-0036-1593882

Sullivan, E. V., and Pfefferbaum, A. (2005). Neurocircuitry in alcoholism: a substrate of disruption and repair. *Psychopharmacology* 180, 583–594. doi: 10.1007/s00213-005-2267-6

Sun, N., Ni, X., Wang, H., Xin, J., Zhao, Y., Pan, K., et al. (2020). Probiotic *Lactobacillus johnsonii* BS15 prevents memory dysfunction induced by chronic high-fluorine intake through modulating intestinal environment and improving gut development. *Probiotics Antimicrob. Proteins* 12, 1420–1438. doi: 10.1007/s12602-020-09644-9

Tang, Y., Zhang, L., Forsyth, C. B., Shaikh, M., Song, S., and Keshavarzian, A. (2015). The role of miR-212 and iNOS in alcohol-Induced intestinal barrier dysfunction and steatohepatitis. *Alcohol. Clin. Exp. Res.* 39, 1632–1641. doi: 10.1111/acer.12813

Thakare, V. N., Dhakane, V. D., and Patel, B. M. (2017). Attenuation of acute restraint stress-induced depressive like behavior and hippocampal alterations with protocatechuic acid treatment in mice. *Metab. Brain Dis.* 32, 401–413. doi: 10.1007/s11011-016-9922-y

Vuong, H. E., Yano, J. M., Fung, T. C., and Hsiao, E. Y. (2017). The microbiome and host behavior. *Annu. Rev. Neurosci.* 40, 21–49. doi: 10.1146/annurev-neuro-072116-031347

Wang, H. S., Xin, J., Zhang, T., Sun, N., Li, L., Ni, X., et al. (2021). Psychoactive effects of *Lactobacillus johnsonii* against restraint stress-Induced memory dysfunction in mice through modulating intestinal inflammation and permeability-a study based on the gut-brain axis hypothesis. *Front. Pharmacol.* 12:662148. doi: 10.3389/fphar.2021.662148

Wang, H., Sun, Y., Xin, J., Zhang, T., Sun, N., Ni, X., et al. (2020). *Lactobacillus johnsonii* BS15 prevents psychological stress-induced memory dysfunction in mice by modulating the gut-brain axis. *Front. Microbiol.* 11:1941. doi: 10.3389/fmicb.2020.01941

Warburton, E. C., and Brown, M. W. (2015). Neural circuitry for rat recognition memory. *Behav. Brain Res.* 285, 131–139. doi: 10.1016/j.bbr.2014.09.050

World Health Organization (2014). Global status report on alcohol and health 2014. *J. Glob. Health* 18, 1–57. doi: 10.1111/tmi.12618

Xin, J., Wang, H., Sun, N., Bughio, S., Zeng, D., Li, L., et al. (2021a). Probiotic alleviate fluoride-induced memory impairment by reconstructing gut microbiota in mice. *Ecotoxicol. Environ. Saf.* 215:112108. doi: 10.1016/j.ecoenv.2021.112108

Xin, J., Sun, N., Wang, H., Ma, H., Wu, B., Li, L., et al. (2021b). Preventive effects of *Lactobacillus johnsonii* on the renal injury of mice induced by high fluoride exposure: insights from colonic microbiota and co-occurrence network analysis. *Ecotoxicol. Environ. Saf.* 228:113006. doi: 10.1016/j.ecoenv.2021.113006

Xin, J., Zeng, D., Wang, H., Ni, X., Yi, D., Pan, K., et al. (2014). Preventing non-alcoholic fatty liver disease through *Lactobacillus johnsonii* BS15 by attenuating inflammation and mitochondrial injury and improving gut environment in obese mice. *Appl. Microbiol. Biotechnol.* 98, 6817–6829. doi: 10.1007/s00253-014-5752-1

Xin, J., Zeng, D., Wang, H., Sun, N., Khalique, A., Zhao, Y., et al. (2020). *Lactobacillus johnsonii* BS15 improves intestinal environment against fluoride-induced memory impairment in mice-a study based on the gut-brain axis hypothesis. *PeerJ* 8:e10125. doi: 10.7717/peerj.10125

Yan, A. W., Fouts, D. E., Brandl, J., Stärkel, P., Torralba, M., Schott, E., et al. (2011). Enteric dysbiosis associated with a mouse model of alcoholic liver disease. *Hepatology* 53, 96–105. doi: 10.1002/hep.24018

Conflict of Interest: JX and HW were employed by the Guangzhou Beneco Biotechnology Co., Ltd.

The remaining authors declare that the research was conducted in the absence of any commercial or financial relationships that could be construed as a potential conflict of interest.

Publisher's Note: All claims expressed in this article are solely those of the authors and do not necessarily represent those of their affiliated organizations, or those of the publisher, the editors and the reviewers. Any product that may be evaluated in this article, or claim that may be made by its manufacturer, is not guaranteed or endorsed by the publisher.

frontiers | Frontiers in Microbiology

ORIGINAL RESEARCH
published: 07 April 2022
doi: 10.3389/fmicb.2022.850687

Gut Bacterial Composition and Functional Potential of Tibetan Pigs Under Semi-Grazing

Hui Niu, Xi-Ze Feng, Chun-Wei Shi, Di Zhang, Hong-Liang Chen, Hai-Bin Huang, Yan-Long Jiang, Jian-Zhong Wang, Xin Cao, Nan Wang, Yan Zeng, Gui-Lian Yang, Wen-Tao Yang* and Chun-Feng Wang**

Jilin Provincial Key Laboratory of Animal Microecology and Healthy Breeding, Key Laboratory of Animal Production and Product Quality Safety of the Ministry of Education, Jilin Provincial Engineering Research Center of Animal Probiotics, College of Veterinary Medicine, College of Animal Science and Technology, Jilin Agricultural University, Changchun, China

Gut bacterial community plays a key role in maintaining host health. The Tibetan pig (*Sus scrofa*), an ancient breed in China, has been known for its high adaptability to harsh environments and for its meat quality. To understand the underlying mechanisms facilitating to shape these unique features, in this study, *16S rRNA* sequencing using pigs feces and subsequent bacterial functional prediction were performed. Also, the gut bacteria of two other breeds of pigs, Barkshire and Landrace, were examined for comparison. It was revealed that the structure of bacterial community in Tibetan pigs appeared to be more complex; the relative abundances of dominant bacterial families varied inversely with those of the other pigs, and the proportion of *Firmicutes* in Tibetan pigs was lower, but *Bacteroides, Fibrobacterota*, *Lachnospiraceae*, *Oscillospiraceae*, and *Ruminococcaceae* were higher. Bacterial functional prediction revealed that the dominant flora in the Tibetan pigs was more correlated with functions regulating the hosts' immune and inflammatory responses, such as NOD-like_receptor_signaling_pathway and vitamin metabolism. In addition, in Tibetan pigs, the taxonomic relationships in the gut bacteria on day 350 were closer than those on earlier stages. Furthermore, gender played a role in the composition and function of bacterial inhabitants in the gut; for boars, they were more correlated to drug resistance and xenobiotics metabolism of the host compared to the sows. In sum, our preliminary study on the gut bacterial composition of the Tibetan pigs provided an insight into the underlying host–microorganism interactions, emphasizing the role of intestinal bacteria in the context of modulating the host's immune system and host development.

Keywords: gut bacteria, Tibetan pigs, bacterial functions, growth stages, genders

OPEN ACCESS

Edited by:
Hesong Wang,
Southern Medical University, China

Reviewed by:
Fahad Nasir,
Northeast Institute of Geography and Agroecology (CAS), China
Ying Li,
Foshan University, China

****Correspondence:***
Gui-Lian Yang
yangguilian@jlau.edu.cn
Wen-Tao Yang
yangwentao@jlau.edu.cn
Chun-Feng Wang
wangchunfeng@jlau.edu.cn

Specialty section:
This article was submitted to Microbial Symbioses, a section of the journal Frontiers in Microbiology

Received: *08 January 2022*
Accepted: *10 February 2022*
Published: *07 April 2022*

Citation:
Niu H, Feng X-Z, Shi C-W, Zhang D, Chen H-L, Huang H-B, Jiang Y-L, Wang J-Z, Cao X, Wang N, Zeng Y, Yang G-L, Yang W-T and Wang C-F (2022) Gut Bacterial Composition and Functional Potential of Tibetan Pigs Under Semi-Grazing. Front. Microbiol. 13:850687. doi: 10.3389/fmicb.2022.850687

INTRODUCTION

Gut microflora plays a vital role in maintaining the health of hosts (Ross et al., 2019). Previous studies revealed that it not only was implicated in the promotion of hosts' mucosal and systemic immunity and hematopoiesis (Staffas et al., 2018), but also was associated with modulation of the host's hypertension-linked metabolic disorders and inflammation (Li J. et al., 2021). In

addition, gut microbiome was recognized as an acquired bacterial defense system (Ross et al., 2019). The interactions between gut microbiota and host immunity exerted effective suppressions of helminth-evoked colitis (Shute et al., 2021). Recent research suggested that adjustment of intestinal microbiota could improve efficacies of treatments of colorectal cancer (Si et al., 2021). In contrast, dysregulated intestinal bacteria and fungi could lead to the loss of intestinal barrier and therefore enhanced disease susceptibility in hosts (Chopyk and Grakoui, 2020). It was reported that alleviation of the imbalance of intestinal microbiota by colonic dialysis could protect the renal function in patients with pre-dialysis chronic kidney disease (Li Y. et al., 2021).

Compared with rodents, swine was considered as a more ideal model for studying human diseases due to its narrow disparities in organ characteristics compared to those of humans (Gehrig et al., 2019). Porcine models were especially adopted for studies of lung cystic fibrosis in humans (Lu and Kolls, 2021) and were also used in the field of pathogenesis of neurodegenerative (Yan et al., 2018) and cardiovascular (Hinkel et al., 2015; Fan et al., 2020; Zhao et al., 2021) diseases. Furthermore, pigs' omnivorous eating behavior contributed to its role in the study of gut microbiota. It was demonstrated that intestinal *Prevotella copri* was a factor for host obesity and fat accumulation (Chen C. et al., 2021). Both biomedical research and agriculture would benefit from enhanced understanding of the pig gut microbiome (Wylensek et al., 2020).

The Tibetan pig, a prototypic breed of pig in China with features of adapting to a wide range of breeding conditions, especially the harsh plateau environment (Ma et al., 2019), was known to possess a high lean meat ratio, and its meat was recognized as green food owing to free range, which made it particularly popular in the high-end market (Huang et al., 2021). As miniature pigs, Tibetan pigs are similar in size to humans, which makes them a superior model for human studies (Lunney, 2007). Previous studies (Cheng et al., 2015) compared respective immune performances in Tibetan and Yorkshire pigs, showing that a stronger innate immunity was exerted in Tibetan pigs, which could trigger comparatively decent local or system immune responses in the hosts to protect against invading pathogens. Interestingly, when Tibetan pigs were introduced and bred in other areas, none ended up with non-acclimatization or sickness (Wu et al., 2007). A DNA recombinant vaccine developed with Tibetan pig *IL-23* gene was shown to enhance the overall immune responses of pigs against infections caused by Porcine circovirus type 2 (Xiao et al., 2020).

There have been some studies on the intestinal microbes of Tibetan pigs. It is reported that there are differences in the intestinal microbes of Tibetan pigs in different living environments and growth stages (Jiang et al., 2018; Zeng et al., 2020). The rich carbohydrate-degrading enzymes in the gut microbes of Tibetan pigs can bring us more benefits in the future microbial production of industrial enzymes (Zhou et al., 2020). To date, limited knowledge was available on the gut bacteria of Tibetan pigs. In this study, *16S rRNA* metagenomic analysis of fresh pigs feces was performed to explore the relation between gut microbiome and host health (Martinez-Guryn et al., 2019). In addition, comparisons of the gut bacteria between Tibetan and Berkshire pigs, which were raised under semi-grazing conditions, and Landrace pigs raised in large-scale houses were conducted to understand the functions of the gut bacterial flora in Tibetan pigs. Besides, gut bacteria underwent dynamic changes in the process of growth (Bäckhed et al., 2015), and were distinct in structure, composition, and diversity between male and female hosts (Wang et al., 2020), which were also investigated in this study to gain an insight into functional gut bacteria in Tibetan pigs.

MATERIALS AND METHODS

Animals and Fecal Sample Collection

In this study, the Tibetan pigs (*Sus scrofa*) used were a cross between hybrid sows (*S. scrofa*) and purebred boar (*S. scrofa*); the parental sows were a progeny of Tibetan pigs crossed with other black pig breeds, including Beijing black pigs and hybrid Tibetan pigs. These second-generation of Tibetan pigs employed in this study could be degenerated into wild type, accelerating farrowing rates, which was in line with actual production needs. Currently, most Tibetan pigs circulating in the market are this second-generation Tibetan pig.

Forty-eight fresh fecal samples were collected from a Tibetan pig farm in Shanxi Province, China (37°30′N, 113°83′E). In this study, three levels of comparisons were performed, including pigs of different breeds, Tibetan pigs of different growth stages, and Tibetan pigs of different sexes. Fresh feces of Landrace pigs were collected under housing conditions, while those of Berkshire pigs and Tibetan pigs were collected under semi-grazing conditions. They are fed all-natural cornmeal and wheat bran. In addition, Berkshire pigs and Tibetan pigs can eat freely on the mountain. For the comparison of gut bacteria between breeds, pigs of different breeds were raised to about 350 days of age, and their feces were collected. The growth of pigs are usually differentiated into phases of lactation, weaning, and fattening. Naturally, the lactation and growing time of Tibetan pigs are relatively long; accordingly, three time points, days 7, 60, and 350, were selected for evaluating the gut bacterial composition in Tibetan pigs. In addition, the feces of Tibetan boars, pregnant sows, and suckling sows were collected and detected. Six parallel samples in each group were set up to eliminate individual differences. Separate stool samples were collected in individual sterilized containers after rectal stimulation and then immediately transported to laboratory on dry ice, and stored at −80°C.

DNA Extraction

The fecal samples were subjected to DNA isolation with PowerSoil DNA Isolation Kit (MoBio Laboratories, Carlsbad, CA) following the manufacturer's instruction. Purity and quality of the genomic DNA were checked by a NanoDrop spectrophotometer (Thermo Fisher Scientific, Massachusetts, United States).

Polymerase Chain Reaction Amplification

After quantification with NanoDrop measurement, 30 ng of DNA was used for Polymerase Chain Reaction (PCR)

amplification. The variable region of *16S rDNA* V3–V4 (338–806) was used to design primers as follows: 338F (5′-ACTCCTACGGGAGGCAGCAG-3′) and 806R (5′-GGACTA CNNGGGTATCTAAT-3′) (Munyaka et al., 2015). PCR was performed in triplicate in 25-μl volumes containing 2.5 μl of 10 × Pyrobest Buffer, 2 μl of 2.5 mM dNTPs, 1 μl of each primer (10 μM), 0.4 U of Pyrobest DNA Polymerase (TaKaRa, Dalian, China), and 15 ng of template DNA (Chen H. et al., 2021). PCR conditions were pre-set as: pre-denaturation was performed at 94°C for 3 min, followed by 25 cycles of denaturation at 94°C for 30 s, then annealed at 50°C for 30 s and extended at 72°C for 60 s (Xing et al., 2021). After this, agarose gel electrophoresis was performed to detect the specificity of the amplification results. The gel was prepared at a concentration of 1%, running at a voltage of 170 V, for 30 min.

Sequencing Library Preparation and Sequencing

Sequencing reactions were carried out at Allwegene Company in Beijing, China using Illumina Miseq PE300 platform (Illumina, Inc., CA, United States).

The off-machine data were divided into samples according to the barcode sequence through the QIIME (v1.8.0), and Pear (v 0. 9. 6) was used to filter and splice the data (Visscher et al., 2019). Ambiguous bases and primer mismatches were removed. The minimum overlap was set as 10 bp, and mismatch rate was set as 0.1. Then, Vsearch (v 2.7.1) was employed to remove sequences less than 230 bp in length, and the uchime method was used to compare and remove chimera sequences according to Gold Database. After these, Uparse algorithm of Vsearch (v 2.7.1) was used for picking up operational taxonomic units (OTUs) cluster, with 97% similarity as the cutoff (Edgar, 2013). Ribosomal Database Project (RDP) Classifier tool was used to classify all sequences into different taxonomic groups against the SILVA128 database (Cole et al., 2009); 70% was used as the confidence threshold.

Diversity and Structural Analysis of the Bacterial of Fecal Samples

QIIME1 (v1.8.0) was used to generate rarefaction curves, α indices (including Shannon, Simpson, Chao1 indices, goods_coverage, observed_species, and PD_whole_tree), and β diversity. The VennDiagram package of R (v3.6.0) was used for making Venn diagrams (Fouts et al., 2012), which allowed for visualizing the number of OTU groups of environmental samples and the overlap between samples or groups. GraphPad Prism (v 9.0.0) was used to estimate alpha-diversity and analyze the dominant phyla. To examine the similarity among Landrace, Berkshire, and Tibetan pigs, R (v3.6.0) was used to perform principal coordinate analysis (PCoA) based on Weighted Unifrace distance (Wang et al., 2012). Based on the species annotation and relative abundance results, R (v3.6.0) software was used to visualize the relative abundance of pig breeds and species composition as boxplots. Besides, the growth dynamics of Tibetan pigs and the composition of intestinal flora were visualized using R. In addition, R software was also used to analyze the histogram of the species composition of Tibetan pigs of different genders. Linear discriminant analysis (LDA) effect size (LEfSe) in galaxy was used to understand the bacterial differences between the breeds of pigs by coupling statistical analysis with examinations of biomarkers and their effect relevance. In this study, an LDA score of 4 was set as the threshold. In addition, to determine the taxonomic relations between bacterial communities in the gut bacteria, the relationship between OTUs was analyzed by Spearman correlation coefficient and R (v3.6.0) software, and the co-occurrence analysis was performed with Cytoscape (Wen et al., 2016). Functional-gene profile was inferred with software package Phylogenetic Investigation of Communities by Reconstruction of Unobserved States (PICRUSt) based on *16S rRNA* gene cluster survey along the samples accompanied by its relative abundance in each of the samples. R was used for heatmap visualization. The top 15 correlated pathways in Tibetan pigs at different growth stages were presented in this study. To determine the correlation between functional pathways and gender, the comparison was visualized with a histogram.

Statistical Analyses

Metastats analysis was performed to determine the significant differences between groups. Kruskal–Wallis tests were conducted to calculate the differences between the means of independent data in multiple groups, and Wilcoxon tests were carried out to compare the differences between two paired groups. Besides, *t*-test and one-way ANOVA are also performed to calculate the significance of data.

RESULTS

16S rRNA Sequencing Data

The *16S rRNA* sequencing generated 4,297,102 raw reads in total. Good_coverage index of the 48 samples in this study was greater than 99%. As shown in the curves of Rarefaction (**Supplementary Figure 1A**), Shannon-Wiener (**Supplementary Figure 1B**), Rank-Abundance (**Supplementary Figure 1C**), and species accumulation (**Supplementary Figure 1D**), the total initial sample reads increased with the sample sizes and then developed into stagnant stages, which indicated that the bacterial complexity in the communities reached its peak and would not enhance sample sizes, suggesting that both sample sizes and sequence reads were sufficient to cover the bacterial inhabitants in the communities.

The Dominant Gut Bacteria in Tibetan Pigs and Its Potential Functions

Overall, 1,426 OTUs were identified in the fecal samples of Tibetan pigs by *16S rRNA* sequencing, of which 311 were unique. The number of OTUs in Tibetan pigs is significantly higher than those in Landrace and Berkshire pigs at age about 1 year (350 days) (**Figure 1A**). Landrace and Berkshire pigs produced 863 and 910 OTUs, respectively. Of the three breeds, the gut bacteria of Landrace and Berkshire pigs were

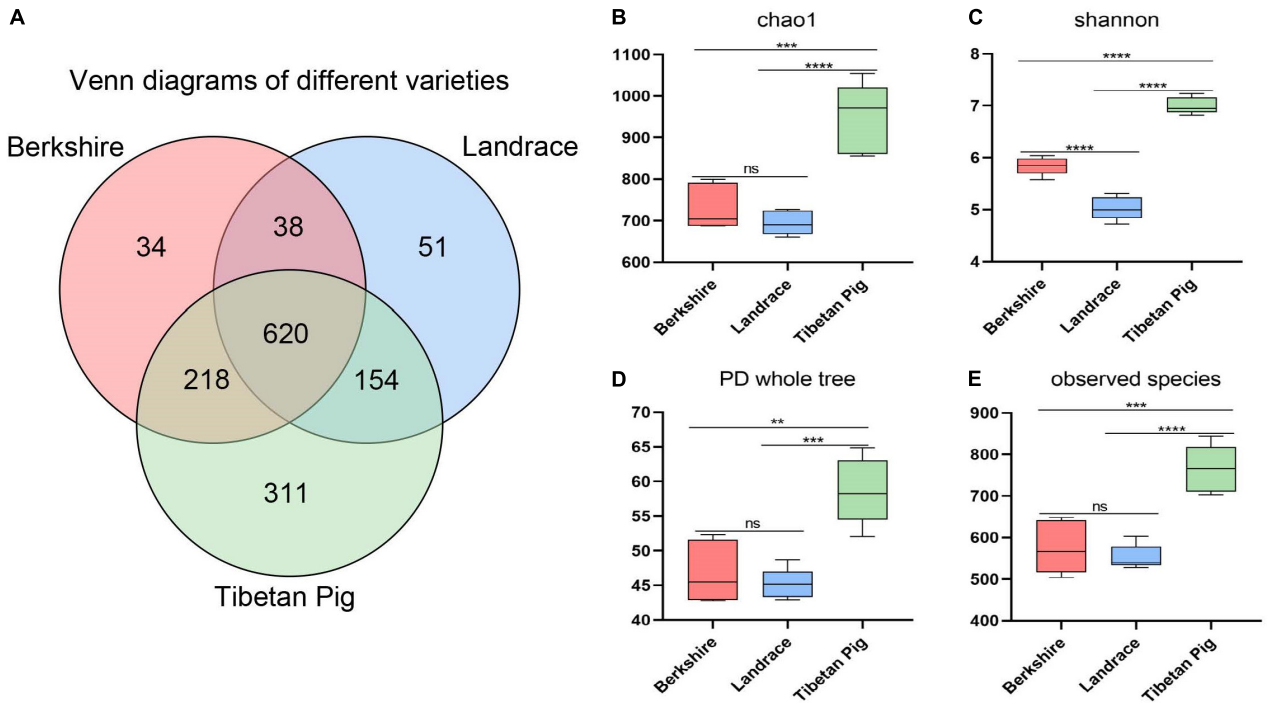

FIGURE 1 | Venn map and alpha-diversity analysis. Venn map of Berkshire pigs, Landrace pigs, and Tibetan pigs on day 350 **(A)**. Chao1 observed number of species **(B)**. Shannon–Wiener index **(C)**. PD whole tree **(D)**. Observed species **(E)**. One-way ANOVA was employed for the statistical analysis (ns, non significant; $^{**}p < 0.01$; $^{***}p < 0.001$; $^{****}p < 0.0001$).

shown to have a similar number of unique OTUs, 51 and 34, respectively. The estimations of alpha diversity of the bacteria for Tibetan pigs were shown to be significantly greater than those for Landrace and Berkshire pigs indicated by indices of Chao1, Shannon, PD_whole_tree, and observed OTUs (observed species) (**Figures 1B–E**), which suggested that the bacterial diversity of Tibetan pigs' gut bacteria was significantly higher than those of the other two breeds, and the Landrace pigs' was the lowest.

Boxplot and PCoA based on the unweighted UniFrac distance of MetaOTUs showed clear differences between the community structures of the three breeds of pigs, and the Landrace pigs samples are most similar to each other (**Figures 2A,B**). The analysis showed that the samples of Tibetan pigs are more similar to the samples of Barkshire pigs than Landrace pigs (**Figures 2A,B**).

Nine phyla were screened out of the three gut bacterial communities after the flora data were subjected to Kruskal–Wallis tests (**Figures 2C–K**). *Firmicutes* and *Bacteroides* were revealed to be the two dominant phyla inhabited in the guts of the three breeds of pigs, yet accounting to varied proportions; *Firmicutes* in Tibetan pigs accounted for 74%, and *Firmicutes* in Barkshire and Landrace pigs accounted for 81 and 91.5%, respectively (**Figure 2C**), while *Bacteroides* was present as the highest in Tibetan pigs at 17.9%, and the lowest in Landrace pigs, approximately 4.5% (**Figure 2D**). Moreover, the proportions of *Fibrobacterota*, *Euryarchaeota*, and *Spirochaetota* in the gut bacteria were pronouncedly higher in Tibetan pigs than the other two breeds (**Figures 2E,G,I**) ($p < 0.01$). However, *Verrucobacteria* and *Desulfobacterota* were higher in Berkshire pigs (**Figures 2F,H**) ($p < 0.05$ and $p < 0.01$), and *Cyanobacteria* and *Actinobacteriota* in Landrace pigs were higher than the other two breeds (**Figures 2J,K**) ($p < 0.05$).

Host–gut bacteria association analyses were performed in the top 13 families and 20 genera of the three pig breeds (**Figure 3**). At the family level, as shown in **Figure 3A**, pronouncedly higher abundance of family *Streptococcus* was presented in the gut of Landrace pigs than in those of Tibetan and Berkshire pigs, while families *Clostridiaceae*, *Erysipelotrichaceae*, and *Peptostreptococcaceae* were higher in Berkshire pigs (**Figure 3A**). Greater proportions of *Christensenellaceae*, *Muribaculaceae*, *Prevotellaceae*, *Spirochaetaceae*, *Lachnospiraceae*, *Oscillospiraceae*, and *Ruminococcaceae* resided in Tibetan pigs than in Berkshire and Landrace pigs. Families *Christensenellaceae*, *Muribaculaceae*, *Prevotellaceae*, and *Spirochaetaceae* in Berkshire pigs were higher in abundance than in Landrace pigs. At the genus level, similar to family distribution, *Streptococcus* and *Clostridium* were significantly higher in proportion in the gut flora of Landrace and Berkshire pigs, respectively. In addition, *Romboutsia, Terrisporobacter*, and *Turicibacter* were most abundant in Berkshire pigs. The scale of *Coprococcus* in Berkshire pigs was lower than in the other two groups. *Lachnospiraceae_XPB1014_group* and *Roseburia* in Tibetan pigs and Berkshire pigs were greater in abundance than in Landrace pigs (**Figure 3B**). The populations of genus *Treponema*,

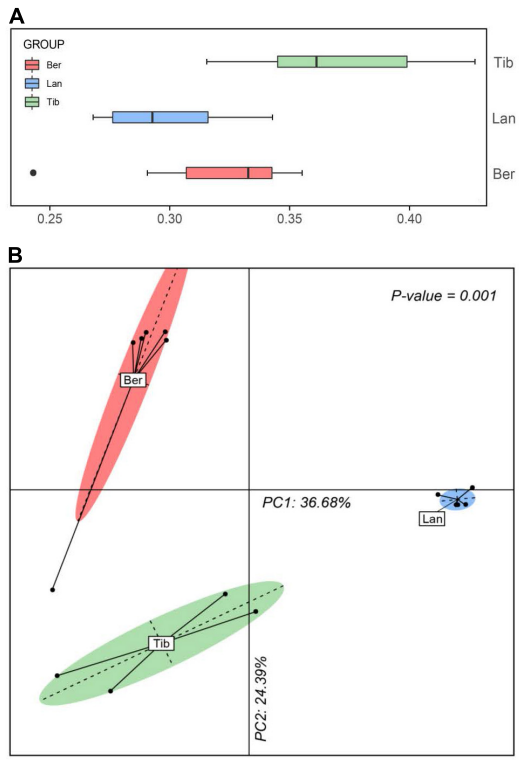

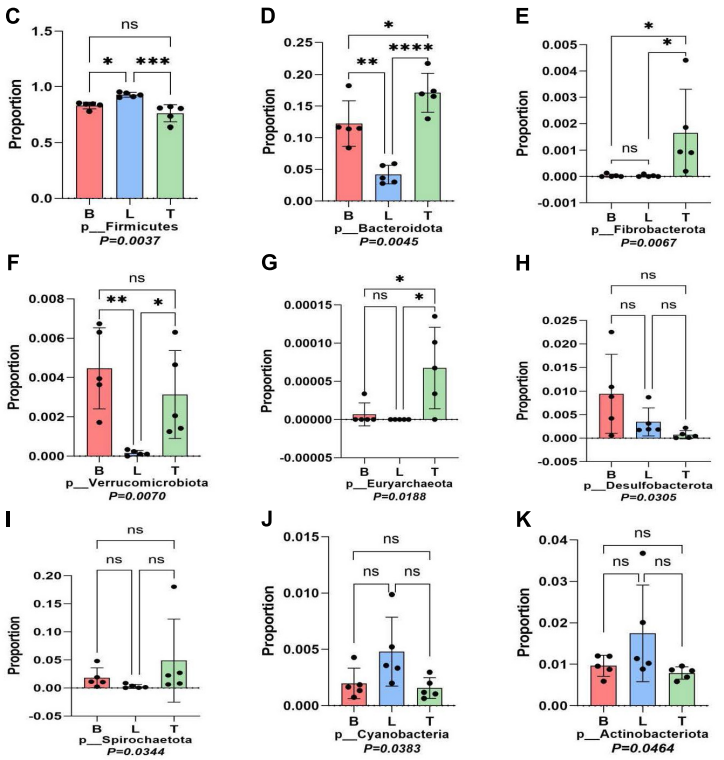

FIGURE 2 | Boxplot, principal coordinate analysis (PCoA), and dominant phylum analysis. Boxplot **(A)** and Principal coordinate analysis (PCoA) based on weighted UniFrac Distances per pig fecal sample **(B)**. Dominant bacteria phyla of three different breeds of pigs were screened out by the Kruskal–Wallis test **(C–K)**. ns was considered insignificant; *$p < 0.05$ was considered as significant difference; **$p < 0.01$, ***$p < 0.001$ and ****$p < 0.0001$ was taken as very significant difference.

NK4A214_group, and *UCG-005* in Tibetan pigs were shown to be significantly higher than those in the other two breeds. The uncultured and unidentified genus presented in Tibetan pigs were obviously higher than in the others (**Figure 3B**).

To further understand the bacterial compositions of gut in detail in each breed of pigs, LDA score was performed using log10 > 4 as the cutoff (**Figure 4A**); cladogram of the LEfSe analyses is shown in **Supplementary Figure 2**. As LEfSe analyses, the dominant inhabitants in the gut bacterial communities of the three breeds of pigs were clearly different between each other, which corresponded with the above host–gut bacteria association analysis.

Subsequently, bacterial metabolic functional predictions were conducted (**Figure 4B**). The seven dominant colonized bacterial species in the gut of Landrace pigs were shown to be highly correlated with the *Staphylococcus_aureus*_infection pathway, and was not correspondent with functions such as Porphyrin_and_chlorophyll_metabolism, Biotin_metabolism, Nicotinate_and_nicotinamide_metabolism, and Protein_digestion_and_absorption. In contrast, the bacterial species that inhabited the Tibetan pigs' gut exerted both anti-*Staphylococcus* and anti-*Helicobacter* functions, and mildly correlated with the NOD-like_receptor_signaling_pathway, which is involved in the recognition of dangerous signals and subsequent regulation of the immune responses in the body, which, however, was missing in the gut community of Landrace pigs. Furthermore, the bacterial communities of Tibetan pigs was highly correspondent to the functions of Pantothenate_and_CoA_biosynthesis, Thiamine_metabolism, and Vitamin_B6_metabolism; in particular, species *Clostridia* and *Oscillospirales* showed significantly higher correlations with Vitamin_B6_metabolism (**Figure 4B**). Besides, the lipid metabolic functions, including Fatty_acid_degradation, Glycerolipid_metabolism, and bile_acid_biosynthesis, were significantly more correlated with the bacterial communities in Berkshire pigs than the other two breeds as shown in **Figure 4B**.

Composition and Functional Potential of Gut Bacteria in Tibetan Pigs at Different Growth Stages

To understand the dynamics of bacterial communities in Tibetan pigs, the gut bacteria were determined at days 7, 60, and 350, respectively. Our results showed that 1,640 OTUs were identified that resided through the three time points in total. Generally, the number of OTUs increased with the growth of the host: 542, 1,206, and 1,390 OTUs were determined at the above time points separately (**Supplementary Figure 3**). Moreover, the scale of individual population of bacterial species was experiencing dynamic variations in the process of the growth of pigs as observed in **Figure 5A**. At the phylum level, *Firmicutes* exhibited a distinct pattern throughout the

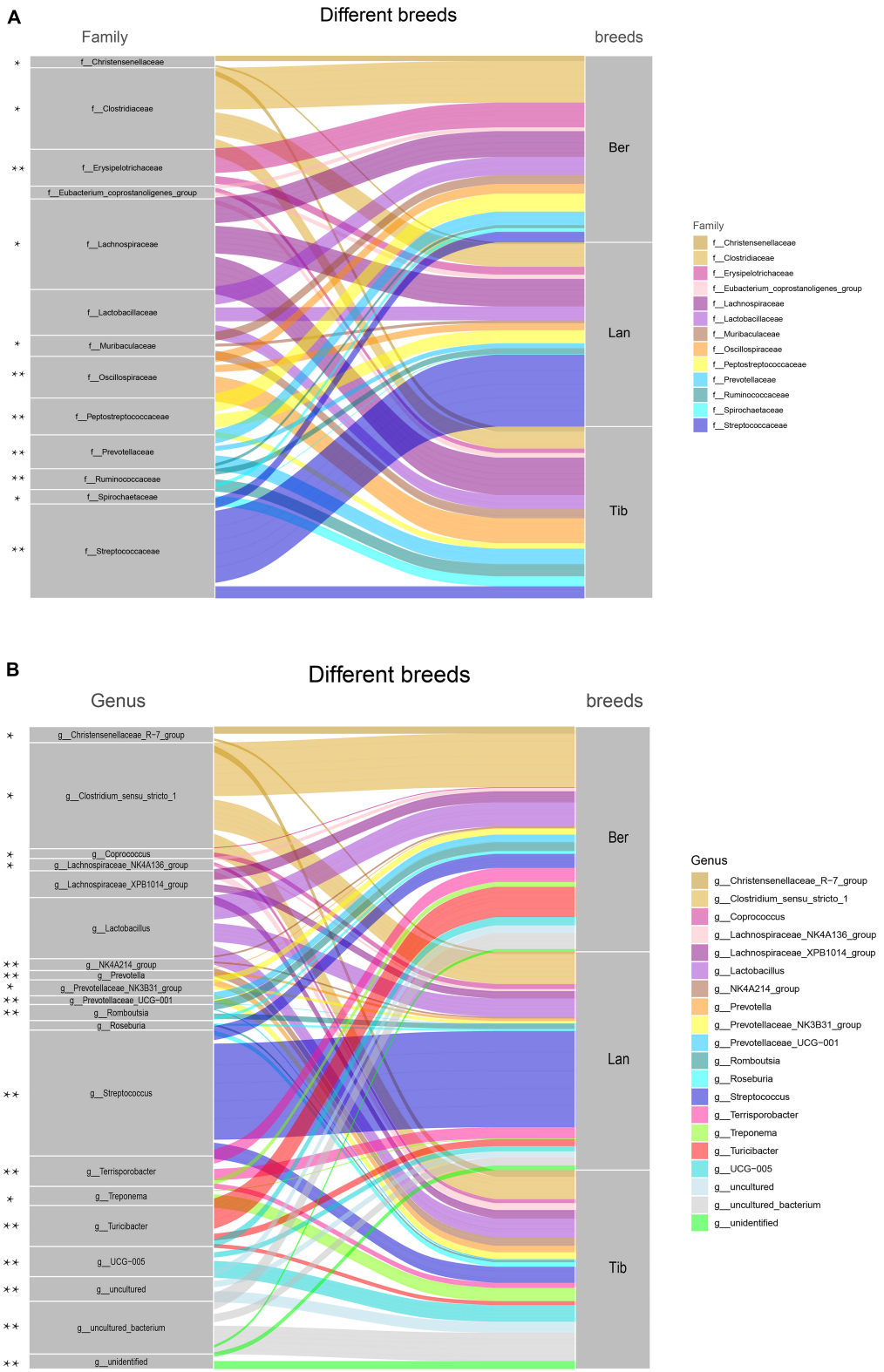

FIGURE 3 | Species composition in the fecal samples of Berkshire, Landrace, and Tibetan pigs. Top 13 dominant family **(A)** and top 20 dominant genus **(B)** were displayed. The color ribbons indicated the associations between families or genus and breeds, of which the colors represented as families or genus. The width of the ribbon reflected the scale of individual connections (the wider the ribbon, the stronger the association) it represented between the families or genus and the breeds. The statistical *p*-values were calculated by Kruskal–Wallis tests. $^{*}p < 0.05$, $^{**}p < 0.01$.

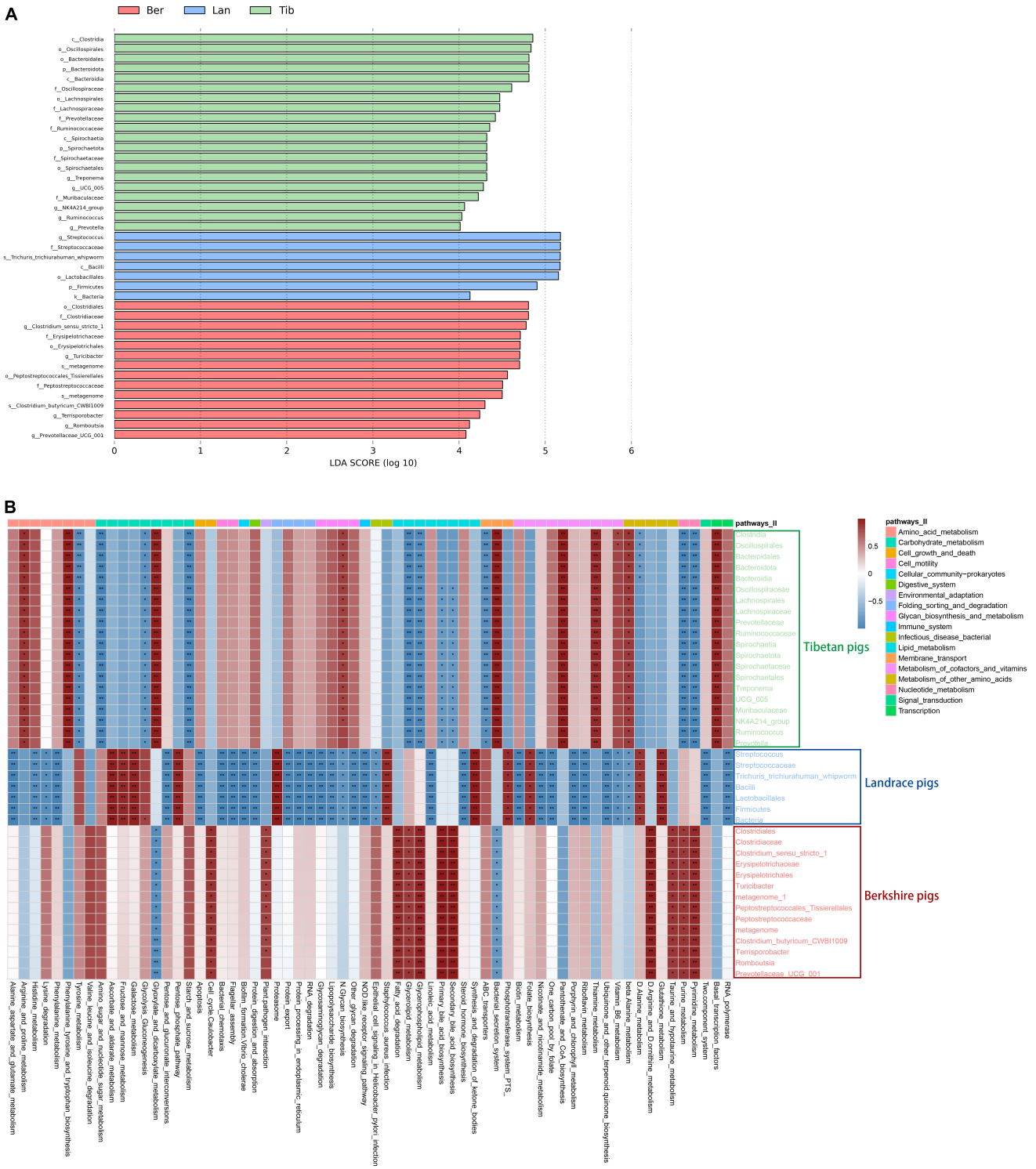

FIGURE 4 | Differences of bacterial species in fecal samples of the three breeds of pigs and heatmap showing the correlation between bacterial species and metabolic pathways. Differences of bacterial species in fecal samples **(A)**. Green, blue, and red represent the bacterial species in Tibetan, Landrace, and Berkshire pigs, respectively. The picture depicts the third-level metabolic pathways annotated against Kyoto Encyclopedia of Genes and Genomes (KEGG). Different colors in the upper part of the picture represent the third-level metabolic pathways annotated to KEGG. Heatmap of correlation between species and metabolic pathways **(B)**. Red represents a positive correlation between species and metabolic pathways, and blue represents a negative correlation. The darker the color, the greater the correlations, $^{*}p < 0.05$, $^{**}p < 0.01$.

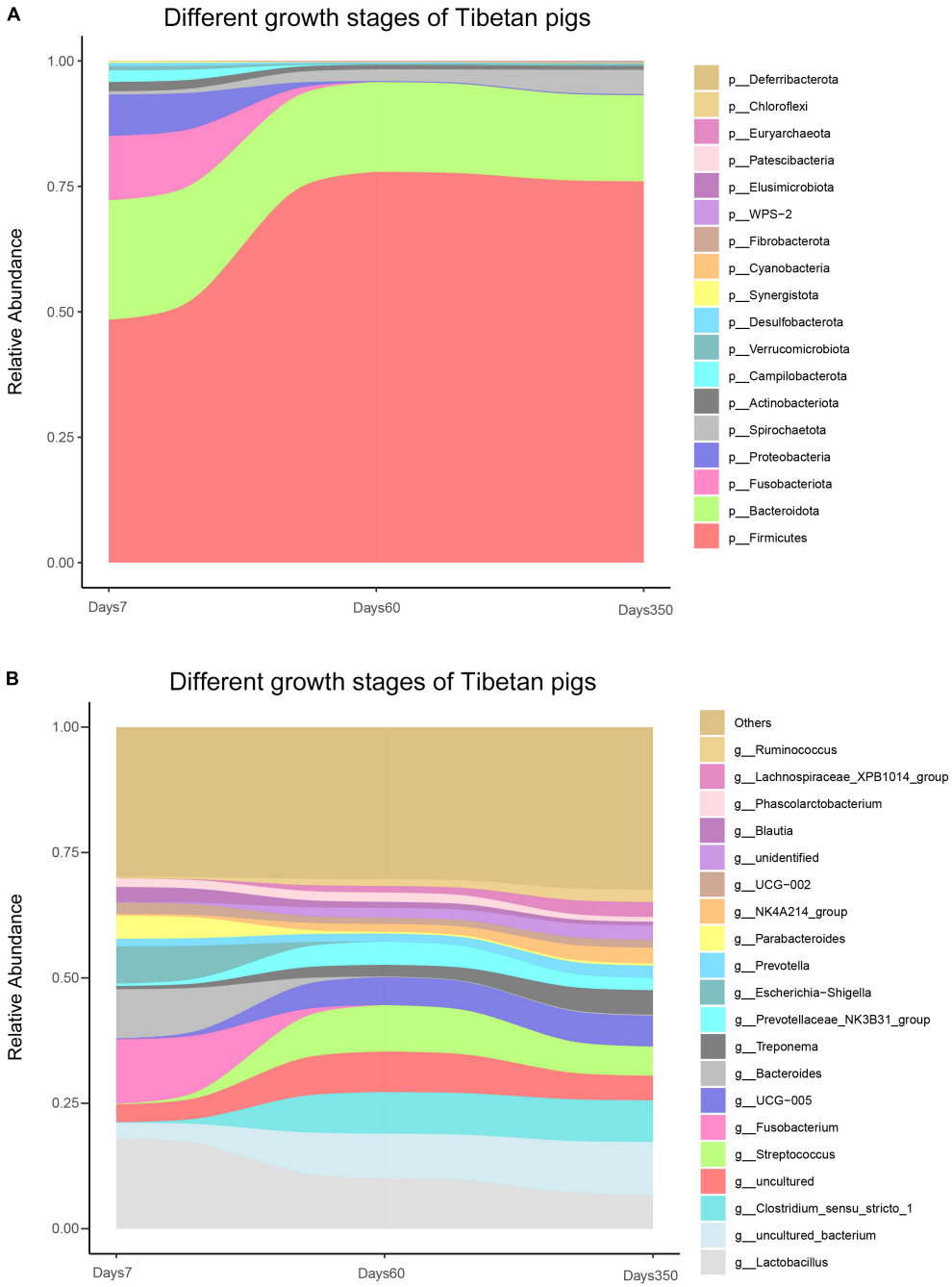

FIGURE 5 | Bacterial composition of Tibetan pigs at different growth stages. Stream-graph displaying the relative abundance of bacterial taxa in days 7, 60, and 350 of Tibetan pigs. Species composition at phylum level **(A)** and top 20 genus **(B)**. Low abundant taxa were grouped as "others".

experimental period, displaying a rising trend in the beginning till around day 60, then started to decline gently, accounting to 48.4, 77.9, and 76.0% at days 7, 60, and 350, respectively. The proportions of *Bacteroidota*, *Proteobacteria*, *Actinobacterota*, *Fusobacteriota*, *Campilobacterota*, *Desulfobacterota*, and *Verrucomicrobiota* had a higher initial relative abundance during the first 7 days, then decreased with the growth of the host, and *Patescibacteria* decreased, while the specific densities of *Spirochaetota*, *Fibrobacterota*, *WPS-2*, *Elusimicrobiota*, and *Deferribacterota* showed increases in the pigs as time passes. Moreover, *Cyanobacteria* and *Chloroflexi* possessed the highest levels of colonized population within the initial 60-day age of pigs.

At the genus level, the analysis showed that the colonized populations of *Clostridium_sensu_stricto_1*, *UCG-005*, *Treponema*, *Prevotella*, *NK4A214_group*,

Lachnospiraceae_XPB1014_group, *Ruminococcus*, unidentified, and other rare species in pigs increased, while those of *Lactobacillus*, *Fusobacterium*, and *Prevoichilauace-ae_NK3* reduced with the aging of the pigs (**Figure 5B**). Moreover, Uncultured_bacterium and *Streptococcus* showed a fluctuation of initial rising and then a decreasing trend. *Bacteroides*, however, showed a reverse trend (**Figure 5B**).

Furthermore, bacterial functional predictions using PICRUSt were performed. Three layers of KEGG functional categories and the top 15 pathways were taken into account, covering the information of genetic processing and metabolisms of lipids, amino acids, and carbohydrates. As shown in **Figure 6**, significantly high abundance of bacterial flora was correlative with the biosynthesis of ansamycin throughout the growth of the pigs. Pronounced increases of bacterial species were related to Valine_leucine_and_isoleucine and Fatty_acid_biosynthetic pathways as the pigs grew. In addition, it was shown that the abundance of gut flora correlated with the biosynthesis of vancomycin and was significantly higher at day 7 than those of days 60 and 350. The bacterial abundances correlated to the Pentose phosphate pathway and One carbon pool by folate pathways were initially exhibited as decreasing trends. Then, with the aging of the pigs, more bacteria became involved, whereas the tendency reversed when it came to the Pantothenate and CoA biosynthesis and Ribosome procession.

As for the colony interactions shown in **Figure 7**, the network of gut bacteria of suckling pigs at day 7 was clearly distributed into three clusters, one of which, with g_*Escherichia-Shigella* as the core genera, extended to comprise g_*Lactobacillus*, g_*Lachnoclostridium*, and g_*Ruminococcus_torques*_group in it (**Figure 7A**). However, the symbiosis network of 60-day pigs was shown to be more independent and simpler (less connected nodes and edges), and not as complicatedly weaved as observed in the pigs at day 350 (more connected nodes and edges) (**Figure 7B**). On day 350, the colonized gut flora was shown a high taxonomic connection in the Tibetan pigs, except that a few genera were separately connected forward or backward (**Figure 7C**).

Composition and Functional Potential of Gut Bacteria Between Two Genders of Tibetan Pigs

The feces of boars and sows in pregnant and lactate phases were collected; 710 shared OTUs were identified among these boars and sows, with 1,016, 984, and 910 OTUs for boars, pregnant sows, and lactating sows, respectively (**Supplementary Figure 4**).

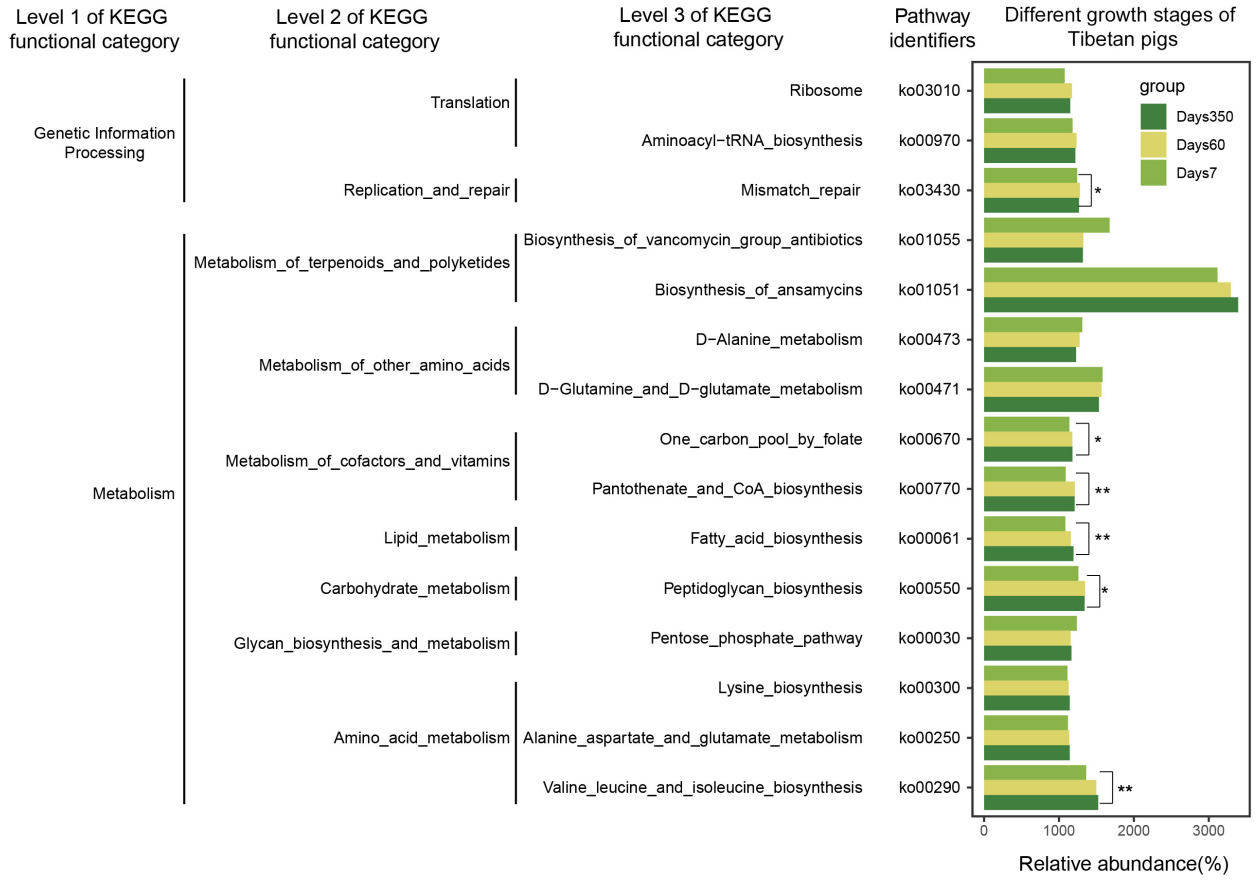

FIGURE 6 | Bacterial functional prediction of Tibetan pigs at three growth stages. The picture shows three levels of KEGG functional category. The gradient colors represent three growth stages. Significant differences were calculated by Kruskal–Wallis tests, $^{*}p < 0.05$, $^{**}p < 0.01$.

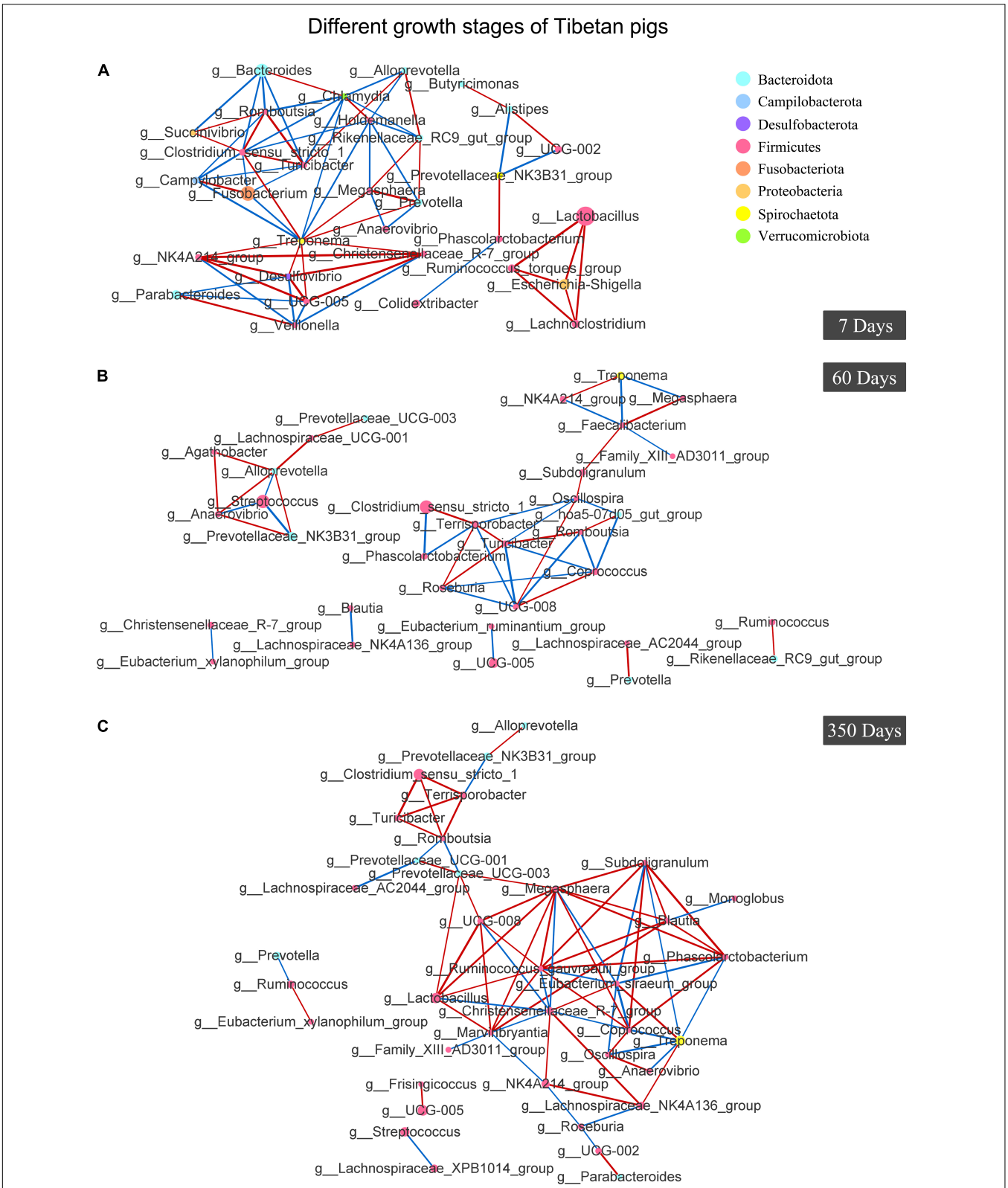

FIGURE 7 | Analysis of Co-occurrence Network of gut bacteria in Tibetan pigs at different growth stages. Co-occurrence Network of Tibetan pigs at day 7 **(A)**, day 60 **(B)**, and day 350 **(C)**. Individual color of dots represented the phyla in the gut. The size of nodes was proportional to the relative abundance of genus. Red lines stood for positive correlations between species, and blue lines represented negative correlations between species. The thickness of the lines indicated the size of the correlation coefficient value.

At the phylum level, *Firmicutes* was the dominant bacteria in both genders. Specifically, a higher abundance of *Firmicutes* and lower *Bacteroidota*, *Proteobacteria*, and *Spirochaetota* inhabited in boars compared to those in sows. The abundances of *Bacteroidota* and *Spirochaetota* in pregnant sows were higher than those of lactating sows. However, the bacterial phylum *Verrucomicrobiota* tended to colonize the gut of lactating rather than pregnant sows, and the least in the boars. *Actinobacteriota*, however, exhibited a reverse trend (**Figure 8A**).

At the genus level, the abundances of colonial *Clostridium_sensu_stricto_1*, *Turicibacter*, *Terrisporobacter*, *Lactobacillus*, and *Romboutsia* in boars were significantly

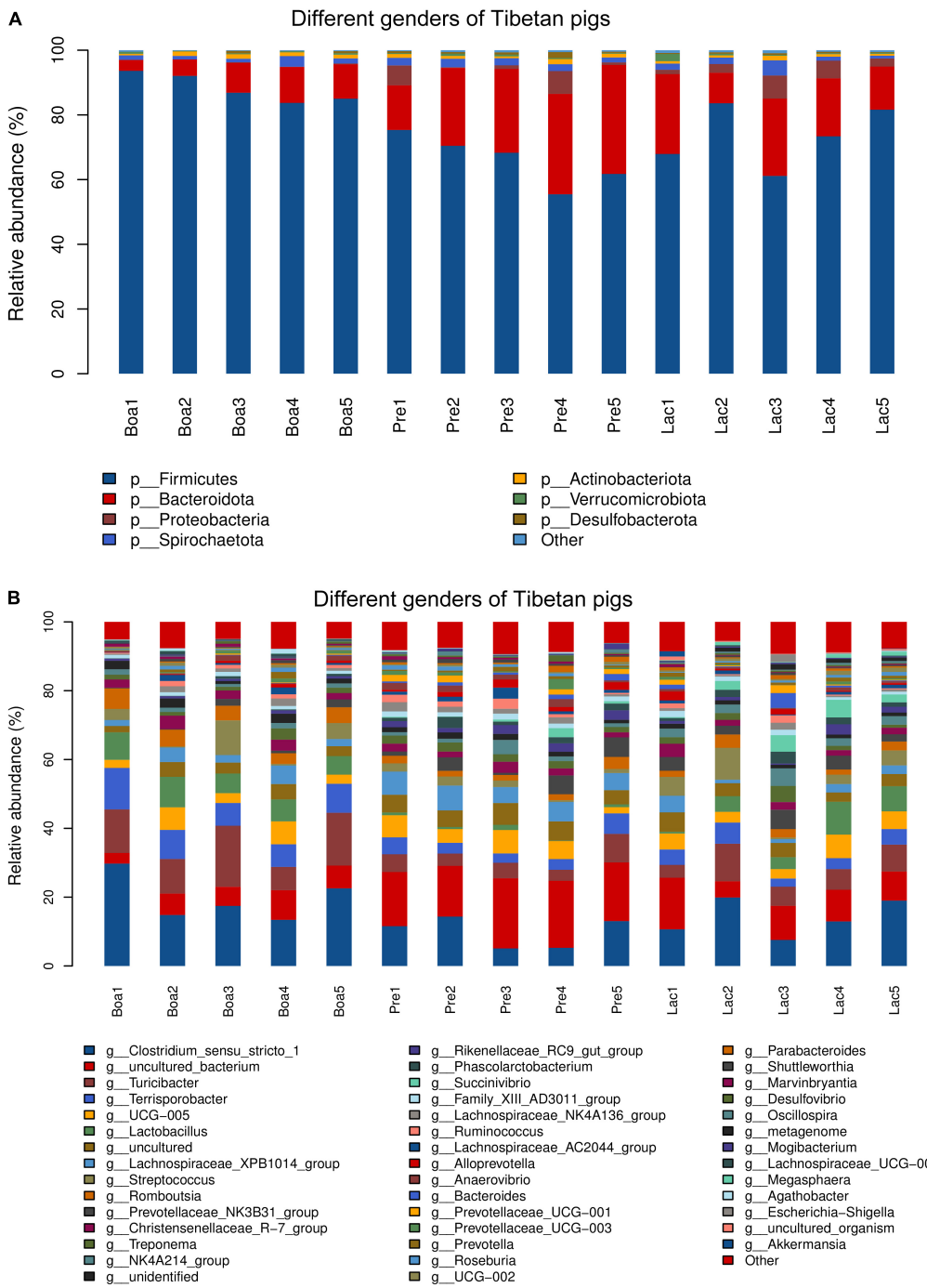

FIGURE 8 | Relative abundance of bacterial species residing in the guts of boars, pregnant sows, and lactating sows. At the phylum level **(A)** and at the genus level **(B)**.

higher than those in sows' gut flora. The genus *Succinivibrio* presented the most in lactating sows and least in boars. Uncultured_bacterium exhibited as the most in pregnant sows and least in boars (**Figure 8B**).

Bacterial functional predictions against 31 relevant KEGG pathways were performed to further understand the effects of gender on gut flora colonization (**Figure 9**). Gut bacteria of boars were more correlative to the pathways of metabolisms of carbohydrate, lipid, drug resistance, environmental adaptation, and xenobiotics biodegradations; pregnant sows were the next for these metabolisms, except for the metabolisms of drug resistance and environmental adaptation (**Figure 9**). However, the bacterial communities of pregnant sows were most correlated with the pathways of metabolisms of amino acid, digestion, energy, glycan biosynthesis and metabolism, immune responses, and vitamins and its cofactors. In particular, the correlation index reached 10 for the metabolism of cofactors and vitamins, significantly higher than those for boars and lactating sows. The gut bacteria in lactating sows were more related to the infectious_disease_bacterial pathway than others. In particular, the relations were significantly lower in the pathways including amino acid, carbohydrate, and lipid metabolism in lactating sows

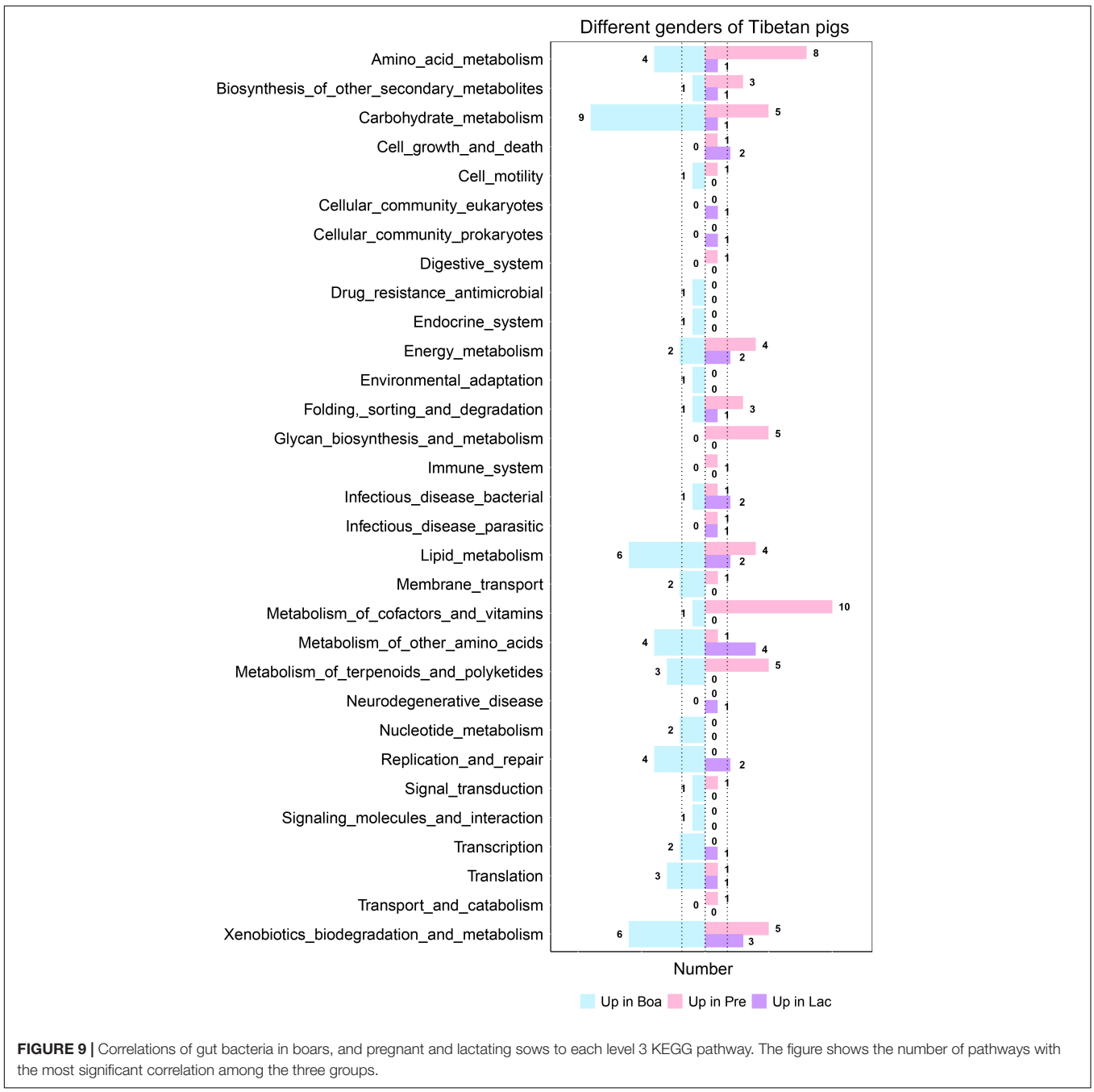

FIGURE 9 | Correlations of gut bacteria in boars, and pregnant and lactating sows to each level 3 KEGG pathway. The figure shows the number of pathways with the most significant correlation among the three groups.

(**Figure 9**). In addition, the intestinal flora of boars was the most respondent to the biosynthesis of ansamycins ($p < 0.05$) (**Supplementary Figure 5**).

DISCUSSION

Compared to previous research (Wang et al., 2012; Jiang et al., 2018; Zeng et al., 2020), the Tibetan pigs under semi-grazing were selected as research subjects. The pigs are introduced and raised in the other areas and circulated in the market. Moreover, they live in semi-grazing conditions and are not fed commercial feed. Perhaps in China, such a "second-generation Tibetan pig" is more likely to be the future development trend. In this study, we determined the bacterial composition of the gut microbiota in Tibetan pigs, and those of Berkshire and Landrace pigs were used for comparison. Furthermore, we found that growth stage, gender, pregnancy, or lactation of sows all affect gut bacteria of Tibetan pigs.

As expected, the structure of gut community in the Tibetan pigs was more complex than the other two breeds. Previous studies had demonstrated that the gut microbiota played an important role on the adaptability of yak to harsh environments of the Qinghai-Tibet Plateau (Guo et al., 2021). Tibetan pigs, similarly, is a breed of highland pig. Studies have supported the hypothesis that the given high-altitude environment helps to shape particular microbiota colonized in the gut, in turn facilitating Tibetan pigs to adapt to the harsh environment (Zeng et al., 2020). The relationship between intestinal bacteria and environmental adaptability of Tibetan pigs in the introduction area remains to be explored.

The Berkshire pig was known for its high-quality meat (Jang et al., 2018) and adaptation to semi-grazing conditions. Landrace pigs, on the contrary, claimed to have a high growth rate (Tang et al., 2007). Comparatively, the gut bacterial structure of the Tibetan pigs was supposed to be more similar to that of Berkshire pigs. Our data showed that the abundance of phylum *Firmicutes* colonized in the gut of Tibetan pigs was significantly lower, whereas *Bacteroides* was much higher than in the other two breeds. The roles of intestinal *Firmicutes* and *Bacteroides* on host's obesity were initially established in 2005, an observation based on the investigation of the microbiota of genetically modified, lean, and wild-type mice, which demonstrated that the colonized *Bacteroidetes* was 50% lower in obese animals than their counterpart in lean mice (Tang et al., 2007). In addition, it was found that a low *Firmicutes*/*Bacteroidetes* ratio was associated with the lean phenotype and a healthy cardiovascular and balanced immune system (Nicholson et al., 2012; Tang et al., 2017). Phylum *Fibrobacteriota* comprises many rumen bacteria, allowing for the degradation of cellulose (Ransom-Jones et al., 2012, 2014). In this study, a higher proportion of *Fibrobacterota* was identified in the gut of Tibetan pigs, which might be ascribed to its herbivory. In addition, human clinical data showed that the abundance of *Verrucomicrobia* in human intestine was inversely associated with the state of host bacterial infections (Dubourg et al., 2013). This may indirectly reflect the high disease-resistant capacity of Tibetan pigs, in which *Verrucomicrobia* had been a long inhabitant. Our data also showed that a number of bacterial families that correlated with anti-inflammation, nutrient metabolism, and absorption pathways resided in the gut of Tibetan pigs in high abundance, such as the probiotic *Christensenellaceae* and *Muribaculaceae*, which had been confirmed to be negatively related to inflammatory and metabolic diseases (Tavella et al., 2021); *Lachnospiraceae* and *Prevotellaceae*, which were related to the synthesis of short-chain fatty acids (SCFAs) responsible for the protection of intestinal mucosae (Purushe et al., 2010; Laffin et al., 2019); and *Methanobrevibacter*, which was an important player in the hydrogen nutrient methane production pathway (St-Pierre and Wright, 2013); moreover, *Muribaculaceae* (S24-7) was shown to be capable of inhibiting inflammatory responses in the animal's intestinal tract, playing an important role in maintaining intestinal health (Ormerod et al., 2016). *Ruminococcaceae*, a producer of butyric acid providing energy for intestinal epithelial cells, is involved in the maintenance of the health of intestine (Serpa et al., 2010) and exerted negative effects on colorectal cancer (Dayama et al., 2020). Besides, *Treponema bryantii* of genus *Treponema*, the most abundant in phylum *Spirochetes*, was identified to be colonized in high abundance in Tibetan pigs and possessed the ability to inhibit intestinal pathogenic bacteria, such as *Escherichia coli* and *Salmonella* (Edrington et al., 2012). All these data evidenced the high capability of disease prevention of Tibetan pigs.

Furthermore, bacterial functional analysis also supported that the gut bacteria of Tibetan pigs was more robustly correspondent to the anti-infection metabolism or pathways. The microflora residing in Landrace pigs was significantly correlated with *Staphylococcus aureus* infections, and the risk of streptococcal infection was high. In contrast, the bacterial communities of Tibetan pigs was vigorously correlated with vitamin B1, B5, and B6 metabolism and synthesis, which facilitated to strengthen its immune system, especially anti-inflammatory responses (Du et al., 2020). The NOD-like receptor was a key factor involved in the regulation of the host's native immune responses and was identified to be significantly correlated with the bacteria in Tibetan pigs. Long-term consumption of green roughage may contribute to the shape of disease-resistant characterization of the gut bacteria in Tibetan pigs.

Taxonomic richness displayed a positively linear correlation with the growth of pigs, which was consistent with previous studies (Jurburg and Bossers, 2021). Specifically, with the increase of age, the intestinal bacteria of Tibetan pigs became more and more abundant. In addition, previous studies revealed that increases in the prevalence of *Fusobacteria* were related to colorectal cancer (Kelly et al., 2018), malnutrition (Pham et al., 2019), impaired human immune recovery (Lee et al., 2018), and biological disorders in suckling pigs (Huang et al., 2019). Our study showed that the abundance of *Fusobacteriota* gradually declined with the aging of the hosts until they disappeared from the gut bacteria on day 360 of Tibetan pigs.

As expected, gut bacteria of Tibetan pigs were more correlated with the perfection of metabolic functions with age; metabolisms of terpenoids and polyketides, amino acids, and lipids, especially

the ability of biosynthesis of ansamycins of the host, were enhanced, which could strengthen the anti-microbial and anti-cancer ability. In addition, the genetic processing was maximized at 60 days of age of the pigs.

Extensive studies showed that diet affected the host's gut microbiota; a stable diet can stabilize the gut microbiota to a certain extent (Han et al., 2020; Gao et al., 2021). Comparatively, the taxonomic relations of gut microbiota in 60-day pigs was unstable, which may be caused by weaning. Previous reports also found high variability in PD whole tree and Shannon index in 56-day-old Tibetan minipigs (Jiang et al., 2018). Instead, a stable gut bacteria relationship was exhibited in 360-day pigs, which were supposed to have more stable body functions and immune responses comparatively (**Figure 7**).

Gender exerted effects on the abundances of the bacterial families residing in the gut of Tibetan pigs. Our analysis showed that the dominant bacteria phyla were the same; the population sizes, however, appeared to be different across boars', pregnant sows', and lactating sows' gut bacteria. Of these, *Lactobacillus* was shown to be significantly higher in boars than sows. *Lactobacillus* species are probiotics, and considered to be beneficial to hosts' health (Gareau et al., 2010). The high abundance of *Succinivibrio* in boars' gut bacteria was also a signature of its high adaptability. *Succinivibrio* species was characterized as high capacity of degradation of cellulose and positively correlated with IL-10, a crucial immunomodulatory cytokine. In contrast, decreases in the abundance of *Succinivibrio* may help maintain the mucosal barrier and prevent chronic immune activation in the natural host (Jasinska et al., 2020) during Simian immunodeficiency virus infection. The exact function of this bacterium needs further study.

Vitamins in the diet were supposed to have beneficial effects on women's fertility (Skoracka et al., 2021). Interestingly, the gut bacteria in pregnant sows appeared to be more correlated to the metabolism of cofactors and vitamins than the other two groups, and lactating sows appeared to have higher responses to bacterial infections, which may be more beneficial to improve the levels of maternal antibodies.

In conclusion, the bacterial composition of Tibetan pigs exhibited a distinct structure, many of which were uncultivated and unidentified bacteria families. These may represent new prokaryotic taxa and increase the phylogenetic diversity of the microbial tree of life (Zhou et al., 2020). In addition, despite individual growth stages, genders and physiological periods difference, bacterial populations of Tibetan pigs exhibited a dynamic equilibrium with varied abundance. This pilot study on the gut bacterial communities in Tibetan pigs may shed light on how we could improve our human adaptability *via* modulating microecology.

DATA AVAILABILITY STATEMENT

Raw sequencing data obtained were deposited in the database SRA under accession number PRJNA768095.

ETHICS STATEMENT

All experiments and procedures were approved by Jilin Agricultural University. All animal experiments in the study complied with the regulations of the Animal Protection and Ethics Committee of Jilin Agricultural University (JLAU20210111001). Written informed consent was obtained from the owners for the participation of their animals in this study.

AUTHOR CONTRIBUTIONS

W-TY, C-FW, G-LY, and C-WS designed the research. HN, X-ZF, DZ, and H-LC performed the research. H-BH, Y-LJ, NW, J-ZW, XC, and YZ analyzed the data. W-TY, C-FW, and G-LY supported the research. HN and W-TY wrote the manuscript. All authors contributed to the article and approved the submitted version.

FUNDING

This work was supported by the National Natural Science Foundation of China (31941018, 31972696, 32072888, and U21A20261), the Science and Technology Development Program of Jilin Province (20190301042NY, YDZJ202102CXJD029, and 20210202102NC), and the China Agriculture Research System of MOF and MARA (CARS-35).

ACKNOWLEDGMENTS

We would like to thank Qing Niu and Jie Niu, Tibetan pig farmers in Dachuankou Village, Heshun County, Shanxi Province for providing animals and assisting in collecting samples.

SUPPLEMENTARY MATERIAL

The Supplementary Material for this article can be found online at: https://www.frontiersin.org/articles/10.3389/fmicb.2022.850687/full#supplementary-material

REFERENCES

Bäckhed, F., Roswall, J., Peng, Y., Feng, Q., Jia, H., Kovatcheva-Datchary, P., et al. (2015). Dynamics and Stabilization of the Human Gut Microbiome during the First Year of Life. *Cell Host Microb.* 17:852. doi: 10.1016/j.chom.2015.05.012

Chen, C., Fang, S., Wei, H., He, M., Fu, H., Xiong, X., et al. (2021). *Prevotella copri* increases fat accumulation in pigs fed with formula diets. *Microbiome* 9:175. doi: 10.1186/s40168-021-01110-0

Chen, H., Mozzicafreddo, M., Pierella, E., Carletti, V., Piersanti, A., Ali, S., et al. (2021). Dissection of the gut microbiota in mothers and children with chronic *Trichuris trichiura* infection in Pemba Island, Tanzania. *Parasit. Vectors* 14:62. doi: 10.1186/s13071-021-04580-1

Cheng, C., Sun, W., Liu, R., Wang, R., Chen, Y., Wang, Y., et al. (2015). Comparison of gene expression of Toll-like receptors and antimicrobial peptides in immune organs and tissues between Yorkshire and Tibetan pigs. *Anim. Genet.* 46, 272–279. doi: 10.1111/age.12286

Chopyk, D. M., and Grakoui, A. (2020). Contribution of the Intestinal Microbiome and Gut Barrier to Hepatic Disorders. *Gastroenterology* 159, 849–863. doi: 10.1053/j.gastro.2020.04.077

Cole, J. R., Wang, Q., Cardenas, E., Fish, J., Chai, B., Farris, R. J., et al. (2009). The Ribosomal Database Project: improved alignments and new tools for rRNA analysis. *Nucleic Acids Res.* 37, D141–D145. doi: 10.1093/nar/gkn879

Dayama, G., Priya, S., Niccum, D. E., Khoruts, A., and Blekhman, R. (2020). Interactions between the gut microbiome and host gene regulation in cystic fibrosis. *Genom. Med.* 12, 12. doi: 10.1186/s13073-020-0710-2

Du, X., Yang, Y., Zhan, X., Huang, Y., Fu, Y., Zhang, Z., et al. (2020). Vitamin B6 prevents excessive inflammation by reducing accumulation of sphingosine-1-phosphate in a sphingosine-1-phosphate lyase-dependent manner. *J. Cell Mol. Med.* 24, 13129–13138. doi: 10.1111/jcmm.15917

Dubourg, G., Lagier, J., Armougom, F., Robert, C., Audoly, G., Papazian, L., et al. (2013). High-level colonisation of the human gut by *Verrucomicrobia* following broad-spectrum antibiotic treatment. *Int. J. Antimicrob. Agents* 41, 149–155. doi: 10.1016/j.ijantimicag.2012.10.012

Edgar, R. (2013). UPARSE: highly accurate OTU sequences from microbial amplicon reads. *Nat. Methods* 10, 996–998. doi: 10.1038/nmeth.2604

Edrington, T., Dowd, S., Farrow, R., Hagevoort, G., Callaway, T., Anderson, R., et al. (2012). Development of colonic microflora as assessed by pyrosequencing in dairy calves fed waste milk. *J. Dairy Sci.* 95, 4519–4525. doi: 10.3168/jds.2011-5119

Fan, W., Jiao, P., Zhang, H., Chen, T., Zhou, X., Qi, Y., et al. (2020). Inhibition of African Swine Fever Virus Replication by Porcine Type I and Type II Interferons. *Front. Microbiol.* 11:1203. doi: 10.3389/fmicb.2020.01203

Fouts, D., Szpakowski, S., Purushe, J., Torralba, M., Waterman, R., MacNeil, M., et al. (2012). Next generation sequencing to define prokaryotic and fungal diversity in the bovine rumen. *PloS One* 7:e48289. doi: 10.1371/journal.pone.0048289

Gao, J., Guo, X., Wei, W., Li, R., Hu, K., Liu, X., et al. (2021). The Association of Fried Meat Consumption With the Gut Microbiota and Fecal Metabolites and Its Impact on Glucose Homoeostasis, Intestinal Endotoxin Levels, and Systemic Inflammation: A Randomized Controlled-Feeding Trial. *Diabet. Care* 44, 1970–1979. doi: 10.2337/dc21-0099

Gareau, M. G., Sherman, P. M., and Walker, W. A. (2010). Probiotics and the gut microbiota in intestinal health and disease. *Nat. Rev. Gastroenterol. Hepatol.* 7, 503–514. doi: 10.1038/nrgastro.2010.117

Gehrig, J., Venkatesh, S., Chang, H., Hibberd, M., Kung, V., Cheng, J., et al. (2019). Effects of microbiota-directed foods in gnotobiotic animals and undernourished children. *Science* 365, eaau4732. doi: 10.1126/science.aau4732

Guo, N., Wu, Q., Shi, F., Niu, J., Zhang, T., Degen, A., et al. (2021). Seasonal dynamics of diet-gut microbiota interaction in adaptation of yaks to life at high altitude. *NPJ Biofilms Microbio.* 7:38. doi: 10.1038/s41522-021-00207-6

Han, M., Yang, K., Yang, P., Zhong, C., Chen, C., Wang, S., et al. (2020). Stratification of athletes' gut microbiota: the multifaceted hubs associated with dietary factors, physical characteristics and performance. *Gut Microb.* 12, 1–18. doi: 10.1080/19490976.2020.1842991

Hinkel, R., Lange, P., Petersen, B., Gottlieb, E., Ng, J., Finger, S., et al. (2015). Heme Oxygenase-1 Gene Therapy Provides Cardioprotection Via Control of Post-Ischemic Inflammation: An Experimental Study in a Pre-Clinical Pig Model. *J. Am. Coll. Cardiol.* 66, 154–165. doi: 10.1016/j.jacc.2015.04.064

Huang, A., Cai, R., Wang, Q., Shi, L., Li, C., and Yan, H. (2019). Dynamic Change of Gut Microbiota During Porcine Epidemic Diarrhea Virus Infection in Suckling Piglets. *Front. Microbiol.* 10:322. doi: 10.3389/fmicb.2019.00322

Huang, Z., Li, Q., Li, M., and Li, C. (2021). Transcriptome analysis reveals the long intergenic noncoding RNAs contributed to skeletal muscle differences between Yorkshire and Tibetan pig. *Sci. Rep.* 11:2622. doi: 10.1038/s41598-021-82126-2

Jang, D., Yoon, J., Taye, M., Lee, W., Kwon, T., Shim, S., et al. (2018). Multivariate genome-wide association studies on tenderness of Berkshire and Duroc pig breeds. *Genes Genom.* 40, 701–705. doi: 10.1007/s13258-018-0672-6

Jasinska, A., Dong, T., Lagishetty, V., Katzka, W., Jacobs, J., Schmitt, C., et al. (2020). Shifts in microbial diversity, composition, and functionality in the gut and genital microbiome during a natural SIV infection in vervet monkeys. *Microbiome* 8:154. doi: 10.1186/s40168-020-00928-4

Jiang, X., Chen, B., Gu, D., Rong, Z., Su, X., Yue, M., et al. (2018). Gut Microbial Compositions in Four Age Groups of Tibetan Minipigs. *Pol. J. Microbiol.* 67, 383–388. doi: 10.21307/pjm-2018-038

Jurburg, S. D., and Bossers, A. (2021). Age Matters: Community Assembly in the Pig Fecal Microbiome in the First Month of Life. *Front. Microbiol.* 12:564408. doi: 10.3389/fmicb.2021.564408

Kelly, D., Yang, L., and Pei, Z. (2018). Gut Microbiota, *Fusobacteria*, and Colorectal Cancer. *Diseases* 6:109. doi: 10.3390/diseases6040109

Laffin, M., Fedorak, R., Zalasky, A., Park, H., Gill, A., Agrawal, A., et al. (2019). A high-sugar diet rapidly enhances susceptibility to colitis via depletion of luminal short-chain fatty acids in mice. *Sci. Rep.* 9:12294. doi: 10.1038/s41598-019-48749-2

Lee, S., Chua, L., Yap, S., Khang, T., Leng, C., Raja Azwa, R., et al. (2018). Enrichment of gut-derived *Fusobacterium* is associated with suboptimal immune recovery in HIV-infected individuals. *Sci. Rep.* 8:14277. doi: 10.1038/s41598-018-32585-x

Li, J., Yang, X., Zhou, X., and Cai, J. (2021). The Role and Mechanism of Intestinal Flora in Blood Pressure Regulation and Hypertension Development. *Antioxi. Redox Signal.* 34, 811–830. doi: 10.1089/ars.2020.8104

Li, Y., Dai, M., Yan, J., Liu, F., Wang, X., Lin, L., et al. (2021). Colonic dialysis can influence gut flora to protect renal function in patients with pre-dialysis chronic kidney disease. *Sci. Rep.* 11:12773. doi: 10.1038/s41598-021-91722-1

Lu, S., and Kolls, J. K. (2021). Early Antibiotics in Cystic Fibrosis: Lessons from the Cystic Fibrosis Pig Model. *Am. J. Respir. Crit. Care Med.* 204, 626–627. doi: 10.1164/rccm.202106-1383ED

Lunney, J. (2007). Advances in swine biomedical model genomics. *Int. J. Biol. Sci.* 3, 179–184. doi: 10.7150/ijbs.3.179

Ma, Y., Han, X., Huang, C., Zhong, L., Adeola, A., Irwin, D., et al. (2019). Population Genomics Analysis Revealed Origin and High-altitude Adaptation of Tibetan Pigs. *Sci. Rep.* 9:11463. doi: 10.1038/s41598-019-47711-6

Martinez-Guryn, K., Leone, V., and Chang, E. B. (2019). Regional Diversity of the Gastrointestinal Microbiome. *Cell Host Microb.* 26, 314–324. doi: 10.1016/j.chom.2019.08.011

Munyaka, P., Eissa, N., Bernstein, C., Khafipour, E., and Ghia, J. (2015). Antepartum Antibiotic Treatment Increases Offspring Susceptibility to Experimental Colitis: A Role of the Gut Microbiota. *PloS One* 10:e0142536. doi: 10.1371/journal.pone.0142536

Nicholson, J., Holmes, E., Kinross, J., Burcelin, R., Gibson, G., Jia, W., et al. (2012). Host-gut microbiota metabolic interactions. *Science* 336, 1262–1267. doi: 10.1126/science.1223813

Ormerod, K., Wood, D., Lachner, N., Gellatly, S., Daly, J., Parsons, J., et al. (2016). Genomic characterization of the uncultured *Bacteroidales* family *S24-7* inhabiting the guts of homeothermic animals. *Microbiome* 4:36. doi: 10.1186/s40168-016-0181-2

Pham, T. P., Tidjani Alou, M., Bachar, D., Levasseur, A., Brah, S., Alhousseini, D., et al. (2019). Gut Microbiota Alteration is Characterized by a *Proteobacteria* and *Fusobacteria* Bloom in Kwashiorkor and a *Bacteroidetes* Paucity in Marasmus. *Sci. Rep.* 9:9084. doi: 10.1038/s41598-019-45611-3

Purushe, J., Fouts, D. E., Morrison, M., White, B. A., Mackie, R. I., Coutinho, P. M., et al. (2010). Comparative genome analysis of *Prevotella ruminicola* and *Prevotella bryantii*: insights into their environmental niche. *Microb. Ecol.* 60, 721–729. doi: 10.1007/s00248-010-9692-8

Ransom-Jones, E., Jones, D. L., Edwards, A., and McDonald, J. E. (2014). Distribution and diversity of members of the bacterial phylum *Fibrobacteres* in environments where cellulose degradation occurs. *Syst. Appl. Microbiol.* 37, 502–509. doi: 10.1016/j.syapm.2014.06.001

Ransom-Jones, E., Jones, D. L., McCarthy, A. J., and McDonald, J. E. (2012). The *Fibrobacteres*: an important phylum of cellulose-degrading bacteria. *Microb. Ecol.* 63, 267–281. doi: 10.1007/s00248-011-9998-1

Ross, B. D., Verster, A. J., Radey, M. C., Schmidtke, D. T., Pope, C. E., Hoffman, L. R., et al. (2019). Human gut bacteria contain acquired interbacterial defence systems. *Nature* 575, 224–228. doi: 10.1038/s41586-019-1708-z

Serpa, J., Caiado, F., Carvalho, T., Torre, C., Gonçalves, L., Casalou, C., et al. (2010). Butyrate-rich colonic microenvironment is a relevant selection factor for metabolically adapted tumor cells. *J. Biol. Chem.* 285, 39211–39223. doi: 10.1074/jbc.M110.156026

Shute, A., Callejas, B., Li, S., Wang, A., Jayme, T., Ohland, C., et al. (2021). Cooperation between host immunity and the gut bacteria is essential for helminth-evoked suppression of colitis. *Microbiome* 9:186. doi: 10.1186/s40168-021-01146-2

Si, H., Yang, Q., Hu, H., Ding, C., Wang, H., and Lin, X. (2021). Colorectal cancer occurrence and treatment based on changes in intestinal flora. *Sem. Cancer Biol.* 70, 3–10. doi: 10.1016/j.semcancer.2020.05.004

Skoracka, K., Ratajczak, A. E., Rychter, A. M., Dobrowolska, A., and Krela-Kaźmierczak, I. (2021). Female Fertility and the Nutritional Approach: The Most Essential Aspects. *Adv. Nutr.* 12, 2372–2386. doi: 10.1093/advances/nmab068

Staffas, A., Burgos, da Silva, M., Slingerland, A., Lazrak, A., Bare, C., et al. (2018). Nutritional Support from the Intestinal Microbiota Improves Hematopoietic Reconstitution after Bone Marrow Transplantation in Mice. *Cell host Microb.* 23, 447.e–457.e. doi: 10.1016/j.chom.2018.03.002

St-Pierre, B., and Wright, A. D. (2013). Diversity of gut methanogens in herbivorous animals. *Animal* 7(Suppl. 1), 49–56. doi: 10.1017/s1751731112000912

Tang, W. H., Kitai, T., and Hazen, S. L. (2017). Gut Microbiota in Cardiovascular Health and Disease. *Circ. Res.* 120, 1183–1196. doi: 10.1161/circresaha.117.309715

Tang, Z., Li, Y., Wan, P., Li, X., Zhao, S., Liu, B., et al. (2007). LongSAGE analysis of skeletal muscle at three prenatal stages in Tongcheng and Landrace pigs. *Genom. Biol.* 8:R115. doi: 10.1186/gb-2007-8-6-r115

Tavella, T., Rampelli, S., Guidarelli, G., Bazzocchi, A., Gasperini, C., Pujos-Guillot, E., et al. (2021). Elevated gut microbiome abundance of *Christensenellaceae*, *Porphyromonadaceae* and *Rikenellaceae* is associated with reduced visceral adipose tissue and healthier metabolic profile in Italian elderly. *Gut Microbes* 13, 1–19. doi: 10.1080/19490976.2021.1880221

Visscher, C., Hankel, J., Nies, A., Keller, B., Galvez, E., Strowig, T., et al. (2019). Performance, Fermentation Characteristics and Composition of the Microbiome in the Digest of Piglets Kept on a Feed With Humic Acid-Rich Peat. *Front. Vet. Sci.* 6:29. doi: 10.3389/fvets.2019.00029

Wang, Y., Sheng, H. F., He, Y., Wu, J. Y., Jiang, Y. X., Tam, N. F., et al. (2012). Comparison of the levels of bacterial diversity in freshwater, intertidal wetland, and marine sediments by using millions of illumina tags. *Appl. Environ. Microbiol.* 78, 8264–8271. doi: 10.1128/aem.01821-12

Wang, Y., Zhang, J., Zhou, Q., Wang, Z., Gao, M., Yang, X., et al. (2020). Monopterus albusAnalysis of the Intestinal Flora in Male Versus Female Swamp Eels *(Monopterus albus)*. *Front. Microbiol.* 11:699. doi: 10.3389/fmicb.2020.00699

Wen, L. M., Wu, W. Z., and Peng, X. C. (2016). Identifying significant pathways of hepatitis B virus-related hepatocellular carcinoma based on crosstalk and network pathways. *Genet. Mol. Res.* 15:gmr8343 doi: 10.4238/gmr.15028343

Wu, T., Li, Z., and Wu, X. (2007). Study on the product adaptability of Tibetan pigs in Guangdong (in Chinese). *Guangdong Vet. Sci. Technol.* 16–18. (In Chinese).

Wylensek, D., Hitch, T., Riedel, T., Afrizal, A., Kumar, N., Wortmann, E., et al. (2020). A collection of bacterial isolates from the pig intestine reveals functional and taxonomic diversity. *Nat. Comm.* 11:6389. doi: 10.1038/s41467-020-19929-w

Xiao, Y., Zhang, H., Chen, J., Chen, Y., Li, J., Song, T., et al. (2020). Cloning and Expression of the Tibetan Pig Interleukin-23 Gene and Its Promotion of Immunity of Pigs to PCV2 Vaccine. *Vaccines* 8:250. doi: 10.3390/vaccines8020250

Xing, J., Zhao, W., Li, Q., Yang, G., Zhang, R., Chen, H., et al. (2021). *Bacillus subtilis* BSH has a protective effect on *Salmonella* infection by regulating the intestinal flora structure in chickens. *Microb. Pathogen.* 155:104898. doi: 10.1016/j.micpath.2021.104898

Yan, S., Tu, Z., Liu, Z., Fan, N., Yang, H., Yang, S., et al. (2018). A Huntingtin Knockin Pig Model Recapitulates Features of Selective Neurodegeneration in Huntington's Disease. *Cell* 173, 989.e–1002.e. doi: 10.1016/j.cell.2018.03.005

Zeng, B., Zhang, S., Xu, H., Kong, F., Yu, X., Wang, P., et al. (2020). Gut microbiota of Tibetans and Tibetan pigs varies between high and low altitude environments. *Microbiol. Res.* 235:126447. doi: 10.1016/j.micres.2020.126447

Zhao, M., Nakada, Y., Wei, Y., Bian, W., Chu, Y., Borovjagin, A., et al. (2021). Cyclin D2 Overexpression Enhances the Efficacy of Human Induced Pluripotent Stem Cell-Derived Cardiomyocytes for Myocardial Repair in a Swine Model of Myocardial Infarction. *Circulation* 144, 210–228. doi: 10.1161/circulationaha.120.049497

Zhou, S., Luo, R., Gong, G., Wang, Y., Gesang, Z., Wang, K., et al. (2020). Characterization of Metagenome-Assembled Genomes and Carbohydrate-Degrading Genes in the Gut Microbiota of Tibetan Pig. *Front. Microbiol.* 11:595066. doi: 10.3389/fmicb.2020.595066

Conflict of Interest: The authors declare that the research was conducted in the absence of any commercial or financial relationships that could be construed as a potential conflict of interest.

frontiers | Frontiers in Microbiology

ORIGINAL RESEARCH
published: 17 June 2022
doi: 10.3389/fmicb.2022.909729

Intestinal Microbes in Patients With Schizophrenia Undergoing Short-Term Treatment: Core Species Identification Based on Co-Occurrence Networks and Regression Analysis

Min Xiang[1†], Liqin Zheng[2†], Daoshen Pu[3†], Feng Lin[1], Xiaodong Ma[1], Huiqian Ye[1], Daoqiong Pu[1], Ying Zhang[1], Dong Wang[4], Xiaoli Wang[5], Kaiqing Zou[6], Linqi Chen[2], Yong Zhang[2], Zhanjiang Sun[2], Tao Zhang[2] and Guolin Wu[1]**

[1] Medical Laboratory, The Fourth People's Hospital of Ya'an, Ya'an, China, [2] MOE Key Lab for Neuroinformation, High-Field Magnetic Resonance Brain Imaging Key Laboratory of Sichuan Province, University of Electronic Science and Technology of China, Chengdu, China, [3] The Fourth People's Hospital of Ya'an, Ya'an, China, [4] Psychiatry Department, The Fourth People's Hospital of Ya'an, Ya'an, China, [5] Internal Medicine, The Fourth People's Hospital of Ya'an, Ya'an, China, [6] The Outpatient Department, The Fourth People's Hospital of Ya'an, Ya'an, China

Schizophrenia, a common mental disorder, has a tremendous impact on the health and economy of people worldwide. Evidence suggests that the microbial-gut-brain axis is an important pathway for the interaction between the gut microbiome and the development of schizophrenia. What is not clear is how changes in the gut microbiota composition and structure during antipsychotic treatment improve the symptoms of schizophrenia. In this study, 25 patients with schizophrenia were recruited. Their fecal samples were collected before and after hospital treatment for 14–19 days. The composition and structure of the intestinal microbiota were evaluated by 16S rRNA sequencing analysis, and the results showed significant differences in fecal microbiota before and after treatment. *Firmicutes* (relative abundances of 82.60 and 86.64%) and *Gemminger* (relative abundances of 14.17 and 13.57%) were the first dominant species at the phylum and genus levels, respectively. The random forest algorithm and co-occurrence network analysis demonstrated that intestinal flora (especially the core species ASV57) could be used as biomarkers to distinguish different clinical states and match treatment regimens accordingly. In addition, after fecal microbiota transplantation, antibiotic-treated recipient mice showed multiple behavioral improvements. These included decreased psychomotor hyperactivity, increased social interaction, and memory. In conclusion, this study suggests that differences in the composition and structure of gut microbiota after treatment are associated with the development and severity of schizophrenia. Results may provide a potential target for the treatment of this disorder.

Keywords: schizophrenia, 16S rRNA sequencing, gut-brain axis, gut microbiota, fecal microbiota transplantation

OPEN ACCESS

Edited by:
Hesong Wang,
Southern Medical University, China

Reviewed by:
Bangyuan Wu,
China West Normal University, China
Wentao Yang,
Jilin Agriculture University, China

***Correspondence:**
Guolin Wu
461102658@qq.com
Tao Zhang
tao.zhang@uestc.edu.cn

†These authors have contributed equally to this work

Specialty section:
This article was submitted to Microbial Symbioses, a section of the journal Frontiers in Microbiology

Received: *31 March 2022*
Accepted: *12 May 2022*
Published: *17 June 2022*

Citation:
Xiang M, Zheng L, Pu D, Lin F, Ma X, Ye H, Pu D, Zhang Y, Wang D, Wang X, Zou K, Chen L, Zhang Y, Sun Z, Zhang T and Wu G (2022) Intestinal Microbes in Patients With Schizophrenia Undergoing Short-Term Treatment: Core Species Identification Based on Co-Occurrence Networks and Regression Analysis. Front. Microbiol. 13:909729. doi: 10.3389/fmicb.2022.909729

INTRODUCTION

Schizophrenia (SCZ) is a common and severe chronic mental disorder, which is manifested as hallucinations, delusions, and abnormal thoughts and behaviors. In addition, apathy and social interaction disorders are also major symptoms (Kahn et al., 2015; Xu et al., 2018). Approximately, 0.5–1% of the population suffers from SCZ globally (Yang et al., 2019), with young adults prone to higher recurrence, disability, and suicide rates (Cacabelos and Martínez-Bouza, 2011; Perez et al., 2021). Due to hallucinations and delusions, patients with SCZ are often unable to distinguish true information from their thoughts accurately. This increases their cognitive burden and leads to a high propensity for violence toward others (Tesli et al., 2020; Tikàsz et al., 2020). Suffering from chronic social interaction disorders, patients with SCZ struggle to maintain a normal life and work more than healthy individuals. Previous studies have indicated that patients with SCZ have a higher unemployment rate (Strassnig et al., 2017) and a shorter life expectancy (Stogios et al., 2021).

Schizophrenia has become a serious public health issue and social problem due to the unknown pathogenesis of the disease, the seriousness of its complications, and the impact of violent behavior by patients. Most conventional standpoints support that genetic (plexin A2 on chromosome 1q32; Mah et al., 2006) and environmental factors (childhood adversity; Wells et al., 2020) substantially influence the development of SCZ (Yue et al., 2011; Birnbaum et al., 2018). Immune system dysfunction, such as abnormal lymphocyte numbers, and neurotransmitter system dysfunction, such as glutamic receptor dysfunction, have been widely reported as the popular causes (Anticevic et al., 2012; Karpiński et al., 2016). Moreover, neuroimaging studies have provided evidence for abnormal nervous system growth, such as differences in prefrontal cortex activation patterns (Takeda et al., 2017) and default mode network functional connection patterns (Wang et al., 2019) between patients with SCZ and healthy controls. Energy metabolism disorders and mitochondrial dysfunction are also associated with SCZ (Gonçalves et al., 2015). Although research on SCZ has not been lacking in recent decades, its pathological mechanism remains largely unknown, and effective interventions for SCZ patients are still limited.

In recent years, the gut microbiota has been associated with cognitive impairment and mental illness. The critical role of the gut-brain axis in various behaviors and brain disorders has been widely acknowledged (Aziz and Thompson, 1998). The concept of the microbiota-gut-brain axis (MGBA) has been introduced in many studies on interactions between gut microbiota and brain functions. For example, the absence of gut microbiota can influence the brain function of germ-free (GF) animals (Diaz Heijtz et al., 2011; Neufeld et al., 2011), while specific strains of bacterial transplants may change animal behavior (De Palma et al., 2017; Tengeler et al., 2020). The gut microbiota is tightly linked to host brain function *via* neural, endocrine, and immune pathways (Järbrink-Sehgal and Andreasson, 2020); the pathways' communication is usually considered a bidirectional line (Rutsch et al., 2020). Transplantation of fecal microbiota from children with autism spectrum disorders (ASD) into GF mice leads to several ASD-like behaviors, a different microbial community structure, and altered tryptophan and serotonin (Xiao et al., 2021) levels. Similarly, mice receiving fecal microbiota from patients with major depression developed depression-like behaviors and altered gut microbiota metabolism compared to "healthy microbiota" colonization (Zheng et al., 2016).

Although the etiology of SCZ is still unclear, MGBA development provides a new perspective to explain the pathophysiological processes relevant to SCZ. Previous studies have shown that gut microbial disorders can be observed in various rodent schizophrenia models. Using metabotropic glutamate receptor 5 (mGlu5) knockout mice as an SCZ model, Gubert et al. (2020) found that SCZ induced significantly different bacterial diversity and taxonomy. Significant genotype alterations in microbial β-diversity also showed decreased relative richness of the *Erysipelotrichaceae* and *Allobaculum* genera (Gubert et al., 2020). In fecal microbiota transplantation (FMT)-induced SCZ mouse models, lower glutamate, higher glutamine, and GABA levels were observed in the hippocampus in addition to SCZ-related behavior. This was similar to other SCZ mouse models involving glutamatergic hypofunction (Zheng et al., 2019). Meanwhile, fecal samples from patients with SCZ had a decreased microbiome α-diversity index and marked disturbances in gut microbial composition (Zheng et al., 2019). A recent study also showed that 19 gut microbiota taxa, such as phylum *Actinobacteria*, were closely associated with SCZ; the microbial dysbiosis index was positively correlated with gut microbiota-associated epitope diversity and gut IgA levels (Xu et al., 2020).

Although the relationship between gut microbiota and SCZ has been widely accepted, whether the changes in schizophrenia severity are also related to gut microbiota remains limited. It is revealing that the characteristic bacteria highly correlated with symptom changes are still lacking. Therefore, the present study compared the gut microbial communities before and after a short treatment period in SCZ patients. We performed FMT on specific pathogen-free (SPF) mice before or after treatment of SCZ patients to test whether gut microbiota was linked with a decrease in schizophrenic symptoms. In addition, to characterize the gut microbial community assembly, the present study used a neutral community model, random forest, and co-occurrence network to determine the potential characteristic bacteria that may influence the host severity of schizophrenic symptoms.

MATERIALS AND METHODS

Subjects and Fecal Sample Collection

Per the Declaration of Helsinki, this study was approved by the Medical Ethics Committee of the Fourth People's Hospital of Ya' an. All participants provided written informed consent and completed a questionnaire with their general information such as age, sex, race, height, weight, anamnesis, history of smoking, and drinking. The participants were recruited from inpatients receiving antipsychotic treatment and were examined and diagnosed according to the ICD-10 by two trained psychiatric physicians. Clinical psychopathological symptoms were evaluated using the Brief Psychiatric Rating Scale (BPRS;

Andersen et al., 1989), Clinical Global Impressions-Severity (CGI-S) Scale, Scale for Assessment of Positive Symptoms (SAPS), and Scale for Assessment of Negative Symptoms (SANS; Malla et al., 1993). An initial stool sample was collected. Then a second stool sample was collected after 14–19 days of treatment (referred to as "before" and "after" treatment). Therapeutic response and side effects were recorded *via* interviews or scales (Clinical Global Impression of Improvement (CGI-I) and Clinical Global Impression of Efficacy (CGI-E). All fresh stool samples obtained from participants were stored at −80°C until DNA extraction.

Supplementary criteria were: (1) age 18–70 years old, male, of Han nationality; (2) absence of any specific drug use for the last 14 days, including antibiotics, probiotics, and prebiotics; (3) absence of any history of gastrointestinal tract disorders or major surgery of the gastrointestinal tract; (4) absence of other psychiatric disorders; (5) completed two-scale assessments before and after treatment (including CGI, BPRS, SAPS, and SANS). After exclusions, 25 of 46 patients met the inclusion criteria for participation. The results of the CGI-I and CGI-E showed that 25 patients showed some improvement after 14–19 days of treatment.

16S rRNA Gene Sequencing and Analysis

A total of 200 μl (final elution volume) of fecal DNA samples were extracted using the E. Z. N. A. TM fecal DNA extraction kit (OMEGA Bio-Tek, Norcross, GA, USA). The extracted DNAs were sent to Shanghai Personal Biotechnology Co., Ltd. (Shanghai, China) after measuring DNA quality and integrity by agarose gel electrophoresis and NanoDrop NC2000 spectrophotometer (Thermo Fisher Scientific, Waltham, MA, USA). The specific barcode was combined into the amplification primers, and pair-end 2 × 250 bp sequencing of the bacterial 16S rRNA gene was measured using the Illumina MiSeq sequencing platform and V3–V4 region fragment. The primer sequences used were 338F (5′-ACTCCTACGGGAGGCAGCA-3′) and 806R (5′-GGACTACHVGGGTWTCTAAT-3′). PCR components contained Buffer (5×, 5 μl), Fast pfu DNA Polymerase (5 U/μl, 0.25 μl), dNTPs (2.5 mM, 2 μl), Forward and Reverse primers (10 uM, 1 μl), DNA Template (1 μl) and ddH_2O (14.75 μl). The amplification procedure consisted of initial denaturation at 98°C for 5 min, degeneration at 98°C for 30 s with 25 cycles, annealing at 53°C for 30 s, extension at 72°C for 45 s, and a final extension at 72°C for 5 min. PCR amplicons were purified and quantified using Vazyme VAHTSTM DNA Clean Beads (Vazyme, Nanjing, China) and a Quant-iT PicoGreen dsDNA Assay Kit (Invitrogen, Carlsbad, CA, USA), respectively.

According to the official tutorial (https://docs.qiime2.org/2020.11/tutorials/), QIIME2 (Bolyen et al., 2018) was used to perform bioinformatics analysis of the sequencing data. The demux plugin, cutadapt plugin (Martin, 2011), and DADA2 plugin (Callahan et al., 2016) were used to demux sequencing and cut primers from the original data, and carry out quality filtering, denoising, merging, as well as the removal of sequences. Non-single-case amplicon sequence variants (ASVs) were aligned to construct a phylogeny between ASVs and fasttree2 (Price et al., 2009). Finally, the species in the abundance table were annotated using the feature-classifier plugin (Price et al., 2009) based on the Navier Bayes classifier and Greengenes 13_8 database.

Alpha Diversity, Beta Diversity, and Microbial Composition Analysis

The even abundance was analyzed with the Wilcoxon sum test for alpha diversity (richness and Shannon diversity) using the *vegan* package (https://CRAN.R.project.org/package=vegan). For in-depth analyses, we selected samples in which at least 20% of the ASVs were present and where the sum of the relative abundances exceeded 2.5% (Ju et al., 2014). Filtering removed species that lacked representation largely suppressed non-zero relationships among low-abundance species, reduced network complexity, and facilitated the identification of communities and core ASVs (Ju et al., 2014). Subsequently, we normalized the filtered ASV sequence counts using the TMM method in the *edgeR* package (Robinson et al., 2010). Based on Bray–Curtis's dissimilarities, principal coordinate analysis (PCoA) was used to visualize the structure of the intestinal microbial communities utilizing the package *Phyloseq* (McMurdie and Holmes, 2013). Permutational multivariate analysis of variance (PERMANOVA) was used to evaluate differences in microbial communities between groups with *adonis* in the *vegan* package. The high-abundance microbiota at the phylum and genus levels were clustered to reveal the taxonomic composition changes of the gut before and after treatment. The Wilcoxon rank-sum test was used to compare specific microbial communities between groups. The above analysis was mainly carried out using the R-studio software (V3.1.2).

Neutral Community Model Analysis

We needed to assess the potential importance of the stochastic process to the intestinal microflora assembly before and after treatment. As such, this study used a neutral community model (Sloan et al., 2006) to predict the relationship between the frequency and relative abundance of ASVs in the sub-communities after treatment. This could determine the stochastic/deterministic interactions during the succession of the original and disturbing ecosystems (Elzhov et al., 2015). Östman's method was used to calculate the R^2, representing the model's goodness of fit. The assembly of the intestinal microbial community conforms to a random process when R^2 is close to 1; otherwise, it conforms to a deterministic process (Östman et al., 2010).

Spaa package (Edgar, 2013) was used to further calculate the Levins niche width index of intestinal microorganisms before and after treatment. A random rearrangement of the *EcolUtils* package simulated the species occurrence frequency. The species whose niche width index exceeded the upper fell below the lower and in the 95% confidence interval as generalist species, specialist species, and neutral taxa, respectively (Wu et al., 2018).

Finally, the empirical C-score was calculated based on the sequential swap randomization algorithm of the *EcoSimR* package (R Core Team, 2018). The zero distribution of the C-score (Stone and Roberts, 1990) was simulated by reassigning the species co-occurrence of the randomization

algorithm. The degree of deviation between the empirical C-score and zero distribution of the C-score was determined to evaluate the standardized effect size (SES) for different microbial communities before and after treatment (Gotelli and Mccabe, 2002; Crump et al., 2009). Generally, positive SES values represent the separated co-occurrence pattern of species. Negative SES values represent the aggregated co-occurrence pattern of species. There is no significant difference between the empirical C-score and null distribution, representing the random co-occurrence pattern of species. In other words, the absolute value of SES is considered to be the degree of influence of deterministic processes on microbial assembly (Swenson, 2014). The calculation was based on 1,000 random permutations simulating a zero-distribution C-score to evaluate the co-occurrence patterns of community species before and after treatment.

Identifying the Key Species by Random Forest

A combination of random forest (RF) algorithms was used to identify the most influential key pathogenic species. It also helped explain the nonlinear relationship and dependence between microbial community characteristics (Zeller et al., 2014). The RF model introduced the standardized abundance of ASV in all major gut microorganisms. Each was assigned two different important scores (mean decrease accuracy, MDA; mean decrease Gini, MDG) and ranked in descending order to obtain the top 20 ASVs.

Co-Occurrence Network and Netshift Analysis

Significant ($p < 0.05$) ASV associations from one sickness state to the other were identified by indicator species analysis to determine the key species that play essential roles in intestinal communities during hospital treatment. These were visualized by the Fruchterman Reingold layout with 10^4 permutations using the *igraph* package. Meanwhile, *Sparcc* correlation (Friedman and Alm, 2012) was calculated among ASV interactions. The significant interactions ($\rho > 0.3$ and $p < 0.05$) were retained, followed by the *greedy optimization of modularity* algorithm (Clauset et al., 2004) to identify and visualize the microbial community modules in the co-occurrence network. The co-occurrence network was visualized using the Fruchterman Reingold layout and 10^4 permutations using the R package *igraph*. Netshift analysis (Kuntal et al., 2019) was used to quantify the community change in the microbial co-occurrence network before and after treatment. Neighbor shift (NESH) scores and Delta betweenness (DelBet) coefficients were used to identify the core microbes that may be considered a "driving force." In addition, the distance matrix of non-metric multidimensional scaling (NMDS) was sorted directly using the *vegan* package. Then the samples (all) and ASVs with DelBet > 0 in Netshift analysis were projected onto the ordination diagram.

Generalized Linear Models

The generalized linear model was conducted using the *mvabund* package. It was used to model the relationship between age, height, weight, education, and six living habits as independent variables, and the abundance of core species as response variables, to analyze the effect of each factor on SCZ development. We used negative binomial regression to make the results more robust and screened out the significant factors for the core pathogenic species based on the significance of 9,999 bootstrap estimates (Benesh and Kalbe, 2016).

Animals and Fecal Microbiota Transplantation

All experiments were conducted with male C57BL/6J mice, which were maintained in a standard SPF environment (12-h light/dark cycle) at temperature (25 ± 2.0°C) and humidity (55 ± 10%), allowed access to food and water freely. According to the core species, 10 subjects were excluded when the fecal samples were subjected to FMT: (1) neither ASV57 nor ASV86 existed in the samples before treatment; and (2) beneficial bacteria (ASV86) decreased or harmful bacteria (ASV57) increased in the samples after treatment. Fecal samples were collected from the rest of 15 SCZ patients for microbiota transplantation, as described in previous studies (Sun et al., 2018; Liang et al., 2019). One spoon of stool (∼1 g) obtained from each patient's fecal sample was suspended and diluted with sterile PBS. The fecal liquid was centrifuged at 800 g for 5 min at 4°C to obtain total bacteria. It was then filtered twice in PBS. About 600 μl of Supernatant fluid was mixed with an equal volume of 40% (volume rate) glycerin-PBS liquid, then diluted. The microbe-containing samples were stored in 20% glycerin-PBS liquid at −80°C until transplantation. The mice were treated with antibiotics to deplete the intestinal flora starting 1 week after habituation by oral gavage once a day for 10 days. After the final gavage of antibiotics for 48 h, mice were randomly divided into two groups. They received oral gavage of the microbiota suspension from patients with SCZ before or after treatment (10 μl/g body weight) for 2 weeks to reconstruct the gut microbiota (hereafter referred to as BT and AT mice). All animal experimental procedures were approved by the Institutional Animal Care and Use Committee of Sichuan Agricultural University.

Behavioral Testing

Behavioral tests were performed using 12 mice per group to ensure the effectiveness of gut microbiota manipulation. All behavioral tests were conducted 48 h after fecal transplantation and were recorded using a video-computerized tracking system (SMART 3.0; Panlab SL, Barcelona, Spain) or evaluated separately by manual observation by two experienced observers. The investigators were blinded to the treatment conditions of the mice during the experiments and outcome assessment. Animals were given 1 h of habituation in the behavioral testing room before testing began to minimize novelty or stress effects. Behavioral tests were performed in the following order: open field test (OFT), elevated plus maze test (EPMT), three-chamber social test (TCST), novel object recognition test (NORT), and forced swimming test (FST). All tests were performed as previously described with minor modifications (Ikeda et al., 2020; Wang et al., 2020; Zhu et al., 2020b). Tests were performed from the least to the most invasive, with a minimum 48 h interval between tests to minimize the influence of previous test history. All objects

used for the tests were cleaned with 70% ethanol between each trial, and the feces and urine in the box were removed.

Open-Field Test

Mice were placed individually in an unfamiliar open-field arena (40 × 40 × 45 cm) and allowed to explore freely for 10 min. The video-computerized tracking system analyzed the total distance traveled (considered an evaluation of locomotor activity) and the time spent in the central zone (15 × 15 cm squared arena). Changes in distance and time in the central zone indicated different anxiety levels (Ikeda et al., 2020).

Elevated Plus-Maze Test

The plus-shaped maze consisted of two open and two closed arms (25 × 5 cm, 20 cm walls, 50 cm above the ground), with arms of the same type facing opposite each other. Mice were placed in the central square (5 × 5 cm) of the maze, facing one of the closed arms. The time spent in the closed and open arms was manually recorded using filmed video during an observation period of 5 min. The ratio of time spent in the open arms was considered a measure of anxiety (Zhu et al., 2020b).

Three-Chamber Sociability Test

The test setup was a box containing three chambers (60 × 40 × 22 cm) separated by Plexiglas walls with openings inside to allow access to each chamber. In the habituation trial, test mice were individually placed in the center chamber and allowed to freely explore all three chambers for 10 min. Subsequently, a small, round wire cage with unfamiliar sex- and strain-matched conspecific (as a stranger) was placed in one of the side chambers, and the same empty cage was placed in another side chamber. In the sociability trial, test mice were placed in the center chamber and allowed to freely explore all three chambers for 10 min. At the end of the 10-min sociability trial, a novel object was placed in an empty cage. The test mice were free to explore the mouse from the previous sociability test (stranger 1) and the novel mouse (stranger 2) for 10 min. The amount of time spent in each cage was recorded using a video camera (Zhu et al., 2020b).

Novel Object Recognition Test

Mice were placed in a 40 × 40 × 45 cm box alone to explore freely for 30 min for habituation under dimly-lit conditions. Two similar objects (smooth pebbles of different colors) were placed in the center of the two halves of the box, and the mice were allowed to explore for 10 min before returning to their home cage. After 24 h, one of the objects was replaced by a tube cap. The mice were placed in the box again for the test session and allowed to explore the familiar and novel objects for 5 min. The discrimination index (DI), a measure of memory function, was defined as the ratio of time spent exploring the novel object to the total time spent exploring both objects during the test session (Wang et al., 2020).

Forced Swim Test

Mice were individually placed in an open, transparent plastic cylinder (diameter: 20 cm; height: 40 cm), which contained 20 cm of water, kept at 24°C ± 1°C. The duration of the mice's immobile behavior was manually recorded in the FST, lasting for 5 min (Zhu et al., 2020b).

Statistical Analysis

All graphs and statistical analyses were performed using the GraphPad Prism software version 8 and IBM SPSS 26.0. Data are expressed as mean ± standard deviation (SD). Differences between the two groups were assessed using a two-tailed Student's *T*-test. Nonparametric tests, including the Kruskal–Wallis test and Wilcoxon rank-sum test, were used to assess the two groups' 16S rRNA gene sequencing data. Statistical significance was set at $p < 0.05$.

RESULTS

The patients' demographic data and clinical parameters are shown in **Supplementay Tables 1**, **2**. There was a significant difference in the BPRS, SAPS, and SANS scores before and after treatment.

DNA Sequencing and Screening

A total of 2,098,961 clean reads were generated from the MiSeq platform and retained after filtering for low-quality reads. The high-quality reads were 2,9319 per sample. In total, 6,667 features (ASVs) were identified. The rarefaction curves showed that all samples reached the platform level (**Figure 1A**), indicating that our sequencing depth was suitable for mining the microbial community in the fecal samples.

Changes in Gut Microbial Alpha Diversity and Beta Diversity Before and After Treatment in SCZ Patients

After treatment in the hospital, the species richness (**Figure 1B**) and Shannon diversity (**Figure 1C**) of the microbiota community increased in patients with SCZ. Still, the differences were not significant compared to before treatment ($p > 0.05$). To compare the structural differences of gut microbiota before and after treatment (referred to as BT and AT groups), the distance matrix based on Bray-Curtis and the PCoA was used to evaluate and visualize beta diversity (**Figure 1D**). **Figure 1D** shows significant differences between the BT and AT groups, and PERMANOVA further confirmed significant differences between the two groups ($p < 0.05$).

Altered Microbial Compositions of the Gut Microbiota After Treatment in SCZ Patients

At the phylum level, 18 taxa were observed in all samples, of which four different taxa were identified as highly abundant phyla (relative abundance >1%). *Firmicutes* (84.61%), *Bacteroidetes* (7.48%), and *Proteobacteria* (4.40%) were the first, second, and third most dominant phyla, respectively. Together with *Actinobacteria* (2.85%), they accounted for 99.26% of the total sequence (**Figure 1E**). *Firmicutes* were the dominant species at the phylum level, with relative abundances of 82.60% and 86.64% before and after treatment, respectively (**Figure 1E**).

At the genus level, 238 taxa were detected in all samples (**Figure 1F**), of which *Gemminger*, *Blautia*, *Facecalibacterium*, *Clostridium*, *Roseburia*, *Bacteroides,* and *Prevotella* accounted for 65.63%. *Gemminger* was the dominant species at the

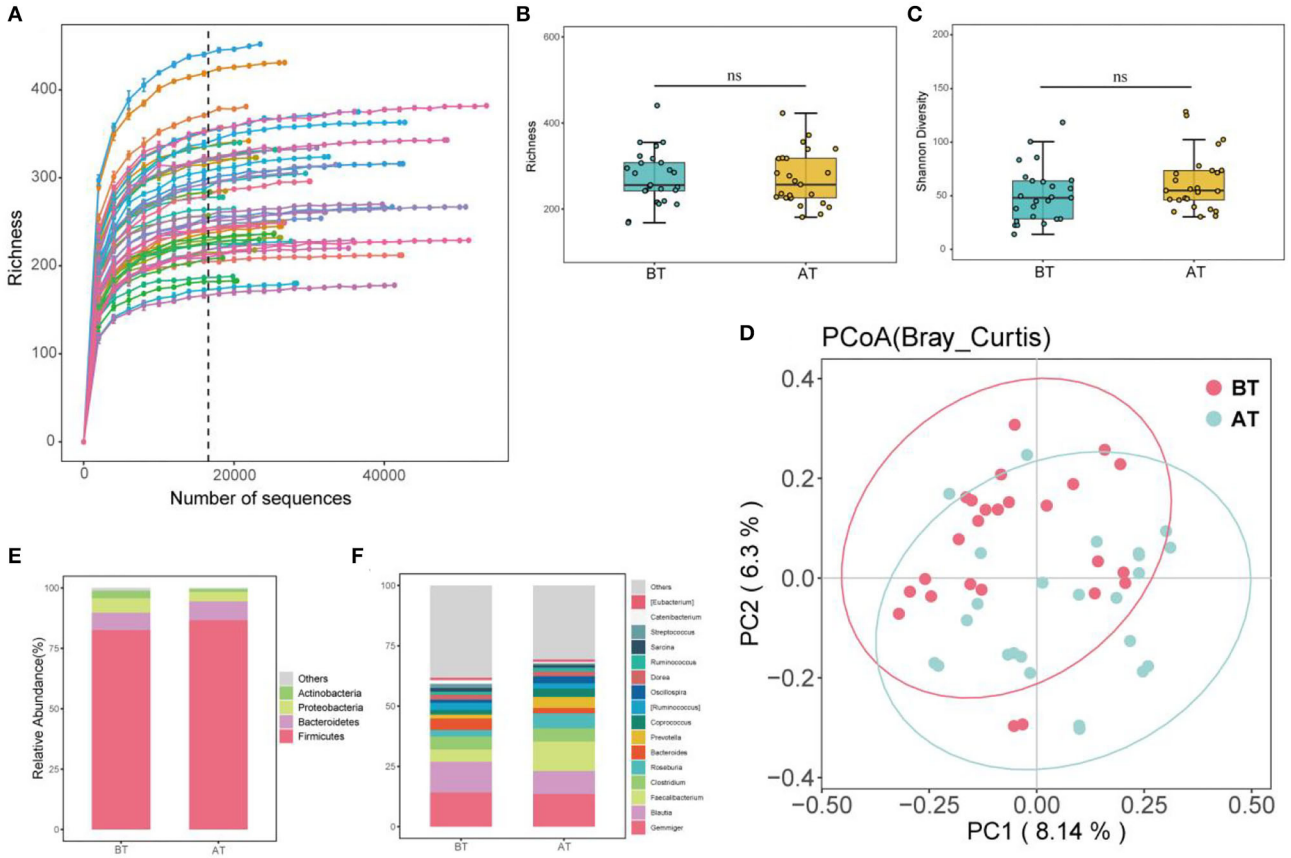

FIGURE 1 | Alpha, Beta diversity, and gut microbial composition. **(A)** Rarefaction curves for intestinal microbiota observed ASV richness. The color lines indicate BT and AT samples, the dashed black line indicates the selected rarefaction depth used to generate the box plots below each curve, 16,589 seqs/sample for microbial communities. **(B)** Community richness of intestinal microbiota in BT and AT samples (Richness); **(C)** Community diversity of intestinal microbiota in BT and AT samples (Shannon diversity), ns, no significant. **(D)** Principal coordinate analysis (PCoA) of intestinal microbiota of mice under different group. **(E)** Relative abundance of dominant phylum taxa (>1%) in intestine from each group. **(F)** Relative abundance of dominant genus taxa (>1%) in intestine from each group.

genus level, with relative abundances of 14.17 and 13.57% before and after treatment, respectively. *Blautia* (a relative abundance of 12.77% and 9.56% before and after treatment) and *Facecalibacterium* (a relative abundance of 5.08% and 12.23%, before and after treatment), respectively, were the second and third dominant species at the genus level. Furthermore, LEfSe was used to identify biomarkers before and after the treatment (**Figures 2A,B**). The biomarkers in the BT group included *Chloracidobacteria*, *Butyricicoccus*, *Oscillospira*, *Bacteroidia*, *Bacteroidales*, *Bacteroidetes*, *Prevotellaceae*, *Prevotella*, *Roseburia*, *Faecalibacterium*, *Ruminocaoccacceae*. *Micrococcaceae* and *Rothia* were biomarkers of the AT group. According to the Metastats analysis, the relative abundance of *Faecalibacterium*, *Butyricicoccus*, *Oscillospira*, *Prevotella,* and *Roseburia* increased significantly after treatment ($p < 0.05$, or $p < 0.01$, **Figures 2C–G**). The relative abundance of *Rothia* decreased significantly after treatment ($p < 0.05$, **Figure 2H**).

The Assembly Mechanism of Gut Microbiota in Patients Before and After Treatment

The neutral community model adequately estimated most of the relationships between the occurrence frequency of ASVs and their relative abundance changes. The explaining rates for the BT and AT groups were 48.1 and 58.1% of community variation, respectively. This indicates that the relative contribution rate of the random process increased significantly after treatment (**Figures 3A,B**). In contrast, the Levins niche width indices of intestinal microorganisms changed indistinctively before and after treatment (**Figure 3C**). Both generalist and specialist species were widespread in the gut microbes of the BT and AT groups. Still, the proportion of specialist species in the gut microbes of the patients was lower after treatment than before treatment (**Figure 3D**). More importantly, the C-score results showed that AT's SES decreased, indicating an increase in the importance of random processes for the gut flora (**Figure 3E**).

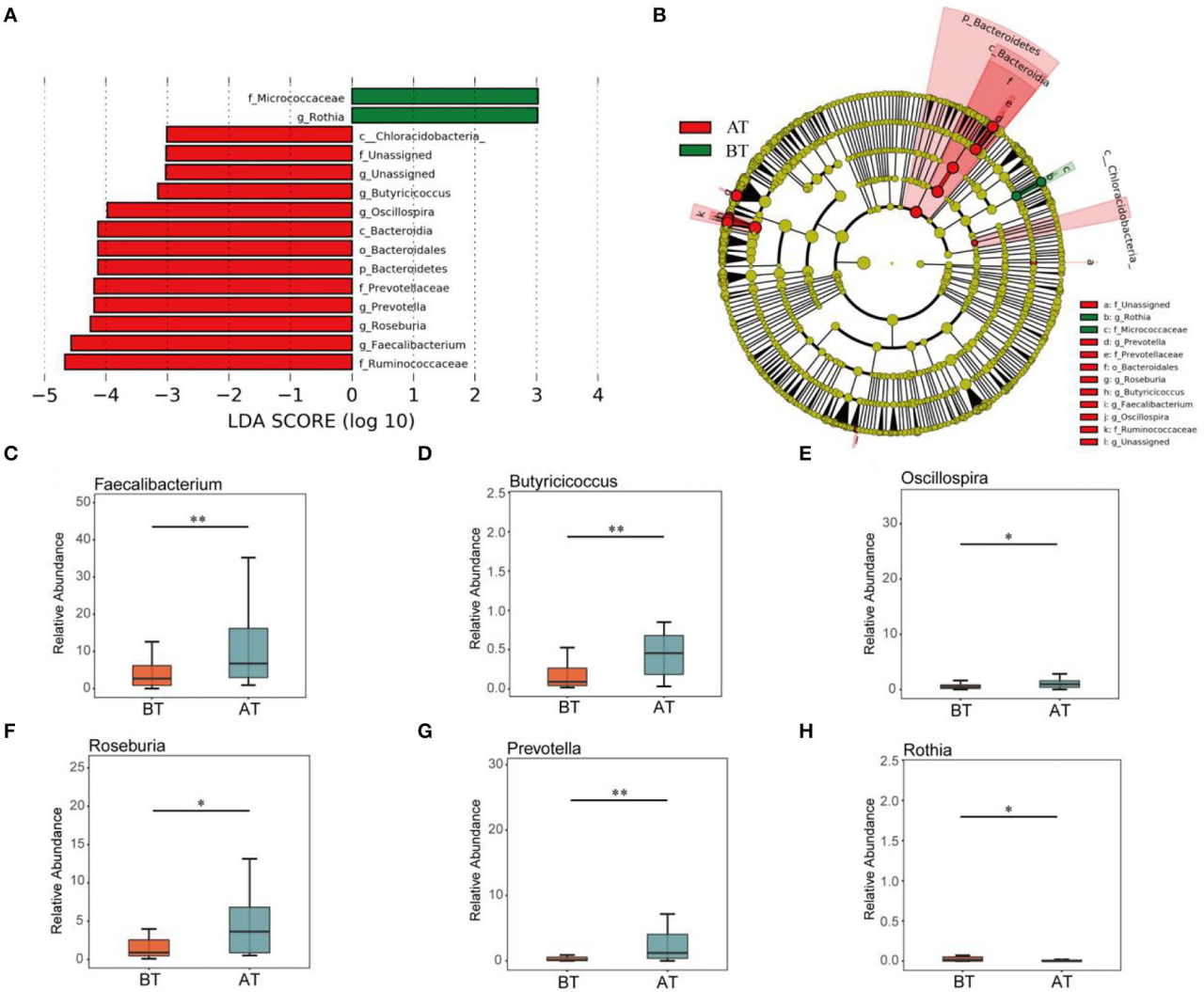

FIGURE 2 | Comparison of intestinal difference groups between BT and AT groups. LEfSe analysis of key taxa of gut microbiota in mice between the BT group and AT group. **(A)** LDA score plot of bacterial taxa with LDA scores higher than 4. **(B)** Taxonomic cladogram derived from LEfSe analysis of 16S rRNA sequences. **(C-H)** Boxplots showing differences in the relative abundance of specific taxa between BT and AT patient. Specific taxa in figure **(C–H)** were *Faecalibacterium* **(C)**, *Butyricicoccus* **(D)**, *Oscillospira* **(E)**, *Roseburia* **(F)**, *Prevotella* **(G),** and *Rothia* **(H)**. $^{*}p < 0.05$, $^{**}p < 0.01$.

Random Forest and Co-Occurrence Network Identified the Key Gut Species

Eighty percent of the samples were randomly selected as the training set for RF analysis. The model was constructed using the training set to classify the two states of patients before and after treatment. Meanwhile, the receiver operating characteristic curve (ROC) was measured by testing set as shown in **Figure 5A**. The area under the curve (AUC) of the testing set reached 0.9, indicating good prediction accuracy on the test dataset. Moreover, the MDA and MDG scores revealed that ASV57 was one of the main features distinguishing the different states before and after treatment (**Figures 4A,B**). According to the indicator species analysis, there were no shared ASVs between the two groups. This indicates that the characteristic bacteria before and after treatment did not have sufficient similarities in terms of habitat preference. Although the numbers of indicator species in the two groups were similar, the species were completely different (**Figure 4C**).

Subsequently, the distribution patterns of the indicator species ASV and its community modules in the gut microbiota symbiotic network were found (**Figures 4D,E**). The observed higher average path length and betweenness centrality of the AT sub-network pointed toward sufficient rewiring compared to the BT sub-network. The lower nodes, connections (edges), average degree, and density in the AT sub-network indicate lower information transport. This might suggest attenuated

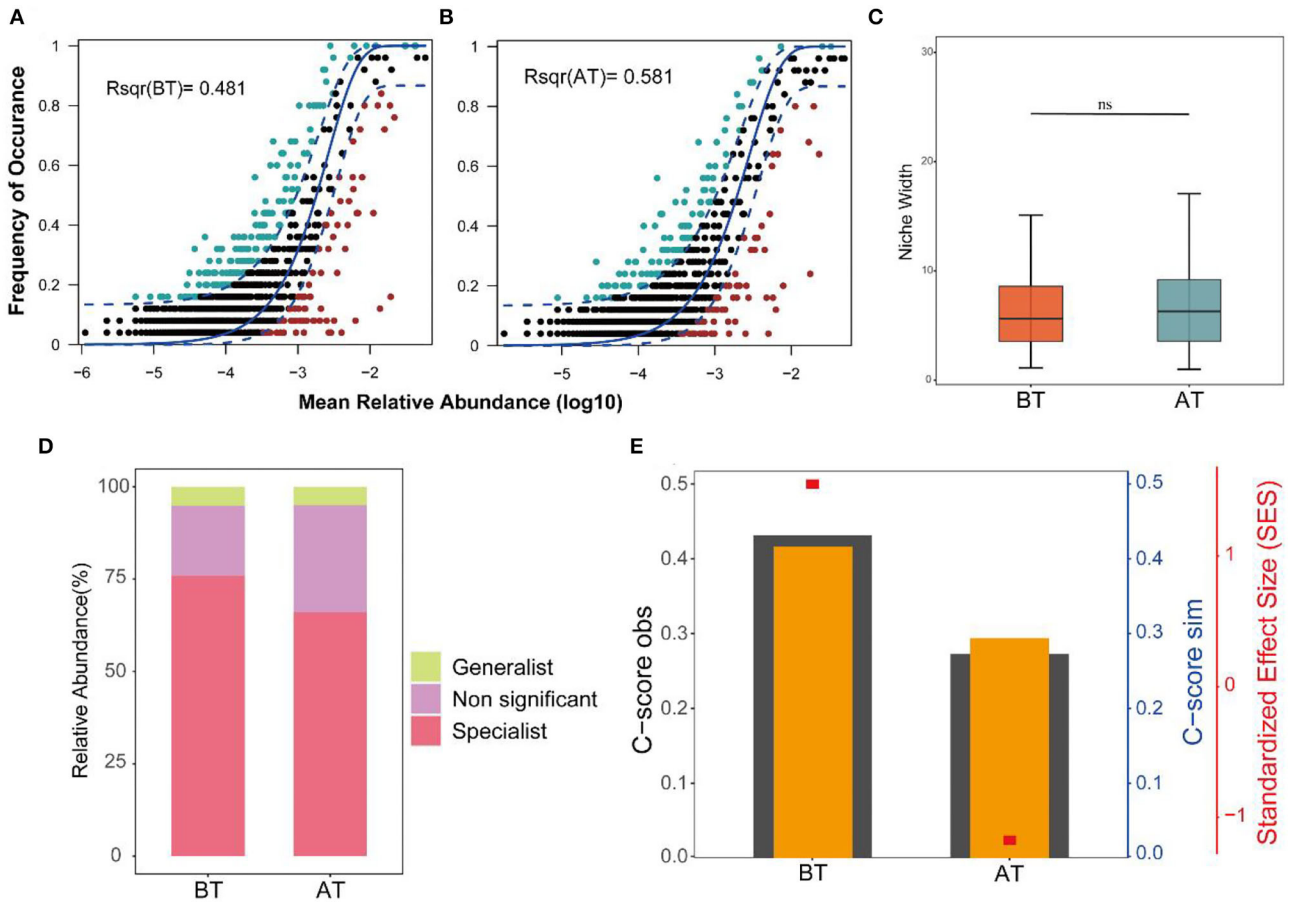

FIGURE 3 | Ecological processes shaping the gut community assembly in BT and AT patients. **(A,B)** Predicted frequency of occurrence of gut microbiota in the BT group **(A)** and AT group **(B)**. The solid blue line is the best fit to the neutral community model (NCM), and the dashed blue line expresses 95% confidence intervals around the NCM prediction. ASVs that occur more or less frequently than predicted by the NCM are shown in lightgreen and lightred, respectively. R^2 indicate the fit to this model. **(C)** Boxplot shows the niche width index distribution of microbial community of gut in BT and AT samples. **(D)** Relative contributions of generalized and specialized species to BT group and AT group of intestinal microbiotas. **(E)** C-score metric using null models. The values of observed C-score (C-score$_{obs}$) > simulated C-score (C-score$_{sim}$) represent non-random co-occurrence patterns. ns, no significant.

colonization activity of harmful microbes (**Table 1**). The microbiome within the module (except for the gray nodes) produced corresponding responses to different states (i.e., BT/AT). Assuming that the colored network nodes were the key regions for further exploring of core species, the key regions of the co-occurrence subnetworks of the AT and BT groups were extracted and subjected to Netshift analysis. The results showed that ASVs with high NESH score were ASV 37, ASV 136, ASV 86, ASV 40, ASV 81, ASV 174, ASV 36, ASV 57, ASV 25, ASV 125, ASV 231; and ASV's with DelBet > 0 were ASV 26, ASV 72, ASV 234, ASV 9, ASV 178 (**Table 2**). These 16 species appeared as large red nodes in the common subnetworks. They were also identified as "driving microbes" that may alter the connections between microbes–ASV 57, which was previously identified as the most important biomarker for different states in the RF model. The red edge connected to ASV 57 indicated that it interacted only in the AT group sub-network, including ASV 86 and ASV 172. The green edge connected to ASV 57 indicated that it interacted only in the BT sub-network, including ASV 15 and ASV 19. The blue edge connected to ASV 57 indicated that it interacted in two groups of sub-networks, including ASV 2 (**Figure 4F**). Similar results were observed in the NMDS analysis (**Figure 5C**), with species scores for ASV 57 predicted across BT samples. These results suggested that ASV 57 may be one of the main causes of schizophrenia development.

The Relationship Between Clinical Parameters and the Key Species

To improve the model accuracy, first, the optimal model for the independent variables in the different subsets was evaluated comprehensively through all-subset regressions (**Figure 5B**). According to the principle of seeking a parsimony model and low collinearity between variables, flavors, and intake of fruits and vegetables were selected from 10 independent variables. Then a negative binomial model was constructed between them and

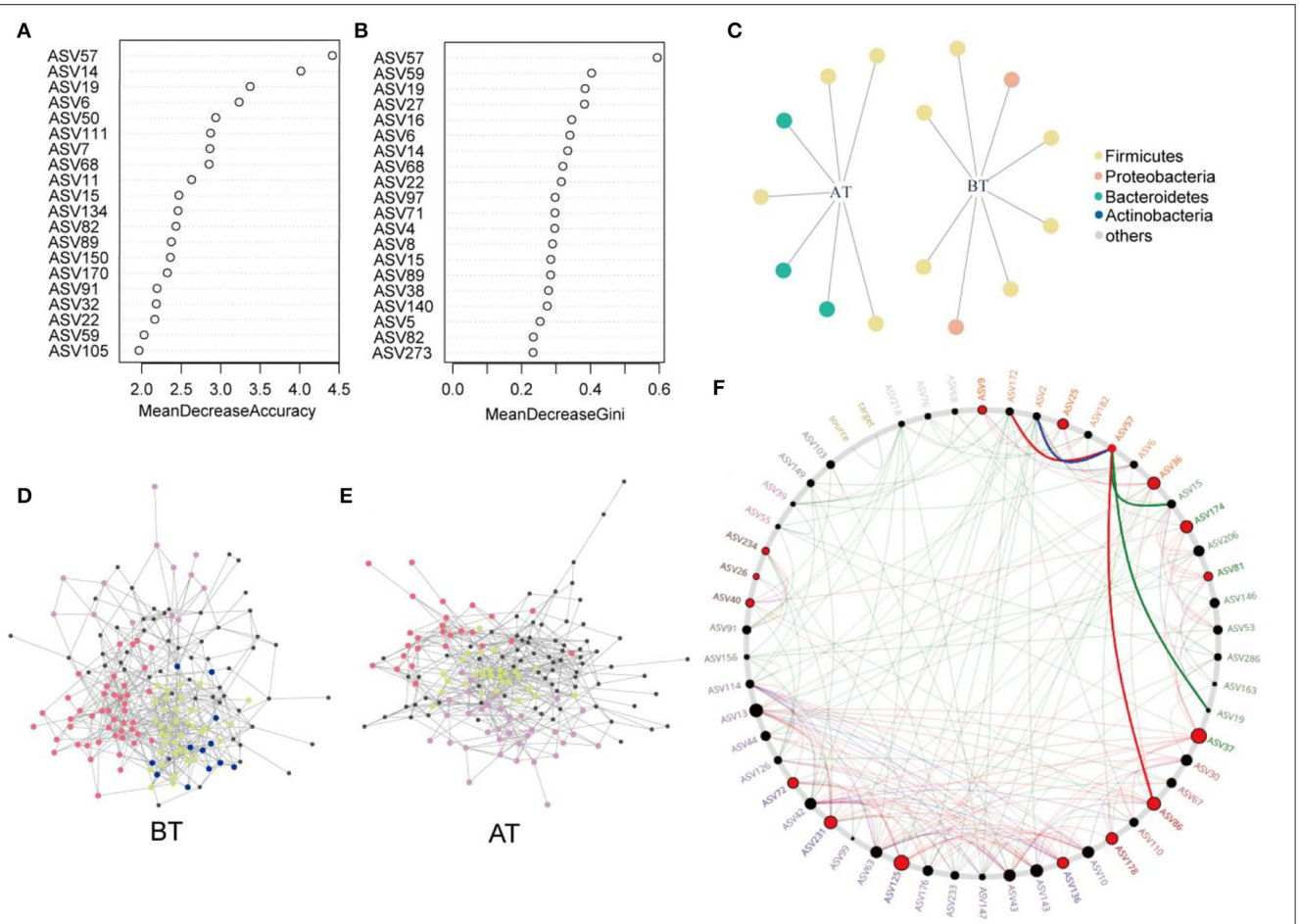

FIGURE 4 | Identification of core ASVs and microbial network analysis. **(A,B)** Random forest showing the top 20 features of the intestinal microenvironment distinguished in the pre- and post-treatment datasets. Each feature (ASV) was assigned two importance score of mean decrease accuracy **(A)** and mean decrease Gini **(B)**. **(C)** Bipartite network showed ASVs specific to before or after treatment identified using indicator species analysis in gut microbial communities. The circle indicates that single species are positively and significantly correlated ($p < 0.05$) with one or more gut microenvironments (the link given by the line). Different ASVs belonging to same phylum level are given the common color. Co-occurrence sub-networks of **(D)** before treatment or **(E)** after treatment. Circles for microbial ASVs are represented by nodes. And partial nodes are colored by association with different modules, which include indicator species corresponding to different gut microenvironment. **(F)** Common sub-networks analysis of BT group and AT group. All nodes belonging to the same community were randomly assigned similar colors. Gray nodes represented ASVs appearing in both the variable group. Big and red node can be considered as "drive microbiota" Red line indicate only in the AT group of sub-networks of interactions. Green line indicates only in the BT group of sub-networks of interactions. And blue line expresses the interactions in both sub-networks.

ASV57 abundance. The whole model was significant, and fruit and vegetable intake and dietary flavors substantially affected the proliferation of ASV 57 ($p < 0.01$). In other words, ASV 57 abundance was associated with fruit and vegetable intake and flavors, regardless of other factors.

Transplantation of SCZ Patient Microbiota Before and After Treatment Induces Different Behaviors in SPF Recipient Mice

A multitude of behavioral tests were performed within 10 days of the FMT on the BT and AT mice (**Figure 6A**). Although there was no difference in the timing at the central area over the 10 min OFT (**Figure 6B**), AT mice showed decreased distance traveled (**Figure 6C**) compared to the BT mice. This indicates lower levels of hyperkinetic behavior. In the TCST, an untreated SPF mouse was used as a stranger. The mice's sociability and preference for social novelty were quantified based on the ratio of the time spent around the wire cage with a stranger mouse vs. the total time spent around the empty wire cage. In the sociability test, AT mice showed a significantly higher ratio of interaction time (around the wire cage with the stranger mouse) than BT mice (**Figure 6E**), indicating an improvement in sociability. In the social novelty preference test, AT mice showed a significantly higher ratio of interaction time (around the wire cage with the novel stranger mouse) than BT mice (**Figure 6F**). This indicates an improved preference for social novelty. The discrimination index of NORT showed that AT mice had improved memory impairment for previously explored objects (**Figure 6G**). In the EPMT, no significant difference was detected in the time spent in

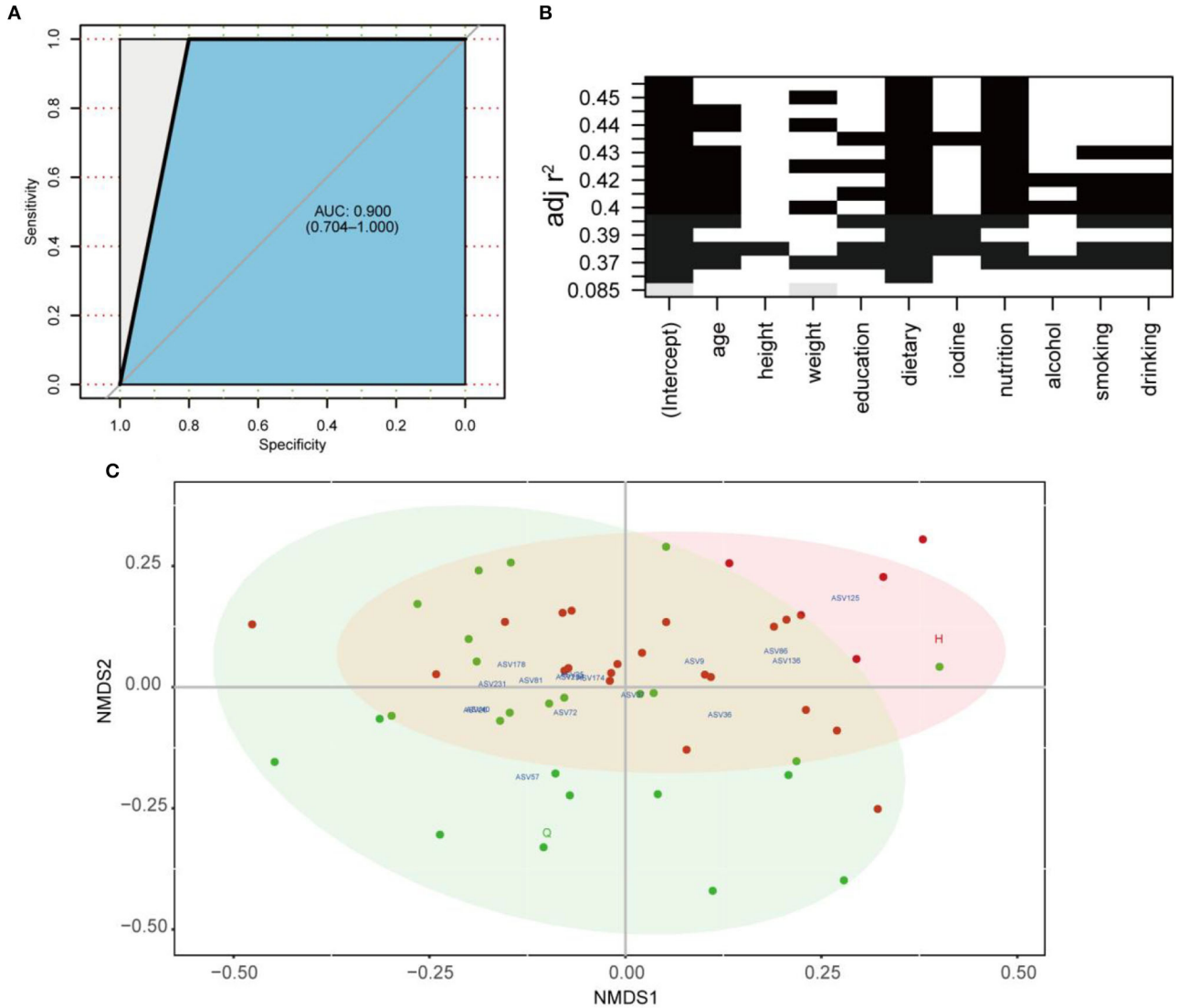

FIGURE 5 | (A) ROC according to 40 samples of the testing set calcualted by cross-validated random forest model. Area under ROC (AUC) and the 95% confidence intervals are also shown. **(B)** All-subsets Regression. The horizontal axis represents the predictive variables, and the vertical axis represents the accuracy of the regression (adjusted R^2), which shows how the accuracy of the regression when different combinations of predictive variables are considered. **(C)** Non-metric multidimensional scaling (NMDS) based on the Bray–Curtis distances. Core ASVs (DelBet > 0) are labeled blue and projected as biomarkers to different locations pre- or post-treatment.

the open areas between the BT and AT mice (**Figure 6D**). During the FST, a similar result was observed for the immobility duration (**Figure 6H**).

DISCUSSION

We used high-throughput 16S rRNA sequencing of fecal samples to conduct microbiome profiling and identified the core species related to SCZ severity. While previous studies have found other evidence of intestinal microbial shift using 16S rRNA sequencing in patients with SCZ, this is the first study to explore the intrinsic changes and core microbes in the gut microenvironment at different baseline phases before and after treatment in the same patients. Although the diversity and composition of the gut microbiome vary greatly among different patients in the same phase, we were able to detect representative community characteristics and variation patterns in almost all samples. Specifically, we have been attempting to analyze the microbial compositions and community assembly before and after treatment in-depth to gain insights into the influence of core species on each of these phases in patients. The combination of treatments is thought to be the greatest source of change in the gut microbiome when other conditions are controlled. Overall, the pattern of separation of the different groups of microbial

TABLE 1 | Properties of before treatment and after treatment co-occurrence sub-networks.

Community	Node	Edge	Ave D	Ave PL	Density	Bet C
BT	107	436	8.15	2.9	0.77	0.05
AT	89	298	6.70	3.1	0.76	0.13

Ave D, average degree; Ave PL, average path length; Bet C, betweenness centralization.

TABLE 2 | Properties of network nodes in BT group and AT group.

S_ID	n(BT)	n(AT)	Core (AT)	Exclusive	Jaccard-score	NESH-score	DelBet
ASV 37	1	11	6	11	0.000	2.650	1.000
ASV 136	4	13	7	9	0.308	1.985	0.723
ASV 86	2	10	5	9	0.091	2.327	0.523
ASV 40	4	4	2	3	0.143	1.486	0.448
ASV 81	3	6	3	4	0.286	1.552	0.441
ASV174	1	5	3	5	0.000	2.167	0.320
ASV 36	3	7	4	7	0.000	2.167	0.316
ASV 57	3	3	2	2	0.200	1.333	0.274
ASV 25	1	5	3	4	0.200	1.867	0.156
ASV 125	1	11	7	11	0.000	2.650	0.144
ASV 231	5	9	6	9	0.000	2.243	0.088
ASV 26	1	2	2	1	0.500	1.067	0.077
ASV 72	2	6	5	5	0.143	1.905	0.064
ASV 234	4	3	2	2	0.167	1.300	0.063
ASV 9	3	4	3	3	0.167	1.533	0.011
ASV 178	1	4	4	4	0.000	2.067	0.003

n(BT/AT), node degree of co-occurrence in the BT/AT group; Core (AT), core degree of nodes in AT group network. Exclusive indicates the new changes of the node in the AT group. Jaccard-score and NESH-Score represent the core degree of nodes in the network. DelBet indicates the betweenness of the node.

structures from baseline to post-treatment was demonstrated by statistical tests using PERMANOVA. Conversely, intestinal community richness and diversity within patients (α-diversity) were not significantly different between the baseline and after treatment. In other studies (Li et al., 2020; Nguyen et al., 2021), we did not observe strong evidence for an obvious difference in the amount or distribution (α-diversity) of the microbiome in patients with schizophrenia compared with controls or after treatment. Those results are consistent with this study. In general, higher α-diversity is regarded as the main characteristic of improved intestinal health. It is widely accepted that greater microbial richness and diversity increase intestinal ecosystem resistance and adaptability due to increased functional redundancy at the metabolic level and a greater level of defense against pathogen invasion (Lozupone et al., 2012; Larsen and Claassen, 2018). Nevertheless, gut microbiota research in humans is increasingly finding that α-diversity data are of limited utility as a reference for intestinal health or for discriminating between different treatments. This has been proven in the intestinal microbiome in other neurological and psychiatric conditions related to autism spectrum disorder (Ho et al., 2020), multiple sclerosis (Mirza et al., 2020), and Parkinson's disease (Nuzum et al., 2020). In addition, the Bray–Curtis distance showed that individual patients after treatment harbored a clearly varied microbial community compared to the composition structure observed before treatment. At the same time, overall distributions had greater variability across the PCoA space in the two groups. According to Nguyen et al. (2021), there was no difference in any alpha diversity of intestinal microbiota between schizophrenias and controls, while significant inter-group differences were observed in unweighted Unifrac and Bray–Curtis distances. Interestingly, similar results were demonstrated for functional analyses in their study. It is well-known that β-diversity distances can display whether variations exist between different treatments. In contrast, they cannot explain what the variations are or at what level of species they occur.

Next, we focused primarily on the microbial composition and comparative analysis of different taxa in the gut. In this study, the intestinal bacteria of patients with schizophrenia mainly consisted of four dominant taxa: *Firmicutes, Bacteroidetes, Proteobacteria,* and *Actinobacteria*, which accounted for more than 90% of the total microbial count in the gut. A similar conclusion was demonstrated in the previous studies (Shen et al., 2018). Meanwhile, the abundance of *Faecalibacterium*, *Butyricicoccus*, *Oscillospira*, *Roseburia*, and *Prevotella* was much higher in the gut of AT patients than in BT patients. In contrast, most other taxa were found to be biomarkers in the AT group, such as *Rothia*. *Faecalibacterium*, an anti-inflammatory butyric-producing taxonomy, has been shown as a common

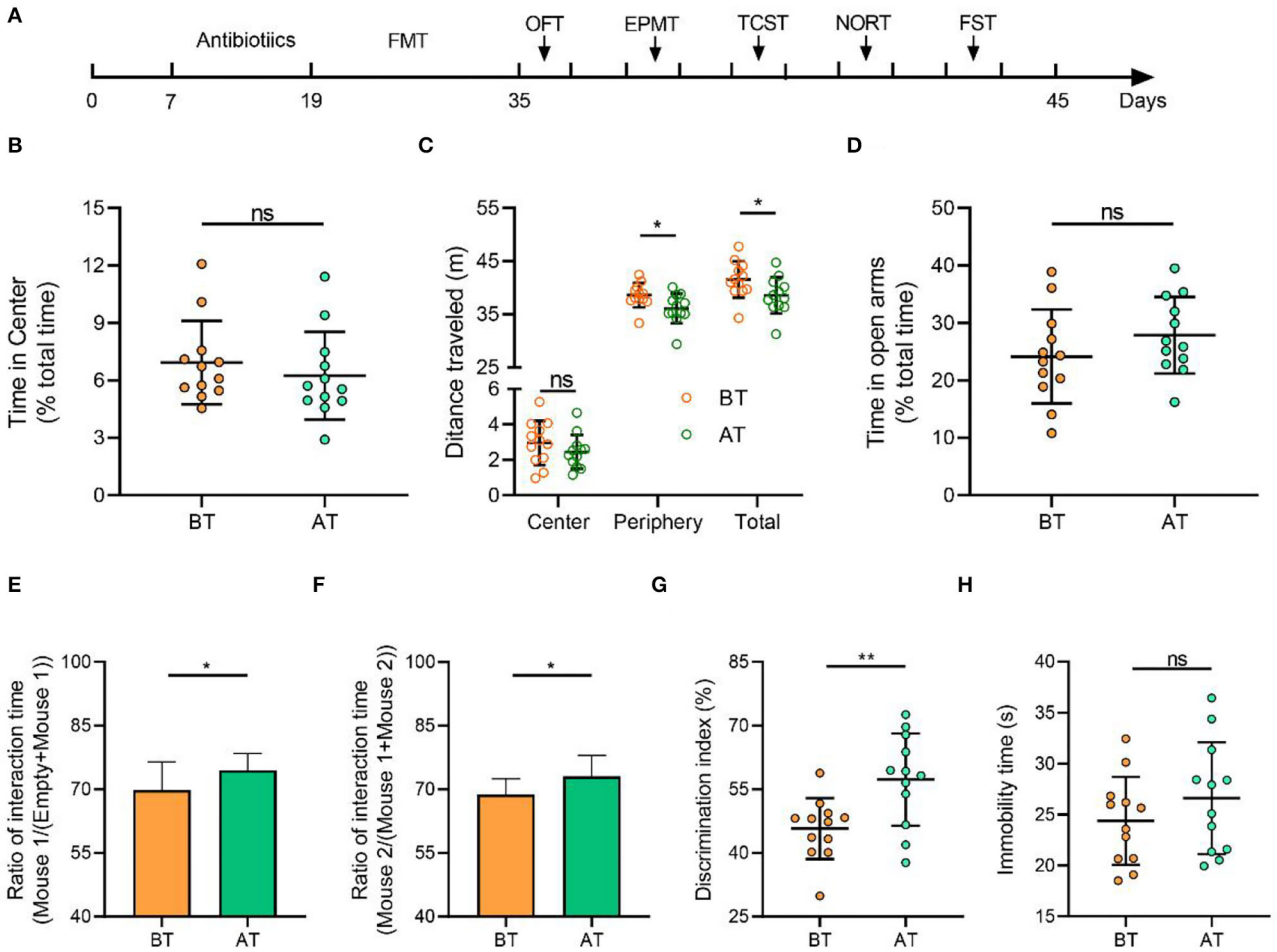

FIGURE 6 | Gut microbiota from patients with SCZ (after treatment) induced a lower level of hyperkinetic behavior and improved sociability, social novelty, and memory in mice than before treatment but had no effects on anxious state and depressive behavior. **(A)** Schematic diagram of mouse treatment and behavioral testing. Mice were given a cocktail of antibiotics to eliminate gut microbiota and received oral gavage of the microbiota suspension from before or after treatment patients with SCZ. A series of behavioral tests were carried out 48 h after the last FMT. OFT open field test, EPMT elevated plus maze test, TCST three-chamber social test, NORT novel object recognition test, FST forced swimming test. **(B)** In the 10-min open field test, both groups of mice spent similar amounts of time in the central arena. **(C)** The cumulative distance (meters) traveled in the different zones, the representative traces of mouse activity. **(D)** Time in open arms of the elevated plus maze during 5-min exploration did not vary between two groups. **(E)** AT mice had obvious changes in sociability compared with BT mice. **(F)** AT mice had obvious changes in social novelty compared with BT mice. **(G)** Novel object recognition test. AT mice spent significantly more time exploring the novel object compared with BT mice, indicating improvement of impaired recognition memory. **(H)** Immobility in the forced swimming test (FST, $p = 0.138$) was similar between BT and AT mice. Means ± SD were presented in **(B–H)** and each circle represents individual mouse ($n = 12$ per group). *P*-values were determined by the Independent Student *T*-test. ns, no significant. $^{*}p < 0.05$, $^{**}p < 0.01$.

bacterial signature in psychiatric disorders, including major depression, anxiety, and schizophrenia (Nikolova et al., 2021). Moreover, lower *Roseburia*, *Butyricicoccus*, *Oscillospira*, and *Prevotella* abundances have also been observed in psychological and behavioral abnormalities (Geirnaert et al., 2015; Shen et al., 2018; Michels et al., 2019; Yang et al., 2021). In this study, the taxa abundance of the above-mentioned microbiota appeared to increase considerably under hospital treatment. It is worth noting that *Oscillospira* and *Butyricicoccus* have been widely considered next-generation probiotic candidates and therefore have great potential for development and application in food, health care, and biopharmaceutical products (Geirnaert et al., 2015; Yang et al., 2021). Finally, gut *Rothia* has been confirmed to be involved in the immune-inflammatory response of the body and is related to the development of allergic diseases and alcoholic fatty liver disease (Simonyte Sjödin et al., 2016; Sverrild et al., 2017; Maccioni et al., 2020).

Unfortunately, the mechanisms of these divergences in gut microbiota composition, the clinical or treatment significance of these changes, and the patterns of psychological disorders that these processes may reveal in patients remain unclear. Therefore, further research will combine more in-depth approaches, including assembly mechanisms of microbial communities (to identify the underlying causes of the gut microbial community),

RF disease classifiers (to evaluate diagnostic values of gut microbes), and microbial interaction network analysis (to identify valuable pathogenic bacteria and potential probiotics). The above results may provide greater insight into the development of schizophrenia and assist in understanding how relevant intestinal core species are related to pathological processes that potentially affect mental health.

Regarding the assembly of gut microbial communities, our study demonstrated that treatment in hospitals has an important effect—it interferes with the balance between stochastic and deterministic processes. The variation in the gut microbial community explained by stochastic processes increased from 48.1% before treatment to 58.1% after treatment. However, the niche breadths of the microbial communities in the AT group did not show significant changes compared to those in the BT group, demonstrating that the microbial community assembly was more strongly influenced by stochastic processes in the AT groups. Deterministic processes are likely to influence habitat specialists with a narrower niche breadth than generalists with a wider niche breadth (Pandit et al., 2009; Wu et al., 2018). In addition, C-score analysis indicated that the SES decreased with hospital treatment. The above findings demonstrated that stochastic processes greatly influenced the gut microbial community assembly with treatment in the hospital. This was likely because treatment processes presented a novel but stable random equilibrium between the loss and gain of taxa in the gut microbial community.

Subsequently, we constructed a prediction model of 164 microbial ASVs to explore specific gut microbes associated with schizophrenia and estimate their diagnostic values. This model indicated high accuracy (AUC = 0.9) and was validated in the testing set, showing that an effective species-based classifier model was not significantly influenced by clinical indicators such as age, height, weight, and gender. Among the 164 ASVs included in the classifier, ASV 57 was significantly enriched in schizophrenia and was annotated as *Ruminococcus*. Previous studies have shown that *Ruminococcus* spp. is significantly associated with Crohn's disease, IBD, and type 2 diabetes (Hall et al., 2017; Baumgartner et al., 2021; Ruuskanen et al., 2022).

Indicator species analysis and Netshift analysis were used to explore the response pattern of the intestinal microbial community for treatment in the hospital and to identify core species. Indicator species analysis is more practical for determining the habitat preferences of species (De Cáceres et al., 2010). Furthermore, we identified key sub-communities (modules) in the co-occurrence network based on the indicator species ASVs. Modularity refers to the natural partitioning of nodes into different groups or modules within a network. Each module is ecologically considered a collection of closely related species and functional units. These species may have ecologically similar functions and can be grouped into the same modules (Baldassano and Bassett, 2016). In the co-occurrence network, we detected four and three microbial community modules in the BT and AT groups, respectively, constituting a common subnetwork under different states. In the present study, we tried to perform an analysis called "Netshift" to understand and identify the "drive microbes" from before and after treatment microbiome datasets from the basis of each subnetwork. It is necessary to consider the abundance of microbes and quantify the variations among the microbial associations to make an intestinal microbiome-based inference. We focused on alterations in the respective associations of nodes between different networks during the reconnection of microbial networks. A node (microbial species) has a similar degree of post-treatment and pre-treatment (total connections to other resident taxa). Still, it might have a completely different set of associations (members participating in the connections). Thus, a centrality index, such as the node degree, is usually used to quantify these changes, but it cannot accurately evaluate associations. In addition, a Jaccard index can be used to quantify the degree of change in the interaction partner of each node between the two networks. However, its results were non-directional. The "Neighbor shift (NESH) score" quantifies specifically enriched interaction partners after treatment, resulting in directional changes of individual node associations. An increase in the medial of a treated gut microbe was used as an index to quantify the increased importance of the considered nodes. A species with a set of altered associations after treatment (determined by high NESH values), but still increasingly important for the entire network (determined by positive DelBet), must be critical in microbial interactions and is predicted to be the "drive microbes" (Kuntal et al., 2019). An increase in delta betweenness (DelBet) of an ASV in the AT group is considered a characteristic to quantify the increase in the importance of this ASV. A gut species in AT patients with a changed set of correlations (high NESH value), while still being increasingly important (positive DelBet) for the microbial network, necessarily holds core importance in microbial interplay and is identified as a key species (Kuntal et al., 2019). According to our results, ASV 57 was also detected as one of the "driver species." ASV57 proved to have negative roles and therefore can be identified as a harmful driver related to schizophrenia. In the common sub-network, the AT patient-specific correlations (displayed as red edges) of ASV 57 pointed toward other core species such as ASV 86, namely *Oscillospira*, which had positive DelBet and high NESH scores and were therefore inferred to have roles in resisting pathogen colonization. *Oscillospira* extensively colonizes the intestinal tracts of animals and humans. Many studies have shown that the gut *Oscillospira* is associated with Parkinson's disease, autism, and colitis disease (Zhai et al., 2019; Liu et al., 2020; Vascellari et al., 2020; Zhang et al., 2020). *Oscillospira* is closely associated with the central nervous system and degenerative diseases. According to a previous study, patients with Parkinson's disease also have a high abundance of *Oscillospira* (Zhang et al., 2020). However, in another study, Zhai et al. (2019) identified the opposite trend by sequencing the intestinal microbiota of children with ASD. They observed that *Oscillospira* increased significantly. In a study of depressed-like mice induced by chronic unpredictable mild stress, the stress induced an increase in the abundance of *Oscillospira;* treatment with *Sophora alopecuroides* (Leguminosae) derived alkaloids reduced the genus abundance (Cao et al., 2020). Johnson (2020) showed that social competence (a comprehensive measure of participants' extraversion, social skills, and communication

ability) was highly correlated with *Akkermansia*, *Lactococcus*, and *Oscillospira*, which were more abundant in individuals with higher social scores. Similarly, the specific correlation between *Oscillospira* and *Ruminococcus* may indicate two independent microbes trying to colonize the microbial network of the AT group. Still, only one species can exert positive effects on patients with schizophrenia. Therefore, the existence of *Oscillospira* might become a "driver microbe" to prevent the colonization of harmful bacteria.

Furthermore, we evaluated the influence of, and changes in, various clinical characteristics on the colonization of *Ruminococcu*s before treatment. This study considered the multicollinearity problem between variables and utilized an all-subset regression to select the clinical variables to simplify the model. In the generalized linear model constructed in our study, the effects of nutrient intake and dietary habits were significant, and the regression coefficients were both positive. This indicates that levels of *Ruminococcus* colonization would decrease as the patients' flavors become weak and vegetables and fruit intake increases. Dietary composition and nutritional status are considered the most important factors in regulating the intestinal microbiota and have been proven as potential new therapies for many neuropsychiatric diseases (Sandhu et al., 2017). Hence, these results provide important and valuable suggestions for future clinical treatment.

Finally, it is feasible to establish animal models by recolonizing the gut of SPF mice with fecal microbiota from patients with SCZ and observing their behavior (Liang et al., 2019; Zhu et al., 2020a). Hyperlocomotion is typical of SCZ-positive symptoms (Akosman et al., 2021). In the open field test, the shorter distance traveled by AT mice than BT mice suggested a decrease in psychomotor hyperactivity in AT mice. Impairment of memory, sociability, and social novelty in SCZ mice, reflects impaired cognitive function and social interaction in SCZ patients (Liu et al., 2017). The memory ability to a familiar object, sociability, and social novelty was seen to be increased in AT mice, demonstrating that negative schizophrenia-like activity was ameliorated. It is notable that, although anxiety-like and depressive-like activity were often the early symptoms of schizophrenia (Lee et al., 2018), the time in open areas and the immobility time are not different in the two mice groups. Similar to our results, a recent study conducted by Zhu et al. did not find anxiety or depressive-like behaviors in mice receiving SCZ microbiota. Moreover, our patients were treated in the hospital for 2 weeks, which may have made these behaviors relatively insensitive to the patients' microbiota. Therefore, these data observed in SPF acceptor mice still provide further evidence for the gut microbes linked to SCZ severity and symptom changes in varying degrees.

In this study, the species composition and structure before and after the treatment were determined by 16S rRNA analysis. The relationship between changes in the intestinal flora and symptom improvement in SCZ patients was preliminarily verified by FMT. However, it is still necessary to provide more evidence to support this conclusion, particularly to reveal the mechanism beyond fecal bacterial transplantation. At the same time, it remains to be confirmed whether there is a causal interaction between changes in the microflora network and differences in symptoms. In addition, the sample size of the participants was small (only 25 patients), and it would be better to have a larger sample size in future studies.

CONCLUSION

These results demonstrated that gut microbiota distributions differ when comparing the fecal samples of patients with SCZ after treatment to before treatment in the hospital. Host antipsychotic treatment could modulate SCZ symptoms by suppressing harmful bacteria and adjusting the assembly structure. The sensitive and well-connected species with marked changes, which might be closely related to decreased schizophrenia severity under antipsychotic treatment, could be considered potential species for future microbiota-directed therapies.

DATA AVAILABILITY STATEMENT

The datasets presented in this study can be found in online repositories. The names of the repository/repositories and accession number(s) can be found at: https://www.ncbi.nlm.nih.gov/, PRJNA821673.

ETHICS STATEMENT

The human experiment was approved by the Medical Ethics Committee of The Fourth People's Hospital of Ya'an (approval number: 2021-1). The patients/participants provided their written informed consent to participate in this study. The animal study was reviewed and approved by All animal experiment procedures were approved by the Institutional Animal Care and Use Committee of the Sichuan Agricultural University (approval number: SYXKchuan2019-187).

AUTHOR CONTRIBUTIONS

MX, LZ, DaosP, TZ, and GW managed project and data. MX, DW, XW, and KZ recruited subjects and saved data. FL, XM, HY, DaoqP, and YiZ collected feces and performed the experiments LZ, LC, YoZ, ZS, DaosP, and GW analyzed and interpreted the results. LZ, MX, and DaosP prepared the draft. LZ, TZ, and GW revised and edited the manuscript. All authors read and approved the final manuscript.

FUNDING

The present study was supported by Sichuan Science and Technology Program (2021YJ0166), which provided funding support for sample collection, parameters

determination, animal purchase, and open access publication fees.

ACKNOWLEDGMENTS

The authors gratefully acknowledge the help from Ms. Zhang Xufei for language correction during drafted the manuscripts. Also, we really appreciate the supports provided by all other students during the animal feeding and behavioral testing.

SUPPLEMENTARY MATERIAL

The Supplementary Material for this article can be found online at: https://www.frontiersin.org/articles/10.3389/fmicb.2022.909729/full#supplementary-material

16S rRNA sequencing reads have uploaded to NCBI. The accession code of sequence reads Archive in the National Center for Biotechnology Information (NCBI) BioProject database: PRJNA821673.

REFERENCES

Akosman, M. S., Türkmen, R., and Demirel, H. H. (2021). Investigation of the protective effect of resveratrol in an MK-801-induced mouse model of schizophrenia. *Environ. Sci. Pollut. Res. Int.* 28, 65872–65884. doi: 10.1007/s11356-021-15664-x

Andersen, J., Larsen, J. K., Schultz, V., Nielsen, B. M., Kørner, A., Behnke, K., et al. (1989). The brief psychiatric rating scale. Dimension of schizophrenia–reliability and construct validity. *Psychopathology* 22, 168–176. doi: 10.1159/000284591

Anticevic, A., Gancsos, M., Murray, J. D., Repovs, G., Driesen, N. R., Ennis, D. J., et al. (2012). NMDA receptor function in large-scale anticorrelated neural systems with implications for cognition and schizophrenia. *Proc. Natl. Acad. Sci. U.S.A.* 109, 16720–16725. doi: 10.1073/pnas.1208494109

Aziz, Q., and Thompson, D. G. (1998). Brain-gut axis in health and disease. *Gastroenterology* 114, 559–578. doi: 10.1016/S0016-5085(98)70540-2

Baldassano, S. N., and Bassett, D. S. (2016). Topological distortion and reorganized modular structure of gut microbial co-occurrence networks in inflammatory bowel disease. *Sci. Rep.* 6:26087. doi: 10.1038/srep26087

Baumgartner, M., Lang, M., Holley, H., Crepaz, D., Hausmann, B., Pjevac, P., et al. (2021). Mucosal biofilms are an endoscopic feature of irritable bowel syndrome and ulcerative colitis. *Gastroenterology* 161, 1245–1256.e20. doi: 10.1053/j.gastro.2021.06.024

Benesh, D. P., and Kalbe, M. (2016). Experimental parasite community ecology: intraspecific variation in a large tapeworm affects community assembly. *J. Anim. Ecol.* 85, 1004–1013. doi: 10.1111/1365-2656.12527

Birnbaum, R., Jaffe, A. E., Chen, Q., Shin, J. H., Kleinman, J. E., Hyde, T. M., et al. (2018). Investigating the neuroimmunogenic architecture of schizophrenia. *Mol. Psychiatry* 23, 1251–1260. doi: 10.1038/mp.2017.89

Bolyen, E., Rideout, J. R., Dillon, M. R., Bokulich, N. A., Abnet, C., Al-Ghalith, G. A., et al. (2018). QIIME 2: Reproducible, interactive, scalable, and extensible microbiome data science. *PeerJ Preprints* 6, e27295v2. doi: 10.7287/peerj.preprints27295v2

Cacabelos, R., and Martínez-Bouza, R. (2011). Genomics and pharmacogenomics of schizophrenia. *CNS Neurosci. Ther.* 17, 541–565. doi: 10.1111/j.1755-5949.2010.00187.x

Callahan, B. J., Mcmurdie, P. J., Rosen, M. J., Han, A. W., Johnson, A. J., and Holmes, S. P. (2016). Dada2: high-resolution sample inference from ilumina amplicon data. *Nat. Methods* 13, 581–583. doi: 10.3086/nmeth.3869

Cao, C., Liu, M., Qu, S., Huang, R., Qi, M., Zhu, Z., et al. (2020). Chinese medicine formula kai-xin-san ameliorates depression-like behaviours in chronic unpredictable mild stressed mice by regulating gut microbiota-inflammation-stress system. *J. Ethnopharmacol.* 261:113055. doi: 10.1016/j.jep.2020.113055

Clauset, A., Newman, M. E., and Moore, C. (2004). Finding community structure in very large networks. *Phys. Rev. E Stat. Nonlin. Soft Matter Phys.* 70(6 Pt 2):066111. doi: 10.1103/PhysRevE.70.066111

Crump, B. C., Peterson, B. J., Raymond, P. A., Amon, R. M. W., Rinehart, A., McClelland, J. W., et al. (2009). Circumpolar synchrony in big river bacterioplankton. *Proc. Natl. Acad. Sci. U.S.A.* 106, 21208–21212. doi: 10.1073/pnas.0906149106

De Cáceres, M., Legendre, P., and Moretti, M. (2010). Improving indicator species analysis by combining groups of sites. *Oikos* 119, 1674–1684. doi: 10.1111/j.1600-0706.2010.18334.x

De Palma, G., Lynch, M. D., Lu, J., Dang, V. T., Deng, Y., Jury, J., et al. (2017). Transplantation of fecal microbiota from patients with irritable bowel syndrome alters gut function and behavior in recipient mice. *Sci. Transl. Med.* 9:379. doi: 10.1126/scitranslmed.aaf6397

Diaz Heijtz, R., Wang, S., Anuar, F., Qian, Y., Björkholm, B., Samuelsson, A., et al. (2011). Normal gut microbiota modulates brain development and behavior. *Proc. Natl. Acad. Sci. U.S.A.* 108, 3047–3052. doi: 10.1073/pnas.1010529108

Edgar, R. C. (2013). UPARSE: highly accurate OTU sequences from microbial amplicon reads. *Nat. Methods* 10, 996–998. doi: 10.1038/nmeth.2604

Elzhov, T. V., Mullen, K. M., Spiess, A. N., and Bolker, B. (2015). *Minpack. lm: R Interface to the Levenberg-Marquardt Nonlinear Least-Squares Algorithm Found in MINPACK, Plus Support for Bounds*. R package version 1.1-8. Available online at: http://CRAN.Rproject.org/package=minpack.lm

Friedman, J., and Alm, E. J. (2012). Inferring correlation networks from genomic survey data. *PLoS Comput. Biol.* 8:e1002687. doi: 10.1371/journal.pcbi.1002687

Geirnaert, A., Wang, J., Tinck, M., Steyaert, A., Van den Abbeele, P., Eeckhaut, V., et al. (2015). Interindividual differences in response to treatment with butyrate-producing Butyricicoccus pullicaecorum 25-3T studied in an *in vitro* gut model. *FEMS Microbiol. Ecol.* 91:fiv054. doi: 10.1093/femsec/fiv054

Gonçalves, V. F., Andreazza, A. C., and Kennedy, J. L. (2015). Mitochondrial dysfunction in schizophrenia: an evolutionary perspective. *Hum. Genet.* 134, 13–21. doi: 10.1007/s00439-014-1491-8

Gotelli, N. J., and Mccabe, D. J. (2002). Species co-occurrence: a meta-analysis of J. M. Diamond s assembly rules model. *Ecology* 83, 2091–2096. doi: 10.1890/0012-9658(2002)083[2091:SCOAMA]2.0.CO;2

Gubert, C., Kong, G., Uzungil, V., Zeleznikow-Johnston, A. M., Burrows, E. L., Renoir, T., et al. (2020). Microbiome profiling reveals gut dysbiosis in the metabotropic glutamate receptor 5 knockout mouse model of schizophrenia. *Front. Cell. Dev. Biol.* 8:582320. doi: 10.3389/fcell.2020.582320

Hall, A. B., Yassour, M., Sauk, J., Garner, A., Jiang, X., Arthur, T., et al. (2017). A novel Ruminococcus gnavus clade enriched in inflammatory bowel disease patients. *Genome Med.* 9:103. doi: 10.1186/s13073-017-0490-5

Ho, L. K. H., Tong, V. J. W., Syn, N., Nagarajan, N., Tham, E. H., Tay, S. K., et al. (2020). Gut microbiota changes in children with autism spectrum disorder: a systematic review. *Gut Pathog.* 12:6. doi: 10.1186/s13099-020-0346-1

Ikeda, K., Nakamoto, C., Kawamura, M., Nakatsukasa, E., Natsume, R., Takao, K., et al. (2020). GluD1 knockout mice with a pure C57BL/6N background show impaired fear memory, social interaction, and enhanced depressive-like behavior. *PLoS ONE* 15:e229288. doi: 10.1371/journal.pone.0229288

Järbrink-Sehgal, E., and Andreasson, A. (2020). The gut microbiota and mental health in adults. *Curr. Opin. Neurobiol.* 62, 102–114. doi: 10.1016/j.conb.2020.01.016

Johnson, K. V. A. (2020). Gut microbiome composition and diversity are related to human personality traits. *Hum. Microbiome J.* 15:100069. doi: 10.1016/j.humic.2019.100069

Ju,. F., Xia, Y., Guo, F., Wang, Z., and Zhang, T. (2014). Taxonomic relatedness shapes bacterial assembly in activated sludge of globally distributed wastewater treatment plants. *Environ. Microbiol.* 16, 2421–2432. doi: 10.1111/1462-2920.12355

Kahn, R. S., Sommer, I. E., Murray, R. M., Meyer-Lindenberg, A., Weinberger, D. R., Cannon, T. D., et al. (2015). Schizophrenia. *Nat. Rev. Dis. Primers* 1:15067. doi: 10.1038/nrdp.2015.67

Karpiński, P., Frydecka, D., Sasiadek, M. M., and Misiak, B. (2016). Reduced number of peripheral natural killer cells in schizophrenia but not in bipolar disorder. *Brain Behav. Immun.* 54, 194–200. doi: 10.1016/j.bbi.2016.02.005

Kuntal, B. K., Chandrakar, P., Sadhu, S., and Mande, S. S. (2019). 'NetShift': a methodology for understanding 'driver microbes' from healthy and disease microbiome datasets. *ISME J.* 13, 442–454. doi: 10.1038/s41396-018-0291-x

Larsen, O. F. A., and Claassen, E. (2018). The mechanistic link between health and gut microbiota diversity. *Sci. Rep.* 8:2183. doi: 10.1038/s41598-018-20141-6

Lee, S., Kang, S., Ang, M. J., Kim, J., Kim, J. C., Kim, S. H., et al. (2018). Deficiency of sterol regulatory element-binding protein-1c induces schizophrenia-like behavior in mice. *Genes Brain Behav.* 18:e12540. doi: 10.1111/gbb.12540

Li, S., Zhuo, M., Huang, X., Huang, Y., Zhou, J., Xiong, D., et al. (2020). Altered gut microbiota associated with symptom severity in schizophrenia. *PeerJ* 8:e9574. doi: 10.7717/peerj.9574

Liang, W., Huang, Y., Tan, X., Wu, J., Duan, J., Zhang, H., et al. (2019). Alterations of glycerophospholipid and fatty acyl metabolism in multiple brain regions of schizophrenia microbiota recipient mice. *Neuropsychiatr. Dis. Treat.* 15, 3219–3229. doi: 10.2147/NDT.S225982

Liu, H., Zhai, J., Wang, B., and Fang, M. (2017). Olig2 silence ameliorates cuprizone-induced schizophrenia-like symptoms in mice. *Med. Sci. Monit.* 23, 4834–4840. doi: 10.12659/MSM.903842

Liu, M., Xie, W., Wan, X., and Deng, T. (2020). Clostridium butyricum modulates gut microbiota and reduces colitis associated colon cancer in mice. *Int. Immunopharmacol.* 88:106862. doi: 10.1016/j.intimp.2020.106862

Lozupone, C. A., Stombaugh, J. I., Gordon, J. I., Jansson, J. K., and Knight, R. (2012). Diversity, stability and resilience of the human gut microbiota. *Nature* 489, 220–230. doi: 10.1038/nature11550

Maccioni, L., Gao, B., Leclercq, S., Pirlot, B., Horsmans, Y., De Timary, P., et al. (2020). Intestinal permeability, microbial translocation, changes in duodenal and fecal microbiota, and their associations with alcoholic liver disease progression in humans. *Gut Microbes* 12:1782157. doi: 10.1080/19490976.2020.1782157

Mah, S., Nelson, M. R., Delisi, L. E., Reneland, R. H., Markward, N., James, M. R., et al. (2006). Identification of the semaphorin receptor PLXNA2 as a candidate for susceptibility to schizophrenia. *Mol. Psychiatry* 11, 471–478. doi: 10.1038/sj.mp.4001785

Malla, A. K., Norman, R. M., and Williamson, P. (1993). Stability of positive and negative symptoms in schizophrenia. *Can. J. Psychiatry* 38, 617–621. doi: 10.1177/070674379303800910

Martin, M. (2011). Cutadapt removes adapter sequences from high-throughput sequencing reads. *Embnet J.* 17, 10–12. doi: 10.14806/ej.17.1.200

McMurdie, P. J., and Holmes, S. (2013). phyloseq: an R package for reproducible interactive analysis and graphics of microbiome census data. *PLoS ONE* 8:e61217. doi: 10.1371/journal.pone.0061217

Michels, N., Van de Wiele, T., Fouhy, F., O'Mahony, S., Clarke, G., and Keane, J. (2019). Gut microbiome patterns depending on children's psychosocial stress: reports versus biomarkers. *Brain Behav. Immun.* 80, 751–762. doi: 10.1016/j.bbi.2019.05.024

Mirza, A., Forbes, J. D., Zhu, F., Bernstein, C. N., Van Domselaar, G., Graham, M., et al. (2020). The multiple sclerosis gut microbiota: a systematic review. *Mult. Scler. Relat. Disord.* 37:101427. doi: 10.1016/j.msard.2019.101427

Neufeld, K. M., Kang, N., Bienenstock, J., and Foster, J. A. (2011). Reduced anxiety-like behavior and central neurochemical change in germ-free mice. *Neurogastroenterol. Motil.* 23, 255–264.e119. doi: 10.1111/j.1365-2982.2010.01620.x

Nguyen, T. T., Kosciolek, T., Daly, R. E., Vázquez-Baeza, Y., Swafford, A., Knight, R., et al. (2021). Gut microbiome in Schizophrenia: altered functional pathways related to immune modulation and atherosclerotic risk. *Brain Behav. Immun.* 91, 245–256. doi: 10.1016/j.bbi.2020.10.003

Nikolova, V. L., Hall, M. R. B., Hall, L. J., Cleare, A. J., Stone, J. M., and Young, A. H. (2021). Perturbations in gut microbiota composition in psychiatric disorders: a review and meta-analysis. *JAMA Psychiatry* 78, 1343–1354. doi: 10.1001/jamapsychiatry.2021.2573

Nuzum, N. D., Loughman, A., Szymlek-Gay, E. A., Hendy, A., Teo, W. P., and Macpherson, H. (2020). Gut microbiota differences between healthy older adults and individuals with Parkinson s disease: a systematic review. *Neurosci. Biobehav. Rev.* 112, 227–241. doi: 10.1016/j.neubiorev.2020.02.003

Östman, Ö., Drakare, S., Kritzberg, E. S., Langenheder, S., Logue, J. B., and Lindstrom, E. S. (2010). Regional invariance among microbial communities. *Ecol. Lett.* 13:1182117. doi: 10.1111/j.1461-0248.2009.01413.x

Pandit, S. N., Kolasa, J., and Cottenie, K. (2009). Contrasts between habitat generalists and specialists: an empirical extension to the basic metacommunity framework. *Ecology* 90, 2253–2262. doi: 10.1890/08-0851.1

Perez, J. M., Berto, S., Gleason, K., Ghose, S., Tan, C., Kim, T. K., et al. (2021). Hippocampal subfield transcriptome analysis in schizophrenia psychosis. *Mol. Psychiatry* 26, 2577–2589. doi: 10.1038/s,41380-020-0696-6

Price, M. N., Dehal, P. S., and Arkin, A. P. (2009). FastTree: computing large minimum evolution trees with profiles instead of a distance matrix. *Mol. Biol. Evol.* 26, 1641–1650. doi: 10.1093/molbev/msp077

R Core Team (2018). *R: A Language and Environment for Statistical Computing*. Vienna: R Foundation for Statistical Computing.

Robinson, M. D., McCarthy, D. J., and Smyth, G. K. (2010). edgeR: a Bioconductor package for differential expression analysis of digital gene expression data. *Bioinformatics* 26, 139–140. doi: 10.1093/bioinformatics/btp616

Rutsch, A., Kantsjö, J. B., and Ronchi, F. (2020). The gut-brain axis: how microbiota and host inflammasome influence brain physiology and pathology. *Front. Immunol.* 11:604179. doi: 10.3389/fimmu.2020.604179

Ruuskanen, M. O., Erawijantari, P. P., Havulinna, A. S., Liu, Y., Méric, G., Tuomilehto, J., et al. (2022). Gut microbiome composition is predictive of incident type 2 diabetes in a population cohort of 5,572 finnish adults. *Diabetes Care*. 45, 811–818. doi: 10.2337/dc21-2358

Sandhu, K. V., Sherwin, E., Schellekens, H., Stanton, C., Dinan, T. G., and Cryan, J. F. (2017). Feeding the microbiota-gut-brain axis: diet, microbiome, and neuropsychiatry. *Transl. Res.* 179, 223–244. doi: 10.1016/j.trsl.2016.10.002

Shen, Y., Xu, J., Li, Z., Huang, Y., Yuan, Y., Wang, J., et al. (2018). Analysis of gut microbiota diversity and auxiliary diagnosis as a biomarker in patients with schizophrenia: a cross-sectional study. *Schizophr. Res.* 197, 470–477. doi: 10.1016/j.schres.2018.01.002

Simonyte Sjödin, K., Vidman, L., Rydén, P., and West, C. E. (2016). Emerging evidence of the role of gut microbiota in the development of allergic diseases. *Curr. Opin. Allergy Clin. Immunol.* 16, 390–395. doi: 10.1097/ACI.0000000000000277

Sloan, W. T., Lunn, M., Woodcock, S., Head, I. M., Nee, S., and Curtis, T. P. (2006). Quantifying the roles of immigration and chance in shaping prokaryote community structure. *Environ. Microbiol.* 8, 732–740. doi: 10.1111/j.1462-2920.2005.00956.x

Stogios, N., Gdanski, A., Gerretsen, P., Chintoh, A. F., Graff-Guerrero, A., Rajji, T. K., et al. (2021). Autonomic nervous system dysfunction in schizophrenia: impact on cognitive and metabolic health. *NPJ Schizophr.* 7:22. doi: 10.1038/s41537-021-00151-6

Stone, L., and Roberts, A. (1990). The checkerboard score and species distributions. *Oecologia* 85, 74–79. doi: 10.1007/BF00317345

Strassnig, M., Cornacchio, D., Harvey, P. D., Kotov, R., Fochtmann, L., and Bromet, E. J. (2017). Health status and mobility limitations are associated with residential and employment status in schizophrenia and bipolar disorder. *J. Psychiatr. Res.* 94, 180–185. doi: 10.1016/j.jpsychires.2017.07.011

Sun, M.-F., Zhu, Y.-L., Zhou, Z.-L., Jia, X.-B., Xu, Y.-D., Yang, Q., et al. (2018). Neuroprotective effects of fecal microbiota transplantation on MPTP-induced Parkinson's disease mice: gut microbiota, glial reaction and TLR4/TNF-α signaling pathway. *Brain Behav. Immun.* 70, 48–60. doi: 10.1016/j.bbi.2018.02.005

Sverrild, A., Kiilerich, P., Brejnrod, A., Pedersen, R., Porsbjerg, C., Bergqvist, A., et al. (2017). Eosinophilic airway inflammation in asthmatic patients is associated with an altered airway microbiome. *J. Allergy Clin. Immunol.* 140, 407–417.e11. doi: 10.1016/j.jaci.2016.10.046

Swenson, N. G. (2014). *Functional and Phylogenetic Ecology in R*. New York, NY: Springer. doi: 10.1007/978-1-4614-9542-0

Takeda, K., Matsumoto, M., Ogata, Y., Maida, K., Murakami, H., Murayama, K., et al. (2017). Impaired prefrontal activity to regulate the intrinsic motivation-action link in schizophrenia. *Neuroimage Clin.* 16, 32–42. doi: 10.1016/j.nicl.2017.07.003

Tengeler, A. C., Dam, S. A., Wiesmann, M., Naaijen, J., van Bodegom, M., Belzer, C., et al. (2020). Gut microbiota from persons with attention-deficit/hyperactivity disorder affects the brain in mice. *Microbiome* 8:44. doi: 10.1186/s40168-020-00816-x

Tesli, N., van der Meer, D., Rokicki, J., Storvestre, G., Røsæg, C., Jensen, A., et al. (2020). Hippocampal subfield and amygdala nuclei volumes in schizophrenia patients with a history of violence. *Eur. Arch. Psychiatry Clin. Neurosci.* 270, 771–782. doi: 10.1007/s00406-020-01098-y

Tikàsz, A., Potvin, S., Dugr,é, J. R., Fahim, C., Zaharieva, V., Lipp, O., et al. (2020). Violent behavior is associated with emotion salience network dysconnectivity in schizophrenia. *Front Psychiatry* 11:143. doi: 10.3389/fpsyt.2020.00143

Vascellari, S., Melis, M., Cossu, G., Melis, M., Serra, A., Palmas, V., et al. (2020). Genetic variants of TAS2R38 bitter taste receptor associate with distinct gut microbiota traits in Parkinson s disease: a pilot study. *Int. J. Biol. Macromol.* 165, 665–674. doi: 10.1016/j.ijbiomac.2020.09.056

Wang, H., Sun, Y., Xin, J., Zhang, T., Sun, N., Ni, X., et al. (2020). *Lactobacillus johnsonii* BS15 prevents psychological stress-induced memory dysfunction in mice by modulating the gut-brain axis. *Front. Microbiol.* 11:1941. doi: 10.3389/fmicb.2020.01941

Wang, Y. M., Zou, L. Q., Xie, W. L., Yang, Z. Y., Zhu, X. Z., Cheung, E. F. C., et al. (2019). Altered functional connectivity of the default mode network in patients with schizo-obsessive comorbidity: a comparison between schizophrenia and obsessive-compulsive disorder. *Schizophr. Bull.* 45, 199–210. doi: 10.1093/schbul/sbx194

Wells, R., Jacomb, I., Swaminathan, V., Sundram, S., Weinberg, D., Bruggemann, J., et al. (2020). The impact of childhood adversity on cognitive development in schizophrenia. *Schizophr. Bull.* 46, 140–153. doi: 10.1093/schbul/sbz033

Wu, W. X., Lu, H. P., Sastri, A., Yeh, Y. C., Gong, G. C., and Chou, W. C. (2018). Contrasting the relative importance of species sorting and dispersal limitation in shaping marine bacterial versus protist communities. *ISME J.* 12, 485–494. doi: 10.1038/ismej.2017.183

Xiao, L., Yan, J., Yang, T., Zhu, J., Li, T., Wei, H., et al. (2021). Fecal microbiome transplantation from children with autism spectrum disorder modulates tryptophan and serotonergic synapse metabolism and induces altered behaviors in germ-free mice. *mSystems* 6:e01343-20. doi: 10.1128/mSystems.01343-20

Xu, J., Jiao, Y., Xing, M., Lin, Y., Su, Y., Ding, W., et al. (2018). Increased plasma leptin as a novel predictor for psychopathological depressive symptoms in chronic schizophrenia. *Gen. Psychiatr.* 31:e100018. doi: 10.1136/gpsych-2018-100018

Xu, R., Wu, B., Liang, J., He, F., Gu, W., Li, K., et al. (2020). Altered gut microbiota and mucosal immunity in patients with schizophrenia. *Brain Behav. Immun.* 85, 120–127. doi: 10.1016/j.bbi.2019.06.039

Yang, J., Li, Y., Wen, Z., Liu, W., Meng, L., and Huang, H. (2021). Oscillospira - a candidate for the next-generation probiotics. *Gut Microbes* 13:1987783. doi: 10.1080/19490976.2021.1987783

Yang, J., Yan, B., Fan, Y., Yang, L., Zhao, B., Zhu, F., et al. (2019). Identification of schizophrenia related biological pathways across eight brain regions. *Behav. Brain Res.* 360, 1–6. doi: 10.1016/j.bbr.2018.11.011

Yue, W. H., Wang, H. F., Sun, L. D., Tang, F. L., Liu, Z. H., Zhang, H. X., et al. (2011). Genome-wide association study identifies a susceptibility locus for schizophrenia in Han Chinese at 11p11.2. *Nat. Genet.* 43, 1228–1231. doi: 10.1038/ng.979

Zeller, G., Tap, J., Voigt, A. Y., Sunagawa, S., Kultima, J. R., Costea, P. I., et al. (2014). Potential of fecal microbiota for early-stage detection of colorectal cancer. *Mol. Syst. Biol.* 10:766. doi: 10.15252/msb.20145645

Zhai, Q., Cen, S., Jiang, J., Zhao, J., Zhang, H., and Chen, W. (2019). Disturbance of trace element and gut microbiota profiles as indicators of autism spectrum disorder: a pilot study of Chinese children. *Environ. Res.* 171, 5186–5189. doi: 10.1016/j.envres.2019.01.060

Zhang, F., Yue, L., Fang, X., Wang, G., Li, C., Sun, X., et al. (2020). Altered gut microbiota in Parkinson s disease patients/healthy spouses and its association with clinical features. *Parkinsonism Relat. Disord.* 81, 84–88. doi: 10.1016/j.parkreldis.2020.10.034

Zheng, P., Zeng, B., Liu, M., Chen, J., Pan, J., Han, Y., et al. (2019). The gut microbiome from patients with schizophrenia modulates the glutamate-glutamine-GABA cycle and schizophrenia-relevant behaviors in mice. *Sci. Adv.* 5:eaau8317. doi: 10.1126/sciadv.aau8317

Zheng, P., Zeng, B., Zhou, C., Liu, M., Fang, Z., Xu, X., et al. (2016). Gut microbiome remodeling induces depressive-like behaviors through a pathway mediated by the host's metabolism. *Mol. Psychiatry* 21, 786–796. doi: 10.1038/mp.2016.44

Zhu, F., Guo, R., Wang, W., Ju, Y., Wang, Q., Ma, Q., et al. (2020a). Transplantation of microbiota from drug-free patients with schizophrenia causes schizophrenia-like abnormal behaviors and dysregulated kynurenine metabolism in mice. *Mol. Psychiatry* 25, 2905–2918. doi: 10.1038/s41380-019-0475-4

Zhu, F., Ju, Y., Wang, W., Wang, Q., Guo, R., Ma, Q., et al. (2020b). Metagenome-wide association of gut microbiome features for schizophrenia. *Nat. Commun.* 11:1612. doi: 10.1038/s41467-020-15457-9

Conflict of Interest: The authors declare that the research was conducted in the absence of any commercial or financial relationships that could be construed as a potential conflict of interest.

Publisher's Note: All claims expressed in this article are solely those of the authors and do not necessarily represent those of their affiliated organizations, or those of the publisher, the editors and the reviewers. Any product that may be evaluated in this article, or claim that may be made by its manufacturer, is not guaranteed or endorsed by the publisher.

frontiers | Frontiers in Microbiology

TYPE Original Research
PUBLISHED 10 November 2022
DOI 10.3389/fmicb.2022.1054504

OPEN ACCESS

EDITED BY
Xueqin Ni,
Sichuan Agriculture University,
China

REVIEWED BY
Bangyuan Wu,
China West Normal University, China
Zahid Naseer,
Pir Mehr Ali Shah Arid Agriculture University, Pakistan

*CORRESPONDENCE
Chunxiao Lai
laichunxiao198610@163.com
Yongmei Huang
kanne111@163.com
Hao Li
futanghu888@126.com

†These authors have contributed equally to this work

SPECIALTY SECTION
This article was submitted to Microbial Symbioses, a section of the journal Frontiers in Microbiology

RECEIVED 26 September 2022
ACCEPTED 24 October 2022
PUBLISHED 10 November 2022

CITATION
Zhao Z, Cui D, Wu G, Ren H, Zhu X, Xie W, Zhang Y, Yang L, Peng W, Lai C, Huang Y and Li H (2022) Disrupted gut microbiota aggravates working memory dysfunction induced by high-altitude exposure in mice.
Front. Microbiol. 13:1054504.
doi: 10.3389/fmicb.2022.1054504

Disrupted gut microbiota aggravates working memory dysfunction induced by high-altitude exposure in mice

Zhifang Zhao[1†], Dejun Cui[1†], Guosong Wu[2†], Hong Ren[3], Ximei Zhu[2], Wenting Xie[3], Yuming Zhang[3], Liu Yang[3], Weiqi Peng[4], Chunxiao Lai[4]*, Yongmei Huang[2]* and Hao Li[3]*

[1]Department of Gastroenterology, National Institution of Drug Clinical Trial, Guizhou Provincial People's Hospital, Medical College of Guizhou University, Guiyang, Guizhou, China, [2]Department of Pharmacy, Baiyun Branch, Nanfang Hospital, Southern Medical University, Guangzhou, China, [3]Plateau Brain Science Research Center, Tibet University, Lhasa, China, [4]Department of Gastroenterology, Baiyun Branch, Nanfang Hospital, Southern Medical University, Guangzhou, China

Background: The widely accepted microbiome-gut-brain axis (MGBA) hypothesis may be essential for explaining the impact of high-altitude exposure on the human body, especially brain function. However, studies on this topic are limited, and the underlying mechanism remains unclear. Therefore, this study aimed to determine whether high-altitude-induced working memory dysfunction could be exacerbated with gut microbiota disruption.

Methods and results: C57BL/6 mice were randomly divided into three groups: control, high-altitude exposed (HAE), and high-altitude exposed with antibiotic treatment (HAE-A). The HAE and HAE-A groups were exposed to a low-pressure oxygen chamber (60–65kPa) simulating the altitude of 3,500–4,000m for 14days, The air pressure level for the control group was maintained at 94.5kPa. Antibiotic water (mixed with 0.2g/L of ciprofloxacin and 1g/L of metronidazole) was provided to the HAE-A group. Based on the results of the novel object test and P300 in the oddball behavioral paradigm training test, working memory dysfunction was aggravated by antibiotic treatment. We determined the antioxidant capacity in the prefrontal cortex and found a significant negative influence (p<0.05) of disturbed gut microbiota on the total antioxidant capacity (T-AOC) and malondialdehyde (MDA) content, as well as the activities of superoxide dismutase (SOD) and glutathione peroxidase (GSH-Px). The same trend was also observed in the apoptosis-related functional protein content and mRNA expression levels in the prefrontal cortex, especially the levels of bcl-2, Bax, and caspase-3. The high-altitude environment and antibiotic treatment substantially affected the richness and diversity of the colonic microbiota and reorganized the composition and structure of the microbial community. *S24-7*, *Lachnospiraceae*, and *Lactobacillaceae* were the three microbial taxa with the most pronounced differences under the stimulation by external factors in this study. In addition, correlation analysis between colonic microbiota and cognitive function in mice demonstrated that *Helicobacteraceae* may be closely related to behavioral results.

Conclusion: Disrupted gut microbiota could aggravate working memory dysfunction induced by high-altitude exposure in mice, indicating the existence of a link between high-altitude exposure and MGBA.

KEYWORDS

gut microbe, probiotic, high altitude, gut-brain axis, antibiotics

Introduction

With the development of highland areas, numerous people from the plains access the plateau every year for work or tourism. High-altitude environments are characterized by lack of oxygen, low pressure, low temperature, and strong ultraviolet radiation; within these features, the reduction in oxygen content plays an important role in affecting human life activities (Li et al., 2015; Tremblay et al., 2021). High-altitude hypoxia has different effects on the digestive, cardiovascular, and nervous systems, and the metabolism of exogenous substances (Pena et al., 2022). The brain is the body's largest oxygen-consuming organ, and its cognitive function is significantly adversely affected by lack of oxygen. Studies have shown that high-altitude hypoxic environments can result in changes to various cognitive processes in the brain, such as decreased attention (Svensson et al., 2015; Zhang D. et al., 2018), inhibitory control (Ma et al., 2015), executive function task correctness, and prolonged reaction times. Although high-altitude exposure can impair brain function, effective methods to prevent such an impact in high-altitude areas remain limited.

Medical researchers have developed the concept of the "microbiome-gut-brain axis (MGBA)," which is gaining increasing attention in the basic biological and physiological studies in the field of psychiatry, neurodevelopment, and age-related and neurodegenerative diseases. MGBA is a two-way information exchange system that integrates brain and gut functions, while the central nervous system communicates with the gut microbiota mainly through metabolites of microbial origin (Bravo et al., 2011; Yano et al., 2015). One study found that mice on a high-fat diet exhibited enhanced systemic and central nervous system inflammatory responses, which, in turn, increased the risk of Alzheimer's disease by affecting the MGBA system, leading to reduced cognitive function and β-amyloid accumulation (Bruce-Keller et al., 2015). In addition, *Bifidobacterium* and *Lactobacillus* have been shown to reduce symptoms associated with anxiety and depression and have a positive effect on memory, learning, and cognition in a variety of animal models (Sun et al., 2015). In addition to the metabolites of the gut microbiota, some of the intermediate products of microbiota metabolism can also cross the blood–brain barrier and act directly on the brain (Haghikia et al., 2016). Thus, modulation of MGBA may be a mechanism for regulating the brain, which provides another potential way to prevent brain dysfunction during high-altitude exposure.

Previous studies have shown that high-altitude environments alter the balance of the intestinal microbiota, causing damage to the intestinal structure and mucosal barrier, ultimately inducing and exacerbating intestinal damage (Zhang W. et al., 2018; Wang et al., 2022). In addition, a study based on 17 healthy men found that the relative abundance of *Prevotella* in the intestines was subject to altitude-dependent changes at 4,300 m, effectively demonstrating that intestinal microbiota may contribute to host variability in response to high-altitude exposure (Ananthakrishnan et al., 2018). The above-mentioned information supports the possibility of considering MGBA as a possible preventive method against brain dysfunction under high-altitude exposure; however, research is needed to demonstrate the role of MGBA during high-altitude exposure.

Therefore, we placed mice in a high-altitude environment simulation device and disrupted the intestinal microbiota of one group of mice using a combination of antibiotics. New object recognition was used to detect working memory impairment and prefrontal oxidative stress markers and apoptotic protein levels were examined. Differences in the composition of intestinal microbiota were analyzed by colonic 16S rDNA sequencing. The present study aimed to provide evidence to answer the following two research questions: (1) Does disturbed gut microbiota exacerbate high-altitude exposure impairment of working memory in mice? (2) The decrease/increase of which gut symbiotic bacteria may play a key role? This study provides a theoretical basis for the application of intestinal commensal bacteria in working memory impairment due to high-altitude exposure.

Materials and methods

Animal treatment and sampling

A total of 36 C57BL/6 mice of the same age (8 weeks old, purchased from SPF Biotechnology Co., Ltd., Beijing, China) were randomly selected and divided into three groups after a week of adjustment. The three groups were as follows: control, high-altitude exposed (HAE), and high-altitude exposed with antibiotic treatment (HAE-A). The air pressure level for the control group was maintained at 94.5 kPa, while the HAE and HAE-A groups were exposed to a low-pressure oxygen chamber simulating an altitude of 3,500–4,000 m for 14 days, with the air pressure set to

60–65 kPa. Antibiotic water (mixed with 0.2 g/L of ciprofloxacin and 1 g/L of metronidazole) was provided to the HAE-A group, and the other two groups were provided with normal drinking water during the 14 experimental days. The temperature and humidity of the low-pressure oxygen chamber were identical to those outside the chamber. The chamber was opened for 1 h per day to supply food (Chengdu Dashuo Institute of Biology, Chengdu, China) and water. All animal experiments were conducted in accordance with the guidelines for the feeding and use of experimental animals and approved by the Committee of Nanfang Hospital Baiyun Branch, Southern Medical University (approval no: SYXK2022-023). All animals were kept in a room with a controlled temperature (22 ± 2°C) and a 12/12-h light/dark cycle (dark period: 7 p.m.–7 a.m.).

After the 14 day experimental period, eight mice from each experimental group were randomly selected. After the behavioral test (novel object test, described below), the mice were immediately sacrificed by cervical dislocation, according to the guidelines of the animal care facility. A portion of the prefrontal cortex was immediately removed. These samples were washed in ice-cold sterile saline, frozen in liquid nitrogen, and then stored at −80°C. The rest of prefrontal cortex and the contents of the colon were removed separately and frozen at −20°C until further analysis. Extraction of samples stored at −80°C and prefrontal cortical RNA was performed using the E.Z.N.A. Total RNA Kit (OMEGA Bio-Tek, Doraville, GA, United States) in accordance with the manufacturer's guidelines. Total RNA (1 μg) was synthesized into first-strand complementary DNA (cDNA) using the PrimeScript™ RT reagent kit with gDNA Eraser (TaKaRa, Dalian, Liaoning, China). The cDNA products were stored at −20°C until subsequent tests.

Novel object test

The schematic diagram of novel object test is shown in Figure 1A. Mice tend to investigate novel objects rather than familiar ones. On this basis, a novel object test of working memory formation was conducted using the method described by Gareau et al. (2011), with minor modifications. Briefly, the mice were placed in a dark open-field arena (40 × 40 × 45 cm, length × width × height) and allowed to explore freely for 1 h for habituation. The mice were shown two distinct objects: a smooth pebble of the right size and blue and orange tube caps of the same size and form. The phases of behavioral assessment included familiarization and testing.

During familiarization, the blue and orange tube caps were placed in the opposing corners of the arena, and the mice were permitted to examine both items for 5 min. After the objects had been removed, the mice were given a 20-min rest before testing.

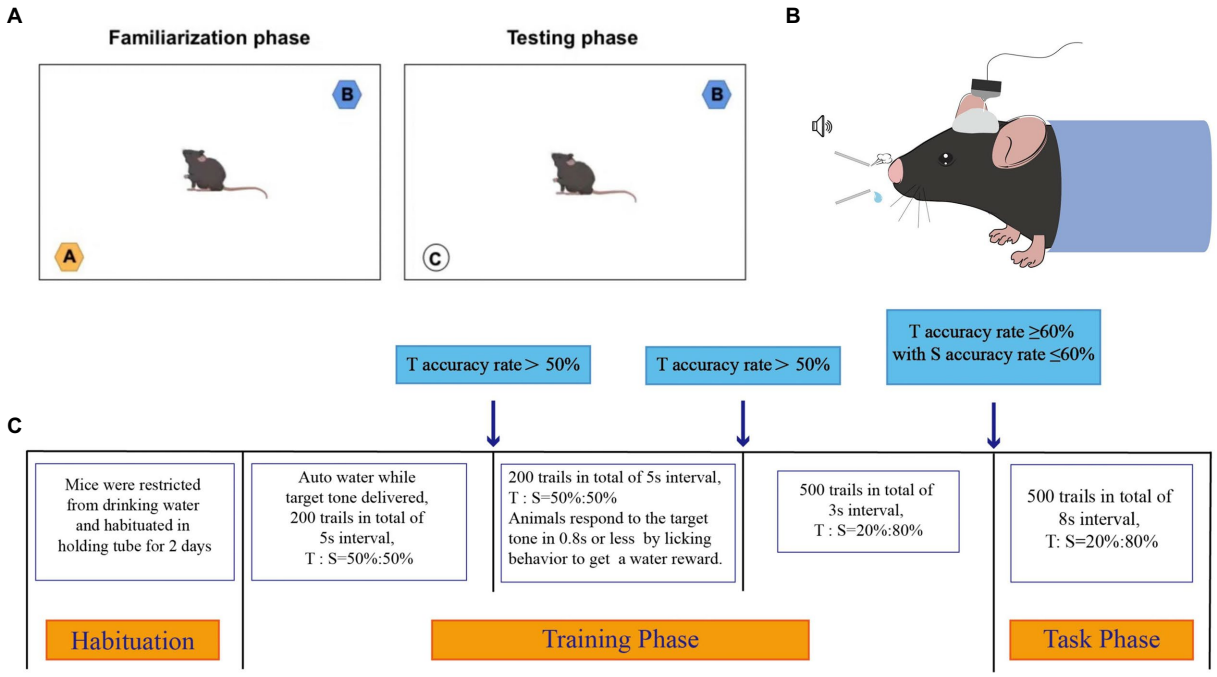

FIGURE 1
The schematic diagram of novel object test and oddball paradigm behavior training. **(A)** Schematic diagram of novel object test. A dark open-field box (40 * 40 * 45cm) was used. The objects shown to the mice were a smooth pebble, a blue cap of the same size and form, and a orange cap of the same size and form, respectively. **(B)** Schematic diagram of oddball paradigm behavior training. **(C)** Schematic presentation of different phases of the Oddball paradigm behavior Training. Animals had to correctly respond to infrequent target (8Hz) tones while correctly ignoring infrequent standard (6Hz) tones. The electrical signals of the mice were recorded during the task phase. T referred to Target tone, S referred to Standard tone.

The orange tube cap was replaced with a smooth pebble during the rest period and during testing, the mice were exposed to the blue tube cap and the smooth pebble. Memory can be assessed as the frequency with which the smooth pebble is explored in comparison with the blue tube cap. The exploration ratio is a measure of how often mice sniff new objects compared to old ones (ratio of the frequency of sniffing the smooth pebble to the total frequency of sniffing the blue tube cap and smooth pebble). No difference between the two objects, or a ratio of 0.5, indicated impaired hippocampus-dependent memory. In the present test, exploration was defined as orientation toward the object with the nose pointing directly at the object within 1–2 cm.

Biochemical analysis

The antioxidant indices in the prefrontal cortex were measured using commercial kits (Jiancheng Bioengineering Institute, Nanjing, Jiangsu, China), including the activities of catalase (CAT), total antioxidant capacity (T-AOC), glutathione peroxidase (GSH-Px), superoxide dismutase (SOD), malondialdehyde (MDA), and GSH content (Zareie et al., 2006). The levels of bcl-2 and Bax in the prefrontal cortex were determined by ELISA using murine-specific reagent kits (MLBIO Biotechnology Co., Ltd., Shanghai, China). Data were analyzed using individual mice. Statistical analyses were performed using one-way ANOVA, followed by Duncan's multiple-range test for multiple comparisons (satisfying both normality and equal variance tests; SigmaPlot for Social Sciences version 12). Differences were considered statistically significant at $p < 0.05$.

Real-time quantitative polymerase chain reaction analysis

The cDNA products generated from the prefrontal cortex were determined by PCR. A CFX96 Real-time PCR Detection System (Bio-Rad, Hercules, CA, United States) with iTaq Universal SYBR Green Supermix (Bio-Rad, Hercules, CA, United States) was used with the following protocol: 5 min at 95°C, 40 cycles of 10 s denaturation at 95°C, and 30 s annealing/extension at optimum temperature (Table 1). The PCR product purity was analyzed using a final melting curve analysis. Standard curves were generated using serial dilutions. Primer sequences for the target genes are shown in Table 1. The mRNA abundance was estimated using the $_{\Delta\Delta}$Ct method. The samples ($n = 6$) in each group were analyzed in triplicate, and Ct was calculated as $(Ct_{target} - Ct_{\beta\text{-actin}})_{treatment} - (Ct_{target} - Ct_{\beta\text{-actin}})_{control.}$ β-actin was used as a eukaryotic housekeeping gene to normalize relative gene expression levels. The measured mean values were used to assess mRNA expression levels of Bcl-2, Bad, Bax, caspase-3, and caspase-9 in the prefrontal cortex. Data were analyzed using individual mice. Statistical analyses were performed using one-way analysis of variance (ANOVA), followed by Duncan's multiple-range test for multiple comparisons (satisfying both normality and equal variance tests; SigmaPlot for Social Sciences version 12). Differences were considered statistically significant at $p < 0.05$.

TABLE 1 Primer sequences for RT-qPCR in the prefrontal cortex.

Gene	Tm (°C)	Sequence
β-actin	60	F: GCTCTTTTCCAGCCTTCCTT
		R: GATGTCAACGTCACACTT
caspase-9	61	F: GAGGTGAAGAACGACCTGAC
		R: AGAGGATGACCACCACAAAG
caspase-3	59	F: ACATGGGAGCAAGTCAGTGG
		R: CGTCCACATCCGTACCAGAG
Bax	61	F: ATGCGTCCACCAAGAAGC
		R: CAGTTGAAGTTGCCATCAGC
Bad	60	F: AGAGTATGTTCCAGATCCCAG
		R: GTCCTCGAAAAGGGCTAAGC
bcl-2	61	F: AGCCTGAGAGCAACCCAAT
		R: AGCGACGAGAGAAGTCATCC

P300 in the oddball behavioral paradigm training test

Surgery and treatment

Before high-altitude exposure, another six mice per group (single-caged) were anesthetized with isoflurane (O.D, 1%–3% in oxygen, R580 anesthesia machine, RWD) and placed on a stereotaxic frame (680303, RWD). A water circulation insulation system (68662, RWD) was used to maintain body temperature at 37°C throughout the experiment. Ophthalmic gel was used to protect the eyes from drying. The heads of the mice were shaved at the surgical area, which was cleaned using 75% ethanol. The skull was exposed horizontal to the bregma and lambda landmarks. Bregma measurement was performed to determine the anterior–posterior (AP) and medial–lateral (ML) coordinates for electrode implantation. Four screws were secured to the skull, one to serve as the recording ground, and the other three to fix the dental cement. A 16-channel Microwire Electrode Array (MEA, arranged in the 2 × 8 configuration, 33 μm diameter nickel-chromium wires with formvar insulation, 0.25 mm inter-electrode spacing, KedouBC), was implanted into the PFC (A/P + 1.0 mm L/M + 0.4 mm D/V −1.8 mm), and secured with dental cement to a home-made metal plate to immobilize the head for oddball behavioral paradigm training. Mice in the HAE and HAE-A groups experienced high-altitude exposure 7 days after recovery from surgery.

Oddball paradigm behavior training

After full recovery from surgery, head-fixed mice were trained in a hearing-based bionic stimulation oddball paradigm. A pair of sound stimuli (~86 db) was used: the target tone (8 kHz) and standard tone (6 kHz). All the tone stimulations were marked

using a microcontroller. The target tone was set to be associated with the water reward, and the standard tone was set to be associated with air puff punishment. In the target trial, the water valve was switched on for 500 ms immediately after the detection of the animal's licking behaviors within the 800 ms response window, and the mouse was rewarded with 10–15 μl water. In the standard trial, the animal's licking behavior triggered an air puff of 500 ms. The training protocol and recording process are shown in Figures 1B,C.

Data acquisition and analysis

Electrophysiological signals were recorded using the Plexon Data Acquisition System (Plexon, United States). Signals were amplified (1,000 Ã–) and bandpass filtered (0.5–30 Hz) and acquired at 2 k Hz for off-line analysis. The LFP responses to the target and standard stimulation were averaged to obtain event-related potentials (ERP). Stimulus-locked trials were extracted for all instances, with each trial comprising up to 800 ms of data and a −200 ms prestimulus. A semi-automated algorithm was used to select discernable ERP peaks, which were baseline-corrected using a 200 ms prestimulus interval. Considering the effect of artifacts on the P3 amplitude/latency estimate, the average of 10 ms before and after the peak in the time window of 250–400 ms was defined as the amplitude of P300, and the time point of the peak was defined as the delay of P300. The peak amplitudes and latencies of P300-like components were calculated for each mouse. Data are presented as mean ± standard deviation (SD). Data between the two groups were compared using paired or unpaired *t*-tests, as appropriate. Repeated-measures (RM) analysis of variance (ANOVA) was used for statistical analyses of the normalized data. Statistical significance was set at $p < 0.05$. If a significant main or interaction effect was found, Newman–Keuls *post-hoc* test was applied.

Bioinformatic analysis of gut microbiota

Total DNA samples of colon contents were obtained using the E. Z. N. A. TM fecal DNA extraction kit (OMEGA Bio-Tek, Norcross, GA, United States), and the final elution volume was 100 μl. The integrity and quality of extracted DNAs were measured using NanoDrop NC2000 spectrophotometer (Thermo Fisher Scientific, Waltham, MA, United States) and agarose gel electrophoresis, respectively. DNA samples were sent to Shanghai Personal Biotechnology Co., Ltd. (Shanghai, China). The specific barcode was incorporated into the amplification primers, and then the bacterial 16S rRNA gene was amplified by PCR and detected by pair-end 2 × 250 bp using the Illumina MiSeq sequencing platform and V3-V4 hypervariable region fragment. The primer sequences used were 338F (5′-ACTCCTACGGGGAGGAGCA-3′) and 806R (5′-GGACTachVGGGTWTCTAAT-3′). PCR amplification system: Fast Pfu DNA Polymerase (5 U/μl) 0.25 μl, dNTPs (2.5 mM) 2 μl, buffer (5×) 5 μl, DNA template 1 μl, ddH2O 14.75 μl forward and reverse primers (10 μM) 1 μl. Amplification program settings consisted of initial denaturation at 98°C for 5 min, 25 cycles; denaturation at 98°C 30 s; annealing at 53°C 30 s; extension 72°C 45 s; and extension at 72°C 5 s. The Quant-iT PicoGreen dsDNA Assay Kit (Invitrogen, Carlsbad, CA, United States) and Vazyme VAHTSTM DNA Clean Beads (Vazyme, Nanjing, China) were used to quantify and purify the PCR amplicons, respectively.

The tool QIIME2 (Bolyen et al., 2018) was used to perform bioinformatic analysis of raw data in reference to the official tutorial.[1] The feature-classifier plugin (Price et al., 2009) based on the Navier Bayes classifier and Greengenes13_8 database was used to annotate the species in the abundance table. Downstream analysis was conducted primarily using Rstudio software (V3.1.2). The alpha diversity index (observed species number and Shannon diversity) was calculated with ASVs abundance, using the vegan package. For in-depth analyses, we filtered sequences with at least eight sequences (number of replicates per treatment) of ASVs counts and relative abundance exceeding 0.1% ASV in all samples as further data for standardized pretreatment. The normalized step for filtered ASV sequence counts was performed using the TMM method in the edgeR package (Robinson et al., 2010). The structure of the gut community was assessed by principal coordinate analysis (PCoA) based on Bray–Curtis dissimilarity using the phyloseq package (McMurdie and Holmes, 2013). Furthermore, permutational multivariate analysis of variance (PERMANOVA) was applied to evaluate the differences in intestinal microbial communities among different treatments using the vegan package with the adonis method. Microbial taxonomy at the phylum and family levels was clustered among the different treatments. In addition, we used indicator species analysis to obtain the point-biserial correlation coefficient (r) of an ASV positively associated with one or more treatments. $p < 0.05$ was set as the filtering threshold to identify the key species, and the bipartite network diagram was visualized. To observe the biomarkers of gut communities in the highland environment and antibiotic treatment, we applied LEfSe analysis to detect differentially abundant taxa across groups (LDA > 4.0, $p < 0.05$). Finally, the Spearman's correlation coefficient ($r > 0.7$ and $p < 0.05$) and Mantel test were calculated to determine the association between the microbial community and behavioral results for all treatments.

Results

Behavioral test and P300 amplitude

Figure 2 shows the results of the behavioral tests for memory capacity in mice. The exploration rate in the NOR

1 https://docs.qiime2.org/

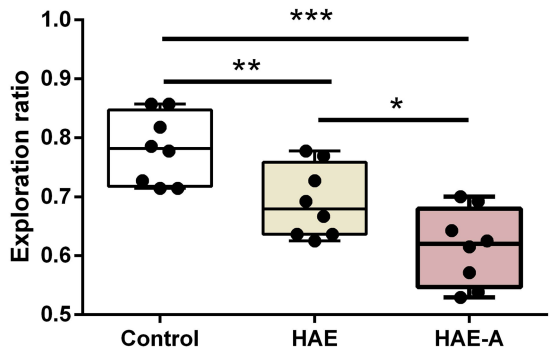

FIGURE 2
Effects of high altitude and antibiotics on exploration ratio by novel object test. Data are presented with the means±standard deviation (n=8). *Difference is significant at the 0.05 level (p<0.05); **difference is significant at the 0.01 level (p<0.01); ***difference is significant at the 0.001 level (p<0.001).

trials was significantly lower in the HAE ($p < 0.01$) and HAE-A groups ($p < 0.001$) than that in the control group. In addition, the exploration rate was significantly lower in the HAE-A group than that in the HAE group ($p < 0.05$). Moreover, we collected the P300 event-related potential (ERP) component during performance of the oddball paradigm behavior training task. After oddball paradigm behavior training, control, HAE, and HAE-A mice exhibited a clear P300 peak amplitude during both standard and target tones. As expected, both amplitude ($n = 6$, $p > 0.005$, control: 170.24 ± 67.91, HAE: 167.04 ± 44.95, HAE-A: 135.64 ± 54.62) and latency ($n = 6$, $p > 0.005$, control: 0.34 ± 0.09, HAE: 0.31 ± 0.07, HAE-A: 0.27 ± 0.09) of standard tone were not significantly different among the three groups. As for target tone, the amplitudes were higher than those of standard tone in all groups. The control group showed the highest P300 peak amplitude (539.30 ± 110.40), while the mean P300 peak amplitude (150.62 ± 71.62) of the HAE-A group was the lowest among the three groups and the average P300 peak amplitude of HAE group was 339.88 ± 85.04. The P300 amplitude of both HAE and HAE-A mice was significantly lower than that of the control mice (HAE vs. control: $p < 0.005$, HAE-A vs. control: $p < 0.001$). In addition, the P300 amplitude in HAE mice was significantly higher than that in HAE-A mice ($p < 0.005$). There was no significant difference in the P300 latency of the target tone between the three groups ($n = 6$, $p > 0.005$, control: 0.32 ± 0.07, HAE: 0.32 ± 0.05, HAE-A: 0.3 ± 0.05). In summary, the changes in normalized amplitude (target amplitude/standard amplitude, control: 3.09 ± 0.86, HAE: 2.03 ± 0.65, HAE-A: 1.02 ± 0.29) in all groups were similar to the target amplitude. Compared to control mice, the normalized amplitudes of HAE and HAE-A were significantly decreased (HAE vs. control: $p < 0.005$, HAE-A vs. control: $p < 0.001$). Furthermore, the normalized amplitude of HAE-A was significantly lower than that of HAE ($n = 6$, $p < 0.005$). The amplitude and latency of the P300 in each group are shown in Figure 3.

Antioxidant capacity in the prefrontal cortex

Figure 4 shows the antioxidant indices in the prefrontal cortex. As shown in Figure 4A, the T-AOC content was significantly lower in the HAE and HAE-A groups than in the control group ($p < 0.001$), whereas the T-AOC content was significantly lower ($p < 0.05$) in the HAE-A group than in the HAE group. Figures 4B,D show that there was no significant difference in SOD activity and GSH-Px activity between the control and HAE groups ($p > 0.05$), but the SOD activity and GSH-Px activity were significantly lower in the control group ($p < 0.01$ and $p < 0.001$, respectively) and HAE group ($p < 0.05$ and $p < 0.001$, respectively) than in the HAE-A group. Figure 4E shows that there was no significant difference ($p > 0.05$) in MDA content between the control and HAE and HAE and HAE-A, but the MDA content was significantly lower in the control ($p < 0.01$) than that in the HAE-A group. In addition, as shown in Figures 4C,F, CAT activity and GSH content were not significantly different between the three groups ($p > 0.05$).

Apoptosis-related proteins in the prefrontal cortex

Figure 5 shows the apoptosis-related functional protein content and mRNA expression levels in the prefrontal cortex. Among them, the bcl-2 content and bcl-2mRNA expression levels in the HAE and HAE-A groups were significantly lower ($p < 0.05$) than those in the control group, whereas the bcl-2 content and bcl-2mRNA expression levels in the HAE group were significantly higher ($p < 0.05$) than those in the HAE-A group (Figure 5A). Bax and Bax mRNA expression levels were not significantly different ($p > 0.05$) between the HAE and HAE-A groups (Figure 5B). As shown in Figure 5D, the mRNA expression levels of caspase-3 were lower in the control and HAE groups those in the HAE-A group ($p < 0.001$), whereas this indicator did not differ between the control and HAE group ($p > 0.05$). Furthermore, the mRNA expression levels of Bax (Figure 5C) and caspase-9 (Figure 5E) were not significantly different among the three groups ($p > 0.05$).

Differences in the gut community in microbial compositions and structure

There were significant differences in the Shannon diversity index of the colon among the three groups ($p < 0.01$ or $p < 0.001$; Figure 6A). With respect to richness (observed_species; Figure 6B), the control group was significantly different from the other two groups ($p < 0.01$ and $p < 0.001$). We tested the separation pattern (β-diversity) between microbial communities using unconstrained principal coordinate analysis (PCoA) of the Bray–Curtis distance (Figure 6C). The colonic microbial communities of the three groups showed clear separation along the first

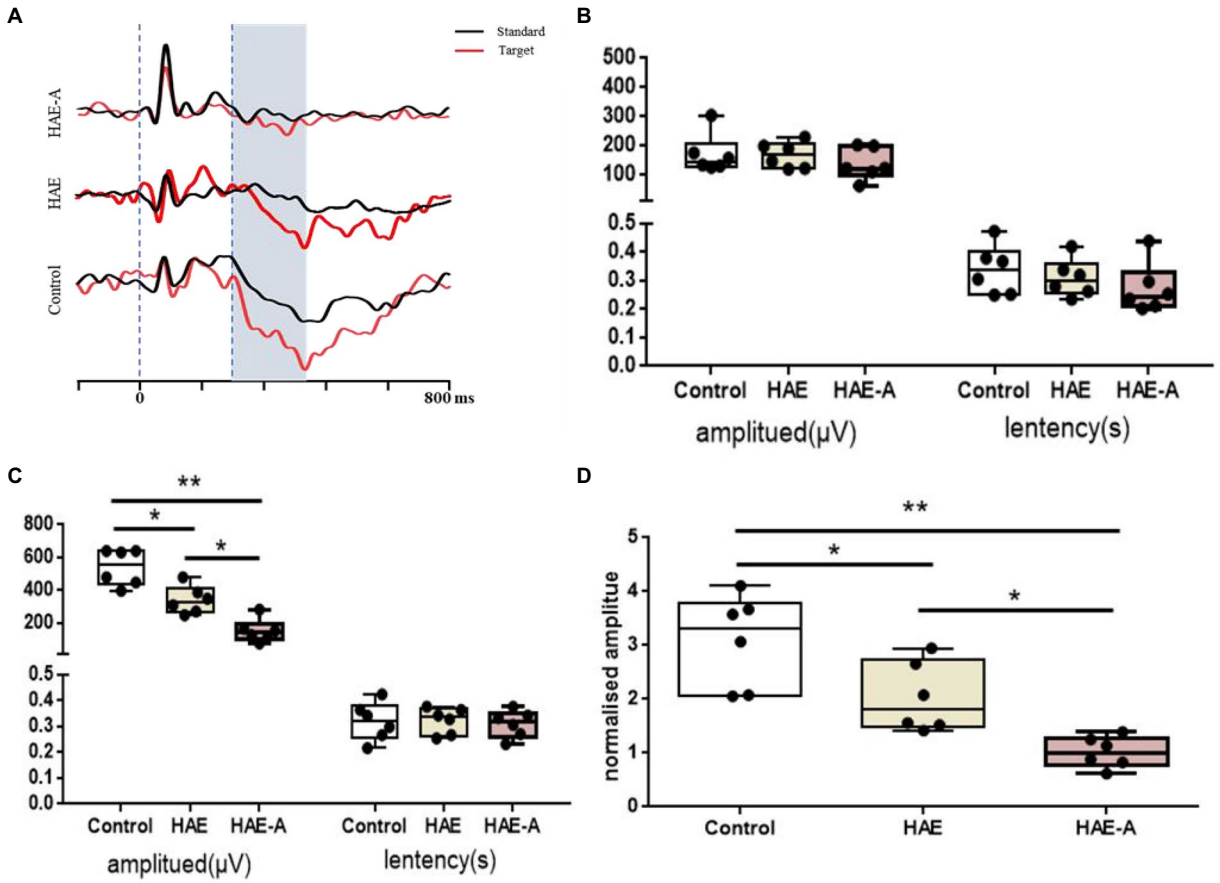

FIGURE 3
Variation of P300 of the oddball behavioral paradigm training test. **(A)** The profile of P300 in control, HAE and HAE-A group, respectively; **(B)** The result of P300 evoked by standard tone stimulation; **(C)** The result of P300 evoked by target tone stimulation; **(D)** The result of normalized P300 amplitude by target/standard. Data are presented with the means±standard deviation (n=6). *Difference is significant at the 0.05 level (p<0.05); **difference is significant at the 0.01 level (p<0.01).

(22.98%) and second (15.89%) principal coordinates. The findings also showed that the treatment methods of the three groups resulted in completely different microbiota structures (Table 2). In the first principal coordinate, the HAE-A group showed significant separation compared to the other two groups, suggesting that antibiotics were the largest source of variation in the colon microbiome of mice. In addition, the second principal coordinate showed a significant separation in all three groups. The results showed that the combined action of plateau and antibiotics was the second major source of variation in distinguishing the different treatments. In the classification analysis of the colon, there were also significant differences in the intestinal microbiota between the control, HAE, and HAE-A groups. Five bacterial phyla (Figure 6D) were identified as the dominant species in colon samples: *Firmicutes*, *Bacteroidetes*, *Verrucomicrobia*, *Proteobacteria*, and *Actinobacteria*. *Firmicutes* were the dominant species, and *Bacteroidetes* was the second most dominant species. In addition, *Verrucomicrobia* was the third most dominant species. At the family level (Figure 6E), *S24-7*, *Lachnospiraceae*, *Lactobacillaceae*, *Verrucomicrobiaceae*, *Erysipelotrichaceae*, *Ruminococcaceae*, *Enterobacteriaceae*, *Desulfovibrionaceae*, *Rikenellaceae*, and *Staphylococcaceae* were the dominant species.

S24-7 was the first dominant species, *Lachnospiraceae* was the second dominant species, and *Lactobacillaceae* was the third dominant species (Figure 6E). Indicator species analysis was also performed to select individual bacteria (ASVs) in the colon microbiota with significant differences in abundance under different treatments, and to perform visual analysis with a bipartite network (Figure 6F). The high number of colonic bacterial ASVs shared between the control and HAE groups reflects the similar clustering of the two sample types in the bacterial community, but bacterial ASVs shared by HAE and control samples, as well as HAE and HAE-A samples, were completely absent. Family-level cluster analysis was conducted for indicator species, and *S24-7*, *Lachnospiraceae*, and *Lactobacillaceae* belonging to indicator species were selected in the colon segment (Figures 6F, 7). Among them, *Lactobacillaceae* was most closely related to the damage caused by the high-altitude environment, and *Lachnospiraceae* was most closely related to the damage caused by antibiotic use in the plateau environment, compared with the control group. *S24-7* was

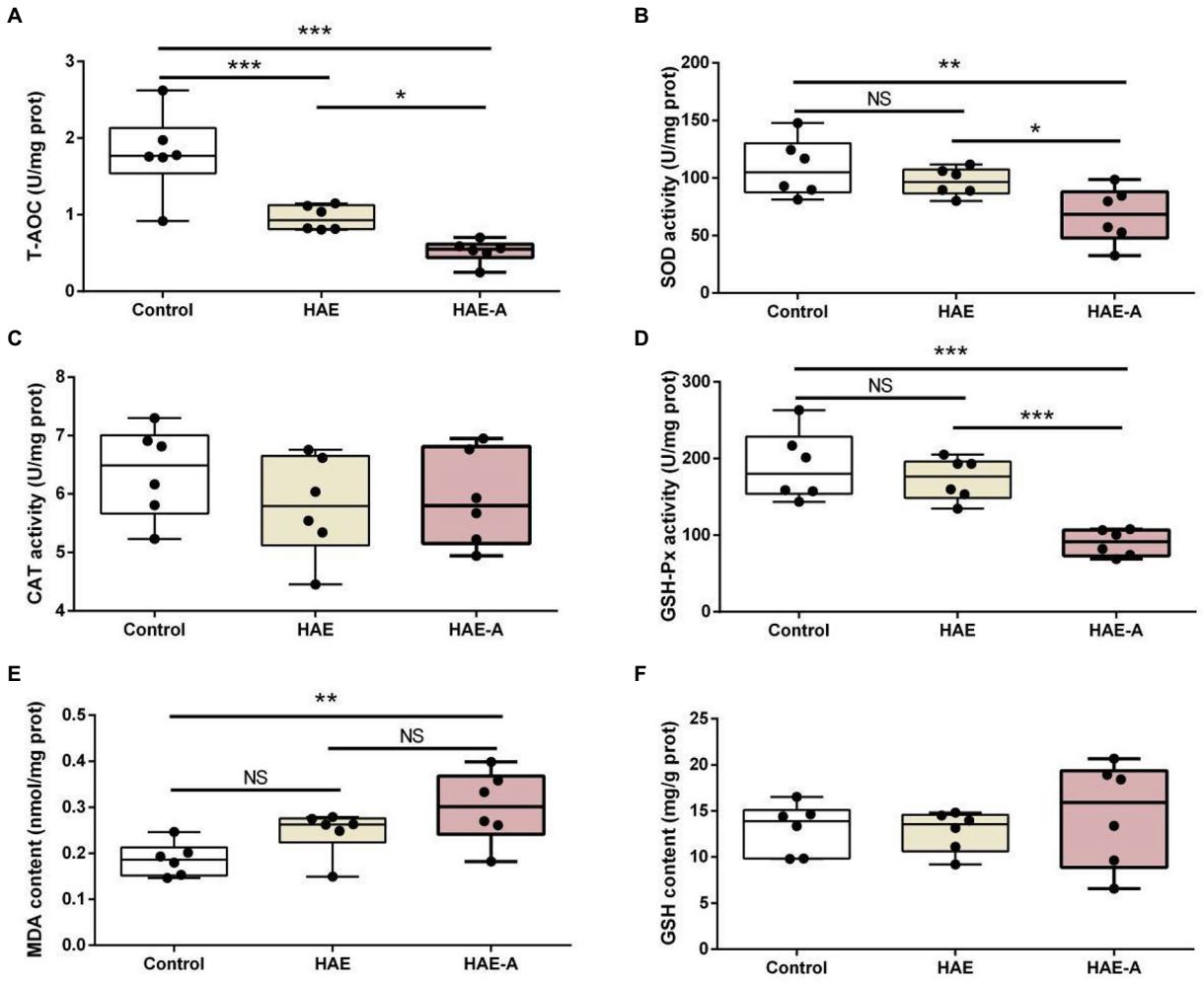

FIGURE 4
Antioxidant capacity in the prefrontal cortex. Data are presented with the means±standard deviation (n=6). NS, not significant (p>0.05); *difference is significant at the 0.05 level (p<0.05); **difference is significant at the 0.01 level (p<0.01); ***difference is significant at the 0.001 level (p<0.001). **(A–F)** Activities or contents of T-AOC, SOD, CAT, GSH-Px, MDA, and GSH, respectively. T-AOC, total antioxidation capacity; SOD, superoxide dismutase; CAT, catalase; GSH-Px, glutathione peroxidase; MDA, malondialdehyde; GSH, glutathione.

the most deficient bacterium in the HAE and HAE-A groups. LEfSe is an algorithm for the discovery of biomarkers that identify genomic features (genes, pathways, or taxa) that characterize the differences between two or more biological conditions. Compared with the HAE group (Figures 8A,B), the significant discriminative taxa in the control group were *Actinomycetales*, *S24-7*, *and Bacteroidales*. Compared with the HAE-A group (Figures 8C,D), the significant discriminative taxa were *Actinomycetales* and *Actinobacteria* in the HAE group.

Correlation between gut community and behavioral test

The results of the Spearman's correlation analysis and heatmaps showed the degree of association of all highly correlated and significant families with the behavioral results (Figure 9A). Subsequently, the combination with the lowest collinearity was selected using the former selection method to construct a linear model. *Helicobacteraceae*, *Porphyromonadaceae*, and *Enterococcaceae* were identified as microbes with high importance (Figure 9A). Further, we conducted separate modeling for the three families and Mantel test analysis (Figures 9B–E). The results showed that the correlation between *Helicobacteraceae* and the exploration ratio was greater than that of the other two families and even greater than the combined effect of the three families. Therefore, it can be assumed that *Helicobacteraceae* is the most important microbe in the colon that affects the results of behavioral tests.

Discussion

As an efficient and flexible assay for investigating various aspects of working memory in rodents, the novel object test was applied in this study to assess working memory deficits associated

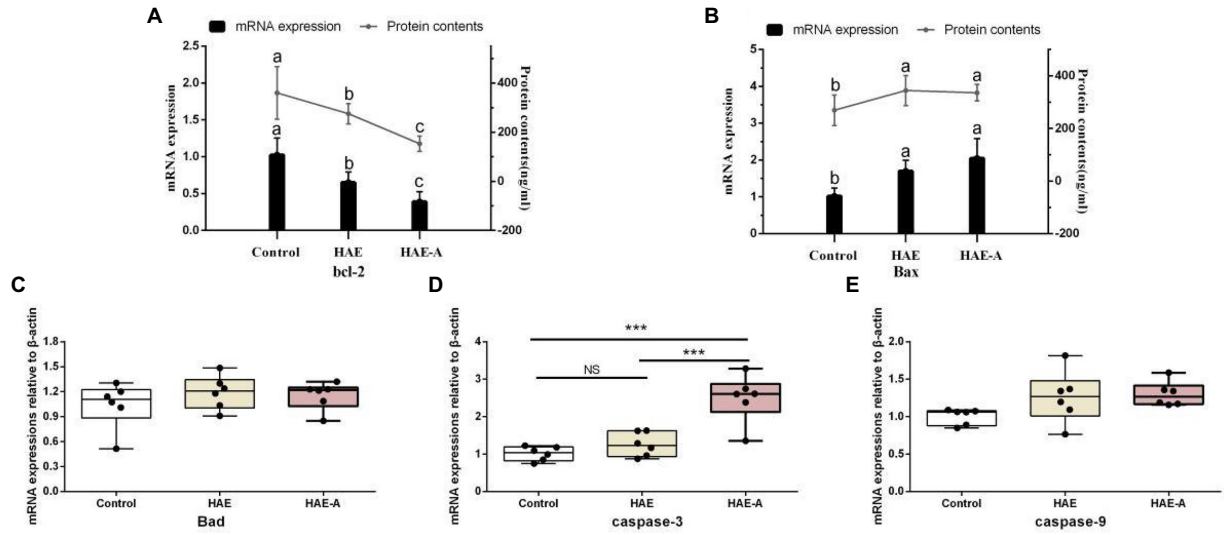

FIGURE 5
Apoptosis-related functional protein contents and mRNA expression levels in the prefrontal cortex. Data are presented with the means±standard deviation (n=6). Bars with different letters are significantly different on the basis of Duncan's multiple-range test (p<0.05). NS, not significant (p>0.05); *difference is significant at the 0.05 level (p<0.05); **difference is significant at the 0.01 level (p<0.01); ***difference is significant at the 0.001 level (p<0.001). **(A,B)**: mRNA expression levels and protein contents of bcl-2 and Bax; **(C–E)**: mRNA expression levels of Bad, caspase-9 and caspase-3, respectively.

TABLE 2 PCoA diversity difference test.

Group1	Group2	Sample size	Permutations	pseudo-*F*	Value of *p*	*q*-value
Control	HAE	16	999	5.294379	0.001	0.001
Control	HAE-A	16	999	7.477914	0.002	0.001
HAE	HAE-A	16	999	6.050981	0.001	0.001

with the prefrontal cortex (Lueptow, 2017). The novel object test relies on the natural predisposition of rodents to explore novelty, and poor working memory ability is reflected by short escape latency and high error (Malekmohamadi et al., 2007; Chen et al., 2014). According to the results of the behavioral tests in this study, high-altitude exposure for 14 days resulted in working memory impairment. The HAE group had a lower exploration rate in the novel object test, indicating lower working memory capacity. This result was consistent with that reported by Ma et al. (2019). Acute exposure to high altitude results in reduced cognitive tasks and working memory, primarily reduced accuracy and responsive behavioral performance, as well as reduced activity in some brain regions, including the medial frontal and visual cortices (Yan et al., 2011). Similar results to acute exposure were found in the long-term exposure group, with subjects who had moved to high altitudes for more than 2 years showing reduced accuracy and slower responses to working memory tasks (Yan et al., 2010). Maintaining the balance of the gut microbiota is considered an effective way to modulate cognitive ability through MGBA (Borre et al., 2014). If the gut microbiota is disturbed, the intestinal environment is affected, which may lead to serious symptoms in the host. For example, damage to the integrity of the intestinal barrier may cause bacteria and/or their metabolites in the lumen to enter blood circulation and eventually impair brain function and cognitive abilities (Julio-Pieper et al., 2014; Sharon et al., 2016). Based on the results of the behavioral test in the present study, MGBA may play an important role during high-altitude exposure, as the mice with antibiotic-disrupted intestinal microbiota performed worse during the novel object test after 14 days of high-altitude exposure. The results of the behavioral test provide new evidence that brain dysfunction caused by high-altitude exposure may be closely related to MGBA.

The P300 results of the oddball behavioral paradigm training test showed the same trend among the three experimental groups in this study. P300 is widely accepted as a marker with positive relativity for all processes of working memory, including formation and retrieval (Ehlers and Somes, 2002). As an event-related potential elicited in response to certain types of stimuli, it is considered a marker of working memory and is closely associated with the formation and retrieval of memories. P300 has also been found to be sensitive to a variety of cognitive processes, including attention, decision-making, and memory encoding, especially in the prefrontal cortex (Eidel and Kübler, 2020). In this study, the P300 evoked by the oddball test in response to rare

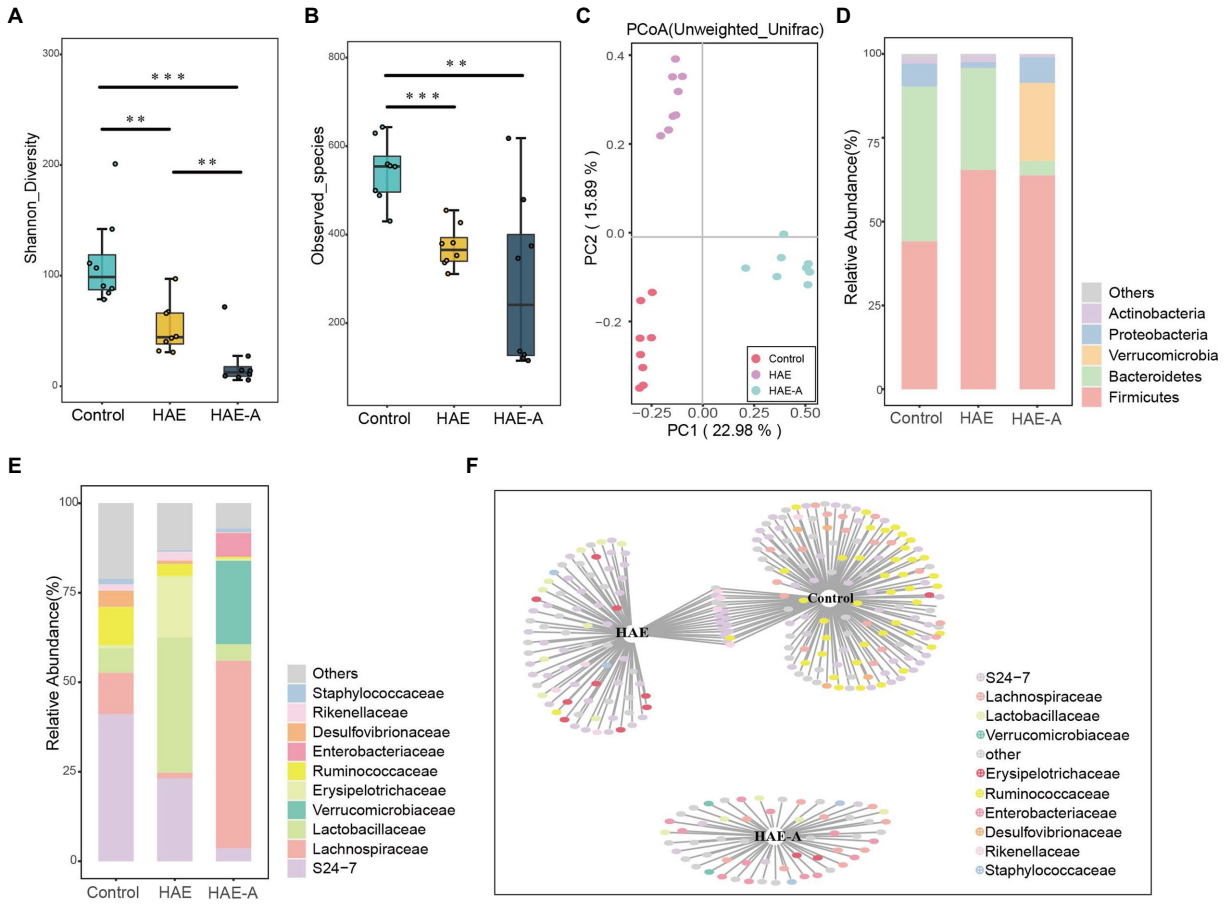

FIGURE 6
Effects of hypoxia on the structure of colon microbiota in normal mice and antibiotic drinking mice. **(A)** Intestinal microbial community diversity in each group (Shannon). Meaning: Wilcoxon. **(B)** Gut microbiome richness (observed species) in colonic luminal samples of each group. Significance: Wilcoxon. **(C)** Principal Coordinate Analysis (PCoA) of Unweighted UniFrac Distance between groups. **(D)** Relative abundance at phylum level in each group (%). **(E)** Relative abundance at each family level (%). **(F)** Bipartite networks of indicator species analysis. It displays different treatment-specific ASVs in the colonic bacterial communities using indicator species analysis. Circles represent individual bacteria and ASVs that are positively and significantly associated ($p<0.05$) with one or more different grouping factors (association(s) given by connecting lines). ASVs are colored according to their Family assignment.

stimulation significantly decreased in amplitude in the HAE and HAE-A groups, suggesting deficits in working memory. In general, a neuron system may recruit more resources to 'mark' an unknown stimulation. By "marking" the stimulation, the neuron system can better process and understand the information, which allows for improved learning and memory formation (Fjell and Walhovd, 2003). Thus, it is more likely that hypoxia may reduce the potential of the brain to recruit more neurons, and this influence of high-altitude exposure is aggravated by disturbed gut microbiota.

The prefrontal cortex is an important brain region for cognition and memory, and growing evidence suggests that prefrontal damage can lead to working memory impairment (Jodo et al., 2004). It is sensitive to pathophysiological changes such as reduced antioxidant capacity, and oxidative damage can impede prefrontal-dependent memory function by reducing the production of new neurons (Huang et al., 2015). A previous study showed that the levels of protein oxidation and catalase activity increased, and serum iron, serum ferritin, and transferrin saturation levels decreased with high-altitude exposure, indicating that the high-altitude environment may affect antioxidant capacity and iron homeostasis (Rytz et al., 2022). The level of antioxidant capacity is closely related to the influence of high altitude, which was also found by Zhang et al. (2015) during research on the effect of hyperbaric oxygen preconditioning in plain migrant plateau personnel. Therefore, we studied the prefrontal cortex to determine the mechanisms by which high-altitude exposure stress induces working memory dysfunction and how intestinal probiotics protect the host from memory dysfunction. CAT, SOD, and GSH-Px are important enzymes that protect against oxidative stress by reducing the activity of superoxide anions and hydrogen peroxide (Thakare et al., 2017). In our study, MDA formation was increased and T-AOC, SOD, GSH-Px, and CAT activities were reduced in the prefrontal cortex

10.3389/fmicb.2022.1054504

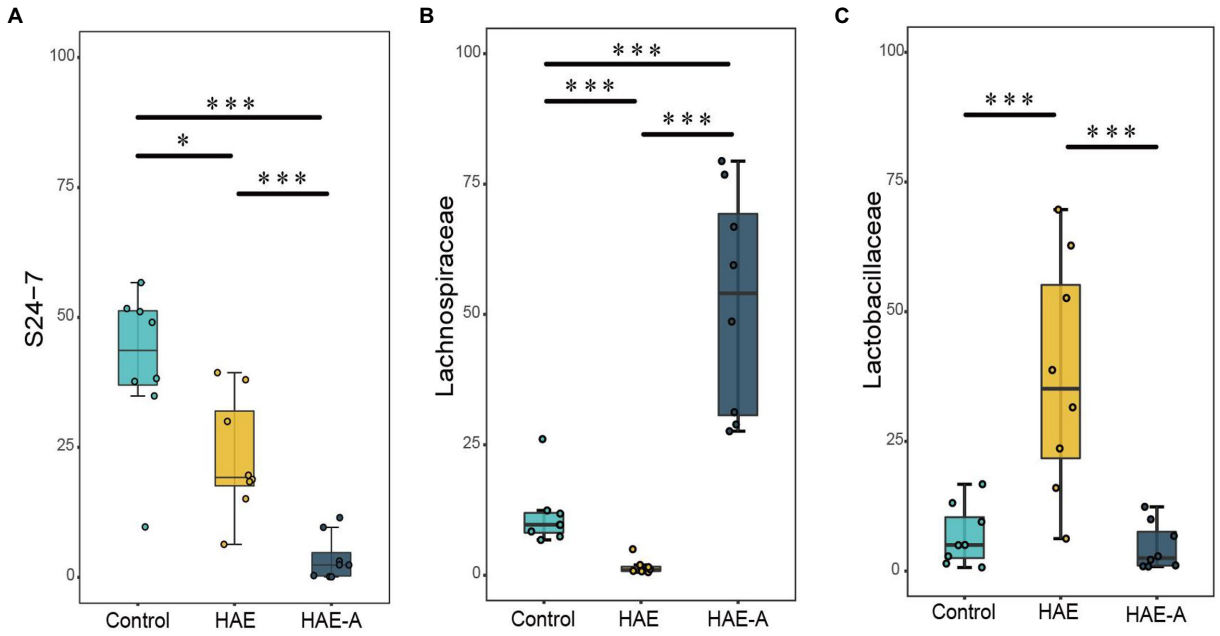

FIGURE 7
Significant altered bacterial taxa in colonic microbes by different treatments at family level. **A–C**: *S24-7*, *Lachnospiraceae*, and *Lactobacillaceae*, respectively. Boxplots showing differences in the relative abundance of significantly discriminant taxa between different treatments. Significance between groups was indicated with asterisk (*p<0.05, **p<0.01, ***p<0.001).

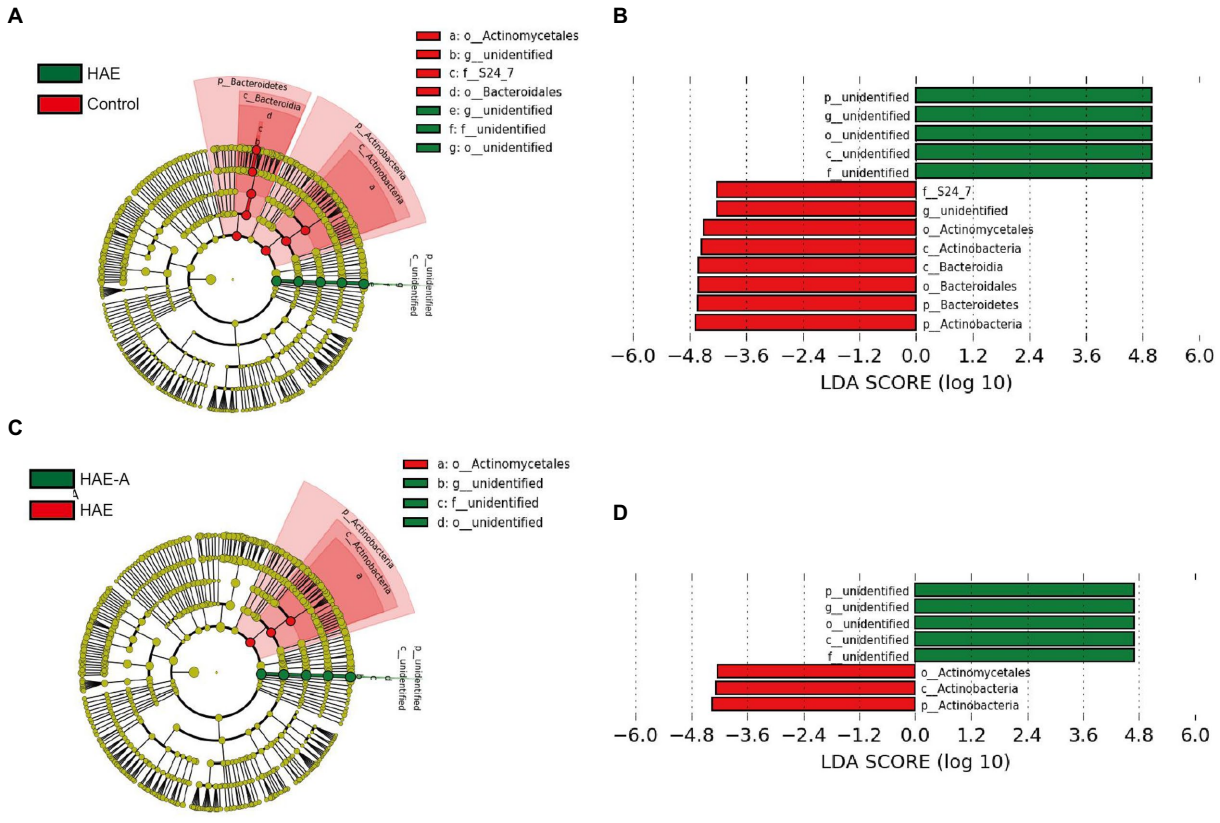

FIGURE 8
LEfSe analysis of colon microbiota in mice. Cladogram **(A,C)** and linear discriminant analysis (LDA) score **(B,D)** and cladogram **(A,C)** were generated from LDA effect size. Taxa with LDA values larger than 4 are shown in the figure.

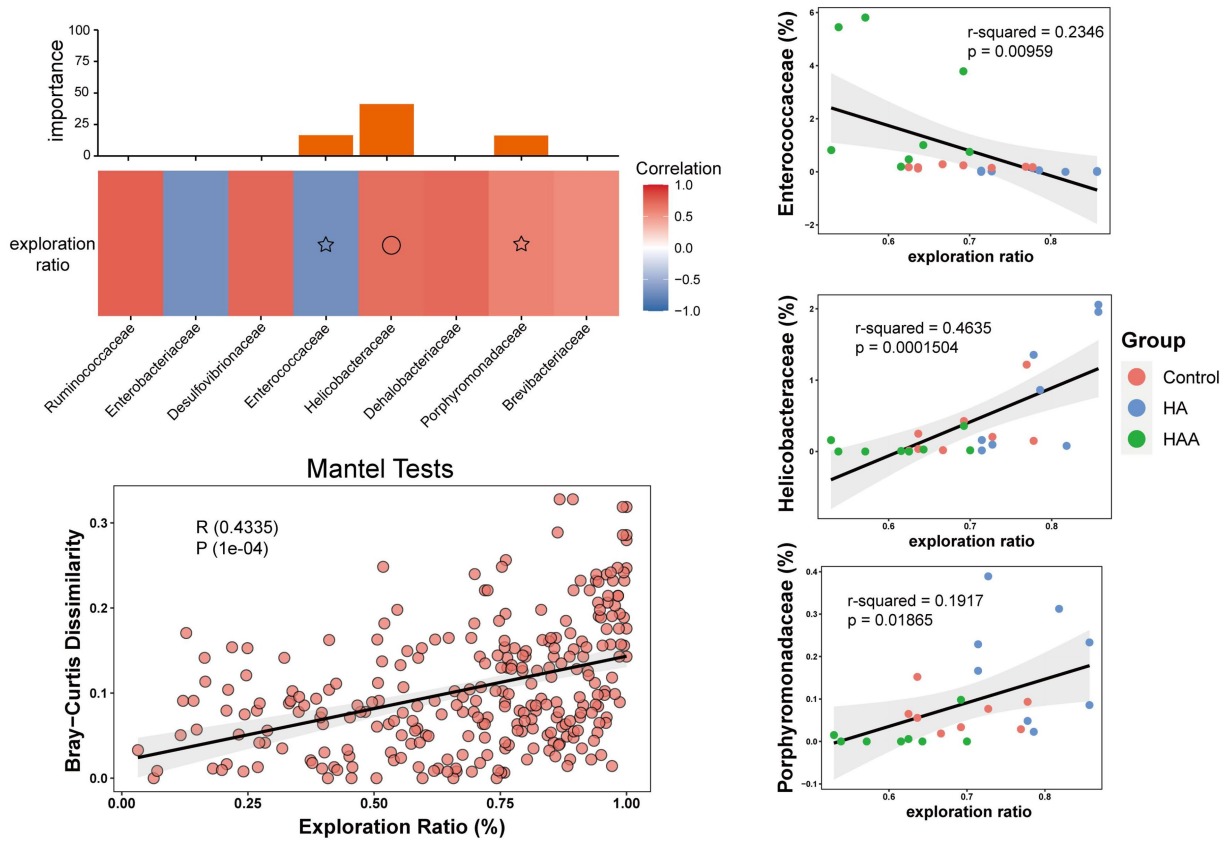

FIGURE 9
Correlation between microbial community and behavioral test in the colon. **(A)** Different colors represent positive (red) or negative (blue) correlation of important family-level microbes with behavioral results. Circles and asterisks represent different levels of importance. **(B–D)** The different results represent the importance of having three species at the family level in behavioral performance. Red circle: control group. Blue circle: HAE group. Green circle: HAE-A group. **(E)** Mantel Test is a correlation test to determine the correlation between two sets of distance measure matrices. And it is used to evaluate whether the sample distance in one matrix is related to the sample distance in the other matrix.

of mice exposed to high-altitude stress, which is consistent with the results of Niki (2012). Similar to many other stressors, acute high-altitude exposure impairs neuronal morphology and prefrontal function, and induces dendritic remodeling in the prefrontal cortex, resulting in impaired working memory in humans and animals (Miller et al., 2018). Thus, our findings clearly indicate that oxidative stress was enhanced. This enhancement is at least partially associated with working memory dysfunction induced by high-altitude stress (Freitas et al., 2014; Passiatore et al., 2014).

Oxidative damage triggers apoptosis and impairs learning- and memory-dependent functions (Schafer and Buettner, 2001). It was also found that oxidative stress caused by reactive oxygen species is an important link to apoptosis protein (Miyamoto et al., 2006). In oxidative stress-mediated apoptosis, caspase activation, changes in Bcl-2-related proteins, and cytochrome C release occur repeatedly and significantly impact the apoptotic process (Maity et al., 2012). By detecting the apoptosis level in murine brain tissues, Van Gossum et al. (2017) found increased caspase-3 and Bax protein expression and decreased Bcl-2 protein expression and the Bc1-2/Bax ratio in plateau hypoxic mice. Thus, changes in the levels of oxidative stress and apoptotic proteins provide a good assessment of the corresponding changes in prefrontal working memory function during acute high-altitude exposure. In oxidative stress-mediated apoptosis, caspase activation, changes in Bcl-2-related proteins, and cytochrome C release occur repeatedly and significantly impact the apoptotic process (Maity et al., 2012). Changes in the levels of oxidative stress and apoptotic proteins provide a good assessment of the corresponding changes in the prefrontal working memory function during acute high-altitude exposure. We evaluated the level of apoptosis in the prefrontal cortex by determining apoptosis-related proteins. The process of mitochondria-mediated apoptosis can be briefly described as follows: The leakage of cytochrome C through Bax-formed holes in the mitochondrial membrane triggers the formation of an apoptosome that activates caspase-9; in turn, caspase-9 triggers the activation of caspase-3 and ultimately causes cell apoptosis (Wang et al., 2017). During this process, the increase in Bax and decrease in Bcl-2 levels are related to high vulnerability to apoptotic activation (Freitas et al., 2014). In the present study, acute high-altitude exposure altered the apoptosis-associated

proteins in the prefrontal cortex. Simultaneously, antibiotic-disrupted intestinal flora exacerbated the reduction in antioxidant capacity and apoptotic levels in the prefrontal cortex after high-altitude exposure stress. This suggests that the modulation of intestinal flora disruption after high-altitude stress may exert beneficial effects on prefrontal oxidative damage and apoptosis.

Previous studies have found that cognitive dysfunction, especially the decline of working memory, is mediated by the gut microbiota in high-altitude environments, which means that the gut microbial structure is closely related to the hypoxic environment. In this study, PCoA analysis of the colonic microbiota revealed that there were different compartments in the colonic microbiota of mice in the control, HA, and HAA groups. Colonic community diversity was significantly higher in the control group than that in the HA group, and the diversity in the HA group was also significantly higher than that in the HAA group. In addition, the microbial richness in the control group was significantly higher than that in the HA group. These results imply that hypoxic exposure and antibiotic treatment have important effects on colonic microbial communities. The analysis of microbial composition demonstrated the differential abundance of taxa among the different environments. Compared to the control group, the relative abundance of dominant colonic microbes in mice was significantly altered in the HA and HAA groups. To further define the most representative microbes in each group of mice, we used indicator species analysis to identify microorganisms that preferred different environments and subsequently clustered taxonomy with similar evolutionary levels into the same family. We observed *Lactobacillaceae*, which prefers a hypoxic environment, *Lachnospiraceae*, which is sensitive to antibiotics in hypoxic environments, and *S24-7*, which was deficient in the HA and HAA groups compared with the control group. The family *Lactobacillaceae* comprises facultative anaerobic gram-positive rods, belonging to the category of lactic acid bacteria (Suissa et al., 2021). Long-term consumption of *Lactobacillaceae* species induces qualitative and quantitative modifications in the microbial ecosystem of the human gastrointestinal tract (Di Cerbo et al., 2015). Specifically, Lactobacillaceae probiotics possess antitumor, antitoxic, cholesterol-lowering, antibacterial, and antiviral activity (Nazir et al., 2018). Hu et al. (2022) found that the abundance of *Lactobacillaceae* changed with prolonged hypoxic exposure in a hypoxic environment. Based on the above studies, we believe that changes in the abundance of *Lactobacilli* may be a defining feature after hypobaric hypoxia exposure, which is of great significance for future studies. *Lachnospiraceae* are present from early infancy. Although taxa of this family have repeatedly shown their ability to produce beneficial metabolites for the host, the number of *Lachnospiraceae* has also increased in the intestinal lumen of subjects with different diseases (Vacca et al., 2020). Juhász et al. (2021) found that antibiotic treatment led to an increase in the abundance of *Lachnospiraceae* bacteria in the gut of mice, which also indicated that the antibiotic treatment was effective in this study. Alterations in the abundance of the *S24-7* family members are related to different environmental conditions. Previous research has found that *S24-7* is more abundant in diabetes-sensitive mice fed a high-fat diet, particularly when the chow is supplemented with glucose oligosaccharides (Serino et al., 2012) and following treatment-induced remission of colitis in mice (Rooks et al., 2014). Moreover, *S24-7* was also demonstrated to be related to L-valine, leucine, and glutarate, and involved in the metabolism of amino acids, low cholesterol, low-density lipoprotein (LDL), and fatty acid content (Seo et al., 2019). Although these observations are currently limited to murine studies, they suggest that *S24-7* is involved in host–microbe interactions that affect gut function and health.

Finally, to further explore the mechanism of impaired working memory after hypoxic exposure, we analyzed the correlations between all microbial families and behavioral cognitions. The selected important microbes were then modeled with the behavioral results, and the Mantel test was used to establish the combined microbial and behavioral modeling analysis. We found that *Helicobacteraceae*, *Porphyromonadaceae*, and *Enterococcaceae* were highly important microorganisms in terms of their correlation with the behavioral results. Then, through separate modeling and Mantel analysis of the three families, we found that the correlation between *Helicobacteraceae* and exploration rate was greater than that of the other two families, and even higher than the comprehensive effect of the three families. Shen et al. (2017) compared the gut microbiota of APP/PS1 transgenic mice with AD and C57/BL6 wild-type (WT) mice and found that the abundance of *Helicobacteraceae* increased significantly in APP/PS1 mice compared to WT mice. Bäuerl et al. (2018) reported the presence of *Helicobacteraceae* and a higher abundance of *Desulfovibrionaceae* in transgenic mice at the family level. Taken together, it is reasonable to assume that *Helicobacteraceae* are the most likely family of colonic bacteria to influence cognitive dysfunction.

Conclusion

Disrupted gut microbiota could aggravate working memory dysfunction induced by high-altitude exposure in mice, indicating the existence of a link between high-altitude exposure and MGBA. The most relevant bacterial family, *Helicobacteraceae,* may play an important role in this process.

Data availability statement

The datasets presented in this study can be found in online repositories. The names of the repository/repositories and accession number(s) can be found at: https://www.ncbi.nlm.nih.gov/, PRJNA884182.

Ethics statement

All animal experiments were conducted in accordance with the guidelines for the feeding and use of experimental animals (approval no: SYXK2022-023) approved by the Committee of Nanfang Hospital Baiyun Branch, Southern Medical University.

Author contributions

ZZ, DC, and GW: conceptualization and methodology. DC, HR, and XZ: project administration and data curation. ZZ, WX, and WP: writing—original draft. ZZ, GW, YZ, and LY: writing—review and editing. CL, YH, and HL: supervision. All authors contributed to the article and approved the submitted version.

Funding

This work is supported by the Scientific Development funds for Local Region from the Chinese Government in 2022 (XZ202201YD0018C), Cultivation Fund of National Nature Science Foundation (grant no. qiankehe2018-5764-11), and Natural Science Foundation of Guangdong Province, China (grant no. 2022A1515011230).

Acknowledgments

We really appreciate the supports provided by all other members in the lab during the animal feeding and sampling.

Conflict of interest

The authors declare that the research was conducted in the absence of any commercial or financial relationships that could be construed as a potential conflict of interest.

Publisher's note

References

Ananthakrishnan, A. N., Bernstein, C. N., Iliopoulos, D., Macpherson, A., Neurath, M. F., Ali, R. A. R., et al. (2018). Environmental triggers in IBD: a review of progress and evidence. *Nat. Rev. Gastroenterol. Hepatol.* 15, 39–49. doi: 10.1038/nrgastro.2017.136

Bäuerl, C., Collado, M. C., Diaz Cuevas, A., Viña, J., and Pérez Martínez, G. (2018). Shifts in gut microbiota composition in an APP/PSS1 transgenic mouse model of Alzheimer's disease during lifespan. *Lett. Appl. Microbiol.* 66, 464–471. doi: 10.1111/lam.12882

Bolyen, E., Rideout, J. R., Dillon, M. R., Bokulich, N. A., Abnet, C., AlGhalith, G. A., et al. (2018). QIIME 2: reproducible, interactive, scalable, and extensible microbiome data science. *PeerJ Preprints.* 6:e27295v2. doi: 10.7287/peerj.preprints27295v2

Borre, Y. E., O'Keeffffe, G. W., Clarke, G., Stanton, C., Dinan, T. G., and Cryan, J. F. (2014). Microbiota and neurodevelopmental windows: implications for brain disorders. *Trends Mol. Med.* 20, 509–518. doi: 10.1016/j.molmed.2014.05.002

Bravo, J. A., Forsythe, P., Chew, M. V., Escaravage, E., Savignac, H. M., Dinan, T. G., et al. (2011). Ingestion of lactobacillus strain regulates emotional behavior and central GABA receptor expression in a mouse *via* the vagus nerve. *Proc. Natl. Acad. Sci. U. S. A.* 108, 16050–16055. doi: 10.1073/pnas.1102999108

Bruce-Keller, A. J., Salbaum, J. M., Luo, M., Blanchard, E. 4th, Taylor, C. M., Welsh, D. A., et al. (2015). Obese-type gut microbiota induce neurobehavioral changes in the absence of obesity. *Biol. Psychiatry* 77, 607–615. doi: 10.1016/j.biopsych.2014.07.012

Chen, X., Cai, F., Guo, S., Ding, F., He, Y., Wu, J., et al. (2014). Protective effect of Flos puerariae extract following acute alcohol intoxication in mice. *Alcohol. Clin. Exp. Res.* 38, 1839–1846. doi: 10.1111/acer.12437

Di Cerbo, A., Palmieri, B., Aponte, M., Morales-Medina, J. C., and Iannitti, T. (2015). Mechanisms and therapeutic effectiveness of lactobacilli. *J. Clin. Pathol.* 69, 187–203. doi: 10.1136/jclinpath-2015-202976

Ehlers, C. L., and Somes, C. (2002). Long latency event-related potentials in mice: effects of stimulus characteristics and strain. *Brain Res.* 957, 117–128. doi: 10.1016/s0006-8993(02)03612-0

Eidel, M., and Kübler, A. (2020). Wheelchair control in a virtual environment by healthy participants using a P300-BCI based on tactile stimulation: training effects and usability. *Front. Hum. Neurosci.* 14:265. doi: 10.3389/fnhum.2020.00265

Fjell, A. M., and Walhovd, K. B. (2003). Effects of auditory stimulus intensity and hearing threshold on the relationship among P300, age, and cognitive function. *Clin. Neurophysiol.* 114, 799–807. doi: 10.1016/s1388-2457(03)00030-0

Freitas, A. E., Bettio, L. E., Neis, V. B., Santos, D. B., Ribeiro, C. M., Rosa, P. B., et al. (2014). Agmatine abolishes restraint stress-induced depressive-like behavior and hippocampal antioxidant imbalance in mice. *Prog Neuropsychopharmacol Biol Psychiatry.* 50, 143–150. doi: 10.1016/j.pnpbp.2013.12.012

Gareau, M. G., Wine, E., Rodrigues, D. M., Cho, J. H., Whary, M. T., Philpott, D. J., et al. (2011). Bacterial infection causes stress-induced memory dysfunction in mice. *Gut* 60, 307–317. doi: 10.1136/gut.2009.202515

Haghikia, A., Jörg, S., Duscha, A., Berg, J., Manzel, A., Waschbisch, A., et al. (2016). Dietary fatty acids directly impact central nervous system autoimmunity *via* the small intestine. *Immunity* 43, 817–829. doi: 10.1016/j.immuni.2015.09.007

Hu, Y., Pan, Z., Huang, Z., Li, Y., Han, N., Zhuang, X., et al. (2022). Gut microbiome-targeted modulations regulate metabolic profiles and alleviate altitude-related cardiac hypertrophy in rats. *Microbiol. Spectr.* 10:e0105321. doi: 10.1128/spectrum.01053-21

Huang, T. T., Leu, D., and Zou, Y. (2015). Oxidative stress and redox regulation on hippocampal-dependent cognitive functions. *Arch. Biochem. Biophys.* 576, 2–7. doi: 10.1016/j.abb.2015.03.014

Jodo, E., Suzuki, Y., Katayama, T., Hoshino, K. Y., Takeuchi, S., Niwa, S., et al. (2004). Activation of medial prefrontal cortex by phencyclidine is mediated *via* a hippocampo-prefrontal pathway. *Cereb. Cortex* 15, 663–669. doi: 10.1093/cercor/bhh168

Juhász, J., Ligeti, B., Gajdács, M., Makra, N., Ostorházi, E., Farkas, F. B., et al. (2021). Colonization dynamics of multidrug-resistant Klebsiella pneumoniae are dictated by microbiota-cluster group behavior over individual antibiotic susceptibility: a Metataxonomic analysis. *Antibiotics (Basel).* 10:268. doi: 10.3390/antibiotics10030268

Julio-Pieper, M., Bravo, J. A., Aliaga, E., and Gotteland, M. (2014). Review article: intestinal barrier dysfunction and central nervous system disorders-a controversial association. *Aliment. Pharmacol. Ther.* 40, 1187–1201. doi: 10.1111/apt.12950

Li, J., He, N., Wei, X., Gao, Y., and Zuo, Y. (2015). Changes in temperature sensitivity and activation energy of soil organic matter decomposition in different Qinghai-Tibet plateau grasslands. *PLoS One* 10:e0132795. doi: 10.1371/journal.pone.0132795

Lueptow, L. M. (2017). Novel object recognition test for the investigation of learning and memory in mice. *J. Vis. Exp.* 126:55718. doi: 10.3791/55718

Ma, H., Wang, Y., Wu, J., Wang, B., Guo, S., Luo, P., et al. (2015). Long-term exposure to high altitude affects conflict control in the conflict-resolving stage. *PLoS One* 10:e0145246. doi: 10.1371/journal.pone.0145246

Ma, H., Zhang, D., Li, X., Ma, H., Wang, N., and Wang, Y. (2019). Long-term exposure to high altitude attenuates verbal and spatial working memory: evidence from an event-related potential study. *Brain Behav.* 9:e01256. doi: 10.1002/brb3.1256

Maity, C., Adak, A., Pathak, T. K., Pati, B. R., and Chandra, M. K. (2012). Study of the cultivable microflora of the large intestine of the rat under varied environmental hyperbaric pressures. *J. Microbiol. Immunol. Infect.* 45, 281–286. doi: 10.1016/j.jmii.2011.12.002

Malekmohamadi, N., Heidari, P., Sahebgharani, M., and Zarrindast, M. R. (2007). Effects of clozapine and sulpiride on morphine state-dependent memory in the step-down passive avoidance test. *Pharmacology* 79, 149–153. doi: 10.1159/000098151

McMurdie, P. J., and Holmes, S. (2013). Phyloseq: an R package for reproducible interactive analysis and graphics of microbiome census data. *PLoS One* 8:e61217. doi: 10.1371/journal.pone.0061217

Miller, E. K., Lundqvist, M., and Bastos, A. M. (2018). Working memory 2.0. *Neuron* 100, 463–475. doi: 10.1016/j.neuron.2018.09.023

Miyamoto, H., Doita, M., Nishida, K., Yamamoto, T., Sumi, M., and Kurosaka, M. (2006). Effects of cyclic mechanical stress on the production of inflammatory agents by nucleus pulposus and anulus fibrosus derived cells in vitro. *Spine (Phila Pa 1976)* 31, 4–9. doi: 10.1097/01.brs.0000192682.87267.2a

Nazir, Y., Hussain, S. A., Abdul Hamid, A., and Song, Y. (2018). Probiotics and their potential preventive and therapeutic role for cancer, high serum cholesterol, and allergic and HIV diseases. *Biomed. Res. Int.* 2018, 3428437–3428417. doi: 10.1155/2018/3428437

Niki, E. (2012). Do antioxidants impair signaling by reactive oxygen species and lipid oxidation products? *FEBS Lett.* 586, 3767–3770. doi: 10.1016/j.febslet.2012.09.025

Passiatore, R., Antonucci, L. A., Bierstedt, S., Saranathan, M., Bertolino, A., Suchan, B., et al. (2014). How recent learning shapes the brain: memory-dependent functional reconfigureuration of brain circuits. *NeuroImage* 245:118636. doi: 10.1016/j.neuroimage.2021.118636

Pena, E., El Alam, S., Siques, P., and Brito, J. (2022). Oxidative stress and diseases associated with high-altitude exposure. *Antioxidants (Basel).* 11:267. doi: 10.3390/antiox11020267

Price, M. N., Dehal, P. S., and Arkin, A. P. (2009). FastTree: computing large minimum evolution trees with profiles instead of a distance matrix. *Mol. Biol. Evol.* 26, 1641–1650. doi: 10.1093/molbev/msp077

Robinson, M. D., McCarthy, D. J., and Smyth, G. K. (2010). edgeR: a bioconductor package for differential expression analysis of digital gene expression data. *Bioinformatics* 26, 139–140. doi: 10.1093/bioinformatics/btp616

Rooks, M. G., Veiga, P., Wardwell-Scott, L. H., Tickle, T., Segata, N., Michaud, M., et al. (2014). Gut microbiome composition and function in experimental colitis during active disease and treatment-induced remission. *ISME J.* 8, 1403–1417. doi: 10.1038/ismej.2014.3

Rytz, C. L., Pun, M., Mawhinney, J. A., Mounsey, C. A., Mura, M., Martin, A., et al. (2022). Differential effects of high-altitude exposure on markers of oxidative stress, antioxidant capacity, and iron profiles. *Am. J. Physiol. Regul. Integr. Comp. Physiol.* 323, R445–R456. doi: 10.1152/ajpregu.00321.2021

Schafer, F. Q., and Buettner, G. R. (2001). Redox environment of the cell as viewed through the redox state of the glutathione disulfifide/glutathione couple. *Free Radic. Biol. Med.* 30, 1191–1212. doi: 10.1016/s0891-5849(01)00480-4

Seo, S. H., Unno, T., Park, S. E., Kim, E. J., Lee, Y. M., Na, C. S., et al. (2019). Korean traditional medicine (Jakyakgamcho-tang) ameliorates colitis by regulating gut microbiota. *Meta* 9:226. doi: 10.3390/metabo9100226

Serino, M., Luche, E., Gres, S., Baylac, A., Bergé, M., Cenac, C., et al. (2012). Metabolic adaptation to a high-fat diet is associated with a change in the gut microbiota. *Gut* 61, 543–553. doi: 10.1136/gutjnl-2011-301012

Sharon, G., Sampson, T. R., Geschwind, D. H., and Mazmanian, S. K. (2016). The central nervous system and the gut microbiome. *Cells* 167, 915–932. doi: 10.1016/j.cell.2016.10.027

Shen, L., Liu, L., and Ji, H. F. (2017). Alzheimer's disease histological and behavioral manifestations in transgenic mice correlate with specific gut microbiome state. *J. Alzheimers Dis.* 56, 385–390. doi: 10.3233/JAD-160884

Suissa, R., Oved, R., Jankelowitz, G., Turjeman, S., Koren, O., and Kolodkin-Gal, I. (2021). Molecular genetics for probiotic engineering: dissecting lactic acid bacteria. *Trends Microbiol.* 30, 293–306. doi: 10.1016/j.tim.2021.07.007

Sun, M. F., Zhu, Y. L., Zhou, Z. L., Jia, X. B., Xu, Y. D., Yang, Q., et al. (2015). Neuroprotective effects of fecal microbiota transplantation on MPTP-induced Parkinson's disease mice: gut microbiota, glial reaction and TLR4/TNF-α signaling pathway. *Brain Behav. Immun.* 70, 48–60. doi: 10.1016/j.bbi.2018.02.005

Svensson, E., Horváth-Puhó, E., Thomsen, R. W., Djurhuus, J. C., Pedersen, L., Borghammer, P., et al. (2015). Vagotomy and subsequent risk of Parkinson's disease. *Ann. Neurol.* 78, 522–529. doi: 10.1002/ana.24448

Thakare, V. N., Dhakane, V. D., and Patel, B. M. (2017). Attenuation of acute restraint stress-induced depressive like behavior and hippocampal alterations with protocatechuic acid treatment in mice. *Metab. Brain Dis.* 32, 401–413. doi: 10.1007/s11011-016-9922-y

Tremblay, J. C., and Ainslie, P. N. (2021). Global and country-level estimates of human population at high altitude. *Proc. Natl. Acad. Sci. U. S. A.* 118:e2102463118. doi: 10.1073/pnas.2102463118

Vacca, M., Celano, G., Calabrese, F. M., Portincasa, P., Gobbetti, M., and De Angelis, M. (2020). The controversial role of human gut Lachnospiraceae. *Microorganisms* 8:573. doi: 10.3390/microorganisms8040573

Van Gossum, A., Pironi, L., Chambrier, C., Dreesen, M., Brandt, C. F., Santarpia, L., et al. (2017). Home parenteral nutrition (HPN) in patients with post-bariatric surgery complications. *Clin. Nutr.* 36, 1345–1348. doi: 10.1016/j.clnu.2016.08.025

Wang, H., Ni, X., Qing, X., Liu, L., Lai, J., Khalique, A., et al. (2017). Probiotic enhanced intestinal immunity in broilers against Ssubclinical necrotic enteritis. *Front. Immunol.* 8:1592. doi: 10.3389/fifimmu.2017.01592

Wang, Y., Shi, Y., Li, W., Wang, S., Zheng, J., Xu, G., et al. (2022). Gut microbiota imbalance mediates intestinal barrier damage in high-altitude exposed mice. *FEBS J.* 289, 4850–4868. doi: 10.1111/febs.16409

Yan, X., Zhang, J., Gong, Q., and Weng, X. (2011). Prolonged high-altitude residence impacts verbal working memory: an fMRI study. *Exp. Brain Res.* 208, 437–445. doi: 10.1007/s00221-010-2494-x

Yan, X., Zhang, J., Shi, J., Gong, Q., and Weng, X. (2010). Cerebral and functional adaptation with chronic hypoxia exposure: a multi-modal MRI study. *Brain Res.* 1348, 21–29. doi: 10.1016/j.brainres.2010.06.024

Yano, J. M., Yu, K., Donaldson, G. P., Shastri, G. G., Ann, P., Ma, L., et al. (2015). Indigenous bacteria from the gut microbiota regulate host serotonin biosynthesis. *Cells* 161, 264–276. doi: 10.1016/j.cell.2015.02.047

Zareie, M., Johnson-Henry, K., Jury, J., Yang, P. C., Ngan, B. Y., McKay, D. M., et al. (2006). Probiotics prevent bacterial translocation and improve intestinal barrier function in rats following chronic psychological stress. *Gut* 55, 1553–1560. doi: 10.1136/gut.2005.080739

Zhang, W., Jiao, L., Liu, R., Zhang, Y., Ji, Q., Zhang, H., et al. (2018). The effect of exposure to high altitude and low oxygen on intestinal microbial communities in mice. *PLoS One* 13:e0203701. doi: 10.1371/journal.pone.0203701

Zhang, Y., Liang, S., He, J., Bai, Y., Niu, Y., Tang, X., et al. (2015). Oxidative stress and antioxidant status in a lizard Phrynocephalus vlangalii at different altitudes or acclimated to hypoxia. *Comp. Biochem. Physiol. A Mol. Integr. Physiol.* 190, 9–14. doi: 10.1016/j.cbpa.2015.08.013

Zhang, D., Zhang, X., Ma, H., Wang, Y., Ma, H., and Liu, M. (2018). Competition among the attentional networks due to resource reduction in Tibetan indigenous residents: evidence from event-related potentials. *Sci. Rep.* 8:610. doi: 10.1038/s41598-017-18886-7

frontiers | Frontiers in Microbiology

TYPE Review
PUBLISHED 23 November 2022
DOI 10.3389/fmicb.2022.960492

OPEN ACCESS

EDITED BY
Hesong Wang,
Southern Medical University,
China

REVIEWED BY
C. Anthony Ryan,
University College Cork, Ireland
Ravinder K. Nagpal,
Florida State University,
United States

*CORRESPONDENCE
Warren C. McNabb
w.mcnabb@massey.ac.nz

SPECIALTY SECTION
This article was submitted to Microbial Symbioses, a section of the journal Frontiers in Microbiology

RECEIVED 03 June 2022
ACCEPTED 01 November 2022
PUBLISHED 23 November 2022

CITATION
Mullaney JA, Roy NC, Halliday C, Young W, Altermann E, Kruger MC, Dilger RN and McNabb WC (2022) Effects of early postnatal life nutritional interventions on immune-microbiome interactions in the gastrointestinal tract and implications for brain development and function. *Front. Microbiol.* 13:960492. doi: 10.3389/fmicb.2022.960492

Effects of early postnatal life nutritional interventions on immune-microbiome interactions in the gastrointestinal tract and implications for brain development and function

Jane A. Mullaney[1,2,3], Nicole C. Roy[1,3,4], Christine Halliday[1,2,5], Wayne Young[1,2,3], Eric Altermann[1,3,6], Marlena C. Kruger[7], Ryan N. Dilger[8] and Warren C. McNabb[1,3]*

[1]Riddet Institute, Massey University, Palmerston North, New Zealand, [2]AgResearch, Palmerston North, New Zealand, [3]High-Value Nutrition National Science Challenge, Auckland, New Zealand, [4]Department of Human Nutrition, University of Otago, Dunedin, New Zealand, [5]School of Food and Advanced Technology, College of Sciences, Massey University, Palmerston North, New Zealand, [6]School of Veterinary Science, Massey University, Palmerston North, New Zealand, [7]School of Health Sciences, College of Health, Massey University, Palmerston North, New Zealand, [8]Department of Animal Sciences, University of Illinois at Urbana-Champaign, Urbana, IL, United States

The gastrointestinal (GI) microbiota has co-evolved with the host in an intricate relationship for mutual benefit, however, inappropriate development of this relationship can have detrimental effects. The developing GI microbiota plays a vital role during the first 1,000days of postnatal life, during which occurs parallel development and maturation of the GI tract, immune system, and brain. Several factors such as mode of delivery, gestational age at birth, exposure to antibiotics, host genetics, and nutrition affect the establishment and resultant composition of the GI microbiota, and therefore play a role in shaping host development. Nutrition during the first 1,000 days is considered to have the most potential in shaping microbiota structure and function, influencing its interactions with the immune system in the GI tract and consequent impact on brain development. The importance of the microbiota-GI-brain (MGB) axis is also increasingly recognized for its importance in these developmental changes. This narrative review focuses on the importance of the GI microbiota and the impact of nutrition on MGB axis during the immune system and brain developmental period in early postnatal life of infants.

KEYWORDS

diet, gastrointestinal microbiota, gastrointestinal-brain development, immune development, early life, microbiota-GI-brain axis

Introduction

The gastrointestinal (GI) tract represents one of the largest sites of interaction between environmental factors, the host, and the microbiota (Thursby and Juge, 2017). The GI microbiota, a collection of microorganisms including bacteria, archaea, and eukarya, resides within the GI tract (mouth to anus) and has co-evolved with the host to form intricate and mutually beneficial or detrimental relationships (Laursen, 2021). Benefits include immune development through strengthening and maintaining epithelial integrity of the small and large intestine, with protective effects against pathogens through physical exclusion. The GI microbiota may also directly influence host metabolism. For example, it directly breaks down foods and food remnants as they progress through the GI tract, altering gene expression of the mucosal cells to facilitate the breakdown of foods, and producing enzymes that are not encoded in the human genome that perform digestion of food remnants (Rowland et al., 2018; Zhao et al., 2019).

There is a critical time window for microbial colonization in early postnatal life, 'setting the scene' for continued GI, immune, and brain development (Tooley, 2020). Disruption of the colonization process or microbiota composition (i.e., dysbiosis) can negatively affect the host, and has significant consequences for the immune system and brain development, thereby impacting cognitive function and behavior (Cussotto et al., 2018; Laursen, 2021). The bidirectional communication pathways between the GI tract and brain are termed the microbiota-gut-brain (MGB) axis; these pathways have been increasingly studied as a potential target for therapeutic applications in preventing or treating a disease or reducing disease symptoms (Brett and de Weerth, 2019). However, the mechanisms underpinning the MGB axis and their roles in the critical window of microbiota colonization during the first 1,000 days of postnatal life warrant more research.

Nutrition is among the foremost determinants of, and directly affects, GI microbiota colonization, composition, and function (Matsuyama et al., 2019). Dietary diversity is positively correlated with greater microbial diversity, due to the increased availability of metabolic substrates for the large intestinal GI microbiota (Heiman and Greenway, 2016). During the first 1,000 days, nutritional intervention is considered to have the most potential in shaping microbiota structure and function and their consequent impact on the GI, immune system, and brain development (Osadchiy et al., 2019; Tooley, 2020).

This narrative review summarizes current knowledge surrounding the importance of the microbiota for development of the GI tract, immune system, and brain during early postnatal life. The review will then discuss the impact of nutrition has on the GI microbiota and its potential role in developing these systems in early postnatal life and highlights new areas of research.

Abbreviations: GI, Gastrointestinal; HMO, Human Milk Oligosaccharides; MAIT , Mucosal-associated invariant T cell; MHC, Major Histocompatibility Complex; MGB, Microbiota-GI-brain; NK cell, Natural Killer cell; Ig, Immunoglobulin.

Microbiota colonization of the gastrointestinal tract and Its effect on host–microbe interactions

While for some time there has been debate over whether the infant is born with a sterile GI tract, recent evidence supports the hypothesis that bacterial DNA are not present within the placenta and almost all microbial DNA detected accounted for by either the introduction during delivery (caesarian) or laboratory reagent contamination (de Goffau et al., 2019).

Following birth, there are broadly four phases of microbial colonization of the GI tract: 1, first exposure as the infant is born; 2, continuous stimulation of the microbiota as a result of oral feeding; 3, additional stimulus of the microbiota with the introduction of solid foods (weaning transition); and 4, stabilization of the composition into an adult-like microbiota (Walker, 2017; Laursen, 2021). These phases are summarized in Figure 1, which also shows the parallel development of the infant's GI tract, immune system, and brain. These various phases of microbiota colonization are affected by different factors: mode of delivery, infant feeding methods, gestational age, weaning duration, frequency and severity of infection, and antibiotic exposure (Rinninella et al., 2019). The composition can therefore fluctuate in response to such factors but stabilizes at around 3 years of age.

Microbial distribution and diversity also increase along the GI tract due to nutrient, chemical and oxygen availability from the proximal to the distal portions. There is a more acidic, oxygenic, and antimicrobial environment in the small intestine than in the colon, where pH is closer to neutral and the colonocytes rapidly consume oxygen (Donaldson et al., 2016). Here, the obligate anaerobes outnumber aerobic and facultative anaerobic bacteria by 100-to 1,000-fold (Donaldson et al., 2016).

Successive pregnancies or maternal parity is also a known risk factor in infant health such as growth, mortality, and even premature birth making parity a significant contributor to the microbiome during pregnancy and infant health (Berry et al., 2021). Because of this, parity should also be considered when designing microbiome studies involving pregnancy and infants.

The microbiota-gut-brain axis

The association of the microbiota with the host, known as the MGB axis, involves bidirectional signaling pathways, and encompasses several organ systems: GI microbiota, enteric nervous system, endocrine system, immune system, central nervous system, autonomic nervous system, hypothalamic–pituitary–adrenal axis, and vagus nerve (Hyland and Cryan, 2016; Martin et al., 2018; Ceppa et al., 2019). Communication within the

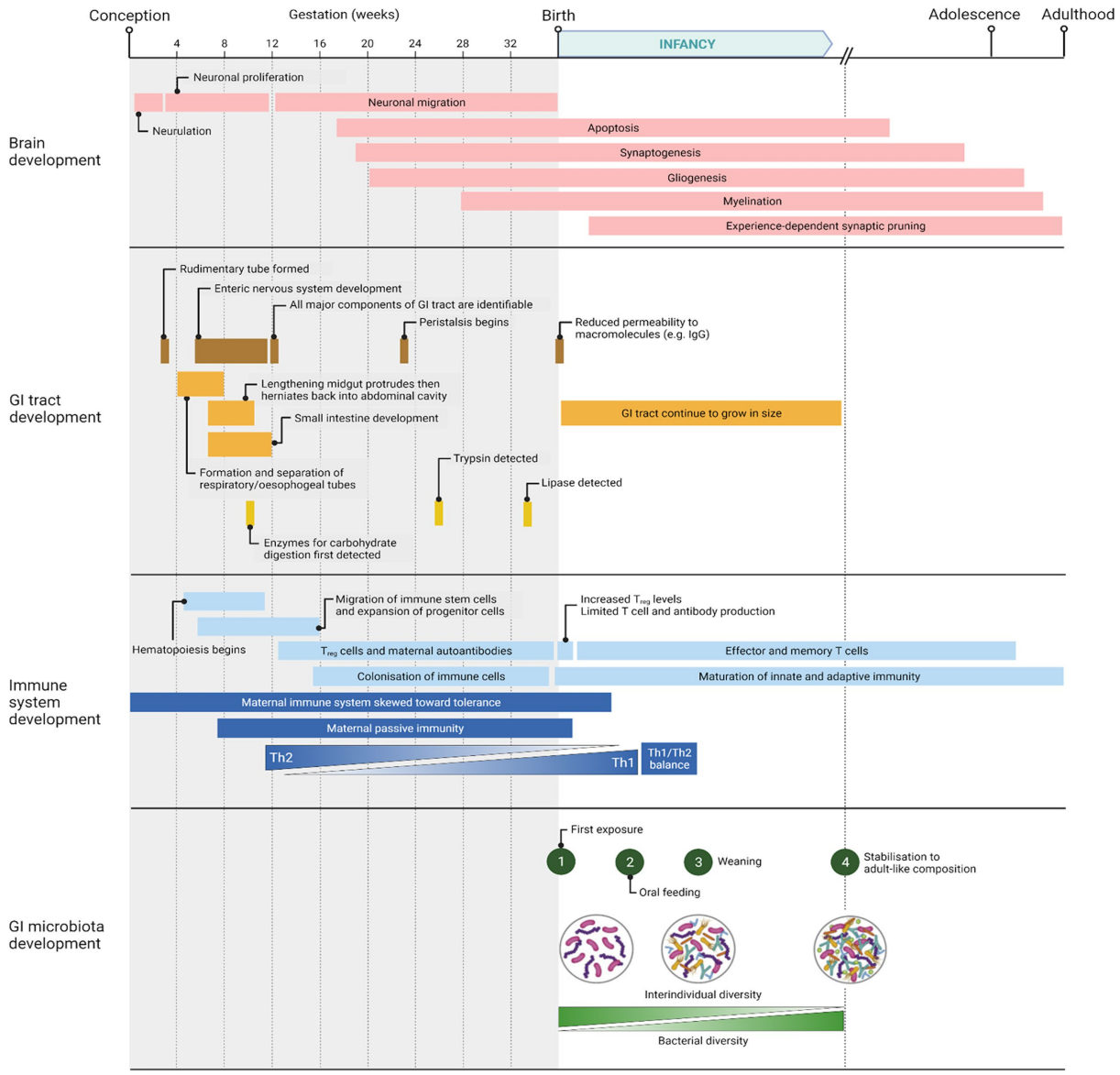

FIGURE 1
Timeline of major events occurring in brain, GI tract, immune system, and GI microbiota development from conception to adulthood. Created with BioRender.com.

MGB axis is regulated using neural, endocrine, immune, and metabolic pathways (Martin et al., 2018; Osadchiy et al., 2019). It involves several neurotransmitters and metabolites (e.g., essential vitamins, secondary bile acids, amino acids, and organic acids) which concentrations must be balanced to maintain homeostasis (Petra et al., 2015; Martin et al., 2018).

Our understanding of the role that the GI microbiota plays within the MGB axis has advanced through research with animal models. While possible, clinical studies performed in humans are difficult, often limited to the collection of fecal samples as a representative of the microbiota composition of the large intestine (Romijn and Rucklidge, 2015). Non-human primates are most comparable to humans; they share physiological, metabolic, and genetic similarities (Zheng et al., 2021). However, their ethical concerns, maintenance cost, and lifespan limit their use for research (Weatheall, 2006; Cowan et al., 2020; Berding et al., 2021; Doifode et al., 2021; Margolis et al., 2021).

Fecal microbiota transplants in humans, which involves the transplant of the fecal microbiota from one individual to another, have also been used to study the MGB axis (Codagnone et al., 2019; Cryan et al., 2019). When successful, the recipient's microbiota compositional signature or profile is more like the donor than the recipient (Cryan et al., 2019). It has been observed in several studies that behavioral phenotypes, for example depression or anxiety, may be transferred along with the microbiota (Bercik et al., 2011; Bruce-Keller et al., 2015; Kelly

et al., 2016; Zheng et al., 2016). Infants may benefit as well. In a proof-of-concept study, the transfer of maternal fecal microbiota was shown to restore normal microbiota development in cesarean-born infants (Korpela et al., 2020).

Of research involving humans, it has been reported that the MGB axis involved in infant development connects general neurocognitive development, socio-emotional behavior, and physical brain structure where function is assumed from neuroimaging (Vaher, 2022). Substantial variation exists across studies, however, most likely due to the methodologies, sample sizes, DNA sequencing methods, and even the statistical models applied. Standardization of sequencing methods and carrying out whole metagenome analyses are required to improve our understanding of the role of the gut microbiome in brain development during those early postnatal development stages (Vaher, 2022). Further research is needed in infants using methods to assess the role of the MGB axis in longitudinal brain development and behavior.

Researchers have applied other methods of studying the MGB axis in mice which includes the use of antibiotics to alter the microbiota composition to elicit behavioral or cognitive changes (Douglas-Escobar et al., 2013; Hoeman et al., 2013; Chu et al., 2019). In another recent study, changes in the microbiota of adult mice brought about with antibiotics or germ-free conditions resulted in behavioral changes, specifically, deficits in fear extinction learning (Chu et al., 2019). This behavior deficit could be restored through by reestablishment of the microbiota suggesting that the microbiota produce compounds that are able to directly affect brain function. It may be also that probiotics can prevent brain injury through blocking the ability of damaging molecules to reach the brain *via* the MGB axis (Douglas-Escobar et al., 2013). Immune systems work in concert. For example, neonates also develop maturation of their dendritic cells, which is brought about through exposure to the microbiota. The dendritic cells produce interleukin (IL)-12 which accumulates in the environment and through a mechanism where IL-12 offsets the bias toward Th1, thereby promoting Th1 differentiation to Th2 (Hoeman et al., 2013).

Pigs are a more suitable and preferable choice over rodents for research focusing on early postnatal life development of the human infant. Pigs and human infants share similar scaled GI and brain developmental timelines as compared to rodents (Mudd and Dilger, 2017). In general, the porcine brain is one-tenth the total volume of the human brain throughout its lifespan with 1 month of human growth being approximately equivalent to 1 week of piglet total brain growth. This is in contrast to rodent brains, which are much smaller, grow and develop with a different trajectory, and would often require pooling tissue to analyze its components (Mudd and Dilger, 2017). Furthermore, the precocial nature of piglets allows for behavioral and cognitive assessments to be performed immediately after birth, which is impossible in either rodents or humans (Mudd and Dilger, 2017; Val-Laillet, 2019). Additionally, most knowledge in immune ontogeny in early postnatal life has stemmed from studies with germ-free rodents, which provide results that are not readily translatable to humans. Pigs are, again, an improved animal model as they share greater similarities with humans in terms of anatomy and function of the immune system (e.g., pigs possess tonsils whereas rodents do not; Pabst, 2020).

Pigs are also the animal model of choice in terms of digestive and associated metabolic processes, as their nutritional requirements when compared with other non-primate animal models are more closely aligned to those of human (infants; Kobek-Kjeldager et al., 2022). Cannulation is also possible for repeated, stress-free digesta sample collection to assess nutrient digestibility and kinetics over the lifetime (Bennell and Husband, 1981a,b). Therefore, the use of pigs in early postnatal life developmental research allows for the determination of the critical time windows of GI, brain, and immune development that may be sensitive to nutrition intervention.

Development of the immune system

Newborn infants need time to develop and mature their innate and adaptive immune systems. There are some transfers of maternal immunity both *in utero* and through breast milk. These processes help to provide immunity to the infant in the first days through transfer of both secretory immunoglobulins and 'milk leukocytes', which produce molecules that migrate to the GI and respiratory tracts (Tuaillon et al., 2009; Houghteling and Walker, 2015; Rudzki et al., 2017). Over time, the components of breast milk change from a primarily protective to a nutritional role (O'Neill et al., 2020; Laursen, 2021).

The maturation of the immune system requires the GI microbiota, the absence of which impacts all aspects of immune system development and function (Mohajeri et al., 2018). Improper development brings about several immunological defects, including increased susceptibility to infections and altered immune homeostasis (Cong et al., 2015; Nash et al., 2017; Eshraghi et al., 2018). It has been observed that mice treated with antibiotics, or gnotobiotic mice colonized by a limited defined consortia of bacteria, showed impaired microglia maturation and immune response upon bacterial stimuli when compared with their conventional counterparts (Erny et al., 2015). Training of the infant immune system is also required for optimal GI function, including vascular supply, epithelial healing, nutrient absorption, and protection from infection.

There is an interface between innate and adaptive immunity, where T or B cells are recruited and work at protecting intestinal mucosal from the resident microbes. The immune system includes the Toll-like receptors (TLRs) that recognize the presence of microbes from their DNA to their surface molecules to the specialized T cells. For a review of 'the interface between innate and adaptive immunity' see Hoebe et al. (2004).

Innate immunity includes the mucosal-associated invariant T (MAIT) cells, abundant in humans and a key immune system component. MAIT cells are atypical T-cells with a limited response repertoire activated by riboflavin-derived molecules (rather than

peptides), which are presented through the major histocompatibility complex (MHC) class I protein MR1 (Godfrey et al., 2019). MAIT cells are absent in germ free mice and become more abundant in microbial-challenged mice, so it is highly likely that exposure to and association with microbes in the GI tract is responsible for their development and maturation (Chen Z. et al., 2017; Godfrey et al., 2019). Similarly, invariant natural killer (NK) T cells are abundant in healthy infants and have a role as 'cytotoxic effectors' and regulation of the adaptive immune system (Wingender et al., 2012; Sagebiel et al., 2019).

Immunoglobulins are also part of the innate and adaptive immune response and are critical to the infant's ability to specifically recognize and bind to antigens, which facilitates their destruction. There are five main classes of immunoglobulins (IgG, IgM, IgA, IgD, and IgE), characterized by the type of heavy chain within their structure, resulting in differences in their function and type of immune response elicited by each molecule. Secretory IgA (sIgA) is transferred through maternal breast milk to the infant where it protects from infection and is critical for homeostasis of the microbiota not only through encouraging colonization but through influencing the microbiota gene expression (Mirpuri et al., 2014; Rogier et al., 2014; Gopalakrishna et al., 2019; Zheng et al., 2020). Maturation of IgA and IgG requires B cell class-switching, and this process does not mature until around 6 months of age. IgE may also be produced through B cell isotype switching at mucosal sites and abnormally high plasma IgE levels have also been observed in germ-free mice compared with conventionally reared mice. A study on this concluded that a sufficient microbial stimulation during early postnatal life is required to maintain baseline IgE levels (Cahenzli et al., 2013). Additionally, it has been demonstrated that the 'allergy phenotype' is transferrable *via* transplantation of the GI microbiota (Walker, 2017; Smeekens et al., 2020). Germ-free mice are inherently susceptible to anaphylactic responses to food, quantified by a drop in body temperature. The colonization of these mice with the microbiota from healthy infants protected the mice from anaphylactic responses, but not when colonized using the microbiota from infants suffering from bovine milk allergy (; Smeekens et al., 2020).

Research in rodents have shown that appropriate innate immune responses are also required for nutrient absorption and metabolism. Shulzhenko et al. identified inter-connecting regulatory signaling networks which balance metabolism and the innate defensive mechanisms in epithelial cells (Shulzhenko et al., 2011). If IgA concentrations are altered, these networks become unbalanced and may cause irregular upregulation of certain pathways (e.g., innate immunity), while downregulating others (e.g., lipid uptake and metabolism; Shulzhenko et al., 2011). Furthermore, bacterial fermentation of indigestible dietary fibers produces organic acids in the colon (Silva et al., 2020). Organic acids promote intestinal barrier integrity, mucus production, and supporting a tolerogenic response over inflammation (O'Keefe, 2016; Parada Venegas et al., 2019; Silva et al., 2020; Laursen, 2021).

Adaptive immunity involves the maturation of T and B cells which begin their development while still *in utero* (Haynes et al., 1988; Haynes and Heinly, 1995; Schonland et al., 2003; Rechavi et al., 2015). Infant responses to antigen by T and B cells are known to be weaker than in adults in most cases except in some vaccines and pathogens (Siegrist and Aspinall, 2009). It is important to acknowledge that much of our understanding early postnatal life immunity in infants has relied on murine models even though they differ substantially in ontogeny as reviewed by Semmes et al. (2020).

Role of the gastrointestinal microbiota in brain development

Brain development begins *in utero* and continues into adolescence (Zuckerkandl and Pauling, 1965), as shown in Figure 1. Major events of brain development in early postnatal life include synaptogenesis, myelination, and synaptic pruning. The GI microbiota is known to affect or be associated with these events, as well as influence neural development, cognition, and behavior. Cognitive functions, including learning capacity and memory, are closely linked with the GI microbiota (Liang et al., 2018b). Cognitive function encompasses the life-long process of learning, which includes both long-and short-term processes (Gareau, 2016). Cognitive impairment has been noted in individuals with GI or neurological disorders (Gareau, 2016; Vuong et al., 2017). Several human studies have been published already, correlative, linking the microbiome with brain function and a summary of these and the findings has been reviewed recently (Tooley, 2020). One recent study looked at the fecal microbiota profiles of 1-year-old infants and correlated these with regional brain volume data and Mullen Scales of Early Learning (indicator of cognitive performance) at 2 years of age, finding differences (Carlson et al., 2018). Although brain volume was not different between groups, the fecal microbiota alpha diversity differed between age groups (Carlson et al., 2018). A key finding in that study was that highest level of cognitive performance could be predicted by the *Bacteroides* genus while the lowest level of performance was predicted by the *Faecalibacterium* genus. While there was a difference in cognitive performance depending on microbiome diversity, there was no evidence of a 'cognitive damage' microbiota profile or nor any cognitive impairment in either age group (Carlson et al., 2018).

Studies using germ-free animal models or antibiotic-induced dysbiosis have been used to demonstrate that without a 'normal' GI microbiota, working and spatial memory are negative influenced (Manderino et al., 2017; Vuong et al., 2017). For instance, elevated hippocampal levels of serotonin (Jameson and Hsiao, 2018) and brain-derived neurotrophic factor (Borrelli et al., 2016; Hoban et al., 2016) were linked with behavioral changes between germ-free and conventional rodents, such as increased depressive-like and decreased anxiety-related behaviors (Cryan and Dinan, 2012; Foster and McVey Neufeld, 2013; Guida et al., 2018; Fulling et al., 2019). The decreased anxiety-like behavior in germ-free mice was observed when subjecting the mice to various

tests that measure the natural aversion of rodents for open and elevated areas and their natural, spontaneous exploratory behavior in novel environments. This cautious versus exploratory behavior must be balanced to ensure survival of the individual for procreation. While decreased anxiety may be advantageous, this may lead to an increased chance of predation and therefore decrease their likelihood of survival. The exhibited aberrant behavior persisted following the colonization of these germ-free mice with a conventional microbiota. These findings show that the GI microbiota plays a role in developing stress pathways and a critical time window exists for reconstitution of the microbiota to normalize behavior (Cryan and Dinan, 2012; Foster and McVey Neufeld, 2013; Guida et al., 2018; Fulling et al., 2019). Similar findings have been reported where a critical time window of colonization exists to avoid negative behavioral changes in adulthood (Sudo et al., 2004; Diaz Heijtz et al., 2011). Furthermore, a study by Bercik et al. showed that behavioral changes are transferable following transplantation of the GI microbiota (Bercik et al., 2011).

The GI microbiota is also linked to changes in neurogenesis (Gareau, 2016; Liang et al., 2017, 2018a; Wei George et al., 2021). In a recent review on how the microbiota composition impacts neurogenesis, possible strategies for using the microbiome to treat neurological disorders is discussed but the mechanisms for microbiome inhibition or promotion of neurogenesis are still not understood (Liu et al., 2022). The primary mode of communication from the GI microbiota to the host's central nervous system is achieved through immune or endocrine mechanisms (Martin et al., 2018). These mechanisms are often mediated by microbially-derived molecules such as organic acids and tryptophan metabolites (Wikoff et al., 2009; Tolhurst et al., 2012; Yano et al., 2015). For example, some 90% of serotonin required for mood, behavior, sleep, and several other functions within the central nervous system and GI tract is produced by the intestinal microbiota (Gershon and Tack, 2007; Gershon, 2013). These metabolites signal enteroendocrine and enterochromaffin cells, which in turn may act directly or indirectly on the central nervous system (Martin et al., 2018). Direct signaling must overcome obstacles such as the epithelial barrier and immune system in the GI tract or blood–brain barrier to exert its effects on the brain (Samuel et al., 2008; Haghikia et al., 2015; Yano et al., 2015). Indirect signaling may induce responses in the central nervous system through long-distance neural signaling by vagal and/or spinal afferents (Goehler et al., 2005; Bravo et al., 2011). Alterations to these signaling pathways within the MGB axis have been implicated in the pathogenesis and pathophysiology of both functional GI and neurological disorders (Rhee et al., 2009; Mayer, 2011). An approach may be developed for prevention and treatment by targeting specific mechanisms through which the GI microbiota interacts and contributes to these disorders (Rhee et al., 2009; Mayer, 2011; Mayer et al., 2014; Cerdó et al., 2017).

Organic acids produced primarily by the colonic microbiota have been observed to exert effects on blood–brain barrier permeability (Braniste et al., 2014). The three most abundant organic acids are the short-chain fatty acids acetate, propionate and butyrate (Rios-Covian et al., 2016). Acetate produced in the intestine crosses the blood brain barrier and is taken up by the brain where it is incorporated into the hypothalamus and eventually has a role in appetite regulation (Frost et al., 2014). Propionate has an effect on the regulation of the sympathetic nervous system, and both propionate and butyrate affect intracellular potassium levels (Oleskin and Shenderov, 2016), and also regulate the expression of tryptophan hydroxylase, which in turn is involved in the biosynthesis of serotonin (Nankova et al., 2014). For a review on the role of the organic acids in the MGB axis see Silva et al. (2020).

The GI microbiota plays a role in the normal development and regulation of the hypothalamic–pituitary–adrenal axis. This axis is a major component of the homeostatic response that mediates the effects of stressors by regulating many physiological processes. Thus, the GI microbiota can influence the host's stress reactivity and anxiety-like behaviors (Saulnier et al., 2013; de Weerth, 2017). For example, maternal separation stress models, e.g., where young are separated from their mothers to stimulate a stress response, have been used to assess how acute and/or chronic stress affects the mouse pups. Stress has resulted in memory dysfunction in germ-free rodents, attributed to altered brain-derived neurotrophic factor expression levels (Gareau et al., 2011). This factor regulates several aspects of the brain, and its altered expression can lead to downstream effects on cognitive functions and intestinal muscle repair, regeneration, and differentiation (Al-Qudah et al., 2014). Germ-free animals also exhibited decreased anxiety and increased stress response with augmented levels of adrenocorticotropic hormone and cortisol (Diaz Heijtz et al., 2011; Neufeld K. A. et al., 2011; Neufeld K. M. et al., 2011; Clarke et al., 2013; Nishino et al., 2013). Following recolonization of the GI tract with a conventional microbiota, normalizing the hypothalamic–pituitary–adrenal axis occurs in an age-dependent manner (Sudo et al., 2004). Reversibility of the increased stress response is achievable only in germ-free mice aged less than 3 weeks, supporting the notion of a critical period during which the plasticity of neural regulation is sensitive to input from the GI microbiota (Sudo et al., 2004).

Stress during early postnatal life has been shown to have long-lasting effects, including altering the MGB axis. A study by O'Mahoney et al., using the maternal separation rat model, showed altered composition of the fecal microbiota following early postnatal life stress as well as altered behavior and systemic immune responses compared to a control group (O'Mahony et al., 2009, 2011). Furthermore, basal adrenocorticotropic hormone levels and increased anxiety-like behaviors were higher in the stressed groups when compared with the control group (Daniels et al., 2004). However, following a subsequent stressor, adrenocorticotropic hormone levels were lower in the stressed groups and were accompanied by altered neurotransmitter levels, indicating that the stressor had detrimental effects on regular stress responses and induced abnormal behaviors (Daniels et al., 2004; Saulnier et al., 2013; Rincel and Darnaudéry, 2019). Psychological stress can

directly affect the integrity of the tight junction proteins responsible for barrier integrity for the intestine and the blood brain barrier and loss of this integrity is also correlated with microbiota dysbiosis (Geng et al., 2019). Chronic stress can also create a loop that affects memory through a feed-forward loop mechanism leading to depressive disorders as shown in Japanese quails (Kraimi et al., 2022). In this animal model study, Japanese quails experienced induced stress with their microbiota transferred to unstressed quails. Again, the *Bacteroides* genus was implicated with the *Alistipes* genus showing increased abundance in the stressed group and this stress response was transferred through the microbiota to the unstressed recipient (Daniels et al., 2004; Saulnier et al., 2013; Rincel and Darnaudéry, 2019; Kraimi et al., 2022).

Early postnatal life nutrition and the microbiota-gastrointestinal-bra in axis

The microbiota is susceptible to modulation by external factors prior to stabilization of its composition at approximately 2–3 years of age. Among these, infant diet has been identified as a major contributor to GI microbiota development in early postnatal life. As such, the effects of infancy diet (namely formula vs. breast milk) on early postnatal life development have been well documented (Colen and Ramey, 2014; Kowalewska-Kantecka, 2016). Comparably, less is known about the effects complementary feeding has on infant microbiota composition (Laursen et al., 2017; Laursen, 2021). Given the dominating influence diet and nutrition has on microbiota composition, and the involvement of the microbiota in regulating immune and brain development, gaining a deeper understanding of the potential microbe-mediated host effects of feeding mode in early infancy is needed (Conlon and Bird, 2014). Also, the complementary feeding period (6–24 months of life) coincides with a critical period in microbiota development, transitioning away from the influence of a milk-based diet (Laursen et al., 2017; Laursen, 2021). The infant microbiota composition stabilizes and resembles an adult-like microbiota at around 3 years of age and attempts at modulation are likely to be more successful if they are conducted before this or early in this period to elicit any beneficial downstream effects.

Early infancy diet

Breast milk is the recommended first nutrition for the infant, providing all necessary nutrients to support growth and development, as well as passive immunity to protect against infectious diseases during infancy. After lactose and lipids, human milk oligosaccharides (HMO) are the third most abundant component of breast milk. These comprise short saccharides composed of five monomeric building blocks (glucose, galactose, fucose, N-acetylglucosamine, and sialic acid), of which over 200 different structures have been identified. These oligosaccharides are responsible for selectively promoting the growth and function of beneficial bacteria As infants lack the necessary enzymes to digest HMOs, the molecules pass into the large intestine and function as a carbon source for commensal bacteria (Yang et al., 2016; Walker, 2017), promoting and stimulating the growth of specific bacterial groups such as *Staphylococci* (Hunt et al., 2011), and from genera *Bifidobacterium* (Zivkovic et al., 2011), *Streptococcus*, *Lactobacillus* (Harmsen et al., 2000) and *Bacteroides*. Only bacteria such as *Bifidobacterium longum* subspecies *infantis* lineage harbor genes to express all enzymes required for degrading and utilizing HMOs (Milani et al., 2017; Taft et al., 2018) However, other bacteria may cleave and utilize specific components of HMOs (Milani et al., 2017). HMOs have been attributed to the two-fold increase of *Bifidobacterium* cells in breastfed infants compared to formula-fed infants (Rinninella et al., 2019). Some bacteria, including *Bacteroides fragilis*, *Bifidobacteria infantis*, and *Lactobacillus acidophilus*, stimulate endogenous production of sIgA, activation of regulatory T cells and anti-inflammatory molecules – all necessary for host homeostasis (Newburg and Walker, 2007; Chichlowski et al., 2012; Jost et al., 2012). Lactoferrin, another component in breast milk, also encourages the proliferation of beneficial bacteria such as *Lactobacillus* and *Bifidobacterium* genera (Mastromarino et al., 2014).

Breastmilk has also been demonstrated to provide passive protection and stimulate the development of the infant's immune system (Schwartz et al., 2012). For example, polymeric IgA and defensins can interfere with pathogen attachment and uptake (Newburg and Walker, 2007), while *n-3* fatty acids (Wijendran et al., 2015) and transforming growth factor-β (Rautava and Walker, 2009) can activate enterocytes to produce anti-inflammatory cytokines, and lactoferrin can interact with the GI tract and promote immune homeostasis (Newburg and Walker, 2007; Walker and Iyengar, 2015).

Comparison of the intestinal microbiota in formula and breast-fed infants showed that at around 40 days, those fed exclusively with formula had greater alpha diversity while both breast-fed and formula-fed infants were colonized predominantly with *Bifidobacterium* species and members of *Enterobacteriaceae* family (Ma J. et al., 2020). While the diversity in the breast-fed infants was lower than formula-fed at day 40, it increased by 4 months and diversity was similar between formula and breast-fed infants. Lower diversity in breast-fed infants was most likely due to the breast milk which requires specific bacteria capable of degrading the oligosaccharides that are in the milk. Although many infant formula products are supplemented with prebiotics such as fructo-oligosaccharides and/or galacto-oligosaccharides, these are not as selective as HMOs since they can be utilized by most *Bifidobacterium* species (Akiyama et al., 2015) and stimulate the growth of various *Lactobacillus*, *Streptococcus*, and *Bacteroides* species (Schwab and Gänzle, 2011; Ma C. et al., 2020). Comparison of metabolic profiles of infants fed either exclusively formula or breastmilk have also confirmed that the metabolic capabilities of the microbiota are primarily proteolytic and saccharolytic, respectively (Chow et al., 2014; He et al., 2019).

Weaning and complementary feeding

Over the course of infancy, a point is reached where milk-based feeding is no longer adequate to cover the nutritional requirements of the infant. Therefore, supplementation with additional foods is required. The introduction of solid foods and the progressive reduction of milk-feeding lead to major GI microbiota compositional and functional changes. Bacteria belonging to families *Bifidobacteriaceae* and *Enterobacteriaceae* are decreased after weaning (Fallani et al., 2011a,b), and any compositional differences between breastfed or formula-fed infants slowly decrease (Yaron et al., 2013; Mastromarino et al., 2014; Rinninella et al., 2019).

Pigs also produce milk oligosaccharides (pMOs); Twenty-nine were described in 2010 and were found to be abundantly sialylated making them more similar to bovine than human (Tao et al., 2010). However, some pMOS are fucosylated, are much more abundant in pigs than in bovine (9% versus 1%) which suggests that pMOs are actually more closely like human than bovine milk and therefore are also influencing the microbiota (Salcedo et al., 2016). In a neonatal piglet model, the fecal microbiota composition stabilized 10 days post-weaning (Chen L. et al., 2017). The sudden change from high-fat, low-carbohydrate milk (pre-weaning) to a high-carbohydrate, low-fat feed (weaning and onward) resulted in a drastic change of available nutrients to the commensal bacteria (Guevarra et al., 2019). The predominant genera post-weaning are microbes efficient in degrading dietary fibers and producing organic acids (Chen L. et al., 2017), resulting in a microbiota composition more adult-like (Chen L. et al., 2017; Guevarra et al., 2018, 2019). Chen et al. observed a shift from a high prevalence of *Lactobacillus* and *Bacteroides* genera, to *Roseburia, Paraprevotella* and *Blautia* genera, post-weaning (Chen L. et al., 2017). Furthermore, Firmicutes and Bacteroidetes remained the most abundant phyla pre-and post-weaning (Alain et al., 2014; Hu et al., 2016; Chen L. et al., 2017). Another study supported these findings, reporting *Bacteroides* as the most abundant genus in nursing pigs (pre-weaning), with *Prevotella* and *Lactobacillus* genera enriched in weaned pigs (Guevarra et al., 2018, 2019).

Interventions with probiotics to improve or maintain good health in early postnatal life have gained much popularity in recent decades (Kapourchali and Cresci, 2020). Some infant formula has been designed to include probiotics, for example *Bifidobacterium* and *Lactobacillus* species, to mimic the composition of human breastmilk. However, probiotic-supplemented infant formula contains a much higher concentration of these probiotic strains when compared with breastmilk (Fernández et al., 2018). Furthermore, not all probiotics are functionally equal, as the effects obtained from one strain cannot be assumed to be replicable with another strain, even if they belong to the same species (McFarland et al., 2018). Even if they are not equal, probiotics have been demonstrated to be safe and effective across multiple studies involving infants. For example, supplementation with probiotics can increase the microbial metabolism of milk oligosaccharides in infants while also reducing intestinal inflammation (Larke et al., 2022). In another recent study, probiotics demonstrated efficacy against the development of antibiotic resistance in preterm infants (Guitor et al., 2022) and in another, probiotics were shown to cause no adverse effects in vulnerable premature infants and decrease the risk of necrotizing enterocolitis (Underwood et al., 2020).

Cognitive impairment is sometimes alleviated through probiotic administration (Liang et al., 2015; Ohsawa et al., 2015; Wang et al., 2015). For example, administration of *Lactobacillus helveticus* improved the stress response and cognitive dysfunction induced by chronic stress in rats (Liang et al., 2015), and *Bifidobacterium longum* strains were observed to be effective in improving memory (Ohland et al., 2013; Savignac et al., 2015). Early postnatal life probiotic intervention has also been observed to reduce sepsis and allergy, as well as having a possible role in reducing the risk of neuropsychiatric disorders such as autism spectrum disorder and attention deficit disorder (Weizman et al., 2005; Indrio et al., 2014; Pärtty et al., 2015; Korpela et al., 2016; Panigrahi et al., 2017). There is also evidence that a combination of *Streptococcus thermophiles* and *Bifidobacterium* genus can be effective in preventing the onset of diarrhea in children following antibiotic treatment (Corrêa et al., 2005). Four *Lactobacillus* strains isolated from breastmilk protected against infection in a mouse model, with potent antimicrobial properties (Olivares et al., 2006). Thus, cultivating microbes from human breastmilk may also prove to provide good probiotic candidates for further research and development.

The application of prebiotics and probiotics in improving health in early postnatal life is promising, but the timing of administration, the quantity administrated, the effect of different strains, combination of strains, engineering, and safety must be carefully considered and continually researched to fully understand how they modulate the GI microbiota composition and exert their effects.

There is a developmental aspect of the growing infant where multiple maturation events are proceeding in the brain; in one direction is synaptogenesis, microglia maturation, with targeted synaptic pruning and myelination. Meanwhile, in the immune system, T and B cells are maturing, innate immune cells are being trained through exposure to the environment, and the immune system is learning to differentiate self from non-self (i.e., foreign). Similarly, in parallel, the microbiota in the GI tract is also maturing, colonizing the intestine, metabolizing nutrients, and releasing microbial products that may be immune modulatory or in the case of butyrate, an energy source for enterocytes lining the intestinal epithelium. The vagus nerve sits right at that junction of the MGB axis and is an integral part of the communication between systems. It accesses the entire digestive wall yet does not cross the epithelial layer and it senses and responds to the signals that come from the microbiota transported across the epithelial layers by host entereroendocrine cells (Wang and Powley, 2007). If this communication system the vagus nerve was targeted, it may be able to affect and restore the homeostasis of the MGB axis (Bonaz et al., 2018).

Future perspectives

The mutualistic relationship that exists between the host and microbes begins at birth and shapes both host health and microbiota composition and function. The development and maturation of the GI tract, immune system, brain, and microbiota are in turn influenced by host genetics and exposure to the environment (e.g., diet, delivery mode, feeding methods, weaning, infection, and antibiotics). There are important interactions between the development and maturation of the immune system that drive the establishment and maturation of the microbiota in the GI tract and potentially affect the brain development and function and associated cognitive behaviors in infants.

The implications of the microbiota and immunological findings discussed in this review for pregnant women, mothers, infants, infant nutrition policy makers, formula manufacturers, and health-conscious consumers are important aspects to consider. The effects of the microbiota on the mental and cognitive state of the infant cannot be ignored. Development and maturation are staged and interdependent processes, with a narrow window of opportunity where nutrition can modulate the microbiota for beneficial effects to be conferred to the infant. Appropriate nutrition might encourage more beneficial bacteria within the microbiota to flourish however, such intervention is a balance between benefits and risks.

Current evidence suggests that the MGB axis is a highway of communication and connections between two complex systems found in the host and the GI tract microbiota. The communication and interactions are complex and manipulating one system might also have unintentional negative outcomes for the other system. For example, high alpha diversity of the microbiota is recognized as an indicator of health. However, in early postnatal life, when the diet is primarily milk based, this diversity is low. The *Bifidobacterium* genus and *Enterobacteriaceae* family are the dominant in the microbiota at that age and these bacteria are critical to the immune development of the infant. The brain also relies on the appropriate immune development to develop.

Another possibility is to encourage the prevalence of fiber-degrading microbes in the infant microbiota by offering fiber-rich foods, but only after the infant transitions to solid foods and thereby has a sufficiently mature microbiota composition. Fiber-rich complementary foods then lead to the increased production of beneficial organic acids which impact positively the colonic epithelium where they are absorbed with specific organic acids (e.g., acetate) affection brain and cognition outcomes. The reverse is inflammatory conditions which can allow translocation of bacteria and their products to the blood where the downstream effects are more inflammation, oxidative stress and may lead to disease.

Increasing the abundance of the *Bacteroides* genus and reducing the abundance of the *Faecalibacterium genus* are counterintuitive to the beneficial effects of the *Faecalibacterium genus* on health. It is known that the methods of assessing the microbiota composition and function lack resolution to characterize which species or bacterial strains are involved. Consequently, some important changes in the microbiota composition that contribute to improve cognition in infants might be undetected in the preweaning period. Sequencing depth and resolution needs to increase to discriminate between bacterial species to better understand these relationships.

Appropriate nutrition in early postnatal life feeds the microbiota in the GI tract sets the baseline for immune, physical and brain health in later life. The microbiota shapes the immune system and is in turn shaped by the immune system. Interactions with any one of these systems impacts on the others. The ability to measure and assess such a dynamic set of systems will involve a cross disciplinary translational approach. It is possible that to reverse or at least mitigate the effects of inadequate nutrition through dietary interventions at that point in time, that narrow window of opportunity before the immune system, the brain and the microbiota mature into the stable adult shape which persists.

Author contributions

CH, NR, JM, WY, EA, MK, RD, and WM have contributed to the work. CH conceived and wrote the initial draft of the manuscript. JM and NR edited and revised the manuscript and in structuring the paper and critically reviewing the manuscript. JM, NR, CH, WY, EA, MK, RD, and WM advised and critically reviewed versions of the paper. All authors contributed to the article and approved the submitted version.

Funding

CH was supported by a fellowship from the Riddet Institute, through funding provided by the NZ Ministry of Business, Innovation & Employment Smarter Lives project. The same grant also supports co-authors JM, WY, EA, and WM.

Conflict of interest

The authors declare that the research was conducted in the absence of any commercial or financial relationships that could be construed as a potential conflict of interest.

Publisher's note

References

Akiyama, T., Kimura, K., and Hatano, H. (2015). Diverse galactooligosaccharides consumption by bifidobacteria: implications of β-galactosidase–LacS operon. *Biosci. Biotechnol. Biochem.* 79, 664–672. doi: 10.1080/09168451.2014.987204

Alain, B. P. E., Chae, J. P., Balolong, M. P., Bum Kim, H., and Kang, D. K. (2014). Assessment of fecal bacterial diversity among healthy piglets during the weaning transition. *J. Gen. Appl. Microbiol.* 60, 140–146. doi: 10.2323/jgam.60.140

Al-Qudah, M., Anderson, C. D., Mahavadi, S., Bradley, Z. L., Akbarali, H. I., Murthy, K. S., et al. (2014). Brain-derived neurotrophic factor enhances cholinergic contraction of longitudinal muscle of rabbit intestine via activation of phospholipase C. *Am. J. Physiol. Gastrointest. Liver Physiol.* 306, G328–G337. doi: 10.1152/ajpgi.00203.2013

Bennell, M. A., and Husband, A. J. (1981a). Route of lymphocyte migration in pigs. I. Lymphocyte circulation in gut-associated lymphoid tissue. *Immunology* 42, 469–474.

Bennell, M. A., and Husband, A. J. (1981b). Route of lymphocyte migration in pigs. II. Migration to the intestinal lamina propria of antigen-specific cells generated in response to intestinal immunization in the pig. *Immunology* 42, 475–479.

Bercik, P., Denou, E., Collins, J., Jackson, W., Lu, J., Jury, J., et al. (2011). The intestinal microbiota affect central levels of brain-derived neurotropic factor and behavior in mice. *Gastroenterology* 141, 599–609.e3. doi: 10.1053/j.gastro.2011.04.052

Berding, K., Vlckova, K., Marx, W., Schellekens, H., Stanton, C., Clarke, G., et al. (2021). Diet and the microbiota-gut-brain Axis: sowing the seeds of Good mental health. *Adv. Nutr.* 12, 1239–1285. doi: 10.1093/advances/nmaa181

Berry, A. S. F., Pierdon, M. K., Misic, A. M., Sullivan, M. C., O'Brien, K., Chen, Y., et al. (2021). Remodeling of the maternal gut microbiome during pregnancy is shaped by parity. *Microbiome* 9:146. doi: 10.1186/s40168-021-01089-8

Bonaz, B., Bazin, T., and Pellissier, S. (2018). The vagus nerve at the interface of the microbiota-gut-brain axis. *Front. Neurosci.* 12:49. doi: 10.3389/fnins.2018.00049

Borrelli, L., Aceto, S., Agnisola, C., De Paolo, S., Dipineto, L., Stilling, R. M., et al. (2016). Probiotic modulation of the microbiota-gut-brain axis and behaviour in zebrafish. *Sci. Rep.* 6:30046. doi: 10.1038/srep30046

Braniste, V., Al-Asmakh, M., Kowal, C., Anuar, F., Abbaspour, A., Tóth, M., et al. (2014). The gut microbiota influences blood-brain barrier permeability in mice. *Sci. Transl. Med.* 6:263ra158. doi: 10.1126/scitranslmed.3009759

Bravo, J. A., Forsythe, P., Chew, M. V., Escaravage, E., Savignac, H. M., Dinan, T. G., et al. (2011). Ingestion of lactobacillus strain regulates emotional behavior and central GABA receptor expression in a mouse via the vagus nerve. *Proc. Natl. Acad. Sci. U. S. A.* 108, 16050–16055. doi: 10.1073/pnas.1102999108

Brett, B. E., and de Weerth, C. (2019). The microbiota–gut–brain axis: a promising avenue to foster healthy developmental outcomes. *Dev. Psychobiol.* 61, 772–782. doi: 10.1002/dev.21824

Bruce-Keller, A. J., Salbaum, J. M., Luo, M., Blanchard, E. T., Taylor, C. M., Welsh, D. A., et al. (2015). Obese-type gut microbiota induce neurobehavioral changes in the absence of obesity. *Biol. Psychiatry* 77, 607–615. doi: 10.1016/j.biopsych.2014.07.012

Cahenzli, J., Koller, Y., Wyss, M., Geuking, M. B., and McCoy, K. D. (2013). Intestinal microbial diversity during early-life colonization shapes long-term IgE levels. *Cell Host Microbe* 14, 559–570. doi: 10.1016/j.chom.2013.10.004

Carlson, A. L., Xia, K., Azcarate-Peril, M. A., Goldman, B. D., Ahn, M., Styner, M. A., et al. (2018). Infant gut microbiome associated with cognitive development. *Biol. Psychiatry* 83, 148–159. doi: 10.1016/j.biopsych.2017.06.021

Ceppa, F., Mancini, A., and Tuohy, K. (2019). Current evidence linking diet to gut microbiota and brain development and function. *Int. J. Food Sci. Nutr.* 70, 1–19. doi: 10.1080/09637486.2018.1462309

Cerdó, T., Ruíz, A., Suárez, A., and Campoy, C. (2017). Probiotic, prebiotic, and brain development. *Nutrients* 9:1247. doi: 10.3390/nu9111247

Chen, Z., Wang, H., D'Souza, C., Sun, S., Kostenko, L., Eckle, S. B., et al. (2017). Mucosal-associated invariant T-cell activation and accumulation after in vivo infection depends on microbial riboflavin synthesis and co-stimulatory signals. *Mucosal Immunol.* 10, 58–68. doi: 10.1038/mi.2016.39

Chen, L., Xu, Y., Chen, X., Fang, C., Zhao, L., and Chen, F. (2017). The maturing development of gut microbiota in commercial piglets during the weaning transition. *Front. Microbiol.* 8:1688. doi: 10.3389/fmicb.2017.01688

Chichlowski, M., De Lartigue, G., German, J. B., Raybould, H. E., and Mills, D. A. (2012). Bifidobacteria isolated from infants and cultured on human milk oligosaccharides affect intestinal epithelial function. *J. Pediatr. Gastroenterol. Nutr.* 55, 321–327. doi: 10.1097/MPG.0b013e31824fb899

Chow, J., Panasevich, M. R., Alexander, D., Vester Boler, B. M., Rossoni Serao, M. C., Faber, T. A., et al. (2014). Fecal metabolomics of healthy breast-fed versus formula-fed infants before and during in vitro batch culture fermentation. *J. Proteome Res.* 13, 2534–2542. doi: 10.1021/pr500011w

Chu, C., Murdock, M. H., Jing, D., Won, T. H., Chung, H., Kressel, A. M., et al. (2019). The microbiota regulate neuronal function and fear extinction learning. *Nature* 574, 543–548. doi: 10.1038/s41586-019-1644-y

Clarke, G., Grenham, S., Scully, P., Fitzgerald, P., Moloney, R., Shanahan, F., et al. (2013). The microbiome-gut-brain axis during early life regulates the hippocampal serotonergic system in a sex-dependent manner. *Mol. Psychiatry* 18:666. doi: 10.1038/mp.2012.77

Codagnone, M. G., Spichak, S., O'Mahony, S. M., O'Leary, O. F., Clarke, G., Stanton, C., et al. (2019). Programming bugs: microbiota and the developmental origins of brain health and disease. *Biol. Psychiatry* 85, 150–163. doi: 10.1016/j.biopsych.2018.06.014

Colen, C. G., and Ramey, D. M. (2014). Is breast truly best? Estimating the effects of breastfeeding on long-term child health and wellbeing in the United States using sibling comparisons. *Soc. Sci. Med.* 109, 55–65. doi: 10.1016/j.socscimed.2014.01.027

Cong, X., Henderson, W. A., Graf, J., and McGrath, J. M. (2015). Early life experience and gut microbiome: the brain-gut-microbiota Signaling system. *Adv. Neonatal Care* 15, 314–323. doi: 10.1097/ANC.0000000000000191

Conlon, M. A., and Bird, A. R. (2014). The impact of diet and lifestyle on gut microbiota and human health. *Nutrients* 7, 17–44. doi: 10.3390/nu7010017

Corrêa, N. B., Péret Filho, L. A., Penna, F. J., Lima, F. M., and Nicoli, J. R. (2005). A randomized formula controlled trial of Bifidobacterium lactis and Streptococcus thermophilus for prevention of antibiotic-associated diarrhea in infants. *J. Clin. Gastroenterol.* 39, 385–389. doi: 10.1097/01.mcg.0000159217.47419.5b

Cowan, C. S. M., Dinan, T. G., and Cryan, J. F. (2020). Annual research review: critical windows – the microbiota-gut-brain axis in neurocognitive development. *J. Child Psychol. Psychiatry* 61, 353–371. doi: 10.1111/jcpp.13156

Cryan, J. F., and Dinan, T. G. (2012). Mind-altering microorganisms: the impact of the gut microbiota on brain and behaviour. *Nat. Rev. Neurosci.* 13, 701–712. doi: 10.1038/nrn3346

Cryan, J. F., O'Riordan, K. J., Cowan, C. S. M., Sandhu, K. V., Bastiaanssen, T. F. S., Boehme, M., et al. (2019). The microbiota-gut-brain Axis. *Physiol. Rev.* 99, 1877–2013. doi: 10.1152/physrev.00018.2018

Cussotto, S., Sandhu, K. V., Dinan, T. G., and Cryan, J. F. (2018). The neuroendocrinology of the microbiota-gut-brain Axis: a behavioural perspective. *Front. Neuroendocrinol.* 51, 80–101. doi: 10.1016/j.yfrne.2018.04.002

Daniels, W. M., Pietersen, C. Y., Carstens, M. E., and Stein, D. J. (2004). Maternal separation in rats leads to anxiety-like behavior and a blunted ACTH response and altered neurotransmitter levels in response to a subsequent stressor. *Metab. Brain Dis.* 19, 3–14. doi: 10.1023/B:MEBR.0000027412.19664.b3

de Goffau, M. C., Lager, S., Sovio, U., Gaccioli, F., Cook, E., Peacock, S. J., et al. (2019). Human placenta has no microbiome but can contain potential pathogens. *Nature* 572, 329–334. doi: 10.1038/s41586-019-1451-5

de Weerth, C. (2017). Do bacteria shape our development? Crosstalk between intestinal microbiota and HPA axis. *Neurosci. Biobehav. Rev.* 83, 458–471. doi: 10.1016/j.neubiorev.2017.09.016

Diaz Heijtz, R., Wang, S., Anuar, F., Qian, Y., Bjorkholm, B., Samuelsson, A., et al. (2011). Normal gut microbiota modulates brain development and behavior. *Proc. Natl. Acad. Sci. U. S. A.* 108, 3047–3052. doi: 10.1073/pnas.1010529108

Doifode, T., Giridharan, V. V., Generoso, J. S., Bhatti, G., Collodel, A., Schulz, P. E., et al. (2021). The impact of the microbiota-gut-brain axis on Alzheimer's disease pathophysiology. *Pharmacol. Res.* 164:105314. doi: 10.1016/j.phrs.2020.105314

Donaldson, G. P., Lee, S. M., and Mazmanian, S. K. (2016). Gut biogeography of the bacterial microbiota. *Nat. Rev. Microbiol.* 14, 20–32. doi: 10.1038/nrmicro3552

Douglas-Escobar, M., Elliott, E., and Neu, J. (2013). Effect of intestinal microbial ecology on the developing brain. *JAMA Pediatr.* 167, 374–379. doi: 10.1001/jamapediatrics.2013.497

Erny, D., Hrabě de Angelis, A. L., Jaitin, D., Wieghofer, P., Staszewski, O., David, E., et al. (2015). Host microbiota constantly control maturation and function of microglia in the CNS. *Nat. Neurosci.* 18, 965–977. doi: 10.1038/nn.4030

Eshraghi, R. S., Deth, R. C., Mittal, R., Aranke, M., Kay, S. S., Moshiree, B., et al. (2018). Early disruption of the microbiome leading to decreased antioxidant capacity and epigenetic changes: implications for the rise in autism. *Front. Cell. Neurosci.* 12:256. doi: 10.3389/fncel.2018.00256

Fallani, M., Amarri, S., Uusijarvi, A., Adam, R., Khanna, S., Aguilera, M., et al. (2011a). Determinants of the human infant intestinal microbiota after the introduction of first complementary foods in infant samples from five European centres. *Microbiology* 157, 1385–1392. doi: 10.1099/mic.0.042143-0

Fallani, M., Amarri, S., Uusijarvi, A., Adam, R., Khanna, S., Aguilera, M., et al. (2011b). The Infabio, determinants of the human infant intestinal microbiota after

the introduction of first complementary foods in infant samples from five European centres. *Microbiology* 157, 1385–1392.

Fernández, L., Ruiz, L., Jara, J., Orgaz, B., and Rodríguez, J. M. (2018). Strategies for the preservation, restoration and modulation of the human milk microbiota. Implications for human milk banks and neonatal intensive care units. *Front. Microbiol.* 9:2676. doi: 10.3389/fmicb.2018.02676

Foster, J. A., and McVey Neufeld, K. A. (2013). Gut-brain axis: how the microbiome influences anxiety and depression. *Trends Neurosci.* 36, 305–312. doi: 10.1016/j.tins.2013.01.005

Frost, G., Sleeth, M. L., Sahuri-Arisoylu, M., Lizarbe, B., Cerdan, S., Brody, L., et al. (2014). The short-chain fatty acid acetate reduces appetite via a central homeostatic mechanism. *Nat. Commun.* 5:3611. doi: 10.1038/ncomms4611

Fulling, C., Dinan, T. G., and Cryan, J. F. (2019). Gut microbe to brain Signaling: what happens in Vagus. *Neuron* 101, 998–1002. doi: 10.1016/j.neuron.2019.02.008

Gareau, M. G. (2016). Cognitive function and the microbiome. *Int. Rev. Neurobiol.* 131, 227–246. doi: 10.1016/bs.irn.2016.08.001

Gareau, M. G., Wine, E., Rodrigues, D. M., Cho, J. H., Whary, M. T., Philpott, D. J., et al. (2011). Bacterial infection causes stress-induced memory dysfunction in mice. *Gut* 60, 307–317. doi: 10.1136/gut.2009.202515

Geng, S., Yang, L., Cheng, F., Zhang, Z., Li, J., Liu, W., et al. (2019). Gut microbiota are associated with psychological stress-induced defections in intestinal and blood-brain barriers. *Front. Microbiol.* 10:3067. doi: 10.3389/fmicb.2019.03067

Gershon, M. D. (2013). 5-Hydroxytryptamine (serotonin) in the gastrointestinal tract. *Curr. Opin. Endocrinol. Diabetes Obes.* 20, 14–21. doi: 10.1097/MED.0b013e32835bc703

Gershon, M. D., and Tack, J. (2007). The serotonin signaling system: from basic understanding to drug development for functional GI disorders. *Gastroenterology* 132, 397–414. doi: 10.1053/j.gastro.2006.11.002

Godfrey, D. I., Koay, H. F., McCluskey, J., and Gherardin, N. A. (2019). The biology and functional importance of MAIT cells. *Nat. Immunol.* 20, 1110–1128. doi: 10.1038/s41590-019-0444-8

Goehler, L. E., Gaykema, R. P., Opitz, N., Reddaway, R., Badr, N., and Lyte, M. (2005). Activation in vagal afferents and central autonomic pathways: early responses to intestinal infection with campylobacter jejuni. *Brain Behav. Immun.* 19, 334–344. doi: 10.1016/j.bbi.2004.09.002

Gopalakrishna, K. P., Macadangdang, B. R., Rogers, M. B., Tometich, J. T., Firek, B. A., Baker, R., et al. (2019). Maternal IgA protects against the development of necrotizing enterocolitis in preterm infants. *Nat. Med.* 25, 1110–1115. doi: 10.1038/s41591-019-0480-9

Guevarra, R. B., Hong, S. H., Cho, J. H., Kim, B. R., Shin, J., Lee, J. H., et al. (2018). The dynamics of the piglet gut microbiome during the weaning transition in association with health and nutrition. *J. Anim. Sci. Biotechnol.* 9:54. doi: 10.1186/s40104-018-0269-6

Guevarra, R. B., Lee, J. H., Lee, S. H., Seok, M. J., Kim, D. W., Kang, B. N., et al. (2019). Piglet gut microbial shifts early in life: causes and effects. *J. Anim. Sci. Biotechnol.* 10:1. doi: 10.1186/s40104-018-0308-3

Guida, F., Turco, F., Iannotta, M., De Gregorio, D., Palumbo, I., Sarnelli, G., et al. (2018). Antibiotic-induced microbiota perturbation causes gut endocannabinoidome changes, hippocampal neuroglial reorganization and depression in mice. *Brain Behav. Immun.* 67, 230–245. doi: 10.1016/j.bbi.2017.09.001

Guitor, A. K., Yousuf, E. I., Raphenya, A. R., Hutton, E. K., Morrison, K. M., McArthur, A. G., et al. (2022). Capturing the antibiotic resistome of preterm infants reveals new benefits of probiotic supplementation. *Microbiome* 10:136. doi: 10.1186/s40168-022-01327-7

Haghikia, A., Jorg, S., Duscha, A., Berg, J., Manzel, A., Waschbisch, A., et al. (2015). Dietary fatty acids directly impact central nervous system autoimmunity via the small intestine. *Immunity* 43, 817–829. doi: 10.1016/j.immuni.2015.09.007

Harmsen, H. J., Wildeboer-Veloo, A. C., Raangs, G. C., Wagendorp, A. A., Klijn, N., Bindels, J. G., et al. (2000). Analysis of intestinal flora development in breast-fed and formula-fed infants by using molecular identification and detection methods. *J. Pediatr. Gastroenterol. Nutr.* 30, 61–67. doi: 10.1097/00005176-200001000-00019

Haynes, B. F., and Heinly, C. S. (1995). Early human T cell development: analysis of the human thymus at the time of initial entry of hematopoietic stem cells into the fetal thymic microenvironment. *J. Exp. Med.* 181, 1445–1458. doi: 10.1084/jem.181.4.1445

Haynes, B. F., Martin, M. E., Kay, H. H., and Kurtzberg, J. (1988). Early events in human T cell ontogeny. Phenotypic characterization and immunohistologic localization of T cell precursors in early human fetal tissues. *J. Exp. Med.* 168, 1061–1080. doi: 10.1084/jem.168.3.1061

He, X., Parenti, M., Grip, T., Lönnerdal, B., Timby, N., Domellöf, M., et al. (2019). Fecal microbiome and metabolome of infants fed bovine MFGM supplemented formula or standard formula with breast-fed infants as reference: a randomized controlled trial. *Sci. Rep.* 9:11589. doi: 10.1038/s41598-019-47953-4

Heiman, M. L., and Greenway, F. L. (2016). A healthy gastrointestinal microbiome is dependent on dietary diversity. *Mol. Metab* 5, 317–320. doi: 10.1016/j.molmet.2016.02.005

Hoban, A. E., Moloney, R. D., Golubeva, A. V., McVey Neufeld, K. A., O'Sullivan, O., Patterson, E., et al. (2016). Behavioural and neurochemical consequences of chronic gut microbiota depletion during adulthood in the rat. *Neuroscience* 339, 463–477. doi: 10.1016/j.neuroscience.2016.10.003

Hoebe, K., Janssen, E., and Beutler, B. (2004). The interface between innate and adaptive immunity. *Nat. Immunol.* 5, 971–974. doi: 10.1038/ni1004-971

Hoeman, C. M., Dhakal, M., Zaghouani, A. A., Cascio, J. A., Wan, X., Khairallah, M. T., et al. (2013). Developmental expression of IL-12Rbeta2 on murine naive neonatal T cells counters the upregulation of IL-13Ralpha1 on primary Th1 cells and balances immunity in the newborn. *J. Immunol.* 190, 6155–6163. doi: 10.4049/jimmunol.1202207

Houghteling, P. D., and Walker, W. A. (2015). Why is initial bacterial colonization of the intestine important to infants' and children's health? *J. Pediatr. Gastroenterol. Nutr.* 60, 294–307. doi: 10.1097/MPG.0000000000000597

Hu, J., Nie, Y., Chen, J., Zhang, Y., Wang, Z., Fan, Q., et al. (2016). Gradual changes of gut microbiota in weaned miniature piglets. *Front. Microbiol.* 7:1727. doi: 10.3389/fmicb.2016.01727

Hunt, K. M., Foster, J. A., Forney, L. J., Schutte, U. M., Beck, D. L., Abdo, Z., et al. (2011). Characterization of the diversity and temporal stability of bacterial communities in human milk. *PLoS One* 6:e21313. doi: 10.1371/journal.pone.0021313

Hyland, N. P., and Cryan, J. F. (2016). Microbe-host interactions: influence of the gut microbiota on the enteric nervous system. *Dev. Biol.* 417, 182–187. doi: 10.1016/j.ydbio.2016.06.027

Indrio, F., Di Mauro, A., Riezzo, G., Civardi, E., Intini, C., Corvaglia, L., et al. (2014). Prophylactic use of a probiotic in the prevention of colic, regurgitation, and functional constipation: a randomized clinical trial. *JAMA Pediatr.* 168, 228–233. doi: 10.1001/jamapediatrics.2013.4367

Jameson, K. G., and Hsiao, E. Y. (2018). Linking the gut microbiota to a brain neurotransmitter. *Trends Neurosci.* 41, 413–414. doi: 10.1016/j.tins.2018.04.001

Jost, T., Lacroix, C., Braegger, C. P., and Chassard, C. (2012). New insights in gut microbiota establishment in healthy breast fed neonates. *PLoS One* 7:e44595. doi: 10.1371/journal.pone.0044595

Kapourchali, F. R., and Cresci, G. A. M. (2020). Early-life gut microbiome—the importance of maternal and infant factors in its establishment. *Nutr. Clin. Pract.* 35, 386–405. doi: 10.1002/ncp.10490

Kelly, J. R., Borre, Y., O'Brien, C., Patterson, E., El Aidy, S., Deane, J., et al. (2016). Transferring the blues: depression-associated gut microbiota induces neurobehavioural changes in the rat. *J. Psychiatr. Res.* 82, 109–118. doi: 10.1016/j.jpsychires.2016.07.019

Kobek-Kjeldager, C., Schönherz, A. A., Canibe, N., and Pedersen, L. J. (2022). Diet and microbiota-gut-brain axis in relation to tail biting in pigs: a review. *Appl. Anim. Behav. Sci.* 246:105514. doi: 10.1016/j.applanim.2021.105514

Korpela, K., Helve, O., Kolho, K. L., Saisto, T., Skogberg, K., Dikareva, E., et al. (2020). Maternal Fecal microbiota transplantation in Cesarean-born infants rapidly restores Normal gut microbial development: a proof-of-concept study. *Cells* 183, 324–334 e5. doi: 10.1016/j.cell.2020.08.047

Korpela, K., Salonen, A., Virta, L. J., Kumpu, M., Kekkonen, R. A., and de Vos, W. M. (2016). Lactobacillus rhamnosus GG intake modifies preschool Children's intestinal microbiota, alleviates penicillin-associated changes, and reduces antibiotic use. *PLoS One* 11:e0154012. doi: 10.1371/journal.pone.0154012

Kowalewska-Kantecka, B. (2016). Breastfeeding – an important element of health promotion. *Dev. Period Med.* 20, 354–357.

Kraimi, N., Lormant, F., Calandreau, L., Kempf, F., Zemb, O., Lemarchand, J., et al. (2022). Microbiota and stress: a loop that impacts memory. *Psychoneuroendocrinology* 136:105594. doi: 10.1016/j.psyneuen.2021.105594

Larke, J. A., Kuhn-Riordon, K., Taft, D. H., Sohn, K., Iqbal, S., Underwood, M. A., et al. (2022). Preterm infant Fecal microbiota and metabolite profiles are modulated in a probiotic specific manner. *J. Pediatr. Gastroenterol. Nutr.* 75, 535–542. doi: 10.1097/MPG.0000000000003570

Laursen, M. F. (2021). Gut microbiota development: influence of diet from infancy to toddlerhood. *Ann. Nutr. Metab.* 77, 21–34. doi: 10.3389/fmicb.2017.00356

Laursen, M. F., Bahl, M. I., Michaelsen, K. F., and Licht, T. R. (2017). First foods and gut microbes. *Front. Microbiol.* 8:356. doi: 10.3389/fmicb.2017.00356

Liang, S., Wang, T., Hu, X., Luo, J., Li, W., Wu, X., et al. (2015). Administration of lactobacillus helveticus NS8 improves behavioral, cognitive, and biochemical aberrations caused by chronic restraint stress. *Neuroscience* 310, 561–577. doi: 10.1016/j.neuroscience.2015.09.033

Liang, S., Wu, X., Hu, X., Wang, T., and Jin, F. (2018a). Recognizing depression from the microbiota–Gut–Brain Axis. *Int. J. Mol. Sci.* 19:1592. doi: 10.3390/ijms19061592

Liang, S., Wu, X., and Jin, F. (2018b). Gut-brain psychology: rethinking psychology from the microbiota-gut-brain Axis. *Front. Integr. Neurosci.* 12:33. doi: 10.3389/fnint.2018.00033

Liang, L., Zhou, H., Zhang, S., Yuan, J., and Wu, H. (2017). Effects of gut microbiota disturbance induced in early life on the expression of extrasynaptic GABA-A receptor α5 and δ subunits in the hippocampus of adult rats. *Brain Res. Bull.* 135, 113–119. doi: 10.1016/j.brainresbull.2017.09.014

Liu, C., Yang, S. Y., Wang, L., and Zhou, F. (2022). The gut microbiome: implications for neurogenesis and neurological diseases. *Neural Regen. Res.* 17, 53–58. doi: 10.4103/1673-5374.315227

Ma, J., Li, Z., Zhang, W., Zhang, C., Zhang, Y., Mei, H., et al. (2020). Comparison of gut microbiota in exclusively breast-fed and formula-fed babies: a study of 91 term infants. *Sci. Rep.* 10:15792. doi: 10.1080/19490976.2020.1785252

Ma, C., Wasti, S., Huang, S., Zhang, Z., Mishra, R., Jiang, S., et al. (2020). The gut microbiome stability is altered by probiotic ingestion and improved by the continuous supplementation of galactooligosaccharide. *Gut Microbes* 12:1785252. doi: 10.1080/19490976.2020.1785252

Manderino, L., Carroll, I., Azcarate-Peril, M. A., Rochette, A., Heinberg, L., Peat, C., et al. (2017). Preliminary evidence for an association between the composition of the gut microbiome and cognitive function in neurologically healthy older adults. *J. Int. Neuropsychol. Soc.* 23, 700–705. doi: 10.1017/S1355617717000492

Margolis, K. G., Cryan, J. F., and Mayer, E. A. (2021). The microbiota-gut-brain Axis: from motility to mood. *Gastroenterology* 160, 1486–1501. doi: 10.1053/j.gastro.2020.10.066

Martin, C. R., Osadchiy, V., Kalani, A., and Mayer, E. A. (2018). The brain-gut-microbiome Axis. *Cell. Mol. Gastroenterol. Hepatol.* 6, 133–148. doi: 10.1016/j.jcmgh.2018.04.003

Mastromarino, P., Capobianco, D., Campagna, G., Laforgia, N., Drimaco, P., Dileone, A., et al. (2014). Correlation between lactoferrin and beneficial microbiota in breast milk and infant's feces. *Biometals* 27, 1077–1086. doi: 10.1007/s10534-014-9762-3

Matsuyama, M., Morrison, M., Cao, K.-A. L., Pruilh, S., Davies, P. S. W., Wall, C., et al. (2019). Dietary intake influences gut microbiota development of healthy Australian children from the age of one to two years. *Sci. Rep.* 9:12476. doi: 10.1038/s41598-019-48658-4

Mayer, E. A. (2011). Gut feelings: the emerging biology of gut-brain communication. *Nat. Rev. Neurosci.* 12, 453–466. doi: 10.1038/nrn3071

Mayer, E. A., Knight, R., Mazmanian, S. K., Cryan, J. F., and Tillisch, K. (2014). Gut microbes and the brain: paradigm shift in neuroscience. *J. Neurosci.* 34, 15490–15496. doi: 10.1523/JNEUROSCI.3299-14.2014

McFarland, L. V., Evans, C. T., and Goldstein, E. J. (2018). Strain-specificity and disease-specificity of probiotic efficacy: a systematic review and meta-analysis. *Front. Med.* 5:124. doi: 10.3389/fmed.2018.00124

Milani, C., Duranti, S., Bottacini, F., Casey, E., Turroni, F., Mahony, J., et al. (2017). The first microbial colonizers of the human gut: composition, activities, and health implications of the infant gut microbiota. *Microbiol. Mol. Biol. Rev.* 81, e00036–e00017. doi: 10.1128/MMBR.00036-17

Mirpuri, J., Raetz, M., Sturge, C. R., Wilhelm, C. L., Benson, A., Savani, R. C., et al. (2014). Proteobacteria-specific IgA regulates maturation of the intestinal microbiota. *Gut Microbes* 5, 28–39. doi: 10.4161/gmic.26489

Mohajeri, M. H., Brummer, R. J. M., Rastall, R. A., Weersma, R. K., Harmsen, H. J. M., Faas, M., et al. (2018). The role of the microbiome for human health: from basic science to clinical applications. *Eur. J. Nutr.* 57:(Suppl 1):S1–S14. doi: 10.1007/s00394-018-1703-4

Mudd, A. T., and Dilger, R. N. (2017). Early-life nutrition and neurodevelopment: use of the piglet as a translational model. *Adv. Nutr.* 8, 92–104. doi: 10.3945/an.116.013243

Nankova, B. B., Agarwal, R., MacFabe, D. F., and La Gamma, E. F. (2014). Enteric bacterial metabolites propionic and butyric acid modulate gene expression, including CREB-dependent catecholaminergic neurotransmission, in PC12 cells--possible relevance to autism spectrum disorders. *PLoS One* 9:e103740. doi: 10.1371/journal.pone.0103740

Nash, M. J., Frank, D. N., and Friedman, J. E. (2017). Early microbes modify immune system development and metabolic homeostasis-the "restaurant" hypothesis revisited. *Front. Endocrinol.* 8:349. doi: 10.3389/fendo.2017.00349

Neufeld, K. A., Kang, N., Bienenstock, J., and Foster, J. A. (2011). Effects of intestinal microbiota on anxiety-like behavior. *Commun. Integr. Biol.* 4, 492–494. doi: 10.4161/cib.4.4.15702

Neufeld, K. M., Kang, N., Bienenstock, J., and Foster, J. A. (2011). Reduced anxiety-like behavior and central neurochemical change in germ-free mice. *Neurogastroenterol. Motil.* 23, 255–e119. doi: 10.1111/j.1365-2982.2010.01620.x

Newburg, D. S., and Walker, W. A. (2007). Protection of the neonate by the innate immune system of developing gut and of human milk. *Pediatr. Res.* 61, 2–8. doi: 10.1203/01.pdr.0000250274.68571.18

Nishino, R., Mikami, K., Takahashi, H., Tomonaga, S., Furuse, M., Hiramoto, T., et al. (2013). Commensal microbiota modulate murine behaviors in a strictly contamination-free environment confirmed by culture-based methods. *Neurogastroenterol. Motil.* 25, 521–528. doi: 10.1111/nmo.12110

O'Neill, I. J., Sanchez Gallardo, R., Saldova, R., Murphy, E. F., Cotter, P. D., McAuliffe, F. M., et al. (2020). Maternal and infant factors that shape neonatal gut colonization by bacteria. *Expert Rev. Gastroenterol. Hepatol.* 14, 651–664. doi: 10.1080/17474124.2020.1784725

Ohland, C. L., Kish, L., Bell, H., Thiesen, A., Hotte, N., Pankiv, E., et al. (2013). Effects of lactobacillus helveticus on murine behavior are dependent on diet and genotype and correlate with alterations in the gut microbiome. *Psychoneuroendocrinology* 38, 1738–1747. doi: 10.1016/j.psyneuen.2013.02.008

Ohsawa, K., Uchida, N., Ohki, K., Nakamura, Y., and Yokogoshi, H. (2015). Lactobacillus helveticus-fermented milk improves learning and memory in mice. *Nutr. Neurosci.* 18, 232–240. doi: 10.1179/1476830514y.0000000122

O'Keefe, S. J. (2016). Diet, microorganisms and their metabolites, and colon cancer. *Nat. Rev. Gastroenterol. Hepatol.* 13, 691–706. doi: 10.1038/nrgastro.2016.165

Oleskin, A. V., and Shenderov, B. A. (2016). Neuromodulatory effects and targets of the SCFAs and gasotransmitters produced by the human symbiotic microbiota. *Microb. Ecol. Health Dis.* 27:30971. doi: 10.3402/mehd.v27.30971

Olivares, M., Díaz-Ropero, M., Martín, R., Rodríguez, J., and Xaus, J. (2006). Antimicrobial potential of four lactobacillus strains isolated from breast milk. *J. Appl. Microbiol.* 101, 72–79. doi: 10.1111/j.1365-2672.2006.02981.x

O'Mahony, S. M., Hyland, N. P., Dinan, T. G., and Cryan, J. F. (2011). Maternal separation as a model of brain-gut axis dysfunction. *Psychopharmacology* 214, 71–88. doi: 10.1007/s00213-010-2010-9

O'Mahony, S. M., Marchesi, J. R., Scully, P., Codling, C., Ceolho, A. M., Quigley, E. M., et al. (2009). Early life stress alters behavior, immunity, and microbiota in rats: implications for irritable bowel syndrome and psychiatric illnesses. *Biol. Psychiatry* 65, 263–267. doi: 10.1016/j.biopsych.2008.06.026

Osadchiy, V., Martin, C. R., and Mayer, E. A. (2019). The gut–brain Axis and the microbiome: mechanisms and clinical implications. *Clin. Gastroenterol. Hepatol.* 17, 322–332. doi: 10.1016/j.cgh.2018.10.002

Pabst, R. (2020). The pig as a model for immunology research. *Cell Tissue Res.* 380, 287–304. doi: 10.1007/s00441-020-03206-9

Panigrahi, P., Parida, S., Nanda, N. C., Satpathy, R., Pradhan, L., Chandel, D. S., et al. (2017). A randomized synbiotic trial to prevent sepsis among infants in rural India. *Nature* 548, 407–412. doi: 10.1038/nature23480

Parada Venegas, D., De la Fuente, M. K., Landskron, G., Gonzalez, M. J., Quera, R., Dijkstra, G., et al. (2019). Short chain fatty acids (SCFAs)-mediated gut epithelial and immune regulation and its relevance for inflammatory bowel diseases. *Front. Immunol.* 10:277. doi: 10.3389/fimmu.2019.00277

Pärtty, A., Kalliomäki, M., Wacklin, P., Salminen, S., and Isolauri, E. (2015). A possible link between early probiotic intervention and the risk of neuropsychiatric disorders later in childhood: a randomized trial. *Pediatr. Res.* 77, 823–828. doi: 10.1038/pr.2015.51

Petra, A. I., Panagiotidou, S., Hatziagelaki, E., Stewart, J. M., Conti, P., and Theoharides, T. C. (2015). Gut-microbiota-brain Axis and its effect on neuropsychiatric disorders with suspected immune Dysregulation. *Clin. Ther.* 37, 984–995. doi: 10.1016/j.clinthera.2015.04.002

Rautava, S., and Walker, W. A. (2009). Academy of breastfeeding medicine founder's lecture 2008: breastfeeding–an extrauterine link between mother and child. *Breastfeed. Med.* 4, 3–10. doi: 10.1089/bfm.2009.0004

Rechavi, E., Lev, A., Lee, Y. N., Simon, A. J., Yinon, Y., Lipitz, S., et al. (2015). Timely and spatially regulated maturation of B and T cell repertoire during human fetal development. *Sci. Transl. Med.* 7:276ra25. doi: 10.1126/scitranslmed.aaa0072

Rhee, S. H., Pothoulakis, C., and Mayer, E. A. (2009). Principles and clinical implications of the brain-gut-enteric microbiota axis. *Nat. Rev. Gastroenterol. Hepatol.* 6, 306–314. doi: 10.1038/nrgastro.2009.35

Rincel, M., and Darnaudéry, M. (2019). Maternal separation in rodents: a journey from gut to brain and nutritional perspectives. *Proc. Nutr. Soc.* 79, 113–132. doi: 10.1017/S0029665119000958

Rinninella, E., Raoul, P., Cintoni, M., Franceschi, F., Miggiano, G. A. D., Gasbarrini, A., et al. (2019). What is the healthy gut microbiota composition? A changing ecosystem across age, environment, diet, and diseases. *Microorganisms* 7:14. doi: 10.3390/microorganisms7010014

Rios-Covian, D., Ruas-Madiedo, P., Margolles, A., Gueimonde, M., de Los Reyes-Gavilan, C. G., and Salazar, N. (2016). Intestinal short chain fatty acids and their link with diet and human health. *Front. Microbiol.* 7:185. doi: 10.3389/fmicb.2016.00185

Rogier, E. W., Frantz, A. L., Bruno, M. E., Wedlund, L., Cohen, D. A., Stromberg, A. J., et al. (2014). Secretory antibodies in breast milk promote long-term intestinal homeostasis by regulating the gut microbiota and host gene expression. *Proc. Natl. Acad. Sci. U. S. A.* 111, 3074–3079. doi: 10.1073/pnas.1315792111

Romijn, A. R., and Rucklidge, J. J. (2015). Systematic review of evidence to support the theory of psychobiotics. *Nutr. Rev.* 73, 675–693. doi: 10.1093/nutrit/nuv025

Rowland, I., Gibson, G., Heinken, A., Scott, K., Swann, J., Thiele, I., et al. (2018). Gut microbiota functions: metabolism of nutrients and other food components. *Eur. J. Nutr.* 57, 1–24. doi: 10.1007/s00394-017-1445-8

Rudzki, L., Pawlak, D., Pawlak, K., Waszkiewicz, N., Małus, A., Konarzewska, B., et al. (2017). Immune suppression of IgG response against dairy proteins in major depression. *BMC Psychiatry* 17:268. doi: 10.1186/s12888-017-1431-y

Sagebiel, A. F., Steinert, F., Lunemann, S., Korner, C., Schreurs, R., Altfeld, M., et al. (2019). Tissue-resident Eomes(+) NK cells are the major innate lymphoid cell population in human infant intestine. *Nat. Commun.* 10:975. doi: 10.1038/s41467-018-08267-72

Salcedo, J., Frese, S. A., Mills, D. A., and Barile, D. (2016). Characterization of porcine milk oligosaccharides during early lactation and their relation to the fecal microbiome. *J. Dairy Sci.* 99, 7733–7743. doi: 10.3168/jds.2016-10966

Samuel, B. S., Shaito, A., Motoike, T., Rey, F. E., Backhed, F., Manchester, J. K., et al. (2008). Effects of the gut microbiota on host adiposity are modulated by the short-chain fatty-acid binding G protein-coupled receptor, Gpr41. *Proc. Natl. Acad. Sci. U. S. A.* 105, 16767–16772. doi: 10.1073/pnas.0808567105

Saulnier, D. M., Ringel, Y., Heyman, M. B., Foster, J. A., Bercik, P., Shulman, R. J., et al. (2013). The intestinal microbiome, probiotics and prebiotics in neurogastroenterology. *Gut Microbes* 4, 17–27. doi: 10.4161/gmic.22973

Savignac, H. M., Tramullas, M., Kiely, B., Dinan, T. G., and Cryan, J. F. (2015). Bifidobacteria modulate cognitive processes in an anxious mouse strain. *Behav. Brain Res.* 287, 59–72. doi: 10.1016/j.bbr.2015.02.044

Schonland, S. O., Zimmer, J. K., Lopez-Benitez, C. M., Widmann, T., Ramin, K. D., Goronzy, J. J., et al. (2003). Homeostatic control of T-cell generation in neonates. *Blood* 102, 1428–1434. doi: 10.1182/blood-2002-11-3591

Schwab, C., and Gänzle, M. (2011). Lactic acid bacteria fermentation of human milk oligosaccharide components, human milk oligosaccharides and galactooligosaccharides. *FEMS Microbiol. Lett.* 315, 141–148. doi: 10.1111/j.1574-6968.2010.02185.x

Schwartz, S., Friedberg, I., Ivanov, I. V., Davidson, L. A., Goldsby, J. S., Dahl, D. B., et al. (2012). A metagenomic study of diet-dependent interaction between gut microbiota and host in infants reveals differences in immune response. *Genome Biol.* 13:r32. doi: 10.1186/gb-2012-13-4-r32

Semmes, E. C., Chen, J. L., Goswami, R., Burt, T. D., Permar, S. R., and Fouda, G. G. (2020). Understanding early-life adaptive immunity to guide interventions for Pediatric health. *Front. Immunol.* 11:595297. doi: 10.3389/fimmu.2020.595297

Shulzhenko, N., Morgun, A., Hsiao, W., Battle, M., Yao, M., Gavrilova, O., et al. (2011). Crosstalk between B lymphocytes, microbiota and the intestinal epithelium governs immunity versus metabolism in the gut. *Nat. Med.* 17, 1585–1593. doi: 10.1038/nm.2505

Siegrist, C.-A., and Aspinall, R. (2009). B-cell responses to vaccination at the extremes of age. *Nat. Rev. Immunol.* 9, 185–194. doi: 10.1038/nri2508

Silva, Y. P., Bernardi, A., and Frozza, R. L. (2020). The role of short-chain fatty acids from gut microbiota in gut-brain communication. *Front. Endocrinol.* 11:25. doi: 10.3389/fendo.2020.00025

Smeekens, J. M., Johnson-Weaver, B. T., Hinton, A. L., Azcarate-Peril, M. A., Moran, T. P., Immormino, R. M., et al. (2020). Fecal IgA, antigen absorption, and gut microbiome composition are associated with food antigen sensitization in genetically susceptible mice. *Front. Immunol.* 11:599637. doi: 10.3389/fimmu.2020.599637

Sudo, N., Chida, Y., Aiba, Y., Sonoda, J., Oyama, N., Yu, X. N., et al. (2004). Postnatal microbial colonization programs the hypothalamic-pituitary-adrenal system for stress response in mice. *J. Physiol.* 558, 263–275. doi: 10.1113/jphysiol.2004.063388

Taft, D. H., Liu, J., Maldonado-Gomez, M. X., Akre, S., Huda, M. N., Ahmad, S. M., et al. (2018). Bifidobacterial dominance of the gut in early life and acquisition of antimicrobial resistance. *mSphere* 3, e00441–e00418. doi: 10.1128/mSphere.00441-18

Tao, N., Ochonicky, K. L., German, J. B., Donovan, S. M., and Lebrilla, C. B. (2010). Structural determination and daily variations of porcine milk oligosaccharides. *J. Agric. Food Chem.* 58, 4653–4659. doi: 10.1021/jf100398u

Thursby, E., and Juge, N. (2017). Introduction to the human gut microbiota. *Biochem. J.* 474, 1823–1836. doi: 10.1042/BCJ20160510

Tolhurst, G., Heffron, H., Lam, Y. S., Parker, H. E., Habib, A. M., Diakogiannaki, E., et al. (2012). Short-chain fatty acids stimulate glucagon-like peptide-1 secretion via the G-protein-coupled receptor FFAR2. *Diabetes* 61, 364–371. doi: 10.2337/db11-1019

Tooley, K. L. (2020). Effects of the human gut microbiota on cognitive performance, brain structure and function: a narrative review. *Nutrients* 12:3009. doi: 10.3390/nu12103009

Tuaillon, E., Valea, D., Becquart, P., Al Tabaa, Y., Meda, N., Bollore, K., et al. (2009). Human milk-derived B cells: a highly activated switched memory cell population primed to secrete antibodies. *J. Immunol.* 182, 7155–7162. doi: 10.4049/jimmunol.0803107

Underwood, M. A., Umberger, E., and Patel, R. M. (2020). Safety and efficacy of probiotic administration to preterm infants: ten common questions. *Pediatr. Res.* 88, 48–55. doi: 10.1038/s41390-020-1080-6

Vaher, K. K. K. (2022). Microbiome-gut-brain axis in brain development, cognition and behavior during infancy and early childhood. *Dev. Rev.* 66:1011038. doi: 10.1016/j.dr.2022.101038

Val-Laillet, D. (2019). Review: impact of food, gut-brain signals and metabolic status on brain activity in the pig model: 10 years of nutrition research using in vivo brain imaging. *Animal* 13, 2699–2713. doi: 10.1017/S1751731119001745

Vuong, H. E., Yano, J. M., Fung, T. C., and Hsiao, E. Y. (2017). The microbiome and host behavior. *Annu. Rev. Neurosci.* 40, 21–49. doi: 10.1146/annurev-neuro-072116-031347

Walker, W. A. (2017). The importance of appropriate initial bacterial colonization of the intestine in newborn, child, and adult health. *Pediatr. Res.* 82, 387–395. doi: 10.1038/pr.2017.111

Walker, W. A., and Iyengar, R. S. (2015). Breast milk, microbiota, and intestinal immune homeostasis. *Pediatr. Res.* 77, 220–228. doi: 10.1038/pr.2014.160

Wang, T., Hu, X., Liang, S., Li, W., Wu, X., Wang, L., et al. (2015). Lactobacillus fermentum NS9 restores the antibiotic induced physiological and psychological abnormalities in rats. *Benef. Microbes* 6, 707–717. doi: 10.3920/BM2014.0177

Wang, F. B., and Powley, T. L. (2007). Vagal innervation of intestines: afferent pathways mapped with new en bloc horseradish peroxidase adaptation. *Cell Tissue Res.* 329, 221–230. doi: 10.1007/s00441-007-0413-7

Weatheall, D. (2006). The Use of Non-Human Primates in Research A Working Group Report Chaired by Sir David Weatherall FRS FmedSci Institution: The Academy of Medical Sciences, Medical Research Council, The Royal Society, Wellcome Trust. Available at: https://royalsociety.org/policy/publications/2006/weatherall-report/

Wei George, Z., Martin Katherine, A., Xing Peter, Y., Agrawal, R., Whiley, L., Wood Thomas, K., et al. (2021). Tryptophan-metabolizing gut microbes regulate adult neurogenesis via the aryl hydrocarbon receptor. *Proc. Natl. Acad. Sci. U. S. A.* 118:e2021091118. doi: 10.1073/pnas.2021091118

Weizman, Z., Asli, G., and Alsheikh, A. (2005). Effect of a probiotic infant formula on infections in child care Centers: comparison of two probiotic agents. *Pediatrics* 115, 5–9. doi: 10.1542/peds.2004-1815

Wijendran, V., Brenna, J. T., Wang, D. H., Zhu, W., Meng, D., Ganguli, K., et al. (2015). Long-chain polyunsaturated fatty acids attenuate the IL-1beta-induced proinflammatory response in human fetal intestinal epithelial cells. *Pediatr. Res.* 78, 626–633. doi: 10.1038/pr.2015.154

Wikoff, W. R., Anfora, A. T., Liu, J., Schultz, P. G., Lesley, S. A., Peters, E. C., et al. (2009). Metabolomics analysis reveals large effects of gut microflora on mammalian blood metabolites. *Proc. Natl. Acad. Sci. U. S. A.* 106, 3698–3703. doi: 10.1073/pnas.0812874106

Wingender, G., Stepniak, D., Krebs, P., Lin, L., McBride, S., Wei, B., et al. (2012). Intestinal microbes affect phenotypes and functions of invariant natural killer T cells in mice. *Gastroenterology* 143, 418–428. doi: 10.1053/j.gastro.2012.04.017

Yang, I., Corwin, E. J., Brennan, P. A., Jordan, S., Murphy, J. R., and Dunlop, A. (2016). The infant microbiome: implications for infant health and neurocognitive development. *Nurs. Res.* 65, 76–88. doi: 10.1097/NNR.0000000000000133

Yano, J. M., Yu, K., Donaldson, G. P., Shastri, G. G., Ann, P., Ma, L., et al. (2015). Indigenous bacteria from the gut microbiota regulate host serotonin biosynthesis. *Cells* 161, 264–276. doi: 10.1016/j.cell.2015.02.047

Yaron, S., Shachar, D., Abramas, L., Riskin, A., Bader, D., Litmanovitz, I., et al. (2013). Effect of high beta-palmitate content in infant formula on the intestinal microbiota of term infants. *J. Pediatr. Gastroenterol. Nutr.* 56, 376–381. doi: 10.1097/MPG.0b013e31827e1ee2

Zhao, J., Zhang, X., Liu, H., Brown, M. A., and Qiao, S. (2019). Dietary protein and gut microbiota composition and function. *Curr. Protein Pept. Sci.* 20, 145–154. doi: 10.2174/1389203719666180514145437

Zheng, P., Wu, J., Zhang, H., Perry, S. W., Yin, B., Tan, X., et al. (2021). The gut microbiome modulates gut-brain axis glycerophospholipid metabolism in a region-specific manner in a nonhuman primate model of depression. *Mol. Psychiatry* 26, 2380–2392. doi: 10.1038/s41380-020-0744-2

Zheng, P., Zeng, B., Zhou, C., Liu, M., Fang, Z., Xu, X., et al. (2016). Gut microbiome remodeling induces depressive-like behaviors through a pathway mediated by the host's metabolism. *Mol. Psychiatry* 21, 786–796. doi: 10.1038/mp.2016.44

Zheng, W., Zhao, W., Wu, M., Song, X., Caro, F., Sun, X., et al. (2020). Microbiota-targeted maternal antibodies protect neonates from enteric infection. *Nature* 577, 543–548. doi: 10.1038/s41586-019-1898-4

Zivkovic, A. M., German, J. B., Lebrilla, C. B., and Mills, D. A. (2011). Human milk glycobiome and its impact on the infant gastrointestinal microbiota. *Proc. Natl. Acad. Sci. U. S. A.* 108, 4653–4658. doi: 10.1073/pnas.1000083107

Zuckerkandl, E., and Pauling, L. (1965). *Evolutionary Divergence and Convergence in Proteins, Evolving Genes and Proteins,* USA: Elsevier, 97–166.

frontiers | Frontiers in Microbiology

TYPE Original Research
PUBLISHED 10 January 2023
DOI 10.3389/fmicb.2022.1069981

OPEN ACCESS

EDITED BY
Hesong Wang,
Southern Medical University,
China

REVIEWED BY
Huaxin Niu,
Inner Mongolia Minzu University, China
Guangzhi Zhang,
Chinese Academy of Agricultural Sciences,
China

*CORRESPONDENCE
Chunwei Shi
shichunwei@jlau.edu.cn
Liping Ye
yeliping1114@163.com
Chunfeng Wang
wangchunfeng@jlau.edu.cn

SPECIALTY SECTION
This article was submitted to
Microbial Symbioses,
a section of the journal
Frontiers in Microbiology

RECEIVED 14 October 2022
ACCEPTED 30 November 2022
PUBLISHED 10 January 2023

CITATION
Niu T, Jiang Y, Fan S, Yang G, Shi C,
Ye L and Wang C (2023) Antiviral effects of
Pediococcus acidilactici isolated from
Tibetan mushroom and comparative
genomic analysis.
Front. Microbiol. 13:1069981.
doi: 10.3389/fmicb.2022.1069981

Antiviral effects of Pediococcus acidilactici isolated from Tibetan mushroom and comparative genomic analysis

Tianming Niu, Yuxin Jiang, Shuhui Fan, Guilian Yang, Chunwei Shi*, Liping Ye* and Chunfeng Wang*

Animal Microecological Engineering Research Center, College of Animal Science and Technology, College of Veterinary Medicine, Jilin Agriculture University, Changchun, China

Rotavirus is one of the main pathogens that cause diarrhoea in young animals, and countless animals have died of rotavirus infection worldwide. Three strains of lactic acid bacteria isolated from Tibetan mushrooms were used to study the inhibition of rotavirus *in vitro* and *in vivo*. One part was to identify and study the biochemical and probiotic characteristics of three isolated lactic acid bacteria, and the other part was to evaluate the inhibitory effect on rotavirus *via in vivo* and *in vitro* experiments. The whole genome of the lactic acid bacteria with the best antiviral effect was sequenced, and the differences between them and the standard strains were analyzed by comparative genomic analysis, so as to provide a theoretical basis for exploring the antiviral effect of lactic acid bacteria.The three strains were identified as *Pediococcus acidilactici*, *Lactobacillus casei* and *Lactobacillus paracasei*. *Pediococcus acidilactici* showed good acid tolerance, bile salt tolerance, survival in artificial intestinal fluid, survival in gastric fluid and bacteriostasis. In *in vitro* experiments, pig intestinal epithelial cells cocultured with *Pediococcus acidilactici* exhibited reduced viral infection. In the *in vivo* experiment, the duodenum of mice fed *Pediococcus acidilactici* had extremely low numbers of virus particles. The total genome size was 2,026,809bp, the total number of genes was 1988, and the total length of genes was 1,767,273bp. The proportion of glycoside hydrolases and glycoside transferases in CAZy was 50.6 and 29.6%, respectively. The Metabolism function in KEEG had the highest number of Global and overview maps. Among the comparative genomes, *Pediococcus acidilactici* had the highest homology with GCF 000146325.1, and had a good collinearity with GCF 013127755.1, without numerous gene rearrangement events such as insertion, deletion, inversion and translocation. In conclusion, *Pediococcus acidilactici* was a good candidate strain for antiviral probiotics.

KEYWORDS

rotavirus, probiotics, *Pediococcus acidilactici*, antiviral effect, whole genome

Introduction

Rotavirus is one of the main pathogens that cause diarrhoea in infants and young animals. Approximately 215,000 infants and young children die from rotavirus infection worldwide each year, and most of these deaths occur in developing countries (Mm et al., 1997). At present, there is no specific drug for rotavirus, and vaccination with a live attenuated vaccine is the most effective way to prevent and control rotavirus-induced diarrhoea, but the vaccine acceptance rate in developing countries is relatively low, so the disease has not been controlled (Omatola et al., 2021; Song, 2021). Probiotics are a group of microorganisms that are beneficial to the host and can maintain the microecological balance of the host body, regulate the immune response, and reduce the occurrence of infectious diseases and intestinal inflammation. Therefore, probiotics are also an important means to prevent rotavirus infection. In recent years, an increasing number of studies have reported that probiotics can effectively shorten the duration of rotavirus-induced diarrhoea, reduce the incidence of diarrhoea and regulate intestinal homeostasis (Mao et al., 2016).

Tibetan mushroom, also known as Tibetan kefir, is the most common natural starter in Tibet, China. It is used to ferment milk at room temperature and has been eaten by Tibetans for hundreds of years. Tibetan mushrooms are rich in lactic acid bacteria, acetic acid bacteria, yeast and other probiotics (Gao and Zhang, 2019), which can produce high concentrations of lactic acid probiotic factors. As a probiotic resource, the Tibetan mushroom not only has rich nutrition but also has many beneficial functions, including the abilities to inhibit pathogenic bacteria (Sun et al., 2019), regulate body immunity, and exert anti-inflammatory and antioxidant effects (Tang et al., 2018). Therefore, Tibetan mushroom has high research value and significance. In clinical practice, Tibetan mushroom fermented milk has obviously alleviated diarrhea, so it is particularly important to explore the type of bacteria that can alleviate diarrhea and its antiviral effect.

An increasing number of probiotics have been reported in antiviral studies. Rather, I et al. used *Lactobacillus plantarum* as an adjuvant drug in the treatment of SARS-CoV-2 infection patients, inhibiting the replication of SARS-CoV-2, regulating the immune response, and reducing the levels of inflammatory factors such as IFN-α, IFN-β, and IL-6. It has a good blocking effect on SARS-CoV-2 (Rather et al., 2021). Salaris,C et al. used *in vitro* experiments combining *Lactobacillus paracasei* with lactoferrin protein, which could significantly inhibit SARS-CoV-2 infection and enhance the ability of Caco-2 intestinal epithelial cells to resist SARS-CoV-2 (Salaris et al., 2021). Huang,S et al. found that metabolites of *Lactobacillus plantarum* (LPM) had a good inhibitory effect on porcine epidemic diarrhoea virus. After treating Vero cells with LPM metabolites, PEDV adsorption could be effectively prevented, the inflammatory response was reduced, and apoptosis of damaged cells was induced (Huang et al., 2021). Watanabe et al. showed that oral immunization of mice with *Enterococcus faecalis* could effectively reduce influenza virus infection, and specific antibodies against influenza virus were detected in the serum of the mice. Therefore, *Enterococcus faecalis* plays an important role in this process (Watanabe et al., 2021). Shin D et al. found that the *Lactobacillus plantarum* product developed in their study could effectively reduce the occurrence of rotavirus enteritis in children and inhibit the adhesion and proliferation of rotavirus in the small intestine (Shin et al., 2020).

In this study, we have isolated and identified three new lactic acid bacterial strains from Tibetan mushrooms and evaluated their probiotic properties, including acid resistance, bile salt resistance, survival in simulated artificial intestinal juice, survival in artificial gastric juice, and inhibition of the growth of pathogenic bacteria. The effects of the three strains on rotavirus replication and immune regulation have also tested *in vitro* and *in vivo* experiments. The best antiviral lactic acid bacteria have selected for all-cause sequencing, and their differences have analyzed by comparing with the model strains to explore their potential antiviral effects. Our goal has to develop the best antiviral lactic acid bacteria into a product for the prevention or treatment of diarrhea caused by rotavirus.

Materials and methods

Isolation and identification of lactic acid bacteria from traditional Tibetan mushrooms

Tibetan mushrooms (20 g) were added to 500 ml of sterilized milk and incubated at room temperature for 24 h. The milk could be fermented into a fermented milk product, which was subsequently fermented into a milky form. In this fermented milk, there were a large number of microbial strains from Tibetan mushrooms, and we used this fermented milk for lactic acid bacterium separation. After 100 μl of Tibetan mushroom fermented milk was serially diluted with 900 μl of phosphate-buffered saline (PBS), it was spread on De Man Rogosa Sharpe (MRS) agar and placed in an anaerobic culture incubator at 37°C for 18 h. After single colonies grew on the medium, a single colony was selected and placed in liquid MRS medium (Hurtado-Romero et al., 2021). After culture, only Gram-positive bacteria and catalase-negative bacteria were selected. Unless otherwise specified, the experiment was repeated three times.

Finally, three strains of Gram-positive bacteria with different colony morphologies were selected, and genomic DNA of the 3 g-positive bacterial strains was extracted. PCR amplification was carried out by using the 16S rDNA method. The general primers used for 16S rDNA amplification are shown in Table 1. The PCR system volume was 20 μl, including PCR enzyme mix (10 μl), the upstream primer and downstream primer (1 μl), the template (2 μl), and sterile water (6 μl). PCR conditions were as follows: 96°C for 3 min, followed by 30 cycles of 96°C for 1 min, 56°C for 30 s, and 72°C for 1 min, and finally 72°C for 7 min. After the PCR was completed, PCR products were subjected to agarose gel electrophoresis to observe the

TABLE 1 Primer sequences and annealing temperatures for polymerase chain reactions.

Gene	Primer sequence (5`-3`)	Product size (bp)	Annealing temp. (°C)
IL-18	Forward:	101	60
	TGAAAACGATGAAGACCTGGAA		
	Reverse:		60
	CCTGGTTAATGAAAAGGACTTGG		
IL-6	Forward:	294	60
	ATGAGAAGTGTGAAAACAGCAAGG		
	Reverse:		60
	CATTTGTGGTGGGGTTAGGG		
IFN-β	Forward:	82	60
	TCGCTCTCCTGATGTGTTTCTC		
	Reverse:		60
	AAATTGCTGCTCCTTTGTTGGT		
TNF-α	Forward:	127	60
	GGCGTGAAGCTGAAAGACAAC		
	Reverse:		60
	GGCTGATGGTGTGAGTGAGG		
IL-1β	Forward:	125	60
	AAGTGGTGTTCTGCATGAGCTTT		
	Reverse:		60
	CAGGGTGGGCGTGTTATCTT		
IFN-α	Forward:	121	60
	ACCTCAGCCAGGACAGCAGTATC		
	Reverse:		60
	TCGCAGCCCAGAGAGCAGATG		
GAPDH	Forward:	150	60
	TGTGTCCGTCGTGGATCTGA		
	Reverse:		60
	TTGCTGTTGAAGTCGCAGGAG		
27F	Forward:	1900	60
	AGAGTTTGATCMTGGCTCAG		
1492R	Reverse: GGTTACCTTGTTACGACTT		60

experimental results. The PCR products were then sent to Shanghai Shenggong Biological Co., Ltd. for sequencing, and the sequencing results were compared on NCBI GenBank. After comparison, the three strains were identified as lactic acid bacteria.

Biochemical identification experiment

The three isolated lactic acid bacteria were inoculated into 10 solutions of biochemical identification reagents, including aescin, cellobiose, maltose, mannitol, salicin, sorbitol, sucrose, raffinose, inulin and lactose (biochemical reagents were purchased from Shandong Qingdao Haibo Biological Co., Ltd.). After anaerobic culture at 37°C for 18 h, the biochemical results were observed, and the data were statistically analyzed. At the same time, the isolated lactic acid bacteria were inoculated into a solution of nitrate reductant, and the experimental results were observed.

Growth curve determination

The three isolated strains of lactic acid bacteria were added to MRS medium at a bacterial density of 1×10^7 CFU/ml. Subsequently, a UV spectrophotometer was used to detect the OD value, which was measured at 0 h. Then, the corresponding OD values at 3 h, 6 h, 9 h, 12 h, 15 h, 18 h, 21 h, 24 h, and 36 h were detected, and the growth curve was drawn.

Artificial gastric and intestinal fluids were simulated

The cultured strains were added to simulated artificial intestinal fluid and artificial gastric juice at a bacterial density of 1×10^7 CFU/ml (artificial intestinal fluid and gastric juice were prepared in accordance with the Chinese pharmacopoeia). After 12 h of culture, MRS plate counting was performed after serial dilution, and the number of colonies was counted.

Tolerance to different concentrations of bile salts and pH 2.5

Lactic acid bacteria (1×10^7 CFU/mL) were added to the MRS liquid medium. After 18 h of anaerobic culture at 37°C, the bacteria were enriched, resuspended in PBS, and added to MRS medium at pH 2.5 for 12 h. The number of single colonies was counted by MRS plate counting. Similarly, resuspended lactic acid bacteria were added to MRS liquid medium with pig bile salt concentrations of 0.30, 0.50 and 1.00% for 12 h, and single colonies of treated lactic acid bacteria were counted.

Inhibition of pathogenic bacteria

One of the most important tests of lactic acid bacteria is whether they can inhibit pathogenic bacteria. Only lactic acid bacteria that can inhibit pathogenic bacteria can be used in further applicantios. We selected *Escherichia coli*, *Salmonella typhimurium* and *Staphylococcus aureus* as pathogenic bacteria to test against the three strains of lactic acid bacteria. First, *Escherichia coli*, *Salmonella typhimurium*, and *Staphylococcus aureus* were plated on nutrient AGAR medium. Then, according to the drilling method, a 6 mm hole was introduced, and the three lactic acid bacteria were added to the holes. At the same time, the antibiotic group and the blank group were established, and the plates were placed in a 37°C anaerobic culture after 18 h. Finally, the size of the bacteriostatic ring was determined to be large or small. The diameter of the antibacterial ring was measured.

Cells and viruses

We used pig intestinal epithelial cells for *in vitro* experiments. The cells were stored in the Animal Microecology Preparation Center of Jilin Agricultural University. In *in vitro* and animal experiments, we used porcine rotavirus (rotavirus is stored in the Animal Microecological Preparation Center of Jilin Agricultural University).

In vitro antiviral experiment

We carried out *in vitro* anti-rotavirus experiments. First, we seeded 1×10^4 IPEC-J2 cells in 6-well plates and then set up 6 experimental groups, namely, the PBS group, challenge group, antiviral drug group, *Pediococcus acidilactici* group, *Lactobacillus casei* group and *Lactobacillus paracasei* group. Next, 1×10^5 CFU/ml lactic acid bacteria were added to IPEC-J2 cells and incubated for 2 h, and then gentamicin was added at a final concentration of 50 μg/ml. After incubation for 1 h, PBS was used for stringent washing 5 times. Then, the cells were infected with RV (virus titre of RV 100 TCID50); after infection for 12 h, then the total RNA of the supernatant and the cells was extracted and reverse transcribed into cDNA. Finally, fluorescence quantitative PCR was used to explore the inhibition of RV replication.

Fluorescence quantitative PCR detection and analysis

We used absolute quantitative methods to conduct real-time PCR in a 20 μl reaction system using constructed plasmids as templates. The 20 μl system consisted of 10 μl of enzyme, 1 μl of upstream primer, 1 μl of downstream primer, 2 μl of template and 6 μl of sterile water. The reaction conditions were as follows: 52°C for 2 min, 95°C for 5 min, and 45 cycles of 95°C for 15 s and 58°C for 1 min. Then, the standard curve was drawn, and the experimental results were interpolated onto the standard curve to calculate the virus copy number for each treatment.

At the same time, a relative quantitative method was used to quantify the changes in the levels of cytokines produced by the cells under different treatments. The reaction system and reaction conditions were the same as those for the absolute quantitative method. Relative quantification of target genes was calculated using the $2^{-\Delta\Delta Ct}$ method (Zhao et al., 2020). The mRNA level of GAPDH was selected as the internal reference, the final results were calculated, and a histogram was drawn. The fluorescence quantitative primers are listed in Table 1.

Antiviral experiment in mice

Specific pathogen-free (SPF) mice (Jeong et al., 2021) aged 3 weeks were used (the mice were from the Animal Center of Jilin Agricultural University), and 6 groups were set with 10 mice in each group, including the blank group, challenge group, antiviral drug group, *Pediococcus acidilactici* group, *Lactobacillus casei* group and *Lactobacillus paracasei* group. The immunization procedure was repeated three times after one insufflation of lactic acid bacteria and 2 days of rest. Finally, 100 TCID50 of rotavirus was administered continuously for 3 days. We measured the weight changes of mice 14 days after infection with the virus and plotted the weight change curve. Additionally, pathological sections of the small intestine and colon of mice in each group were made, and RNA of two intestinal segments was extracted. All the mice were finally euthanized, which was in line with ethical approval.

Elisa

In the animal experiments, the serum and faeces of mice were collected before feeding bacteria, after feeding bacteria and 3 days after challenge. According to the instructions of the ELISA kits, IFN-β, IL-6, and TNF-α in serum and SIgA in faeces were quantified (ELISA kits were purchased from Jiangsu MEIMIAN Industry Co., Ltd.). For treatment of faeces, the faeces samples were weighed at low temperature, and then an equivalent amount of sterile PBS was added to dissolve the faeces. After overnight incubation at 4°C, the faeces samples were centrifuged at 12000 r/min for 2 min, and the supernatant was transferred. The concentration of tested samples was analyzed statistically, and a histogram was drawn.

The intestinal tract of mice was examined by pathology

The duodenum and colon of mice under various treatments were collected, and the treated duodenum and colon were dyed with haematoxylin and eosin and then made into pathological sections for pathological examination. See the Supplementary materials for the specific steps.

Whole genome sequencing

Pediococcus acidilactici was activated, and the bacteria were collected. The total bacterial DNA was extracted by using the bacterial DNA gene extraction kit and sent to Beijing Nuohe Source Technology Co., LTD for sequencing. After passing the library test, Pac Bio Sequel and Illumina Nova Seq PE150 sequencing were performed. After filtering and quality control of the original disembarkation data, SMRT Link V5.0.1 software was used to preliminarily assemble the original disembarkation data, and the assembled data were corrected to obtain the genome assembly data. The optimized assembly data were compared and analyzed with the assembly results, and the sequencing results

were corrected. Glimmer V3.02 and Gene Mark S V4.3 software were used to predict the coding genes of the Mycococcus lactis genome. The Clusters of Orthologous Groups of proteins (COG) database was annotated by EGG NOG V4.5.1 software. KEGG was annotated through the Kyoto Encyclopedia of Genes and Genomes (KEGG) online database. The database of CAZy is annotated through rum-active En Zymes (CAZy) V6.0 software. Secondary metabolites were annotated by Anti SMASH V4.0.2 software.

Comparative genome analysis

Phylogenetic trees of homologous single copy genes were constructed using IQ-Tree V1.6.12 software, and the TREE construction method was Maximum Likelihood. Mummer V4.0 analysis software was used for collinearity analysis with default software parameters. To calculate the similarity or evolutionary distance between different genomes for species classification and relative comparison. Therefore, by comparing the Average Nucleotide Identity (ANI), the genetic relationship of two genomes was compared at the Nucleotide level. In order to find out the conserved features of the genome, and thus the phenotypic variation of the genome, the relationship between the very conserved core genome and the number of genes in the pan genome was analyzed.

Statistical analysis

Values are expressed as the mean ± standard deviation (SD). Statistical significance was assessed at $p < 0.05$ for all comparisons. Statistical analysis was performed with Statistical Product and Service Solutions (SPSS.19) statistical software.

Results

Results of isolation and identification of lactic acid bacteria

Single colonies on MRS solid medium were selected for Gram staining, and finally, three strains of Gram-positive Lactobacillus were identified. Based on observation, one strain was a Gram-positive coccus, and two were Gram-positive *Bacillus brevis*. According to 16S rDNA identification, the Gram-positive coccus was *Pediococcus acidilactici*, and the Gram-positive short bacilli were *lactobacillus casei* and *lactobacillus paracasei* (see the Supplementary material S1 for the comparison results, 200X).

Biochemical identification experiment

The three isolated and identified lactobacillus strains (*Pediococcus acidilactici*, *Lactobacillus casei* and *Lactobacillus paracasei*) were inoculated with 10 biochemical identification reagents. The results of the experiment showed that *Pediococcus acidilactici* was positive for cellobiose, salicin, and inulin fermentation, while it was negative for aescin, maltose, mannitol, sorbitol, sucrose, raffinose and lactose fermentation. The biochemical identification results for *Lactobacillus casei* and *Lactobacillus paracasei* were the same. Both *Lactobacillus casei* and *Lactobacillus paracasei* could ferment aescin, cellobiose, maltose, mannitol, salicin, sorbitol, sucrose, inulin and lactose, while they were negative for raffinose fermentation. The results are shown in Table 2.

Growth curve drawing

According to the growth of the three strains of lactic acid bacteria, a growth curve was drawn. The results showed that in the growth process of the three strains of lactic acid bacteria, the growth of the three strains was different in the logarithmic phase. The growth rate of *Pediococcus acidilactici* was higher than that of *Lactobacillus paracasei*, and that of *Lactobacillus casei* was the slowest. However, in the plateau phase, the growth of the three strains of lactic acid bacteria was relatively identical, as shown in Figure 1A.

Artificial gastric and intestinal fluids were simulated

We compared the tolerance of the three strains of lactic acid bacteria by simulating the gastric juice and intestinal juice environments. In the gastric juice environment, the tolerance of *Pediococcus acidilactici* was significantly higher than that of *Lactobacillus casei* ($p < 0.001$) and that of *Lactobacillus paracasei* ($p < 0.01$). However, the tolerance of *Lactobacillus casei* in the intestinal fluid environment was significantly higher than that of *Pediococcus acidilactici* and *Lactobacillus paracasei* ($p < 0.01$). The results are shown in Figure 1B.

Acid and bile salt tolerance results

We prepared MRS liquid medium with a pH of 2.5, added lactic acid bacteria at a concentration of 1×10^6 CFU/ml to the medium to allow them to tolerate the conditions for 12 h, and then carried out counting and statistical analysis through the drop plate experiment. The results showed that the tolerance of *Lactobacillus paracasei* was stronger than that of *Pediococcus acidilactici* and *Lactobacillus casei* in the medium with pH = 2.5, and the tolerance percentage was 69%.

Pig bile salt was used to prepare MRS liquid media with bile salt concentrations of 0.30, 0.50 and 1%, and lactic acid bacteria at a concentration of 1×10^6 CFU/ml were added to the MRS liquid media. After 12 h of culture, drop plate

TABLE 2 Biochemical test.

Strain/ biochemical reagent	Aescin	Cellobiose	Maltose	Mannitol	Salicin	Sorbitol	Sucrose	Raffinose	Inulin	Lactose	Reducing nitrate
Pediococcus acidilactici	–	+	–	–	+	–	–	–	+	–	+
Lactobacillus casei	+	+	+	+	+	+	+	–	+	+	–
Lactobacillus paracasei	+	+	+	+	+	+	+	–	+	+	–

(+) was positive, indicating a reaction. (–) was negative, indicating no reaction.

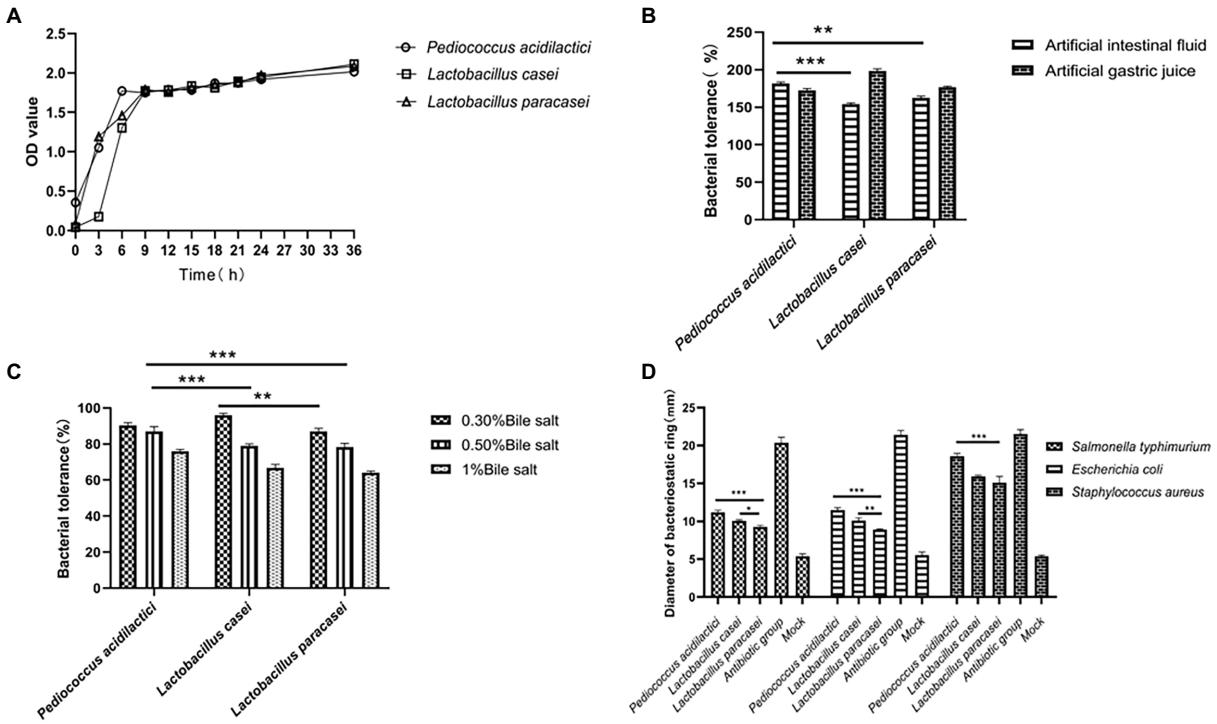

FIGURE 1
Growth characteristics and tolerance of isolated bacteria. **(A)** Growth curve of three isolated lactic acid bacteria. **(B)** Tolerance of three strains under artificial simulated intestinal fluid and gastric juice conditions. **(C)** Tolerance of three strains of bacteria under different concentrations of bile salt. **(D)** Inhibitory effects of three strains on three pathogens (the pathogenic bacteria were *Escherichia coli, Salmonella* and *Staphylococcus aureus*).

counting and statistical analysis were used. The results showed that the tolerances of *Pediococcus acidilactici* and *Lactobacillus casei* in MRS with 0.30% bile salt was similar, and both were stronger than that of *Lactobacillus paracasei*. The tolerance of *Pediococcus acidilactici* in MRS with 0.50% bile salt and 1% bile salt was higher than that of *Lactobacillus casei* and *Lactobacillus paracasei*. The experimental results are shown in Figure 1C.

Inhibition of pathogenic bacteria

We selected *Escherichia coli*, *Salmonella typhimurium* and *Staphylococcus aureus* as the three pathogenic bacteria for the resistance testing of *Pediococcus acidilactici*, *Lactobacillus casei* and *Lactobacillus paracasei*. The antibacterial ability was determined by the diameter of the antibacterial ring. We measured the diameter of the bacteriostatic ring (mm), and the experimental

results showed that the three strains of lactic acid bacteria showed good inhibitory effects on Salmonella, *Escherichia coli* and *Staphylococcus aureus*, among which *Pediococcus acidilactici* showed good inhibitory effects on the three pathogenic bacteria and was significantly more potent than *Lactobacillus casei* and *Lactobacillus paracasei* ($p < 0.01$). The experimental results are shown in Figure 1D.

In vitro antiviral experiment

In the *in vitro* assessment, we divided the experiment into 6 groups, They were PBS group, challenge group, antiviral drug group, *Pediococcus acidilactici* group, *Lactobacillus casei* group and *Lactobacillus paracei* group. The RNA of the virus was extracted and reverse transcribed into cDNA. The number of virions in cells treated by each condition was determined by absolute quantification. The experimental results showed that the virus copy number in the cells treated with the three strains of lactic acid bacteria was reduced. Compared with that in the challenge group, the virus copy number was significantly lower in the *Pediococcus acidilactici* group, *Lactobacillus casei* group and *Lactobacillus paracasei* group ($p < 0.001$), and the virus copy number under the *Pediococcus acidilactici* treatment was the lowest, indicating the best inhibitory effect, followed by that with *Lactobacillus casei*. The experimental results are shown in Figure 2.

Total RNA was extracted from IPEC-J2 cells after each treatment, and the relative expression levels of IFN-α, IFN-β, IL-1β, IL-6, IL-18, and TNF-α were quantitatively determined. The experimental results showed that when quantifying IFN-α and IFN-β in IPEC-J2 cell cultures, the relative expression levels of IFN-α and IFN-β in the *Pediococcus acidilactici* group, *Lactobacillus casei* group, *Lactobacillus paracasei* group and the challenge group were significantly increased compared with those in the PBS group ($p < 0.01$), and the relative expression levels in the *Pediococcus acidilactici* group were the highest (Figures 3A,B). When quantifying IL-1β, IL-6, IL-18 and TNF-α in IPEC-J2 cell culture, the relative expression levels of L-1β, IL-6, IL-18 and TNF-α were significantly decreased in the *Pediococcus acidilactici* group, *Lactobacillus casei* group and *Lactobacillus paracasei* group compared with those in the challenge group (Figures 3C,F), among which the relative expression levels in the *Pediococcus acidilactici* group were the lowest. The experimental results are shown in Figure 3.

In vivo antiviral experiment

In *in vivo* experiments, we performed absolute quantitative comparisons of virus copy numbers in the duodenum of mice under different treatments. The results showed that immunization of mice with the three lactic acid bacteria strains could prevent rotavirus infection. The virus copy number in the duodenum of

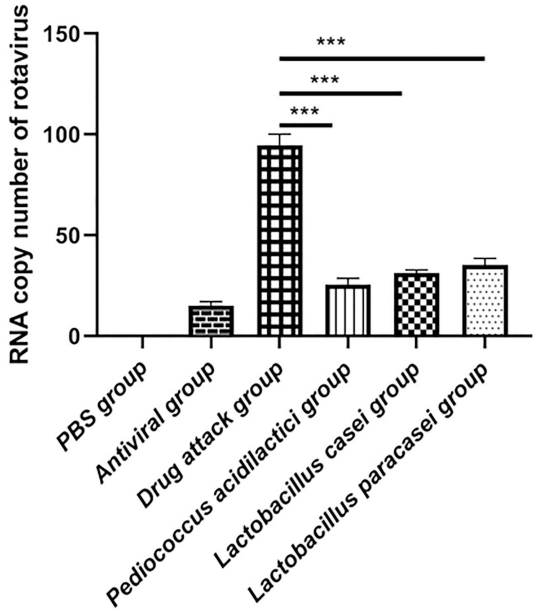

FIGURE 2
The number of virus copies was quantified in cultures of lactic acid bacteria and porcine intestinal epithelial cells.

mice in the *Pediococcus acidilactici* group, *Lactobacillus casei* group and *Lactobacillus paracasei* group was significantly lower than that in the challenge group ($p < 0.01$). The virus copy number of mice treated with *Pediococcus acidilactici* was the lowest, indicating that *Pediococcus acidilactici* could effectively inhibit virus infection and replication. The experimental results are shown in Figure 4A.

After challenge, the body weight of the mice under different treatments changed significantly. The results showed that the body weight of the mice treated with the three strains of lactic acid bacteria gradually recovered after the second day after challenge, and the body weight of the mice immunized with *Lactobacillus paracasei* increased faster than that of the mice in the *Pediococcus acidilactici* group and *Lactobacillus casei* group, but there was no significant difference. The weight loss of mice in the challenge group was obvious, and the weight change of mice in the antiviral drugs group was also obvious. The experimental results are shown in Figure 4B.

ELISA results

We collected the blood and faeces of each group of mice before feeding with the bacteria, after feeding with the bacteria and after challenge and detected the levels of IFN-β, IL-6, TNF-α in serum and of SIgA in faeces by ELISA to study the changes. The results showed that the serum IFN-β content in the three lactic acid bacterium groups changed little after feeding with the bacteria and challenge but increased significantly in challenge

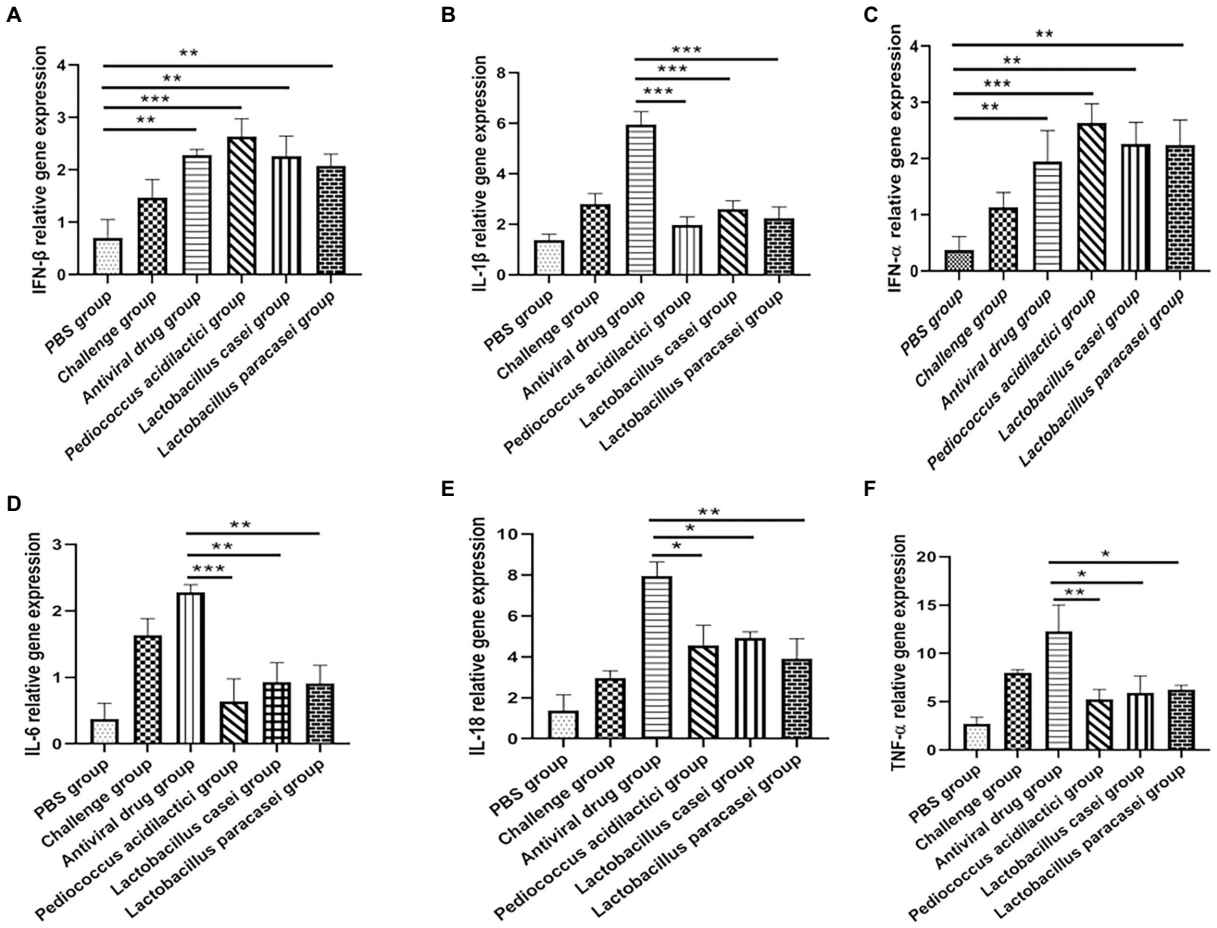

FIGURE 3
Lactobacillus and porcine intestinal epithelial cell cultures were used to quantify the cytokines produced by cells. **(A)**, IFN-β relative gene expression. **(B)**, IFN-α relative gene expression. **(C)**, IL-1β relative gene expression. **(D)**, IL-6 relative gene expression. **(E)**, IL-18 relative gene expression. **(F)**, TNF-α relative gene expression.

group (Figure 5A). Compared with that in the blood of the PBS group, the IL-6 content in the blood of all treatment groups after challenge was significantly increased ($p < 0.05$; Figure 5B). When detecting TNF-α in blood, compared with that in the challenge group, TNF-α content in all treatment groups was significantly decreased ($p < 0.01$; Figure 5C). When detecting SIgA in faeces, the content of SIgA in faeces of the *Pediococcus acidilactici* group was significantly higher than that of the challenge group ($p < 0.01$; Figure 5D). The experimental results are shown in Figure 5.

The pathological examination results

Pathological examination of the duodenum and colon in mice showed that in the challenge group, the virus destroyed the integrity of the duodenal villi of the mice and appeared at the top of the intestinal villus injury. Inflammatory cell infiltration was accompanied by interstitial oedema, inflammatory cell infiltration in the colon submucosa was visible, and goblet cell numbers increased at the same time. However, there were no obvious pathological changes in the three groups with the lactic acid bacteria, and the intestinal villi of mice in the *Pediococcus acidilactici* group were relatively intact. The experimental results are shown in Figures 6, 7.

Whole genome sequencing results

The whole genome of *Pediococcus acidilactici* was composed of a ring structure with chromosome 2,026,809.The number of genes was 1988, the total length of genes was 1,767,273 bp, and the average length of genes was 889 bp. Using CRISPRdigger for genome CRISPR prediction, the number of CRISPR was 6, with a full length of 1,070 bp and an average length of 178.333 bp. The number of tRNA was 57, with an average length of 75 bp and a full length of 4,310 bp (Figure 8A). By comparison and analysis of evolutionary trees, PA of *Pediococcus acidilactici* was similar to GCF 000146325.1 (Figure 8B).

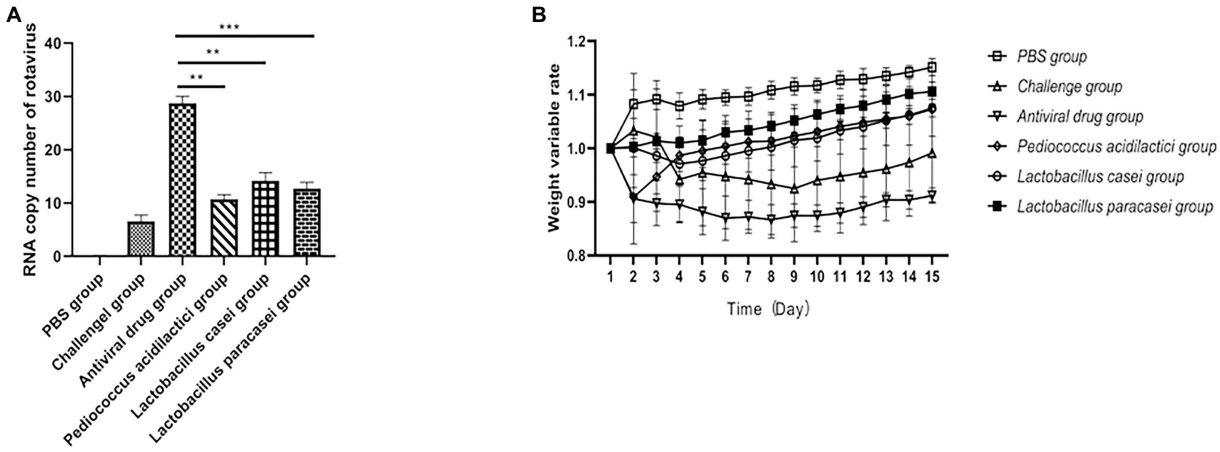

FIGURE 4
Lactic acid bacteria inhibit rotavirus replication *in vivo*. **(A)**, The number of viral RNA copies in the small intestine of mice after challenge. **(B)**, Weight loss rate of mice after challenge.

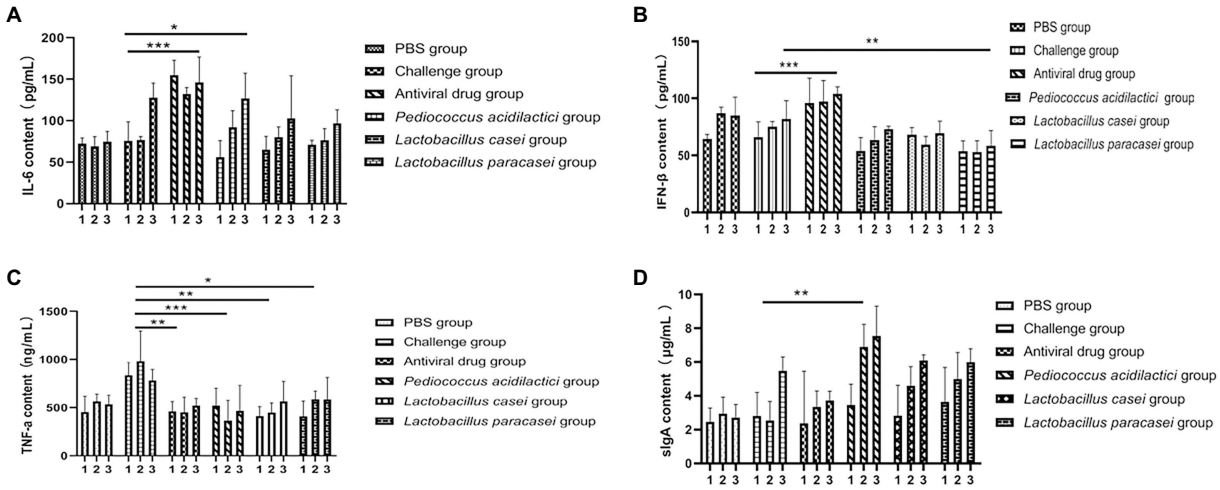

FIGURE 5
Cytokines and secretory sIgA in the blood of mice were detected by ELISA. **(A)** The change in IFN-β concentration in the blood of mice in three time periods. **(B)** The change of the concentration of IL-6 in the three stages. **(C)** The change in TNF-α concentration in the three stages. **(D)** Changes in the sIgA concentration in faeces (1 means before feeding lactic acid bacteria, 2 means after feeding Lactobacillus, 3 indicates after rotavirus infection).

A total of 81 genes were annotated to 5 active enzymes by CAZy of PA of *Pediococcus acidilactici*, among which 50.62% of genes were annotated as glycoside hydrolases (GH), 29.63% were annotated as glycosyl transferases (GT). 6.17% genes were annotated as carbohydrate esterases(CE), 4.83% genes were annotated as auxiliary activity(AA). And 12.35% genes were annotated as rum-binding modules (CBM; Figure 9A). A total of 1,333 genes were annotated to functional information in KEGG annotation of *Pediococcus acidilactici*. The number of genes related to cellular process was 2.63%, the number of genes related to metabolism was 69.84% and the number of genes related to human diseases was 3.68%. The number of genes related to genetic information processing was 11.85%, and the number of genes related to biological systems was 1.65%. The number of genes associated with environmental information processing was 10.35%. In the KEGG functional annotation, the most genes were related to metabolic pathways, among which the proportion of Global and Overview maps was 25.66%, followed by the proportion of metabolism 14.18% (Figure 9B); COG annotation of *Pediococcus acidilactici* has a total of 1910 genes annotated to four COG functions, Its functions were mainly concentrated in Carbohydrate transport and metabolism

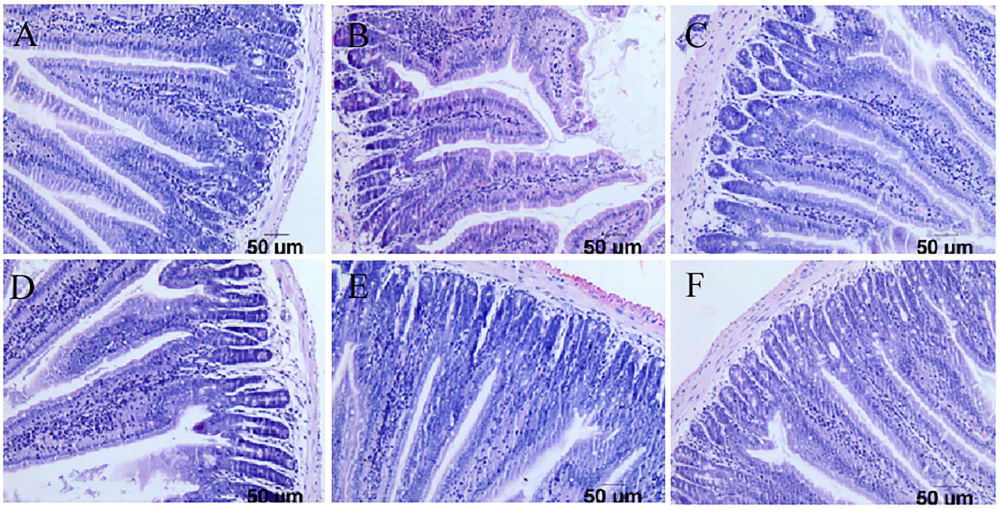

FIGURE 6
Pathological sections of the small intestine in mice. **(A)** Pathological sections of the small intestine in the PBS group. **(B)** Pathological sections of the small intestine in the challenge group. **(C)** Pathological sections of the small intestine in the antiviral drug group. **(D)** Pathological sections of the small intestine in the *Pediococcus acidilactici* group. **(E)** Pathological sections of the small intestine in the *Lactobacillus casei* group. **(F)** Pathological sections of the small intestine in the *Lactobacillus paracasei* group.

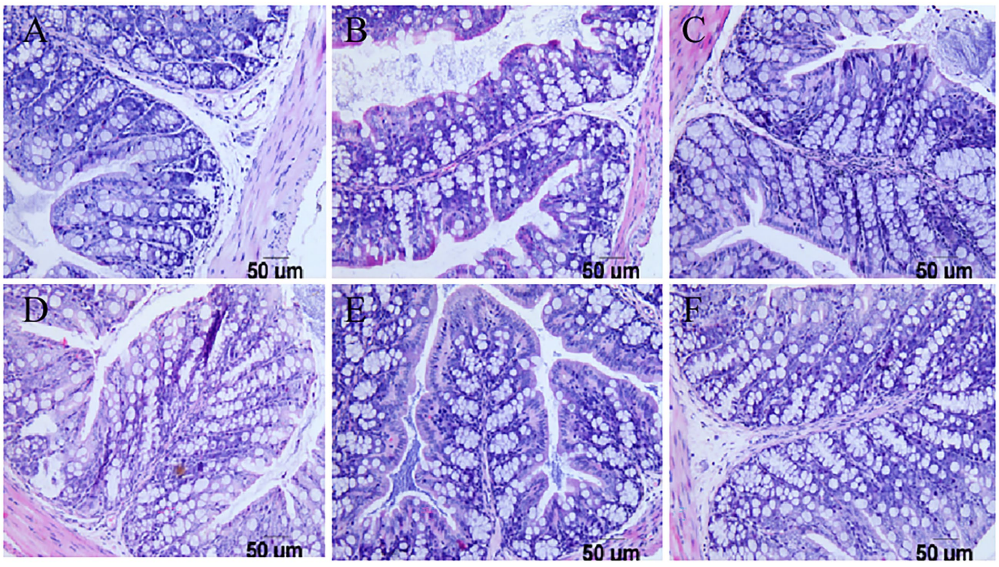

FIGURE 7
Pathological sections of the large intestine in mice. **(A)** Pathological sections of the large intestine in the PBS group. **(B)** Pathological sections of the large intestine in the challenge group. **(C)** Pathological sections of the large intestine in the antiviral drug group. **(D)** Pathological sections of the large intestine in the *Pediococcus acidilactici* group. **(E)** Pathological sections of the large intestine in the *Lactobacillus casei* group. **(F)** Pathological sections of the large intestine in the *Lactobacillus paracasei* group.

(9.58%), Ribosomal structure and Transcription(6.86%) and biogenesis(6.91%). In addition, 1.10% of the genes were annotated to be related to secondary metabolites biosynthesis (transport and catabolism) (Figure 9C).

Comparative genomic results

The whole genome of *Pediococcus acidilactici* was compared. In the pan-genome analysis, with the increase of the number of

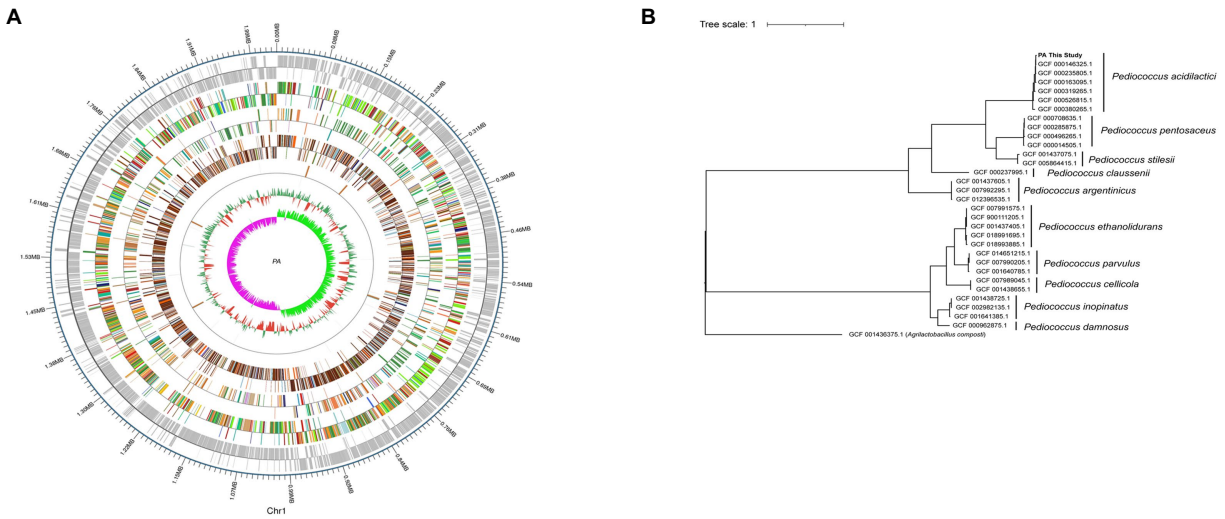

FIGURE 8
Whole gene sequencing of *Pediococcus acidilactici*. **(A)** A complete diagram of bacteria. **(B)** Comparison of evolutionary trees of *Pediococcus acidilactici*.

genes, the total number of genes in the pan-genome gradually increased, and the increase amplitude gradually decreased, while the number of core genome gradually decreased, and tended to be stable (Figure 10). In order to assess the relatability of the species, the average nucleotide identity analysis (ANI) showed that the ANI values of the 100 isolates were all above 97%, which was greater than the threshold of 96% for conspecific identification. It indicated that these strains belonged to *Pediococcus acidilactici*, and there was no subspecies (Figure 11). In order to explain the evolutionary relationship and multiploidy events among strains, the collinearity analysis was used to compare *Pediococcus acidilactici* with the GCF-013127755.1-genomic. Fna strain with high homology. The experimental results showed that gene insertion occurred in the red base sequence, while the yellow base sequence caused and translocated. However, for most base sequence comparisons, there was a good collinearity relationship (Figure 12).

Discussion

Tibetan mushrooms have existed in China for many years and are called kefir in the West. Studies have reported that Tibetan mushrooms are extremely rich in lactic acid bacteria. Different types of fermented milk and different geographical locations have different structures of lactic acid bacteria, with some yeast as the dominant microorganism and some lactobacillus as the dominant bacterium. Therefore, researchers research results on Tibetan mushrooms are also inconsistent (Georgalaki et al., 2021). Some researchers isolated *Lactobacillus paracasei* from Tibetan kefir and found that the extracellular polysaccharide produced by it had good probiotic properties (Bengoa et al., 2021). It has been reported that *Saccharomyces cerevisiae* isolated from Tibetan mushrooms can prevent and treat gastrointestinal and other infectious diseases and can be used as an excellent fermentation preparation for production (Ansari et al., 2021). In this study, three strains of lactic acid bacteria, *Pediococcus acidilactici*, *Lactobacillus casei* and *Lactobacillus paracasei*, were isolated from Tibetan mushrooms, and their physiological and biochemical characteristics, probiotic properties and antiviral properties were studied. The inhibitory effects of the three strains on rotavirus were compared *in vitro* and *in vivo*.

Adikari, AMMU et al. isolated several strains of lactic acid bacteria from traditional fermented milk gel and evaluated their morphological, biochemical, physiological and probiotic properties (Adikari et al., 2021). In this study, three strains of lactic acid bacteria isolated from Tibetan mushrooms were sequenced by 16S rDNA sequencing, and the results confirmed *Pediococcus acidilactici*, *Lactobacillus casei* and *Lactobacillus paracasei* after comparison. There are no literature reports that *Pediococcus acidilactici* has been isolated from Tibetan mushrooms. Therefore, three strains of lactic acid bacteria were tested for their resistance to acid, bile salt, artificial gastric juice and artificial intestinal juice. In the acid resistance test, *Lactobacillus paracasei* showed a strong tolerance; under the condition of pH 2.5, it still had 69% tolerance. In the article of Falfan, Cotes RN et al., *Lactobacillus paracasei* also showed excellent acid resistance (Falfán-Cortes et al., 2021) In the bile salt tolerance test, *Pediococcus acidilactici* showed good tolerance, which was stronger than that of *Lactobacillus casei* and *Lactobacillus paracasei*. In the experiment assessing tolerance to artificial gastric juice, *Pediococcus acidilactici* could tolerate artificial gastric juice, and the loss of *Pediococcus acidilactici* in gastric juice was low. *Lactobacillus casei* showed strong tolerance in the artificial intestinal fluid experiment. *Pediococcus acidilactici* has a good inhibitory effect on *Escherichia coli*, *Salmonella typhimurium*, and *Staphylococcus aureus*, and its inhibitory ability was stronger than

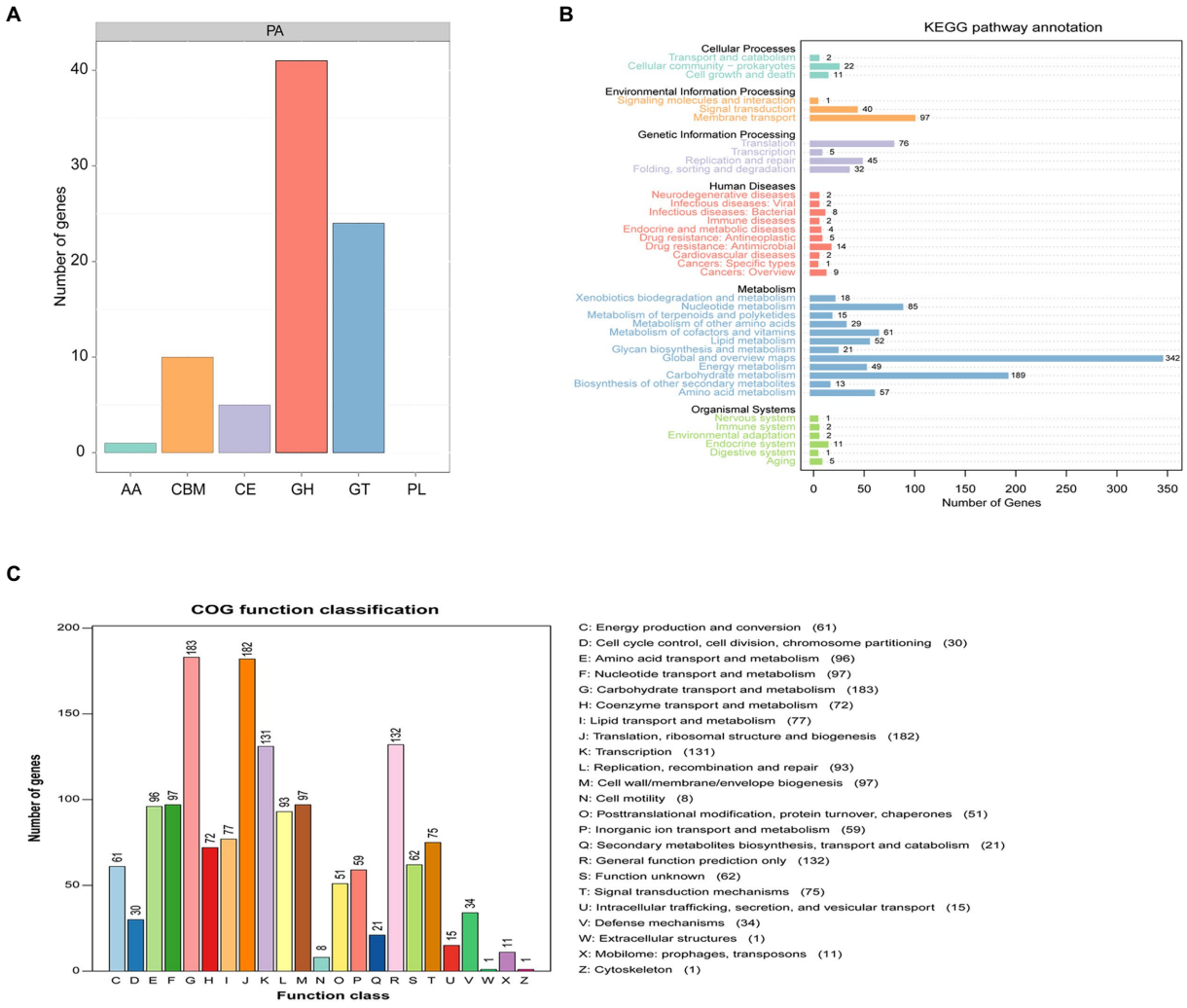

FIGURE 9
Functional prediction of *Pediococcus acidilactici*. **(A)** CAZy analysis of *Pediococcus acidilactici*. **(B)** Analysis of KEGG signaling pathway in *Pediococcus acidilactici*. **(C)** COG function prediction analysis of *Pediococcus acidilactici*.

that of *Lactobacillus casei* and *Lactobacillus paracasei*. *Pediococcus acidilactici* isolated by Pei et al. had a significant inhibitory effect on *Salmonella typhimurium* (Pei et al., 2021).

In the *in vitro* experiment, under different treatments of IPEC-J2 cells, the copy number of virions in each group was compared to determine the inhibitory effect on virion proliferation. Compared with other treatments, *Pediococcus acidilactici* showed a strong inhibitory effect. It has been reported that *Lactobacillus casei* can prevent rotavirus adhesion on the MA104 cell surface (Olaya Galán et al., 2016; Fernandez-Duarte et al., 2018), and *Lactobacillus paracasei* can also inhibit virus replication. This is the first time that *Pediococcus acidilactici* has been shown to inhibit the virus, which may be related to the physiological characteristics of *Pediococcus acidilactici*. In the *in vivo* experiment, the rotavirus particle copy number in the duodenum of mice in the *Pediococcus acidilactici* group was the lowest, indicating that immunization with *Pediococcus acidilactici* could effectively prevent virus infection. In the statistical analysis of the body weight loss rate, lactic acid bacteria could effectively alleviate the weight loss caused by virus infection in mice and gradually promote body weight gain (Glubokova et al., 2021). Through the duodenum and colon pathological examination for each group of mice, we found that rotavirus can destroy the integrity of the mouse duodenum villi, appearing at the top of the intestinal villus damage; cause a small amount of inflammatory cell infiltration accompanied by tissue interstitial oedema and inflammatory cell infiltration in the colon submucosa visible; and increase the number of goblet cells (Liu et al., 2013; Tada et al., 2016). However, there were no obvious pathological changes induced by the three *lactobacillus* strains, and the intestinal villi of mice in the *Pediococcus acidilactici* group were relatively intact (Wu et al., 2013). Overall, the lactic acid bacteria isolated from Tibetan mushrooms had an inhibitory effect on the virus, among which *Pediococcus acidilactici* had the best inhibitory effect. In animal experiments, the levels of cytokines in blood and SIgA in the faeces of mice in each group were detected. After immunization

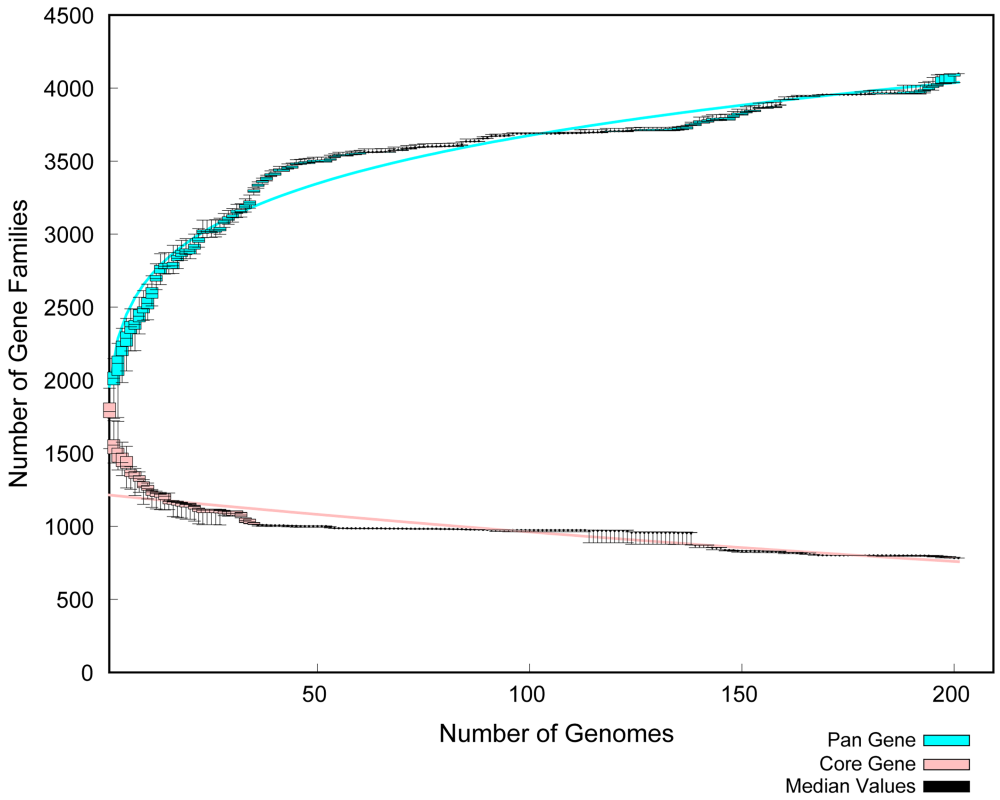

FIGURE 10
Comparative analysis of Pan Gene and Core Gene in *Pediococcus acidilactici*.

with lactic acid bacteria, the changes in IFN-β levels in blood were not significant, but the levels of IL-6 increased, those of TNF-α decreased, and those of SIgA in faeces showed an upwards trend, indicating that lactic acid bacteria can activate T cells. IL-6 can activate the lymphokines produced by T cells and fibroblasts, make the precursor of B cells become antibody producing cells, and cooperate with colony stimulating factors to promote the growth and differentiation of original bone marrow derived cells, and enhance the cleavage function of natural killer cells. In this experiment, the level of IL-6 increased significantly, which may be a factor for the role of *Pediococcus acidilactici* in the antiviral process. These effects of reducing inflammatory factor levels and increasing nonspecific antibody content to address viral infection were similar to those reported in the literature (Xie et al., 2021).

With the reduction of sequencing cost and the rapid development of sequencing technology, whole genome sequencing has become the most concise, effective, and rapid powerful tool to discover specific genes and explore the mechanism of action. Singh et al. compared the genome and phenotype of *Acinetobacter baumannii* AB030 with the highly resistant pathogen LAC-4 and found that AB030 contained many genes related to antibiotic resistance and virulence that were absent from LAC-4 (Singh et al., 2020). In this study, the second - and third-generation sequencing technologies were used to perform fine sequencing, analysis and functional annotation of the whole genome of *Pediococcus acidilactici* strain, and to analyze the biological characteristics and gene function of the strain at the molecular level.The collinearity analysis of the genome showed that the differences between the isolated *Pediococcus acidilactici* and GCF-013127755.1 strains were small, but there were still a small number of translocations and inversions, indicating that under long-term selection pressure, the strains expanded genes in the local collinear regions through gene horizontal transfer or directed evolution to add new functions and better adapt to the complex and variable environment.

Pediococcus acidilactici, *Lactobacillus casei*, and *Lactobacillus paracasei* isolated from Tibetan mushrooms have good probiotic properties and inhibitory effects on rotavirus infection. This study provided a feasible scheme for further understanding the infection process of rotavirus and the mechanism by which probiotics such as *Pediococcus acidilactici* inhibit virus replication.

Data availability statement

All data generated or analyzed in this study are included in the article (and its supplementary information file) published here in. 16S rDNA sequencing data have been uploaded to NCBI, and GenBank submitted: OM390598.1, OM390600.1, OM390599.1. Pig rotavirus was donated by Professor Ren Xiaofeng of Northeast Agricultural University. The number is DN30209. *Escherichia coli* (ATCC 25922), *Salmonella typhimurium* (ATCC 14028) and *Staphylococcus aureus* (ATCC 25923).

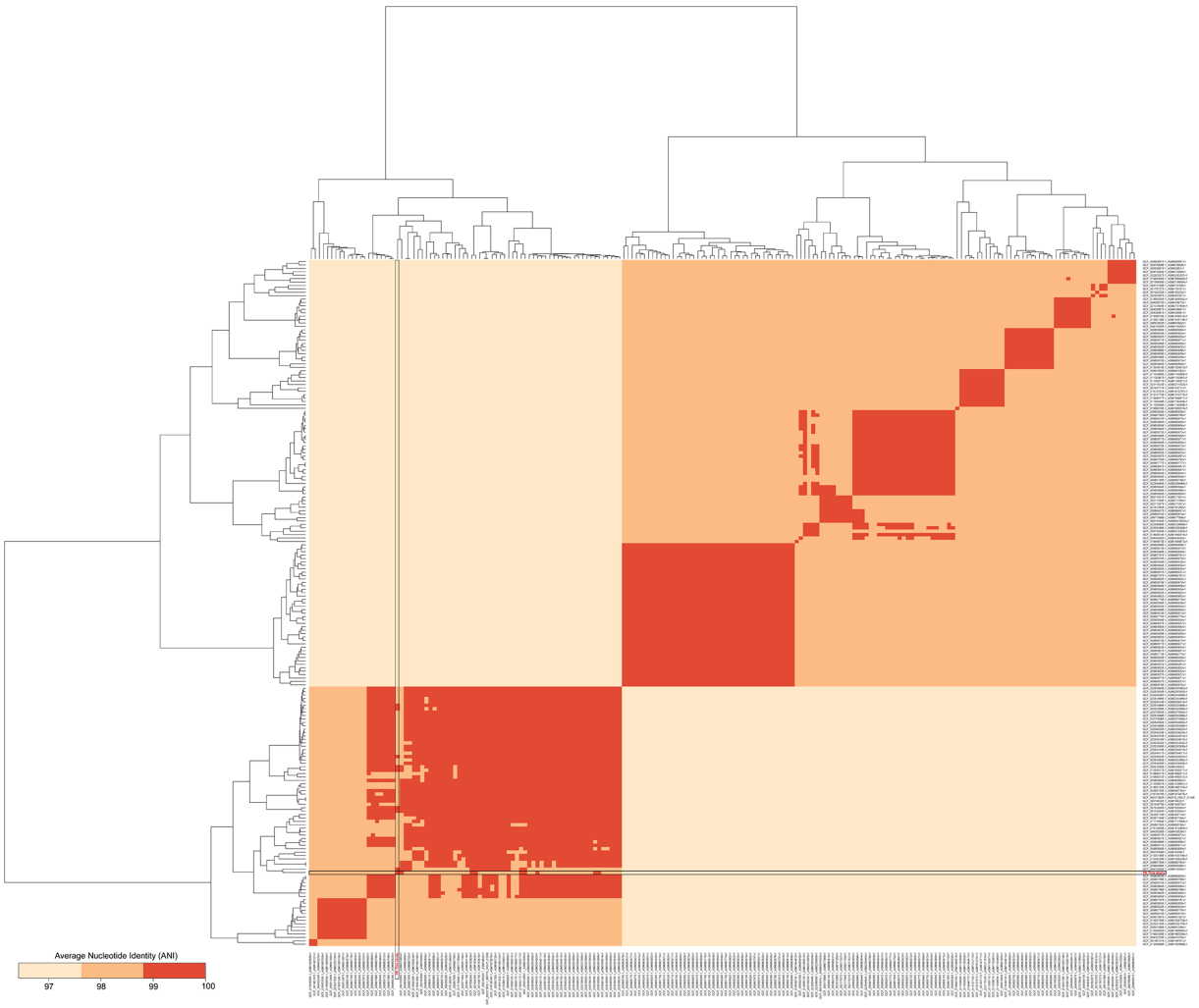

FIGURE 11
Nucleotide levels were compared between two genomic relatedness.

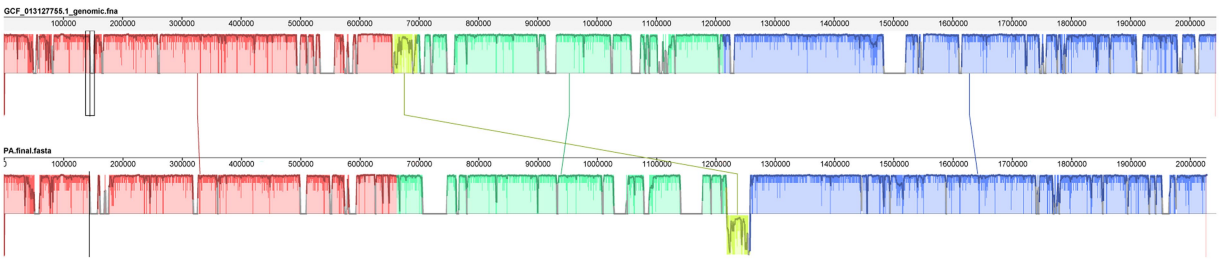

FIGURE 12
Collinearity analysis of *Pediococcus acidilactici* and GCF-013127755.1.

Ethics statement

The experiment was conducted in strict accordance with animal welfare and ethics guidelines.

Author contributions

Dr. Niu TM designed this research and completed most of the experimental work. Master Jiang YX wrote the first draft of the

manuscript, Master Fan SH, assisted in completing most of the experimental work. Teachers Yang GL, Shi CW, Ye LP, Wang CF provided theoretical guidance and technical support for this experiment. All authors have read and approved the manuscript.

Funding

This work was supported by the National Natural Science Foundation of China (31941018, 32072888, and U21A20261), China Agriculture Research System of MOF and MARA (CARS35), Science and Technology Development Program of Jilin Province (YDZJ202102CXJD029, 20190301042NY, and 20220202057NC) and the Science and Technology Project of the Education Department of Jilin Province (JJKH20220366KJ).

Acknowledgments

We thank the Jilin Provincial Animal Microecological Agent Engineering Research Center of Jilin Agricultural University for providing animal experimental knowledge and an SPF animal room.

Conflict of interest

The authors declare that the research was conducted in the absence of any commercial or financial relationships that could be construed as a potential conflict of interest.

Publisher's note

All claims expressed in this article are solely those of the authors and do not necessarily represent those of their affiliated organizations, or those of the publisher, the editors and the reviewers. Any product that may be evaluated in this article, or claim that may be made by its manufacturer, is not guaranteed or endorsed by the publisher.

Supplementary material

The Supplementary material for this article can be found online at: https://www.frontiersin.org/articles/10.3389/fmicb.2022.1069981/full#supplementary-material

References

Adikari, A., Priyashantha, H., Disanayaka, J., Jayatileka, D. V., Kodithuwakku, S. P., et al. (2021). Lisolation, identification and characterization of species diversity from: traditional fermented buffalo milk gels in Sri Lanka. *Heliyon* 7:e8136. doi: 10.1016/j.heliyon.2021.e08136

Ansari, F., Alian Samakkhah, S., Bahadori, A., Jafari, S. M., Ziaee, M., et al. (2021). Saccharomyces cerevisiae var. Boulardiihealth-promoting properties of as a probiotic; characteristics, isolation, and applications in dairy products. *Crit. Rev. Food Sci. Nutr.*, 1–29. doi: 10.1080/10408398.2021.1949577

Bengoa, A. A., Dardis, C., Garrote, G. L., and Abraham, A. G. (2021). Health-promoting properties of lacticaseibacillus paracasei: a focus on kefir isolates and exopolysaccharide-producing strains. *Foods* 10:2239. doi: 10.3390/foods10102239

Falfán-Cortes, R. N., Mora-Peñaflor, N., Gómez-Aldapa, C. A., Rangel-Vargas, E., Acevedo-Sandoval, O. A., et al. (2021). Characterization and evaluation of probiotic potential in vitro and in situ of lacticaseibacillus paracasei isolated from tenate cheese. *Journal of Food Protection*. doi: 10.4315/JFP-21-021

Fernandez-Duarte, K. P., Olaya-Galán, N. N., Salas-Cárdenas, S. P., Lopez-Rozo, J., and Gutierrez-Fernandez, M. F. (2018). Bifidobacterium adolescentis (dsm 20083) and lactobacillus casei (lafti l26-dsl): probiotics able to block the in vitro adherence of rotavirus in ma104 cells. *Prob. Antimicrob. Proteins* 10, 56–63. doi: 10.1007/s12602-017-9277-7

Gao, W., and Zhang, L. (2019). Comparative analysis of the microbial community composition between tibetan kefir grains and milks. *Food Res. Int.* 116, 137–144. doi: 10.1016/j.foodres.2018.11.056

Georgalaki, M., Zoumpopoulou, G., Anastasiou, R., Kazou, M., and Tsakalidou, E. (2021). Lactobacillus kefiranofaciens: from isolation and taxonomy to probiotic properties and applications. *Microorganisms* 9. doi: 10.3390/microorganisms9102158

Glubokova, E. A., Leneva, I. A., Kartashova, N. P., Falynskova, I. N., Tikhov, R. M., et al. (2021). Efficacy of (r)-6-adamantane-derivatives of 1,3-oxazinan-2-one and piperidine-2,4-dione in the treatment of mice infected by the a/California/04/2009 influenza virus. *Acta Nat.* 13, 116–125. doi: 10.32607/actanaturae.11020

Huang, S., Yu, Q., Xie, L., Ran, L., Wang, K., et al. (2021). Inhibitory effects of lactobacillus plantarum metabolites on porcine epidemic diarrhea virus replication. *Res. Vet. Sci.* 139, 32–42. doi: 10.1016/j.rvsc.2021.07.002

Hurtado-Romero, A., Del Toro-Barbosa, M., Gradilla-Hernández, M. S., Garcia-Amezquita, L. E., and García-Cayuela, T. (2021). Probiotic properties, prebiotic fermentability, and gaba-producing capacity of microorganisms isolated from mexican milk kefir grains: a clustering evaluation for functional dairy food applications. *Foods* 10:2275. doi: 10.3390/foods10102275

Jeong, Y. Y., Lee, G. Y., and Yoo, Y. C. (2021). Bovine lactoferricin induces intestinal epithelial cell activation through phosphorylation of fak and paxillin and prevents rotavirus infection. *J. Microbiol. Biotechnol.* 31. doi: 10.4014/jmb.2106.06044

Liu, F., Li, G., Wen, K., Wu, S., Zhang, Y., et al. (2013). Lactobacillus rhamnosus gg on rotavirus-induced injury of ileal epithelium in gnotobiotic pigs. *J. Pediatr. Gastroenterol. Nutr.* 57, 750–758. doi: 10.1097/MPG.0b013e3182a356e1

Mao, X., Gu, C., Hu, H., Tang, J., Chen, D., et al. (2016). Dietary lactobacillus rhamnosus gg supplementation improves the mucosal barrier function in the intestine of weaned piglets challenged by porcine rotavirus. *PLoS One* 11:e146312. doi: 10.1371/journal.pone.0146312

Mm, M., Mt, Y., Mo, R., and Ms, A. (1997). Non-seasonal viral and bacterial episode of diarrhoea in the Jordan Valley, west of Jordan. *FEMS Immunol. Med. Microbiol.* 18, 133–138. doi: 10.1111/j.1574-695X.1997.tb01038.x

Olaya Galán, N. N., Ulloa Rubiano, J. C., Velez Reyes, F. A., Fernandez Duarte, K. P., Salas Cárdenas, S. P., et al. (2016). In vitro antiviral activity of lactobacillus casei and bifidobacterium adolescentis against rotavirus infection monitored by nsp4 protein production. *J. Appl. Microbiol.* 120, 1041–1051. doi: 10.1111/jam.13069

Omatola, C. A., Ogunsakin, R. E., and Olaniran, A. O. (2021). Prevalence, pattern and genetic diversity of rotaviruses among children under 5 years of age with acute gastroenteritis in South Africa: a systematic review and meta-analysis. *Viruses* 13. doi: 10.3390/v13101905

Pei, L., Liu, J., Huang, Z., Iqbal, M., and Shen, Y. (2021). Effects of lactic acid bacteria isolated from equine on salmonella-infected gut mouse model. *Prob. Antimicrob. Proteins*. doi: 10.1007/s12602-021-09841-0

Rather, I. A., Choi, S. B., Kamli, M. R., Hakeem, K. R., Sabir, J., et al. (2021). Lactobacillus plantarumpotential adjuvant therapeutic effect of probio-88 postbiotics against SARS-cov-2. *Vaccine* 9. doi: 10.3390/vaccines9101067

Salaris, C., Scarpa, M., Elli, M., Bertolini, A., Guglielmetti, S., et al. (2021). Lacticaseibacillus paracasei dg enhances the lactoferrin anti-SARS-cov-2 response in caco-2 cells. *Gut Microbes* 13:1961970. doi: 10.1080/19490976.2021.1961970

Shin, D. Y., Yi, D. Y., Jo, S., Lee, Y. M., Kim, J. H., et al. (2020). Effect of a new lactobacillus plantarum product, lrcc5310, on clinical symptoms and virus reduction in children with rotaviral enteritis. *Medicine* 99:e22192. doi: 10.1097/MD.0000000000022192

Singh, M., De Silva, P. M., Al-Saadi, Y., Switala, J., Loewen, P. C., et al. (2020). Acinetobacter baumanniicharacterization of extremely drug-resistant and hypervirulent ab030. *Antibiotics* 9. doi: 10.3390/antibiotics9060328

Song, J. M. (2021). Parenteral, non-live rotavirus vaccine: recent history and future perspective. *Clin. Exp. Vacc. Res.* 10, 203–210. doi: 10.7774/cevr.2021.10.3.203

Sun, Y., Geng, W., Pan, Y., Wang, J., Xiao, P., et al. (2019). Supplementation with lactobacillus kefiranofaciens zw3 from tibetan kefir improves depression-like behavior in stressed mice by modulating the gut microbiota. *Food Funct.* 10, 925–937. doi: 10.1039/c8fo02096e

Tada, A., Zelaya, H., Clua, P., Salva, S., Alvarez, S., et al. (2016). Immunobiotic lactobacillus strains reduce small intestinal injury induced by intraepithelial lymphocytes after toll-like receptor 3 activation. *Inflamm. Res.* 65, 771–783. doi: 10.1007/s00011-016-0957-7

Tang, W., Li, C., He, Z., Pan, F., Pan, S., et al. (2018). Probiotic properties and cellular antioxidant activity of lactobacillus plantarum ma2 isolated from tibetan kefir grains. *Prob. Antimicrob. Proteins* 10, 523–533. doi: 10.1007/s12602-017-9349-8

Watanabe, T., Hayashi, K., Kan, T., Ohwaki, M., and Kawahara, T. (2021). Enterococcus faecalisanti-influenza virus effects of kh2 and snk12 rna. *Biosci. Microb. Food Health* 40, 43–49. doi: 10.12938/bmfh.2020-019

Wu, S., Yuan, L., Zhang, Y., Liu, F., Li, G., et al. (2013). Probiotic lactobacillus rhamnosus gg mono-association suppresses human rotavirus-induced autophagy in the gnotobiotic piglet intestine. *Gut Pathogens* 5:22. doi: 10.1186/1757-4749-5-22

Xie, P., Fang, Y., Shen, Z., Shao, Y., Ma, Q., et al. (2021). Broad antiviral and anti-inflammatory activity of qingwenjiere mixture against SARS-cov-2 and other human coronavirus infections. *Phytomed. Int. J. Phytother. Phytopharmacol.* 93:153808. doi: 10.1016/j.phymed.2021.153808

Zhao, L., Li, M., Sun, K., Su, S., Geng, T., et al. (2020). Hippophae rhamnoides polysaccharides protect ipec-j2 cells from lps-induced inflammation, apoptosis and barrier dysfunction in vitro via inhibiting tlr4/nf-κb signaling pathway. *Int. J. Biol. Macromol.* 155, 1202–1215. doi: 10.1016/j.ijbiomac.2019.11.088

frontiers | Frontiers in Microbiology

TYPE Original Research
PUBLISHED 16 March 2023
DOI 10.3389/fmicb.2023.1094071

OPEN ACCESS

EDITED BY
Hesong Wang,
Southern Medical University,
China

REVIEWED BY
Hajie Lotfi,
Tabriz University of Medical Sciences,
Iran
Mengfei Ye,
Shaoxing No.7 People's Hospital, China

*CORRESPONDENCE
Susana Ruiz-Ruiz
✉ ruiz_susrui@gva.es

†These authors have contributed equally to this work and share first authorship

SPECIALTY SECTION
This article was submitted to Microbial Symbioses, a section of the journal Frontiers in Microbiology

RECEIVED 09 November 2022
ACCEPTED 13 February 2023
PUBLISHED 16 March 2023

CITATION
Pesantes N, Barberá A, Pérez-Rocher B, Artacho A, Vargas SL, Moya A and Ruiz-Ruiz S (2023) Influence of mental health medication on microbiota in the elderly population in the Valencian region. *Front. Microbiol.* 14:1094071. doi: 10.3389/fmicb.2023.1094071

Influence of mental health medication on microbiota in the elderly population in the Valencian region

Nicole Pesantes[1,2†], Ana Barberá[1†], Benjamí Pérez-Rocher[3], Alejandro Artacho[1], Sergio Luís Vargas[4], Andrés Moya[1,2,3] and Susana Ruiz-Ruiz[1,2*]

[1]Fundación para el Fomento de la Investigación Sanitaria y Biomédica de la Comunitat Valenciana (FISABIO), València, Spain, [2]Consorcio de Investigación Biomédica en Red de Epidemiología y Salud Pública (CIBEResp), Madrid, Spain, [3]Instituto de Biología Integrativa de Sistemas (I2Sysbio), CSIC-Universitat de València, València, Spain, [4]Programa de Microbiología y Micología, Instituto de Ciencias Biomédicas, Facultad de Medicina, Universidad de Chile, Santiago, Chile

Spain has an aging population; 19.93% of the Spanish population is over 65. Aging is accompanied by several health issues, including mental health disorders and changes in the gut microbiota. The gut-brain axis is a bidirectional network linking the central nervous system with gastrointestinal tract functions, and therefore, the gut microbiota can influence an individual's mental health. Furthermore, aging-related physiological changes affect the gut microbiota, with differences in taxa and their associated metabolic functions between younger and older people. Here, we took a case–control approach to study the interplay between gut microbiota and mental health of elderly people. Fecal and saliva samples from 101 healthy volunteers over 65 were collected, of which 28 (EE|MH group) reported using antidepressants or medication for anxiety or insomnia at the time of sampling. The rest of the volunteers (EE|NOMH group) were the control group. 16S rRNA gene sequencing and metagenomic sequencing were applied to determine the differences between intestinal and oral microbiota. Significant differences in genera were found, specifically eight in the gut microbiota, and five in the oral microbiota. Functional analysis of fecal samples showed differences in five orthologous genes related to tryptophan metabolism, the precursor of serotonin and melatonin, and in six categories related to serine metabolism, a precursor of tryptophan. Moreover, we found 29 metabolic pathways with significant inter-group differences, including pathways regulating longevity, the dopaminergic synapse, the serotoninergic synapse, and two amino acids.

KEYWORDS

aging, microbiota, gut-brain axis, mental health disorders, 16S rRNA gene sequencing, metagenomics, tryptophan

1. Introduction

Spain has an aging population. In 2000, according to data from INE, the Spanish national statistics office (Instituto Nacional de Estadistica, 2021a)[1], the population over 65 years of age was 16.53% and in 2022 that percentage will rise to 20.22%. In fact, demographic projections made by INE suggest that this trend is accelerating, and by 2,068 people, over 65 years of age could represent 29.4% of the population (García et al., 2021). The increase in elderly population over recent years, and the aging rate (i.e., ratio of people over 65 vs. those under 16) is currently 129.11% in Spain and the Comunidad Valenciana (Instituto Nacional de Estadistica, 2021b). This circumstance is a clear indicator of the improvement in the quality of life in post-industrial countries, but we cannot ignore the fact that the quantity of life alone is not a sufficient indicator of quality of life.

According to the World Health Organization, over 20% of adults aged 60 and over suffer from a mental or neurological disorder. Mental disorders are defined as "health conditions characterized by alterations in thinking, mood, or behavior (or a combination thereof) associated with distress and impaired functioning." Mental health disorders affect mood, thinking, and behavior. These also include depression, anxiety, insomnia, eating disorders, and addictive behaviors. In the Comunidad Valenciana (Spain), there is a 24.6% risk of mental health disorders in adulthood, which can rise to 50% in people over 84 years old (Conselleria de Sanitat Universal i Salut Pública, 2020). Geriatric depression often remains undiagnosed and untreated and its symptoms are commonly attributed to normal aging; however, the lack of treatment has important consequences for both the patients' quality of life and the primary care system (Park and Unützer, 2011).

The elderly may experience life stressors common to all people, but also other stressors that are more common in later life, like a significant ongoing loss in capacities and a decline in functional ability. For example, older adults may experience reduced mobility, chronic pain, frailty, or other health problems, for which they require some form of long-term care (Chen et al., 2020). In addition, older people are more likely to experience events such as bereavement, or a decline in socioeconomic status with retirement (Venkatapuram et al., 2017). All of these stressors can result in isolation, loneliness, or psychological distress in the elderly, for which they may require long-term care (Harman, 2006).

There is growing evidence that the gut-brain axis, a bidirectional communication network that links the emotional and cognitive centers of the brain with peripheral intestinal functions, plays a role in promoting mental health or disorders (Richards et al., 2021). It regulates, for instance, appetite and feeding, glucose and metabolite homeostasis, and gut motility (Cryan and O'Mahony, 2011). Several factors can influence the bidirectional interplay between the gut and the brain, including: (i) neurological diseases like Parkinson, autism spectrum disorder or Alzheimer; (ii) psychological disorders, including depression, anxiety and insomnia; and (iii) gastrointestinal (GI) disorders such as irritable bowel syndrome and obesity (Liang et al., 2018; Suganya and Koo, 2020; Richards et al., 2021).

The transmission of sensory information from the gut to the brain is mediated by hormonal and neural circuits (Suganya and Koo, 2020). After a stimulus such as ingestion, the passage of nutrients from the duodenum and jejunum produces chemical and mechanical stimuli that are detected by enteroendocrine cells (EECs). These cells will then secrete signaling peptides detected by sensory cells from the enteric nervous system (ENS) or the central nervous system (CNS) (Liang et al., 2018). There are intestinal microorganisms with the ability to produce metabolites, such as serotonin and Gamma-aminobutyric acid (GABA), which are active neurotransmitters in the human nervous system (Mazzoli and Pessione, 2016). These metabolites, once secreted by the microbiota, induce intestinal epithelial cells to release neural modulating molecules that signal the ENS, which, in turn, signals the brain function and therefore influences the hosts' demeanor. GABA is the most abundant inhibitory neurotransmitter in the mammalian CNS. It is produced by microorganisms, plants, and animals and plays an important role in regulating blood pressure, sleep, cognition, and obesity, among other physiological functions. Therefore, it has been used as an antidepressant, hypotensive, insulin secretagogue, and as insomnia medication (Kalueff and Nutt, 2007).

It is also interesting to mention the functional role of essential amino acids produced by gut microbes, in particular tryptophan. The majority of tryptophan in the human body circulates in the blood attached to albumin, while only 10–20% can be found circulating freely (Gao et al., 2020). Studies have shown that changes in the gut microbiota affect the gut-brain axis by modulating the tryptophan metabolism and that metabolic products of tryptophan metabolism can interact with the gut-brain axis and the CNS. These metabolites include 5-hydroxytryptamine (5-HT or serotonin), indolic compounds, and kynurenines (KYN) (Gao et al., 2020). Only 1–2% of available ingested tryptophan goes through the 5-HT pathway. This has important implications as 5-HT is the neurotransmitter mainly responsible for regulating mood and anxiety.

Low serotonin levels in the CNS contribute to significantly increased depression and anxiety (Lindseth et al., 2015). The 5-HT pathway is involved in modulating emotions, food intake, sleep, sexual behavior, and pain management. Indeed, 8.95% of serotonin is synthesized in the GI tract by enterochromaffin cells (EC), which are the most common type of EECs, and help regulate intestine permeability, motility, secretion, epithelial development, mucosal inflammation, and the development and neurogenesis of the enteric nervous system (Liu et al., 2021). It is estimated that 95% of the produced serotonin is found in the GI tract (Richard et al., 2009).

The biosynthesis of 5-HT is entirely dependent on the enzyme tryptophan hydroxylase (TPH), which converts tryptophan into 5-hydroxytryptophan (5-HTP) (Gao et al., 2020). TPH is a rate-limiting enzyme that exists in TPH1 and TPH2. TPH1 is expressed in the EC cells in the GI tract and the pineal gland while TPH2 is mainly expressed in the myenteric plexus of the ENS and the serotonergic neurons of the brainstem (Pelosi et al., 2015). Dysregulation in TPH expression is believed to play a role in psychiatric disorders such as anxiety and GI diseases such as irritable bowel syndrome (Gao et al., 2020).

More than 90% of tryptophan is metabolized through the kynurenine pathway (KP). Indolamine 2, 3-dioxygenase (IDO), expressed in various organs such as the brain, the GI tract, and the liver, and tryptophan 2, 3-dioxygenase (TDO), mainly expressed in the liver, are the enzymes that catalyze the first step of tryptophan metabolism on KP (Gao et al., 2020). These enzymes transform tryptophan into N-formylkynurenine, which is subsequently

1 https://www.ine.es/

metabolized into KYN. Of these enzymes, TDO mediates the metabolism of KP at a basal level, while IDO is activated in an immune-activated environment (Chen et al., 2021). After KYN biosynthesis, it will continue to form other KYN such as kynurenic acid (KYNA) and quinolinic acid (QUIN). These compounds can cross the Blood–Brain Barrier (BBB) and reach the CNS, where they can act as neuromodulators and exert either neuroprotective or neurotoxic effects (Gao et al., 2020).

Ruiz-Ruiz et al. (2020) identified a link between aging and the microbial pathway associated with tryptophan and indole (tryptophan degradation product) production and metabolism by the commensal microbiota. The key proteins involved in tryptophan-to-indole metabolism, tryptophanase (TnaA), and tryptophan synthase (TrpB) are more abundant and expressed at higher levels in the gut microbiota of infants, whereas they are expressed at significantly lower levels in adults and even lower levels or below the detection limit in the elderly. From the age of 11 years, the human gut microbiota may exhibit a decreased capacity to produce these metabolites, and from the age of 34 years, this capacity may drop by over 90% compared to childhood (Ruiz-Ruiz et al., 2020). Tryptophan deficiency from a certain age could be associated with a high risk of mental health disorders in adulthood.

Oral health is also influenced by aging, with an increased prevalence of periodontal disease (Clark et al., 2021). There are studies that have shown that the composition and diversity of the oral microbiota are related to the general health state and frailty in aging (Ogawa et al., 2018; Singh et al., 2019). Furthermore, there is strong evidence that elderly people who have a relatively high number of missing teeth are more likely to develop dementia and mild cognitive impairment (Batty et al., 2013). Also, it has been suggested that transition of bacteria from the oral mucosa to the gut is more frequent in the elderly than in adults (Iwauchi et al., 2019), which increases when volunteers suffer from inflammatory oral or intestinal diseases (Kitamoto et al., 2020). Another studies demonstrated the significance of the oral microbiome in the development or progression of a number of systemic disorders, including type 2 diabetes (Arimatsu et al., 2014) and colorectal cancer Komiya et al., 2019, which might suggest a possible effect of the oral microbiota over other disorders including mental health disorders.

In the present study, we carried out 16S rRNA gene and metagenomic sequencing to determine differences in the taxa, functions, and metabolic pathways of intestinal and oral microbiota in a cohort of over 65-year-olds in the Comunidad Valenciana (Spain). The study included individuals treated with medication for anxiety, depression, and/or insomnia and those who were not diagnosed with any mental health disorders.

2. Materials and methods

2.1. Study participants

A case–control study was performed. Fecal and saliva samples from 101 volunteers over 65 were collected (EE cohort). All participants were residents of the Comunidad Valenciana (Spain) and filled out a questionnaire about their diet, general health, habits, weight and height (with which the body mass index (BMI) has been calculated), employment situation, medical history, and vaccinations. Some of this information is collected in Supplementary Table 1. The EE cohort was composed of 37 males and 63 females (average age 71.29 ± 5.83), 28 of whom (27.72%) reported being treated with antidepressants, anxiety, or insomnia medication (EE|MH group). Of these, 24 were women corresponding to 85.7% of the group (23.8% of the complete EE cohort), and 4 were men corresponding to 14.3% of the group (4% of the complete EE cohort). The remaining 73 were controls (EE|NOMH group). All procedures were reviewed and approved by the Ethics Committee (Reference: 20210305/07) of Fundación para el Fomento de la Investigación Sanitaria y Biomédica de la Comunitat Valenciana (FISABIO). All the volunteers provided written informed consent before their participation.

2.2. Sample preparation

Fecal samples were collected from each volunteer in sterile tubes, containing 10 mL of RNAlater Solution (Ambion) to stabilize and preserve the integrity of nucleic acids prior analysis. Samples were homogenized by adding 10 mL phosphate-buffered saline (PBS) (containing, per liter, 8 g of NaCl, 0.2 g of KCl, 1.44 g of Na2HPO4, and 0.24 g of KH2PO4 [pH 7.2]) and then centrifuged to eliminate solid waste. The obtained fecal microbial suspension was aliquoted and stored at −80°C until further processing. With respect to saliva samples, 3 mL was collected from each volunteer in sterile containers, aliquoted, and stored at −80°C until further processing.

2.3. DNA extraction of fecal samples

A total of 500 µL of fecal suspension was pelleted and weighted and the total genomic DNA was extracted using the QIAamp DNA mini stool kit (Qiagen). The fecal suspension pellet was resuspended in 1 mL of inhibitEX Buffer from the extraction kit and then 20 µL of lysozyme (10 mg/mL) was added for cellular lysis, followed by 30 min incubation at 37°C. The lysate was subjected to mechanical treatment with 200 µL of 150–212 µm diameter Glass Beads (Sigma) and heated to 95°C for 5 min. The samples were then centrifuged and 600 µL of the supernatant was treated with 45 µL of proteinase K. The following steps were carried out according to the manufacturers' recommendations.

2.4. DNA extraction of saliva samples

A total of 250 µL of saliva was pelleted at 4°C, weighted, and total genomic DNA was extracted using the QIAamp DNA mini kit (Qiagen) with a few preliminary steps. The pellet was resuspended in the leftover supernatant and incubated for 45 s in a 37°C ultrasonic cleaner (Raypa). Then, 130 µL of AL Buffer from the extraction kit was added to each sample and then 10 µL of "enzyme mix" containing 2.5 µL of lysozyme (100 mg/mL), 2.5 µL of lysostaphin (5 mg/mL), 2.5 µL of mutanolysin, and 2.5 µL of nuclease-free water was also added and incubated for one-hour at 37°C. Subsequently, 20 µL of proteinase K from the extraction kit was added to the lysate and the samples were incubated for 10 min at 56°C, followed by 10 min at 70°C, and 3 min at 95°C incubation. The lysate was then mixed with 200 µL of 100% ethanol and placed on the kit mini-column. Finally,

the washing steps were performed according to the manufacturers' recommendations.

2.5. 16S rRNA gene amplification, library, and sequencing

For fecal and saliva samples, V3-V4 hypervariable regions of the 16S rRNA gene were amplified by PCR using primers: 5′-TCGTCGGCAGCGTCAGATGTGTATAAGAGACAGCCTACG GGNGGCWGCAG-3′ (forward); and 5′-GTCTCGTGGGCTCGGA GATG TGTATAAGAGACAGGACTACHVGGTATCTAATCC-3′ (reverse). Amplicons were purified using NucleoMag NGS Clean-up and Size Select magnetic beads (Macherey-Nagel) and then Illumina sequencing adapters using the Nextera XT Index Kit (Illumina) were attached. Quantification of DNA was performed with a Qubit 3.0 fluorometer using the Qubit dsDNA HS assay kit (Thermo Fisher Scientific). Amplicon libraries were pooled in equimolar ratios for sequencing on a MiSeq platform of Illumina (2 × 300 bp paired-end reads) following the manufacturers' recommendations.

2.6. Metagenome library and sequencing

For fecal samples, whole-genome sequencing was also performed from total DNA. Metagenome libraries were obtained with Illumina's Nextera XT DNA Library Preparation Kit. Short fragments were eliminated using NucleoMag NGS Clean-up and Size Select magnetic beads (Macherey-Nagel) and the obtained purified libraries were sequenced in a MiSeq platform of Illumina (2 × 150 bp paired-end reads) following the manufacturers' recommendations.

2.7. Bioinformatics and statistical analysis

In-house bioinformatic analysis pipelines were applied. For 16S rDNA gene analysis, we obtained the amplicon sequence variant (ASV) data with the DADA2 pipeline (Callahan et al., 2016), which removed the forward and reverse primers, filtered low-quality reads, and trimmed reads by length. Paired reads were merged to obtain the full denoised sequences, combined and abundance matrices were obtained. Chimeric ASVs as well as host (human) ASVs were removed. Finally, taxonomy was assigned to each variant by comparing them against the SILVA database (Quast et al., 2012) (naive Bayesian classifier to assign up to genus level and 97% blast matching for species level).

For metagenomic analysis, once the raw sequencing data were obtained, the sequencing adaptors were removed by Cutadapt software. Low-quality reads were eliminated using PRINSEQ, as well as short reads, and reads with a high percentage of ambiguous bases, in addition to low entropy reads. To join overlapping pairs to obtain longer sequences, the FLASH software was used. Non-overlapping forward pairs were also taken into account while non-overlapping reverse pairs were discarded. The host (human) genome and the non-coding ribosomal RNA sequences were filtered out using Bowtie2 with the SILVA database. The reads were then assembled into contigs using Megahit and mapped against the contigs using Blast. Open reading frames (ORF) were predicted using the Prodigal software and abundance tables were created. Functional annotation was performed by mapping each ORF against protein family database using the program HMMER and the KEGG Orthology database. Finally, Kaiju was used for taxonomical annotation of metagenome data. Once the functional compositional matrix was obtained, the results were grouped into functional categories and metabolic pathways.

Each matrix, including the ASV, phylum, genus, and functional compositional matrices were then analyzed. The R statistics software was applied to obtain alpha (Shannon and Chao1 indexes) and beta diversity (Canonical Correspondence Analysis (CCA), Permanova test, and Wilcoxon non-parametric test). Correlation analysis between the saliva and fecal samples was obtained using the sPCA mixomics approach for a single omic (Kim-Anh et al., 2016).

2.8. Robustness analysis: attenuation and buffering

Functional capacities of microbiomes are dependent on the taxonomic structure of the microbial community, because each taxon is associated to putatively different functions and abundances. The functional metagenome could be inferred considering the taxonomic composition of the microbial community. Changes in the composition and/or abundance of one or more taxa can cause changes in functional capacities. This has recently been described as taxa-function relationships (Vieira-Silva et al., 2016; Eng and Borenstein, 2018).

Two main systemic parameters can be estimated to determine the functional robustness of microbial communities: attenuation and buffering. The determination was done using the microbial community taxa-function robustness estimation pipeline developed by Eng and Borenstein (2018).[2] To calculate changes in functional capacities or, more formally, to quantify the changes in gene composition induced by changes in taxonomical structure, the abovementioned work describes an approach to evaluate the taxa-function robustness and quantify the two abovementioned parameters. Attenuation measures how rapidly the functional shift increases as perturbation magnitude increases and buffering is defined as how large a taxonomic perturbation must be before noticeable functional shifts occur. These two parameters can be measured globally and for particular superpathways or pathways, thereby detecting the weakest points in the global microbiota metabolism when a stochastic change in the microbial community occurs, generating deviations in the functional profile.

We have implemented some modifications in the original pipeline in order to improve sensitivity and accuracy. First, we used PICRUSt2 (Douglas et al., 2020) to derive a 16S copy number table, a genomic content annotation table, and a phylogenetic tree. Second, those files were used to replace the ones provided by the original pipeline. Manipulation of data and its graphical representation, as well as and statistical tests, was done using R scripts using libraries dplyr, ggplot, and ggpubr. Attenuation and Buffering measurements, graphical

2 https://github.com/borenstein-lab/robustness

10.3389/fmicb.2023.1094071

representation, and statistical tests were done using R scripts and libraries dplyr (Wickham et al., 2022) and ggplot2 (Wickham, 2016).

2.9. Data availability statement

The curated sequences from 16S rRNA gene and metagenomes were deposited in the EBI Short Read Archive under the study accession number PRJEB56919, with accession numbers ERS13596619- ERS13596719 and ERS13596821-ERS13596921 for the16S rRNA gene from fecal and saliva samples, respectively, and ERS13596720-ERS13596820 for metagenomes.

3. Results

3.1. Clinical and biochemical characteristics

We obtained samples from a cohort of 101 volunteers over 65 years old (EE cohort) from the Comunidad Valenciana (Spain), 28 of whom were treated with medication for anxiety, depression, and/or insomnia (EE|NOMH group) and 73 not treated for any mental health disorders (EE|NOMH group). The medication of the EE|MH group included modulators of GABA receptors, modulators of serotonin availability, or sleep regulators (Table 1). Some participants combined more than one type of medication at the same time. In addition, some of them suffer common age-related diseases (hypercholesterolemia, hypertension, diabetes, and coronary diseases) and take medication for its treatment. Both groups had a similar representation of these most common diseases.

TABLE 1 Volunteers over 65years from the Valencian Community which were treated with medication for anxiety, depression, and insomnia (EE|MH).

Identification number	Age	Gender	Group
EE13	67	Female	1
EE24	68	Female	1
EE25	68	Female	2
EE26	65	Male	2
EE27	68	Female	4
EE34	70	Female	3
EE37	75	Female	1
EE38	83	Female	1
EE40	69	Female	2
EE42	65	Female	1
EE50	65	Female	2
EE54	73	Female	1
EE62	66	Female	3
EE64	81	Male	1
EE71	82	Female	2
EE72	68	Female	2
EE74	88	Female	1
EE75	74	Female	3
EE79	68	Female	3
EE83	74	Female	3
EE89	71	Female	1
EE90	90	Male	1
EE91	89	Female	1
EE95	66	Female	4
EE102	65	Female	3
EE107	65	Female	1
EE108	71	Male	1
EE113	66	Female	1

Groups: 1: Modulators of GABA receptors; 2: Modulators of serotonin availability; 3: Combination of groups 1 and 2; 4: Sleep regulators.

3.2. 16S taxonomy from fecal samples

A total 7,050,645 reads were sequenced from fecal samples, 18.23% of which were removed after quality check and host filtering, obtaining an average of 57,086 reads per sample (maximum length = 109,272, minimum length = 12,168, total number reads = 5,822,728). Taxonomic annotation showed two phyla with main representation in the EE cohort: Firmicutes (48.92%) and Bacteroidota (40.76%). Other phyla with lower representation included: Proteobacteria (4.25%), Actinobacteriota (2.82%), Verrucomicrobiota (1.31%), Desulfobacterota (0.70%), Cyanobacteria (0.15%), and Synergistota (0.12%).

Alpha diversity analyses at genus and ASV levels showed that Shannon and Chao indexes were not statistically significant between EE|MH and EE|NOMH groups (Figures 1A,B). However, regarding beta diversity, the distribution of genera and ASV in the two groups was statistically significant (Adonis test, value of $p = 0.003$ and 0.038, respectively; Figure 1C). Because the EE/NOMH group has a clearly higher number of individuals than the EE/NOMH group (73 versus 28 volunteers), the analysis was repeated three times, each time choosing a group of 30 EE/NOMH individuals at random, in order to avoid bias due to the difference in the members of each group. In the three comparisons, the result was statistically significant with value of *ps* of 0.04, 0.021, and 0.002, respectively. The Wilcoxon non-parametric test also showed statistically significant differences (value of $p < 0.05$) between the two groups in the following eight genera (Figure 2A): *Bilophila*, *Bacteroides*, *Colidextribacter*, *Flavonifractor*, *Parabacteroides*, *Oscillibacter*, *Alistipes*, and *Coprococcus* and in five ASVs (Figure 2B), which correspond to the species *Flavonifractor plautii, Bilophila wadsworthia, Lachnospira pectinoschiza*, and two with *Faecalibacterium prausnitzii*. Of these, the genus *Coprococcus* and the ASVs corresponding to the species *Flavonifractor plautii* and *Bilophila wadsworthia* were more abundant in the EE|NOMH group.

3.3. 16S taxonomy from saliva samples

A total of 9,050,887 reads were sequenced from saliva samples, 24.47% of which were removed after quality check and host filtering, obtaining an average of 68,358.57 reads per sample (maximum length = 488,613, minimum length = 28,571, total number of reads = 6,835,857). Taxonomic annotation showed that the most

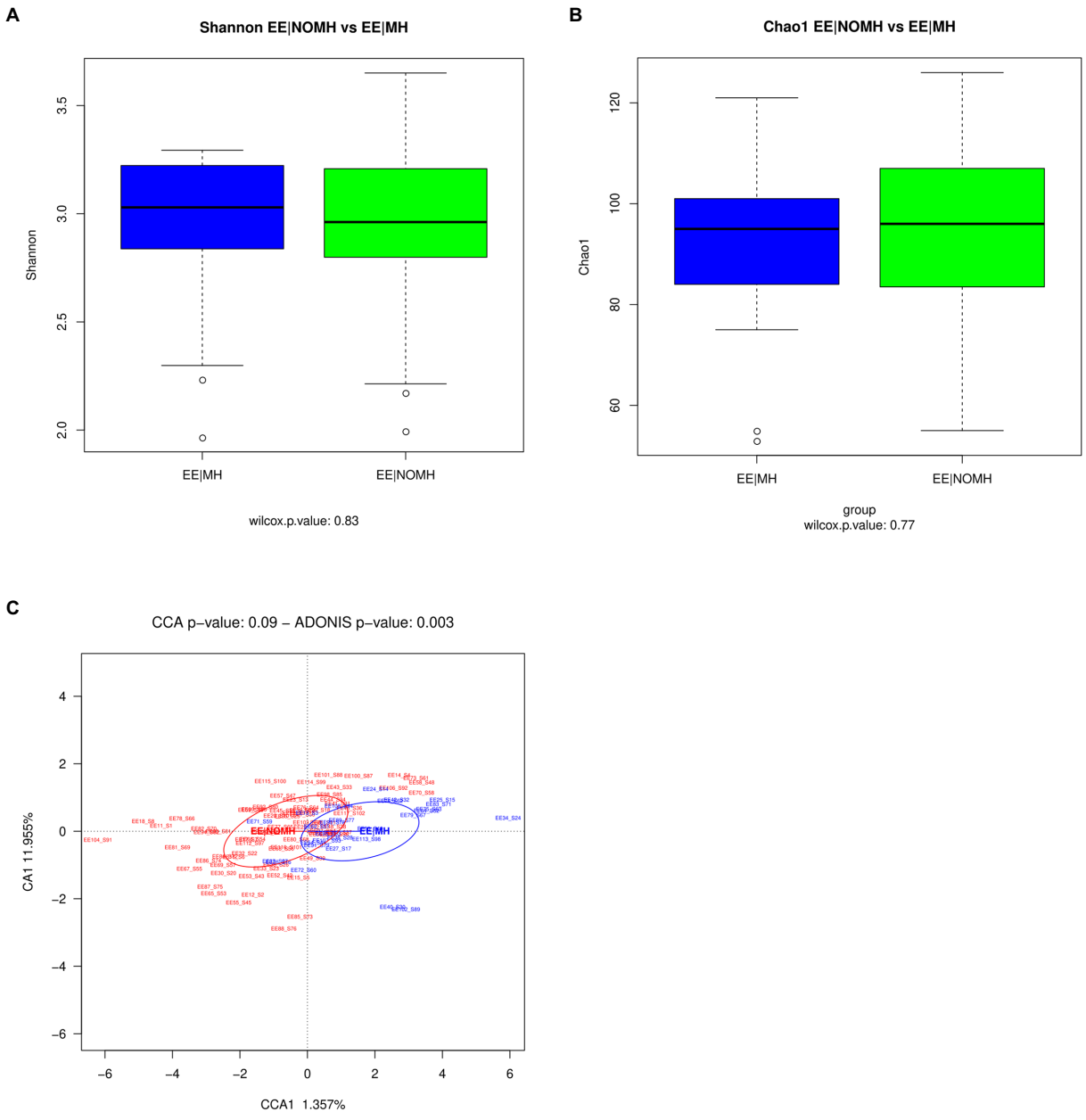

FIGURE 1
16S alpha and beta diversity of fecal samples. **(A)** Shannon diversity index and **(B)** richness estimator Chao1 analysis between EE|MH and EE|NOMH groups. **(C)** Canonical Correspondence Analysis (CCA) of EE|MH (blue) and EE|NOMH (red) groups at genus level.

represented phyla were Firmicutes (30.22%), Bacteroidota (28.91%), and Proteobacteria (20.48%), and other phyla with lower representation that included Fusobacteriota (8.15%), Actinobacteriota (5.82%), Patescibacteria (2.97%), Campilobacterota (2.21%), and Spirochaetota (0.83%). Similar results to those obtained with fecal samples were detected for the alpha diversity at the genus and ASV levels of saliva samples. Shannon and Chao indexes were not significantly different with p values >0.05 between EE|MH and EE|NOMH (Figures 3A,B). However, significant differences were found in the beta diversity between groups (Adonis test value of $p = 0.02$) (Figure 3C). We identified statistically significant differences (Wilcoxon test) for five genera (Figure 4A): *Veillonella*, Neisseria, *Porphyromonas*, *Lactobacillus*, and *Treponema*, and five ASV (Figure 4B), which corresponded to the species *Oribacterium asaccharolyticum, Stomatobaculum longum, Fusobacterium periodonticum, Veillonella rogosae*, and *Porphyromonas pasteri*. Only the genus *Veillonella* and the ASV corresponding to *Oribacterium asaccharolyticum* and *Stomatobaculum longum* were more abundant in EE|MH, while the rest were more abundant in EE|NOMH.

3.4. Correlation analysis between gut and saliva microbiota

Correlation analysis between the gut and the saliva microbiota at genus level was performed using the Mixomics single omic approach.

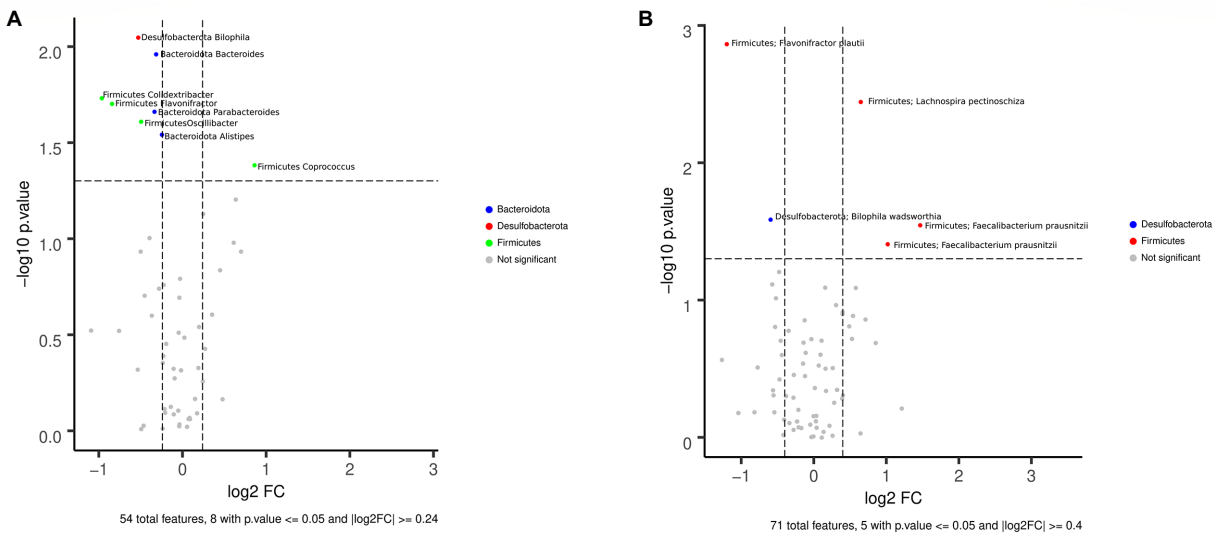

FIGURE 2
Volcano plots showing the differential abundance of **(A)** genera and **(B)** ASVs between EE|MH (right) and EE|NOMH (left) groups in fecal samples.

The correlation analyses showed differences between both groups. In the EE|MH group the genus *Lachnospira* (gut) with the genera *Megasphaera* and *Atopobium* (saliva) and the genus *Subdoligranulum* (gut) with the genus *Lachnoanaerobaculum* (saliva) showed significant negative correlations, while the genus *Odoribacter* (gut) with the genera *Alloprevotella* and *Haemophilus* (saliva) and the genera *Lachnoclostridium*, and *Colidextribacter* (gut) with the genus *Megasphaera* (saliva) showed positive correlation (Figure 5A). By contrast, the genus *Alistipes* (gut) had significant negative correlation with the genera *Veillonella* and *Prevotella* (saliva) in the EE|NOMH group (Figure 5B).

3.5. Functional orthologs analysis from metagenome data of fecal samples

A total 554,768,576 reads were sequenced, 19.09% of which were removed after quality check and host filtering, obtaining an average of 4,444,094.52 reads per sample (maximum length = 15,434,500, minimum length = 924,728, number of total reads = 448,853,547); of these 270,608,848 were correctly assigned to KEGG Orthology (KO) categories (maximum number of reads assigned per sample = 10,033,384; minimum number of reads assigned per sample = 330,178).

No significant differences were found in the CCA analysis between EE|MH and EE|NOMH for KO categories (Adonis test value of $p = 0.24$; Supplementary Figure 1). However, the Wilcoxon test identified 382 KO categories that showed significant differences (value of $p < 0.05$). It is worth mentioning that five are involved in tryptophan metabolism (K00382, K03781, K01692, K00658, and K01667) (see Supplementary Figure 2) and six in serine metabolism (K00382, K02437, K01079, K00281, K00605, and K18348/K12235). Serine is used by bacteria to convert indole into tryptophan- (see Supplementary Figure 3), which were higher in EE|MH than in EE|NOMH (Figure 6). Furthermore, 19 KO categories involved in the synthesis of metabolic products related to GABA production was higher in the EE|MH group (K13746, K03474, K00294, K00175, K01425, K03473, K09758, K05275, K00174, K17865, K05597, K01580, K00262, K01640, K00634, K01692, K13051, K01470, and K09472). Three of these KO categories correspond to the arginine and proline metabolism pathway (K00294, K01470, and, K09472), five to the alanine aspartate and glutamate metabolism (K00262, K00294, K01425, K01580, and K05597), seven to the butanoate metabolism (K00174, K00175, K00634, K01580, K01640, K01692, and K17865), and three to the vitamin B6 metabolism (K03473, K03474, and K05275) which, as a co-factor, is also involved in the biosynthesis and catabolism of amino acids and neurotransmitters like GABA (Table 2). Finally, two more KO categories were shared by the arginine and proline metabolism and the alanine, aspartate, and glutamate metabolism pathways (K00294) and by the alanine, aspartate, and glutamate metabolism, and the butanoate metabolism pathways (K01580). The genus contribution to these KOs was obtained using taxonomy information from metagenomic data through Kaiju. The genera *Bacteroides* and *Alistipes* were the most representative in most of the KOs analyzed. It is noteworthy that the percentage of the *Bacteroides* contribution was higher in the EE|MH group in all but one KO and that the genus *Alistipes* had a higher contribution in most of the KOs in the EE|NOMH group (Table 2).

3.6. Analysis of KEGG metabolic pathways

CCA analysis carried out between EE|MH and EE|NOMH showed no statistically significant differences in KEGG pathways (Adonis test $p-$value = 0.25; see Supplementary Figure 4). However, 29 KEGG pathways showed significant differences in the Wilcoxon test. Interestingly, considering that both groups consisted of individuals over the age of 65, the pathway regulating longevity was significantly higher in EE|MH than in EE|NOMH (path 04211, value of $p = 0.02$; Figure 7A). In addition, two amino acid metabolism pathways also showed higher abundance in the EE|MH group: valine, leucine, and isoleucine degradation (path 00280, value of $p = 0.0084$)

10.3389/fmicb.2023.1094071

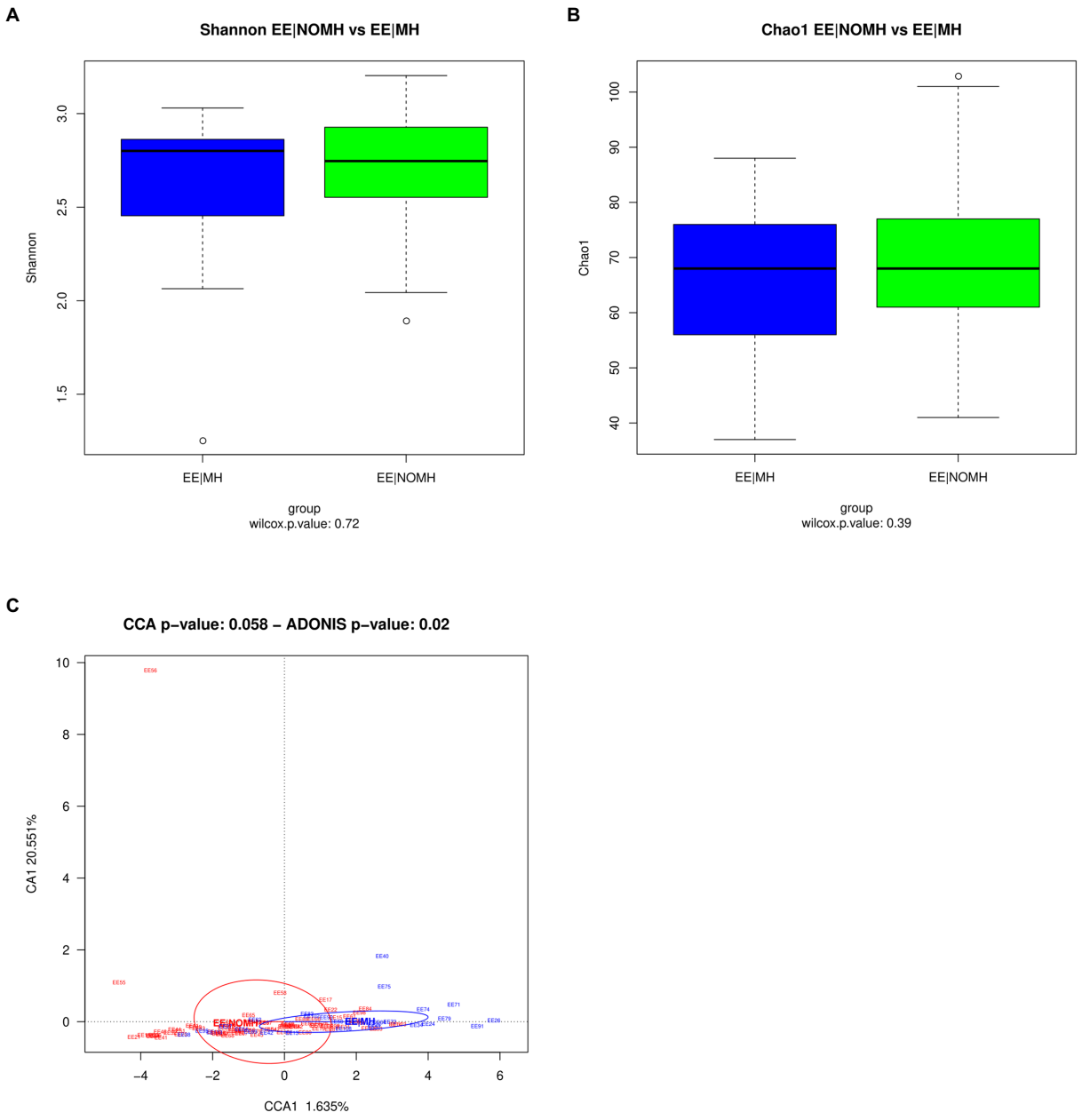

FIGURE 3
16S alpha and beta diversity of saliva samples. **(A)** Shannon diversity index and **(B)** richness estimator Chao1 analysis between EE|MH and EE|NOMH groups. **(C)** Canonical Correspondence Analysis (CCA) of EE|MH (blue) and EE|NOMH (red) groups at genus level.

and phenylalanine metabolism (path: 00360, value of $p = 0.0088$; Figure 7B). Finally, the other two significant KEGG pathways related to the CNS and tryptophan metabolism were higher in the EE|MH group, the dopaminergic synapse (path: 04728 value of $p = 0.015$) and serotoninergic synapse (path 04726, value of $p = 0.019$; Figure 7C).

3.7. Robustness analysis of samples

EE|MH and EE|NOMH groups showed no differences in either attenuation (Mann–Whitney test value of $p = 0.072$) or buffering (Mann–Whitney test p value = 0.15) in fecal samples. Attenuation and buffering for each individual are shown in Supplementary Table 2. In addition, values of attenuation and buffering for each individual within each group (Supplementary Figure 5A) are not correlated after applying Pearson's correlation coefficient. In some cases, individual pathways start from a common precursor, or produce a common product, but they can also have other relationships. Superpathways can have individual reactions due to their components in addition to other pathways. Moreover, distribution curves of attenuation and buffering (Supplementary Figures 5B,C, respectively) were similar for both groups, controls and treated individuals. Similar results to those observed in fecal samples were observed for saliva. Attenuation and buffering for each individual saliva sample are shown in

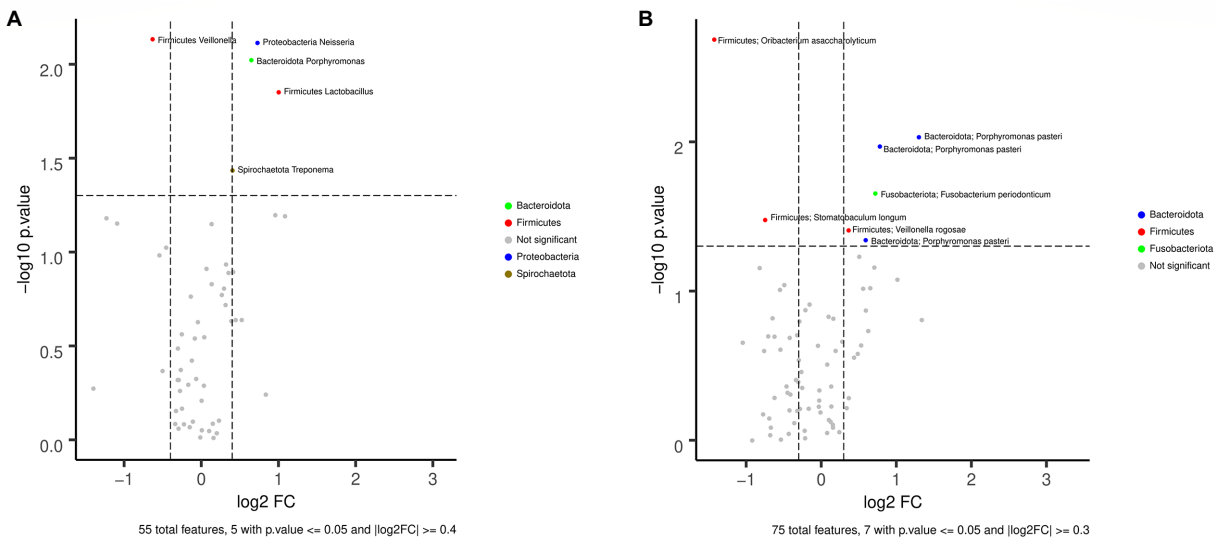

FIGURE 4
Volcano plots showing the differential abundance of **(A)** genera and **(B)** ASVs between EE|MH (right) and EE|NOMH (left) in saliva samples.

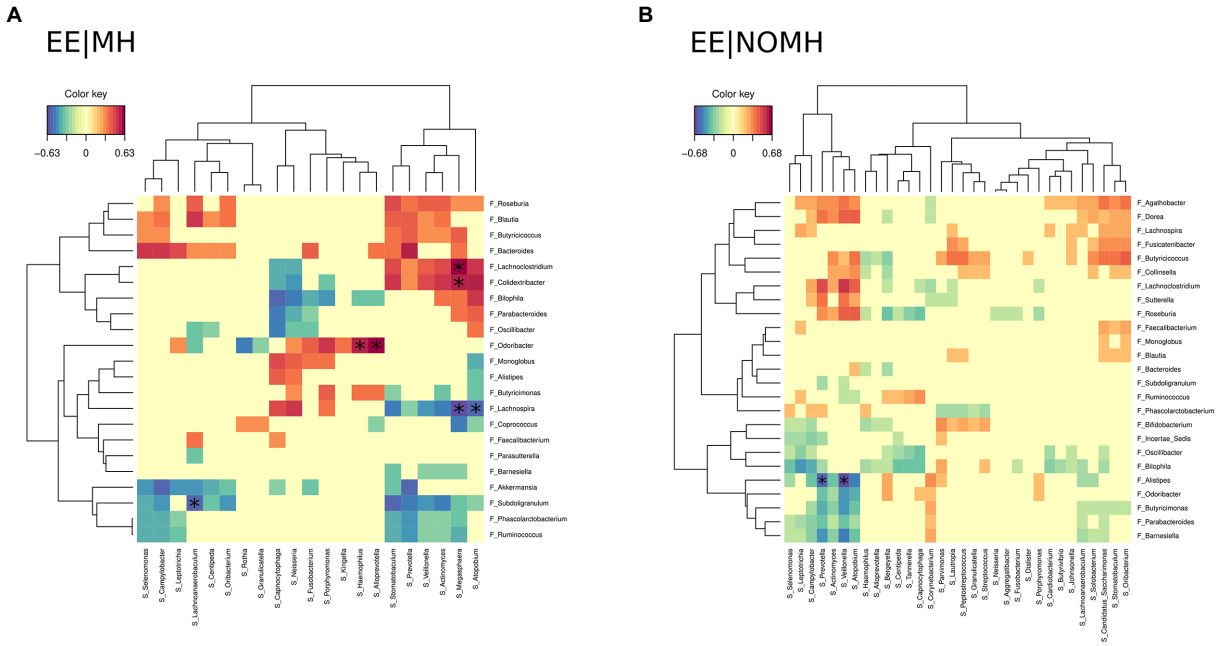

FIGURE 5
Heatmaps charts showing the correlations between gut and saliva microbiota in **(A)** EE|MH and **(B)** EE|NOMH groups.

Supplementary Table 3. Attenuation (Mann–Whitney test, p value = 0.41) and buffering (Mann–Whitney test, p value = 0.95 for Buffering) were not significant between groups. Moreover, values of attenuation and buffering for each individual within each group (Supplementary Figure 6A) did not correlate after applying Pearson's correlation coefficient. Furthermore, distribution curves of attenuation and buffering (Supplementary Figures 6B,C, respectively) were also similar for both groups, controls and treated.

Of the 20 main superpathways, most will have an additional parent class within the pathway ontology to define their biological role. Statistical differences for attenuation were found for fecal and saliva samples in superpathways for both groups (Supplementary Figures 7A,B, respectively). In fecal samples only in superpathway cell motility (lower attenuation in treated group, value of p in Kruskal–Wallis test 0.0428) while in saliva samples, we found differences in attenuation for four superpathways (higher for treated group in superpathways for lipid metabolism and translation and lower in metabolism of terpenoids and polyketides, and cell growth and death). In case of buffering, no differences were found in fecal samples (Supplementary Figure 7C), while differences were recorded

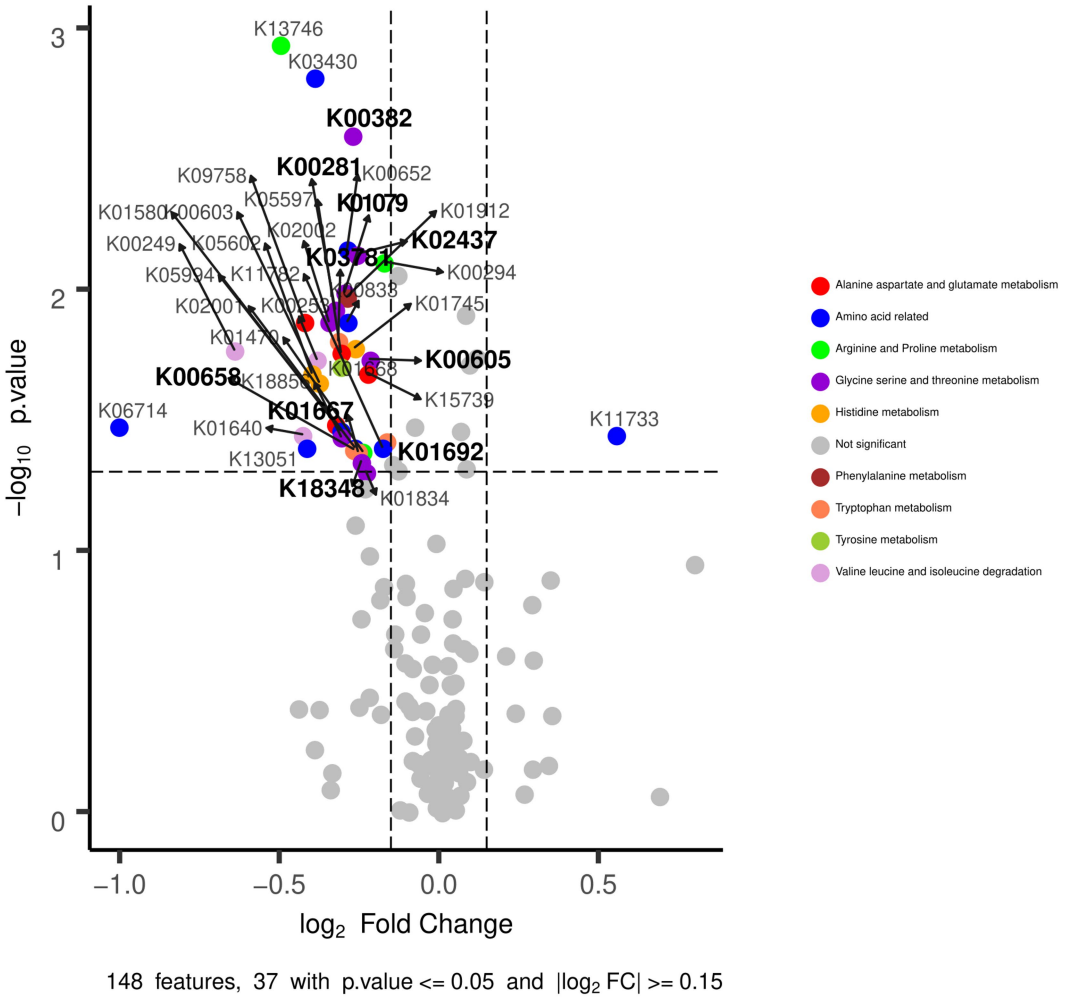

FIGURE 6
Significant differences in KEGG categories, in bold those related to tryptophan and serine metabolism between EE|NOMH (right) and EE|MH (left) groups.

in only four superpathways in saliva samples: lipid metabolism, metabolism of other amino acids and folding, sorting and degradation (lower for treated group) and, finally, metabolism of terpenoids and polyketides (higher in treated group; Supplementary Figure 7D).

4. Discussion

Tryptophan is an essential amino acid for protein synthesis, and the least abundant amino acid in proteins and cells (Gao et al., 2020). Certain bacterial products of tryptophan metabolism, including serotonin, indolic compounds, and kynurenines, can interact with the gut-brain axis and the CNS of the host, thereby modulating physiology (Agus et al., 2018). Changes affecting the gut-brain axis are thought to be connected to a number of neurological disorders, such as Parkinson's disease, Autism spectrum disorder, and Alzheimer's disease, as well as some gastrointestinal (GI) disorders, such as irritable bowel syndrome and obesity, and even some psychological disorders, such as depression, anxiety, and insomnia (Liang et al., 2018; Richards et al., 2021). Other authors have focused on the role of the microbiota in the development of mental health-related conditions, discussing that conditions characterized by acute or chronic inflammation, depression, decreased quality of life or cognitive impairment are related to the metabolic alteration of amino acid precursors of neurotransmitters, such as tryptophan and phenylalanine among others Strasser et al., 2017.

Around 90–95% of available tryptophan goes through the KP, 1–2% of it forms 5-HT and melatonin through the serotonin pathway, and 4–6% is metabolized into indole and other indolic derivates by bacteria (Gao et al., 2018), that can be transferred across the blood–brain barrier to reduce neuroinflammation Cox and Weiner, 2018. The microbiota plays an important role, for instance, it is crucial for the gut's amino acid metabolism, which has an impact on neuroinflammatory illnesses. The ability of the microbiota to access gut-brain signaling pathways and modify the host's behavior depends on bidirectional communication along the gut-brain axis. TPH2 is the protein that catalyzes the first step in serotonin biosynthesis from tryptophan in the brain. An imbalance in serotonin levels has been widely associated with neuropsychiatric disorders such as depression and anxiety (Pelosi et al., 2015). Shishkina et al. showed that TPH2 expression increases in the midbrain in animal models of depression treated with antidepressants (Shishkina et al., 2007). In our study, the

10.3389/fmicb.2023.1094071

TABLE 2 Significantly different KO categories and the genera with the highest contribution to them in both groups.

KO	*p*-value	Pathway	Most abundant	Genera with the highest contribution in EE|MH	Genera with the highest contribution in EE|NOMH
K03781	0.016	Tryptophan metabolism	EE|MH	*Bacteroides* (45.5%) *Alistipes* (21.6%)	*Bacteroides* (36%) *Alistipes* (24%)
K00658	0.041	Tryptophan metabolism	EE|MH	*Bacteroides* (57.4%)	*Bacteroides* (52.3%)
K01667	0.042	Tryptophan metabolism	EE|MH	*Bacteroides* (29%) *Alistipes* (23.1%)	*Bacteroides* (22.6%) *Alistipes* (23.3%)
K02437	0.007	Glycine, serine and threonine metabolism	EE|MH	*Bacteroides* (31.5%) *Alistipes* (9.9%)	*Bacteroides* (27.1%) *Alistipes* (11.5%)
K01079	0.01	Glycine, serine and threonine metabolism	EE|MH	*Bacteroides* (36.8%) *Alistipes* (9.3%)	*Bacteroides* (34.5%) *Alistipes* (12.4%)
K00281	0.011	Glycine, serine and threonine metabolism	EE|MH	*Bacteroides* (43%) Alistipes (12.3%)	*Bacteroides* (39.7%) *Alistipes* (12.4%)
K00605	0.018	Glycine, serine and threonine metabolism	EE|MH	*Bacteroides* (46.7%) *Alistipes* (14.3%) *Prevotella* (6.2%)	*Bacteroides* (38.1%) *Alistipes* (13.1%) *Prevotella* (9.4%)
K18348 K12235	0.046	Glycine, serine and threonine metabolism	EE|MH	*Bacteroides* (16.1%) *ParaBacteroides* (6.2%) *Faecalibacterium* (6.2%)	*Bacteroides* (14.1%) *ParaBacteroides* (8.7%)
K13746	0.001	Arginine and proline metabolism	EE|MH	*Bacteroides* (60%)	*Bacteroides* (40%) *Roseburia* (20%)
K01470	0.042	Arginine and proline metabolism	EE|MH	*Bacteroides* (36.6%)	*Bacteroides* (34.8%)
K09472	0.049	Arginine and proline metabolism	EE|MH	*Bilophila* (16.7%) *Enterobacter* (16.7%) *Escherichia* (16.7%)	not assigned
K01425	0.009	Alanine, aspartate and glutamate metabolism	EE|MH	*Bacteroides* (41.6%) *Alistipes* (8.1%)	*Bacteroides* (31.6%) *Alistipes* (9.6%)
K09758	0.013	Alanine, aspartate and glutamate metabolism	EE|MH	*Bacteroides* (47.5%)	*Bacteroides* (43.7%)
K05597	0.017	Alanine, aspartate and glutamate metabolism	EE|MH	*Bacteroides* (62%) *Sutterella* (11%) *Phascolarctobacterium* (5.8%)	*Bacteroides* (59.8%) *Sutterella* (5%) *Phascolarctobacterium* (6.3%)
K00262	0.033	Alanine, aspartate and glutamate metabolism	EE|MH	*Bacteroides* (23.1%) *Faecalibacterium* (6.1%) *Alistipes* (4.3%)	*Bacteroides* (16.9%) *Faecalibacterium* (6.1%) *Alistipes* (4.8%)
K13051	0.04	Alanine, aspartate and glutamate metabolism	EE|MH	*Bacteroides* (68.4%) *Bifidobacterium* (5.3%)	*Bacteroides* (64.4%) *Bifidobacterium* (4.4%)
K00175	0.009	Butanoate metabolism	EE|MH	*Bacteroides* (34.6%) *Alistipes* (8.4%) *Prevotella* (7.5%)	*Bacteroides* (28.7%) *Alistipes* (8.4%) *Prevotella* (8.9%)
K00174	0.015	Butanoate metabolism	EE|MH	*Bacteroides* (38%) *Alistipes* (9.8%) *Prevotella* (6.3%)	*Bacteroides* (33.6%) *Alistipes* (11%) *Prevotella* (8%)
K17865	0.016	Butanoate metabolism	EE|MH	*Bacteroides* (33.3%) *Alistipes* (55.6%)	*Bacteroides* (5.9%) *Alistipes* (52.9%)
K01640	0.036	Butanoate metabolism	EE|MH	*Faecalibacterium* (46.7%) *Phascolarctobacterium* (26.7%)	*Faecalibacterium* (9.1%) *Phascolarctobacterium* (45.5%) *Cloacibacillus* (9.1%)

(Continued)

10.3389/fmicb.2023.1094071

TABLE 2 (Continued)

KO	*p*-value	Pathway	Most abundant	Genera with the highest contribution in EE|MH	Genera with the highest contribution in EE|NOMH
K00634	0.037	Butanoate metabolism	EE|MH	*Bacteroides* (32.3%) *Alistipes* (11.1%) *Prevotella* (5.5%)	*Bacteroides* (26.5%) *Alistipes* (9.4%) *Prevotella* (8.7%)
K00170	0.042	Butanoate metabolism	EE|NOMH	*Clostridium* (29.2%) *Roseburia* (12.5%) *Sutterella* (12.5%)	*Clostridium* (62.7%) *Sutterella* (7.2%)
K03474	0.003	Butanoate metabolism	EE|MH	*Bacteroides* (46.2%) *Alistipes* (8.8%)	*Bacteroides* (38.3%) *Alistipes* (10.4%) *Prevotella* (10.4%)
K03473	0.013	Butanoate metabolism	EE|MH	*Bacteroides* (31.8%) *Alistipes* (11.5%) *Prevotella* (6.5%)	*Bacteroides* (55.6%) *Alistipes* (10.6%) *Prevotella* (8.4%)
K05275	0.014	Butanoate metabolism	EE|MH	*Bacteroides* (36%)	*Bacteroides* (31.6%) *Prevotella* (5.8%)
K08681	0.039	Butanoate metabolism	EE|NOMH	*Roseburia* (15.9%) *Butyrivibrio* (7.9%) *Eubacterium* (7.9%)	*Prevotella* (25.6%) *Butyrivibrio* (6.6%)
K00382	0.0026	Tryptophan metabolism Glycine, serine and threonine metabolism	EE|MH	*Bacteroides* (56.6%) *Alistipes* (6.5%)	*Bacteroides* (49.1%) *Alistipes* (8%)
K01692	0.038	Tryptophan metabolism Butanoate metabolism	EE|MH	*Clostridium* (14.3%) *Oscillibacter* (14.3%) *Sutterella* (14.3%)	*Clostridium* (7.1%) *Coprococcus* (7.1%) *Oscillibacter* (7.1%) *Faecalibacterium* (7.1%) *Phascolarctobacterium* (7.1%) *Sutterella* (7.1%) *Klebsiella* (7.1%)
K00294	0.007	Arginine and proline metabolism Alanine, aspartate and glutamate metabolism	EE|MH	*ParaBacteroides* (20%) *Coprococcus* (6.7%) *Butyricimonas* (6.7%)	*ParaBacteroides* (20%) *Coprococcus* (8%) *Odoribacter* (8%)
K01580	0.032	Alanine, aspartate and glutamate metabolism Butanoate metabolism	EE|MH	*Bacteroides* (41.5%) *Alistipes* (16.7%)	*Bacteroides* (34.7%) *Alistipes* (17.5%)

volunteers with depression were also taking antidepressant medication, which might increase the abundance of genera strongly correlated with TPH2, such as *Bilophila* (Liu G. et al., 2020). In fact, the genus *Bilophila* proved significantly higher in the EE|MH group. These bacteria are reported to be significantly increased in anhedonia (loss of pleasure) in mouse models. Anhedonia is one of the two core symptoms of depression (Yang et al., 2019) and was also found to be increased in a mouse model of depression, subjected to chronic unpredictable mild stress (Zhang M. et al., 2021). *Bilophila* has also been described as positively correlated with tryptophan hydroxylase 2 (TPH2) gene expression (Liu G. et al., 2020).

Over 90% of the whole tryptophan is metabolized through the KP. IDO and tryptophan 2, 3-dioxygenase (TDO) are the enzymes that catalyze the first step of tryptophan metabolism in this pathway (Maes et al., 2011). On the one hand, TDO activation is normally stable and is regulated by tryptophan availability (Gao et al., 2020). On the other hand, IDO is induced by interferon-gamma (IFN-γ) and tumor necrosis factor-alpha (TNF-α) among other pro-inflammatory cytokines, and its activation is correlated with the intensity of depressive symptoms (Höglund et al., 2019; Gao et al., 2020; Chen et al., 2021). IDO activation by inflammation caused by bacteria such as *Flavonifractor* and *Alistipes* and promoting KYN formation through KP can decrease tryptophan availability, negatively impacting serotonin synthesis and neurotransmission. *Flavonifractor* and *Alistipes* were significantly higher in the mental-health treatment group (EE|MH). *Flavonifractor* has previously been reported as higher in individuals with major depressive disorder (Jiang et al., 2015; Valles-Colomer et al., 2019), generalized anxiety disorder (Jiang et al., 2015), affective disorders (Coello et al., 2019), and bipolar disorder (Lindseth et al., 2015; Wang et al., 2021). *Flavonifractor* has also been

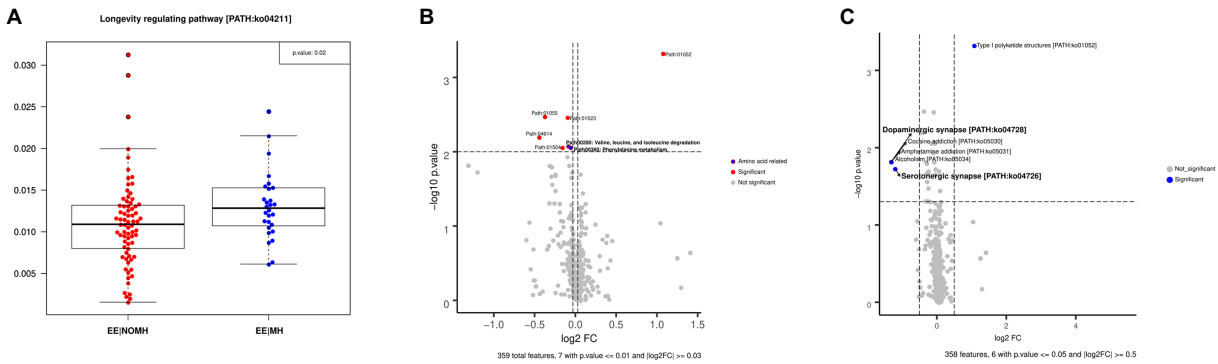

FIGURE 7
(A) Differences in the longevity regulating pathway between EE|NOMH (red) and EE|MH (blue). **(B)** Significant differences in the metabolism of amino acids between EE|NOMH (right) and EE|MH (left). **(C)** Significant differences in neuronal synapses between EE|NOMH (right) and EE|MH (left) groups.

described as a pro-inflammatory genus and studies show a negative association between this genus and quality of life scores (Jiang et al., 2018). Parker et al. (2020) and Jiang et al. (2015) also described *Alistipes* to be higher in patients with depression (Jiang et al., 2018; Parker et al., 2020). This genus is believed to be associated with stress, fatigue syndrome, and depressive disorders through inflammatory pathways (Naseribafrouei et al., 2014).

Bacteroides were also significantly higher in the EE/MH mental-health treatment group. The role of *Bacteroides* in mental health is highly controversial, with some authors observing the genus to be lower in patients suffering from mental health disorders (Jiang et al., 2015), while others find it to be higher in this group (Yang et al., 2019). This genus has previously been studied for its ability to produce cytokines and its role in inflammation, as gut inflammation has a clear association with depression (Schiepers et al., 2005; Dantzer, 2009). By contrast, *Flavonifractor* is reported to be higher in patients with remitted geriatric depression (Lee et al., 2022), which might explain why it is higher in the EE|MH group, where elderly subjects are medicated for mental health. In this case, the medication might be responsible for remission.

During aging, elderly individuals suffer from systematic inflammation and, as stated above, mental illness is generally associated with an inflammatory state of the patient. Oral health is also influenced by aging and inflammation, with an increased prevalence of periodontal disease (Clark et al., 2021). Several studies suggest that some psychiatric diseases, such as Alzheimer's or bipolar disorder, are related to leakage of pro-inflammatory oral bacteria triggering neuroinflammation (Leira et al., 2017). Furthermore, mental health issues such as anxiety and depression are related to a decrease in oral hygiene and dental check-ups (Anttila et al., 2006; Okoro et al., 2012; Simpson et al., 2020). Periodontal diseases (mainly periodontitis and gingivitis) are caused by bacterial-induced inflammation. *Porphyromonas* is a well-known periodontal pathogen whose virulence factors cause deregulation in inflammatory and immune responses of the host (Mysak et al., 2014; Leira et al., 2017). Studies of Alzheimer's disease show inflammatory cytokines such as TNF-α, IL-1, IL-6, and IL-8 are released from the host cells that have been infected with *Porphyromonas* (Mei et al., 2020). Similarly, *Treponema denticola* is known to cause gingivitis in cases of oral dysbiosis, despite being a normal component of human oral microbiota (Simpson et al., 2020).

Porphyromonas and *Treponema* were both higher in our EE|NOMH group saliva. Both bacteria can form synergistic biofilms and are positively associated with chronic periodontitis and severe periodontal disease (Ng et al., 2019). The genus *Veillonella*, which was found to be higher in the EE|MH group, was previously correlated with anti-inflammatory mediators and maintains oral pH by metabolizing lactate into weaker acids (Rosier et al., 2018). In the case of oral microbiota, we also observed the influence of mental health medicine in restoring elderly participants to a healthier state, as the medicated EE|MH group had significantly lower abundances of these pro-inflammatory genera.

Correlation analysis of both oral and intestinal microbiota, showed similar results. In the EE|NOMH group, the genus *Alistipes* from the gut was negatively correlated with the oral genera Veillonella and *Prevotella*. As stated above, *Alistipes* is a pro-inflammatory genus that has previously been correlated with mental health problems while oral *Veillonella* and *Prevotella* were negatively correlated with pro-inflammatory markers, *Prevotella* has been even negatively associated with distress (Kohn et al., 2020). Meanwhile, in the EE|MH group the gut genus *Lachnospira* showed a negative correlation with the oral genera *Megasphaera* and *Atopobium*. Previous studies report *Lachnospira* to be lower in animal models of depression and stress (Flux and Lowry, 2020), and in a cohort of patients suffering major depressive disorder (Rosier et al., 2018). By contrast, *Megasphaera* and *Atopobium* are found to be higher in cohorts with mental health disorders (McGuinness et al., 2022). Similarly, the oral genus *Lachnoanaerobaculum* and the intestinal genus *Subdoligranulum* showed significant negative correlations in the EE|MH group. Liu R. T. et al. (2020) reported that the abundance of *Subdoligranulum* was reduced in subjects who had more severe symptoms of depression (Liu R. T. et al., 2020), while Wang et al. described an augmented abundance of *Lachnoanaerobaculum* in depression and anxiety (Wang et al., 2022).

On the other hand, *Odoribacter* in gut microbiota with the oral genera *Alloprevotella* and *Haemophilus* had a positive correlation in the EE|MH group, all three of these genera are related with bad health. *Odoribacter* is one of the gut microbes associated with mental health issues, including major depressive disorder (Zhang M. et al., 2021).

Oral *Alloprevotella* is described to be involved in periodontal disease (Sun et al., 2020) and *Haemophilus* is a well-known oral pathogen (Nørskov-Lauritsen, 2014). A similar positive correlation was obtained in the EE|MH group between *Lachnoclostridium*, and *Colidextribacter* from the intestinal microbiota with the oral genus *Megasphaera* that, as stated above, is elevated in mental health disorders. *Lachnoclostridium* has been associated with higher depressive symptoms in an induced animal model of depression (Zhang Y. et al., 2021), while *Colidextribacter* was associated with a positive response to antidepressant treatment in a mouse model of depression (Duan et al., 2021). Together these results again indicate that the mental-health treatment the EE|MH group may be restoring the microbiota to a healthier state, even though some genera related with mental health disorders are still present.

Parabacteroides, another genus involved in tryptophan metabolism, was significantly higher in the EE|MH group. Deng et al. (2021) showed that the genus plays an important role in tryptophan metabolism, where it has a strong correlation between the KP and depressive-like behavioral changes in a rat model of chronic restraint stress (Wu et al., 2014; Deng et al., 2021). Moreover, Li et al. (2016) described that a decrease in the abundance of *Parabacteroides* correlated with an improvement in the mood of adults.

Functional analysis of metagenome data showed five KEGG Orthology categories that are significantly higher in the EE|MH group and are related to tryptophan metabolism. Interestingly, tryptophanase (K01667) was markedly higher in the EE|MH group. This enzyme carries out the first step in the indolic pathway, transforming tryptophan into indole (Agus et al., 2018). Indole is a signaling molecule that can control bacteria antibiotic resistance, sporulation, and biofilm formation. It can also inhibit quorum sensing and modulate virulence factors (Agus et al., 2018). Indolic compounds are AhR ligands; AhR activation influences immune homeostasis *via* receptor anti-inflammatory effect by regulating intraepithelial lymphocytes and innate lymphoid cells (Li et al., 2011; Qiu et al., 2012; Jin et al., 2014). They are known to extend the health-span of several models of aging, such as *C. elegans*, *D. melanogaster*, and mouse (Sonowal et al., 2017).

Ruiz-Ruiz et al. (2020) showed the loss of the tryptophanase enzyme during aging and describe how the microbiota diminishes its ability to produce indole and tryptophan in old age, compromising the health status of the elderly (Ruiz-Ruiz et al., 2020). Our EE|NOMH group, comprising over 65-year-olds who are not taking mental-health medication, had a significantly lower abundance of tryptophanase. This would indicate that medication, such as antidepressants and anti-anxiolytic drugs, restore these individuals to a healthier state, which might also explain the significant difference in the longevity regulating pathway between the EE|MH and EE|NOMH groups.

GABA is the principal inhibitory neurotransmitter in the brain. It affects the control of homeostasis during stress and has been associated with mental health disorders such as anxiety and depression (Geuze et al., 2008). GABA and several other GABA analogs have been shown to have anxiolytic and hypnotic effects. Positive modulators to GABA receptors have been used to treat anxiety disorders and insomnia (Kalueff and Nutt, 2007). Classic mental-health treatments include benzodiazepines, these are positive allosteric modulators of GABA receptors (Sigel and Ernst, 2018).

Oscillibacter, which we found to be enriched in the EE|MH group, has valeric acid as its main metabolic product; this metabolite mimics GABA. Valeric acid can bind with the GABAa receptor, which explains the association between valeric acid-producing bacteria and depression (Naseribafrouei et al., 2014). Rong et al. (2019) reported similar results, finding an increase of this genus in treated patients suffering from major depressive disorder or bipolar disorder (Rong et al., 2019). Similarly, the GABA producing genus *Bacteroides* (Otaru et al., 2021) was also higher in the EE|MH group. The contribution of genera to the analyzed KOs showed that *Bacteroides* and *Alistipes* were the ones contributing most to the production of these KOs in the EE|MH group. It is noteworthy that these genera were also significantly higher in the EE|MH group.

The dopaminergic synapse, which includes alcoholism, the amphetamine addiction, and the cocaine addiction pathways, was higher in our EE|MH group. Dopamine is a neurotransmitter responsible for several functions in the body, including learning, memory, reward, and motor control. It has been implicated in psychiatric and psychological disorders (Ko and Strafella, 2012). Dopamine availability is higher in cocaine and amphetamine users, and the reward system in the brain was active in animal models of addiction (Di Chiara et al., 2004). The use of benzodiazepines as mental-health medication in the EE|MH group also explains the difference in synaptic pathways between both groups. Benzodiazepines are positive allosteric modulators of GABA receptors, and it has been suggested that the activation of GABA receptors enhances dopamine release (Kramer et al., 2020).

The results show that treatment-related changes in taxonomic composition of microbiota modifies robustness parameters, in other words, eventual changes in taxonomic composition modify functional capacity of the bacterial community, at least in some superpathway functions. However, it is important remark that this functional capacity is based only on the content of all genes of prokaryotic organisms living in microbiota, without considering the expression levels of every gene.

In the fecal microbiota, there are differences in taxonomic abundances in treated and not treated subjects, with a relevant impact on functional capacity and robustness for at least for some superpathways. For attenuation, differences were observed only in superpathway cell motility, while in buffering, no differences were found. Particularly interesting are the results for saliva samples, which show some differences in buffering. These were lower for at least three superpathways related with metabolism, which can induce variations in the metabolite landscape if alterations occur. These corresponded to the superpathway of lipid metabolism, superpathway of metabolism of terpenoids and polyketides and superpathway of metabolism of other amino acids. Also changes in attenuation were found (higher for superpathway of lipid metabolism and lower for superpathway of metabolism of terpenoids and polyketides). For the remaining superpathways not directly related with metabolism the differences observed could induce variations in cell division and growth of prokaryotic cells, without obvious consequences in community taxonomic composition dynamics, which could finally modify the values of those parameters of robustness.

Therefore, at least in oral microbiota, in-depth studies should address the relationship between changes induced in functional capacity by alteration or disturbances of the microbial community, and the medication to treat pathologies. In this respect, there are numerous references on the role of medication in Xerostomia related with salivary gland dysfunction, and oral diseases associated to diazepine (De Almeida et al., 2008) and other mental-health drugs

(Koller et al., 2000; Arany et al., 2021) or medication commonly used by the elderly population (Leal et al., 2010).

Spain has an aging population, with 19.93% of the whole population over 65 years of age, in 2021. This age range corresponds to a higher risk of suffering mental health issues, reaching around 25% in 65-year-olds and up to 55% in 85-year-olds (Conselleria de Sanitat Universal i Salut Pública, 2020). It is important to identify the reasons underlying this increase in mental health issues in a population that registered 1,281 suicides in people over 65 in 2020 in Spain (Instituto Nacional de Estadistica, 2020). Here, we have demonstrated that there are significant differences in the microbiome composition and function of older people in the Comunidad Valenciana being medicated for mental health issues. Our results also indicated that the medication might help to recover the microbiome to a healthier state and aid patient remission by remodeling the gut microbiota and bacterial tryptophan metabolism.

Data availability statement

The datasets presented in this study are deposited in the European Nucleotide Archive repository (https://www.ebi.ac.uk/ena), accession number PRJEB56919.

Ethics statement

The studies involving human participants were reviewed and approved by all procedures were reviewed and approved by the Ethics Committee (Reference: 20210305/07) of Fundación para el Fomento de la Investigación Sanitaria y Biomédica de la Comunitat Valenciana (FISABIO). All the volunteers provided written informed consent before their participation. The patients/participants provided their written informed consent to participate in this study.

Author contributions

NP and AB carried out the experiments and processed sequencing data. BP-R developed the robustness analysis. AA performed the bioinformatic analyses. SR-R and AM designed the experiments and wrote the manuscript. All authors contributed to the article and approved the submitted version.

Funding

This research was funded by the Spanish Ministry of Science and Innovation (PID2019-105969GB-I00) and supported by a grant (Programa Santiago Grisolía, GRISOLIAP/2019/080) from the Generalitat Valenciana.

Acknowledgments

We are grateful to Javi Pons for the contributions with the bioinformatics and statistical analysis and Nuria Jiménez for the technical support with the libraries and sequencing.

Conflict of interest

The authors declare that the research was conducted in the absence of any commercial or financial relationships that could be construed as a potential conflict of interest.

Publisher's note

Supplementary material

The Supplementary material for this article can be found online at: https://www.frontiersin.org/articles/10.3389/fmicb.2023.1094071/full#supplementary-material

References

Agus, A., Planchais, J., and Sokol, H. (2018). Gut microbiota regulation of tryptophan metabolism in health and disease. *Cell Host Microbe* 23, 716–724. doi: 10.1016/j.chom.2018.05.003

Anttila, S., Knuuttila, M., Ylostalo, P., and Joukamaa, M. (2006). Symptoms of depression and anxiety in relation to dental health behavior and self-perceived dental treatment need. *Eur. J. Oral Sci.* 114, 109–114. doi: 10.1111/j.1600-0722.2006.00334.x

Arany, S., Kopycka-Kedzierawski, D. T., Caprio, T. V., and Watson, G. E. (2021). Anticholinergic medication: related dry mouth and effects on the salivary glands. *Oral Surg. Oral Med. Oral. Pathol. Oral Radiol.* 132, 662–670. doi: 10.1016/j.oooo.2021.08.015

Arimatsu, K., Yamada, H., Miyazawa, H., Minagawa, T., Nakajima, M., Ryder, M. I., et al. (2014). Oral pathobiont induces systemic inflammation and metabolic changes associated with alteration of gut microbiota. *Sci. Rep.* 4:4828. doi: 10.1038/srep04828

Batty, G. D., Li, Q., Huxley, R., Zoungas, S., Taylor, B. A., Neal, B., et al. (2013). Oral disease in relation to future risk of dementia and cognitive decline: prospective cohort study based on the Action in Diabetes and Vascular Disease: Preterax and Diamicron Modified-Release Controlled Evaluation (ADVANCE) trial. *Eur. Psychiatry* 28, 49–52. doi: 10.1016/j.eurpsy.2011.07.005

Callahan, B. J., McMurdie, P. J., Rosen, M. J., Han, A. W., Johnson, A. J. A., and Holmes, S. P. (2016). DADA2: High-resolution sample inference from Illumina amplicon data. *Nat. Methods* 13, 581–583. doi: 10.1038/nmeth.3869

Chen, L. M., Bao, C. H., Wu, Y., Liang, S. H., Wang, D., Wu, L. Y., et al. (2021). Tryptophan-kynurenine metabolism: A link between the gut and brain for depression in inflammatory bowel disease. *J. Neuroinflammation* 18, 1–13. doi: 10.1186/s12974-021-02175-2

Chen, L., Zhang, L., and Xu, X. (2020). Review of evolution of the public long-term care insurance (LTCI) system in different countries: influence and challenge. *BMC Health Serv. Res.* 20:1057. doi: 10.1186/s12913-020-05878-z

Clark, D., Kotronia, E., and Ramsay, S. E. (2021). Frailty, aging, and periodontal disease: basic biologic considerations. *Periodontol.* 87, 143–156. doi: 10.1111/prd.12380

Coello, K., Haldor, T., Sørensen, N., Munkholm, K., and Vedel, L. (2019). Brain, Behavior, and Immunity Gut microbiota composition in patients with newly diagnosed bipolar disorder and their unaffected first-degree relatives. *Brain Behav. Immun.* 75, 112–118. doi: 10.1016/j.bbi.2018.09.026

Conselleria de Sanitat Universal i Salut Pública (Ed.). (2020). Estrategía Autonómica de Salud mental 2016-2020.pdf. Available at: http://www.san.gva.es/documents/156344/6700482/Estrateg%C3%ADa+Auton%C3%B3mica+de+Salud+mental+2016+2020+.pdf

Cox, L. M., and Weiner, H. L. (2018). Microbiota signaling pathways that influence neurologic disease. *Neurotherapeutics* 15, 135–145. doi: 10.1007/s13311-017-0598-8

Cryan, J. F., and O'Mahony, S. M. (2011). The microbiome-gut-brain axis: from bowel to behavior: from bowel to behavior. *Neurogastroenterol. Motil.* 23, 187–192. doi: 10.1111/j.1365-2982.2010.01664.x

Dantzer, R. (2009). Cytokine, sickness behavior, and depression. *Immunol. Allergy Clin. N. Am.* 29, 247–264. doi: 10.1016/j.iac.2009.02.002

De Almeida, P. D. V., Grégio, A. M., Brancher, J. A., Ignácio, S. A., Machado, M. A., de Lima, A. A., et al. (2008). Effects of antidepressants and benzodiazepines on stimulated salivary flow rate and biochemistry composition of the saliva. *Oral Surg. Oral Med. Oral Pathol. Oral Radiol.* 106, 58–65. doi: 10.1016/j.tripleo.2007.11.008

Deng, Y., Zhou, M., Wang, J., Yao, J., Yu, J., Liu, W., et al. (2021). Involvement of the microbiota-gut-brain axis in chronic restraint stress: disturbances of the kynurenine metabolic pathway in both the gut and brain. *Gut Microbes* 13, 1–16. doi: 10.1080/19490976.2020.1869501

Di Chiara, G., Bassareo, V., Fenu, S., De Luca, M. A., Spina, L., Cadoni, C., et al. (2004). Dopamine and drug addiction: the nucleus accumbens shell connection. *Neuropharmacology* 47, 227–241. doi: 10.1016/j.neuropharm.2004.06.032

Douglas, G. M., Maffei, V. J., Zaneveld, J. R., Yurgel, S. N., Brown, J. R., Taylor, C. M., et al. (2020). PICRUSt2 for prediction of metagenome functions. *Nat. Biotechnol.* 38, 685–688. doi: 10.1038/s41587-020-0548-6

Duan, J., Huang, Y., Tan, X., Chai, T., Wu, J., Zhang, H., et al. (2021). Characterization of gut microbiome in mice model of depression with divergent response to escitalopram treatment. *Transl. Psychiatry* 11:303. doi: 10.1038/s41398-021-01428-1

Eng, A., and Borenstein, E. (2018). Taxa-function robustness in microbial communities. *Microbiome* 6:45. doi: 10.1186/s40168-018-0425-4

Flux, M. C., and Lowry, C. A. (2020). Finding intestinal fortitude: Integrating the microbiome into a holistic view of depression mechanisms, treatment, and resilience. *Neurobiol. Dis.* 135:104578. doi: 10.1016/j.nbd.2019.104578

Gao, K., Mu, C., Farzi, A., and Zhu, W. (2020). Tryptophan metabolism: a link between the gut microbiota and brain. *Adv. Nutr.* 11, 709–723. doi: 10.1093/advances/nmz127

Gao, J., Xu, K., Liu, H., Liu, G., Bai, M., Peng, C., et al. (2018). Impact of the gut microbiota on intestinal immunity mediated by tryptophan metabolism. *Front. Cell. Infect. Microbiol.* 8:13. doi: 10.3389/fcimb.2018.00013

García, A. A., Nieto, P. A., Díaz, J. P., Fariñas, D. R., García, A. A., and Rodríguez, R. P. (2021). Indicadores estadísticos básicos. *Informes Envejecimiento en Red* 22:38.

Geuze, E., van Berckel, B. N. M., Lammertsma, A. A., Boellaard, R., de Kloet, C. S., Vermetten, E., et al. (2008). Reduced GABAA benzodiazepine receptor binding in veterans with post-traumatic stress disorder. *Mol. Psychiatry* 13, 74–83. doi: 10.1038/sj.mp.4002054

Harman, D. (2006). Aging: overview. *Ann. N. Y. Acad. Sci.* 928, 1–21. doi: 10.1111/j.1749-6632.2001.tb05631.x

Höglund, E., Øverli, Ø., and Winberg, S. (2019). Tryptophan metabolic pathways and brain serotonergic activity: a comparative review. *Front. Endocrinol.* 10:158. doi: 10.3389/fendo.2019.00158

Instituto Nacional de Estadistica (2020). Defunciones por suicidios. Available at: https://www.ine.es/dynt3/inebase/es/index.htm?padre=5453&capsel=5454

Instituto Nacional de Estadistica (2021a). Indicadores de crecimiento y estructura de la población. Total Nacional. INE. Available at: https://www.ine.es/consul/serie.do?d=true&s=IDB55727&c=2&

Instituto Nacional de Estadistica (2021b). Índice de Envejecimiento por comunidad autónoma. INE. Available at: https://www.ine.es/jaxiT3/Datos.htm?t=1452

Iwauchi, M., Horigome, A., Ishikawa, K., Mikuni, A., Nakano, M., Xiao, J., et al. (2019). Relationship between oral and gut microbiota in elderly people. *Immun. Inflamm. Dis.* 7, 229–236. doi: 10.1002/iid3.266

Jiang, H., Ling, Z., Zhang, Y., Mao, H., Ma, Z., Yin, Y., et al. (2015). Altered fecal microbiota composition in patients with major depressive disorder. *Brain Behav. Immun.* 48, 186–194. doi: 10.1016/j.bbi.2015.03.016

Jiang, H., Ruan, B., Yu, Z., Zhang, Z., Deng, M., and Zhao, J. (2018). Altered gut microbiota profile in patients with generalized anxiety disorder. *J. Psychiatr. Res.* 104, 130–136. doi: 10.1016/j.jpsychires.2018.07.007

Jin, U.-H., Lee, S.-O., Sridharan, G., Lee, K., Davidson, L. A., Jayaraman, A., et al. (2014). Microbiome-derived tryptophan metabolites and their aryl hydrocarbon receptor-dependent agonist and antagonist activities. *Mol. Pharmacol.* 85, 777–788. doi: 10.1124/mol.113.091165

Kalueff, A. V., and Nutt, D. J. (2007). Role of GABA in anxiety and depression. *Depress. Anxiety* 24, 495–517. doi: 10.1002/da.20262

Kim-Anh, L. C., Rohart, F., Gonzalez, I., and Dejean, S. (2016). MixOmics: Omics Data Integration Project. R package version 6.1.1. Available at: https://CRAN.R-project.org/package=mixOmics

Kitamoto, S., Nagao-Kitamoto, H., Jiao, Y., Gillilland, M. G., Hayashi, A., Imai, J., et al. (2020). The intermucosal connection between the mouth and gut in commensal pathobiont-driven colitis. *Cells* 182, 447–462.e14. doi: 10.1016/j.cell.2020.05.048

Ko, J. H., and Strafella, A. P. (2012). Dopaminergic neurotransmission in the human brain: new lessons from perturbation and imaging. *Neuroscientist* 18, 149–168. doi: 10.1177/1073858411401413

Kohn, J. N., Kosciolek, T., Marotz, C., Aleti, G., Guay-Ross, R. N., Hong, S. H., et al. (2020). Differing salivary microbiome diversity, community and diurnal rhythmicity in association with affective state and peripheral inflammation in adults. *Brain Behav. Immun.* 87, 591–602. doi: 10.1016/j.bbi.2020.02.004

Koller, M. M., Purushotham, K. R., Maeda, N., Scarpace, P. J., and Humphreys-Beher, M. G. (2000). Desipramine induced changes in salivary proteins, cultivable oral microbiota and gingival health in aging female NIA Fischer 344 rats. *Life Sci.* 68, 445–455. doi: 10.1016/s0024-3205(00)00951-6

Komiya, Y., Shimomura, Y., Higurashi, T., Sugi, Y., Arimoto, J., Umezawa, S., et al. (2019). Patients with colorectal cancer have identical strains of *Fusobacterium nucleatum* in their colorectal cancer and oral cavity. *Gut* 68, 1335–1337. doi: 10.1136/gutjnl-2018-316661

Kramer, P. F., Twedell, E. L., Shin, J. H., Zhang, R., and Khaliq, Z. M. (2020). Axonal mechanisms mediating γ-aminobutyric acid receptor type A (GABA-A) inhibition of striatal dopamine release. *eLife* 9:e55729. doi: 10.7554/eLife.55729

Leal, S. C., Bittar, J., Portugal, A., Falcão, D. P., Faber, J., and Zanotta, P. (2010). Medication in elderly people: its influence on salivary pattern, signs and symptoms of dry mouth. *Gerodontology* 27, 129–133. doi: 10.1111/j.1741-2358.2009.00293.x

Lee, S. M., Dong, T. S., Krause-Sorio, B., Siddarth, P., Milillo, M. M., Lagishetty, , et al. (2022). The intestinal microbiota as a predictor for antidepressant treatment outcome in geriatric depression: a prospective pilot study. *Int. Psychogeriatr.* 34, 33–45. doi: 10.1017/S1041610221000120

Leira, Y., Domínguez, C., Seoane, J., Seoane-Romero, J., Pías-Peleteiro, J. M., Takkouche, B., et al. (2017). Is periodontal disease associated with Alzheimer's disease? A systematic review with meta-analysis. *Neuroepidemiology* 48, 21–31. doi: 10.1159/000458411

Li, Y., Innocentin, S., Withers, D. R., Roberts, N. A., Gallagher, A. R., Grigorieva, E. F., et al. (2011). Exogenous stimuli maintain intraepithelial lymphocytes via aryl hydrocarbon receptor activation. *Cells* 147, 629–640. doi: 10.1016/j.cell.2011.09.025

Li, L., Su, Q., Xie, B., Duan, L., Zhao, W., Hu, D., et al. (2016). Gut microbes in correlation with mood: case study in a closed experimental human life support system. *Neurogastroenterol. Motil.* 28, 1233–1240. doi: 10.1111/nmo.12822

Liang, S., Wu, X., and Jin, F. (2018). Gut-brain psychology: rethinking psychology from the microbiota–gut–brain axis. *Front. Integr. Neurosci.* 12:33. doi: 10.3389/fnint.2018.00033

Lindseth, G., Helland, B., and Caspers, J. (2015). The effects of dietary tryptophan on affective disorders. *Arch. Psychiatr. Nurs.* 29, 102–107. doi: 10.1016/j.apnu.2014.11.008

Liu, G., Chong, H. X., Chung, F. Y. L., Li, Y., and Liong, M. T. (2020). *Lactobacillus plantarum* DR7 modulated bowel movement and gut microbiota associated with dopamine and serotonin pathways in stressed adults. *Int. J. Mol. Sci.* 21, 1–16. doi: 10.3390/ijms21134608

Liu, R. T., Rowan-Nash, A. D., Sheehan, A. E., Walsh, R. F. L., Sanzari, C. M., Korry, B. J., et al. (2020). Reductions in anti-inflammatory gut bacteria are associated with depression in a sample of young adults. *Brain Behav. Immun.* 88, 308–324. doi: 10.1016/j.bbi.2020.03.026

Liu, N., Sun, S., Wang, P., Sun, Y., Hu, Q., and Wang, X. (2021). The mechanism of secretion and metabolism of gut-derived 5-hydroxytryptamine. *Int. J. Mol. Sci.* 22:7931. doi: 10.3390/ijms22157931

Maes, M., Leonard, B. E., Myint, A. M., Kubera, M., and Verkerk, R. (2011). The new '5-HT' hypothesis of depression: cell-mediated immune activation induces indoleamine 2,3-dioxygenase, which leads to lower plasma tryptophan and an increased synthesis of detrimental tryptophan catabolites (TRYCATs), both of which contribute to the onset of depression. *Prog. Neuro Psychopharmacol. Biol. Psychiatry* 35, 702–721. doi: 10.1016/j.pnpbp.2010.12.017

Mazzoli, R., and Pessione, E. (2016). The neuro-endocrinological role of microbial glutamate and GABA signaling. *Front. Microbiol.* 7:1934. doi: 10.3389/fmicb.2016.01934

McGuinness, A. J., Davis, J. A., Dawson, S. L., Loughman, A., Collier, F., O'Hely, M., et al. (2022). A systematic review of gut microbiota composition in observational studies of major depressive disorder, bipolar disorder and schizophrenia. *Mol. Psychiatry* 27, 1920–1935. doi: 10.1038/s41380-022-01456-3

Mei, F., Xie, M., Huang, X., Long, Y., Lu, X., Wang, X., et al. (2020). Porphyromonas gingivalis and its systemic impact: current status. *Pathogens* 9:944. doi: 10.3390/pathogens9110944

Mysak, J., Podzimek, S., Sommerova, P., Lyuya-Mi, Y., Bartova, J., Janatova, T., et al. (2014). *Porphyromonas gingivalis*: major periodontopathic pathogen overview. *J. Immunol. Res.* 2014, 1–8. doi: 10.1155/2014/476068

Naseribafrouei, A., Hestad, K., Avershina, E., Sekelja, M., Linløkken, A., and Wilson, R. (2014). Correlation between the human fecal microbiota and depression. *Neurogastroenterol. Motil. Neurogastroenterol Motil.* 26, 1155–1162. doi: 10.1111/nmo.12378

Ng, H. M., Slakeski, N., Butler, C. A., Veith, P. D., Chen, Y.-Y., Liu, S. W., et al. (2019). The role of *Treponema denticola* motility in synergistic biofilm formation with *Porphyromonas gingivalis*. *Front. Cell. Infect. Microbiol.* 9:432. doi: 10.3389/fcimb.2019.00432

Nørskov-Lauritsen, N. (2014). Classification, identification, and clinical significance of *Haemophilus* and *Aggregatibacter* species with host specificity for humans. *Clin. Microbiol. Rev.* 27, 214–240. doi: 10.1128/CMR.00103-13

Ogawa, T., Hirose, Y., Honda-Ogawa, M., Sugimoto, M., Sasaki, S., Kibi, M., et al. (2018). Composition of salivary microbiota in elderly subjects. *Sci. Rep.* 8:414. doi: 10.1038/s41598-017-18677-0

Okoro, C. A., Strine, T. W., Eke, P. I., Dhingra, S. S., and Balluz, L. S. (2012). The association between depression and anxiety and use of oral health services and tooth loss: depression and anxiety and oral health. *Community Dent. Oral Epidemiol.* 40, 134–144. doi: 10.1111/j.1600-0528.2011.00637.x

Otaru, N., Ye, K., Mujezinovic, D., Berchtold, L., Constancias, F., Cornejo, F. A., et al. (2021). GABA production by human intestinal *Bacteroides* spp.: prevalence, regulation, and role in acid stress tolerance. *Front. Microbiol.* 12:656895. doi: 10.3389/fmicb.2021.656895

Park, M., and Unützer, J. (2011). Geriatric depression in primary care. *Psychiatr. Clin. North Am.* 34, 469–487. doi: 10.1016/j.psc.2011.02.009

Parker, B. J., Wearsch, P. A., Veloo, A. C. M., Rodriguez-palacios, A., and Rodriguez-palacios, A. (2020). The genus *Alistipes*: gut bacteria with emerging implications to inflammation, cancer, and mental health. *Front. Immunol.* 11:906. doi: 10.3389/fimmu.2020.00906

Pelosi, B., Pratelli, M., Migliarini, S., Pacini, G., and Pasqualetti, M. (2015). Generation of a Tph2 conditional knockout mouse line for time- and tissue-specific depletion of brain serotonin. *PLoS One* 10:e0136422. doi: 10.1371/journal.pone.0136422

Qiu, J., Heller, J. J., Guo, X., Chen, Z. E., Fish, K., Fu, Y. X., et al. (2012). The aryl hydrocarbon receptor regulates gut immunity through modulation of innate lymphoid cells. *Immunity* 36, 92–104. doi: 10.1016/j.immuni.2011.11.011

Quast, C., Pruesse, E., Yilmaz, P., Gerken, J., Schweer, T., Yarza, P., et al. (2012). The SILVA ribosomal RNA gene database project: improved data processing and web-based tools. *Nucleic Acids Res.* 41, D590–D596. doi: 10.1093/nar/gks1219

Richard, D. M., Dawes, M. A., Mathias, C. W., Acheson, A., Hill-Kapturczak, N., and Dougherty, D. M. (2009). Tryptophan: basic metabolic functions, behavioral research and therapeutic indications. *Int. J. Tryptophan Res.* 2:IJTR.S2129. doi: 10.4137/IJTR.S2129

Richards, P., Thornberry, N. A., and Pinto, S. (2021). The gut–brain axis: identifying new therapeutic approaches for type 2 diabetes, obesity, and related disorders. *Mol. Metabol.* 46:101175. doi: 10.1016/j.molmet.2021.101175

Rong, H., Xie, X. H., Zhao, J., Lai, W. T., Wang, M. B., Xu, D., et al. (2019). Similarly, in depression, nuances of gut microbiota: evidences from a shotgun metagenomics sequencing study on major depressive disorder versus bipolar disorder with current major depressive episode patients. *J. Psychiatr. Res.* 113, 90–99. doi: 10.1016/j.jpsychires.2019.03.017

Rosier, B. T., Marsh, P. D., and Mira, A. (2018). Resilience of the oral microbiota in health: mechanisms that prevent dysbiosis. *J. Dent. Res.* 97, 371–380. doi: 10.1177/0022034517742139

Ruiz-Ruiz, S., Sanchez-Carrillo, S., Ciordia, S., Mena, M. C., Méndez-García, C., Rojo, D., et al. (2020). Functional microbiome deficits associated with ageing: chronological age threshold. *Aging Cell* 19:e13063-11. doi: 10.1111/acel.13063

Schiepers, O. J. G., Wichers, M. C., and Maes, M. (2005). Cytokines and major depression. *Prog. Neuro Psychopharmacol. Biol. Psychiatry* 29, 201–217. doi: 10.1016/j.pnpbp.2004.11.003

Shishkina, G. T., Kalinina, T. S., and Dygalo, N. N. (2007). Up-regulation of tryptophan hydroxylase-2 mRNA in the rat brain by chronic fluoxetine treatment correlates with its antidepressant effect. *Neuroscience* 150, 404–412. doi: 10.1016/j.neuroscience.2007.09.017

Sigel, E., and Ernst, M. (2018). The benzodiazepine binding sites of GABAA receptors. *Trends Pharmacol. Sci.* 39, 659–671. doi: 10.1016/j.tips.2018.03.006

Simpson, C. A., Adler, C., du Plessis, M. R., Landau, E. R., Dashper, S. G., Reynolds, E. C., et al. (2020). Oral microbiome composition, but not diversity, is associated with adolescent anxiety and depression symptoms. *Physiol. Behav.* 226:113126. doi: 10.1016/j.physbeh.2020.113126

Singh, H., Torralba, M. G., Moncera, K. J., DiLello, L., Petrini, J., Nelson, K. E., et al. (2019). Gastro-intestinal and oral microbiome signatures associated with healthy aging. *GeroScience* 41, 907–921. doi: 10.1007/s11357-019-00098-8

Sonowal, R., Swimm, A., Sahoo, A., Luo, L., Matsunaga, Y., Wu, Z., et al. (2017). Indoles from commensal bacteria extend healthspan. *Proc. Natl. Acad. Sci. U. S. A.* 114, E7506–E7515. doi: 10.1073/pnas.1706464114

Strasser, B., Sperner-Unterweger, B., Fuchs, D., and Gostner, J. M. (2017). Mechanisms of inflammation-associated depression: immune influences on tryptophan and phenylalanine metabolisms. *Curr. Top. Behav. Neurosci.* 31, 95–115. doi: 10.1007/7854_2016_23

Suganya, K., and Koo, B.-S. (2020). Gut–brain axis: role of gut microbiota on neurological disorders and how probiotics/prebiotics beneficially modulate microbial and immune pathways to improve brain functions. *Int. J. Mol. Sci.* 21:7551. doi: 10.3390/ijms21207551

Sun, X., Li, M., Xia, L., Fang, Z., Yu, S., Gao, J., et al. (2020). Alteration of salivary microbiome in periodontitis with or without type-2 diabetes mellitus and metformin treatment. *Sci. Rep.* 10:15363. doi: 10.1038/s41598-020-72035-1

Valles-Colomer, M., Falony, G., Darzi, Y., Tigchelaar, E. F., Wang, J., Tito, R. Y., et al. (2019). The neuroactive potential of the human gut microbiota in quality of life and depression. *Nat. Microbiol.* 4, 623–632. doi: 10.1038/s41564-018-0337-x

Venkatapuram, S., Ehni, H.-J., and Saxena, A. (2017). Equity and healthy ageing. *Bull. World Health Organ.* 95, 791–792. doi: 10.2471/BLT.16.187609

Vieira-Silva, S., Falony, G., Darzi, Y., Lima-Mendez, G., Garcia Yunta, R., Okuda, S., et al. (2016). Species–function relationships shape ecological properties of the human gut microbiome. *Nat. Microbiol.* 1:16088. doi: 10.1038/nmicrobiol.2016.88

Wang, H., Foong, J. P. P., Harris, N. L., and Bornstein, J. C. (2021). Enteric neuroimmune interactions coordinate intestinal responses in health and disease. *Mucosal Immunol.* 15, 27–39. doi: 10.1038/s41385-021-00443-1

Wang, Z., Liu, S., Xu, X., Xiao, Y., Yang, M., Zhao, X., et al. (2022). Gut microbiota associated with effectiveness and responsiveness to mindfulness-based cognitive therapy in improving trait anxiety. *Front. Cell. Infect. Microbiol.* 12:719829. doi: 10.3389/fcimb.2022.719829

Wickham, H. (2016). *ggplot2: Elegant Graphics for Data Analysis*. Springer-Verlag: New York.

Wickham, H., François, R., Henry, L., and Müller, K. (2022). dplyr: A Grammar of Data Manipulation. Available at: https://github.com/tidyverse/dplyr

Wu, H. Q., Okuyama, M., Kajii, Y., Pocivavsek, A., Bruno, J. P., and Schwarcz, R. (2014). Targeting kynurenine aminotransferase II in psychiatric diseases: promising effects of an orally active enzyme inhibitor. *Schizophr. Bull.* 40, S152–S158. doi: 10.1093/schbul/sbt157

Yang, C., Fang, X., Zhan, G., Huang, N., Li, S., Bi, J., et al. (2019). Key role of gut microbiota in anhedonia-like phenotype in rodents with neuropathic pain. *Transl. Psychiatry* 9:57. doi: 10.1038/s41398-019-0379-8

Zhang, Y., Huang, J., Xiong, Y., Zhang, X., Lin, Y., and Liu, Z. (2021). Jasmine tea attenuates chronic unpredictable mild stress-induced depressive-like behavior in rats via the gut-brain axis. *Nutrients* 14:99. doi: 10.3390/nu14010099

Zhang, M., Li, A., Yang, Q., Li, J., Wang, L., Liu, X., et al. (2021). Beneficial effect of alkaloids from *Sophora alopecuroides* L. on CUMS-induced depression model mice via modulating gut microbiota. *Front. Cell. Infect. Microbiol.* 11, 1–14. doi: 10.3389/fcimb.2021.665159

Frontiers in Microbiology

Explores the habitable world and the potential of microbial life

The largest and most cited microbiology journal which advances our understanding of the role microbes play in addressing global challenges such as healthcare, food security, and climate change.

Discover the latest Research Topics

See more →

Frontiers

Avenue du Tribunal-Fédéral 34
1005 Lausanne, Switzerland
frontiersin.org

Contact us

+41 (0)21 510 17 00
frontiersin.org/about/contact